

**Design and synthesis of novel bioactive
steroids and beta-lactam based molecules by
click chemistry and application of steroidal
organocatalyst for aldol reaction**

Thesis Submitted to AcSIR

For the Award of the Degree of

DOCTOR OF PHILOSOPHY

In

CHEMICAL SCIENCES



BY

Jaisingh Manohar Divse
(Registration Number: 10CC11A26020)

Under the guidance of
Dr. Santosh B. Mhaske

Organic Chemistry Division
CSIR-National Chemical Laboratory
Pune - 411008, India.

November 2017

सीएसआईआर - राष्ट्रीय रासायनिक प्रयोगशाला

(वैज्ञानिक तथा औद्योगिक अनुसंधान परिषद)

डॉ. होमी भाभा मार्ग, पुणे - 411 008, भारत



CSIR - NATIONAL CHEMICAL LABORATORY

(Council of Scientific & Industrial Research)


Dr. Homi Bhabha Road, Pune - 411 008, India


Dr. Santosh B. Mhaske
Sr. Scientist
Organic Chemistry Division
sb.mhaske@ncl.res.in
+9120 2590 2440

November 2017


Thesis Certificate

This is to certify that the work incorporated in this Ph.D. thesis entitled “**Design and synthesis of novel bioactive steroids and β -lactam based molecules by click chemistry and application of steroidal organocatalyst for aldol reaction.**” submitted by **Mr. Jaisingh Manohar Divse** to Academy of Scientific and Innovative Research (AcSIR) in fulfilment of the requirements for the award of the Degree of Doctor of Philosophy, embodies original research work under my supervision. I further certify that this work has not been submitted to any other University or Institution in part or full for the award of any degree or diploma. Research material obtained from other sources has been duly acknowledged in the thesis. Any text, illustration, table etc., used in the thesis from other sources, have been duly cited and acknowledged.


Mr. Jaisingh Manohar Divse
(Research Student)


Dr. Santosh B. Mhaske
(Research Supervisor)

Communication Channels


NCL Level DID : 2590
NCL Board No. : +91-20-25902000
EPABX : +91-20-25893300
: +91-20-25893400

FAX

Director's Office : +91-20-25902601
COA's Office : +91-20-25902660
SPO's Office : +91-20-25902664

WEBSITE
www.ncl-india.org

Declaration by the Candidate

I hereby declare that the original research work embodied in this thesis entitled **“Design and synthesis of novel bioactive steroids and β -lactam based molecules by click chemistry and application of steroidal organocatalyst for aldol reaction.”** Submitted to Academy of Scientific and Innovative Research for the award of degree of Doctor of Philosophy (Ph. D.) is the outcome of experimental investigations carried out by me under the supervision of **Dr. Santosh B. Mhaske**, Senior Scientist, Organic Chemistry Division, CSIR-National Chemical Laboratory, Pune. I affirm that the work incorporated is original and has not been submitted to any other academy or institute for the award of any degree or diploma.

November 2017

Organic Chemistry Division

CSIR-National Chemical Laboratory

Pune-411008


Jaisingh Manohar Divse
(Research Fellow)



Dedicated to
My family and Teachers

ACKNOWLEDGEMENTS

This thesis represents the amalgamation of my work with the good and bad moments in the past six years in Organic Chemistry Division, NCL. Dozens of people have helped and taught me immensely in life as well as during my Ph. D. stint, I would like to take this as an opportunity to thank all those people.

*First of all, I would like to express my enormous gratitude to my ex-research supervisor **Dr. (Mrs.) Vandana S. Pore** for her cherished guidance, understanding and patience which added considerably to my graduate experience. I am thankful to her for giving me freedom at work place and made my dream. I must also mention that she has had so much patience during my PhD work. My sincere regards and reverence for her will remain forever.*

*I would also like to express my gratitude to my current research supervisor **Dr. Santosh Mhaske** under whom I have completed my rest of the work. I am especially thankful to him for giving me the freedom to continue my research from the previous group. His mentoring and patience towards my work will always be appreciated. The disciplines whatever he taught me, I will follow them throughout my life.*

Dr. Hanumant Borate, for his advice, guidance, supports and encouragements during every stage of this research work and also providing his lab for me.

I also like to acknowledge the efforts taken by Mrs. S. Kunte to help me throughout my research for chiral separations wherever needed.

I also thank Head of the OCD, Dr. Subhash P. Chavan and the former Head of the OCD, Dr. Pradeep K. Tripathi and also the Director of NCL for providing infrastructural facilities. I am also thankful to UGC New Delhi for the financial assistance in the form of fellowship.

I gratefully acknowledge the valuable suggestions and timely help of DAC committee, Dr. H. B. Borate, Dr. N. P. Argade, and Dr. Mrs. S. K. Asha. Suggestions offered during assessments and other presentations are also gratefully acknowledged.

My sincere thanks to the people in various parts of the institute, Mrs. Katharine Raphael, and all OCD and SAC office staff for their cooperation. I would also like to acknowledge all the staff members of GC, HPLC, IR, NMR, Mass, Microanalysis, X-ray analysis, Library, Administration and technical divisions of NCL for their assistance during the course of my work.

I would like to offer thanks to my friends and beloved seniors Dr. Deepak Salunke, Dr. Nilkanth, Dr. Suleman Maujan, Dr. Prakash Chavan, Dr. Ashish Chinchunsure, Dr. Sandip Agalave, Dr. Rohan Erande, Dr. Nagnath Patil, Dr. Manik Bhosale, Dr. Satej Dharmapurikar and Dr. Vivek Humane, for their love and affection.

I would like to thank all my colleagues for always maintaining cheerful and healthy work environment inside as well as outside the Lab. My special thanks to Shrikant, Chaitanya, Vikram, Jaydeep,

ACKNOWLEDGEMENTS

Anand, Dattatray, Vitthal, Suhas, Milind, Pankaj, Jyoti, Dnyaneshwar, Virat, Sachin, Mahesh, Sandip wagh, Manoj, Revan, Ritesh, Namita, Sandhya, Supriya, Nitin and Dr. Kavita whom I shared my most precious moments during my Ph.D.

No words will be sufficient to express my thanks to my friends Ranjeet, Ruby, Mayur, Sachin, Macchindra, Shehabaaz, Vijay, Neha, Dinesh, Sanket, Nitin, Shahaji, Atul and Kunal for the cherished friendships and creating such wonderful atmosphere around me with their support outside the lab.

I especially thanks to Mr. Kamlesh Nerkar and Dr. Vijay Khedkar who stood up behind me throughout my Ph.D career and became my strong moral support.

My family is always source of inspiration and great moral support for me in perceiving my education, I am thankful to God for having me such a supportive family. The words are insufficient to express my gratitude towards my family. I take this opportunity to express gratitude to my parents, Mrs. Padmini and Mr. Manohar Divse for their tons of love, sacrifice, blessings, unconditional support and encouragement. I express my deep and paramount gratitude to my wife Priyanka and brother Anil. Without their constant support and encouragement, I could not stand with this dissertation. I would also like to show my deep gratitude to my parents in law.

At last but not the least, I thank whole heartedly, the omnipotent God, the illimitable superior spirit, for the strength and determination to put my chin up when faced with hardships in life.

Jaisingh Manohar Divse

TABLE OF CONTENTS

❖	General remarks	i
❖	Abbreviations	ii
❖	Synopsis	iv

PRESENT WORK: DIVIDED INTO FOUR CHAPTERS

Chapter 1

Synthesis and biological evaluation of new fluconazole β -lactam conjugates linked *via* 1, 2, 3-triazole through click chemistry as anti-fungal agents.

1.1	Abstract	1
1.2	Introduction	1
1.3	Review of literature	2
1.4	Present Work	8
1.4.1	Objective	8
1.4.2	Result and discussion	9
1.5	Conclusion	20
1.6	Experimental section	21
1.7	NMR spectra	32
1.8	HRMS	38
1.9	References	41

Chapter 2

Design and synthesis of 11 α -substituted bile acid derivatives as potential anti-tuberculosis agents

2.1	Abstract	47
2.2	Introduction	47

TABLE OF CONTENTS

2.3	Review of literature	48
2.4	Present work	59
2.4.1	Objective	59
2.4.2	Result and discussion	59
2.5	Conclusion	72
2.6	Experimental Section	73
2.7	NMR spectra	81
2.8	References	90

Chapter 3

Cholic acid based *trans*-4-hydroxy-(L)- proline derivative as recyclable organocatalyst for highly *diastereo*- and *enantioselective* asymmetric direct aldol reactions in water

3.1	Abstract	97
3.2	Introduction	97
3.3	Review of literature	98
3.4	Present work	103
3.4.1	Objective	103
3.4.2	Result and discussion	104
3.5	Conclusion	114
3.6	Experimental section	114
3.7	HPLC Spectra	123
3.8	NMR Spectra	140
3.9	HRMS	151
3.10	References	158

TABLE OF CONTENTS

Chapter 4

**Design and synthesis of one-pot click derivatives of pregnenolone by
epoxide opening of 20'(*R*)-spiro[oxirane-2,20'-pregn-5'-en]-3' -ol and
their bioevaluation as anti-cancer agents**

4.1	Abstract	163
4.2	Introduction	163
4.3	Review of literature	164
4.4	Present work	170
4.4.1	Objective	170
4.4.2	Result and discussion	171
4.5	Conclusion	181
4.6	Experimental section	181
4.7	NMR spectra	195
4.8	HRMS	219
4.9	References	224

	List of Publications	225
	Erratum	226

GENERAL REMARKS

- ¹H NMR spectra were recorded on AV-200 MHz, AV-400 MHz, JEOL AL-400 (400 MHz) and DRX-500 MHz spectrometer using tetramethylsilane (TMS) as an internal standard. Chemical shifts have been expressed in ppm units downfield from TMS.
- ¹³C NMR spectra were recorded on AV-50 MHz, AV-100 MHz, JEOL AL-100 (100 MHz) and DRX-125 MHz spectrometer.
- Mass spectroscopy was carried out on PI QStar Pulsar (Hybrid Quadrupole-TOF/MS/MS) and High-resolution mass spectra (HRMS) were recorded on a Thermo Scientific Q-Exactive, Accela 1250 pump and also EI Mass spectra were recorded on Finnigan MAT-1020 spectrometer at 70 eV using a direct inlet system.
- Infrared spectra were scanned on Shimadzu IR 470 and Perkin-Elmer 683 or 1310 spectrometers with sodium chloride optics and are measured in cm⁻¹.
- Optical rotations were measured with a JASCO DIP 370 digital polarimeter.
- All reactions are monitored by Thin Layer Chromatography (TLC) carried out on 0.25 mm E-Merck silica gel plates (60F-254) with UV light, I₂, and anisaldehyde in ethanol as developing agents.
- All reactions were carried out under nitrogen or argon atmosphere with dry, freshly distilled solvents under anhydrous conditions unless otherwise specified. Yields refer to chromatographically and spectroscopically homogeneous materials unless otherwise stated.
- All evaporations were carried out under reduced pressure on Buchi rotary evaporator below 50 °C unless otherwise specified.
- Silica gel (60-120), (100-200), and (230-400) mesh were used for column chromatography.
- **Each chapter and section has different compounds, may contain same numbers and reference numbers.**


DEFINITIONS AND ABBREVIATIONS

Ac	Acetyl
Ac ₂ O	Acetic anhydride
AlCl ₃	Aluminium chloride
AIBN	2,2'-Azobisisobutyronitrile
aq	Aqueous
b	Broad
Bn	Benzyl
BnBr	Benzyl bromide
CDCl ₃	Deuterated chloroform
cm	Centimeter
(COCl) ₂	Oxalyl chloride
DCM	Dichloromethane
d	Doublet
dm	Decimeter
DMF	Dimethylformamide
DMSO	Dimethyl sulfoxide
DMSO-d ₆	Deuterated dimethyl sulfoxide
EDC	Ethylene dichloride
EtOAc	Ethyl acetate
Et ₃ N	Triethyl amine
g	Grams
h	Hour/s
HPLC	High performance liquid chromatography
IR	Infrared
K ₂ CO ₃	Potassium carbonate
L	Liter
m	Multiplet
M ⁺	Molecular ion
mg	Milligrams
MHz	Megahertz
min	Minutes

DEFINATIONS AND ABBREVIATIONS

ml	Milliliter
mmol	Millimole
MP	Melting point
MTCC	Microbial type culture collection
n-BuLi	<i>n</i> -Butyllithium
Na ₂ SO ₄	Sodium sulfate
NaHCO ₃	Sodium bicarbonate
NaH	Sodium hydride
NaI	Sodium iodide
NBS	<i>N</i> -Bromosuccinimide
NMR	Nuclear Magnetic Resonance
psi	Per square inch
<i>P-TSA</i>	<i>para</i> toluene sulfonic acid
q	Quartet
rt	Room temperature
RT	Retention time
R _f	Retention factor
s	Singlet
t	Triplet
TBAB	Tetrabutylammonium bromide
TBDMS	<i>tert</i> -Butyldimethylsilyl
TEA	Triethyl amine
THF	Tetrahydrofuran
TLC	Thin layer chromatography

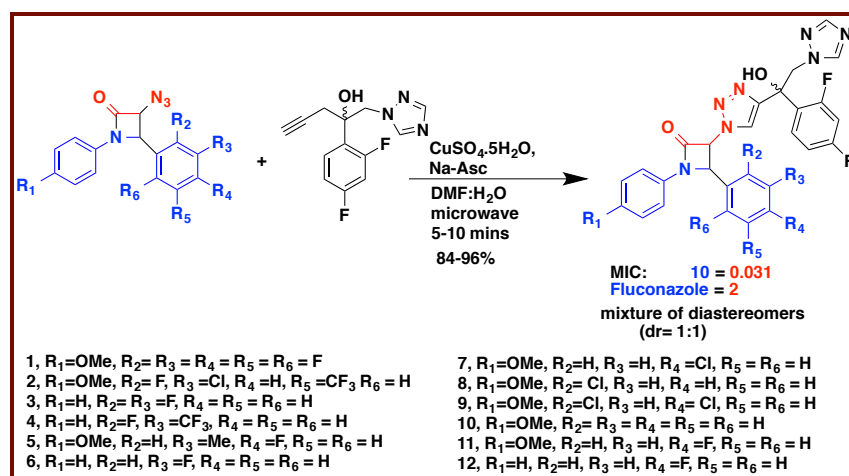
Synopsis

	Synopsis of the Thesis to be submitted to the Academy of Scientific and Innovative Research for Award of the Degree of Doctor of Philosophy in Chemistry
	Name of the Candidate Mr. Jaisingh M. Divse
	Degree Enrolment No. & Date Ph.D in Chemical Sciences (10CC11A26020); August 2011
	Title of the Thesis Design and synthesis of novel bioactive steroids and beta-lactam based molecules by click chemistry and application of steroidal organocatalyst for aldol reaction
	Research Supervisor Dr. Santosh B. Mhaske (AcSIR, CSIR-NCL, Pune)

Introduction:

The thesis is divided into four different working chapters. Chapter 1 involves design and synthesis of novel 1, 2, 3-triazole-linked β -lactam–fluconazole conjugates linked *via* 1, 2, 3-triazole and also deals with its biological evaluation as potent antifungal. Chapter 2 involves design and synthesis of 11α -substituted bile acid derivatives as potential anti-tuberculosis agents and molecular docking study supports the biological findings. Chapter 3 deals with synthesis of efficient bile acid based *trans*-4-hydroxy-(L)- proline derivative as recyclable organocatalyst for highly diastereo- and enantioselective asymmetric direct aldol reactions in water. Finally, Chapter 4 involves design and synthesis of novel one pot click derivatives of pregnenolone from epoxide opening of 20'(R)-Spiro[oxirane-2,20'-pregn-5'-en]-3' -ol, and their biological evaluation as anticancer agents.

Chapter 1: Synthesis and biological evaluation of new fluconazole β -lactam conjugates linked *via* 1, 2, 3-triazole as antifungal agents:

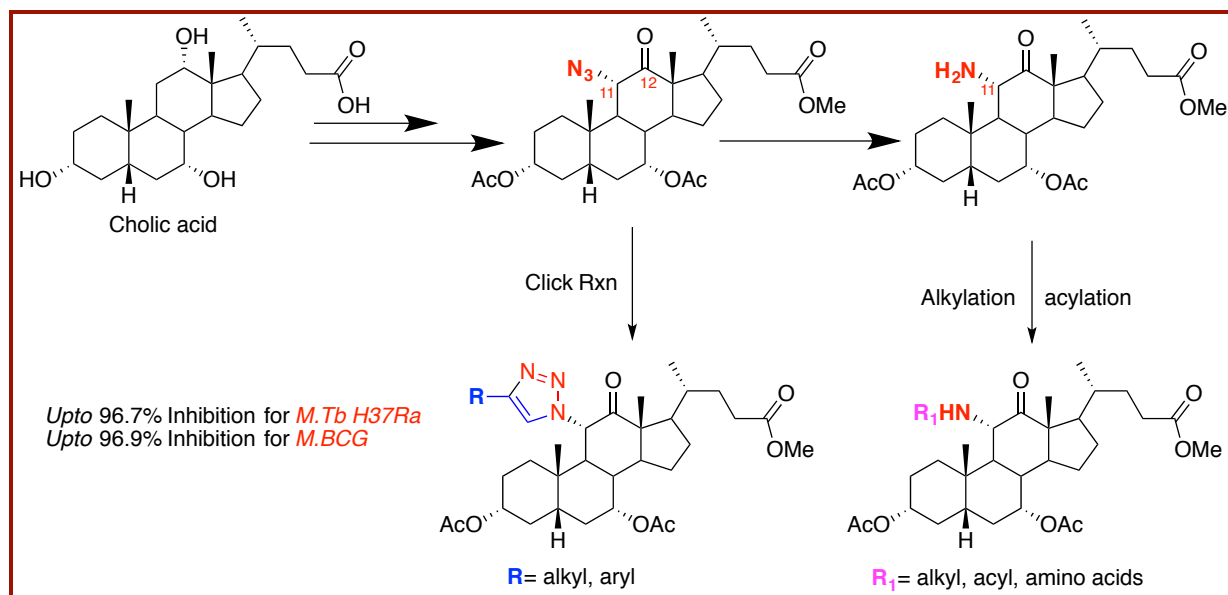


Novel 1, 2, 3-triazole-linked β -lactam–fluconazole conjugates were designed and synthesized.¹ The compounds showed potent antifungal activity against two pathogenic *Candida* strains;

Candida albicans ATCC 24433 and *Candida albicans* ATCC 10231 with MIC values in the range of 0.0625–2 µg/mL. Compounds showed promising antifungal activity against all the tested fungal pathogens except *C. neoformans* ATCC 34554 compared to fluconazole. Compound in which the β-lactam ring was formed using *para*-anisidine and benzaldehyde was found to be more potent than fluconazole against all the fungal strains with an IC₅₀ value of <0.015 µg/mL for *Candida albicans* (ATCC 24433). Mechanistic studies for active compounds revealed that the antifungal action was due to ergosterol inhibition. Two compounds at a concentration of 0.125 µg/mL caused 91.5 and 96.8% ergosterol depletion, respectively, compared to fluconazole which at the same concentration caused 49% ergosterol depletion. The molecular docking study revealed that all the fluconazole β-lactam conjugates could snugly fit into the active site of lanosterol 14α-demethylase (CYP51) with varying degrees of affinities. As anticipated, the binding energy for most potent compound (-58.961 kcal mol⁻¹) was much smaller than that for fluconazole (-52.92 kcal mol⁻¹). The synthesized compounds have therapeutic potential for the control of candidemia.

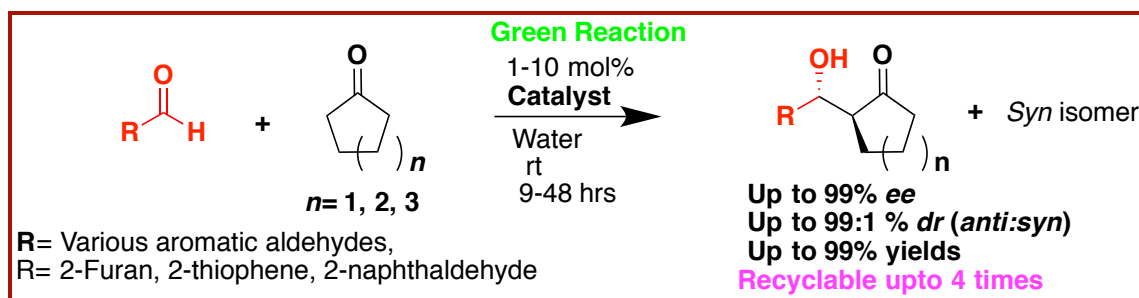
Chapter 2: Design and synthesis of 11α-substituted bile acid derivatives as potential anti-tuberculosis agents.

This chapter involves design and synthesis of a series of novel 11α-triazoyl bile acid derivatives.^{2,3} In addition, we also have synthesized N-alkyl and N-acyl derivatives of C-11 amino bile acid esters. All the compounds were evaluated for the inhibitory activity against *Mycobacterium tuberculosis* H37Ra (*MTB*) at 30 µg/mL level. Four lead compounds were further confirmed from their dose dependent effect against *MTB*. These compounds were found to be active against Dormant and active stage *MTB* under both in *vitro* as well as within THP1 host macrophages. The most promising compound showed strong anti-tubercular activities against *MTB* under *in-vitro* and *ex-vivo* (IC₉₀ value of ≈3 µg/mL) conditions and almost insignificant cytotoxicity up to 100 µg/mL against THP-1, A549 and PANC-1 human cancer cell lines. Inactivity of all these compounds against Gram positive and Gram negative bacteria indicates their specificity. Molecular docking studies of these compounds into the active site of *DprE1* enzyme revealed a similar binding mode to native ligands in the crystal structure thereby helping to establish a structural basis of inhibition of *MTB*. The synthesized compounds were analyzed for ADME properties and showed potential to develop good oral drug candidates. Our results clearly indicate the identification of some novel, selective and specific inhibitors against *MTB* that can be explored further for potential anti-tubercular drug.



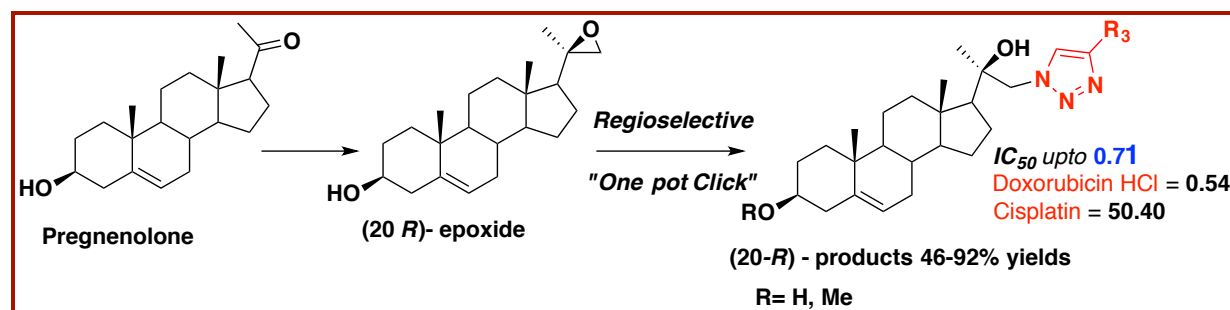
Chapter 3: Cholic acid based *trans*-4-hydroxy-(L)- proline derivative as recyclable organocatalyst for highly diastereo- and enantioselective asymmetric direct aldol reactions in water.

A new cholic acid derived organocatalyst was prepared by linking *trans*-4-hydroxy-L-proline through 1, 2, 3-triazole linkage using click chemistry. The resulting organocatalyst was found to be most active against asymmetric direct aldol reaction between *para*-nitro benzaldehyde and cyclohexanone in water without the need for organic solvents and toxic co-catalysts and additives. The results obtained were excellent giving >98% yields, >99% *ee* and 98:2 *dr* in just 9 hours using 10 mol % of the catalyst. Such efficiency is attributed to the fact that the cholic acid moiety containing amide and a triazole ring facilitated the accessibility of hydrophobic reactants to active sites in water and stabilized the formed enamine intermediate during the reaction. Low catalyst loading *i.e.*, just 1 mol % of the catalyst was also found to achieve >88% yield and >99.5% *ee* for *para*-nitrobenzaldehyde and cyclohexanone. Furthermore, the catalyst can be recycled atleast three times affording similar results in terms of enantioselectivity and diastereoselectivity, but in reducing yields.



Chapter 4: Synthesis of novel one-pot click derivatives of pregnenolone from epoxide opening of 20'(R)-Spiro[oxirane-2,20'-pregn-5'-en]-3' -ol, and their biological evaluation as anti-cancer agents.

A series of new 1, 2, 3-triazole derivatives based on 20(R)-hydroxycholesterol skeleton, starting from 16-dehydropregnenolone acetate (16-DPA) were synthesized by three component "one-pot" reaction protocol. The reaction is regioselective in terms of epoxide opening in in-situ conditions followed by click reaction. The regioselective formation of intermediate azide and the final product is confirmed by single X-ray crystallography. All the synthesized compounds showed potent anticancer activity against one of the breast cancer cell line (MDA-MB-231) with IC₅₀ value upto 0.71 µg/mL. Molecular docking study also supports the biological findings.



References:

1. Synthesis and biological evaluation of new fluconazole β -lactam conjugates linked via 1, 2, 3-triazole, Jaisingh M. Divse, Santosh B. Mhaske, Chaitanya R. Charolkar, Duhita G. Sant, Santosh G. Tupe, Mukund V. Deshpande and Vandana S. Pore, *New J. Chem.*, **2017**, *41*, 470-479.
2. Design and synthesis of 11 α -substituted bile acid derivatives as potential anti-tuberculosis agents, Vandana S. Pore, Jaisingh M. Divse, Chaitanya R. Charolkar, Laxman U. Nawale, Vijay M. Khedkar, Dhiman Sarkar, *Bioorganic & medicinal chemistry letters*, **2015**, *25* (19), 4185-4190.
3. 11-Substituted Bile acid derivatives, process for the preparation thereof and use of these compounds as medicaments, Jaisingh Divse, Vandana S. Pore, C. Charolkar , **WO Patent WO 2015/087340 A1, US 20160311848 A1**

Chapter 1

Synthesis and biological evaluation of new fluconazole β -lactam conjugates linked *via* 1, 2, 3-triazole through click chemistry as antifungal agents.

Chapter 1

Synthesis and biological evaluation of new fluconazole β -lactam conjugates linked via 1, 2, 3-triazole through click chemistry as antifungal agents.

1.1 Abstract

Applications of 'click chemistry' are frequently found in all aspects of drug discovery, ranging from lead developments through combinatorial chemistry and target-templated *in vitro* chemistry, to proteomics and DNA research, using bioconjugation reactions. The triazole products are more than just idle linkers; they easily correlate with biological targets, through hydrogen bonding and dipole interactions. In this chapter, novel 1, 2, 3-triazole-linked β -lactam-fluconazole conjugates **31(a-l)** were designed and synthesized.¹ The compounds showed potent antifungal activity against two pathogenic *Candida* strains; *Candida albicans* ATCC 24433 and *Candida albicans* ATCC 10231 with MIC values in the range of 0.0625–2 $\mu\text{g/mL}$. Compounds **31h**, **31j** and **31k** showed promising antifungal activity against all the tested fungal pathogens except *C. neoformans* ATCC 34554 as compared to fluconazole.¹ Compound **31j** in which β -lactam ring was formed using *para*-anisidine and benzaldehyde was found to be more potent than fluconazole against all the fungal strains with an IC_{50} value of $<0.015 \mu\text{g/mL}$ for *Candida albicans* (ATCC 24433). Mechanistic studies for active compounds revealed that the antifungal action was due to ergosterol inhibition. Compounds **31h** and **31j** at 0.125 $\mu\text{g/mL}$ concentration caused 91.5 and 96.8% ergosterol depletion respectively as compared to fluconazole which at same concentration caused 49% ergosterol depletion. Molecular docking study revealed that all the fluconazole β -lactam conjugates **31(a-l)** could snugly fit into the active site of lanosterol 14 α -demethylase (CYP51) with varying degree of affinities.¹ As anticipated, binding energy for compound **31j** (-58.961 kcal/mol) was much lesser than fluconazole (-52.92 kcal/mol). The synthesized compounds have therapeutic potential for the control of candidemia.¹

1.2 Introduction

Click chemistry is a modular synthetic approach towards the assembly of new molecular entities. It's used firmly demonstrates a broad scope of Copper-catalyzed azide-alkyne cycloaddition (CuAAC) in different areas of life and material chemistry such as drug discovery,² bioconjugation,² polymer science,⁴ and related fields⁵ including supramolecular chemistry.⁶ The presence of heterocyclic rings in the various medicinal entities most often

contain 1, 2, 3-triazole and 1, 2, 4-triazole moiety. A lot of research has been carried out on triazole and their derivatives, which has proved the pharmacological importance of this heterocyclic nucleus. Kharb *et al.* have reviewed⁷ the pharmacological activities of triazole derivatives with an update of recent research findings. Sheng and Zhang present a focused review on the most significant achievements in the discovery of antifungal lead structures within last few years.⁸ Mainly, the structure-activity relationship of antifungal leads and scope for future antifungal drug discovery is provided. Fungal infections caused by *Candida*, *Aspergilli* and *Cryptococcus* have continued to be a major medical problem since past two decades especially involving immunocompromised patients.^{9,10} Four major types of drugs including azoles (e.g. fluconazole), allyamines (e.g. naftifine), polyene macrolides (e.g. amphotericin B) and echinocandins (e.g. caspofungin) are most frequently used antifungal agents for treatment of fungal infections.¹¹ The current antifungal drugs are either highly toxic (amphotericin B) or are becoming ineffective due to emergence of resistant strains (flucytosine and azoles). In spite of significant research on antifungal agents, the azoles continue to be the mainstay of therapy for systemic life threatening fungal infections as they can be administered orally and have broad-spectrum activities against most of the pathogenic yeasts and filamentous fungi. Fluconazole, a 1, 2, 4-triazole has shown an exceptional therapeutic performance against *Candida* infections. It is a drug of choice for the treatment of infections by *Candida albicans* and *Cryptococcus neoformans* due to its potent activity; excellent safety profile, and favorable pharmacokinetics characteristics.¹² However, fluconazole is not fungicidal and extensive use of fluconazole has increased the number of fluconazole-resistant *C. albicans* isolates.¹³ Therefore; great efforts have been made to modify the chemical structure of fluconazole, in order to broaden its antifungal spectrum of activity and to increase its potency.

1. 3. Review of Literature

1. 3.1 Cu catalysed azide alkyne cycloaddition “Click reaction”

The 1, 3-dipolar cycloaddition reactions (DCR) for the synthesis of five membered heterocycles are well known transformations in synthetic organic chemistry.¹⁴ This reaction produces two regioisomers namely 1, 4- and 1, 5-disubstituted-1, 2, 3-triazole products in 1:1 ratio. Sharpless^{15a} and Meldal^{15b} groups have already reported the rate improvement (up to 107 times) and enhanced regioselectivity of the Huisgen 1, 3-DCR of an organic azide to terminal acetylene to afford, regiospecifically, the 1, 4-disubstituted, 1, 2, 3-triazole in the

presence of Cu(I) catalyst (Figure 1). The Cu (I)-catalyzed 1, 3-DCR has strongly satisfied the requirement of “click chemistry” as mentioned by Sharpless and within the past few years, it has become a premier element of synthetic organic chemistry.¹⁶

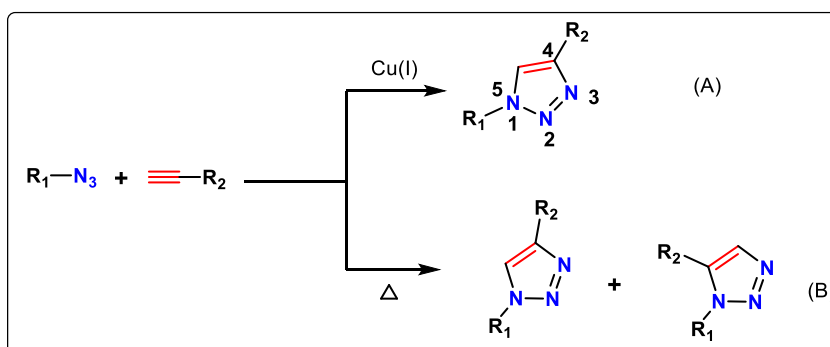


Figure 1. 1, 3-Dipolar cycloaddition between organic azides and terminal alkynes

The classical non-catalyzed process proceeds by a concerted mechanism under thermal conditions to afford a mixture 1, 4- and 1, 5-disubstituted, 1, 2, 3-triazole regioisomers. The relative proportion of regioisomers and rate can be predicted from electronic and steric effects.¹⁷ The Cu(I)-catalysed (“click”) process has been postulated to occur in a step wise mechanism from recent thermal and kinetic studies.¹⁷ A substantial rise in the rate of the Cu(I)-catalysed process in the aqueous solvents is justified regarding stepwise process which lowers the activation barrier relative to that of the non-catalysed process by as much as 11.8 kcal/mol.^{18,19} The proposed catalytic cycle involves several postulated and transient Cu(I)-acetylide complexes, starting with complexation of the alkyne to the Cu(I) metal centre to form a Cu(I)-alkyn π -complex (A) (Figure 2).²⁰

1.3.2 Click reaction and pharmacological applications of 1, 2, 3-triazoles

Click chemistry offers a novel approach to the synthesis of 1, 2, 3-triazole containing molecules. Azides and alkynes are basically inert to most of the biological conditions, oxygen, water, and the majority of common reaction conditions in the modern organic synthesis.²¹ 1, 2, 3-Triazole moiety does not occur in nature, although the synthetic molecules containing 1, 2, 3-triazole units show diverse biological activities (Figure 3). 1, 2, 3-Triazole moieties are engaging connecting units, as they are stable to metabolic degradation and also capable of hydrogen bonding, which can be complimentary in the binding of biomolecular targets and enhance the solubility.²² The importance of triazole containing compounds in medicinal chemistry is indisputable. Contrary to other azaheterocycles, the 1, 2, 3-triazole ring is unprotonated at physiological *pH* because of its

poor basicity. Hence, the unprotonated sp^2 -hybridized nitrogen atoms of 1, 2, 3-triazoles may better mimic the partial positive charge at the anomeric carbon in the transition state of the glucosidase catalyzed reaction than the corresponding basic nitrogen atoms of iminosugars.²³

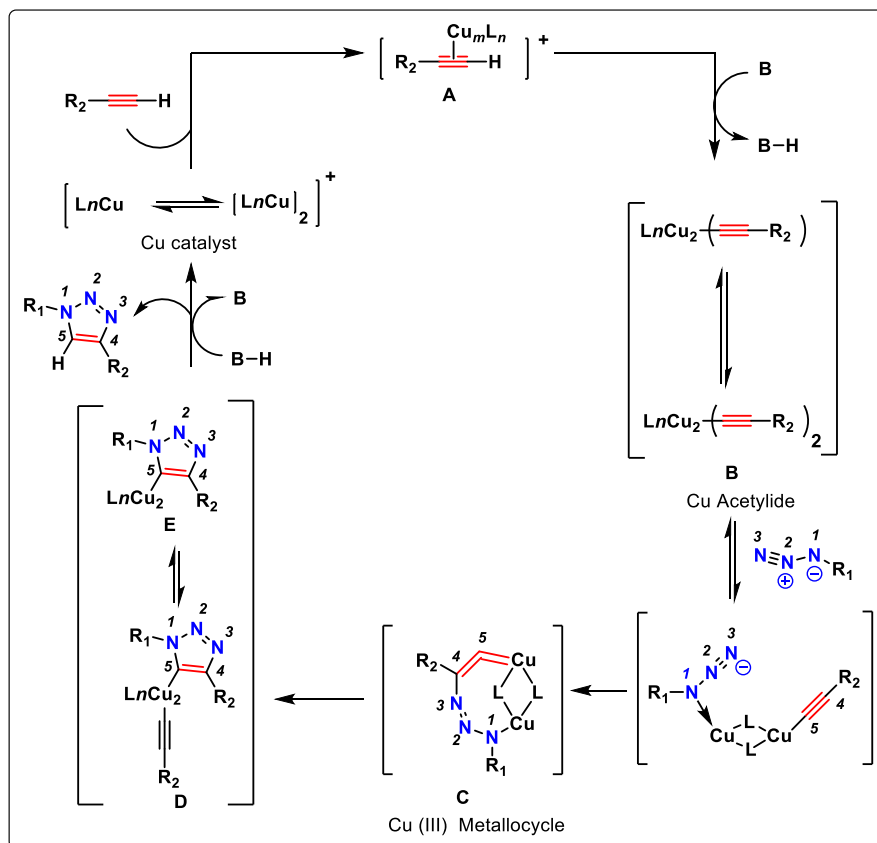


Figure 2. Outline of plausible mechanisms for the Cu(I) catalyzed reaction between organic azides and terminal alkynes

1.3.3 Antifungal and Antibacterials

Based on the structure of the active site of lanosterol 1, 4 α -demethylase (CYP51) and the extensive investigation of the structure–activity relationships ofazole antifungals, it was found that 1, 2, 4-triazole ring and 2, 4-difluorophenyl group are essential for the promising antifungal activity.²⁴ Dangerous fungal infections has tremendously raised in last two decades due to greater use of immunosuppressive drugs, prolonged use of broad-spectrum antibiotics. The antifungal and antibacterial drugs presently marketed are either highly toxic or becoming ineffective due to the emergence of resistant strains and necessitates continuing research into new classes of antimicrobial agents. 1, 2, 3-Triazole containing molecules is one of these categories.

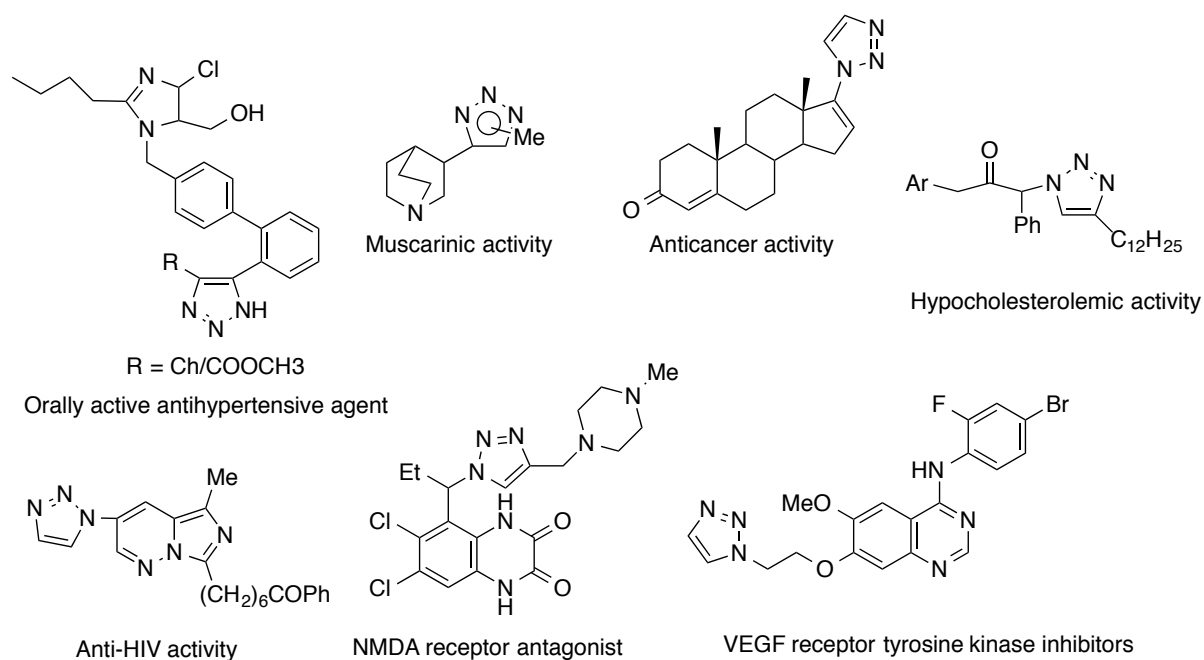


Figure 3. 1, 2, 3-Triazole containing molecules with different biological activities.

From our group, we have designed, and synthesized^{25a} fluconazole/bile acid conjugates at C-3 and C-24 positions of bile acids under microwave assisted Cu (I) catalyzed cycloaddition reaction. These 1, 4-disubstituted fluconazole/bile acid conjugates, linked with 1, 2, 3-triazole, were synthesized in excellent yield and in lesser reaction time. These new entities were found to be antifungal against *Candida* species having MIC ranging from 3.12 to 6.25 $\mu\text{g}/\text{mL}$. It was considered that bile acid part acts as a drug carrier and fluconazole part acts as an inhibitor of 14-demethylase enzymes in the fungal cell. Our group also reported synthesis^{25b} of fluconazole based novel mimics containing 1, 2, 3-triazole with or without substitution at C-4 (Figure 4, **1** and **2**). Some of the compounds were observed to be more potent against *Candida* fungal pathogens than fluconazole and amphotericin B. It was observed that a compound having long alkyl chain reduced fungal load in mice by 97.4% and did not show any profound proliferative effect at lower dose (0.001 mg/mL). We also reported^{25c} synthesis of new fluconazole analogues (Figure 4, **3**, **4**) containing two different 1, 2, 3-triazole units in the side chain component. All the compounds were found to show potent antifungal activity.

There is a report²⁶ from our group on synthesis of novel 1, 2, 3-triazole-linked β -lactam–bile acid conjugates (Figure 4, **5**) and some dimeric compounds (Figure 4, **6**) by 1,3-dipolar cycloaddition reaction of azido β -lactam and terminal alkyne of bile acids. Most of

the compounds exhibited vital antifungal and moderate antibacterial activity against all the tested strains. One of the compounds showed excellent antifungal activity with MIC value of 16 $\mu\text{g/mL}$ against *C. albicans* and 8 $\mu\text{g/mL}$ against *B. poitrasii*.

Chaudhary *et al.* Synthesized²⁷ several novel 1, 4-disubstituted-1, 2, 3-triazolyluridine derivatives (Figure 4, 7) by ‘click chemistry’ approach, most of which showed significant antifungal activity. One of the compounds showed potent antifungal activity against *C. neoformans* with MIC of 8 $\mu\text{g/mL}$ (0.018 $\mu\text{g/mL}$ for Fluconazole).

Sangshetti and Shinde developed²⁸ a new, convenient, simple and efficient method for the synthesis of novel series of 3-(1-(1-substituted piperidin-4-yl)-1H-1, 2, 3-triazol-4-yl)-5,6-diphenyl-1, 2, 4-triazines (Figure 5, 8) using $\text{ZrOCl}_2 \cdot 8\text{H}_2\text{O}$ as a catalyst. A novel series of 1, 2, 3 triazole compounds possessing 1, 2, 4-oxadiazole ring (Figure 5, 9) was also efficiently synthesized by these authors.²⁹ Some of the synthesized compounds were found to be as active as or potent than miconazole and comparable to that of fluconazole.

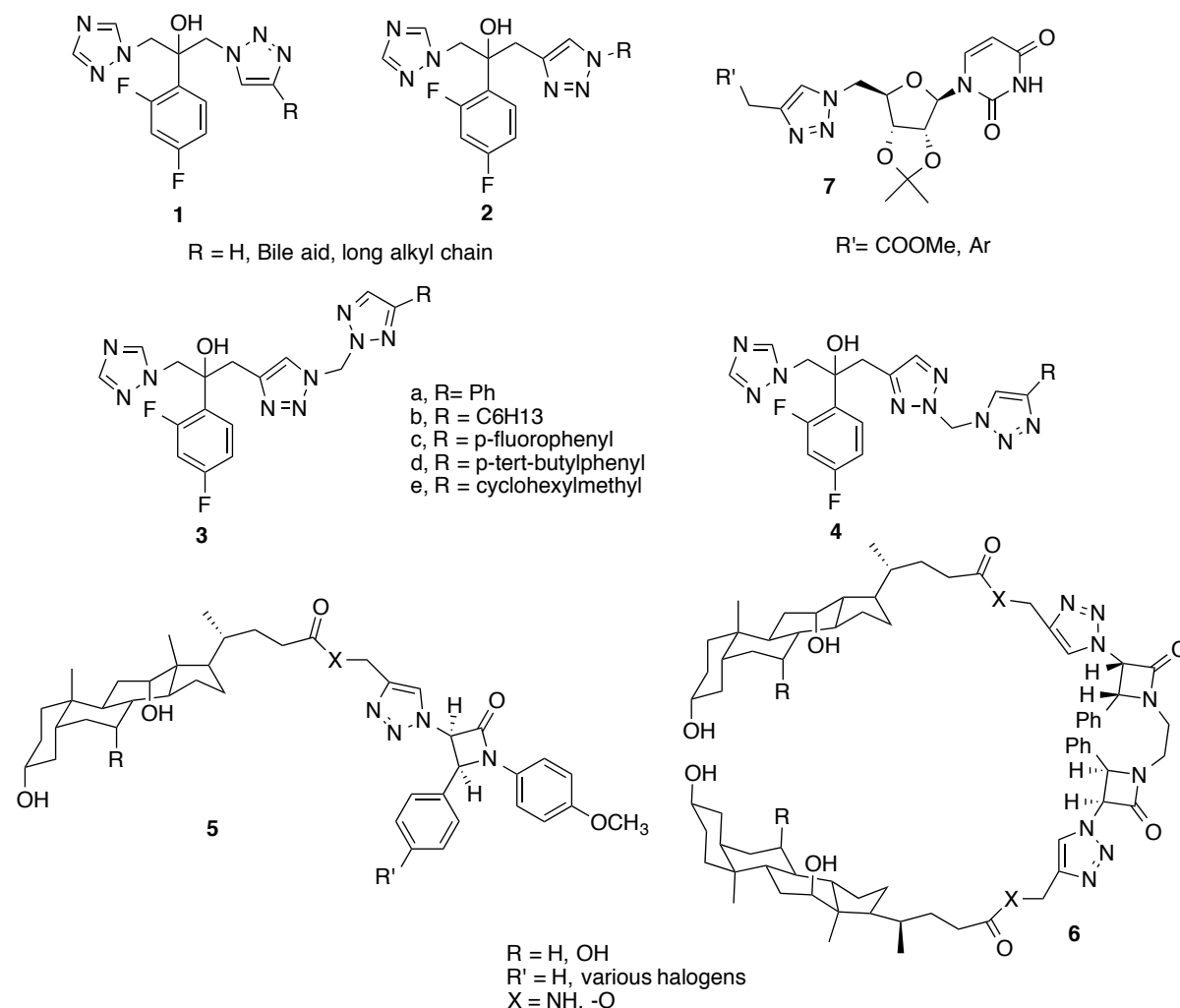


Figure 4. Structures 1-7

To find new antileishmanial drugs activity Ferreira *et al.* Synthesized³⁰ new imidazole and triazole containing compounds and tested them against promastigote forms of *Leishmania amazonensis*. The results showed that the introduction of the difluoromethylene moieties (Figure 5, **10**) turned the inactive carbaldehydes into active antileishmanial compounds with IC₅₀ below 3.0 μM. Kategaonkar and coworker's reported³¹ antimicrobial activities of new 2-chloro-3-((4-phenyl-1*H*-1, 2, 3-triazol-1-yl) methyl) quinoline derivatives (Figure 5, **11**) against a large number of fungal and bacterial strains.

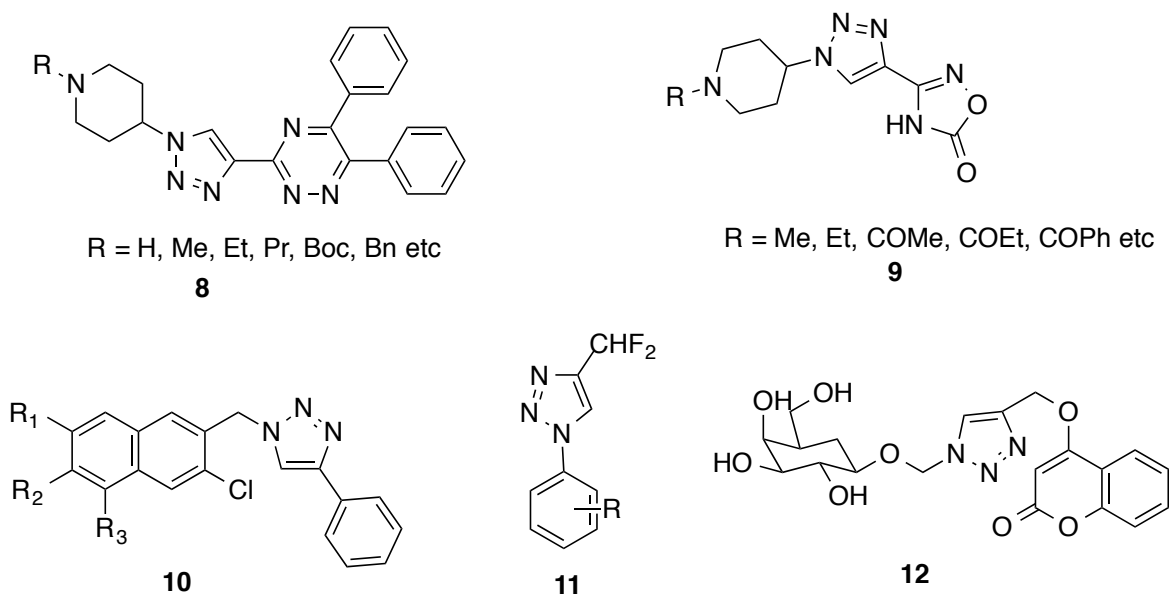


Figure 5. Structures 8-12

A series of sugar derivatives bearing two kinds of reactive handles (alkynyl and azide) were synthesized enzymatically from unprotected sugars giving rise to triazole-containing glycosides³² (Figure 5, **12**). The activities of triazole glycosides were found to be antifungal.

Luesse *et al.*³³ synthesized a library of nonactive acid-derived triazoloamide derivatives (Figure 6, **13**) and evaluated as antimicrobial agents. Sumangala and his co-worker's synthesized³⁴ 1, 2, 3-triazoles containing quinoline moiety (Figure 6, **14**). They studied their antimicrobial and antifungal activity using cyclo-piroxolamine as a standard antifungal agent. Investigation of the structure activity relationships revealed that nature of the substituent on position 4 of triazole ring influences the antimicrobial activity.

Substituted 1, 2, 3-triazoles such as N-[1-arylmethylen e]-1-[8-(trifluoromethyl)quinolin-4-yl]-5-methyl-1*H*-1, 2, 3-triazole-4-carbohydrazides and [1-aryl-4-{1-[8-(trifluoromethyl)quinolin-4-yl]-5-methyl-1*H*-1, 2, 3-triazol-4-yl}prop-2-en-1-ones showed

good antimicrobial activity.³⁵ Thomas and his co-workers reported antimicrobial activities of new quinoline derivatives (Figure 6, **15**) having 1, 2, 3-triazole moiety.³⁶

Reddy *et al.*³⁷ reported the synthesis and antimicrobial evaluation of glycol-derived novel tetrahydrofuran 1, 2, 3-triazoles (Figure 6, **16 and 17**).³⁷ The most potent molecule showed antibacterial and antifungal activities with MIC value of 12.5 $\mu\text{g/mL}$.

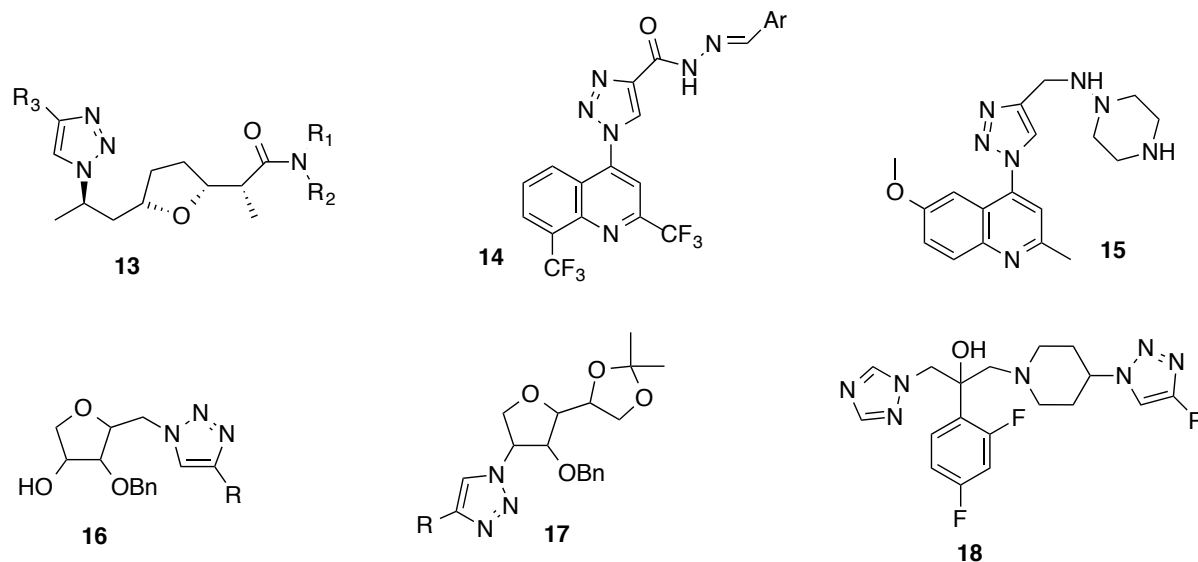


Figure 5. Structures 13-18

Due to rising incidence of invasive fungal infections and critical drug resistance to triazole antifungal agents, Z. Jiang *et al.*³⁸ designed and synthesized a series of novel antifungal triazoles with substituted triazole-piperidine side chains **18** (Figure 6). Most of the target compounds were found to be potent against a variety of clinically important fungal pathogens. In particular, some compounds were highly active against *Candida albicans* and *Cryptococcus neoformans* with MIC values in the range of 0.125 mg/mL to 0.0125 mg/mL. They represent promising leads for the development of new generation of triazole antifungal agents. Molecular docking studies revealed that the target compounds interacted with CACYP51 mainly through hydrophobic and Vander Waals interactions.

1.4 Present work

1.4.1 Objective

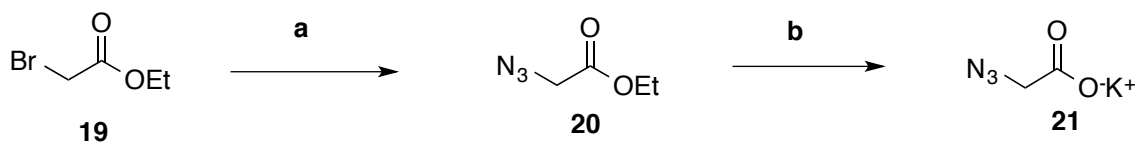
As can be seen from above discussion, there is rise in the incidence of invasive fungal infections and critical drug resistance to various antifungal agents including fluconazole itself. Hence, there is always a scope for improvement in the existing drugs through their modification in terms of introducing new and effective pharmacophores or

making their hybrids by associating them with novel molecules with new biological potentials. A beta-lactam (β -lactam) ring is a four-membered lactam cyclic amide, and the β -lactam ring is part of the nucleus structure of several antibiotic classes, the important ones being the penicillins, carbapenems, cephalosporins, and monobactams, which are, hence, also called β -lactam antibiotics. Almost all of these antibiotics work by inhibiting bacterial cell wall biosynthesis. Here, we have introduced β -lactam moiety to the fluconazole linked through 1, 2, 3- triazole to enhance its biological potential.

1.4.2 Results and discussion

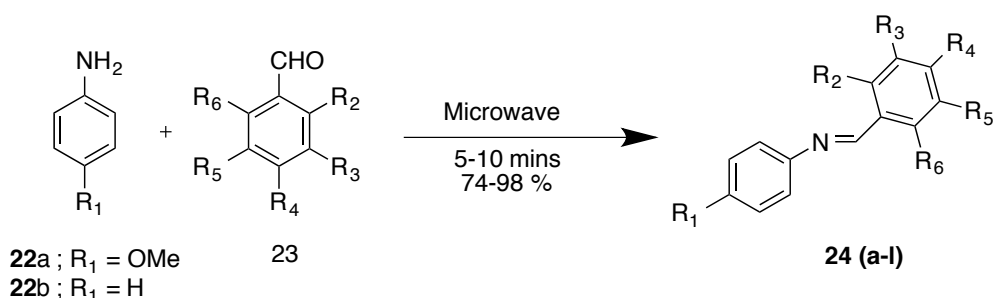
1.4.2.1 Chemistry

Target molecules **30 (a-l)** were synthesized by click reaction of β -lactam containing the racemic mixture of azides **25 (a-l)** and with fluconazole based intermediate **29** having terminal alkyne, in the presence of Cu(I) catalys. Synthesis of potassium salt of azido acetic acid **21** was started from ethyl bromoacetate **19** (Scheme 1). Compound **19** on treatment with sodium azide afforded ethyl azidoacetate **20** with 82% of yield. Subsequent saponification of ester functionality of compound **20** with KOH in methanol gave the potassium salt of azidoacetic acid **21** with 96% yield (Scheme 1).



Scheme 1. a) NaN_3 , Dry DMF, 80 °C, 8 h, 82%; b) KOH, MeOH, rt, 3 h, 96%

Imines **24 (a-l)** were conveniently prepared in a microwave without any solvents or catalysts within 5-10 minutes in excellent yields (90-95%), from the amines **22 (a and b)** and aldehydes **23 (a-l)**. These imines were used to prepare intermediate azides **24 (a-l)** without any further purification (Scheme 2).

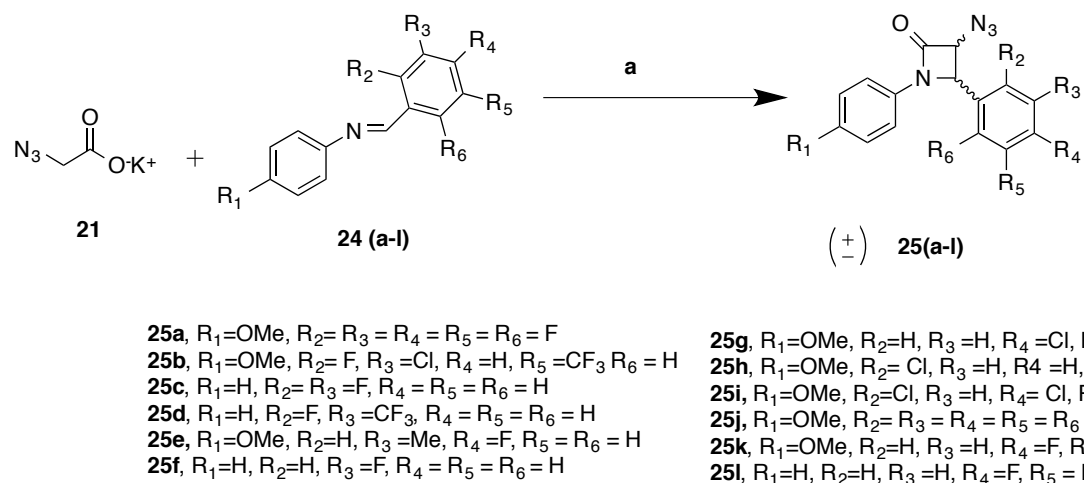


24a, R₁=OMe, R₂= R₃ = R₄ = R₅ = R₆ = F
24b, R₁=OMe, R₂= F, R₃ =Cl, R₄ =H, R₅=CF₃ R₆ = H
24c, R₁=H, R₂= R₃ =F, R₄ = R₅ = R₆ = H
24d, R₁=H, R₂=F, R₃ =CF₃, R₄ = R₅ = R₆ = H
24e, R₁=OMe, R₂=H, R₃ =Me, R₄ =F, R₅ = R₆ = H
24f, R₁=H, R₂=H, R₃ =F, R₄ = R₅ = R₆ = H

24g, R₁=OMe, R₂=H, R₃ =H, R₄ =Cl, R₅ = R₆ = H
24h, R₁=OMe, R₂= Cl, R₃ =H, R₄ =H, R₅ = R₆ = H
24i, R₁=OMe, R₂=Cl, R₃ =H, R₄ = Cl, R₅ = R₆ = H
24j, R₁=OMe, R₂= R₃ = R₄ = R₅ = R₆ = H
24k, R₁=OMe, R₂=H, R₃ =H, R₄ =F, R₅ = R₆ = H
24l, R₁=H, R₂=H, R₃ =H, R₄ =F, R₅ = R₆ = H

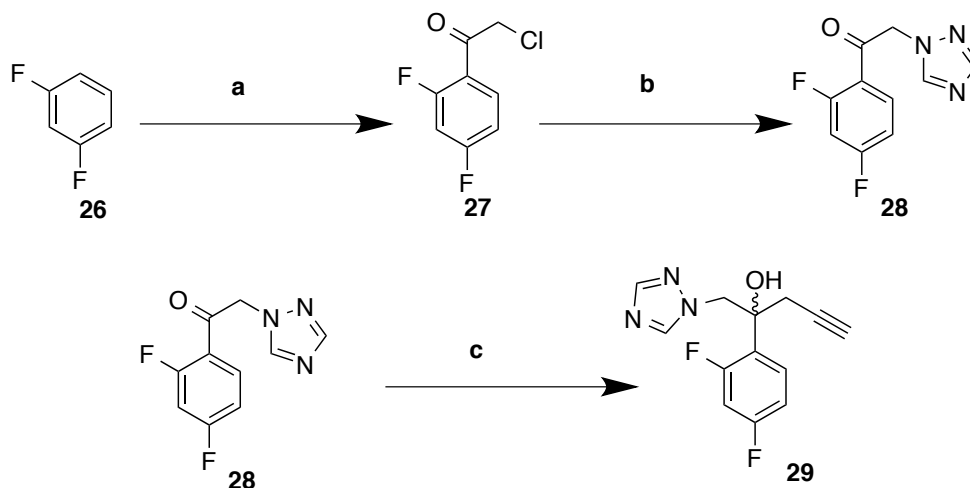
Scheme 2. Synthesis of Imines **24 (a-l)** using microwave 360-540W for 5-10 mins.

The diastereomeric mixture azides **25 (a-l)** were prepared by using the ketene–imine cycloaddition (Staudinger reaction)³⁹ of potassium azidoacetate **21** and imines **24 (a-l)** in the presence of triphosgene and triethylamine in anhydrous dichloromethane with good yields (Scheme 3). Compounds **25 (a-l)** were obtained as diastereomeric mixture which was inseparable by crystallization or column chromatography.^{40,41}



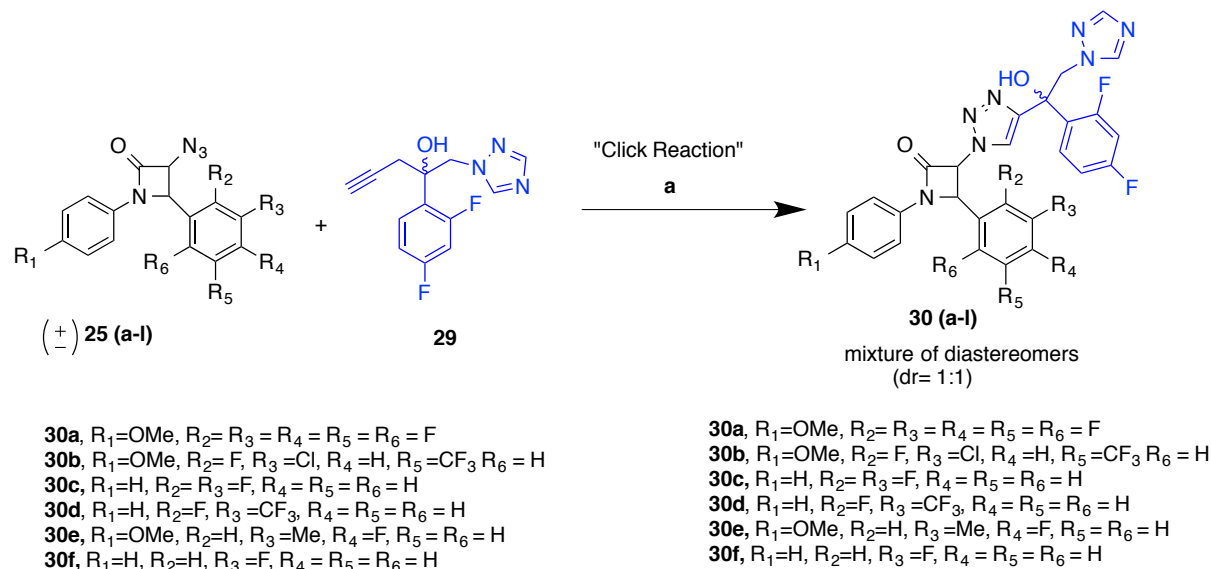
Scheme 3. a) Triphosgene, triethylamine, Dry DCM, 0 °C to rt, 18 h, 62-93%

Keto compound **28** was synthesized starting from *m*-difluorobenzene **26** by Friedel-Crafts acylation using chloroacetyl chloride and AlCl₃ followed by substitution of chlorine by 1, 2, 4-triazole. Further reaction of **28** with propargyl bromide under Barbier type reaction conditions using activated zinc and propargyl bromide in only DMF afforded product alkyne **29** as racemic mixture (Scheme 4).⁴²



Scheme 4. a) Chloroacetyl chloride, AlCl₃, 1, 2-DCE, rt, 7 h; b) 1, 2, 4-triazole, NaHCO₃, Toluene, reflux, 4 h, 55% overall in two steps; c) propargyl bromide, activated Zn, Dry DMF: THF (1:1), rt, 3-4 h, 95%

Our next objective was to synthesize 1, 2, 3-triazole-linked β -lactam-fluconazole conjugates **30 (a-l)**. The cycloaddition reaction of alkyne **29**, with a diastereomeric mixture of azide **25 (a-l)**, in the presence of Cu(I) catalyst as per reported procedure⁴⁰ under microwave irradiation furnished diastereomeric mixture of novel conjugates **30 (a-l)** in excellent yields (Scheme 5). These diastereomers were inseparable by flash column chromatography and also by crystallization. Their separation by preparative HPLC was also unsuccessful. All the synthesized molecules were characterized by FTIR, ¹H NMR, ¹³C NMR and HR-MS.



Scheme 5. a) CuSO₄.5H₂O, Sodium ascorbate, DMF: H₂O (4:1), microwave 540W 5-10 mins, 84-96%

1.4.2.2 Biological activity

A. Antibacterial activity

As all the synthesized compounds **30 (a-l)** had β -lactam pharmacophore as a one of the functional group, they were tested for *in vitro* antibacterial activity at concentrations 0.39-50 $\mu\text{g/mL}$ against *Escheirchia coli*, *Pseudomonas aeruginosa* and *Staphylococcus aureus* by broth microdilution method.⁴³ None of the compounds showed antibacterial activity against the tested strains.

B. Antifungal activity

The antifungal activity of the final compounds **30(a-l)** was evaluated by CLSI standard broth microdilution assay against different fungal pathogens, viz. *Candida albicans* ATCC 24433, *C. albicans* ATCC 10231, *Cryptococcus neoformans* ATCC 34554, *Candida glabrata* NCYC 388, *Candida tropicalis* ATCC 750, *Aspergillus niger* ATCC 10578 and *Aspergillus fumigatus* NCIM 908.⁴⁴ Antifungal activity data of 1, 2, 3-triazole-linked β -lactam fluconazole conjugates **30(a-l)** is given in Table 1 in terms of IC_{50} (concentration causing 50% growth inhibition) and MIC (minimum inhibitory concentration causing >90% growth inhibition). Fluconazole was used as a standard antifungal drug.

All the compounds showed better antifungal activity than fluconazole with MIC values ranging from 16 – 0.031 $\mu\text{g/mL}$ against both *C. albicans* strains with an exception of **30a** and **30d** which exhibited 2X MIC than fluconazole against *C. albicans* ATCC 10231. Compound **30j** with β -lactam ring containing *para*-anisidine and benzaldehyde was most effective with MIC values 0.031 and 0.5 $\mu\text{g/mL}$ against *C. albicans* ATCC 24433 and *C. albicans* ATCC10231, respectively. It also showed good activity against all other fungal pathogens tested. Good to moderate activity was observed for the synthesized compounds **30 (a-l)** against *Cryptococcus neoformans* ATCC 34554, *Candida glabrata* NCYC 388 and *Candida tropicalis* ATCC 750, whereas they were found least susceptible against *A. niger* ATCC 10578 and *A. fumigatus* NCIM 908. Four compounds **30h**, **30i**, **30j** and **30k** showed good antifungal activity against *C. tropicalis* ATCC 750 (MIC values in the range of 64 – 32 $\mu\text{g/mL}$) where fluconazole proved to be ineffective. Based on these results, **30h**, **30j** and **30k** were identified as leads and used for further mechanistic studies.

Table 1. Antifungal activity of the 1, 2, 3-triazole-linked β -lactam fluconazole conjugates **30 (a-l)**.

Compounds	<i>C. albicans</i> ATCC 24433		<i>C. albicans</i> ATCC10231		<i>C. neoformans</i> ATCC 34554		<i>C. glabrata</i> NCYC 388		<i>C. tropicalis</i> ATCC 750		<i>A. niger</i> ATCC 10578		<i>A. fumigatus</i> NCIM 908	
	IC ₅₀ [*]	MIC ^{**}	IC ₅₀	MIC	IC ₅₀	MIC	IC ₅₀	MIC	IC ₅₀	MIC	IC ₅₀	MIC	IC ₅₀	MIC
30a	0.28	0.5	9.2	16	110.5	>256	57	128	83.45	>256	120.4	>256	63.62	>256
30b	0.11	0.25	1.34	4	41.83	64	8.68	16	46.81	128	83.2	>256	202.9	>256
30c	0.1	0.25	3.95	8	107.2	256	20.63	64	14.26	32	96	>256	220.9	>256
30d	0.29	0.5	6.18	16	68.01	128	32.23	64	69.79	128	54.04	>256	118	>256
30e	0.16	0.25	3.74	8	102	>256	73.6	>256	71.31	>256	41.63	>256	56	>256
30f	0.083	0.125	2.9	4	169	>256	36.24	64	8.15	16	189.8	>256	164.4	>256
30g	0.086	0.125	0.74	2	59.73	128	18.22	32	6.52	32	133.1	256	139.1	>256
30h	0.1	0.25	1.93	4	45.91	128	16.97	32	17.92	32	64	>256	52.62	>256
30i	0.21	0.5	1.1	4	73.79	128	6.23	16	14.67	32	80.9	>256	67.11	>256
30j	<0.015	0.031	0.1	0.5	16.26	32	8	16	36.09	64	12.57	64	91.25	>256
30k	0.041	0.0625	0.56	2	66.66	128	17.02	32	15.52	64	90.14	256	112.2	>256
30l	0.17	0.25	1.7	4	32.34	64	11.93	32	14.2	32	113.7	256	90.43	>256
Fluconazole	0.150	2	3.29	8	8.05	16	68.4	128	89.9	>256	75.9	128	96.7	>256

* IC₅₀: concentration (in $\mu\text{g/mL}$) causing 50% growth inhibition; **MIC: Minimum Inhibitory Concentration causing >90% growth inhibition.

1.4.2.3 Ergosterol quantification assay

The cellular target of azole antifungals is lanosterol 14 α -demethylase, an enzyme of ergosterol biosynthesis pathway. Inhibition of lanosterol 14 α -demethylase results in accumulation of methylated sterol intermediates and depletion of ergosterol. This results in membrane instability, loss in cellular integrity and subsequent death of the fungus.^{45,46} In spectrophotometric sterol analysis, ergosterol and late sterol intermediate 24(28)-dehydroergosterol gives a characteristic four peak curve for a 230-300 nm scan. For the *Candida* cells samples treated with **30h**, **30i**, **30j** and **30k**, the peak intensity decreased with increase in the concentration of the compounds (Figure 6) indicating depletion of ergosterol.

Table 2. Depletion of total ergosterol content of *C. albicans* ATCC 24433 when exposed to $\frac{1}{2}$ MIC, MIC and 2X MIC concentration of 1, 2, 3-triazole-linked β -lactam fluconazole conjugates

Compound	Concentration ($\mu\text{g/mL}$)	% Ergosterol depletion
30h	0.0625	12.459
	0.125	91.598
	0.25	92.459
30i	0.125	68.033
	0.25	92.049
	0.5	93.238
30j	0.03125	39.385
	0.0625	59.795
	0.125	96.885
30k	0.0625	41.270
	0.125	67.787
	0.25	94.344
Fluconazole	0.125	49.057
	0.25	67.254
	0.5	81.475

Compounds **30h** and **30j** at 0.125 $\mu\text{g}/\text{mL}$ concentration produced >90% ergosterol depletion, whereas, same concentration of fluconazole could cause only 49% ergosterol depletion (Table 2). The results indicated that the newly synthesized 1, 2, 3-triazole-linked β -lactam fluconazole conjugates exerted their antifungal action through inhibition of lanosterol 14 α -demethylase and concomitant ergosterol depletion.

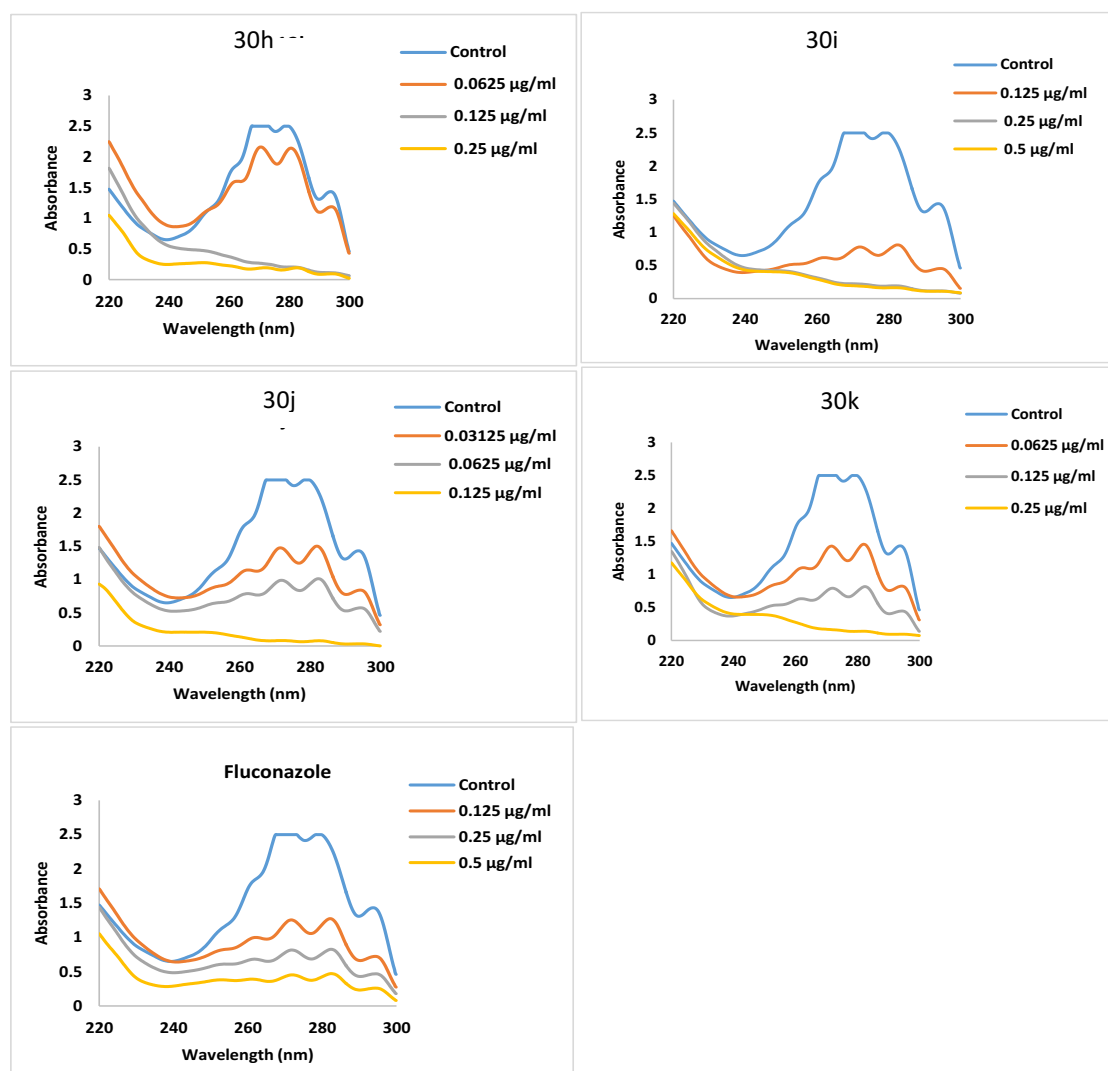


Figure 6. Spectrophotometric analysis of sterol composition of *C. albicans* ATCC 24433 exposed to different concentrations of **30h**, **30i**, **30j**, **30k** and fluconazole.

1.4.2.4 Molecular Docking

Molecular docking study has become an integral part of drug discovery research in recent times to identify the potential targets for different ligands and their associated thermodynamic interactions with the target enzyme governing the inhibition of the pathogen. This structure-

based drug design approach imparts knowledge on binding affinities, binding modes and types of interactions guiding the enzyme–inhibitor complexation which provides an ample opportunity to medicinal chemists for generating and analyzing the potential of designed molecules. Thus, with the aim to rationalize the promising antifungal activity portrayed by the title compounds **30 (a-l)** and to gain an insight into their binding interactions at the molecular level, a molecular docking study was carried out with *Candida albicans* sterol 14 α -demethylase (CYP51) as target enzyme. Molecular docking study revealed that all the fluconazole β -lactam conjugates **30 (a-l)** could snugly fit into the active site of CYP51 with varying degree of affinities adopting a very similar orientation and at co-ordinates close to that of the native ligand - fluconazole in the crystal structure (Figure 7).

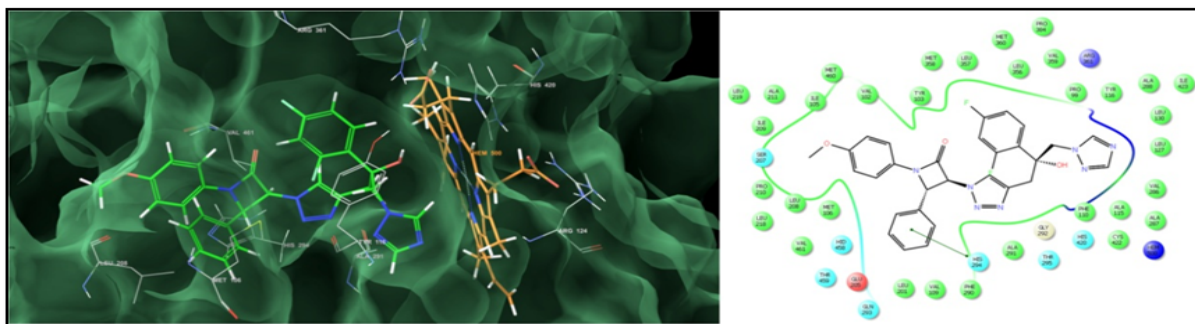


Figure 7. Binding mode of **30j** into the active site of lanosterol 14 α -demethylase (CYP51) (the π - π stacking interaction)

Their complexation was stabilized through a network of significant steric and electrostatic interactions. The minimum energy for the formation of complex between ligand and receptor (Glide energy) for each of these analogues was observed to be negative ranging from -58.961 kcal/mol to -53.125 kcal/mol with an average docking score of -7.74 while the docking score for Fluconazole was -7.34 with binding energy of -52.92 kcal/mol. This was in harmony with the experimental finding where we found the MIC of these compounds better than Fluconazole. Also a significant correlation was observed between the docking score and the antifungal activity- the active compounds having higher scores while those with relatively low activity were also predicted to have a lower score (Table 3). A higher negative value for docking score and the binding energy signifies a good binding affinity of the ligand towards the target and vice versa. The binding energy signifies the energy required for a ligand to cover the entire enzyme surface and its putative interactions at the active site. A detailed quantitative analysis of the per-residue interaction between the compounds **30 (a-l)** and the

residues lining the active site of the enzyme was carried out to identify the most significantly interacting residues and the type of interactions (bonded and non-bonded interactions) that govern the binding of these molecules to CYP51. However, to maintain the brevity of text, this analysis is elucidated in the section only for the most active compound **30j** while the results for the remaining compounds are summarized in Table 3.

Table 3. Quantitative estimates of the per-residue interaction analysis of the fluconazole β -lactam conjugates **30 (a-l)** with lanosterol 14 α -demethylase (CYP51).

Antifungal activity in $\mu\text{g/mL}$				
Compound	MIC	IC ₅₀	Docking Score	Binding Energy (kcal/mol)
30a	0.50	0.28	-7.46	-53.38
30b	0.25	0.11	-7.61	-55.12
30c	0.25	0.1	-7.58	-55.54
30d	0.50	0.29	-7.40	-53.12
30e	0.25	0.16	-7.54	-55.10
30f	0.125	0.083	-7.95	-56.27
30g	0.125	0.086	-7.91	-56.79
30h	0.25	0.1	-7.59	-55.99
30i	0.5	0.21	-7.45	-53.95
30j	0.031	<0.015	-8.50	-58.96
30k	0.0625	0.041	-8.28	-57.89
30l	0.25	0.17	-7.69	-55.82

The lowest energy docked conformation of the most active **30j** into the active site of CYP51 showed that the inhibitor binds at the same co-ordinates as the native ligand with a significantly higher binding affinity (Table 3). The compound binds with the highest affinity with a docking score of -8.501 and binding energy -58.961 kcal/mol. The higher binding affinity can be attributed to the specific bonded and non-bonded per residue interactions with the residues lining the active site of CYP51. A detailed analysis of the per-residual interactions revealed that the van der Waals interactions are more prevalent over the electrostatic contribution in its overall binding affinity towards CYP51. An extensive network of favorable van der Waals interactions with Val359 (-1.47 kcal/mol), Leu356 (-2.74 kcal/mol), Ala291 (-1.79 kcal/mol), Tyr116 (-4.21 kcal/mol), Phe110 (-2.13 kcal/mol) through

the Fluconazole component of the β -lactam conjugate stabilized the compound into the active site while the para-methoxy substituted aromatic ring attached to the β -lactam was engaged in similar interactions with Met460 (-3.75 kcal/mol), Leu208 (-3.48 kcal/mol), Met106 (-2.03 kcal/mol), Ile105 (-2.40 kcal/mol) and Tyr103 (-2.95 kcal/mol) residues. Furthermore the second aromatic ring attached to β -lactam was also involved in significant van der Waals interactions with Val461 (-2.59 kcal/mol), Thr459 (-2.28 kcal/mol), His294 (-2.84 kcal/mol), Phe290 (-4.15 kcal/mol) and Glu205 (-2.54 kcal/mol) residues lining the active site stabilizing the enzyme-inhibitor complex. The compound was engaged in a set of relatively few but significant electrostatic interactions as well with Ala291 (-1.36 kcal/mol), Phe290 (-1.41 kcal/mol), Glu205 (-2.51 kcal/mol), Tyr116 (-1.94 kcal/mol) and Tyr103 (-1.23 kcal/mol) residues. The enhanced binding affinity of **30j** can also be attributed to a very strong van der Waals (-8.82 kcal/mol) as well as electrostatic (-5.734 kcal/mol) interaction with Heme moiety present in the active site of CYP51. This is a very important observation considering the fact that even Fluconazole is coordinated with the iron metal in the active site of CYP51 indicating that these compounds may as well share the same inhibition mechanism of action as Fluconazole. A very prominent pi-pi (π - π) stacking interaction was also observed between the aromatic ring attached to the β -lactam and His294 residue in the active site. While **30j** displayed only single pi-pi stacking interaction, the other molecules in the dataset were engaged in such interaction with Tyr116, Tyr103, Phe110, Phe290 residues as well. Such pi-pi stacking interactions not only serve the function of an "anchor" guiding the 3D orientation of the ligand in its active site but also facilitate the steric and electrostatic interactions adding to the stability of the enzyme-inhibitor complex.

The per-residue ligand interaction analysis revealed that the primary driving forces for mechanical interlocking was the steric complementarity between these ligands and the active site residues of CYP51 which is reflected in the relatively higher number of favorable van der Waals interactions than the other components contributing to the overall binding affinity. Overall, it is evident from the docking simulations and more specifically from the per-residue interaction energy distribution that these molecules have excellent affinity for the lanosterol 14 α -demethylase (CYP51) enzyme making them pertinent starting points for structure-based lead optimization.

1.4.2.5 Cytotoxicity testing of the compounds **30 (a-l)**

Compounds **30 (a-l)** were checked for cytotoxicity by MTT assay using MCF-7, A-431 and HUVEC (Human umbilical vein endothelial cells) cell line⁴⁷ and hemolysis assay.⁴⁸ All the

compounds at tested concentration (up to 100 µg/mL) were found to be non-toxic to the HUVEC cells (Table 4). For hemolysis assay, the concentrations tested were in the range of 2–256 µg/mL. None of the compounds showed hemolysis at these concentrations except for **30b**. Even for **30b**, the hemolysis observed was negligible and at much higher concentrations than MIC i.e. 1.94% and 1.21% hemolysis at 256 and 128 µg/mL, respectively (Table 4).

Table 4. Cytotoxicity testing of the compounds 30 (a-l)

Sr. No.	Code	Cytotoxic Effect of inhibitors: MCF-7		Cytotoxic Effect of inhibitors: A431		Cytotoxic Effect of inhibitors: HUVEC	
		IC50	MIC	IC50	MIC	IC50	MIC
1	30a	>100	>100	80.43	>100	63.17	>100
2	30b	31.71	89.67	23.21	83.56	73.83	>100
3	30c	>100	>100	73.74	>100	>100	>100
4	30d	>100	>100	85.76	>100	>100	>100
5	30e	>100	>100	>100	>100	>100	>100
6	30f	>100	>100	>100	>100	>100	>100
7	30g	>100	>100	77.99	>100	>100	>100
8	30h	>100	>100	86.25	>100	>100	>100
9	30i	29.85	97.44	67.77	>100	>100	>100
10	30j	>100	>100	>100	>100	>100	>100
11	30k	>100	>100	>100	>100	>100	>100
12	30l	37.09	88.2	>100	>100	74.14	>100

1.4.2.6 Antifungal susceptibility assay

Antifungal activities of the synthesized compounds (in terms of IC₅₀ and MIC) against *C. albicans* ATCC 24433, *C. albicans* ATCC 10231, *C. glabrata* NCYC 388, *C. neoformans*

ATCC 34664, *C. tropicalis* ATCC 750 (CLSI - Clinical Laboratory Standards Institute document M27-A3)⁴⁴ and *A. fumigatus* NCIM 908, *A. niger* ATCC 10578 (CLSI M38-A2)²⁵ were determined by CLSI broth microdilution assay.⁴⁵

1.4.2.7 Effect of triazoles on sterol profile of *C. albicans* ATCC 24433

Inhibition of lanosterol 14 α -demethylase by azoles was analyzed by spectrophotometric quantification of ergosterol depletion as described previously.^{45,46} The concentrations of **30h**, **30i**, **30j**, **30k** and fluconazole used in the assay were 1/2 MIC, MIC and 2X MIC concentrations.

1.4.2.8 Cytotoxicity assays

The active compounds **30 (a-l)** were studied for cytotoxicity (MTT assay)⁴⁷ against two human cancer cell lines (MCF-7 and A431) and were found to be non-cytotoxic. The cytotoxic effect of lead compounds **30 (a-l)** was checked at the concentrations of 100, 50, 25, 12.5, 6.25, 3.125, 1.5625 and 0.7813 $\mu\text{g/mL}$ to determine the GI_{50} and GI_{90} . These compounds **30 (a-l)** were further evaluated against human primary cells (HUVECs) to check the selectivity of these compounds. The GI_{90} ($>100 \mu\text{g/mL}$) values of the compounds **30 (a-l)** indicate that the compounds are potent and specific inhibitors against *Candida* strains. Compound **30 b** has exhibited highest cytotoxicity ($\text{GI}_{50} <25; >32 \mu\text{g/mL}$) against MCF-7 and A431 cells.

1.4.2.9 Hemolysis study

All the compounds were tested for RBC hemolysis as described previously.⁴⁸ The concentrations tested were in the range of 4–512 $\mu\text{g/mL}$. (Pl. give available data)

1.5 Conclusion

In conclusion, 12 new fluconazole- β -lactam conjugates linked *via* 1, 2, 3-triazole were synthesized and evaluated for antifungal potential.¹ Compounds **31h**, **31i**, **31j** and **31k** were found to be most potent compounds and exhibited better antifungal activity than fluconazole against pathogenic strains of *C. albicans* and *C. tropicalis*. Mode of action studies revealed that the antifungal action of the compounds was through inhibition of lanosterol 14 α -demethylase enzyme of ergosterol biosynthesis pathway. Results of spectrophotometric sterol analysis corroborated with that of the molecular docking studies confirming the mode of

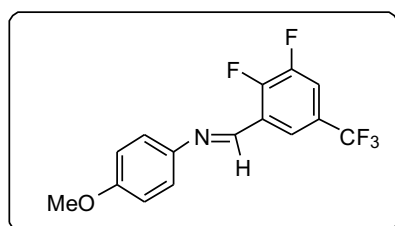
action of the lead compounds. The compounds were non-hemolytic and non-cytotoxic. The synthesized fluconazole- β -lactam conjugates hold promise for the control of *Candidemia*. Further optimization of lead compounds and pre-clinical evaluation of the series will help in the discovery of potential antifungal drug candidate.

1. 6 Experimental

1.6.1 General procedure for synthesis of Imines (24a-l)

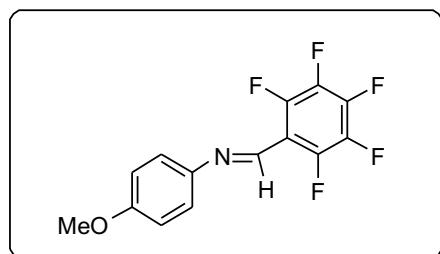
Amine (1mmol), and aldehyde (1-1.2mmol) was taken in a conical flask and kept it inside ordinary domestic microwave oven for 5-8 mins under 540 W. The conical flask was removed out and kept for 15-20 mins at room temperature. The reaction mixture in liquid form was slowly became solid. The solid obtained was then first washed with pet ether and then by 5:95 ethyl acetate: pet ether solution. The solid was obtained in high yeilds (80-98%) and used further without any purification.

(E)-*N*-(4-methoxyphenyl)-1-(perfluorophenyl) methanimine (24a)



Yield: 92%; M.P 122-123 °C; IR (CHCl₃, cm⁻¹) 1617, 3019; ¹H NMR (CDCl₃, 200 MHz) δ 8.50 (s, 1H), 7.64-7.71 (m, 1H), 7.45-7.52 (m, 1H), 7.19-7.31 (m, 1H), 6.94-7.0 (m, 1H), 3.88 (s, 3H); ¹³C NMR (CDCl₃, 50 MHz) δ 165.5, 160.6, 158.5, 156.6, 144.2, 138.8, 130.2, 124.7, 122.2, 114.6, 55.45. ESI-MS (m/z): 302.14[M+H]⁺.

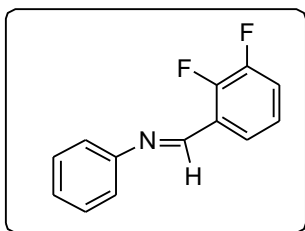
(E)-1-(2,3-difluoro-5-(trifluoromethyl)phenyl)-*N*-(4-methoxyphenyl)methanimine (24b)



Yield: 89%; M.P 58-59 °C; IR (CHCl₃, cm⁻¹) 1617, 3019; ¹H NMR (CDCl₃, 200 MHz) δ 8.78 (s, 1H), 8.42 (dd, J = 5.56 Hz, 1H), 7.75 (d, J = 6.44 Hz, 1H), 7.30-7.35 (m, 2H), 6.94-6.99 (m, 2H), 3.86 (s, 3H); ¹³C NMR (CDCl₃, 50 MHz) δ 162.0, 159.3, 156.9, 147.9, 143.4, 129.2, 123.5, 122.7, 120.2, 114.5, 55.5; ESI-MS (m/z): 316.24[M+H]⁺.

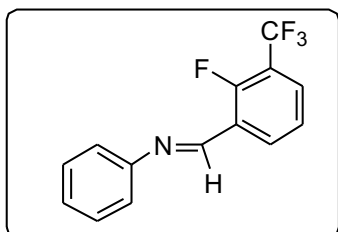
(E)-1-(2,3-difluorophenyl)-*N*-phenylmethanimine (24c)

Yield: 80%; sticky solid; IR (CHCl₃, cm⁻¹) 1617, 3019; ¹H NMR (CDCl₃, 200 MHz) δ 8.65 (s, 1H), 7.80-7.87 (m, 1H), 7.28-7.35 (m, 1H), 7.04-7.26 (m, 6H); ¹³C NMR (CDCl₃, 50



MHz) δ 153.1, 152.1, 151.3, 148.4, 146.2, 129.2, 126.6, 122.5, 120.9, 118.5, 115.0; ESI-MS (m/z): 218.24[M+H]⁺.

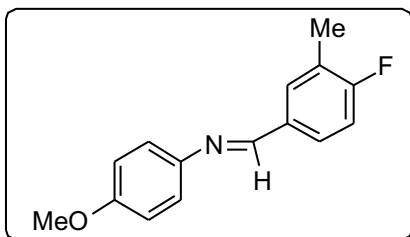
(E)-1-(2-fluoro-3-(trifluoromethyl)phenyl)-N-phenylmethanimine (24d)



Yield: 75%; sticky solid; IR (CHCl₃, cm⁻¹) 1617, 3019; ¹H NMR (CDCl₃, 400 MHz) δ 8.82 (s, 1H), 8.44 (t, *J*= 7.34 Hz, 1H), 7.75 (t, *J* = 7.34 Hz, 1H), 7.43-7.47 (m, 2H), 7.35-7.39 (m, 1H), 7.28-7.31 (m, 3H); ¹³C NMR (CDCl₃, 50 MHz) δ 151.6, 151.2, 131.8, 129.2, 126.8, 125.3, 124.2, 123.7, 120.9;

ESI-MS (m/z): 268.08[M+H]⁺.

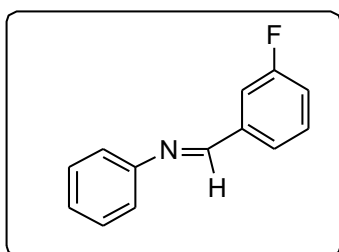
(E)-1-(4-fluoro-3-methylphenyl)-N-(4-methoxyphenyl)methanimine (24e)



Yield: 93%; M.P 74-75 °C; IR (CHCl₃, cm⁻¹) 1617, 3019; ¹H NMR (CDCl₃, 200 MHz) δ 8.46 (s, 1H), 7.68-7.86 (m, 2H), 7.25-7.30 (m, 2H), 7.12-7.18 (m, 1H), 6.97-7.01 (m, 2H), 3.89 (s, 1H), 2.39 (s, 3H); ¹³C NMR (CDCl₃, 50 MHz) δ 190.7, 165.5, 160.6, 158.2,

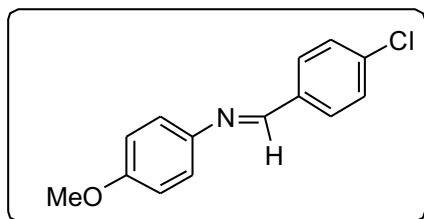
157.2, 144.6, 132.3, 131.4, 131.3, 128.2, 125.3, 122.0, 115.5, 114.3, 55.4, 14.4; ESI-MS (m/z): 244.28[M+H]⁺.

(E)-1-(3-fluorophenyl)-N-phenylmethanimine (24f)

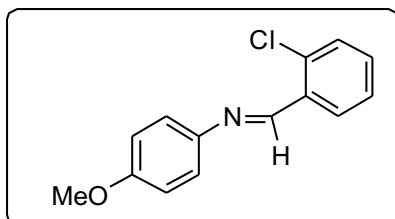


Yield: 88%; sticky solid; IR (CHCl₃, cm⁻¹) 1617, 3019; ¹H NMR (CDCl₃, 400 MHz) δ 8.48 (s, 1H), 7.66-7.73 (m, 2H), 7.43-7.51 (m, 3H), 7.18-7.32 (m, 4H); ¹³C NMR (CDCl₃, 50 MHz) δ 165.5, 160.6, 158.8, 151.4, 138.5, 138.4, 130.3, 129.1, 126.2, 120.8, 118.5, 115.1 ; ESI-MS (m/z):

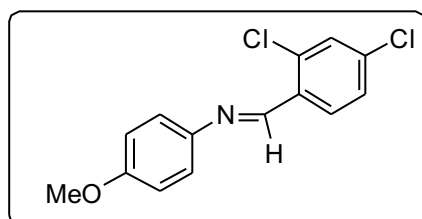
200.08[M+H]⁺.

(E)-1-(4-chlorophenyl)-N-(4-methoxyphenyl)methanimine (24g)

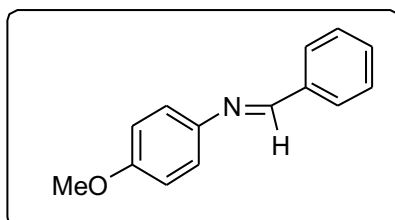
Yield: 98%; M.P 115-116 °C; IR (CHCl₃, cm⁻¹) 1617, 3019; ¹H NMR (CDCl₃, 200 MHz) δ 8.49 (s, 1H), 7.88 (d, *J* = 8.46 Hz, 2H), 7.49 (d, *J* = 8.46, 2H), 7.29 (d, *J* = 8.84, 2H), 6.99 (d, *J* = 6.69, 2H), 3.89 (s, 3H); ¹³C NMR (CDCl₃, 50 MHz) δ 158.4, 156.5, 144.2, 136.8, 134.8, 129.6, 128.9, 122.1, 114.3, 55.3; ESI-MS (m/z): 246.08[M+H]⁺.

(E)-1-(2-chlorophenyl)-N-(4-methoxyphenyl)methanimine (24h)

Yield: 98%; M.P 56-57 °C; IR (CHCl₃, cm⁻¹) 1617, 3019; ¹H NMR (CDCl₃, 200 MHz) δ 8.95 (s, 1H), 8.22-8.26 (m, 1H), 7.27-7.41 (m, 5H), 6.93-6.98 (m, 2H), 3.85 (s, 3H); ¹³C NMR (CDCl₃, 50 MHz) δ 158.5, 154.6, 144.4, 135.7, 131.7, 129.8, 128.2, 122.4, 114.3, 55.4; ESI-MS (m/z): 246.08[M+H]⁺.

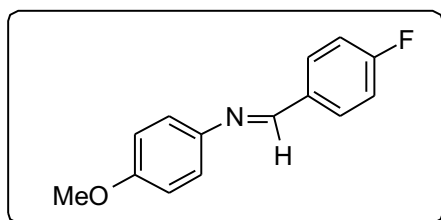
(E)-1-(2,4-dichlorophenyl)-N-(4-methoxyphenyl)methanimine (24i)

Yield: 96%; M.P 94-95 °C; IR (CHCl₃, cm⁻¹) 1617, 3019; ¹H NMR (CDCl₃, 200 MHz) δ 8.88 (s, 1H), 8.20 (d, *J* = 8.46 Hz, 1H), 7.45 (d, *J* = 2.02Hz, 1H), 7.27-7.37 (m, 3H), 6.94-6.98 (m, 2H), 3.86(s, 3H); ¹³C NMR (CDCl₃, 50 MHz) δ 158.8, 153.1, 144.1, 137.0, 136.1, 132.0, 129.5, 129.1, 122.5, 114.4, 55.4; ESI-MS (m/z): 280.04[M+H]⁺.

(E)-N-(4-methoxyphenyl)-1-phenylmethanimine (24j)

Yield: 98%; M.P 70-71 °C; IR (CHCl₃, cm⁻¹) 1617, 3019; ¹H NMR (CDCl₃, 200 MHz) δ 8.48 (s, 1H), 7.86-7.91 (m, 2H), 7.44-7.49 (m, 3H), 7.20-7.26 (m, 2H), 6.89-6.97 (m, 2H), 3.83 (s, 3H); ¹³C NMR (CDCl₃, 50 MHz) δ 158.2, 158.1, 144.7, 136.3, 130.9, 128.6, 122.1, 114.2, 55.3; ESI-MS (m/z): 212.08[M+H]⁺.

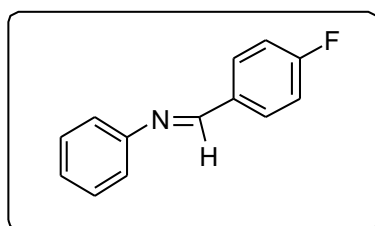
(E)-1-(4-fluorophenyl)-N-(4-methoxyphenyl)methanimine (24k)



Yield: 97%; M.P 86-87 °C; IR (CHCl₃, cm⁻¹) 1617, 3019; ¹H NMR (CDCl₃, 200 MHz) δ 8.45 (s, 1H), 7.86-7.93 (m, 2H), 7.16-7.27 (m, 4H), 6.92-6.97 (m, 2H), 3.85 (s, 3H); ¹³C NMR (CDCl₃, 50 MHz) δ 165.6, 158.2, 156.6, 144.5, 132.7, 130.3, 122.1,

115.8, 114.3, 55.3; ESI-MS (m/z): 230.08[M+H]⁺.

(E)-1-(4-fluorophenyl)-N-phenylmethanimine (24l)



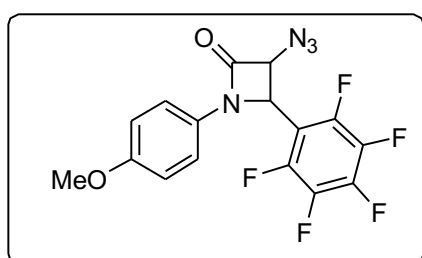
Yield: 80%; M.P 37-38 °C; IR (CHCl₃, cm⁻¹) 1617, 3019; ¹H NMR (CDCl₃, 200 MHz) δ 8.47 (s, 1H), 7.92-7.99 (m, 2H), 7.41-7.49 (m, 2H), 7.17-7.32 (m, 5H); ¹³C NMR (CDCl₃, 50 MHz) δ 167.1, 162.1, 158.7, 151.7, 135.5, 130.8, 129.1, 125.9, 120.8, 116.0, 115.0 ; ESI-MS (m/z):

200.08[M+H]⁺.

1.6.2 General procedure for synthesis of β-lactams (25 a-l)

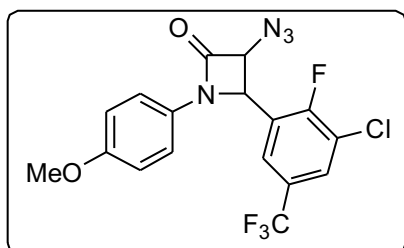
A solution of triphosgene (0.296 g, 1 mmol), in anhydrous CH₂Cl₂ (15 ml), was added slowly to a mixture of potassium salt of azidoacetic acid **21** (2 mmol), imine **24a-l** (2 mmol) and triethyl amine (0.84 ml, 6 mmol) in anhydrous CH₂Cl₂ (20 mL) at 0 °C. After the addition, the reaction mixture was allowed to warm up to room temperature (28 °C) and stirred for 15 h. The reaction mixture was then washed with water (20 ml), saturated sodium bicarbonate solution (2×15 ml) and brine (15 ml). The organic layer was dried over anhydrous sodium sulphate and concentrated to get crude product, which was purified by column chromatography to give pure β-lactams **25(a-l)**.

3-azido-1-(4-methoxyphenyl)-4-(perfluorophenyl)azetidin-2-one (25a)

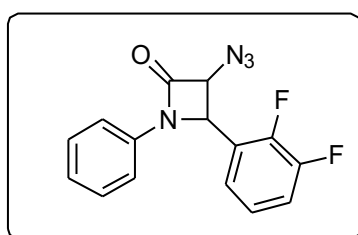


Yield: 81%; IR (CHCl₃, cm⁻¹) 2115 (N₃), 1763 (CO); ¹H NMR (CDCl₃, 200 MHz) δ 7.20 (d, *J* = 9.09 Hz, 2H), 6.85 (d, *J* = 9.10 Hz, 2H), 5.61 (d, *J* = 5.43, 1H), 5.24 (d, *J* = 5.3, 1H), 3.78 (s, 3H, OCH₃); ¹³C NMR (CDCl₃, 50 MHz) δ 159.7, 157.0, 129.5, 118.1, 114.7,

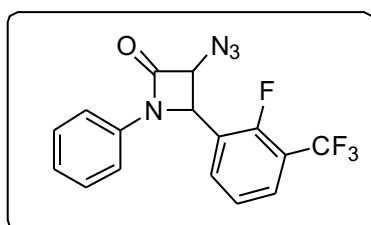
66.6, 55.4, 51.7; ESI-MS (m/z): 349.06[M+H]⁺.

3-azido-4-(3-chloro-2-fluoro-5-(trifluoromethyl)phenyl)-1-(4-methoxyphenyl)azetidin-2-one (25b)

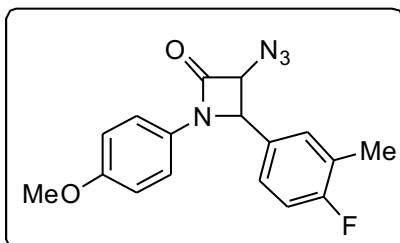
Yield: 80%; IR (CHCl₃, cm⁻¹) 2115 (N₃), 1751 (CO); ¹H NMR (CDCl₃, 200 MHz) δ 7.72-7.76 (m, 1H), 7.33-7.36 (m, 1H), 7.22-7.26 (m, 2H), 6.84-6.89 (m, 2H), 5.58 (d, *J* = 5.43, 1H), 5.20 (d, *J* = 5.43, 1H), 3.79 (s, 3H, OCH₃); ¹³C NMR (CDCl₃, 50 MHz) δ 160.2, 157.0, 129.4, 128.6, 124.1, 118.4, 114.7, 67.2, 55.4, 54.6; ESI-MS (m/z): 415.06[M+H]⁺.

3-azido-4-(2,3-difluorophenyl)-1-phenylazetidin-2-one (25c)

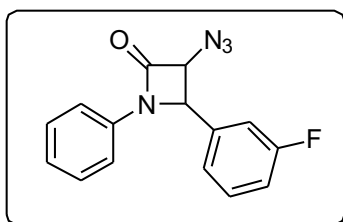
Yield: 77%; IR (CHCl₃, cm⁻¹) 2115 (N₃), 1751 (CO); ¹H NMR (CDCl₃, 200 MHz) δ 7.12-7.25 (m, 5H), 6.91-7.10 (m, 3H), 5.56 (d, *J* = 5.44, 1H), 5.09 (d, *J* = 5.55, 1H); ¹³C NMR (CDCl₃, 50 MHz) δ 161.0, 136.3, 129.3, 129.2, 125.1, 117.3, 117.2, 67.1, 60.1, 54.6; ESI-MS (m/z): 301.06[M+H]⁺.

3-azido-4-(2-fluoro-3-(trifluoromethyl)phenyl)-1-phenylazetidin-2-one (25d)

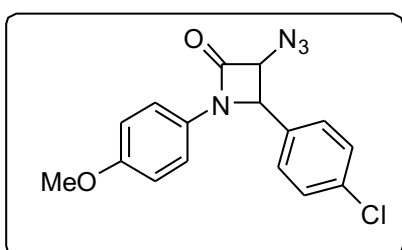
Yield: 75%; IR (CHCl₃, cm⁻¹) 2115 (N₃), 1751 (CO); ¹H NMR (CDCl₃, 200 MHz) δ 7.63-7.70 (m, 1H), 7.36-7.42 (m, 1H), 7.31-7.35 (m, 3H), 7.27-7.30 (m, 1H), 7.14-7.26 (m, 2H), 5.69 (d, *J* = 5.43, 1H), 5.15 (d, *J* = 5.43 Hz, 1H); ¹³C NMR (CDCl₃, 50 MHz) δ 160.9, 136.2, 132.2, 129.4, 125.2, 124.4, 124.3, 117.1, 67.2, 54.2; ESI-MS (m/z): 351.08[M+H]⁺.

3-azido-4-(4-fluoro-3-methylphenyl)-1-(4-methoxyphenyl)azetidin-2-one (25e)

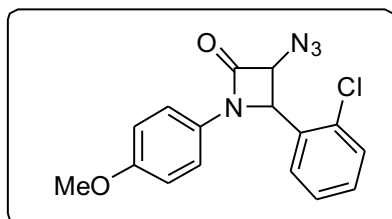
Yield: 52%; IR (CHCl₃, cm⁻¹) 2115 (N₃), 1751 (CO); ¹H NMR (CDCl₃, 200 MHz) δ 7.26-7.30 (m, 2H), 7.07-7.20 (m, 3H), 6.83-6.87 (m, 2H), 5.26 (d, *J* = 5.31 Hz, 1H), 5.04 (d, *J* = 5.18 Hz, 1H), 3.80 (s, 3H), 2.31 (s, 3H); ¹³C NMR (CDCl₃, 50 MHz) δ 164.0, 160.9, 159.1, 156.6, 130.6, 130.5, 130.0, 127.9, 126.6, 126.4, 118.7, 115.7, 114.4, 67.3, 60.2, 55.4, 49.9, 14.6; ESI-MS (m/z): 326.08[M+H]⁺.

3-azido-4-(3-fluorophenyl)-1-phenylazetidin-2-one (25f)

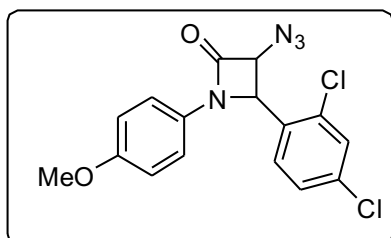
Yield: 81%; IR (CHCl₃, cm⁻¹) 2115 (N₃), 1751 (CO); ¹H NMR (CDCl₃, 200 MHz) δ 7.37-7.43 (m, 1H), 7.28-7.32 (m, 4H), 7.12-7.16 (m, 1H), 7.03-7.11 (m, 3H), 5.32 (d, *J* = 5.43, 1H), 5.07 (d, *J* = 5.44 Hz, 1H); ¹³C NMR (CDCl₃, 50 MHz) δ 165.4, 161.1, 160.5, 136.4, 135.3, 130.7, 129.3, 125.0, 123.1, 117.3, 114.4, 67.3, 60.1; ESI-MS (*m/z*): 283.08[M+H]⁺.

3-azido-4-(4-chlorophenyl)-1-(4-methoxyphenyl)azetidin-2-one (25g)

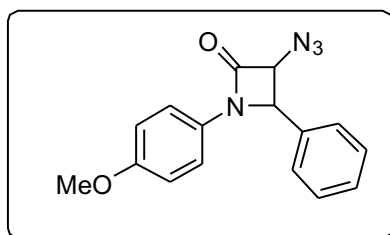
Yield: 90%; IR (CHCl₃, cm⁻¹) 2115 (N₃), 1751 (CO); ¹H NMR (CDCl₃, 400 MHz) δ 7.41 (d, *J* = 7.82 Hz, 1H), 7.23-7.29 (m, 4H), 6.83 (d, *J* = 8.81 Hz, 1H), 5.27 (d, *J* = 5.38 Hz, 1H), 5.05 (d, *J* = 5.38 Hz, 1H), 3.77 (s, 3H); ¹³C NMR (CDCl₃, 50 MHz) δ 160.6, 156.7, 135.1, 131.2, 129.2, 128.9, 118.7, 114.4, 67.3, 60.1, 55.4; ESI-MS (*m/z*): 329.08[M+H]⁺.

3-azido-4-(2-chlorophenyl)-1-(4-methoxyphenyl)azetidin-2-one (25h)

Yield: 91%; IR (CHCl₃, cm⁻¹) 2115 (N₃), 1751 (CO); ¹H NMR (CDCl₃, 200 MHz) δ 7.48-7.53 (m, 1H), 7.28-7.36 (m, 2H), 7.21-7.26 (m, 3H), 6.84-6.88 (m, 2H), 5.67 (d, *J* = 5.31, 1H), 5.15 (d, *J* = 5.31 Hz, 1H), 3.79 (s, 3H); ESI-MS (*m/z*): 329.08[M+H]⁺.

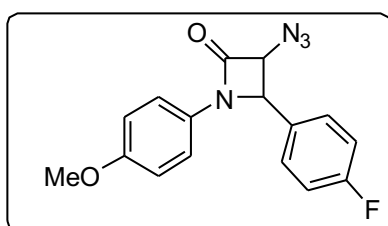
3-azido-4-(2,4-dichlorophenyl)-1-(4-methoxyphenyl)azetidin-2-one (25i)

Yield: 90%; IR (CHCl₃, cm⁻¹) 2115 (N₃), 1751 (CO); ¹H NMR (CDCl₃, 200 MHz) δ 7.51 (d, *J* = 1.89 Hz, 1H), 7.20-7.26 (m, 3H), 7.08-7.13 (m, 1H), 6.82-6.87 (m, 2H), 5.59 (d, *J* = 5.31, 1H), 5.15 (d, *J* = 5.30 Hz, 1H), 3.78 (s, 3H); ¹³C NMR (CDCl₃, 50 MHz) δ 160.4, 156.8, 135.3, 129.7, 127.5, 118.5, 114.5, 67.5, 57.9, 55.4; ESI-MS (*m/z*): 363.04[M+H]⁺.

3-azido-1-(4-methoxyphenyl)-4-phenylazetididin-2-one (25j)

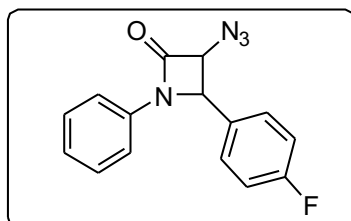
Yield: 94%; IR (CHCl₃, cm⁻¹) 2115 (N₃), 1751 (CO); ¹H NMR (CDCl₃, 200 MHz) δ 7.25-7.41 (m, 6H), 6.68-6.84 (m, 3H), 5.30 (d, *J* = 5.30, 1H), 5.03 (d, *J* = 5.31 Hz, 1H), 3.76 (s, 3H); ¹³C NMR (CDCl₃, 50 MHz) δ 160.8, 156.5, 132.6, 129.1, 128.8, 127.5, 118.7, 114.4, 67.3, 60.7, 55.4;

ESI-MS (*m/z*): 295.14[M+H]⁺.

3-azido-4-(4-fluorophenyl)-1-(4-methoxyphenyl)azetididin-2-one (25k)

Yield: 92%; IR (CHCl₃, cm⁻¹) 2115 (N₃), 1751 (CO); ¹H NMR (CDCl₃, 200 MHz) δ 7.29-7.36 (m, 2H), 7.07-7.22 (m, 3H), 6.68-6.84 (m, 3H), 5.28 (d, *J* = 5.31, 1H), 5.03 (d, *J* = 5.31 Hz, 1H), 3.77 (s, 3H); ¹³C NMR (CDCl₃, 50 MHz) δ 164.3, 161.8, 160.6, 156.6, 129.9, 129.4, 128.4,

118.7, 114.4, 67.3, 60.1, 55.4; ESI-MS (*m/z*): 313.14[M+H]⁺.

3-azido-4-(4-fluorophenyl)-1-phenylazetididin-2-one (25l)

Yield: 72%; IR (CHCl₃, cm⁻¹) 2115 (N₃), 1751 (CO); ¹H NMR (CDCl₃, 200 MHz) δ 7.28-7.51 (m, 5H), 7.05-7.25 (m, 4H), 5.30 (d, *J* = 5.43, 1H), 5.03 (d, *J* = 5.30 Hz, 1H); ¹³C NMR (CDCl₃, 50 MHz) δ 165.4, 161.1, 160.5, 136.4, 135.3,

130.7, 129.3, 125.0, 123.1, 117.3, 114.4, 67.3, 60.1; ESI-MS (*m/z*): 283.10[M+H]⁺.

1.6.3 General procedure for synthesis of fluconazole β-lactam conjugates 31 (a-l).

The alkyne of fluconazole **29** (1 equiv) and the azides **25 (a-l)** (1 equiv) were dissolved in DMF: H₂O (7:3). To this solution CuSO₄·5H₂O (0.05 equiv) and sodium ascorbate (0.5 equiv) were added. The reaction mixture was placed in a microwave reactor and irradiated for 5-8 mins at 540 W. It was then cooled to room temperature, quenched with crushed ice and extracted with ethyl acetate. The extract was washed with water and brine, dried over anhydrous sodium sulphate. Solvent was evaporated under reduced pressure and crude product was purified by column chromatography to obtain β-lactam-bile acid conjugates **30a** to **30l** with 88-93% yields.

3-(4-(2-(2,4-difluorophenyl)-2-hydroxy-3-(1H-1, 2, 4-triazol-1-yl)propyl)-1H-1, 2, 3-triazol-1-yl)-1-(4-methoxyphenyl)-4-(perfluorophenyl)azetidin-2-one; 30a. Brown colored solid; Yield: 90%; IR (CHCl₃, cm⁻¹) 3415, 1761; ¹H NMR (CDCl₃, 400 MHz) δ 8.05-8.09 (m, 1H), 7.85 (d, J = 7.3 Hz, 1H), 7.71 (d, J = 9.5 Hz, 1H), 7.29 (d, J = 8.0 Hz, 2H, Ar-H), 7.31-7.40 (m, 1H, Ar-H), 6.89 (d, J = 9.0 Hz, 2H), 6.70-6.80 (m, 2H), 6.26-6.33 (m, 1H), 5.91-5.93 (m, 1H), 5.21 (bs, 1H), 4.70-4.76 (m, 1H), 4.28-4.50 (m, 1H), 3.81 (s, 3H), 3.37-3.49 (m, 1H), 3.09-3.23 (m, 1H); ¹³C NMR (CDCl₃, 50 MHz) δ 163.9, 157.5, 156.5, 146.5, 142.4, 142.3, 129.7, 129.3, 124.4, 123.2, 118.3, 114.8, 111.6, 111.3, 105.6, 104.5, 104.2, 104.0, 74.9, 66.5, 56.5, 55.5, 52.9, 52.8, 33.9, 33.7, 29.7, 14.1; ESI-MS (m/z): 648.15 [M+H]⁺; HRMS (ESI-qTOF): calcd for C₂₉H₂₁F₇N₇O₃ [M+H]⁺, 648.1589: found: 648.1583.

4-(3-chloro-2-fluoro-5-(trifluoromethyl)phenyl)-3-(4-(2-(2,4-difluorophenyl)-2-hydroxy-3-(1H-1, 2, 4-triazol-1-yl)propyl)-1H-1, 2, 3-triazol-1-yl)-1-(4-methoxyphenyl)azetidin-2-one; 30b. Brown colored solid; Yield: 89%; IR (CHCl₃, cm⁻¹) 3415, 1761; ¹H NMR (CDCl₃, 500 MHz) δ 8.02-8.06 (m, 2H), 7.81 (s, 1H), 7.47-7.51 (m, 1H, Ar-H), 7.28-7.36 (m, 3H, Ar-H), 7.23-7.26 (m, 1H, Ar-H), 6.89 (t, J = 8.54 Hz, 2H), 6.67-6.78 (m, 2H), 6.25-6.39 (m, 1H), 5.83-5.84 (m, 1H), 5.18 (bs, 1H), 4.63-4.69 (m, 1H), 4.05-4.19 (m, 1H), 3.81 (s, 3H), 3.18-3.27 (m, 1H), 3.03-3.11 (m, 1H); ¹³C NMR (CDCl₃, 50 MHz) δ 162.6, 157.4, 157.1, 142.8, 142.7, 129.8, 129.1, 124.5, 123.6, 123.0, 118.6, 114.8, 111.6, 111.4, 104.3, 104.1, 103.9, 74.7, 67.1, 56.5, 55.8, 55.5, 55.3, 36.5, 33.8, 33.6, 31.4, 29.7, 29.1, 14.1; ESI-MS (m/z): 678.14 [M+H]⁺; HRMS (ESI-qTOF): calcd for C₃₀H₂₃ClF₆N₇O₃ [M+H]⁺, 678.1450: found: 678.1454.

4-(2,3-difluorophenyl)-3-(4-(2-(2,4-difluorophenyl)-2-hydroxy-3-(1H-1, 2, 4-triazol-1-yl)propyl)-1H-1, 2, 3-triazol-1-yl)-1-phenylazetidin-2-one; 30c. Yellow colored solid; Yield: 91%; IR (CHCl₃, cm⁻¹) 3415, 1761; ¹H NMR (CDCl₃, 400 MHz) δ 8.03-8.07 (m, 1H), 7.82 (s, 1H), 7.33-7.40 (m, 5H, Ar-H), 7.28-7.31 (m, 1H, Ar-H), 7.18-7.23 (m, 1H, Ar-H), 6.85-6.98 (m, 3H), 6.68-6.76 (m, 2H), 6.25-6.34 (m, 1H), 5.86-5.89 (m, 1H), 5.18 (bs, 1H), 4.60-4.65 (m, 1H), 4.01-4.22 (m, 1H), 3.20-3.29 (m, 1H), 2.99-3.12 (m, 1H); ¹³C NMR (CDCl₃, 50 MHz) δ 165.2, 158.2, 158.0, 151.2, 142.5, 136.1, 129.8, 129.5, 125.6, 123.0, 117.3, 111.4, 104.1, 98.0, 67.0, 56.6, 56.3, 55.5, 49.6, 33.9, 33.6, 29.7, 14.1; ESI-MS (m/z): 564.14 [M+H]⁺; HRMS (ESI-qTOF): calcd for C₂₈H₂₂F₄N₇O₂ [M+H]⁺, 564.1766: found: 564.1769.

3-(4-(2-(2,4-difluorophenyl)-2-hydroxy-3-(1H-1, 2, 4-triazol-1-yl)propyl)-1H-1, 2, 3-triazol-1-yl)-4-(2-fluoro-3-(trifluoromethyl)phenyl)-1-phenylazetidin-2-one; 30d. Wine red colored solid; Yield: 90%; IR (CHCl₃, cm⁻¹) 3415, 1761; ¹H NMR (CDCl₃, 400 MHz) δ 8.02-8.07 (m, 3H), 7.80 (s, 1H), 7.33-7.41 (m, 6H, Ar-H), 7.20-7.24 (m, 1H, Ar-H), 7.00-7.21 (m, 1H, Ar-H), 6.67-6.74 (m, 2H), 6.25-6.33 (m, 1H), 5.90-5.93 (m, 1H), 5.21 (bs, 1H), 4.60-4.65 (m, 1H), 3.99-4.17 (m, 1H), 3.17-3.25 (m, 1H), 3.02-3.10 (m, 1H); ¹³C NMR (CDCl₃, 50 MHz) δ 162.5, 158.0, 157.8, 151.3, 142.7, 136.0, 132.16, 129.6, 125.7, 123.0, 117.3, 111.5, 104.1, 74.8, 67.1, 56.5, 56.3, 55.2, 36.5, 33.7, 31.4, 29.7; ESI-MS (m/z): 614.18 [M+H]⁺; HRMS (ESI-qTOF): calcd for C₂₉H₂₂F₆N₇O₂ [M+H]⁺, 614.1734: found: 614.1727.

3-(4-(2-(2,4-difluorophenyl)-2-hydroxy-3-(1H-1, 2, 4-triazol-1-yl)propyl)-1H-1, 2, 3-triazol-1-yl)-4-(4-fluoro-3-methylphenyl)-1-(4-methoxyphenyl)azetidin-2-one; 30e. cream colored solid; Yield: 88%; IR (CHCl₃, cm⁻¹) 3415, 1761; ¹H NMR (CDCl₃, 400 MHz) δ 7.99-8.06 (m, 1H), 7.15-7.40 (m, 6H), 6.67-7.02 (m, 6H), 6.29 (d, *J* = 10.9 Hz, 1H), 5.33-5.53 (m, 1H), 4.13-4.84 (m, 4H), 3.76 (m, 3H), 3.11-3.46 (m, 2H), 2.26 (s, 1H), 2.05-2.10 (m, 3H); ¹³C NMR (CDCl₃, 50 MHz) δ 169.7, 158.2, 157.0, 141.9, 130.0, 129.7, 126.5, 125.6, 119.1, 118.8, 115.4, 114.5, 67.5, 60.6, 55.4, 33.7, 14.6, 14.4; HRMS (ESI-qTOF): calcd for C₃₀H₂₇F₃N₇O₃ [M+H]⁺, 590.2122: found: 590.2108.

3-(4-(2-(2,4-difluorophenyl)-2-hydroxy-3-(1H-1, 2, 4-triazol-1-yl)propyl)-1H-1, 2, 3-triazol-1-yl)-4-(3-fluorophenyl)-1-phenylazetidin-2-one; 30f. Brown colored solid; Yield: 91%; semi-solid; IR (CHCl₃, cm⁻¹) 3415, 1761; ¹H NMR (CDCl₃, 400 MHz) δ 7.89-8.01 (m, 1H), 7.73 (d, *J* = 7.82 Hz, 1H), 7.30-7.37 (m, 2H, Ar-H), 7.0-7.24 (m, 7H, Ar-H), 6.84-6.87 (m, 1H, Ar-H), 6.63-6.78 (m, 3H), 6.20-6.29 (m, 1H), 5.53-5.56 (m, 1H), 5.26 (bs, 1H), 4.47-4.72 (m, 2H), 3.02-3.43 (m, 2H); ¹³C NMR (CDCl₃, 50 MHz) δ 163.7, 161.2, 158.5, 158.4, 154.3, 151.4, 144.2, 142.4, 136.2, 130.4, 129.8, 129.5, 125.6, 123.2, 117.4, 116.3, 113.8, 111.5, 104.1, 75.1, 74.8, 67.4, 60.4, 56.5, 534.1, 33.9, 29.6, 21.0, 14.1; ESI-MS (m/z): 546.14 [M+H]⁺; HRMS (ESI-qTOF): calcd for C₂₈H₂₃F₃N₇O₃ [M+H]⁺, 546.1860: found: 546.1860.

4-(4-chlorophenyl)-3-(4-(2-(2,4-difluorophenyl)-2-hydroxy-3-(1H-1, 2, 4-triazol-1-yl)propyl)-1H-1, 2, 3-triazol-1-yl)-1-(4-methoxyphenyl)azetidin-2-one; 30g. Wine red colored semi-solid; Yield: 90%; IR (CHCl₃, cm⁻¹) 3415, 1761; ¹H NMR (CDCl₃, 500 MHz) δ 7.99-8.03 (m, 1H), 7.80 (s, 1H), 7.31-7.37 (m, 3H, Ar-H), 7.23-7.26 (m, 1H, Ar-H), 7.07-7.15 (m, 1H), 6.81-6.93 (m, 5H), 6.68-6.74 (m, 2H), 6.26-6.34 (m, 1H), 5.56-5.59 (m, 1H), 5.15

(bs, 1H), 4.56-4.63 (m, 1H), 3.87-4.16 (m, 1H), 3.80 (s, 3H), 2.99-3.25 (m, 2H); ^{13}C NMR (CDCl_3 , 50 MHz) δ 163.5, 161.5, 157.8, 157.1, 151.4, 142.4, 133.8, 130.4, 129.7, 129.5, 123.2, 122.4, 118.7, 114.6, 113.8, 113.7, 111.5, 111.4, 104.0, 74.6, 67.45, 60.5, 66.5, 55.4, 34.0, 33.5, 29.6; ESI-MS (m/z): 592.14 $[\text{M}+\text{H}]^+$; HRMS (ESI-qTOF): calcd for $\text{C}_{29}\text{H}_{25}\text{ClF}_2\text{N}_7\text{O}_3$ $[\text{M}+\text{H}]^+$, 592.1670: found: 592.1663.

4-(2-chlorophenyl)-3-(4-(2-(2,4-difluorophenyl)-2-hydroxy-3-(1H-1, 2, 4-triazol-1-yl)propyl)-1H-1, 2, 3-triazol-1-yl)-1-(4-methoxyphenyl)azetidin-2-one; 30h. Cream colored solid; Yield: 92%; IR (CHCl_3 , cm^{-1}) 3415, 1761; ^1H NMR (CDCl_3 , 500 MHz) δ 7.99-8.01 (m, 1H), 7.79 (s, 1H), 7.28-7.35 (m, 3H, Ar-H), 7.23-7.24 (m, 1H, Ar-H), 7.02-7.17 (m, 4H), 6.87-6.89 (m, 2H), 6.67-6.72 (m, 2H), 6.27-6.36 (m, 1H), 5.90-5.93 (m, 1H), 5.13 (bs, 1H), 4.52-4.59 (m, 1H), 3.91-4.0 (m, 1H), 3.80 (s, 3H), 3.01-3.22 (m, 2H); ^{13}C NMR (CDCl_3 , 50 MHz) δ 163.5, 161.8, 161.5, 158.0, 157.8, 157.1, 151.4, 142.4, 132.8, 130.0, 129.7, 129.5, 128.4, 123.2, 122.4, 118.7, 114.6, 113.8, 113.7, 111.5, 111.4, 104.0, 74.6, 74.8, 67.45, 59.0, 56.4, 56.2, 36.4, 33.8, 14.4; ESI-MS (m/z): 592.14 $[\text{M}+\text{H}]^+$; HRMS (ESI-qTOF): calcd for $\text{C}_{29}\text{H}_{25}\text{ClF}_2\text{N}_7\text{O}_3$ $[\text{M}+\text{H}]^+$, 592.1670: found: 592.1663.

4-(2,4-dichlorophenyl)-3-(4-(2-(2,4-difluorophenyl)-2-hydroxy-3-(1H-1, 2, 4-triazol-1-yl)propyl)-1H-1, 2, 3-triazol-1-yl)-1-(4-methoxyphenyl)azetidin-2-one; 30i. Brown colored solid; Yield: 90%; IR (CHCl_3 , cm^{-1}) 3415, 1761; ^1H NMR (CDCl_3 , 400 MHz) δ 8.01 (s, 1H), 7.83 (s, 1H), 7.30-7.36 (m, 4H, Ar-H), 7.21-7.25 (m, 1H, Ar-H), 7.05-7.14 (m, 2H), 6.86-6.90 (m, 2H), 6.72-6.76 (m, 2H), 6.23-6.33 (m, 1H), 5.83-5.89 (m, 1H), 5.14 (bs, 1H), 4.58-4.65 (m, 1H), 3.95-3.99 (m, 1H), 3.80 (s, 3H), 3.07-3.26 (m, 2H); ^{13}C NMR (CDCl_3 , 50 MHz) δ 163.8, 161.3, 161.2, 157.8, 157.6, 157.1, 142.2, 165.5, 135.4, 129.7, 129.6, 127.7, 127.2, 118.7, 114.6, 111.6, 111.4, 104.3, 103.7, 74.9, 71.0, 67.0, 60.3, 58.6, 58.5, 55.4, 34.1, 33.8, 29.6; ESI-MS (m/z): 626.14 $[\text{M}+\text{H}]^+$; HRMS (ESI-qTOF): calcd for $\text{C}_{29}\text{H}_{24}\text{Cl}_2\text{F}_2\text{N}_7\text{O}_3$ $[\text{M}+\text{H}]^+$, 626.1280: found: 626.1269.

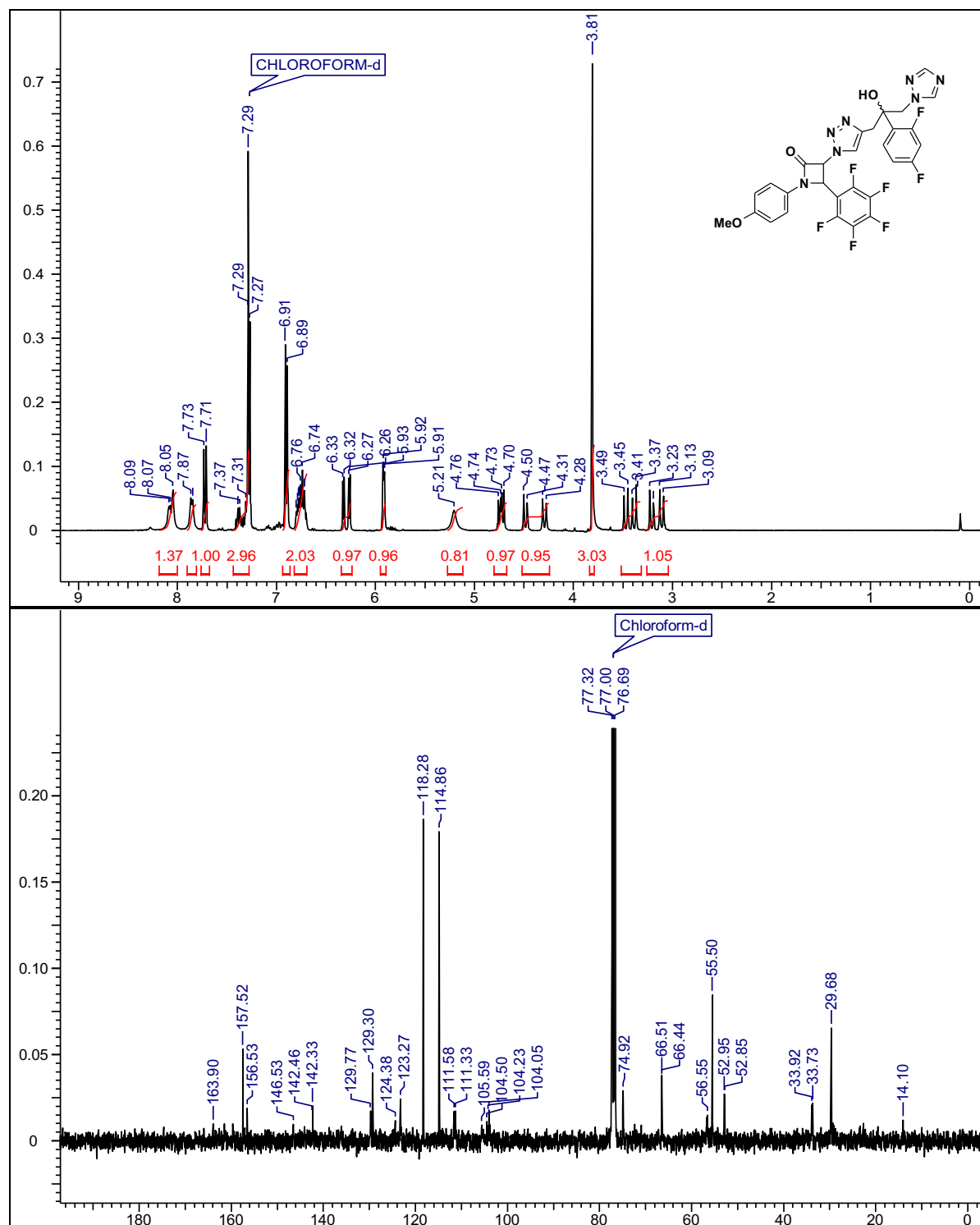
3-(4-(2-(2,4-difluorophenyl)-2-hydroxy-3-(1H-1, 2, 4-triazol-1-yl)propyl)-1H-1, 2, 3-triazol-1-yl)-1-(4-methoxyphenyl)-4-phenylazetidin-2-one; 30j. Yellow colored solid; Yield: 90%; IR (CHCl_3 , cm^{-1}) 3415, 1761; ^1H NMR (CDCl_3 , 500 MHz) δ 7.96-8.03 (m, 1H), 7.79 (s, 1H), 7.41-7.52 (m, 1H), 7.33-7.35 (m, 2H, Ar-H), 7.22-7.26 (m, 1H, Ar-H), 7.07-7.16 (m, 4H), 6.80-6.87 (m, 2H), 6.66-6.74 (m, 2H), 6.28-6.34 (m, 1H), 5.58-5.61 (m, 1H), 5.07 (bs, 1H), 4.49-4.58 (m, 1H), 4.0-4.02 (m, 1H), 3.78 (s, 3H), 2.97-3.19 (m, 2H); ^{13}C NMR (CDCl_3 , 50

MHz) δ 163.6, 158.1, 157.9, 157.0, 142.2, 131.1, 129.8, 129.0, 128.6, 126.6, 126.5, 126.1, 119.0, 118.8, 114.5, 114.4, 111.5, 111.3, 104.0, 103.8, 74.6, 67.5, 61.04, 56.5, 55.9, 55.4, 34.2, 29.6; ESI-MS (m/z): 558.18 [M+H]⁺; HRMS (ESI-qTOF): calcd for C₂₉H₂₆F₂N₇O₃ [M+H]⁺, 558.2060: found: 558.2057.

3-(4-(2-(2,4-difluorophenyl)-2-hydroxy-3-(1H-1, 2, 4-triazol-1-yl)propyl)-1H-1, 2, 3-triazol-1-yl)-4-(4-fluorophenyl)-1-(4-methoxyphenyl)azetidin-2-one; 30k. White colored solid; Yield: 93%; semi-solid; IR (CHCl₃, cm⁻¹) 3415, 1761; ¹H NMR (CDCl₃, 500 MHz) δ 7.96-8.0 (m, 1H), 7.79-7.81 (m, 1H), 7.35-7.38 (m, 1H), 7.29-7.33 (m, 2H, Ar-H), 7.22-7.26 (m, 2H, Ar-H), 7.09-7.13 (m, 2H), 6.80-6.88 (m, 4H), 6.67-6.78 (m, 2H), 6.22-6.29 (m, 1H), 5.55-5.59 (m, 1H), 5.11 (bs, 1H), 4.56-4.61 (m, 1H), 3.87-4.20 (m, 1H), 3.79 (s, 3H), 3.19-3.26 (m, 1H), 2.99-3.13 (m, 1H); ¹³C NMR (CDCl₃, 50 MHz) δ 163.7, 163.6, 161.6, 157.8, 151.5, 142.4, 129.6, 128.5, 126.9, 123.2, 122.9, 119.0, 118.8, 115.9, 115.7, 114.6, 111.5, 104.0, 74.9, 74.8, 67.5, 62.5, 60.4, 56.4, 34.0, 29.6, 14.1; ESI-MS (m/z): 576.19 [M+H]⁺; HRMS (ESI-qTOF): calcd for C₂₉H₂₅F₃N₇O₃ [M+H]⁺, 576.1965: found: 576.1968.

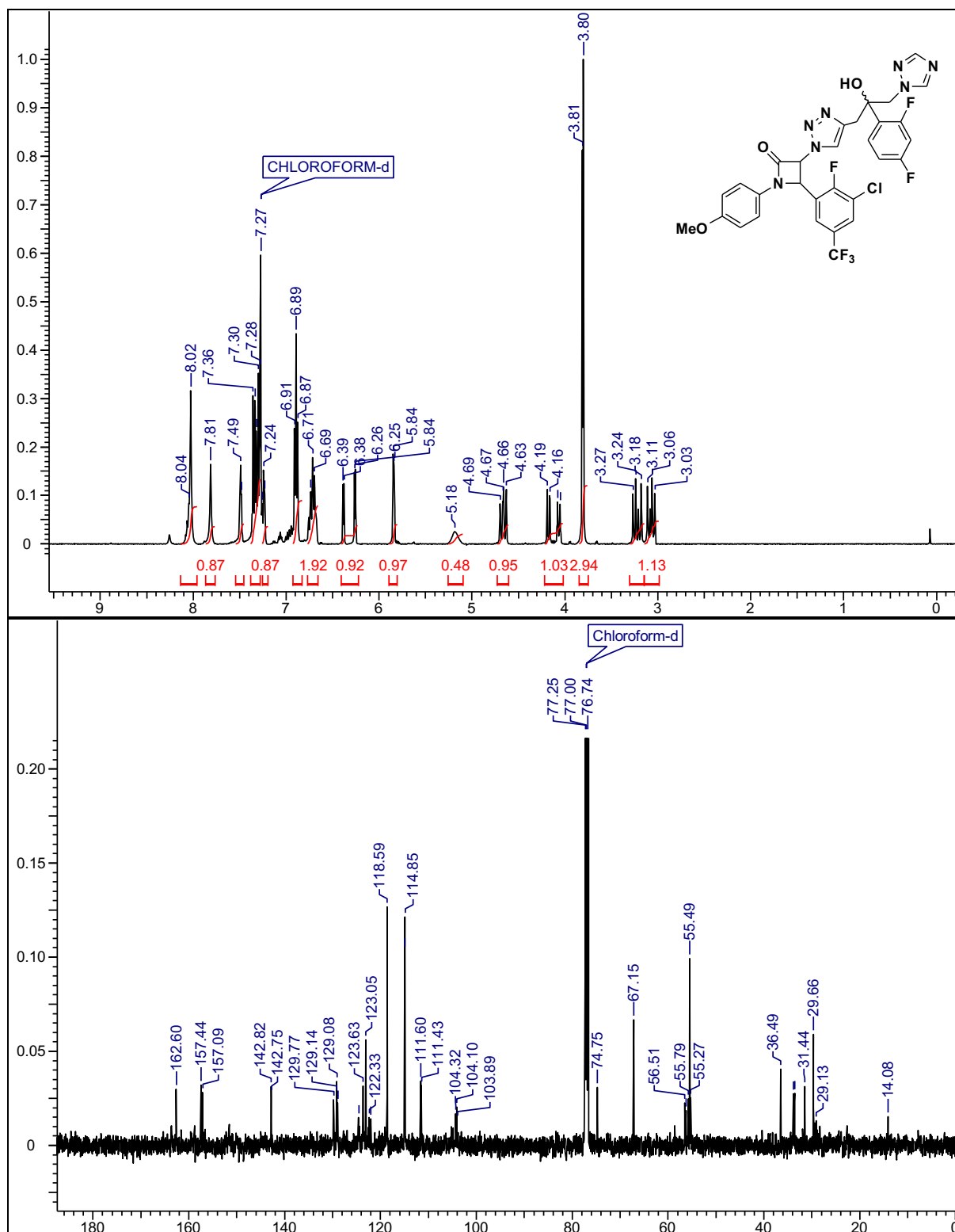
3-(4-(2-(2,4-difluorophenyl)-2-hydroxy-3-(1H-1, 2, 4-triazol-1-yl)propyl)-1H-1, 2, 3-triazol-1-yl)-4-(4-fluorophenyl)-1-phenylazetidin-2-one; 30l. Dark brown semi-solid; Yield: 90%; semi-solid; IR (CHCl₃, cm⁻¹) 3415, 1761; ¹H NMR (CDCl₃, 400 MHz) δ 7.96-8.0 (m, 1H), 7.79-7.83 (m, 1H), 7.32-7.40 (m, 5H, Ar-H), 7.20-7.25 (m, 2H, Ar-H), 7.09-7.18 (m, 2H, Ar-H), 6.78-6.87 (m, 2H), 6.69-6.73 (m, 2H), 6.24-6.31 (m, 1H), 5.59-5.63 (m, 1H), 5.11-5.22 (m, 1H), 4.54-4.61 (m, 1H), 3.88-4.20 (m, 1H), 3.03-3.26 (m, 2H); ¹³C NMR (CDCl₃, 50 MHz) δ 164.0, 163.9, 161.4, 158.6, 158.4, 151.4, 144.2, 142.4, 136.2, 129.7, 129.4, 128.4, 125.5, 122.9, 117.4, 116.0, 115.7, 111.5, 104.3, 104.0, 74.92, 74.8, 74.7, 67.4, 60.4, 56.5, 34.0, 33.6, 29.3. ESI-MS (m/z): 546.18 [M+H]⁺; HRMS (ESI-qTOF): calcd for C₂₈H₂₃F₃N₇O₂ [M+H]⁺, 546.1860: found: 546.1865.

1.7 Selected spectra

 ^1H & ^{13}C of compound 30 a (400 MHz, 50 MHz; CDCl_3)

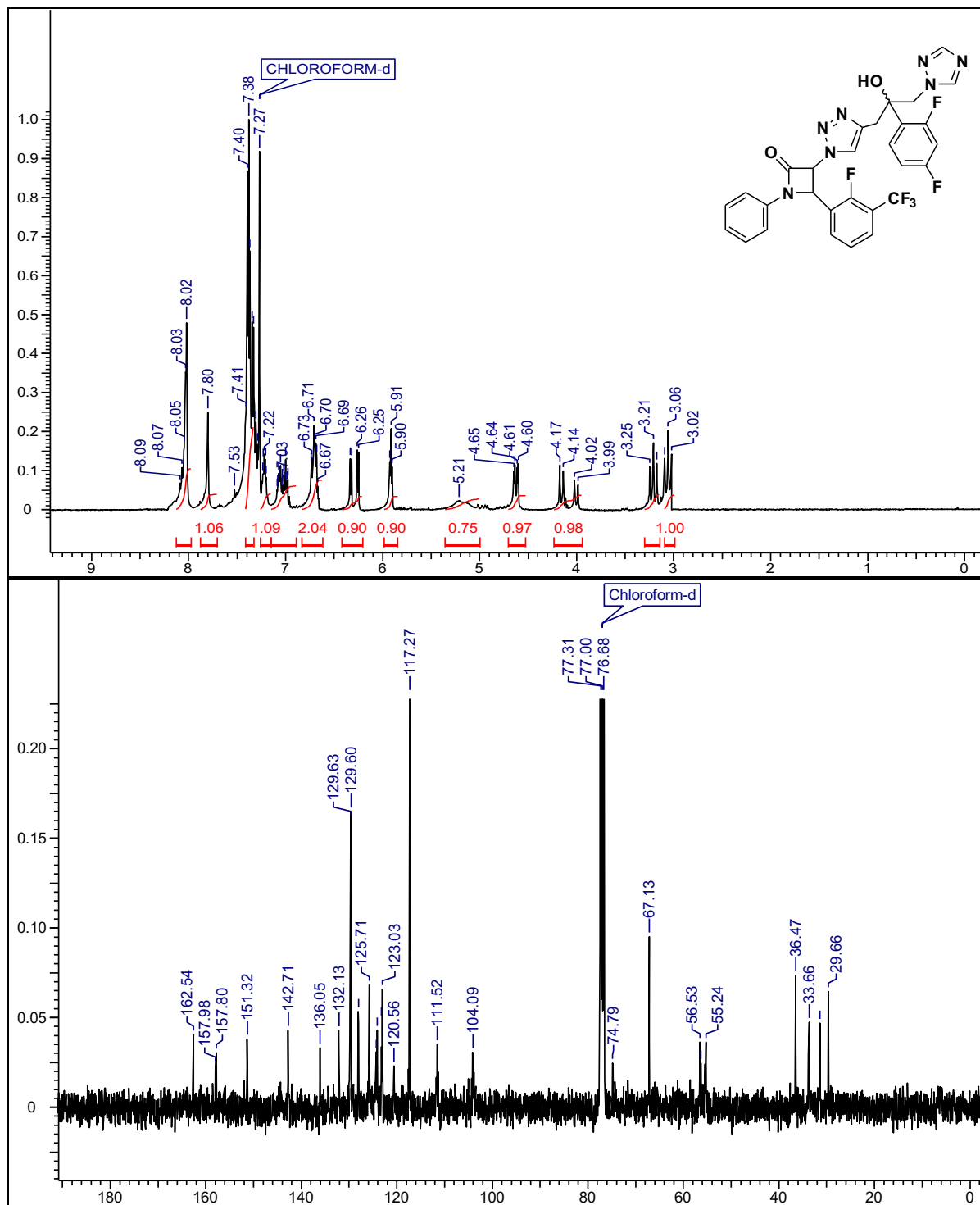
Chapter 1

^1H & ^{13}C of compound 30 b (500 MHz, 50 MHz; CDCl_3)



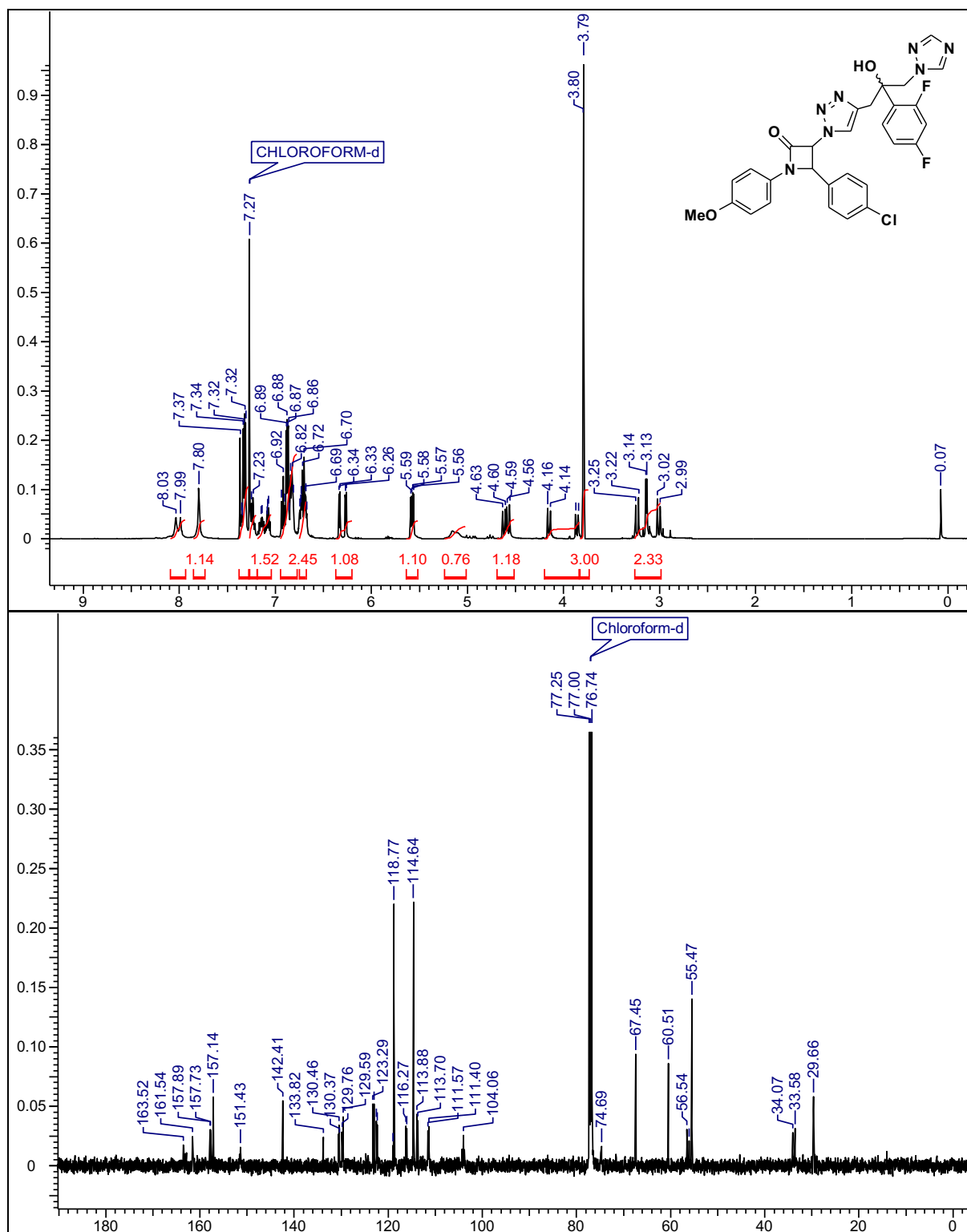
Chapter 1

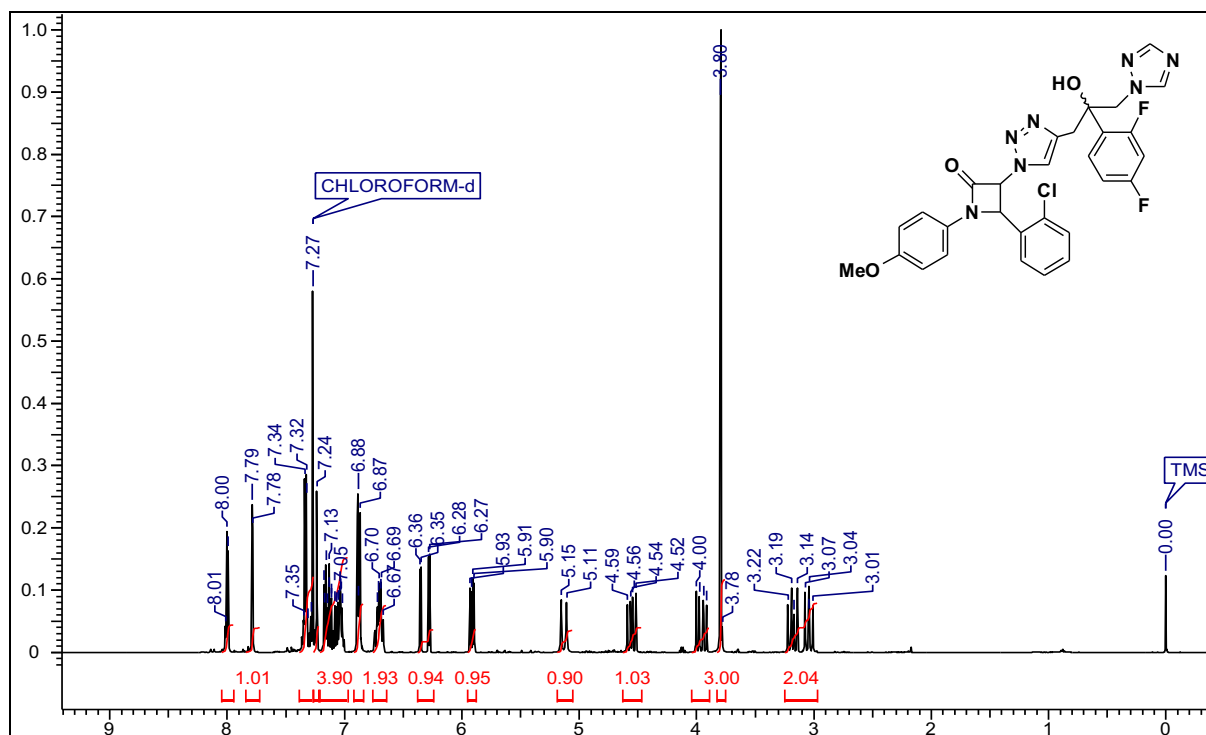
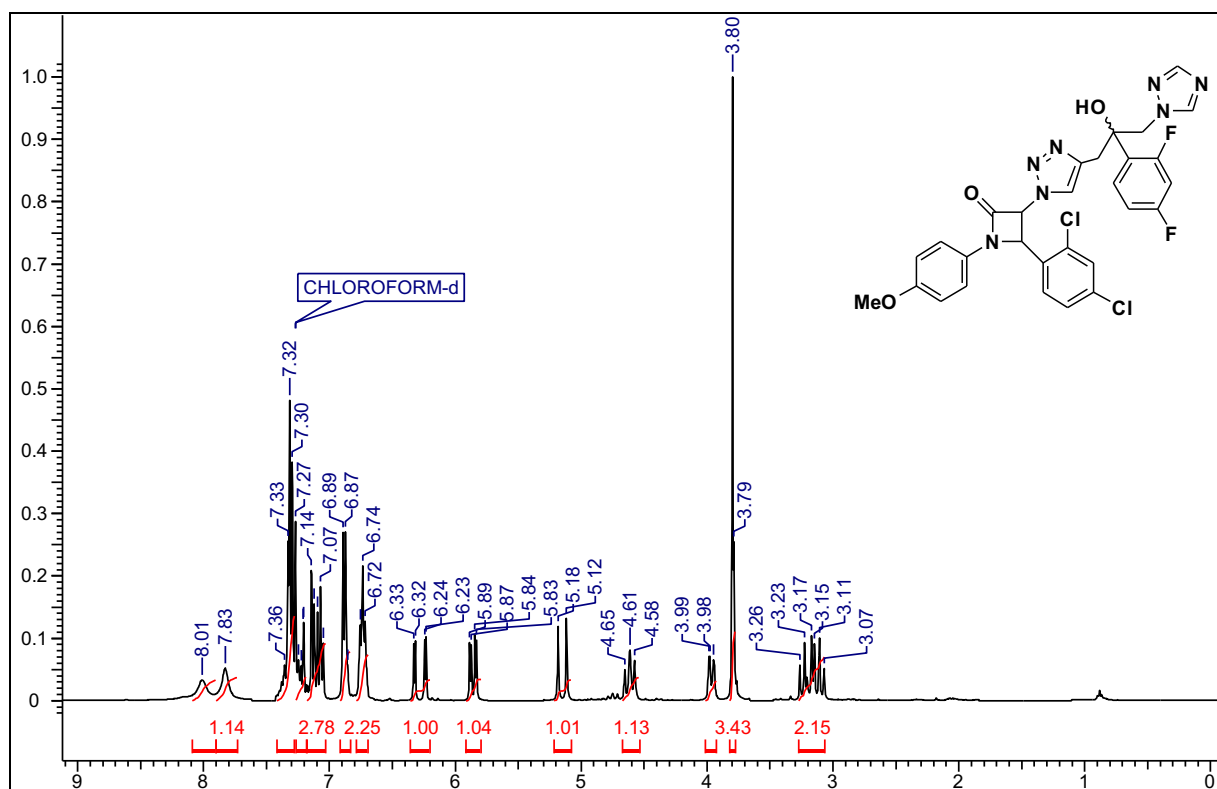
^1H & ^{13}C of compound 30 d (400 MHz, 50 MHz; CDCl_3)

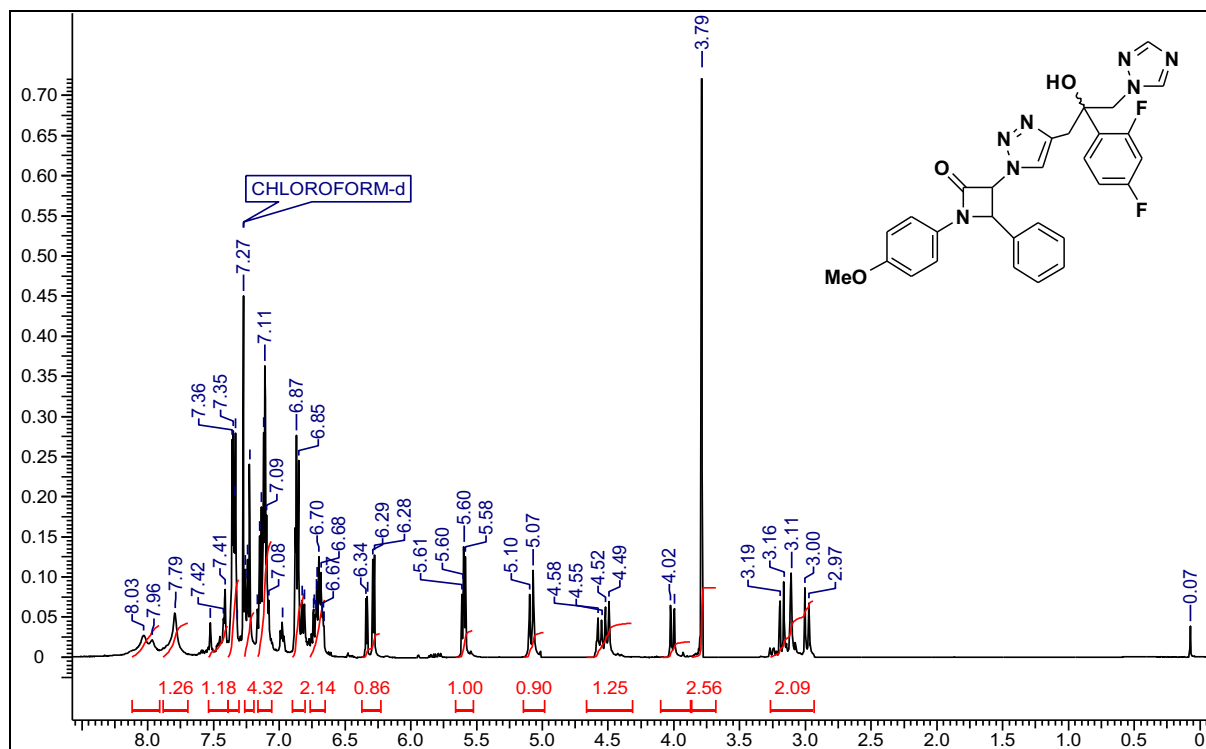
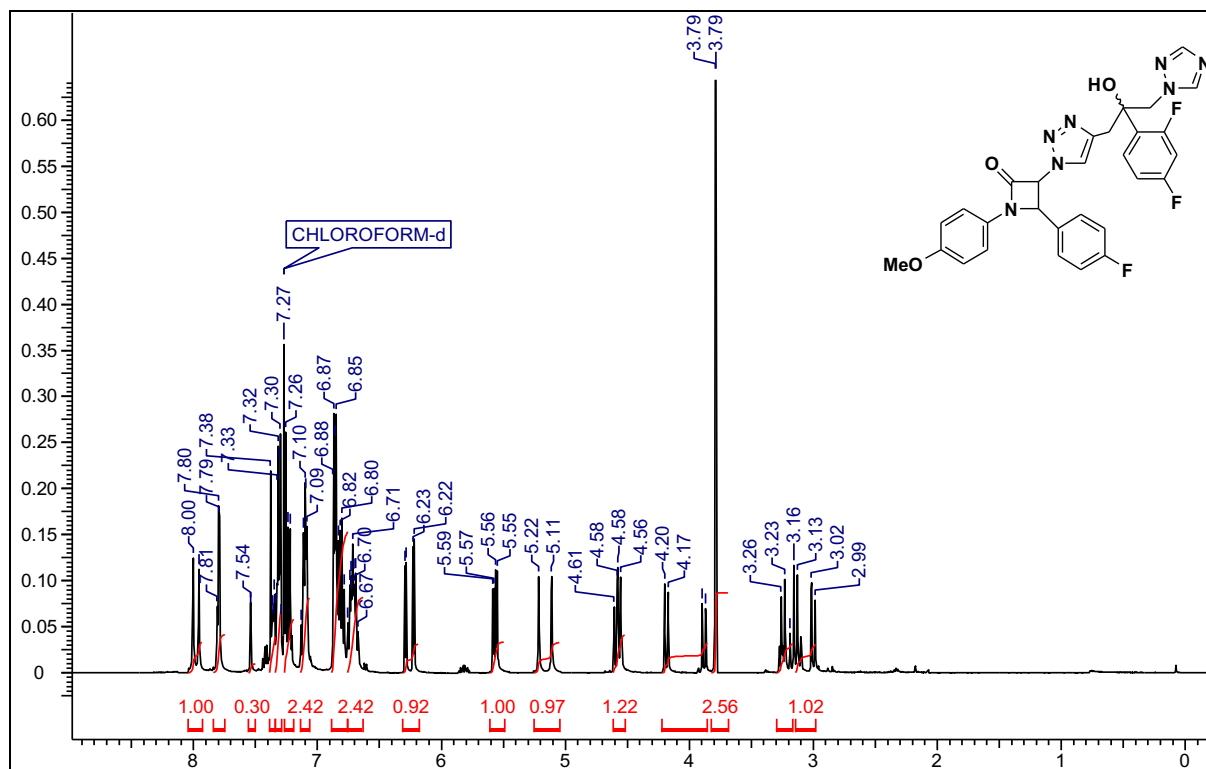


Chapter 1

^1H & ^{13}C of compound 30 g (500 MHz, 50 MHz; CDCl_3)

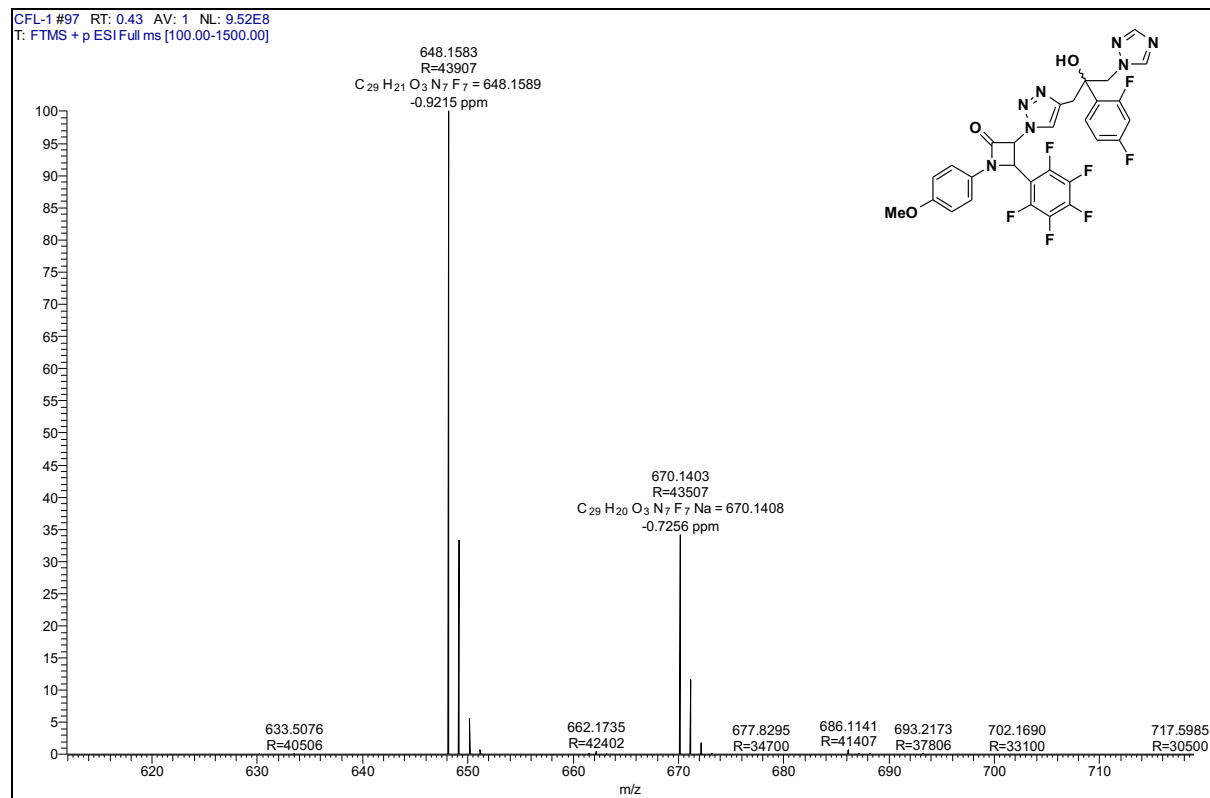


¹H of compound 30 h (500 MHz; CDCl₃)**¹H of compound 30 i (400 MHz; CDCl₃)**

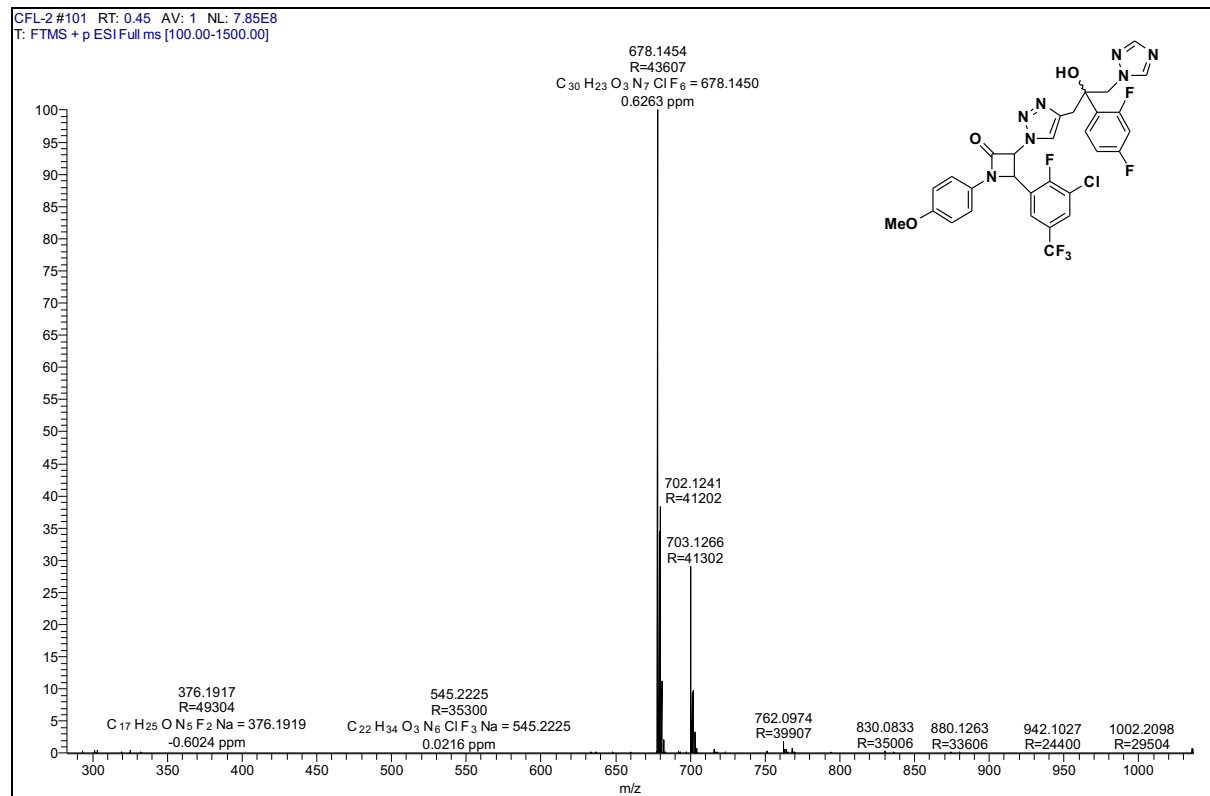
¹H of compound 30 j (500 MHz; CDCl₃)**¹H of compound 30 k (500 MHz; CDCl₃)**

1.8 Selected HRMS Spectra

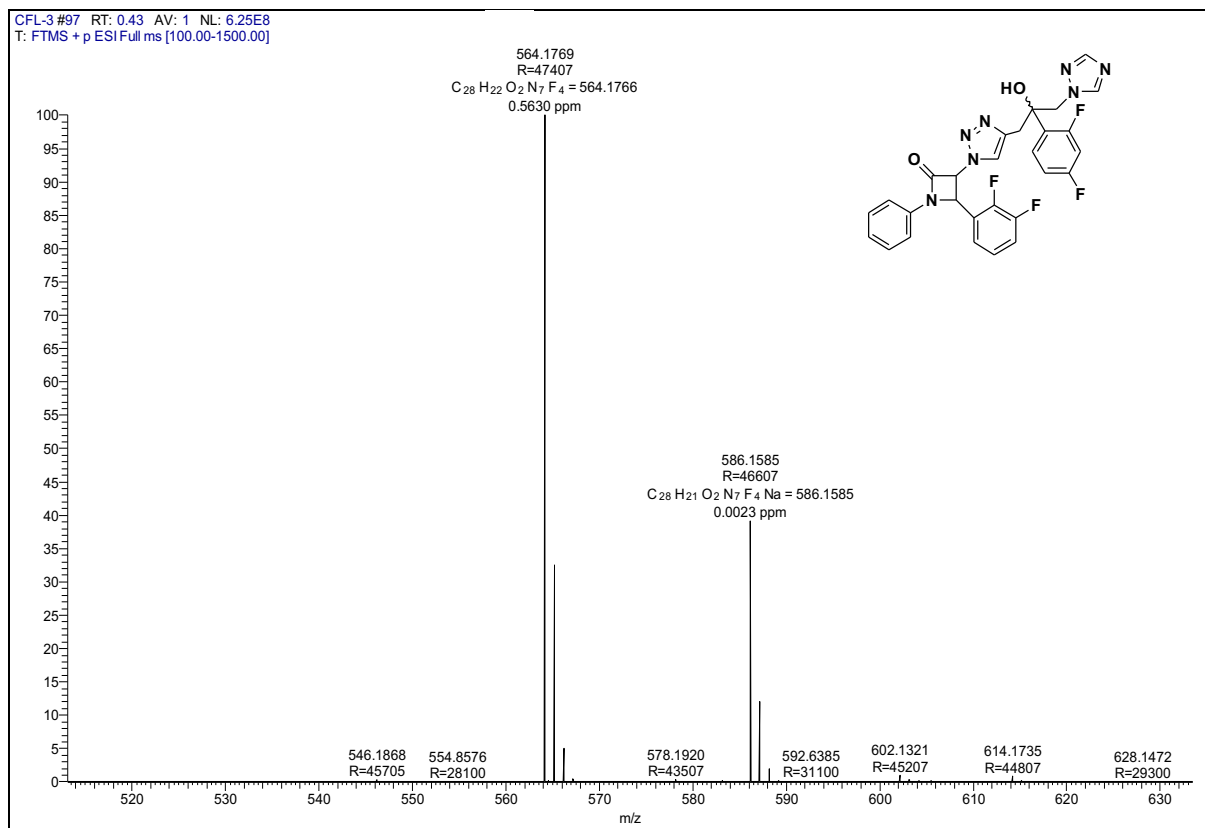
30 a



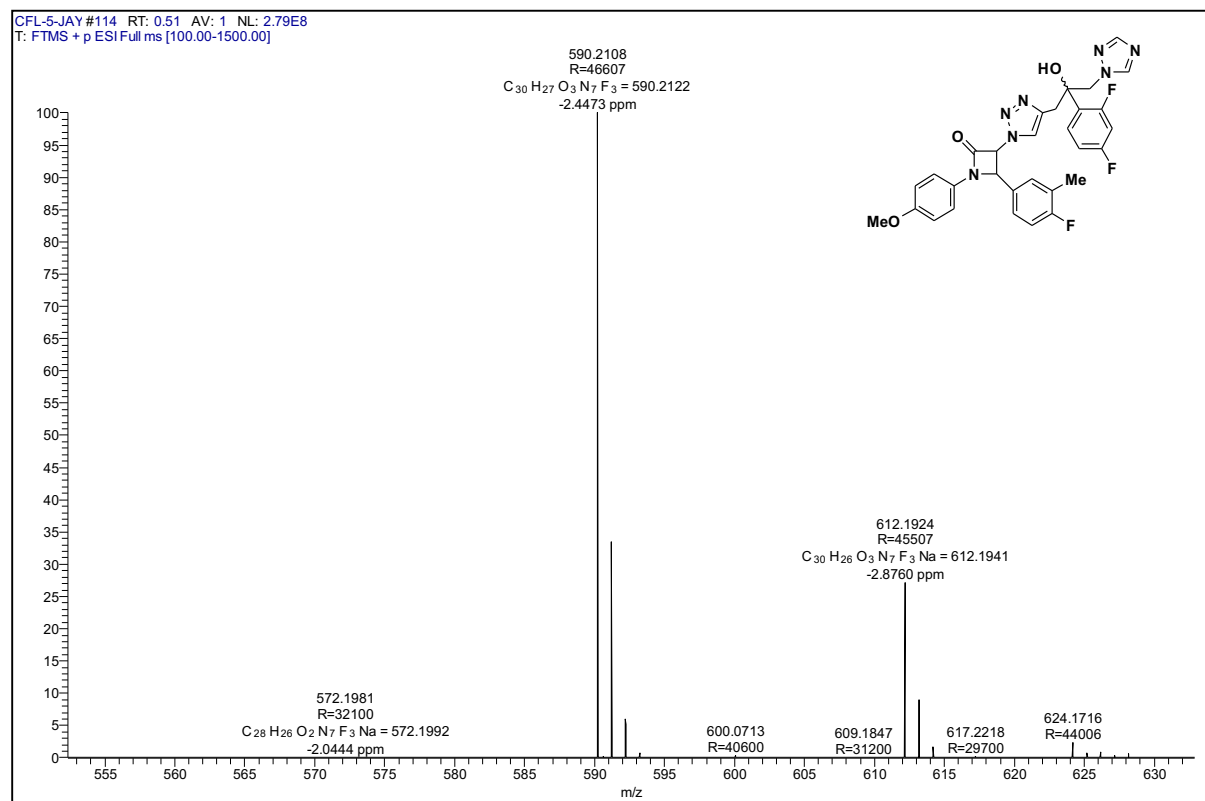
30 b



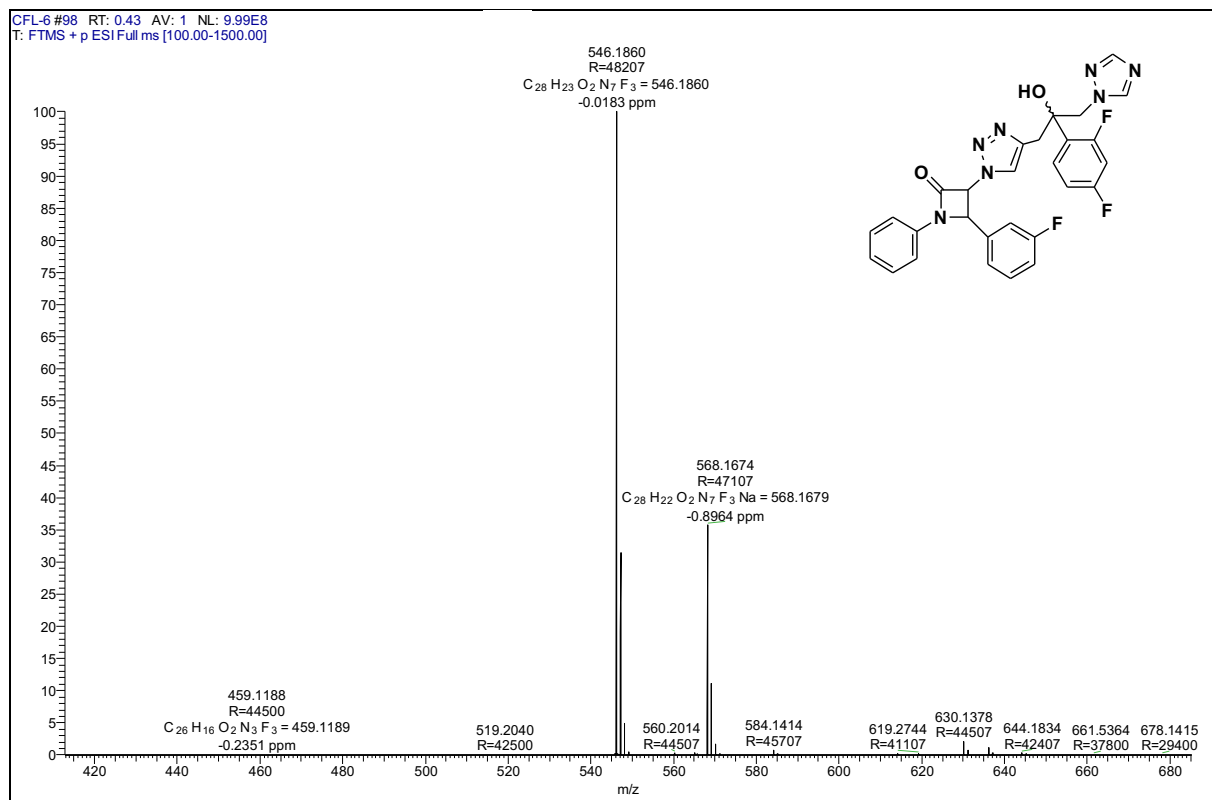
30 c



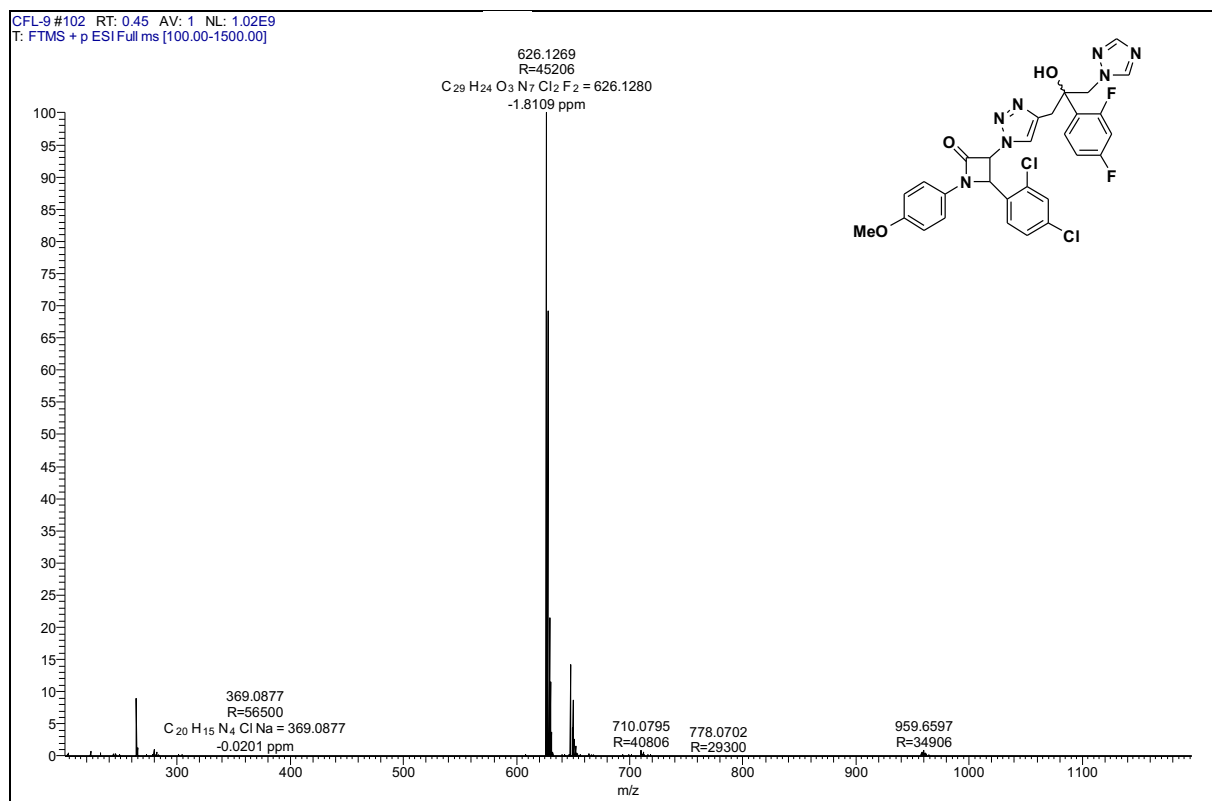
30 e



30 f



30 i



1.9 References

1. J. M. Divse, S. B. Mhaske, C. R. Charolkar, D. G. Sant, S. G. Tupe, M. V. Deshpande, V. M. Khedkar, L. U. Nawale, D. Sarkar, V. S. Pore, *New J. Chem.*, **2017**, 41, 470-479.
2. a) S. Roper, H. C. Kolb, in *Fragment-Based Approaches in Drug Discovery: Methods and Principles in Medicinal Chemistry Vol. 34*, (Eds: H. Baltes, W. Göpel, J. Hesse), Wiley-VCH: Weinheim, 2006; p 313-339; b) K. B. Sharpless, R. Manetsch, *Expert Opin. Drug Discovery* **2006**, 1, 525-538; c) G. C. Tron, T. Pirali, R. A. Billington, P. L. Canonico, G. Sorba, A. A. Genazzani, *Med. Res. Rev.* **2008**, 28, 278-308.
3. a) R. J. Pieters, D. T. S. Rijkers, R. M. J. Liskamp, *QSAR Comb. Sci* **2007**, 26, 1181-1190; b) A. J. Dirks, J. Cornelissen, F. L. van Delft, J. C. M. van Hest, R. J. M. Nolte, A. E. Rowan, F. Rutjes, *QSAR Comb. Sci.* **2007**, 26, 1200-1210; c) C. M. Salisbury, B. F. Cravatt, *QSAR Comb. Sci.* **2007**, 26, 1229-1238; d) J. M. Baskin, C. R. Bertozzi, *QSAR Comb. Sci.* **2007**, 26, 1211-1219; e) J. F. Lutz, *Angew. Chem., Int. Ed.* **2008**, 47, 2182-2184 (*Angew. Chem.*, **2008**, 120, 5749-5752); f) J. F. Lutz, H. G. Börner, *Prog. Polym. Sci.* **2008**, 33, 1-39.
4. a) W. H. Binder, C. Kluger, *Curr. Org. Chem.* **2006**, 10, 1791-1815; b) H. Nandivada, X. W. Jiang, J. Lahann, *Adv. Mater.* **2007**, 19, 2197-2208; c) D. Fournier, R. Hoogenboom, U. S. Schubert, *Chem. Soc. Rev.* **2007**, 36, 1369-1380; d) P. L. Golas, K. Matyjaszewski, *QSAR Comb. Sci.* **2007**, 26, 1116-1134; e) N. K. Devaraj, J. P. Collman, *QSAR Comb. Sci.* **2007**, 26, 1253.
5. a) Z. Zhou, C. J. Fahrni, *J. Am. Chem. Soc.* **2004**, 126, 8862-8863; b) A. J. Link, M. K. S. Vink, D. A. Tirrell, *J. Am. Chem. Soc.* **2004**, 126, 10598-10602; c) W. G. Lewis, F. G. Magallon, V. V. Fokin, M. G. Finn, *J. Am. Chem. Soc.* **2004**, 126, 9152-9153; d) K. Sivakumar, F. Xie, B. M. Cash, S. Long, H. N. Barnhill, Q. Wang, *Org. Lett.* **2004**, 6, 4603-4606; e) V. D. Bock, H. Hiemstra, J. H. van Maarseveen, *Eur. J. Org. Chem.* **2005**, 51-68; f) P. Wu, V. V. Fokin, *Aldrichimica Acta* **2007**, 40, 7-17; g) K. A. Kalesh, P. Y. Yang, R. Srinivasan, S. Q. Yao, *QSAR Comb. Sci.* **2007**, 26, 1135-1144; h) F. Santoyo-Gonzalez, F. Hernandez-Mateo, *Top. Heterocycl. Chem.* **2007**, 7, 133-177; i) J. F. Lutz, H. Schlaad, *Polymer* **2008**, 49, 817-824.
6. For selected reviews, see: (a) O. S. Miljanic, W. R. Dichtel, I. Aprahamian, R. D. Rohde, H. D. Agnew, J. R. Heath, J. F. Stoddart, *QSAR Comb. Science* **2007**, 26, 1165-1174; (b) I. Aprahamian, O. S. Miljanic, W. R. Dichtel, K. Isoda, T. Yasuda, T.

- Kato, J. F. Stoddart, *Bull. Chem. Soc. Jpn.* **2007**, *80*, 1856-1869; (c) A. B. Braunschweig, W. R. Dichtel, O. S. Miljanic, M. A. Olson, J. M. Spruell, S. I. Khan, J. R. Heath, J. F. Stoddart, *Chem. Asian J.* **2007**, *2*, 634-647; For selected papers see:
- d) V. Aucagne, K. D. Haenni, D. A. Leigh, P. J. Lusby, D. B. Walker, *J. Am. Chem. Soc.* **2006**, *128*, 2186-2187; e) R. K. O'Reilly, M. J. Joralemon, C. J. Hawker, K. L. Wooley, *Polym. Sci. Polym. Chem.* **2006**, *44*, 5203-5217; f) D. D. Diaz, K. Rajagopal, E. Strable, J. Schneider, M. G. Finn, *J. Am. Chem. Soc.* **2006**, *128*, 6056-6057; g) M. V. Gil, M. J. Arevalo, O. Lopez, *Synthesis* **2007**, 1589-1620; h) W. B. Zhang, Y. Tu, R. Ranjan, R. M. VanHorn, S. Leng, J. Wang, M. J. Polce, C. Wesdemiotis, R. P. Quirk, G. R. Newkome, S. Z. D. Cheng, *Macromol.* **2008**, *41*, 515-517; i) J. S. Marois, K. Cantin, A. Desmarais, J. F. Morin, *Org. Lett.* **2008**, *10*, 33-36.
7. R. Kharb, P. C. Sharma, M. S. Yar, *Enzyme Inhib. Med. Chem.* **2011**, *26*, 1-21
 8. R. S. Bohacek, C. McMartin, W. C. Guida, *Med. Res. Rev.* **1996**, *16*, 3-50
 9. D. Kontoyannis, E. Mantadakis, G. Samonis, *J. Hosp. Infect.*, 2003, **53**, 243.
 10. B. Monk, A. Goffeau, *Science*, 2008, **321**, 367.
 11. (a) B. E. De Pauw, F. Meunier, *Chemotherapy*, 1999, **45**, 1; (b) A. Chakrabarti, *J. postgrad. Med.*, 2005, **51**, S16; (c) R. Cha, J. D. Sobel, *Expert Rev. Anticancer Ther.*, 2004, **2**, 357; (d) N. H. Shear, V. Villars, C. Marsolais, *Clin. Dermatol.*, 1991, **9**, 487; (e) L. K. Ostrosky-Zeichner, A. Marr, J. H. Rex and S. H. Cohen, *Clin. Infect. Dis.*, 2003, **37**, 415.
 12. (a) C. A. Kauffman, P. L. Carver, *Drugs*, 1997, **53**, 539; (b) N. C. Karyotakis, E. J. Anaissie, *Curr. Opin. Inf. Dis.* 1994, **7**, 658; (c) M. Zervos, F. Meunier, *Int. J. Antimicrob. Agents*, 1993, **3**, 147.
 13. J. H. Rex, M. G. Rinaldi, M. A. Pfaller, *Antimicrob. Agents Chemother.*, 1995, **39**, 1.
 14. (a) Huisgen, R. *J. Org. Chem.* **1976**, *41*, 403-419; (b) Gothelf, K. V.; Jørgensen, K. A. *Chem.. Rev.* **1998**, *98*, 863-909.
 15. a) V. V. Rostovsev, L. G. Green, V. V. Fokin, K. B. Sharpless, *Angew. Chem., Int. Ed. Engl.* **2002**, *41*, 2596-2599 (*Angew. Chem.* **2002**, *114*, 2708-2711); b) C. W. Tornøe, C. Christensen, M. Meldal, *J. Org. Chem.* **2002**, *67*, 3057-3062.
 16. H. C. Kolb, M. G. Finn, K. B. Sharpless, *Angew. Chem., Int. Ed.* **2001**, *40*, 2004-2021 (*Angew. Chem.* **2001**, *113*, 2056-2075).
 17. (a) Sustmann, R. *Tetrahedron Lett.* **1971**, *29*, 2717-2720.; (b) Bräse, S.; Gil, C.; Knepper, K.; Zimmermann, V. *Angew. Chem. Int. Ed.* **2005**, *44*, 5188-5240.
 18. (a) Weber, L. *Drug Disc. Today* **2004**, *1*, 261-267.

19. (a) Genin, M. J.; Allwine, D. A.; Anderson, D. J.; Barbachyn, M. R.; Emmert, D. E.; Garmon, S. A.; Graber, D. R.; Grega, K. C.; Hester, J. B.; Hutchinson, D. K.; Morris, J.; Reischer, R. J.; Ford, C. W.; Zurenko, G. E.; Hamel, C. J.; Schaadt, R. D.; Stapert, D.; Yagi, B. H. *J. Med. Chem.* **2000**, *43*, 953-970.; (b) Dabak, Ö.; Sezer, A.; Akar, O. *Eur. J. Med. Chem.* **2003**, *38*, 215-218.
20. (a) Himo, F.; Lovell, T.; Hilgraf, R.; Rostovtsev, V. V.; Noodleman, L.; Sharpless, K. B.; Fokin, V. V. *J. Am. Chem. Soc.* **2005**, *127*, 210-216.; (b) Bock, V. D.; Hiemstra, H.; Van Maarseveen, J. H. *Eur. J. Org. Chem.* **2006**, 51-68.
21. a) E. Saxon, C. R. Bertozzi, *Science* **2000**, *287*, 2007–2010; b) K. L. Kiick, E. Saxon, D. A. Tirrel, C. R. Bertozzi, *Proc. Natl. Acad. Sci. U. S. A.* **2002**, *99*, 19–24.
22. a) D. K. Dalvie, A. S. Kalgutkar, S. C. Khojasteh-Bakht, R. S. Obach, J. P. O'Donnell, *Chem. Res. Toxicol.* **2002**, *15*, 269-299; b) W. S. Horne, M. K. Yadav, C. D. Stout, M. R. Ghadiri, *J. Am. Chem. Soc.* **2004**, *126*, 15366-15367.
23. M. I. Garcia-Moreno, D. Rodriguez-Lucena, C. O. Mellet, J. M. G. Fernandez, *J. Org. Chem.* **2004**, *69*, 3578–3581.
24. (a) S. M. Michael, R. Kenneth, In *Recent Trends in the Discovery, Development and evaluation of Antifungal Agents*; R. A. Fromtling, Ed., Prous Science Publishers: SA, 1987, 81; (b) G. Aperis, E. Mylonakis, *Expert Opin. Investig. Drugs*, 2006, *15*, 579; (c) A. Chen, J. D. Sobel, *Expert Opin. Emerg. Drugs*, 2005, *10*, 21.
25. a) V. S. Pore, N. G. Aher, M. Kumar, P. K. Shukla, *Tetrahedron* **2006**, *62*, 11178–11186; b) N.G. Aher, V. S. Pore, N. N. Mishra, A. Kumar, P. K. Shukla, A. Sharma, M. K. Bhat, *Bioorg. Med. Chem. Lett.* **2009**, *19*, 759–763; c) V. S. Pore, S. G. Agalave, P. Singh, P. K. Shukla, V. Kumar, M.I. Siddiqi, *Org. Biomol. Chem.* **2015**, *13*, 6551-6561.
26. a) N. S. Vatmurge, B. G. Hazra, V. S. Pore, F. Shirazi, P. S. Chavan, M. V. Deshpande, *Bioorg. Med. Chem. Lett.* **2008**, *18*, 2043–2047; b) N. S. Vatmurge, B. G. Hazra, V. S. Pore, F. Shirazi, M. V. Deshpande, S. Kadreppa, S. Chattopadhyay, *Org. Biomol. Chem.* **2008**, *6*, 3823-3830.
27. P. M. Chaudhary, S. R. Chavan, F. Shirazi, M. Razdan, P. Nimkar, S. P. Maybhate, A. P. Likhite, R. Gonnade, B. G. Hazara, M. V. Deshpande, S. R. Deshpande, *Bioorg. Med. Chem. Lett.* **2009**, *17*, 2433–2440.
28. J. N. Sangshetti, D. B. Shinde, *Bioorg. Med. Chem. Lett.* **2010**, *20*, 742–745.
29. J. N. Sangshetti, R. R. Nagawade, D. B. Shinde, *Bioorg. Med. Chem. Lett.* **2009**, *19*, 3564–3567.

30. S. B. Ferreira, M. S. Costa, N. Boechat, R. J. S. Bezerra, M. S. Genestra, M. M. Canto-Cavalheiro, W. B. Kover, V. F. Ferreira, *Eur. J. Med. Chem.* **2007**, *42*, 1388-1395.
31. A. H. Kategaonkar, P. V. Shinde, S. K. Pasale, B. B. Shingate, M. S. Shingare, *Eur. J. Med. Chem.*, **2010**, *45*, 3142-3146.
32. W-Y Lu, X-W Sun, C. Zhu, J-H Xu, G-Q Lin, *Tetrahedron* **2010**, *66*, 750-757.
33. S. B. Luesse, G. Wells, A. Nayek, A. E. Smith, B. R. Kusche, S. C. Bergmeier, M. C. McMills, N. D. Priestley, D. L. Wright, *Bioorg. Med. Chem. Lett.* **2008**, *18*, 3946-3949.
34. V. Sumangala, B. Poojary, N. Chidananda, J. Fernandes, N. S. Kumari, *Arch. Pharmcal Res.* **2010**, *33*, 1911-1918.
35. B. S. Holla, M. Mahalinga, M. S. Karthikeyan, B. Poojary, P. M. Akberali, N. S. Kumari, *Eur. J. Med. Chem.* **2005**, *40*, 1173-1178.
36. K. D. Thomas, A. V. Adhikari, N. S. Shetty, *Eur. J. Med. Chem.* **2010**, *45*, 3803-3810.
37. L. V. R. Reddy, P.V. Reddy, N. N. Mishra, P. K. Shukla, G. Yadav, R. Srivastava, A. K. Shaw, *Carbohydr. Res.* **2010**, *345*, 1515-1521.
38. Z. Jiang, J. Gu, C. Wang, S. Wang, N. Liu, Y. Jiang, G. Dong, Y. Wang, Y. Liu, J. Yao, Z. Miao, W. Zhang, C. Sheng, *Eur. J. Med. Chem.*, **2014**, *82*, 490-497.
39. D. Krishnaswamy, V. V. Govande, V. K. Gumaste, B. M. Bhawal, A. R. Deshmukh, *Tetrahedron*, 2002, **58**, 2215.
40. (a) B. G. Hazra, N. S. Vatmurge, V. S. Pore, F. Shirazi, P. Chavan, M. Deshpande, *Bioorg. Med. Chem. Lett.*, 2008, **18**, 2043; (b) N. S. Vatmurge, B. G. Hazra, V. S. Pore, F. Shirazi, M. Deshpande, S. Kadreppa, S. Chattopadhyay, *Org. Biomol. Chem.*, 2008, **6**, 3823.
41. R. S. Upadhyaya, S. Jain, N. Sinha, N. Kishore, R. Chandra and S. K. Arora, *Eur. J. Med. Chem.*, 2004, **39**, 579.
42. V. S. Pore, N. G. Aher, M. Kumar, P. K. Shukla, *Tetrahedron*, 2006, **62**, 11178.
43. (a) B. G. Hazra, N. S. Vatmurge, V. S. Pore, F. Shirazi, P. Chavan, M. Deshpande, *Bioorg. Med. Chem. Lett.*, 2008, **18**, 2043; (b) N. S. Vatmurge, B. G. Hazra, V. S. Pore, F. Shirazi, M. Deshpande, S. Kadreppa, S. Chattopadhyay, *Org. Biomol. Chem.*, 2008, **6**, 3823.
44. Clinical and Laboratory Standards Institute. Approved Standard. Document M27-A; CLSI: Wayne, PA, USA, 1997; (b) Clinical and Laboratory Standards Institute. Document M38-P; CLSI: Wayne, PA, USA, 1998; (c) Clinical and Laboratory

- Standards Institute. Approved Standard M7–A5, 5th ed.; CLSI: Wayne, PA, USA, 2000.
45. S. Pulya, Y. Kommagalla, D. G. Sant, S. U. Jorwekar, S. G. Tupe, M. V. Deshpande, C.V. Ramana, *RSC adv.*, 2016, **6**, 11691.
 46. B. A. Arthington-Skaggs, H. Jradi, T. Desai, C. J. Morrison, *J. Clin. Microbiol.*, 1999, **37**, 3332.
 47. T. Mosmann, Rapid colorimetric assay for cellular growth and survival: application to proliferation and cytotoxicity assays. *Journal of immunological methods*, 1983,**65**,55.
 48. M. S. A. Khan and I. Ahmad, *Appl. Microbiol. Biotech.*, 2011, **90**, 1083.

Chapter 2

Design and synthesis of 11 α -substituted bile acid derivatives as potential anti-tuberculosis agents

Chapter 2

Design and synthesis of 11 α -substituted bile acid derivatives as potential anti-tuberculosis agents

2.1 Abstract

We have synthesized a series of novel 11 α -triazoyl bile acid derivatives.¹ In addition, we also have synthesized N-alkyl and N-acyl derivatives of C-11 amino bile acid esters.¹ All the compounds were evaluated for the inhibitory activity against *Mycobacterium tuberculosis* H37Ra (*MTB*) at 30 μ g/mL level. Four lead compounds (**36b**, **35**, **47** and **48**) were further confirmed from their dose dependent effect against *MTB*. These compounds were found to be active against Dormant and active stage *MTB* under both *in vitro* as well as within THP1 host macrophages. The most promising compound **36b** showed strong antitubercular activities against *MTB* under *in-vitro* and *ex-vivo* (IC₉₀ value of \approx 3 μ g/mL) conditions and almost insignificant cytotoxicity up to 100 μ g/mL against THP-1, A549 and PANC-1 human cancer cell lines. Inactivity of all these compounds against Gram positive and Gram negative bacteria indicates their specificity. Molecular docking studies of these compounds into the active site of *DprE1* enzyme revealed a similar binding mode to native ligands in the crystal structure thereby helping to establish a structural basis of inhibition of *MTB*. The synthesized compounds were analyzed for Adsorption, distribution, metabolism and excretion (ADME) properties and showed potential to develop good oral drug candidates. Our results clearly indicate the identification of some novel, selective and specific inhibitors against *MTB* that can be explored further for potential antitubercular drug.

2.2 Introduction

Mycobacterium tuberculosis is a huge threat to the world nowadays, which is caused by acid-fast, Gram-positive bacterium. *Mycobacterium tuberculosis* is listed as global emergency by WHO due to its latent haven in about one third of the global population. Despite the availability of many drugs (isoniazid, rifampin, pyrazinamide, and ethambutol) including vaccines like Bovine Calmette–Guerin (BCG) in the market, TB continues to be the leading bacterial infection. This is due to emergence of drug resistance occurring due to inappropriate use of antibiotics. 1, 2, 3-Triazole moieties are effective linking units and modified synthetic molecules bearing them show diverse biological activities.^{2,3}

Steroids derivatized at C-11 are well known for biological activity and are found in many naturally occurring molecules such as cortisone, hydrocortisone and corticosterone.⁴ Much more potent synthetic corticosteroids such as dexamethasone, triamcinolone and fluticasone also possess C-11 hydroxyl functionality.⁵ There is a recent report on synthesis of sterically hindered 11 β -amino-progesterone derivatives and their evaluation as 11- β -hydroxysteroid dehydrogenase inhibitors and mineralocorticoid receptor antagonists.⁶

In the exploration of developing novel inhibitors which may conquer the complexity and duration of the current therapeutic approach, as well as efficiently treat MDR and XDR tuberculosis, we thought of making a combination of steroids and 1, 2, 3-triazole at C-11 position. 1, 2, 3-Triazole moieties are stable to metabolic degradation and also improve hydrogen bonding, which can be beneficial in binding of biomolecular targets and for solubility.⁷ Huisgen's 1, 3- dipolar cycloaddition of terminal acetylenes and organic azides gives a mixture of 1, 4- and 1, 5-disubstituted-1, 2, 3-triazoles and require higher temperature and large reaction period.^{7a} Cu(I) catalyzed 1, 3-dipolar cycloaddition has been a method of choice for the synthesis of 1, 4-disubstituted-1, 2, 3-triazoles.^{7b-d} Among the various reaction conditions, microwave assisted Cu(I) catalyzed reaction was found to be suitable for this conjugation as it gives the product in less reaction time.⁸

Bile acids are naturally facial amphiphilic in nature due to the stereochemical orientation of one to three hydroxyl groups.⁹ Polymyxin B is an antimicrobial essentially used for resistant Gram-negative infections. It is obtained from the bacterium *Bacillus polymyxa*. It has a bactericidal response against almost all Gram-negative bacilli as it binds to the cell membrane and alters its structure, makes it more permeable. Cholic acid derived cationic anti-microbial agents were synthesized by Savage and co-workers that possessed a higher affinity for lipid A of bacterial membranes as compared to polymyxin B.^{10b} In this chapter, we propose that incorporating 1, 2, 3-triazole rings with several alkyl or acyl amines on bile acid amphiphiles modulate their specificity against mycobacteria. We unraveled that hard-charged amphiphiles specifically destroy mycobacteria as the hydrophobic, rigid, waxy outer membranes of the mycobacteria may allow penetration of these hydrophobic amphiphiles.

2.3 Review of literature

2.3.1 Bile acid and its importance

Bile acids are natural products consisting of a facially amphiphilic steroid nucleus and a polar side chain and obtained from the digestive systems of vertebrates.¹¹ Bile acids participate in

the digestion and resorption of lipids and lipophilic vitamins. In the salt form, they act as emulsifiers, assisting in the solubilization and absorption of fats and lipids in the small intestine. It is now well recognized that besides their biological importance, these molecules are useful starting materials in designing novel structures with potential applications in supramolecular science.¹² The synthesis of bile acid derived dendritic structures was first reported by Kolehmainen *et al.*¹³ They have been used in the treatment of bile acid deficiency, liver diseases, and in dissolving of cholesterol gallstones,¹⁴ and also have many medical applications.¹⁵⁻¹⁸

Because of large, rigid, and curved steroidal skeletons, having chemically different hydroxy groups, unique amphiphilicity, and their enantiomeric purities, together with easy availability and low cost, make bile acids important and ideal building blocks for the design and synthesis of novel bioactive molecules and supramolecular assemblies.

Bile salts are biosynthesized from cholesterol in the liver and stored in the gall bladder. The human liver produces 600-800 mL of bile per day. After food intake and subsequent gall bladder emptying, bile is secreted into the small intestine, where the bile acids perform their essential function in the digestion and resorption of fat, fatty acids and lipid-soluble vitamins. These nutrients are insoluble in water which dispersed in micelles of bile acids and lipids. The bile acids recirculate to the liver *via* the portal vein, undergoing this enterohepatic circulation 6-15 times per day. Bile acids are manufactured from cholesterol in hepatocytes. This catabolic pathway represents the major metabolic fate of cholesterol (Figure 1).

The most abundant primary bile salts in humans are cholate, chenodeoxycholate and deoxycholate, and they are normally conjugated with either glycine (75%) or taurine (25%). Conjugation increases the aqueous solubility of bile salts under physiological conditions. All primary bile acids appear to have three features in common: (i) they are the major end-products of cholesterol metabolism, (ii) they are secreted into the bile largely in a conjugated form, and (iii) these conjugates are membrane-impermeable, water-soluble, amphiphilic molecules having a powerful ability to transform lamellar arrays of lipids into mixed micelles.^{19,20}

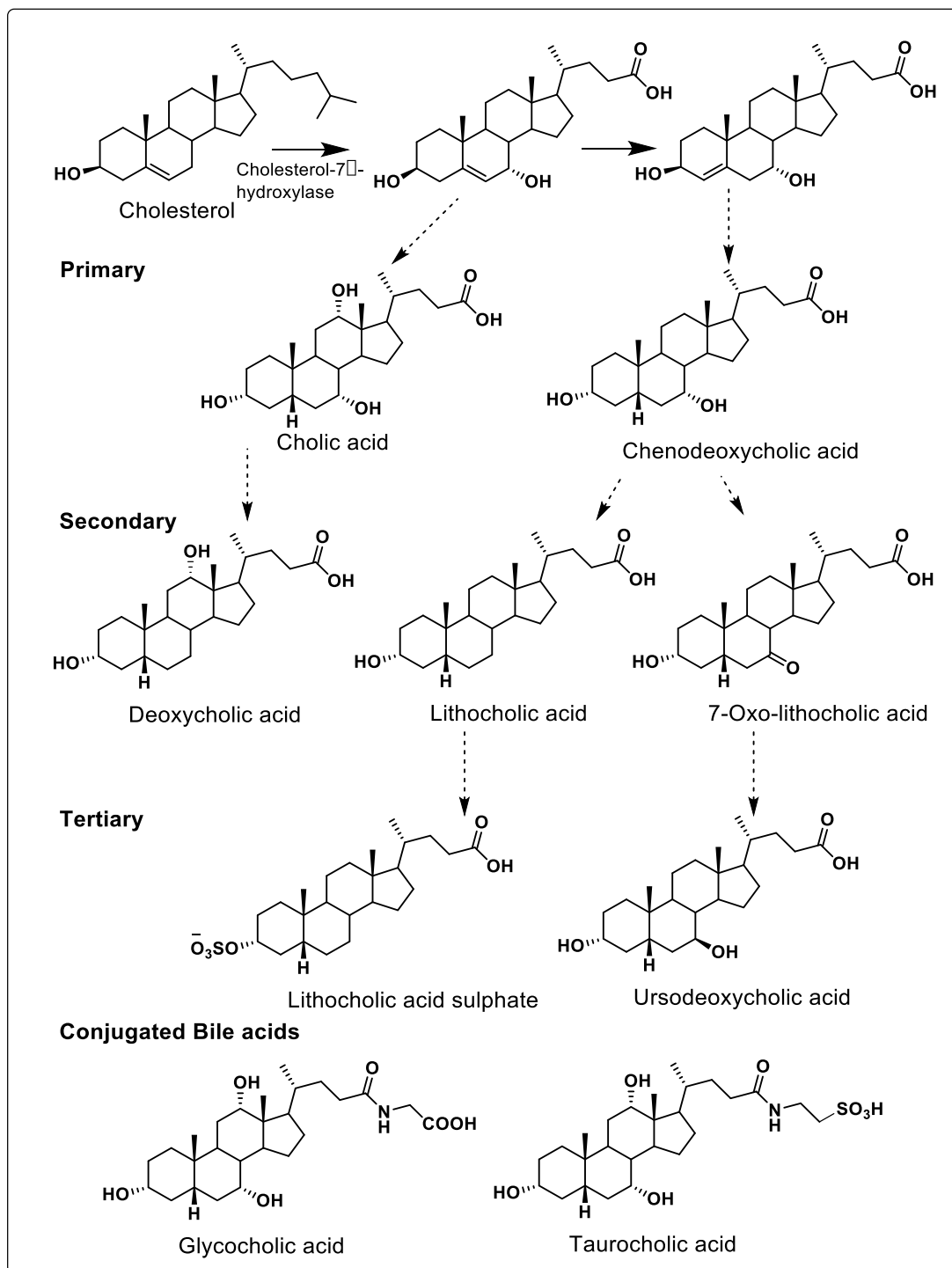


Figure 1. Bile acid metabolism-production of primary, secondary and tertiary bile acids occurs in the liver and by intestinal bacteria. Structures of conjugated bile acids: glycocholic acid and taurocholic acid.

Recently, there has been an increasing interest in using bile acids as enhancing the absorption for drug delivery. Bile acids have a unique ability to promote drug penetration

through biological membranes. Bile acids also have a unique ability to improve the epithelial carrier of hydrophilic drugs through the paracellular route and that of hydrophobic compounds through both paracellular and transcellular routes. The role of bile acids in promoting drug permeation has been experimentally illustrated in various pharmaceutical formulations including oral, nasal, ocular, buccal, pulmonary and rectal delivery as well as through the blood–brain barrier. Recently, bile acids have drawn attention in the field of drug delivery due to their ability to act as a drug carrier system in the form of mixed micelles, bilosomes and chemical conjugates with drug molecules.²¹

2.3.2 Chemical Structures of Bile Acids

All bile acids consist of two connecting units, a rigid steroid nucleus and a short aliphatic side chain (Figure 2).^{19,20} The steroid nucleus of bile acids has the saturated tetracyclic hydrocarbon perhydrocyclopentanophenanthrene, containing three six-member rings (A, B and C) and a five-member ring D. In addition, there are angular methyl groups at positions C-18 and C-19. The bile acid nucleus in higher vertebrates is curved (beaked) because rings A and B are *cis* fused (Figure 2).

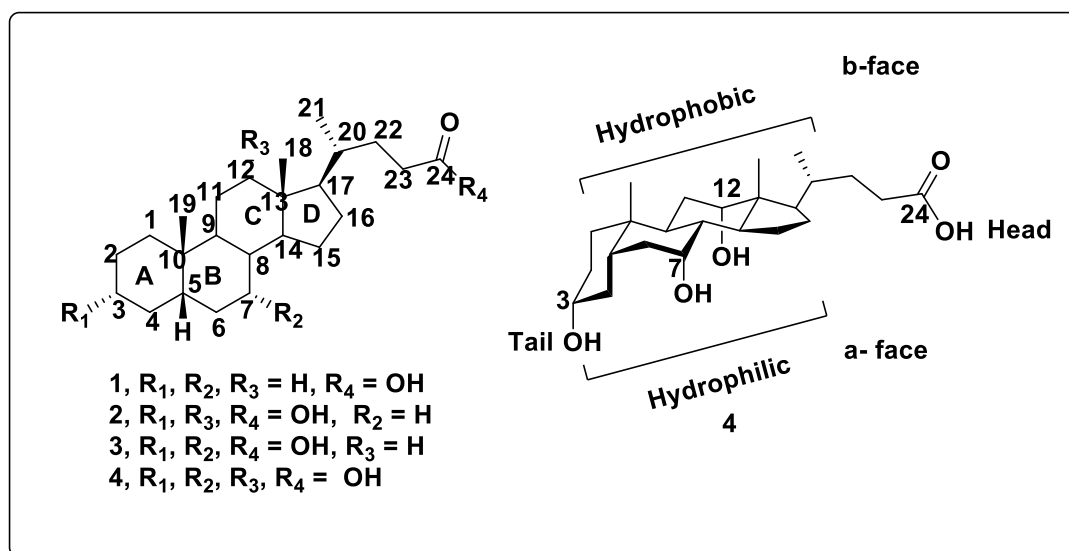


Figure 2. Chemical structures of different bile acids.

The human bile acid pool consists mainly (~90%) of cholic acid, **4** (3 α ,7 α ,12 α -trihydroxy-5 β -cholan-24-oic acid), chenodeoxycholic acid, **3** (3 α ,7 α -dihydroxy-5 β -cholan-24-oic acid), and deoxycholic acid, **2** (3 α ,12 α -dihydroxy-5 β -cholan-24-oic acid). The bile acid nucleus possesses angular methyl groups at positions C-10 and C-13 on the convex

hydrophobic β -face and the hydroxyl groups on the concave hydrophilic α -face which makes these compounds facially amphipathic.²²⁻²⁹

2.3.3 Influence of bile acids on drug bioavailability

The development of technologies that enable poorly membrane permeable drugs to efficiently penetrate biological membranes is one of the prominent challenges in the pharmaceutical industry.³⁰ The oral bioavailability of the inadequately water-soluble, lipid-lowering drug fenofibrate, was increased significantly by five times using liposomes containing a bile salt, NaDC, compared to the fast release formulation of micronized fenofibrate.³¹ Guan *et al.*³² improved the oral bioavailability of cyclosporine A by developing liposomes containing a bile salt, NaDC, as oral drug delivery systems. The low oral bioavailability of this drug is due to its high molecular weight and poor water solubility. The importance of bile acids for molecular drug delivery is described by their unique combination of rigidity and chirality, high availability, biocompatibility, and the various possibilities of functionalization.³³ To use bile acids as carriers for drugs, the corresponding drug can be coupled either to a hydroxyl group at positions 3, 7 or 12 of the bile acid molecule or to the carboxyl group at position 24, and in most initial studies drugs have been attached to the bile acid side chain, C-24, due to the relatively simple synthesis process.³⁴ Some studies demonstrated that oral bioavailability of the valine ester prodrug of acyclovir in mice was increased remarkably (two fold) by coupling to chenodeoxycholic acid at position C-24, compared to the parent drug itself.³⁵ Some researchers have investigated the attachment of a bile acid moiety to the cis-platinum molecule, in order to achieve liver selectivity for the treatment of liver tumors and to reduce undesired toxic effects.³⁶ The experiments with drug–bile acid conjugates having attached the drug moiety to the C-24 carboxylic acid function showed that a certain liver selectivity could be achieved, but their intestinal absorption, however, was low.³⁴

2.3.4 Bile acids based conjugates and their pharmacological applications

A variety of low molecular weight antibiotics have been isolated from diverse animal species in last few decades. These molecules include peptides, lipids, alkaloids, etc and exhibit antibiotic activity against environmental microbes and are thought to play a role in innate immunity. Michael Zasloff reported the discovery of a broad-spectrum steroidal antibiotic isolated from tissues of the dogfish shark *Squalus acanthias*.³⁷ This water-soluble

antibiotic, which they named squalamine (Fig.3), exhibits potent bactericidal activity against both Gram-negative and Gram-positive bacteria.

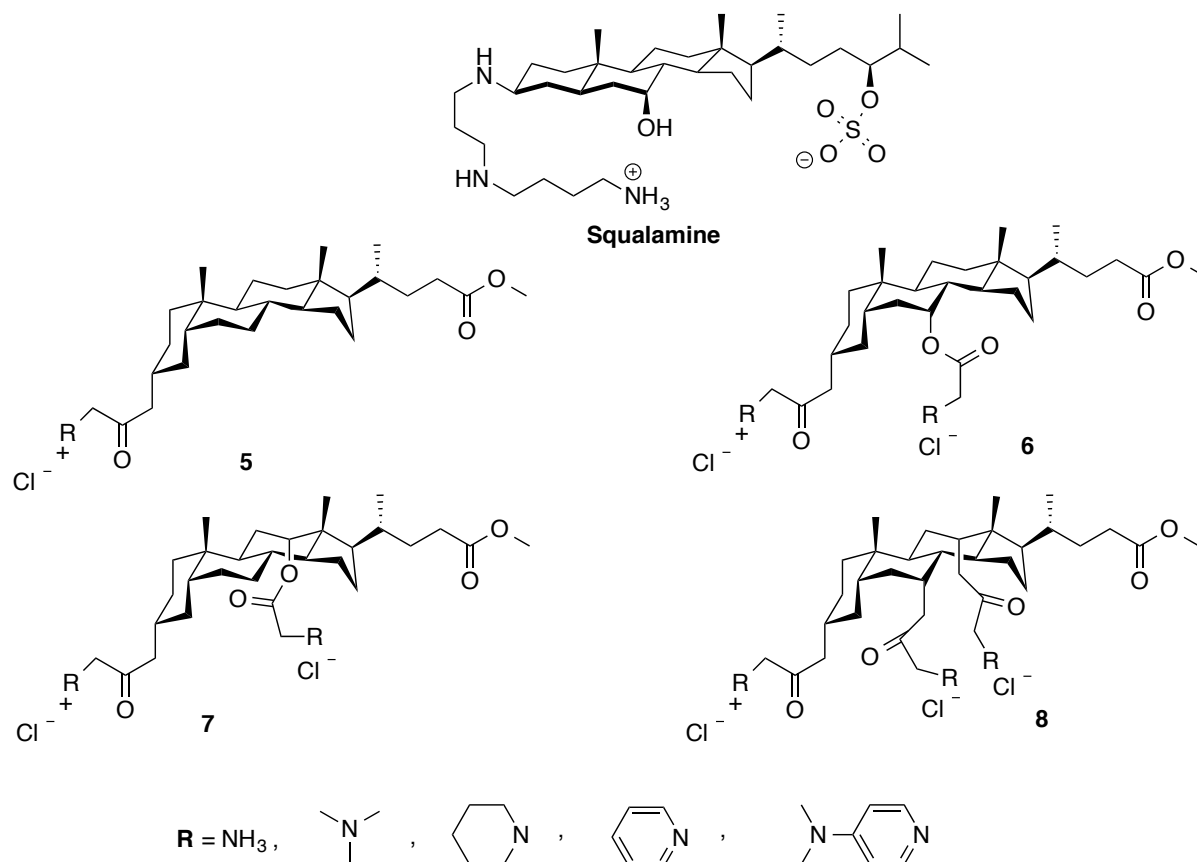


Fig.3 Squalamine and Molecular structures of lithocholic acid **5** (LCA)-, chenodeoxycholic acid **6** (CDCA)-, deoxycholic acid **7** (DCA)-, and cholic acid **8** (CA)-based amphiphiles; with different charged head groups

Squalamine is a cationic steroid characterized by a condensation of an anionic bile salt intermediate with spermidine. The discovery of squalamine in the shark implicates a steroid as a potential host-defense agent in vertebrates and provides insights into the chemical design of a family of broad-spectrum antibiotics. Avinash Bajaj *et al.*³⁸ found that fine-tuning charged head groups on a bile acid scaffold modulates their specificity against bacteria. Soft-charged primary amine amphiphiles interact with Gram-positive and Gram-negative bacterial membranes, whereas hard-charged head groups provide efficient and selective interactions with hydrophobic mycobacterial membranes (Fig.3).

Antinarelli *et al.*³⁹ synthesized aminoquinoline/steroid conjugates regioselectively via 1, 3-dipolar cycloaddition of alkynes of aminoquinolines. This addition of a steroid group to aminoquinoline molecules was found to enhance the leishmanicidal and antitubercular

activities **9-11** (fig. 4).³⁹

In one of the previous reports from our group⁴⁰ tetrapeptides derived from glycine and β -alanine were pinned at the C-3 β position of the developed cholic acid to obtain novel tetrapeptide-linked cholic acid based derivatives **12** and **13** (fig. 4). These generic structures have been designed utilizing amphiphilic nature of cholic acid. It was observed that incorporation of linear tetrapeptide fragment on the cholic acid skeleton not only reduced its toxicity to the tested cell lines but also demonstrated excellent synergism effect with the known antibiotics. The synergism of the most active compounds **12** (1 and 4 $\mu\text{g/mL}$) and **13** (6 and 8 $\mu\text{g/mL}$) significantly improves the activity of fluconazole and erythromycin against *C. albicans* and *E. coli*, respectively.

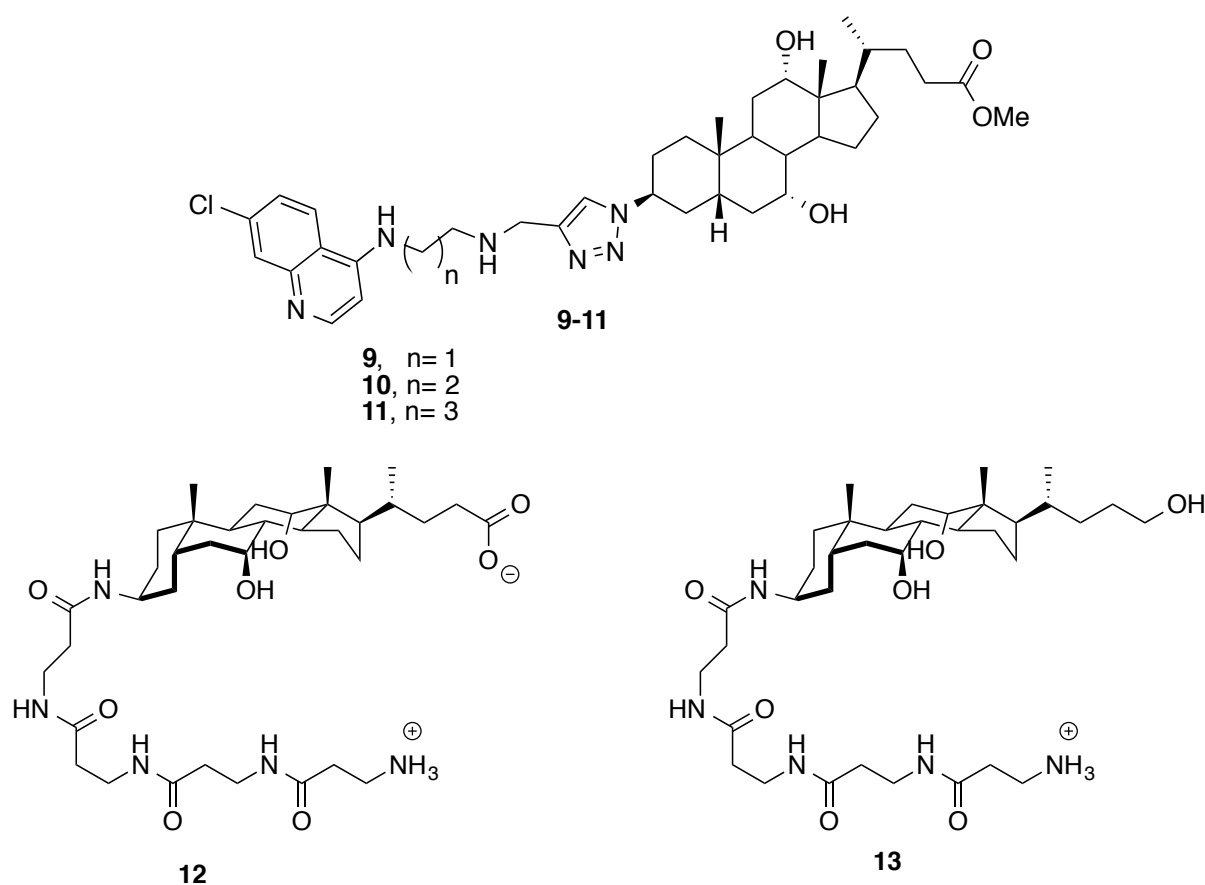


Fig 4. Aminoquinoline/steroids conjugates **9-11** and tetrapeptides linked cholic acid derivatives **12** and **13**.

Again from our group, new steroidal dimers exhibiting antifungal and antiproliferative activity *in-vitro* were synthesized.⁴¹ *N1, N3*-diethylenetriaminebis[cholic acid amide] was found to be active against *C. albicans*, *Y. lipolytica*, and *B. poitrassi* at nanomolar concentration and did not show any effect on cell proliferation (**14, 15** Fig 5). *N1, N2*-

ethylenediaminebis[deoxycholic acid amide] totally inhibited the growth of human oral cancer (HEp-2) and human breast cancer (MCF-7) cells (**16**, **17** Fig.5). Based on novel C-11 amino functionalized steroidal inhibitor structures namely, 11-amino-12-(oxo/ hydroxy) steroids **18** and **19** by Marples and co-workers.⁴² Our group has synthesized A/B ring cis steroidal enamine **20a**, N-benzyloxycarbonyl (N-Cbz) **20b**, N-pivaloyl **20c**, and N-ethoxycarbonyl **20d** derivatives (Fig. 5).⁴³ These compounds were expected to be HIV-1 protease inhibitors based on their modest activity against HIV in cell culture. This was the first report of syncytia induction and enhancement of viral replication in HIV-1 infected T cells by cholic acid derivatives.

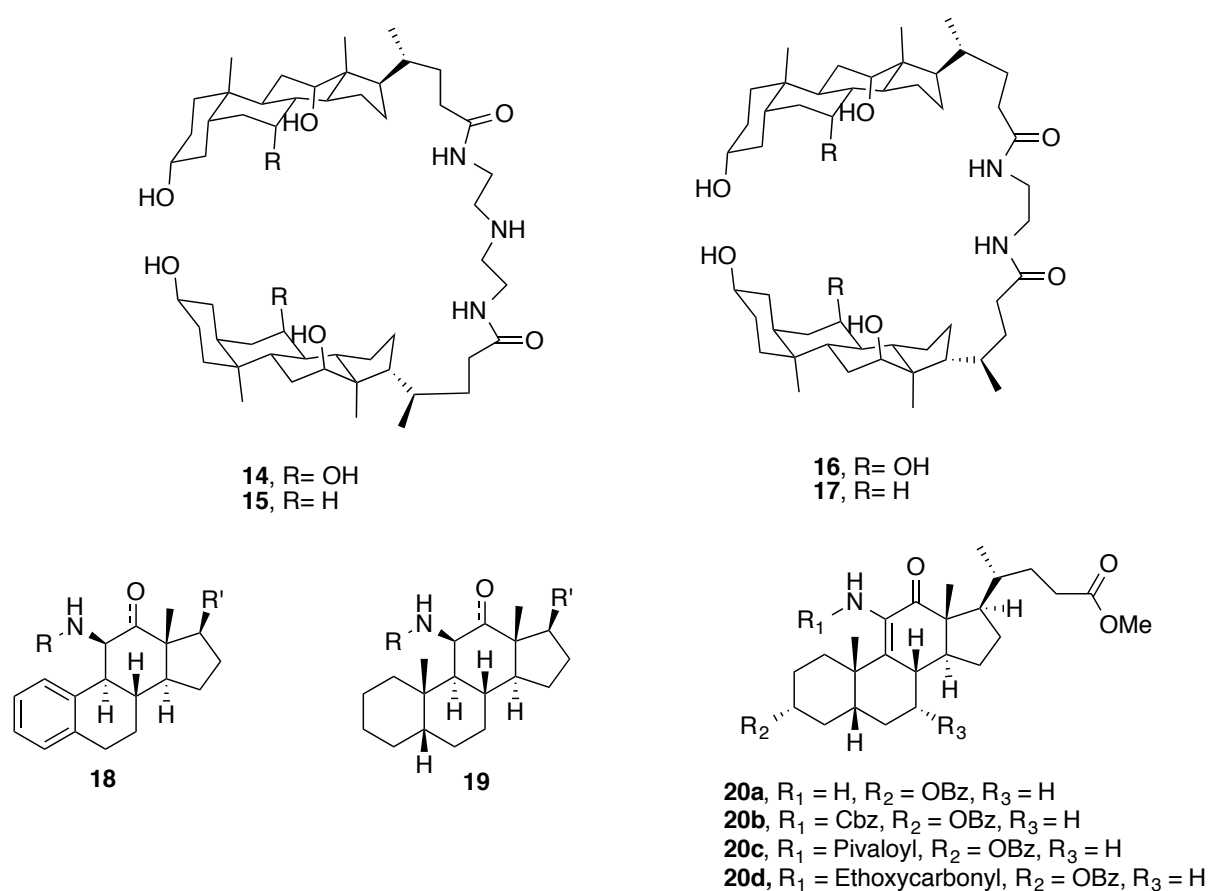


Fig. 5 Structure of various bile acid derivatives **14-20(a-d)**

Recently, there is a report in which A. Alsayari *et al.*⁴⁴ synthesized series of estrone based analogs at positions C-9, C-11, C-16, and C-17 positions and investigated to be estrogenic/ anti-estrogenic activity. Compounds **22** and **23** revealed their potential to show inhibitory estrogenic profile (Fig.6). They also showed potent inhibition of cell growth stimulated by estradiol, suggesting that they may have potential for treatment of breast cancer.

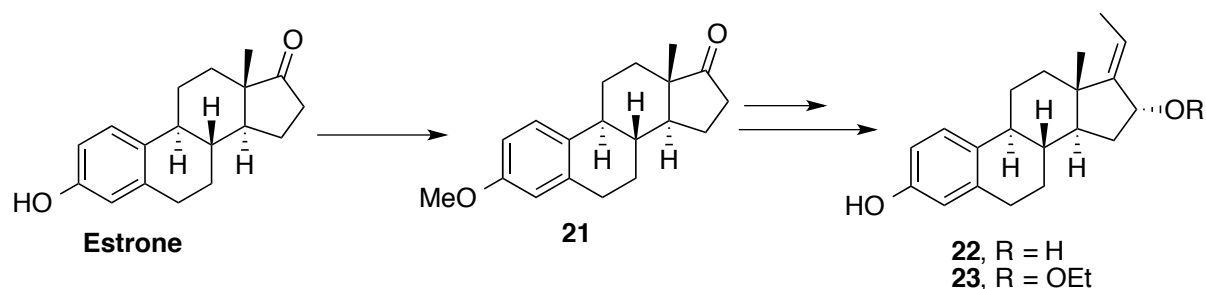


Fig. 6 Estrone based derivatives 21-23

2.3.5 Antituberculosis molecules containing 1, 2, 3-triazole moiety

Tuberculosis (TB) is one of the leading causes of mortality. The current WHO-approved treatment for TB, known as directly observed therapy short-course (DOTS), involves three- or four-drug regimen comprising isoniazid, rifampin, pyrazinamide, and/or ethambutol for a minimum of 6 months. While these first-line agents remain useful in treating susceptible *Mycobacterium tuberculosis* strains, the emergence of multidrug resistant tuberculosis demands the development of new drugs.

Somu *et al.* reported⁴⁵ the synthesis of rationally designed nucleoside (Fig. 7, 24). Compound **24** was found to be the inhibitor of *Mycobacterium tuberculosis* which disturbs siderophore biosynthesis.

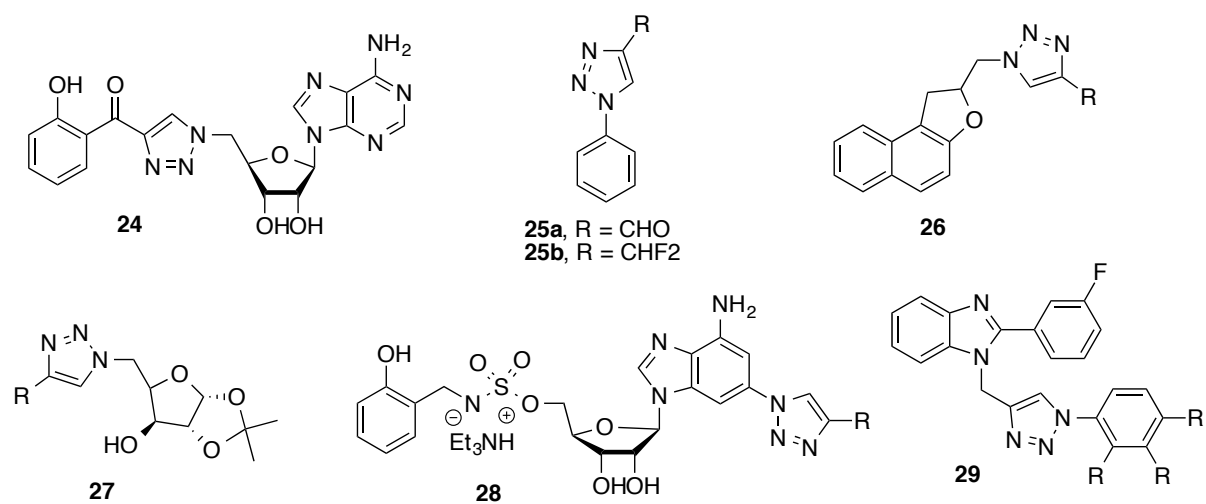


Fig. 7. Structure 24-29

Two series of 1, 2, 3-triazoles compounds with antimycobacterial profile were reported by Costa *et al.*⁴⁶ The in vitro anti-tuberculosis screening of these series showed that the triazole-4-carbaldehyde derivatives (Fig. 7, **25a**) were more active than the 4-difluoro-

methyl derivatives (Fig. 7, **25b**). SAR study indicated the importance of hydrogen bond acceptor subunit, its place in the aromatic ring, the planarity of triazole and phenyl rings in these compounds for the anti-tubercular activity.

Tripathi *et al.*⁴⁷ have carried out the synthesis of 1-(2,3-dihydro benzofuran-2-yl)-methyl [1, 2, 3]-triazoles (Fig. 7, **26**) and studied their antitubercular activity against *Mycobacterium tuberculosis* H37Rv.⁴⁷ Most of the compounds exhibited antitubercular activities with MIC ranging from 12.5 to 3.12 g/mL.

Dabak and his co-workers⁴⁸ studied the antitubercular activity of 4-acyl-1H-1, 2, 3-triazole derivatives, which were synthesized by condensation of α -diazo- β -oxoaldehyde compounds with different amines. 5-Azido-5-deoxy-xylo-, ribo-, and arabinofuranoses (Fig. 7, **27**) were found⁴⁹ to show antitubercular activity against *Mycobacterium tuberculosis* H37Rv. The best compound disclosed antitubercular activity with MIC 12.5 g/mL.

A series of 1, 2, 3-triazole derivatives of 5'-O-[N-(salicyl)sulfamoyl]adenosine (Fig. 7, **28**) (Sal-AMS) was synthesized by M. L. Konte *et al.*⁵⁰ as inhibitors of aryl acid adenylating enzymes (AAAE) involved in siderophore biosynthesis by *Mycobacterium tuberculosis*. Structure activity relationships revealed remarkable ability to tolerate a broad range of substituents at the 4-position of the triazole moiety, and the most of the compounds showed subnanomolar activity.

From promising results of the preliminary study, novel H37Rv strain inhibitors with fluorine and 1, 2, 3-triazole containing benzimidazoles (Fig. 7, **29**) for the treatment of tuberculosis were disclosed by Gill *et al.*⁵¹

A modular approach has been established by Dondoni *et al.*⁵² for the preparation of a set of C-oligomannosides (Fig. 8, **30**) featuring 1, 2, 3-triazole ring as the inter-glycosidic linker as *Mycobacterium tuberculosis* cell wall synthase inhibitors. The biological

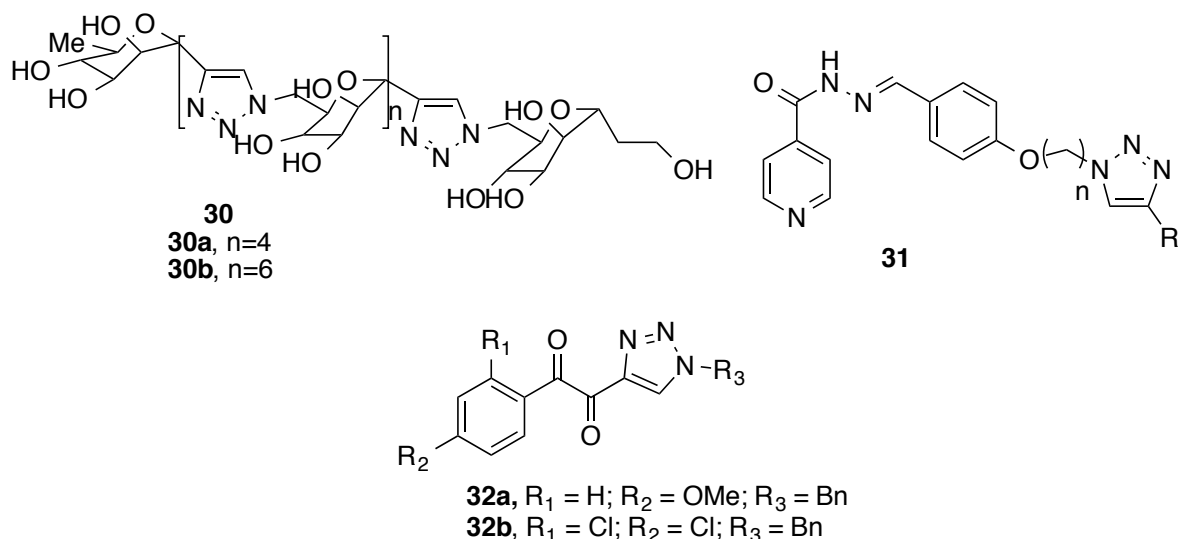


Fig. 8. Structures 30-32

experiments indicated that triazole bound oligomannosides (TOM) (Fig. 8, **30**) endowed with the optimal chain lengths (**30A** and **30B**) for the interaction with PPM-dependent R-(1,6)-mannosyltransferases showed the highest activity ($IC_{50} = 0.14-0.22\text{mM}$). It was proposed that triazole ring spacers provide mainly to the overall length of these oligomannosides.

D. Kumar *et al.* Reported⁵³ the synthesis and antimycobacterial activity of 1, 2, 3-triazole derivatives **31** of isoniazid (Fig. 8). Most of the synthesized compounds exhibited potent activity against *Mycobacterium tuberculosis* H37Rv strain with MIC99 values ranging from 0.195 to 1.56 μM *in vitro*. All the synthesized compounds showed good antimycobacterial activity as compared to reference compound isoniazid. The cytotoxicity of all the compounds was studied against THP-1 cell line, and no toxicity was observed even at 50 μM concentration.

Two series of α -ketotriazole and α , β -diketotriazole derivatives were synthesized⁵⁴ by C. Menendez *et al.*⁵⁴ and evaluated for antitubercular and cytotoxic activities. Among them, two α , β -diketotriazole compounds (**32**, Fig. 8) showed good activities with (minimum inhibitory concentration = 7.6 μM and 6.9 μM , respectively) on *MTb* and multi-drug resistant *MTb* strains and exhibited no cytotoxicity ($IC_{50} > 50 \mu\text{M}$) on colorectal cancer HCT116 and normal fibroblast GM637H cell lines. These two compounds represent promising leads for further optimization.

2.4 Present work

2.4.1 Objective

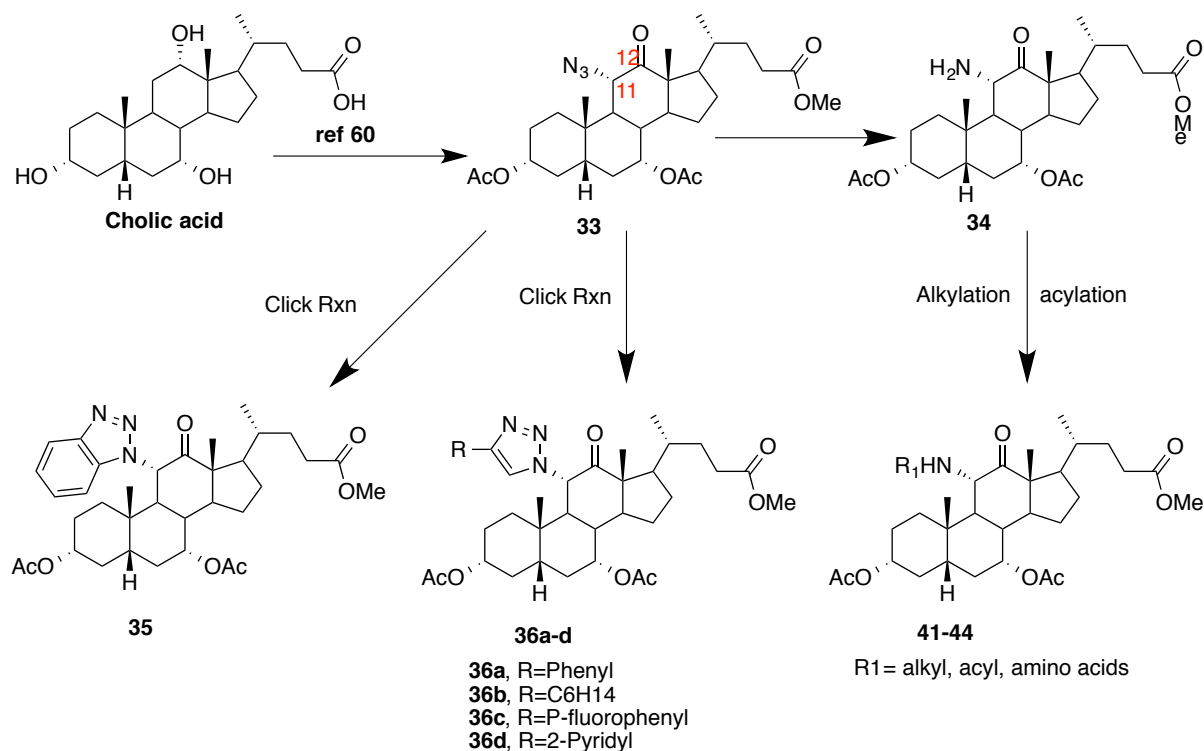
As can be seen from the above discussion, there are several reports on synthesis of steroid/bile acid based conjugates which exhibited various biological activities. As discussed earlier in this chapter, C-11 derivatized steroids are well known for biological activity and are found in many naturally occurring steroidal drugs. It is reported that 1, 2, 3-triazole moieties are effective linking units and modified synthetic molecules bearing them show diverse biological activities.⁵⁵⁻⁵⁸ By keeping these aspects in mind and to overcome the current challenges regarding resistance *MTb*, we planned to design and synthesize a few novel C-11 functionalized molecules having both the necessary moieties (Bile acid and 1, 2, 3-triazole) which may show antitubercular activity. This chapter deals with the synthesis of cholic acid-based novel C-11 α -triazoyl derivatives having 1, 4-disubstituted 1, 2, 3-triazoles and also having some molecules with alkylation and acylation at C-11 amino position of cholic acid and their bioevaluation as antitubercular agents.

2.4.2 Results and discussion

2.4.2.1 Synthesis of Target Compounds **35** and **36a-d**.

In addition to our work on microwave assisted 1, 2, 3- triazole containing biologically active bile acid derivatives,⁵⁹ now we report here the synthesis of new bile acid derivatives substituted at C-11 α -position with 1, 2, 3-triazoyl moiety as potential antituberculosis agents. Besides, we have also synthesized N- alkyl and N-acyl derivatives at 11 α -position of cholic acid to study structure activity relationships.

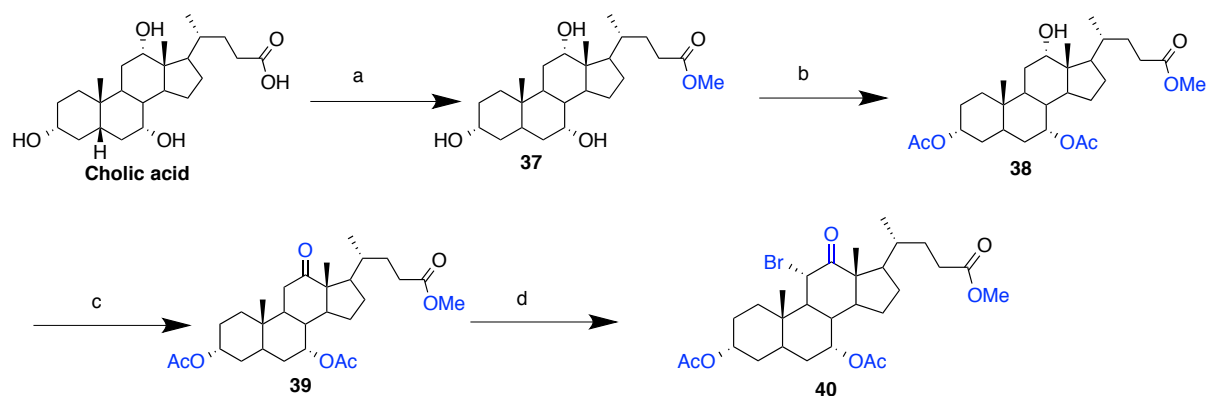
A general route for the synthesis of all the 11 α -triazoyl cholic acid derivatives **35**, **36(a-d)** and various alkylated and acylated on the amino group at the C-11 position of cholic acid is depicted in Scheme 1. The key intermediate 11 α -azido-12-oxo methyl cholate **33** was synthesized from cholic acid by our reported procedure⁶⁰ with some modifications. 11 α -azido group in compound **33** on microwave assisted copper catalyzed 1,3-dipolar cycloaddition reaction (Click reaction) with four different alkynyl compounds gave 1,4-disubstituted-1, 2, 3- triazole ring containing new compounds in good yields (Compounds **36a-d**). Reaction of azide **33** with 2-(trimethylsilyl) phenyltrifluoromethanesulfonate and cesium fluoride in acetonitrile at room temperature afforded benzotriazole **35**.



Scheme 1. Synthesis of Target Compounds **35**, **36a-d** and **41-44**

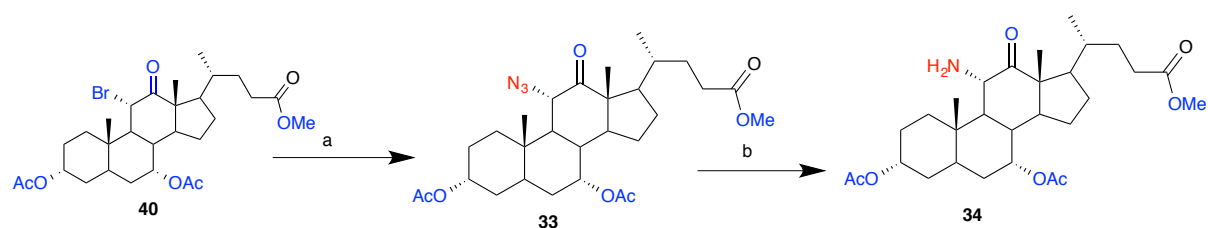
To carry out synthesis of N-alkyl and N-acyl derivatives at C- 11 position, azido functionality in compound **33** was reduced with Pd/C or using Staudinger reaction with triphenyl phosphine and water or with catalytic hydrogenation to get the known amino compound **34** which was further alkylated or acylated with different reagents (Scheme 1).

Cholic acid on methyl esterification by using PTSA in methanol gives **37** with 95% yield, which on further treated with acetic anhydride in dichloromethane using dimethylamino pyridine (DMAP) as a catalyst and triethyl amine as base gives acetate protected **38** ester of cholic acid at C-3 & C-7 positions selectively keeping C-12 hydroxy group unprotected (Scheme 2). Compound **38** on Jones oxidation using chromium trioxide, sulphuric acid in acetone at 0 to 10 °C afforded C-12 keto compound **39** with 77% yield (Scheme 2). Bromination at C-11 position was done by using bromine in benzene at room temperature for six days afforded **40** with 81% yield. It must be noted that by allowing bromination using bromine in benzene for 1-2 days, the C-11 α - and β -brominated product will obtained as a mixture. Besides, by allowed it to kept for 6-7 days, α -bromo C-11 derivative of cholic acid was obtained as major product. Although, we have not succeeded to separate or get exclusive β -bromo C-11 derivative of cholic acid.



Scheme 2. a) PTSA, MeOH, 24 h, rt, 95%; b) Ac₂O, DMAP, TEA, Dry DCM, rt, 4-5 h, 86%; c) Jones Oxidation, CrO₃, H₂SO₄, Acetone, 0 - 10 °C, 10 mins, 77%; d) Br₂, Benzene, rt, 6 days, 81%

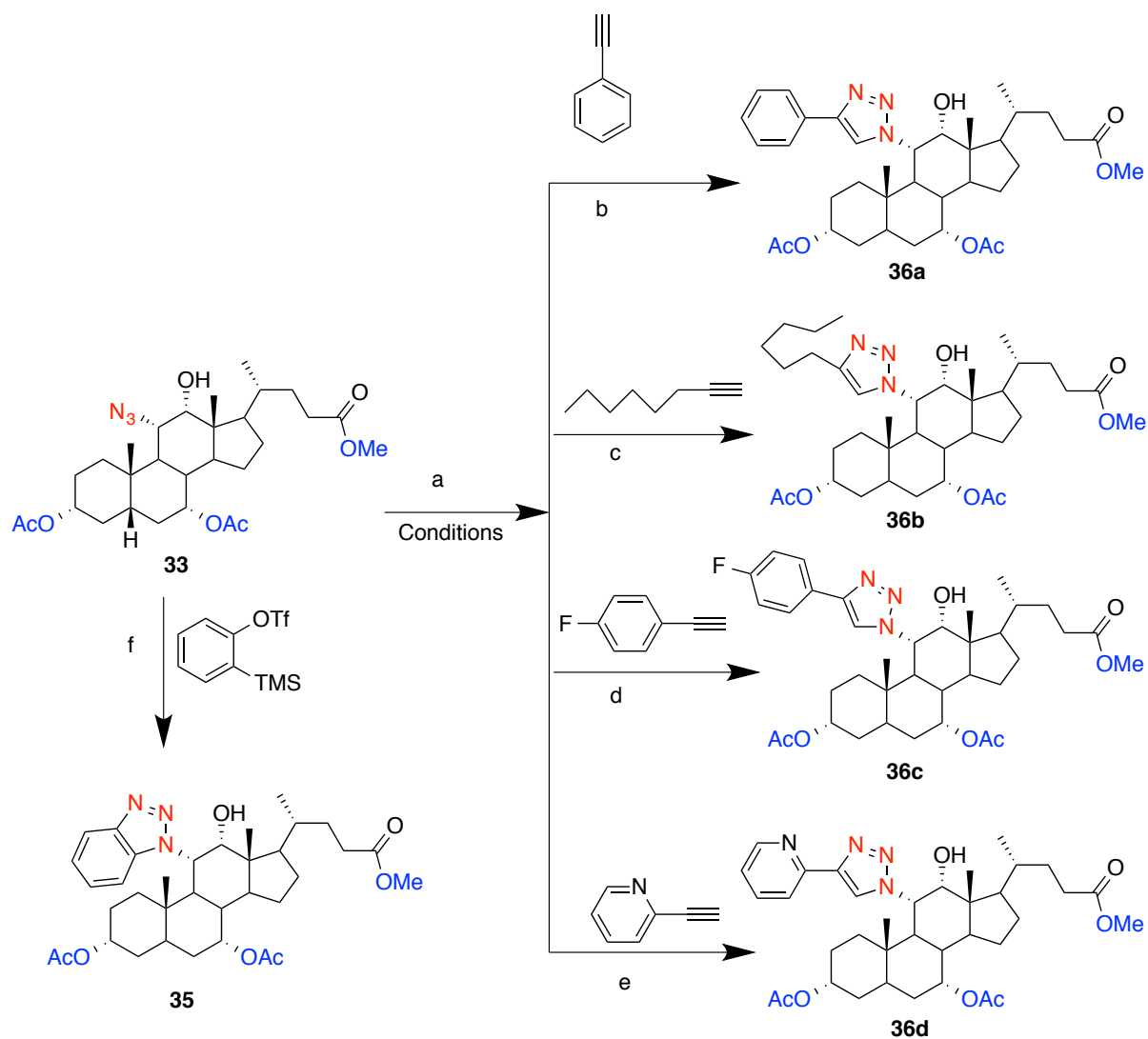
Further, C-11 α -bromo derivative of cholic acid on treatment with sodium azide in DMF at 60 °C afforded C-11 α -azido compound **33** in 55% yield, which was further reduced to C-11 amino using triphenyl phosphine in THF and water (Staudinger reaction) to give amino compound **34** with 79% yield or can be obtained by reduction using H₂/Pd in MeOH (Scheme 3).



Scheme 3. a) NaN₃, DMF, 60 °C, 16 h, 55%; b) i) PPh₃, THF; ii) H₂O, rt, 24 h, 79% or H₂/Pd-C, Methanol, 8-10 h.

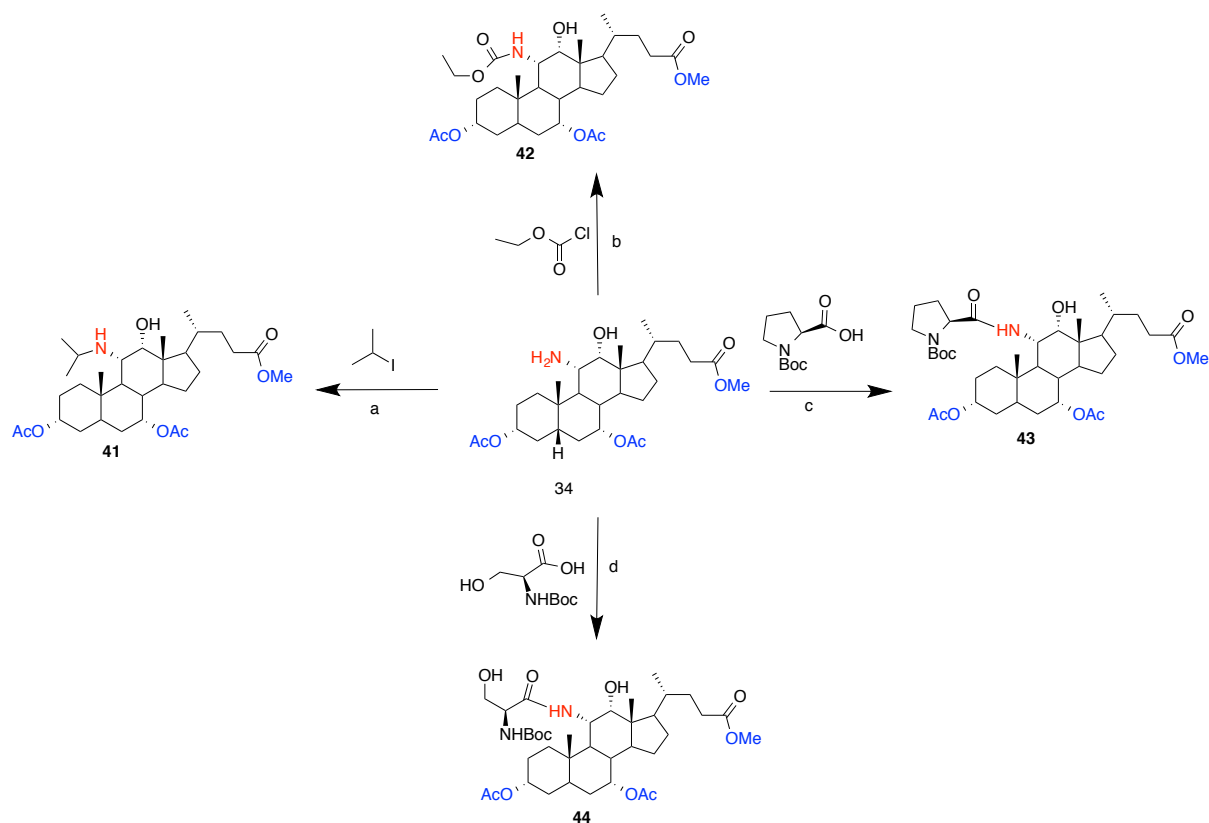
1, 2, 3- triazole derivatives at C- 11 position were prepared by Cu(I) catalyzed 1,3-dipolar cycloaddition reaction (Click reaction) with various terminal alkynes *i.e.* phenyl acetylene, 1-octyne, *p*-fluorophenyl acetylene, 2-pyridyl acetylene afforded products **36a-d** respectively with excellent yields. In addition to that category, one more compound with 1, 2, 3-triazole was prepared by click of intermediate **33** with precursor of benzyne *i.e.* 2-(trimethylsilyl)phenyltrifluoromethanesulfonate using cesium fluoride in acetonitrile afforded

35 containing substituted benzotriazole at C-11 with 82% yield (Scheme 4).



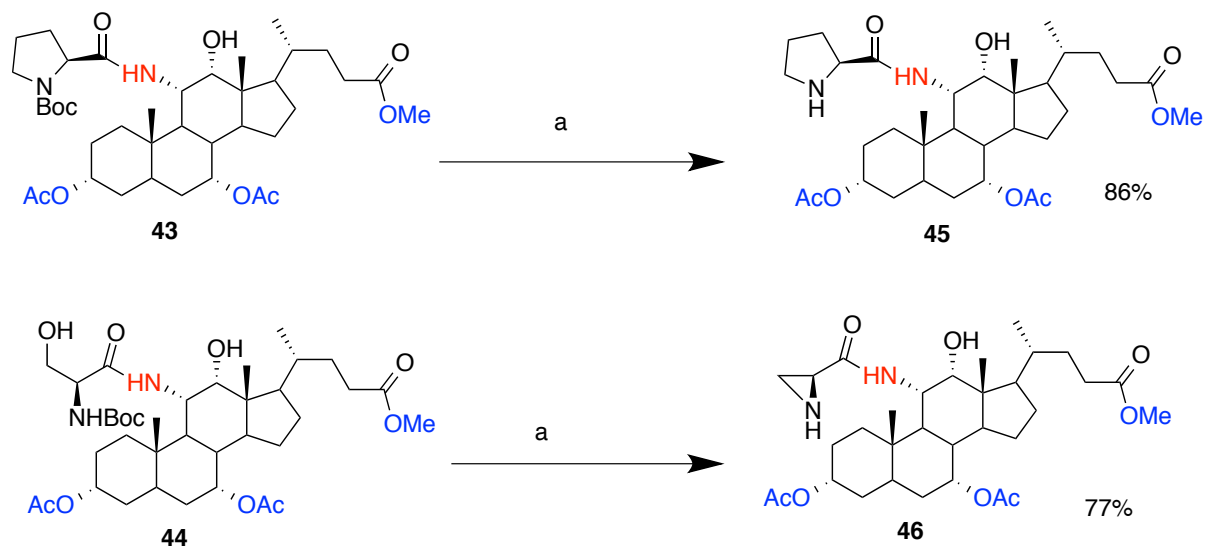
Scheme 4. a) $\text{CuSO}_4 \cdot 5\text{H}_2\text{O}$, Sodium ascorbate, DMF: H_2O (4:1), Microwave 50-100W (4-8mins); b) phenyl acetylene, 5 min, 71%; c) 1-octyne, 8 min, 31%; d) *p*-fluoroacetylene, 4 min, 81%; e) 2-pyridyl, 5 min, 87%; f) 2-(trimethylsilyl)phenyltrifluoromethanesulfonate, CsF, ACN, rt, 18 h, 82%

C-11 Amino compound **34** was treated with isopropyl iodide in the presence of potassium carbonate to afford N-isopropyl compound **41** at C-11 position (Scheme 5). Compound **42** was obtained from C-11 amino compound by treating it with ethyl chloroformate in the presence of N-methyl morpholine in dry DCM at -20°C yielding 70%. Compound **34** on reaction with N-Boc protected amino acids Proline and Serine under peptide coupling conditions, resulted into compounds **43** and **44**, respectively (Scheme 5).



Scheme 5. a) Isopropyl iodide, K₂CO₃, Dry DMF, 60-70 °C, 24 h, 81%; b) Ethyl chloroacetate, NMM, Dry DCM, -20 °C to rt, 3 h, 70%; c) *N*-*boc* proline, EDC, HOBT, DMAP, Dry DMF, rt, 3 h, 77%; d) *N*-*boc* serine, EDC, HOBT, DMAP, Dry DMF, rt, 3 h, 85%

Deprotection of Boc in proline derivative **43** using TFA in DCM at 0 °C resulted into compound **45** while that of serine derivative **44** resulted into cyclization of formed amino alcohol to give aziridine containing compound **46** (Scheme 6). All the synthesized compounds were fully characterized by spectroscopic analysis and were studied for their anti-tuberculosis and antibacterial activity. Their toxicity was also studied against three human cancer cell lines.



Scheme 6. a) TFA, DCM, 0 °C, 1-2 h, 86%(45), 77%(46)

2.4.2.2 Antibacterial activity

Anti-bacterial activity of all the compounds was tested against *Escherichia coli*, *Pseudomonas fluorescens*, *Staphylococcus aureus*, and *Bacillus subtilis* (Table 1). However all the compounds were found to show very poor or no activity against all the tested bacteria.

Table 1: Antibacterial screening results of synthesized compounds and their % Inhibition at 30 µg/mL against different bacterial strains.

Compound ID	<i>E.coli</i>	<i>Pseudomonas fluorescens</i>	<i>Staphylococcus aureus</i>	<i>Bacillus subtilis</i>
36a	17.84	NA	NA	20.01
36b	NA	NA	NA	22.93
36c	43.82	23.16	NA	20.04
36d	32.10	47.14	NA	NA
35	33.80	46.81	NA	8.94
41	31.93	37.17	16.36	4.79
42	46.74	54.48	17.26	NA
43	26.83	61.50	NA	NA
44	43.22	29.89	11.94	NA
45	23.93	20.09	NA	NA

2.4.2.3 Anti-tubercular activity: primary screening

The biological activity for each compound 1 to 10 was determined by measuring inhibition of growth against the avirulent strain of *M. tuberculosis* (MTB H37Ra; ATCC 25177) in liquid medium (Table 2 and Table 3). In a preliminary screening, the antimycobacterial activity of these compounds was assessed at concentrations of 30, 10, 3 $\mu\text{g/mL}$ using XRMA antitubercular screening protocol.^{61,62} The antimycobacterial activity results are summarized in Table 2.

The compounds which showed more than 90 % inhibition (Table 2) at 30 $\mu\text{g/mL}$ were confirmed by carrying out dose-dependent effect using a range from 30 to 0.23 (Compounds **35**, **43**, **44**) and 10 to 0.078 (compound **36b**) $\mu\text{g/mL}$ to determine IC₅₀ and IC₉₀ with serial dilution in DMSO of compounds (Table 3).

Table 2. Anti-tubercular activity of compounds against dormant *Mycobacterium tuberculosis* H37Ra.

Compound ID	% Inhibition of <i>Mycobacterium tuberculosis</i> H37Ra growth in presence of compounds		
	30 $\mu\text{g/mL}$	10 $\mu\text{g/mL}$	3 $\mu\text{g/mL}$
33	12	NA	NA
36a	74	68	67
36b	97	96	91
36c	79	75	71
36d	71	48	38
35	96	94	76
34	<1	<1	NA
41	84	71	66
42	86	73	66
43	94	80	66
44	91	73	68
45	71	66	55
39	34	28	13
Cholic acid	53	36	NA

Compounds **36b**, **35**, **43** and **44** were found to be particularly active against *Mycobacterium tuberculosis* H37Ra strain. The % Inhibition in the presence of test material is calculated by following formula. % inhibition = (Average of Control-Average of Compound)/ (Average of Control-Average of Blank) X 100) Where Control is culture medium with cells and DMSO and blank is culture medium without cells.

Compounds were considered inactive if % I < 90 at 30 $\mu\text{g/mL}$.

For all samples, each compound concentration was tested in triplicates in a single experiment.

NA: Not active

Table 3. Antitubercular activity of active compounds 36b, 35, 43 and 44 against *M. Tuberculosis* H37Ra under *in-vitro*, *ex-vivo* conditions^a

IC ₅₀ and IC ₉₀ values (µg/mL) of compounds against <i>M. Tuberculosis</i> H37Ra with SD values							
Compound ID		36b	35	43	44	Rifampicin	Isoniazid
<i>Invitro</i> (Dormant)	IC ₅₀	0.17±0.02	1.27±0.06	2.25±0.51	6.16±0.56	0.0014±0.0005	0.0023±0.0004
	IC ₉₀	2.43±0.06	7.15±0.56	27.01±0.08	26.31±0.08	0.043±0.015	0.075±0.002
<i>Invitro</i> (Active)	IC ₅₀	0.64±0.04	1.08±0.23	3.62±0.43	2.70±0.48	0.0018±0.0004	0.0019±0.0005
	IC ₉₀	2.63±0.35	9.79±0.12	27.49±0.66	28.85±0.22	0.048±0.002	0.074±0.007
<i>Ex Vivo</i> (Dormant)	IC ₅₀	0.13±0.02	1.65±0.27	1.32±0.09	3.44±0.94	0.0018±0.0004	0.0024±0.0001
	IC ₉₀	1.55±0.23	8.16±1.12	23.84±0.56	26.30±0.66	0.048±0.014	0.0078±0.043
<i>Ex Vivo</i> (Active)	IC ₅₀	0.25±0.04	1.11±0.35	1.96±0.21	3.98±0.49	0.0021±0.0002	0.0024±0.0001
	IC ₉₀	2.80±0.34	8.60±0.65	27.30±1.50	26.85±0.32	0.051±0.0042	0.075±0.007

^aIC₅₀ /IC₉₀ in µg/mL. Antitubercular activity of each agent were determined by serial dose dependent dilutions.

Compound 36b was found to be more active than compounds 35, 47, 48 at an IC₉₀, IC₅₀ value against both dormant and active phase of *Mycobacterium tuberculosis* H37Ra.

Standard antitubercular drugs and positive controls.

Intracellular antitubercular activities of each agent in differentiated THP-1 cells.

Data were expressed as the means of triplication.

SD (±): Standard Deviation.

All calculations were performed using Origin 8 statistical software. Compounds **36b**, **35**, **43**, and **44** tested in this study exhibited high antitubercular activities against both dormant and active stages of *Mycobacterium tuberculosis* H37Ra under both *in-vitro* and *ex-vivo* conditions. Minimum Inhibitory Concentration (MIC) values of the most active compound (**36b**) determined against the dormant state were 2.43 and 1.55 µg/mL respectively when measured under *in-vitro*^{61,61} and *ex-vivo*⁶³ conditions. Interestingly, compound **36b** was found to be almost equally effective against the actively growing *Mtb bacilli*. Other compounds also had significant antitubercular activity (both IC₉₀ and IC₅₀) against dormant and active phages (ranging between 1.1 to 28.8 µg/mL). The antitubercular activity shown by these molecules may be due to inhibition of decaprenylphosphoryl-β-D-ribose-2'-epimerase (*DprE1*) enzyme of MTB as 1, 2, 3-triazole derivatives are reported to inhibit this enzyme.⁶⁴ *DprE1* is involved in the biosynthesis of decaprenylphosphoryl-D-arabinose (DPA), as an essential component

of the mycobacterial cellwall⁶⁵ Overallse compounds exhibited weak to significant antitubercular activity.

2.4.3.4 Cytotoxicity

The lead compounds (**36b**, **35**, **43** and **44**) were assayed for their cytotoxicity against three different human cancer cell lines, THP-1 (Human acute monocytic leukemia cell line), Panc-1 (Human pancreas carcinoma cell line) and A549 (Human lung adenocarcinoma epithelial cell line) using MTT assay.^{66,67} The cells were exposed to test compounds for 48 h. Paclitaxel was used as positive control. The cytotoxic effect of these compounds was checked at the concentrations of 100, 50, 25, 12.5, 6.25, 3.125, 1.5625 and 0.7813 µg/mL to determine the GI₅₀ and GI₉₀. Compound **36b** did not show any cytotoxicity up to 100 µg/mL on all the three cell lines used Table 4.

Table 4. Cytotoxicity of most active compounds **36b**, **35**, **43** and **44** against 3 human cancer cell lines after 48 h of Exposure^a

Compound ID	Cytotoxic profile against human cancer cell lines					
	<i>THP-1</i>		<i>PANC-1</i>		<i>A549</i>	
	GI ₅₀	GI ₉₀	GI ₅₀	GI ₉₀	GI ₅₀	GI ₉₀
36b ^b	>100	>100	>100	>100	>100	>100
35	29.9	>100	50.02	>100	20.04	>100
43	45.95	>100	15	>100	52	>100
44	76.18	>100	>100	>100	>100	>100
^c Paclitaxel	0.1374	5.8140	0.1279	5.7150	0.0035	0.0706

^aIC₅₀ /IC₉₀ in µg/mL, after 48 h. Human cancer cell lines: *THP-1* from acute monocytic leukemia, *PANC-1* from pancreas carcinoma and *A549* from lung adenocarcinoma.

^bCell viability >80 % at the highest concentration of 100 µg/mL.

^c Standard anticancer drug and positive control.

The GI₅₀ values were indicated as mean calculated from three independent experiments.

2.4.3.6 Computational Studies

Molecular docking study

Molecular docking study was carried out to identify the potential target for these bile acid analogues and thereby try to understand the key molecular mechanisms in exerting inhibitory activity against *Mycobacterium tuberculosis*. In the absence of available resources to carry out the experimental studies, computational chemistry approaches like molecular docking have become quite essential to identify the targets for different ligands and the associated

thermodynamic interactions with the target enzyme governing the inhibition of the pathogen. Antitubercular activity portrayed by the 11 α -substituted bile acid derivatives motivated us to investigate if they are suitable ligands to the known targets crystallographically resolved for *Mycobacterium tuberculosis*. After scanning through the available crystal structures for mycobacterium targets, we could find a enough good agreement between the experimental antitubercular data and docking results against DprE1 enzyme. Decaprenylphosphoryl-D-ribose oxidase (DprE1) of *Mycobacterium tuberculosis* is an essential enzyme involved in the biosynthesis of decaprenylphosphoryl-D-arabinose (DPA).⁶⁸ According to the literature reports, DPA is the only known donor of D-arabinofuranosyl residues for the synthesis of arabinogalactan, a basic precursor for the mycobacterial cell wall core.⁶⁹ In this regards, DprE1 is also shown to be essential for cell growth and survival.⁷⁰ Recent literature report on 1, 2, 3-triazole conjugates as novel antitubercular agents acting through inhibition of DprE1 strengthened our efforts to investigate the probable binding mode of 11 α -substituted bile acid derivatives discussed herein into the active site of this enzyme.⁷¹

We have tried to investigate the thermodynamic interactions involved in the binding of 11 α -substituted bile acid derivatives to DprE1 enzyme via computational docking methods for gaining insights into the experimentally observed antitubercular activity pattern. The most appropriate approach for evaluating the accuracy of a docking protocol is to determine how closely the lowest energy binding pose predicted by the scoring function resembles the binding mode determined by X-ray crystallography. In the present study, the docking protocol was validated by extracting the native ligand from the crystal structure and docking it back into binding site of the DprE1. The root mean square deviation (RMSD) between the original conformation of native ligand and the conformation obtained from its re-docking into crystal structure was found to be less than 1Å, validating the reliability of and reproducibility of the docking procedure in reproducing the experimentally observed binding mode for molecules investigated herein. Figure 9 shows the overlay of the crystallographically observed binding mode of the native ligand over its best docked conformation.

From the ensuing docked structures, it is clear that with all the 11 α -substituted bile acid derivatives showed similar orientation in the DprE1 active site and the complexes formed were stabilized by formation of several steric and electrostatic interactions. The results of the docking calculations have been analyzed based on four main parameters- Glidescore, Glide energy, H-bonds and non-bonded interactions (Van der Waals and Coulombic). Considering

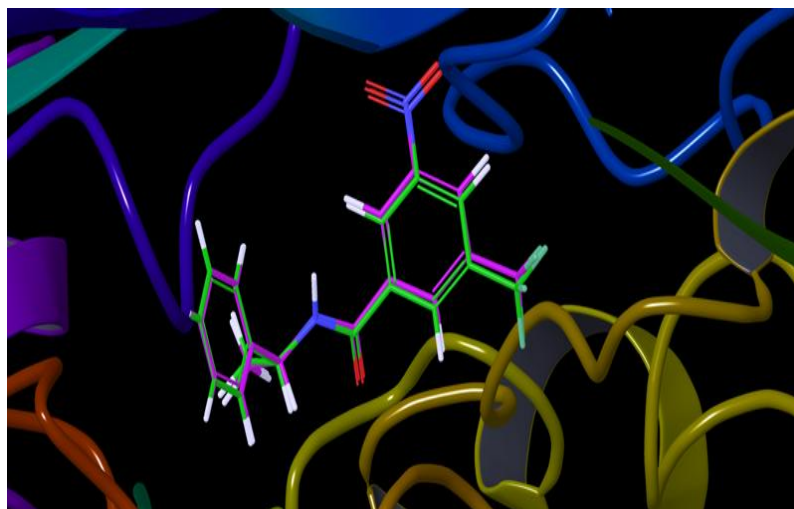


Figure 9: Superimposition of the X-ray binding mode of the native ligand (green carbon) over its best docked conformation (pink carbon) in the active site of DprE1

the variation in these parameters, the binding affinity of different 11α -substituted bile acid derivatives towards receptor has been discussed. The intermolecular interaction energy values between 11α -substituted bile acid derivatives and DprE1 enzyme obtained from the docking simulation are summarized in Table 5. Visual inspection of the docked complexes revealed that all the ligands could snugly fit into the active site of the enzyme occupying positions very close to that of the native ligand in the crystal structure with an average docking score of -7.685. Their docking score varied from -9.951 to -4.995 while the docking score for the native ligand was found to be -7.953. A statistically significant correlation was observed between the experimental antitubercular activity and the theoretical predictions from molecular docking calculations with the active compounds having high scores while those with relatively low inhibition were also predicted to have a lower docking score. A detailed per-residue interaction analysis between the protein and the 11α -substituted bile acid derivatives, was carried out through which we can speculate regarding the detailed binding patterns in the cavity. However for the sake of brevity we have elucidated the per-residue interactions analysis only for the most active compound **36b**. The level of anti-tubercular activities obtained for 11α -substituted bile acid derivatives prompted us to perform molecular docking studies to understand the ligand–protein interactions in detail. The binding mode of the most active analogue (**36b**) into the DprE1 binding site observed at the end of docking simulation is shown in **Figure 10**. The lower interaction energy observed for **36b** rationalizes the tighter binding of this molecule into the DprE1. Visual inspection of the docking pose revealed that the inhibitor snugly fits the active site of DprE1 making various close contacts

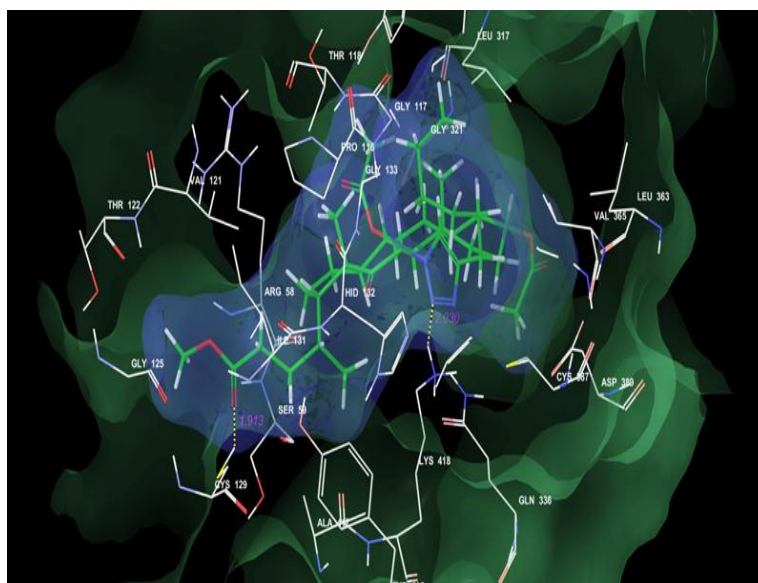


Figure 3. Binding mode of **36b** into the active site of *Mycobacterium tuberculosis* DprE1.

with the active site residues. The per residue-ligand interaction energy distribution showed that the Van der Waals interactions (-66.324) are more prevalent over the electrostatic contribution (-11.707) in the overall binding affinity.

The compound was found to be stabilized through an extensive chain of Van der Waals interactions with Ala 417 (-1.765 kcal/mol), Tyr415 (-2.428 kcal/mol), Asp389 (-1.481 kcal/mol), Cys387 (-3.532 kcal/mol), Val365 (-4.01 kcal/mol), Leu317 (-4.55 kcal/mol), Lys134 (-1.539 kcal/mol), Gly133 (-1.371 kcal/mol), His132 (-3.687 kcal/mol), Ile131 (-1.61 kcal/mol), Val 121 (-3.211 kcal/mol), Gly 117 (-4.367 kcal/mol), Pro 116(-2.844 kcal/mol), Tyr 60(-3.757 kcal/mol), Ser 59(-2.15 kcal/mol), Arg58 (-2.895 kcal/mol) and Trp16 (-2.689 kcal/mol) residues lining the active site. Furthermore, it also showed significant electrostatic interactions with Lys367 (-1.351 kcal/mol), Asp318 (-2.975 kcal/mol), Arg58 (-1.679 kcal/mol), Lys134 (-1.384 kcal/mol) residues. A very prominent pi-pi stacking interaction was observed between the triazole moiety in **36b** and the imidazole ring in His132 (3.10Å). In addition to this, two crucial hydrogen bonding interactions were observed within the active site; the first one is in between the carbonyl oxygen of the inhibitor and Cys129 (1.91 Å), and the second, hydrogen bond was observed between the triazole backbone of inhibitor and Lys418 (2.03 Å). These hydrogen-bonding interactions function as an "anchor", guiding the 3D orientation of the ligand in its active site, thereby aiding the steric and electrostatic interactions. Analysis of the molecular docking results for the remaining 11 α -substituted bile acid derivatives also revealed a similar binding profile making them pertinent starting points for second-generation drug development.

Table 3: The intermolecular interaction energy values between 11 α -substituted bile acid derivatives and DprE1 enzyme obtained from the docking simulation

Code	Glide score	Glide Energy	Van der Waals energy (kcal/mol)	Code	Glide score	Glide Energy	Van der Waals energy (kcal/mol)
33	-5.935	-40.387	-34.796	41	-7.830	-56.815	-51.181
36a	-8.190	-58.418	-51.875	42	-8.153	-58.00	-50.498
36b	-9.951	-78.031	-66.324	43	-9.012	-67.982	-58.68
36c	-8.210	60.969	-54.063	44	-8.970	-63.742	-56.003
36d	-6.236	-53.806	-48.695	45	-7.310	-57.115	-50.99
34	-4.995	-26.326	-22.187				

In silico ADME predictions

Absorption, distribution, metabolism, excretion and toxicity (ADMET) data is now-a-days considered to be very essential in the drug discovery process since approximately 40% of drug candidates fail in clinical trials owing to poor pharmacokinetics and toxicity properties. This late-stage failures contribute significantly to the cost of new drug discovery endeavors. Therefore, ability to detect problematic candidates in the early stage of drug discovery significantly reduces the amount of time and resources being wasted on molecules that are doomed to fail and focus lead optimization efforts to enhance the desired ADMET profiles. With this objective, we have carried out in silico ADME predictions for the active molecules (**36b**, **35**, **43** and **44**) to gauge their drug-likeness using the QikProp tool (Schrödinger, LLC., New York) incorporated in Schrodinger molecular modeling suite. The in silico ADME prediction data is summarized in Table 4. In this study, we have calculated % Human oral absorption, logarithm of partition coefficient (LogP), predicted brain/blood partition coefficient, molecular volume (MV), binding to human serum albumin, molecular weight (MW), number of hydrogen bond acceptors and donors, Caco-2 cell permeability and MDCK cell permeability.

The molecules investigated herein displayed fairly good oral bioavailability with very low susceptibility to acid hydrolysis in the stomach as reflected from the % Human oral absorption data. Inspection of the partition coefficient values ($\log P_{O/W}$) and prediction of

binding to human serum albumin suggested that these molecules are hydrophobic in nature. We found that there exists a direct correlation between the oral bioavailability and the hydrophobicity. As the hydrophobicity of these compounds is increasing from compounds **44** to **43** to **35** to **36b** there is linear rise in the oral bioavailability. So was the trend for the observed anti-tubercular activity. Compound **36b** which is the most hydrophobic, showed the highest antitubercular activity. The predicted values of apparent Caco-2 cell permeability, which accounts for the gut-blood barrier, further support these findings. Drugs targeting the central nervous system (CNS) are expected to cross the blood-brain barrier in order to reach their destination while drugs with peripheral site of actions are expected to have no brain penetration to avoid related side effects. Low values predicted for brain/blood partition coefficient signify that these molecules have very low propensity to cross the brain/blood brain barrier thereby eliminating the chances of CNS related toxicity. This is further supported by the predicted apparent MDCK cell permeability data which is also regarded as a good model for the blood brain barrier permeability. Therefore, the overall *in silico* ADME predictions appear to be interesting for future lead optimization.

Table 4. ADME (*In silico*) prediction data.

Molecule ID	M.Wt.	%Human Oral Absorption	Caco-2 cell permeability	MDCK cell permeability
36b	655.87	75.74	110.36	45.68
35	621.77	72.10	150.47	63.86
43	706.87	51.46	60.23	29.82
44	714.93	64.83	151.99	64.56

2.5 Conclusions

In conclusion, we have synthesized a series of new 11 α -triazoyl, 11 α -N-alkyl and N-acyl bile acid derivatives.¹ All the compounds exhibited potent antimycobacterial activity against *Mycobacterium tuberculosis* H37Ra among which compounds **36b**, **35**, **43** and **44** were found to show better activity. The following are the highlights of our results,

1. Among all, Compound **36b** displayed the most potent overall antitubercular activity against dormant as well as active phase of *Mycobacterium tuberculosis* H37Ra by *in vitro* and *ex-vivo* (MIC / IC₅₀ value of <3 μ g/mL / <0.7 μ g/mL).
2. Compounds **36b** also showed low cytotoxicity (nil up to 100 μ g/mL) against human cancer cell lines THP-1, A549 and PANC-1.

- All the compounds did not show any antibacterial activity.
- The theoretical predictions derived from molecular docking studies were found to be in harmony with the experimental anti-tubercular data thereby suggesting that these 11 α -substituted bile acid derivatives may be acting as DprE1 inhibitors.
- ADME analysis of the synthesized compounds showed potential as good oral drug candidates.
- This is the first report of steroidal molecules containing 1, 2, 3-triazole showing antituberculosis activity.
- Compound **36b** may be the best candidate for further investigation as a potential lead molecule among all the compounds studied here.

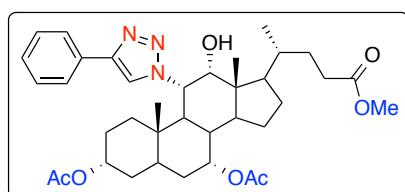
In further studies of these 11 α -substituted bile acid derivatives, diverse structural modifications are currently being investigated through iterative synthesis and computational modeling and the results will be communicated in due course.

2.6 Experimental section

General procedure for the synthesis of compounds 36a - 36d.

Alkyne (0.3 mmol) and the azide **33** (0.1g, 0.18 mmol) were dissolved in DMF: H₂O (4:1) 5 mL. To this solution CuSO₄·5H₂O (0.002g, 0.01 mmol) and sodium ascorbate (0.015g, 0.08 mmol) were added. The reaction mixture was placed in domestic microwave reactor and irradiated for 5 min. at 360W. The reaction mixture was cooled, diluted with cold water and then extracted with ethyl acetate. Organic phase was dried over anhydrous Na₂SO₄. Solvent was evaporated under reduced pressure and the crude product was purified by column chromatography on silica gel using ethyl acetate/hexane (1:4) to get the pure product **36a-d**.

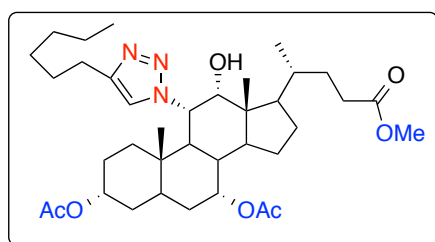
(3R,5S,7R,10S,11S,13R)-17-((R)-5-methoxy-5-oxopentan-2-yl)-10,13-dimethyl-12-oxo-11-(4-phenyl-1H-1, 2, 3-triazol-1-yl)hexadecahydro-1H-cyclopenta[a]phenanthrene-3,7-diyl diacetate (36a).



Colorless solid, Yield: 71%; mp. 108-109 °C; [α]_D²⁵+153.38 (c = 1, CHCl₃); IR (Nujol, cm⁻¹): 3404, 3307, 1737; ¹H NMR (200 MHz, CDCl₃): δ 7.96 (s, 1H), 7.85 (d, 2H), 7.42 (t, 2H), 7.35 (t, 1H), 5.95 (bs, 1H), 5.04 (s, 1H), 4.31-4.43 (m, 1H), 3.66 (s, 3H), 2.10 (s, 1H), 1.98 (s, 1H), 1.29 (s, 3H), 1.24 (s, 3H), 1.20 (s, 3H), 0.74 (d, 3H);

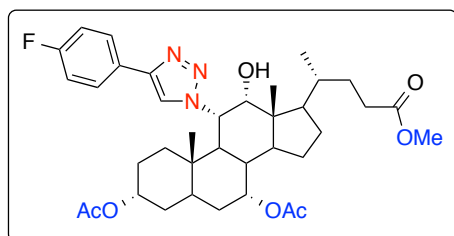
^{13}C NMR (101 MHz, CDCl_3): δ 204.6 (C=O at C-12), 174.4 (C=O of C-24 ester), 170.4 (C=O of C-3 acetate), 169.9 (C=O of C-7 acetate), 147.6 (benzylic C), 130.6 (aromatic C), 128.8 (aromatic C) 128.2 (aromatic C), 125.8 (aromatic C), 121.6 (Triazole C-H), 73.2 (C-3), 70.5 (C-7), 65.8 (C-11), 56.6, 51.6, 47.4, 42.3, 38.1, 37.4, 35.5, 35.3, 31.9, 31.3, 31.0, 30.2, 29.7, 29.4, 28.2, 27.2, 24.7, 24.1, 22.7, 22.6, 21.5, 21.4, 18.2, 14.1, 11.3; HRMS (ESI): Calculated for $[\text{M} + \text{H}]^+$ ($\text{C}_{37}\text{H}_{49}\text{N}_3\text{O}_7$) requires m/z 648.3644; found 648.3643.

(3R,5S,7R,10S,11S,13R)-11-(4-hexyl-1H-1, 2, 3-triazol-1-yl)-17-((R)-5-methoxy-5-oxopentane-2-yl)-10,13-dimethyl-12-oxohexadecahydro-1H-cyclopenta[a]phenanthrene-3,7-diyl diacetate (36b).



Colourless solid. Yield: 31.6 %; mp. 77-78 °C; $[\alpha]_{\text{D}}^{25} +137.14$ ($c = 1$, CHCl_3); IR (Nujol, cm^{-1}): 2926.36, 2856.41, 1734.78; ^1H NMR (200 MHz, CDCl_3): δ 7.48 (s, 1H), 5.86 (s, 1H), 5.02 (s, 1H), 4.42 (m, 1H), 3.66 (s, 3H), 2.75 (t, 2H), 2.08 (s, 3H), 1.99 (s, 3H), 1.27 (s, 3H), 1.26 (s, 3H), 1.18 (s, 3H), 0.89 (s, 3H), 0.74 (d, 1H); ^{13}C NMR (CDCl_3 , 101 MHz): δ 204.5 (C=O at C-12), 174.1 (C=O of C-24 ester), 170.1 (C=O of C-3 acetate), 169.6 (C=O of C-7 acetate), 147.9 (quaternary C of triazole), 122.2 (Triazole C-H), 72.8 (C-3), 70.2 (C-7), 65.2 (C-11), 56.9, 52.9, 51.8, 47.7, 42.6, 38.4, 37.7, 35.6, 35.0, 31.9, 31.3, 30.0, 29.8, 29.3, 28.8, 27.5, 26.1, 24.4, 22.8, 21.7, 21.6, 18.7, 14.3, 11.6; HRMS (ESI): Calculated for $[\text{M} + \text{H}]^+$ ($\text{C}_{37}\text{H}_{58}\text{N}_3\text{O}_7$) requires m/z 656.4260; found 656.4259.

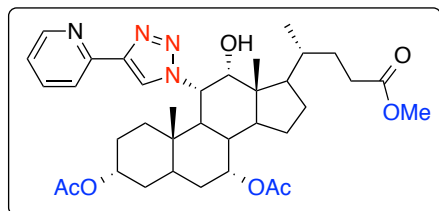
(3R,5S,7R,10S,11S,13R)-11-(4-(4-fluorophenyl)-1H-1, 2, 3-triazol-1-yl)-17-((R)-5-methoxy-5-oxopentane-2-yl)-10,13-dimethyl-12-oxohexadecahydro-1H-cyclopenta[a]phenanthrene-3,7-diyl diacetate (36c).



Colorless solid. Yield: 81%; mp. 105-106 °C; $[\alpha]_{\text{D}}^{25} +173.96$ ($c = 1$, CHCl_3); IR (Nujol, cm^{-1}): 2927.64, 2873.97, 1738; ^1H NMR (200 MHz, CDCl_3): δ 7.93 (s, 1H), 7.81 (m, 2H), 7.12 (m, 2H), 5.91 (d, 1H), 5.03 (d, 1H), 4.40 (m, 1H), 3.66 (s, 3H), 2.09 (s, 3H), 1.97 (s, 3H), 1.30 (s, 3H), 1.26 (s, 3H), 1.21 (s, 3H), 0.76 (d, 3H); ^{13}C NMR (CDCl_3 , 101 MHz): δ 204.6 (C=O at C-12), 174.5 (C=O of C-24 ester), 170.5 (C=O of C-3 acetate), 170.0 (C=O of C-7 acetate), 164.0, 146.8, 127.6, 126.9, 121.5 (Triazole C-H), 116.0, 115.8, 73.1 (C-3), 70.5 (C-7), 65.9 (C-11), 56.7, 51.7, 47.5, 42.3, 38.1, 37.5, 35.6, 35.4, 32.0, 31.4, 31.1,

29.8, 27.3, 24.1, 21.6, 21.5, 18.5, 14.2, 11.4; HRMS (ESI): Calculated for $[M + H]^+$ ($C_{37}H_{48}FN_3O_7$) requires m/z 666.3352; found 666.3352.

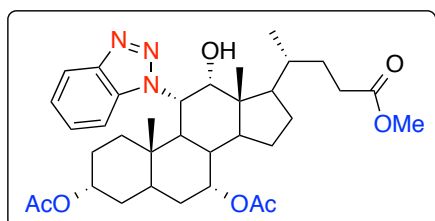
(3R,5S,7R,10S,11S,13R)-17-((R)-5-methoxy-5-oxopentan-2-yl)-10,13-dimethyl-12-oxo-11-(4-(pyridin-2-yl)-1H-1, 2, 3-triazol-1-yl)hexadecahydro-1H-cyclopenta[a]phenanthrene-3,7-diyl diacetate (36d).



Colorless solid. Yield: 87%; mp. 98-99°C; $[\alpha]_D^{25} +122.56$ ($c=1$, $CHCl_3$); IR (Nujol, cm^{-1}): 2926.38, 2873.04, 1732.87; 1H NMR (200 MHz, $CDCl_3$): δ 8.58 (d, 1H), 8.39 (s, 1H), 8.21 (d, 1H), 7.81 (t, 1H), 5.05 (s, 1H), 4.38 (m, 1H), 3.65 (s, 3H), 2.11 (s, 3H), 1.94 (s, 3H), 1.32 (s, 3H), 1.26 (s, 3H), 1.19 (s, 3H), 0.75 (d, 3H); ^{13}C NMR ($CDCl_3$, 101 MHz): δ 203.9 (C=O at C-12), 174.4 (C=O of C-24 ester), 170.6 (C=O of C-3 acetate), 170.1 (C=O of C-7 acetate), 122.9 (Triazole C-H), 120.40, 73.1 (C-3), 70.5 (C-7) 66.0 (C-11), 56.4, 51.5, 47.4, 42.0, 38.0, 37.7, 36.7, 35.5, 35.3, 31.9, 31.6, 31.0, 30.3, 29.7, 29.4, 27.8, 27.2, 24.7, 24.1, 22.8, 21.5, 21.4, 18.3, 14.1, 11.1; HRMS (ESI): Calculated for $[M + H]^+$ ($C_{36}H_{49}N_4O_7$) requires m/z 649.3593; found 649.3696.

(3R,5S,7R,10S,11S,13R)-11-(1H-benzo[d][1, 2, 3]triazol-1-yl)-17-((R)-5-methoxy-5-oxopentan-2-yl)-10,13-dimethyl-12-oxohexadecahydro-1H-cyclopenta[a]phenanthrene-3,7-diyl diacetate (35).

To a solution of 2-(trimethylsilyl)phenyltrifluoromethane sulfonate (0.35 mL 1.5 mmol) in anhydrous acetonitrile, Cesium fluoride (0.9 g 2.4mmol) was added. The reaction mixture was stirred at 25 °C for 30 min and to this reaction mixture azide 1 (0.7 g 1.2 mmol) in dry acetonitrile was added drop wise. The reaction mixture was stirred at 25 °C for 16 h. It was then treated with ice water and extracted with ethyl acetate. Organic phase was separated and dried over anhydrous Na_2SO_4 . Solvent was removed under reduced pressure and crude product was purified by column chromatography on silica gel using ethyl acetate/hexane (1:4) to get the pure product **35** as light yellow solid; Yield 88%; mp. 111-112 °C;



$[\alpha]_D^{25} +78.20$ ($c=0.2$, $CHCl_3$); IR (Nujol, cm^{-1}): 3021.01, 2970.93, 1728.58, 1216.44; 1H NMR (200 MHz, $CDCl_3$): δ 8.9 (m, 1H), 7.51 (s, 1H), 7.36-7.4 (m, 2H), 6.25 (d, 1H), 5.1 (s, 1H), 4.31 (m, 1H), 3.64 (s, 3H) 2.14 (s, 3H), 2.05 (s, 3H), 1.95 (s, 2H), 1.86 (s, 2H), 1.26 (s, 3H), 1.22 (s, 3H), 0.73 (d, 3H); ^{13}C -NMR: (101 MHz, $CDCl_3$): δ 203.9 (C=O at C-12), 174.4 (C=O of C-24 ester), 170.4 (C=O of C-3

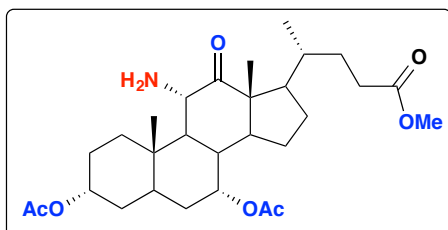
acetate), 169.9 (C=O of C-7 acetate), 139.3, 133.6, 127.7, 127.5, 124.1, 123.9 (Triazole C-H), 73.2 (C-3), 70.9 (C-7), 66.1 (C-11), 62.7, 56.3, 56.2, 51.9, 51.5, 50.2, 47.3, 41.98, 38.5, 37.7, 35.4, 31.9, 29.7, 29.4, 27.4, 26.7, 14.1, 11.1; HRMS (ESI): Calculated for $[M + H]^+$ ($C_{35}H_{48}O_7N_3$) requires m/z 622.3487; found 622.3477 and also for $[M + 23]^+$ ($C_{35}H_{48}O_7N_3Na$) requires m/z 644.3306; found 644.3295.

General procedures for the synthesis of compound 34.

Methyl 11 α -amino-3 α ,7 α -diacetoxo-12-oxo-5 β -cholan-24-oate (34).

Method A: Methyl 11 α -azido-3 α ,7 α -diacetoxo-12-oxo-5 β -cholan-24-oate **33** (0.25 g, 0.46 mmol) in EtOAc (15 mL) was hydrogenated at 28 °C and 40 psi pressure using 10 % Pd/C (0.025 g) for 5 h. After filtration of the catalyst and evaporation of the solvent, afforded methyl 11 α -amino-3 α ,7 α -diacetoxo-12-oxo-5 β -cholan-24-oate **34** (0.224 g, 95 %) as white solid.

Method B (Stradinger reaction): A solution of methyl 11 α -azido-3 α ,7 α -diacetoxo-12-oxo-5 β -cholan-24-oate **33** (0.11 g, 0.2 mmol) was stirred with triphenylphosphine (0.08 g, 0.3 mmol) in dry THF (5 mL) for 24 h. Water (0.1 mL) was added and the solvent was removed after additional 24 h. After dilution with EtOAc (100 mL), the organic layer was separated, washed with water (2x20 mL), brine (20 mL), dried and solvent was evaporated under reduced pressure. Chromatography of the residue on alumina (10 % EtOAc/PE) afforded methyl 11 α -amino-3 α ,7 α -diacetoxo-12-oxo-5 β -cholan-24-oate **34** as white solid. Yield 80%; mp 154 °C; $[\alpha]_D^{28} + 61.84$ ($c = 1.52$, $CHCl_3$); IR (Nujol, cm^{-1}): 3389, 2954, 1731, 1714 cm^{-1} ;



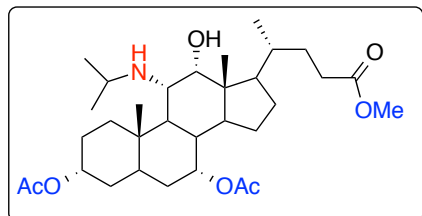
1H NMR (500 MHz, $CDCl_3$): δ 4.94 (bs, 1H), 4.64 (m, 1H), 3.76 (d, 1H), 3.66 (s, 3H), 2.72 (dt, 1H), 2.40 (m, 1H), 2.27 (m, 1H), 2.02 (s, 3H), 2.01 (s, 3H), 1.19 (s, 3H), 1.01 (s, 3H), 0.85 (d, 3H).

General procedure for the synthesis of compounds 41 to 44.

(3R,5S,7R,10S,11S,13R,17R)-11-(isopropylamino)-17-((R)-5-methoxy-5-oxopentan-2-yl)-10,13-dimethyl-12-oxohexadecahydro-1H-cyclopenta[a]phenanthrene-3,7-diyl diacetate (41).

To a solution of amine **34** (0.4 g, 0.75 mmol) in anhydrous DMF, anhydrous potassium carbonate (0.63 g, 4.6 mmol) and isopropyl iodide (0.15 mL, 1.5 mmol) were added. The reaction mixture was then allowed to stir at 60-70 °C for 24 h. The reaction mixture was

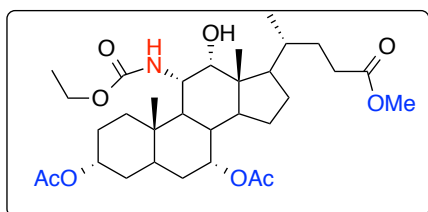
treated with ice water and was extracted with ethyl acetate. Organic phase was separated and dried over anhydrous Na_2SO_4 . The solvent was removed under vacuo and the residue purified by column chromatography on silica gel using ethyl acetate/hexane (2:1) to give the pure product **45** as thick yellow liquid. Yield (0.35 g, 81 %); mp 83-84 °C; $[\alpha]_D^{28} +94.76$ ($c=1.00$, CHCl_3); IR (Nujol, cm^{-1}): 3347.42, 2949.83, 1722.29; ^1H NMR (500 MHz, CDCl_3): δ 4.91 (bs, 1H), 4.63 (m, 1H), 3.67 (s, 3H), 3.60 (d, 1H), 3.03 (d, 1H), 2.02 (s, 3H), 2.01 (s, 3H), 1.59 (d, 6H), 1.16 (s, 3H), 1.05 (s, 3H), 0.79 (d,



3H); ^{13}C NMR (101 MHz, CDCl_3): δ 215.1 (C=O at C-12), 174.6 (C=O of ester at C-24), 170.8 (C=O of C-3 acetate), 170.3 (C=O of C-7 acetate), 74.4 (C-3), 71.1 (C-7), 62.0 (C-11), 56.9, 54.1, 51.5, 46.9, 44.5, 42.6, 38.3, 37.7, 37.1, 35.3, 31.6, 31.2, 30.3, 29.7, 27.8, 27.3, 24.6, 23.5, 23.2, 22.7, 21.5, 18.4, 14.1, 10.7; LCMS Calculated for ($\text{C}_{32}\text{H}_{51}\text{N O}_7$) : 561.37; found ($\text{M} + \text{Na}$) m/z : 584.15.

(3R,5S,7R,10S,11S,13R,17R)-11-((ethoxycarbonyl)amino)-17-((R)-5-methoxy-5-oxopentan-2-yl)-10,13-dimethyl-12-oxohexadecahydro-1H-cyclopenta[a]phenanthrene-3,7-diyl diacetate (42**).**

To a solution of amine **34** (0.5 g, 1 mmol) in anhydrous CH_2Cl_2 , N-methylmorpholine (0.12 mL, 1.1 mmol) was added and the mixture cooled to -20 °C, after which ethylchloroformate (0.1 mL, 1 mmol) was added. The reaction temperature was maintained at -20 °C for 5 min, it was allowed to stir at 0 °C for 2-3 hrs. Finally, the reaction mixture was treated with aq. HCl, aq. NaHCO_3 , aq. NaCl and then dried over anhydrous Na_2SO_4 . The organic phase was concentrated in vacuo and the residue was purified by column chromatography on silica gel by using ethyl acetate/hexane (2:1) to give the pure product **42** as colorless solid. Yield (0.35g, 70%); mp 107-108 °C; $[\alpha]_D^{25} +82.64$ ($c=1.00$, CHCl_3); IR

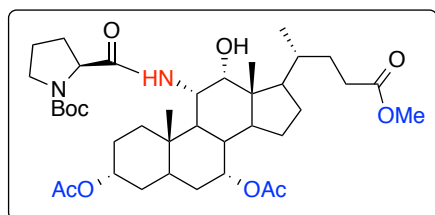


(Nujol, cm^{-1}): 3362.18, 2936.19, 1727.05; ^1H NMR (200 MHz, CDCl_3): δ 5.31 (d, 1H), 4.95 (bs, 1H), 4.77 (t, 2H), 4.58-4.61 (m, 1H), 4.05-4.16 (m, 2H), 3.66 (s, 3H), 2.03 (s, 3H), 2.02 (s, 3H), 1.23 (s, 3H), 1.07 (s, 3H), 0.79 (d, 3H); ^{13}C NMR (101 MHz, CDCl_3): δ 210.6 (C=O at C-12), 174.5 (C=O of ester at C-24), 170.6 (C=O of C-3 acetate), 170.1 (C=O of C-7 acetate), 156.8 (Amide C=O), 73.8 (C-3), 70.8 (C-7), 60.9 (OCH_2), 56.2, 56.0, 52.7, 51.2, 46.8, 41.9, 37.8, 37.0, 34.9, 34.8, 31.1, 30.8, 29.9, 29.3, 28.0, 27.3, 26.9, 24.0, 22.4, 21.1, 18.1, 14.2, 10.3; HRMS (ESI): Calculated for [$\text{M} + \text{H}$] $^+$ ($\text{C}_{32}\text{H}_{50}\text{N O}_9$) requires m/z - 592.3480; found 592.3471.

General procedure for the synthesis of compounds (43) and (44).

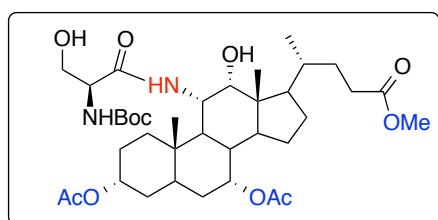
To a solution of N-Boc protected amino acid (1.2 mmol) in anhydrous DMF, 1-Ethyl-3-(3-dimethylaminopropyl)-carbodiimide (EDC, 0.27 g, 1.4 mmol), hydroxybenzotriazole (0.06 g, 0.5 mmol) and DMAP (0.02 g, 0.2 mmol) were added and the mixture was cooled to 0 °C. The reaction temperature was maintained at 0 °C for 5-10 mins, and then DMF solution of amine **34** (0.5 g, 1 mmol) was added dropwise over 5 min at 0 °C. The reaction mixture was allowed to attain room temperature and then it was stirred for 3 hrs at room temperature. Finally, the reaction mixture was treated with aq. HCl, aq. NaHCO₃, aq. NaCl and then dried over anhydrous Na₂SO₄. The organic phase was concentrated in vacuo and the residue purified by column chromatography on silica gel by using ethyl acetate/hexane (2:1) to give the pure products **43** and **44**.

(3R,5S,7R,10S,11S,13R,17R)-11-(2-((tert-butoxycarbonyl)amino)-3-hydroxypropanamido)-17-((R)-5-methoxy-5-oxopentan-2-yl)-10,13-dimethyl-12-oxohexadecahydro-1H-cyclopenta[a]phenanthrene-3,7-diyl diacetate (43).



Colorless solid; Yield 77 %; mp 93-94 °C; $[\alpha]_D^{28} +25.72$ ($c= 1.00$; CHCl₃); IR (Nujol, cm⁻¹) 3356.67, 2938.40, 1714.91; ¹H NMR (500 MHz, CDCl₃): 5.07 (t, 1H), 4.94 (s, 1H), 4.59 (m, 1H), 4.36 (bd, 1H), 3.66 (s, 3H), 3.31 (m, 2H), 2.03 (s, 3H), 2.01 (s, 3H), 1.51 (s, 9H), 1.25 (s, 3H), 1.07 (s, 3H), 0.78 (d, 3H); ¹³C NMR (101 MHz, CDCl₃) δ 212.3, 209.4, 174.5, 173.0, 170.5, 170.0, 73.8, 70.8, 56.3, 54.6, 52.7, 51.5, 47.1, 43.2, 38.1, 37.3, 35.7, 35.3, 31.9, 31.4, 31.1, 30.3, 29.7, 28.3, 27.8, 27.2, 24.3, 22.8, 21.4, 18.7, 14.1, 10.7; HRMS-(ESI): Calculated for $[M + H]^+$ (C₃₇H₅₉N₂O₁₁) requires m/z ; 707.4113; found 707.4108.

(3R,5S,7R,10S,11S,13R,17R)-11-((R)-1-(tert-butoxycarbonyl)pyrrolidine-2-carboxamido)-17-((R)-5-methoxy-5-oxopentan-2-yl)-10,13-dimethyl-12-oxohexadecahydro-1H-cyclopenta[a]phenanthrene-3,7-diyl diacetate (44).



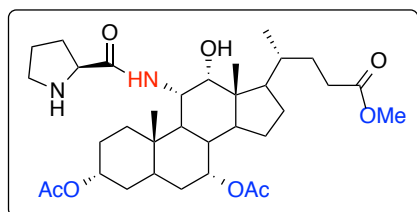
Colourless solid; Yield 85 %; mp 113-114 °C; $[\alpha]_D^{28} +53.00$ ($c= 1$; CHCl₃); IR (Nujol, cm⁻¹): 3356.67, 2938.40, 1714.91; ¹H NMR (400 MHz, CDCl₃): δ 6.69 (d, $J = 9.76$ Hz, 1H), 5.42 (m, 1H), 4.96 (d, 1H), 5.04 (m, 1H), 4.58 (m, 1H), 4.04-4.20 (m, 2H), 3.66 (s, 3H), 3.62-3.70 (m, 1H), 2.02 (s, 3H), 2.05 (s, 3H), 1.46

(s, 9H), 1.23 (s, 3H), 1.08 (s, 3H), 0.76 (d, $J = 6.41$ Hz, 3H); ^{13}C NMR (101 MHz, CDCl_3): δ 210.6 (C=O at C-12), 174.5 (C=O of ester at C-24), 171.1 (Boc C=O), 170.6 (C=O of C-3 acetate), 170.0 (C=O of C-7 acetate), 155.6 (amide C=O), 80.3 (CH_2OH), 73.5 (C-3), 70.6 (C-7), 63.1 (C=11), 60.3 (CH of NHBOC), 56.3, 56.3, 55.2, 52.5, 51.5, 47.2, 42.8, 41.9, 38.2, 37.4, 36.1, 35.2, 31.9, 31.5, 31.1, 30.3, 29.7, 28.3, 27.8, 27.2, 24.3, 22.9, 21.5, 18.4, 14.2, 10.6; HRMS (ESI): Calculated for $[\text{M} + \text{H}]^+$ ($\text{C}_{39}\text{H}_{61}\text{N}_2\text{O}_{10}$) requires m/z 717.4321; found 717.4315.

General procedure for Boc deprotected compounds (45) and (46)

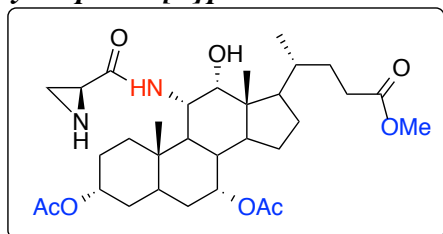
A solution of *N*-*boc* protected amino acid derivative **43** or **44** (0.24mmol) in anhydrous DCM was cooled to 0°C . To this solution trifluoroacetic acid (0.09 mL, 1.22 mmol) was added drop wise keeping the temperature 0°C . The reaction mixture was stirred at this temperature for 1-2 hrs and was treated with cold NaHCO_3 . The reaction mixture was extracted with DCM. Organic phase was separated and dried over anhydrous Na_2SO_4 . Solvent was removed under vacuo and the residue purified by column chromatography on silica gel using methanol/DCM (1:9) to give the pure product.

(3R,5S,7R,10S,11S,13R,17R)-17-((*R*)-5-methoxy-5-oxopentan-2-yl)-10,13-dimethyl-12-oxo-11-((*R*)-pyrrolidine-2-carboxamido)hexadecahydro-1H-cyclopenta[*a*]phenanthrene-3,7-diyl diacetate (45).



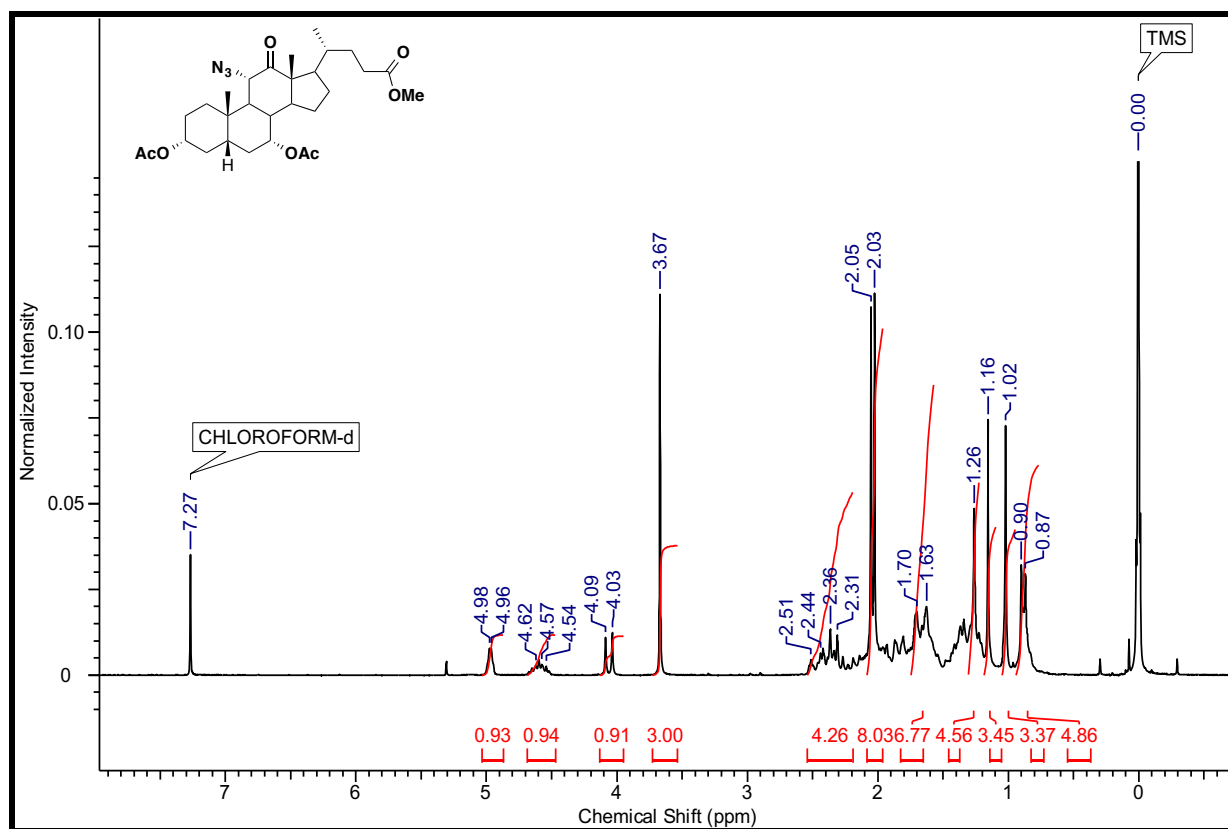
Yellowish solid; Yield 86 %; mp. $102-103^\circ\text{C}$; $[\alpha]_{\text{D}}^{28} +124.40$ ($c = 1.00$; CHCl_3); IR (Nujol, cm^{-1}): 3317.67, 2944.93, 1713.60; ^1H NMR (200 MHz, CDCl_3): δ 8.13 (d, 1H), 4.96 (m, 2H), 4.56-4.62 (m, 1H), 3.82-3.86 (m, 1H), 3.66 (s, 3H), 3.05-3.10 (m, 1H), 2.91-2.95 (m, 1H), 2.04 (s, 3H), 2.03 (s, 3H), 1.24 (s, 3H), 1.09 (s, 3H), 0.76 (d, 3H); ^{13}C -NMR (101 MHz; CDCl_3): δ 209.9 (C=O at C-12), 175.5 (amide C=O), 174.5 (C=O of ester at C-24), 170.6 (C=O of C-3 acetate), 170.1 (C=O of C-7 acetate) 73.7 (C-3), 70.9 (C-7), 60.7 (C-11), 56.3, 54.6, 51.4, 48.9, 47.3, 44.4, 42.7, 41.1, 38.2, 37.4, 35.2, 31.1, 30.0, 26.5, 22.8, 21.3, 18.4, 14.1, 10.8; HRMS (ESI): Calculated for $[\text{M} + \text{H}]^+$ ($\text{C}_{34}\text{H}_{53}\text{N}_2\text{O}_8$) requires m/z 617.3787; found 617.3796.

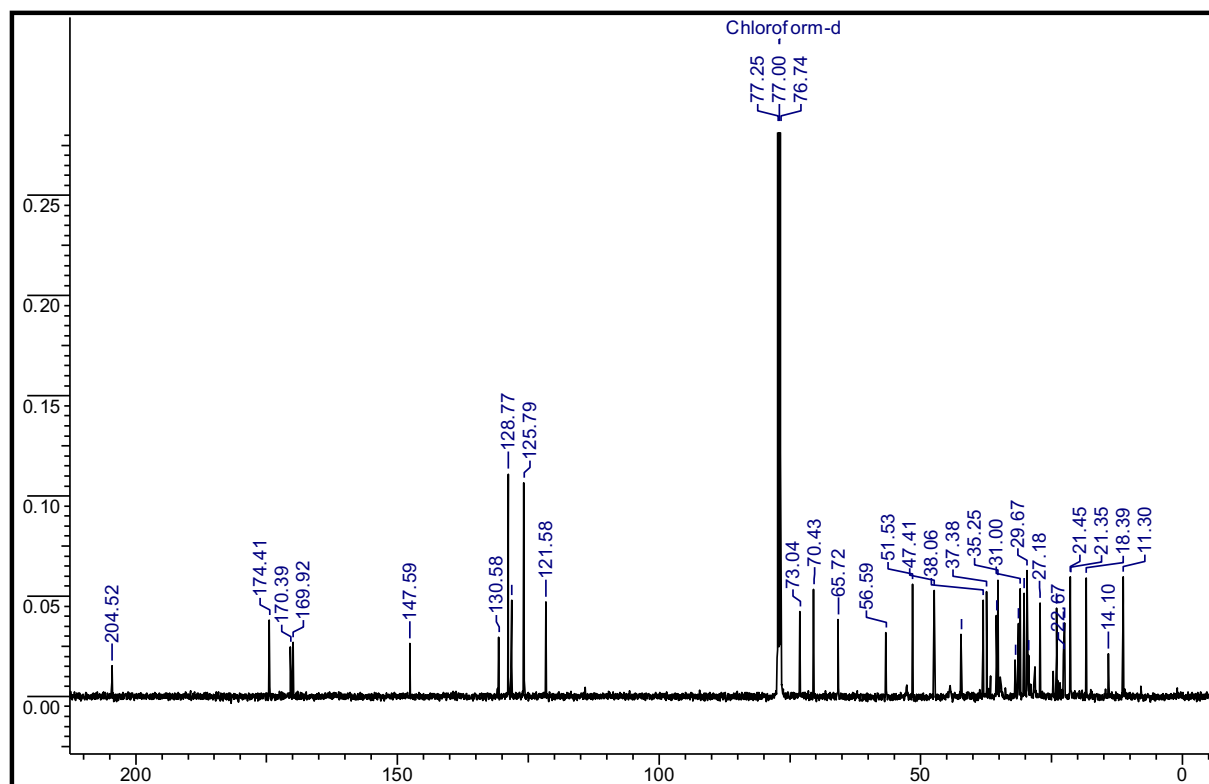
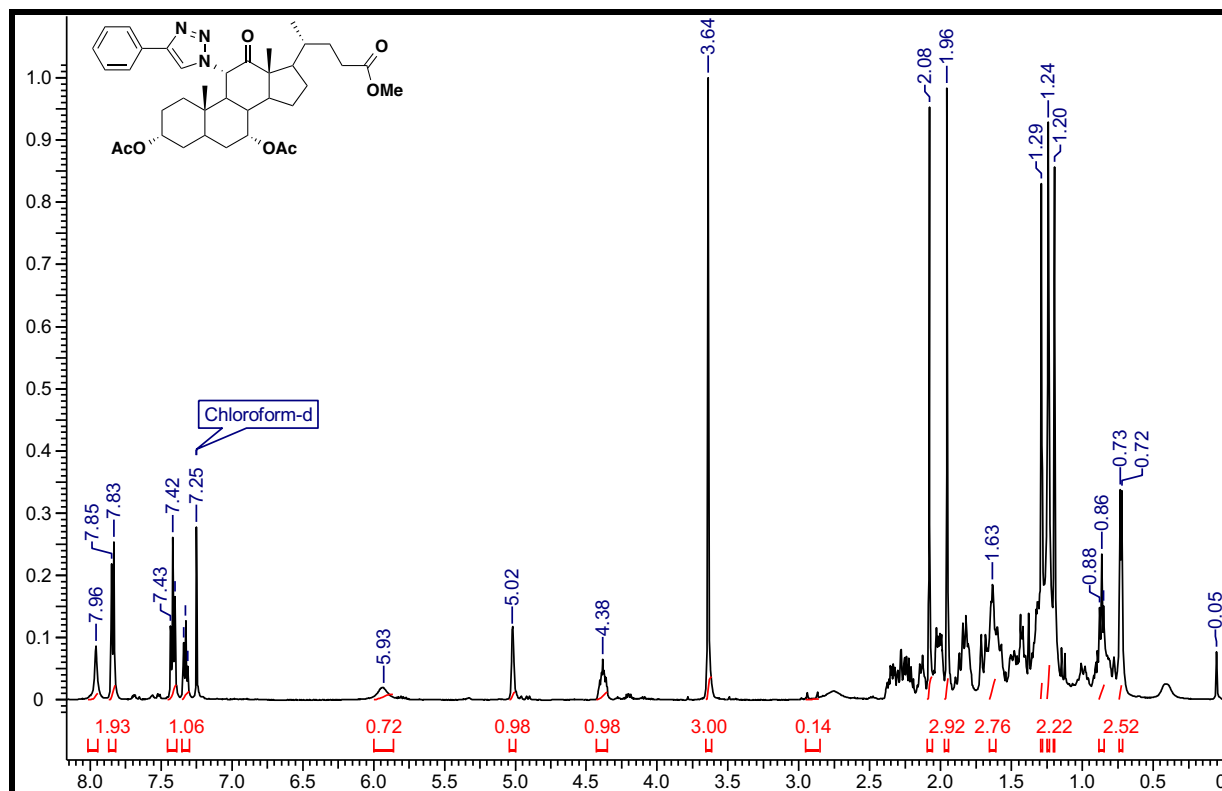
(3R,5S,7R,10S,11S,13R,17R)-11-(aziridine-2-carboxamido)-17-((R)-5-methoxy-5-oxopentane-2-yl)-10,13-dimethyl-12-oxohexadecahydro-1H-cyclopenta[a]phenanthrene-3,7-diyl diacetate (46).

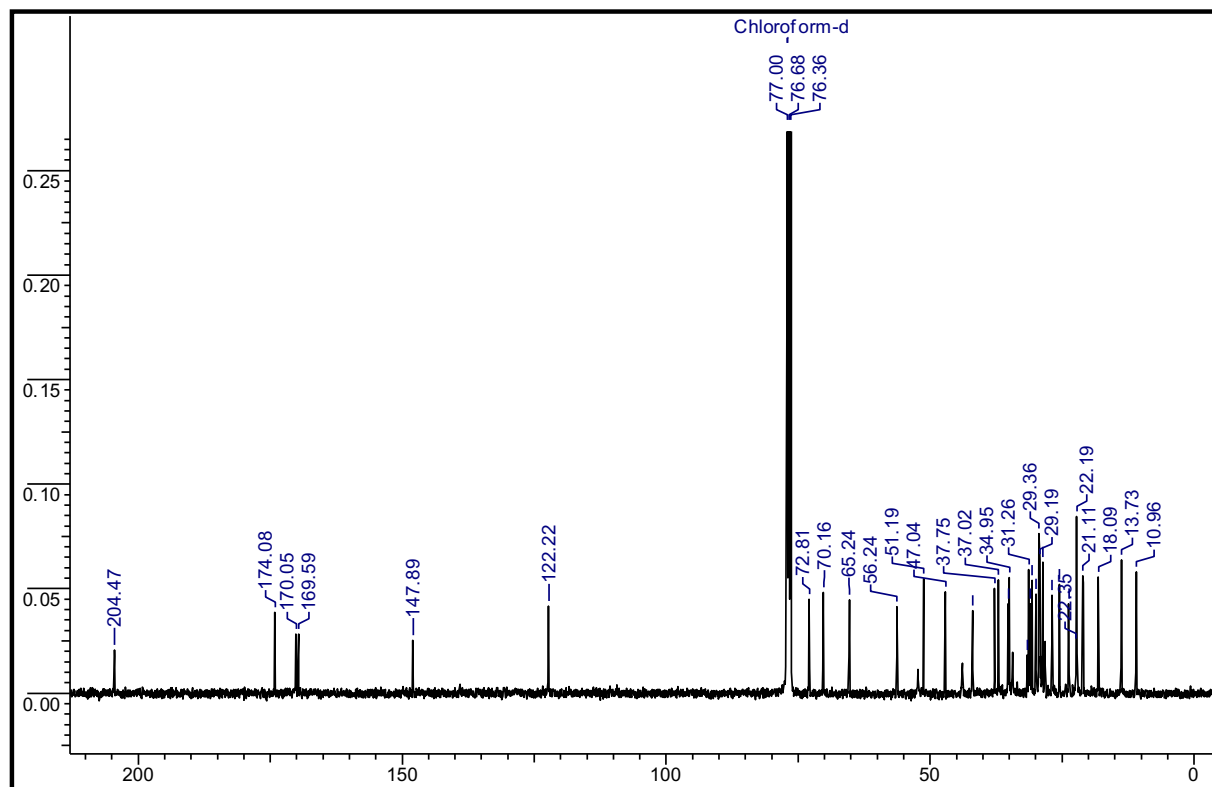
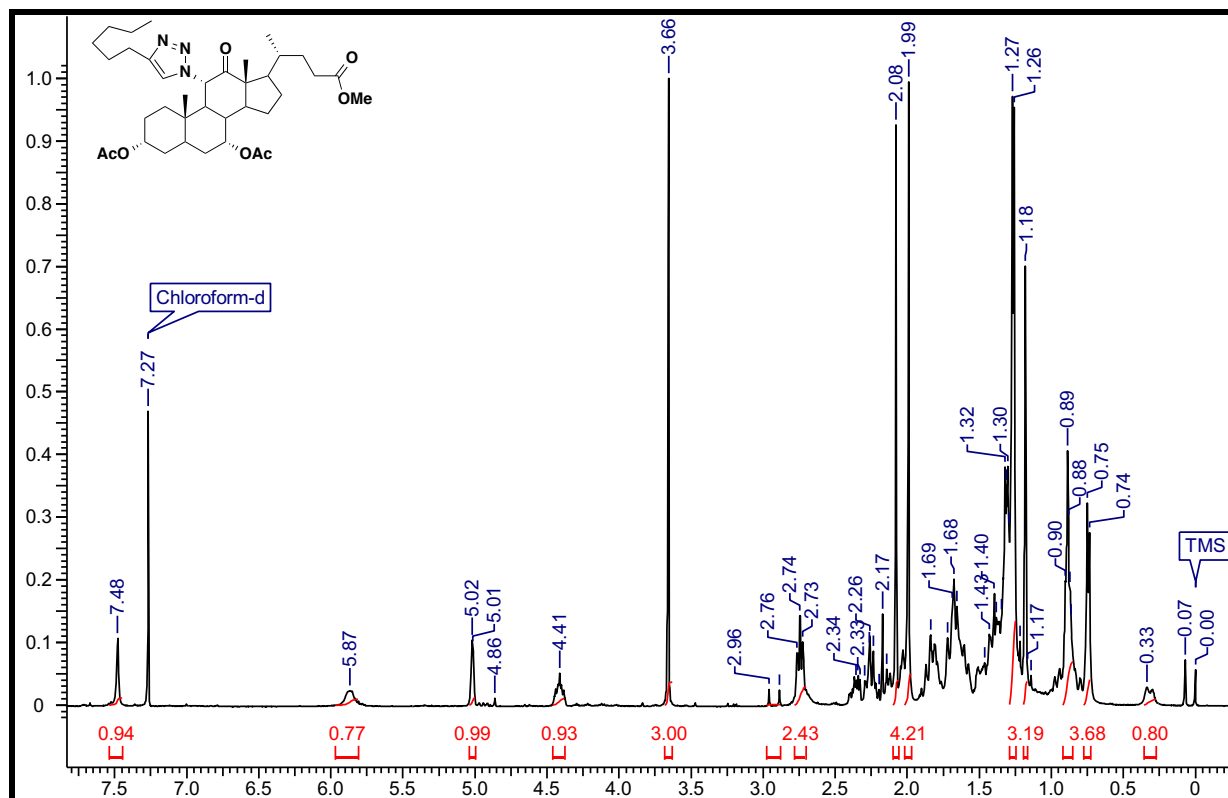


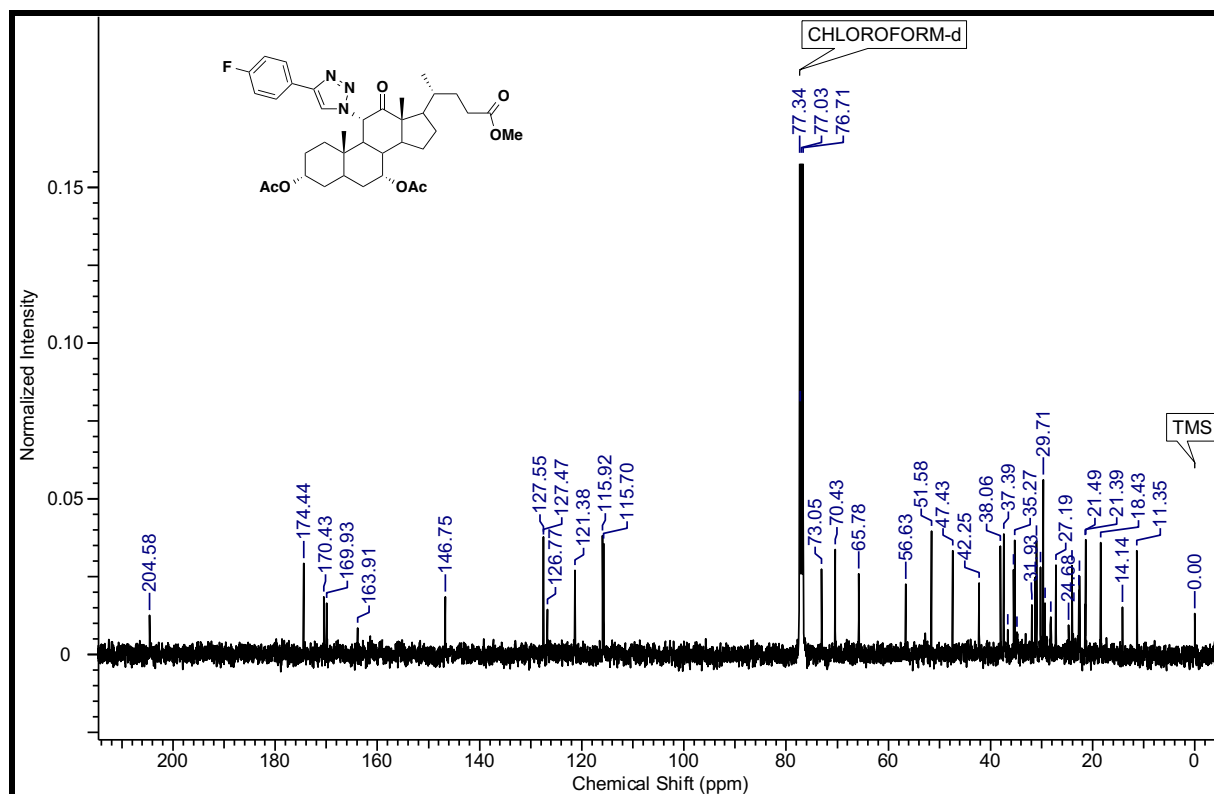
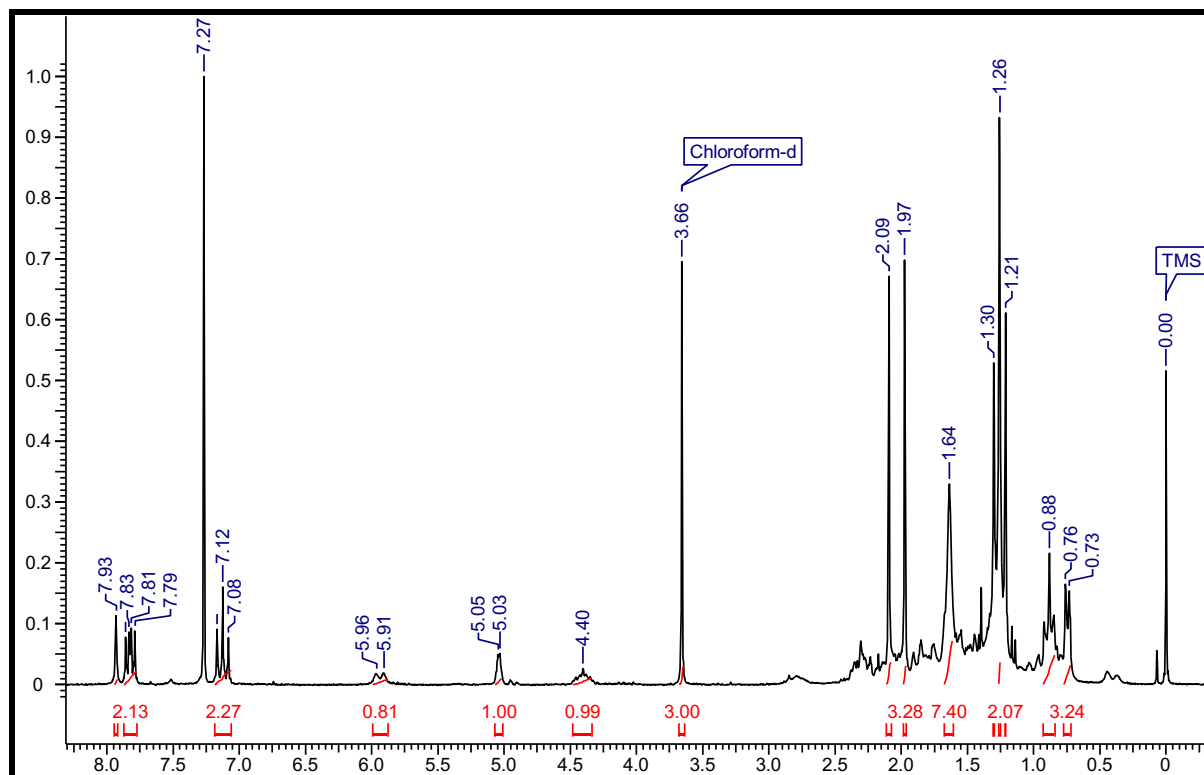
Colourless solid; Yield 77%; mp. 112-113 °C; $[\alpha]_D^{28} +89.56$ ($c=1$; CHCl_3); IR (Nujol, cm^{-1}): 3020.66, 2975.18, 1728.45, 1215.90; ^1H NMR (200 MHz, CDCl_3): δ 7.75 (d, 1H), 4.94 (m, 2H), 4.57 (m, 1H), 3.83-3.91 (m, 1H), 3.49-3.54 (m, 1H), 3.66 (s, 3H), 2.26-2.41 (m, 4H), 2.05 (s, 3H), 2.03 (s, 3H), 1.24 (d, 3H), 1.09 (s, 3H), 0.78 (d, 3H); ^{13}C NMR (101 MHz; CDCl_3): δ 209.7 (C=O at C-12), 174.3 (C=O of ester at C-24), 171.5 (CH of aziridine ring), 170.3 (C=O of C-3 acetate), 169.8 (C=O of C-7 acetate), 162.22 (amide C=O), 73.3 (C-3), 70.5 (C-7), 63.8 (C-11), 60.8 (CH_2 of aziridine ring), 54.2, 52.7, 51.9, 51.52, 47.4, 45.9, 42.4, 38.5, 37.5, 35.5, 35.1, 31.6, 31.4, 30.4, 29.69, 27.0, 24.4, 22.9, 21.4, 19.1, 12.0; HRMS (ESI): Calculated for $[\text{M} + \text{H}]^+$ ($\text{C}_{32}\text{H}_{49}\text{N}_2\text{O}_8$) requires m/z 589.3482 ; found 589.3483.

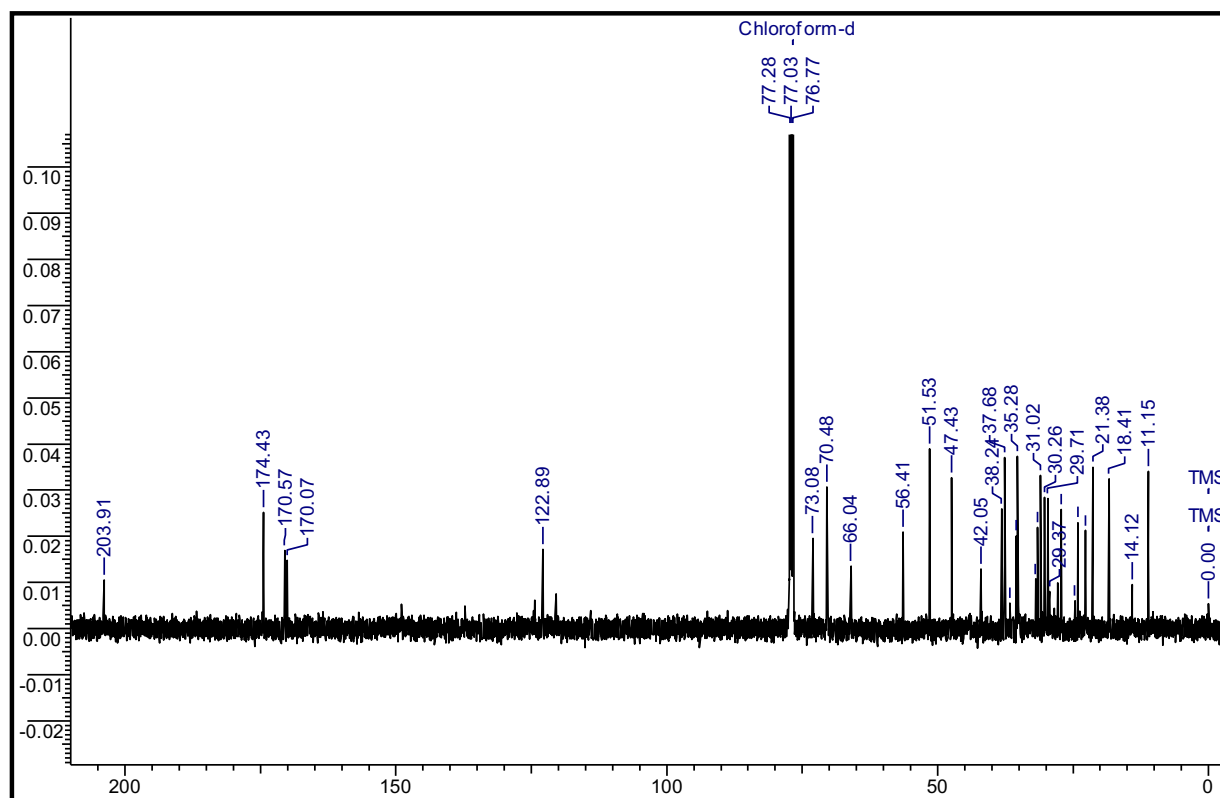
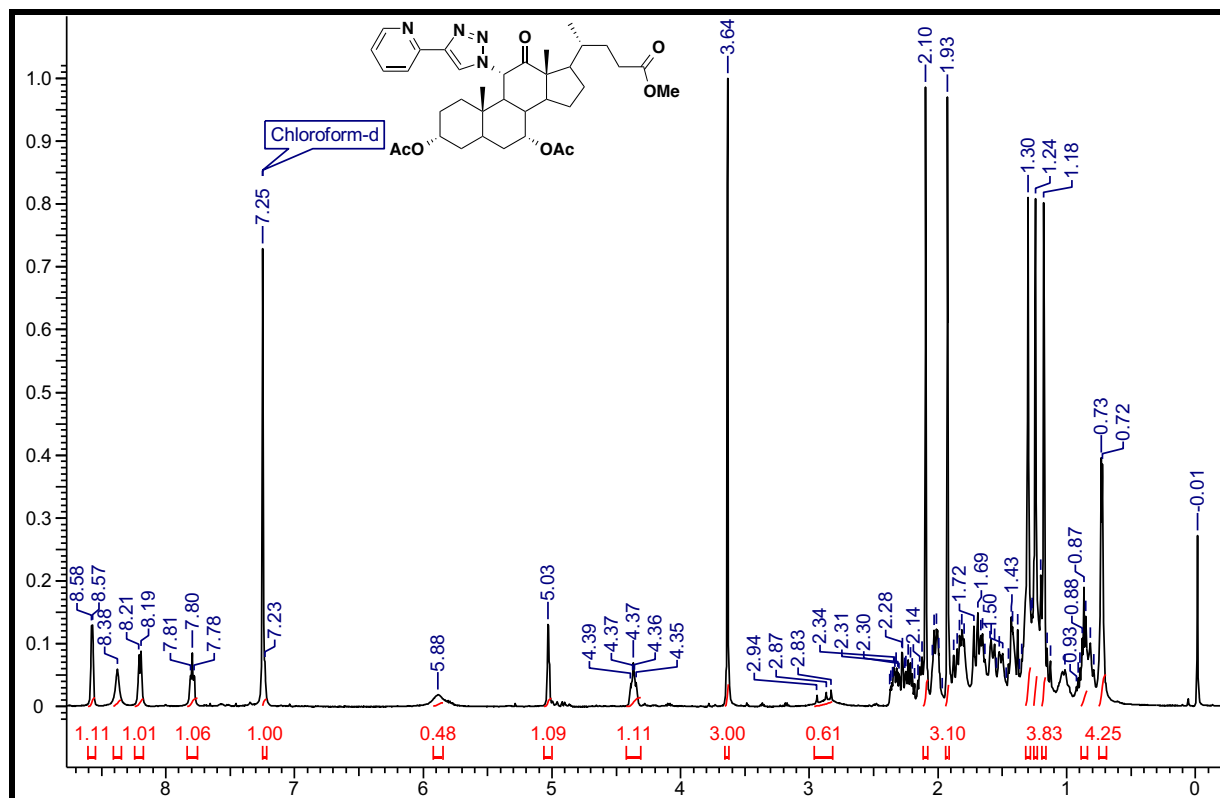
2.7 Selected NMR Spectras

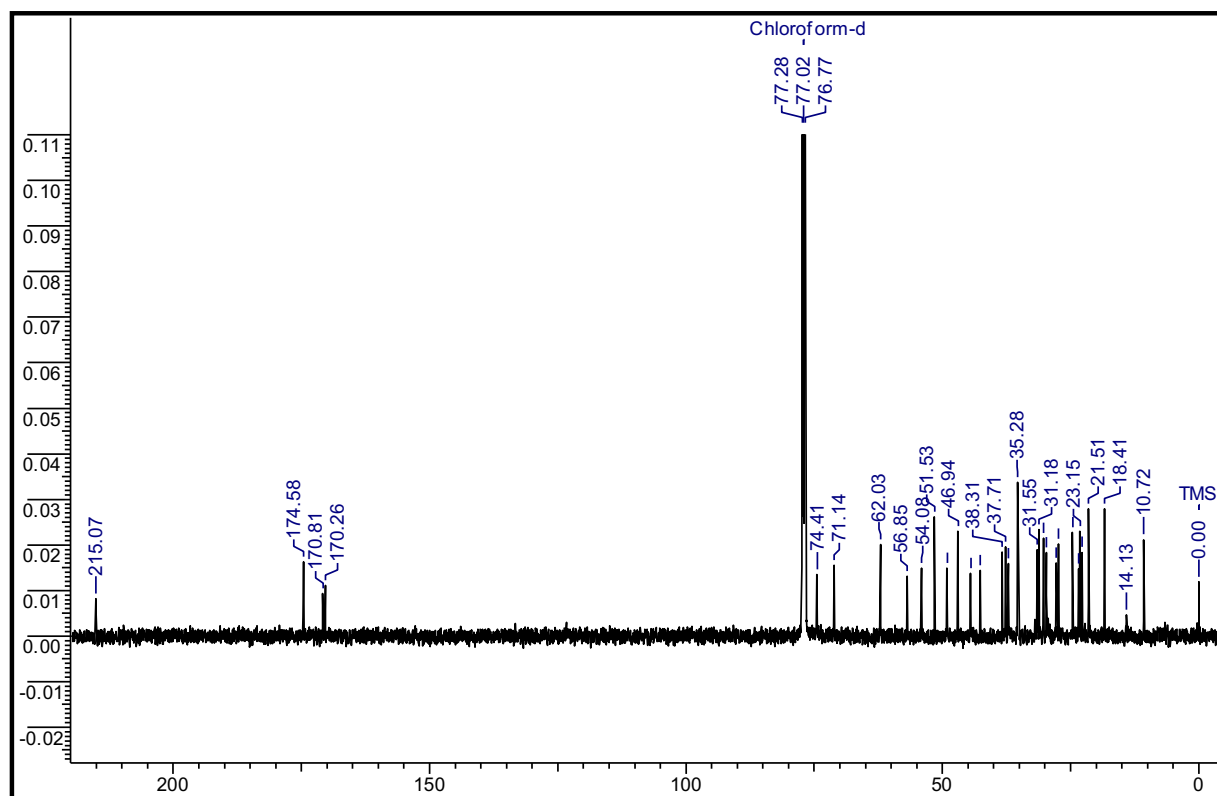
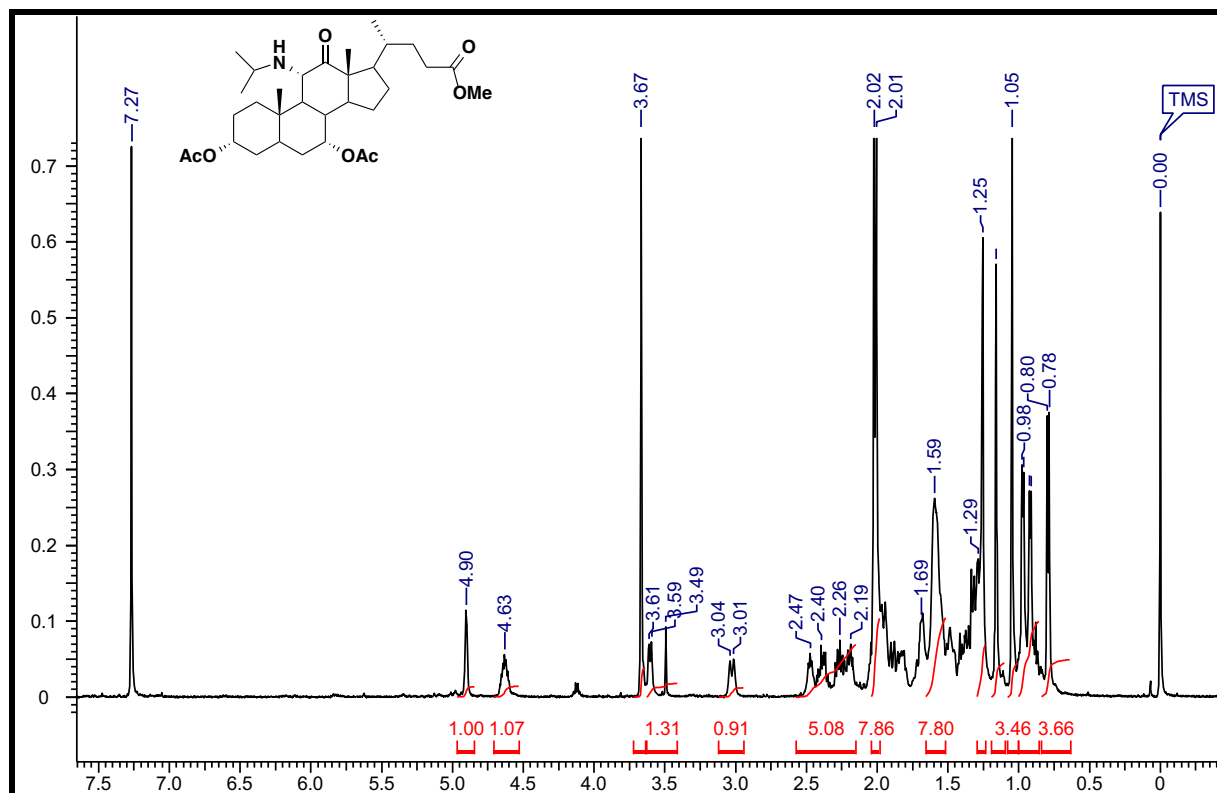
 ^1H NMR Spectra of 33 (200 MHz; CDCl_3)

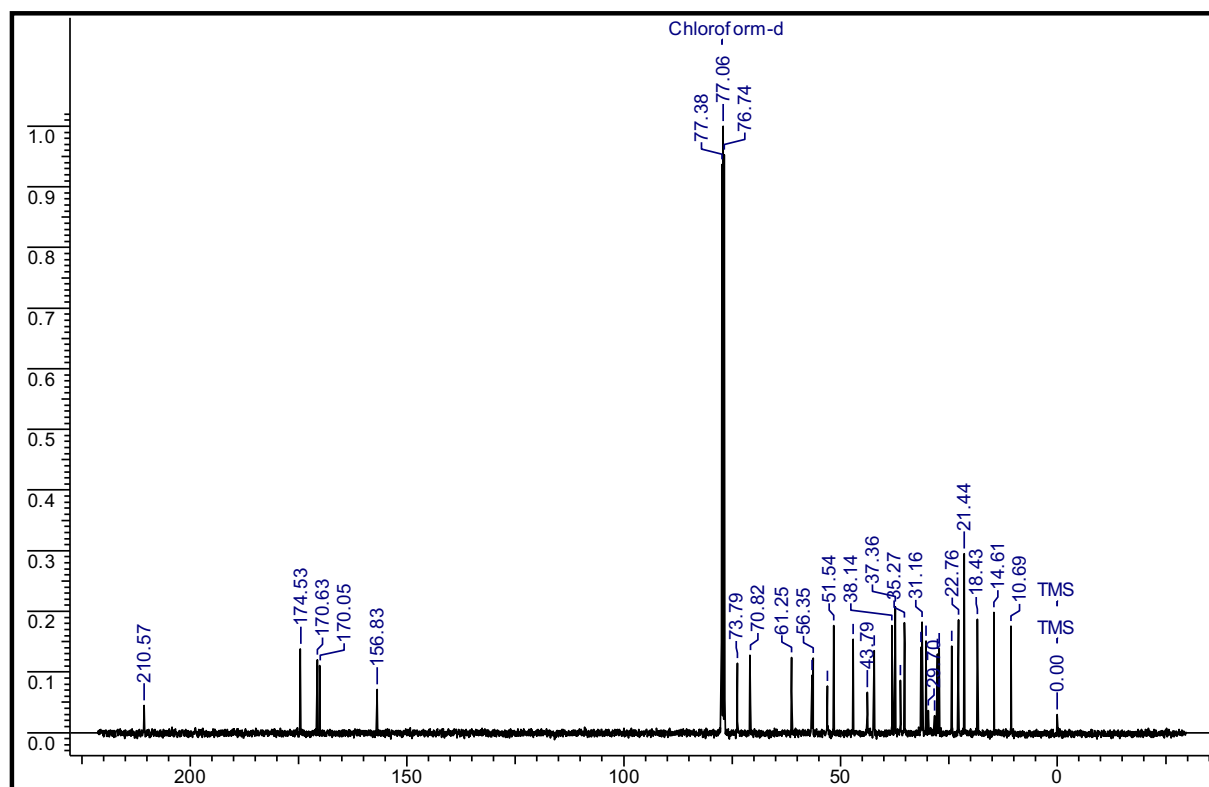
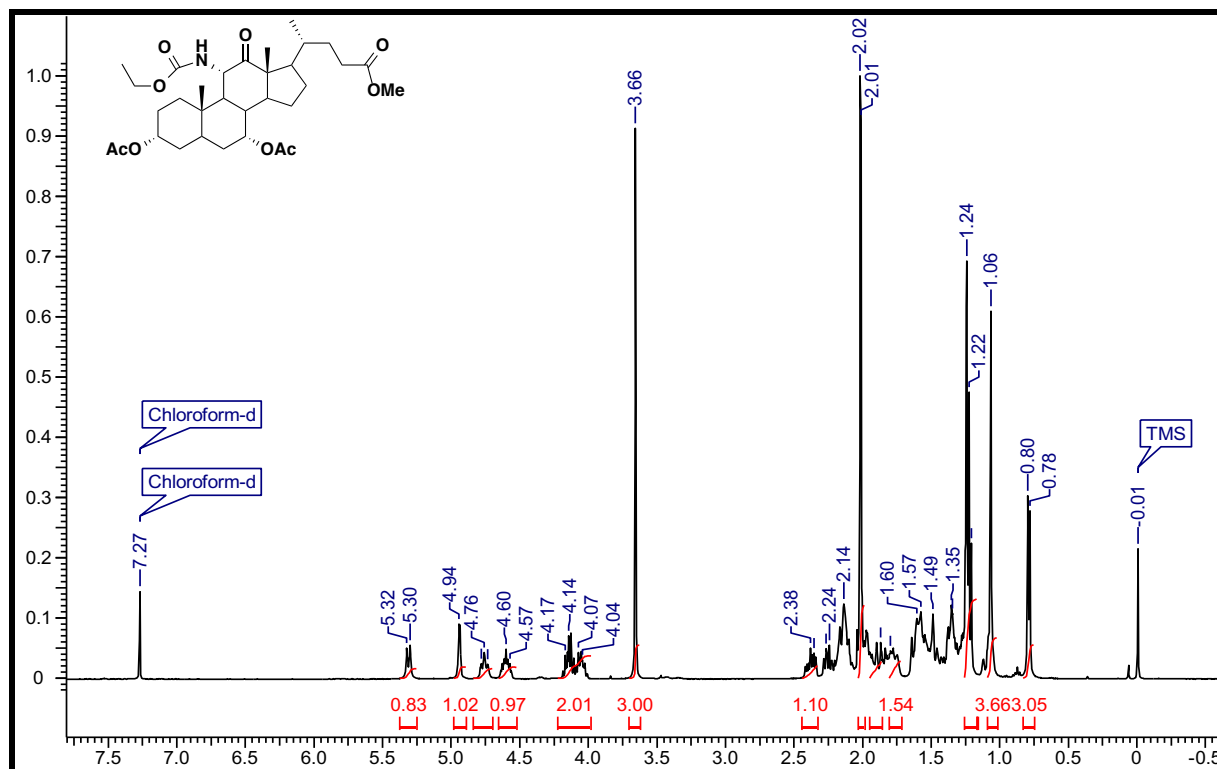
^1H and ^{13}C NMR of 36a (200 MHz, 101 MHz; CDCl_3)

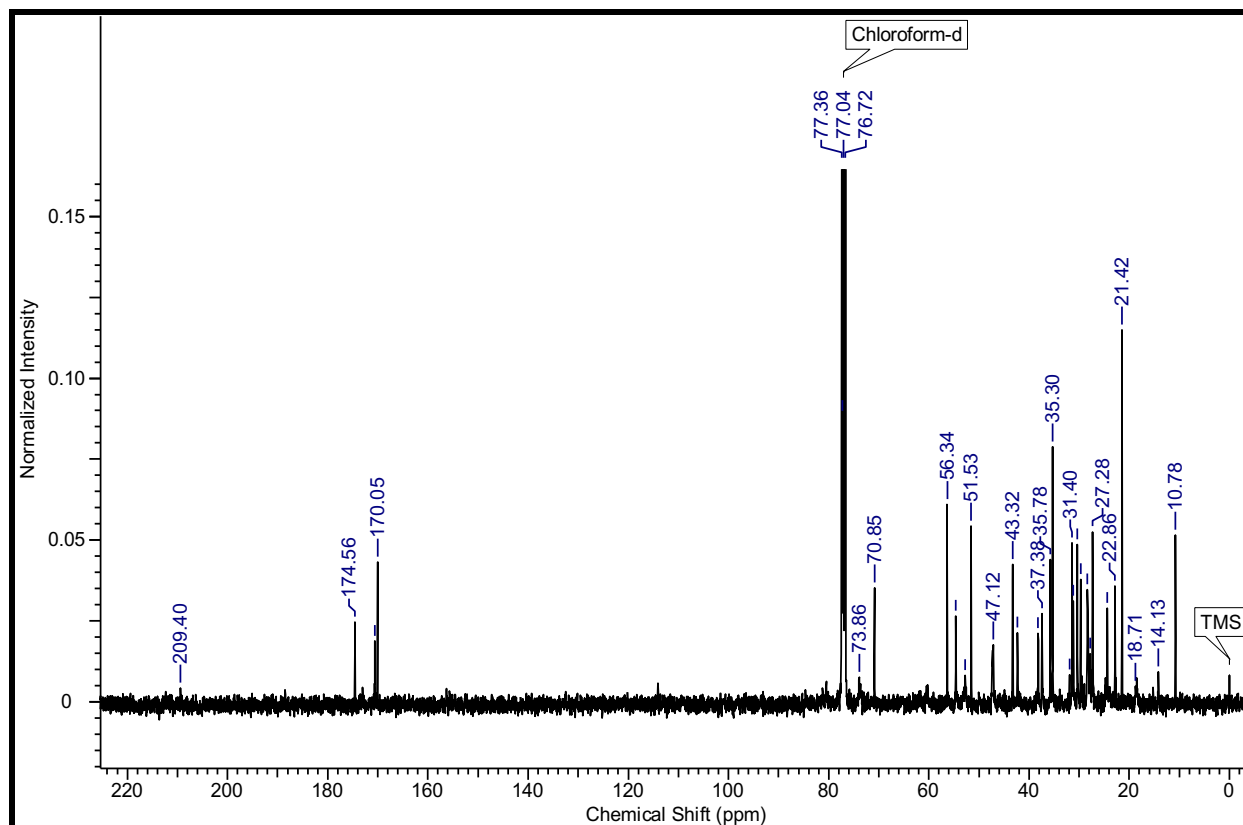
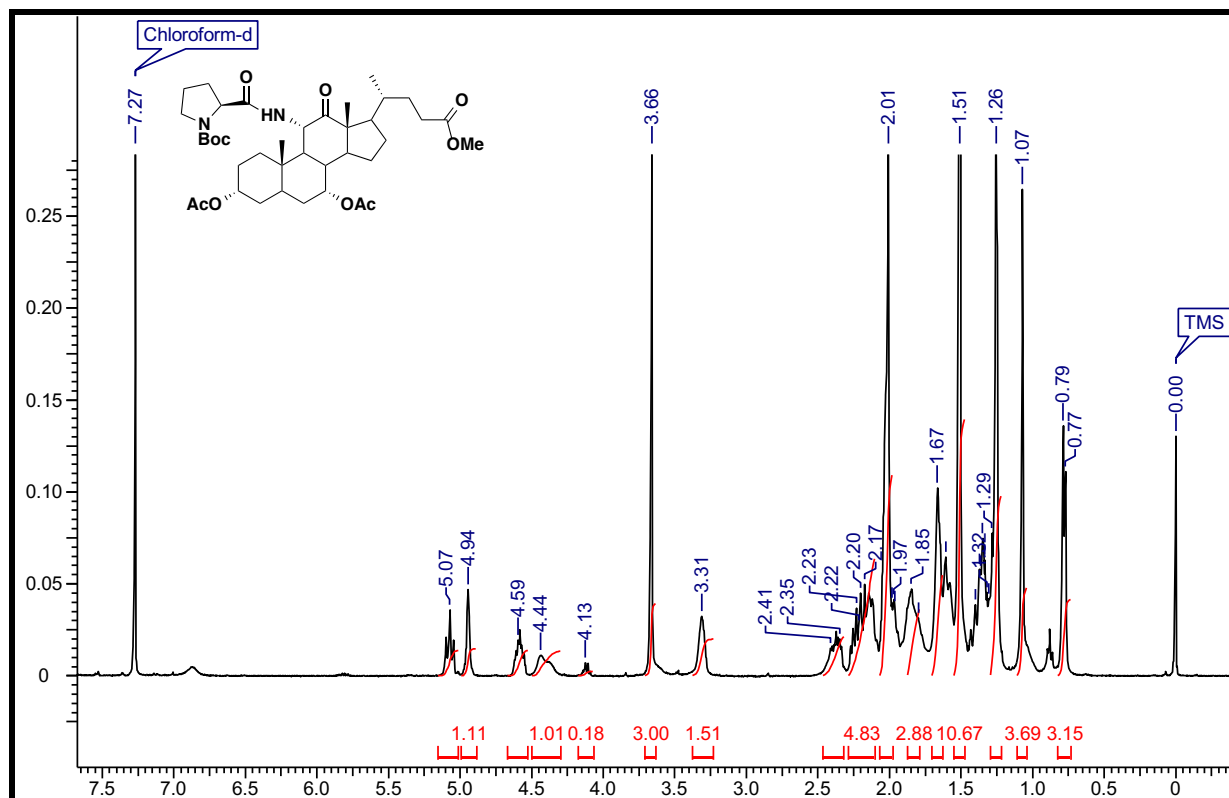
^1H and ^{13}C NMR of 36b (200 MHz, 101 MHz; CDCl_3)

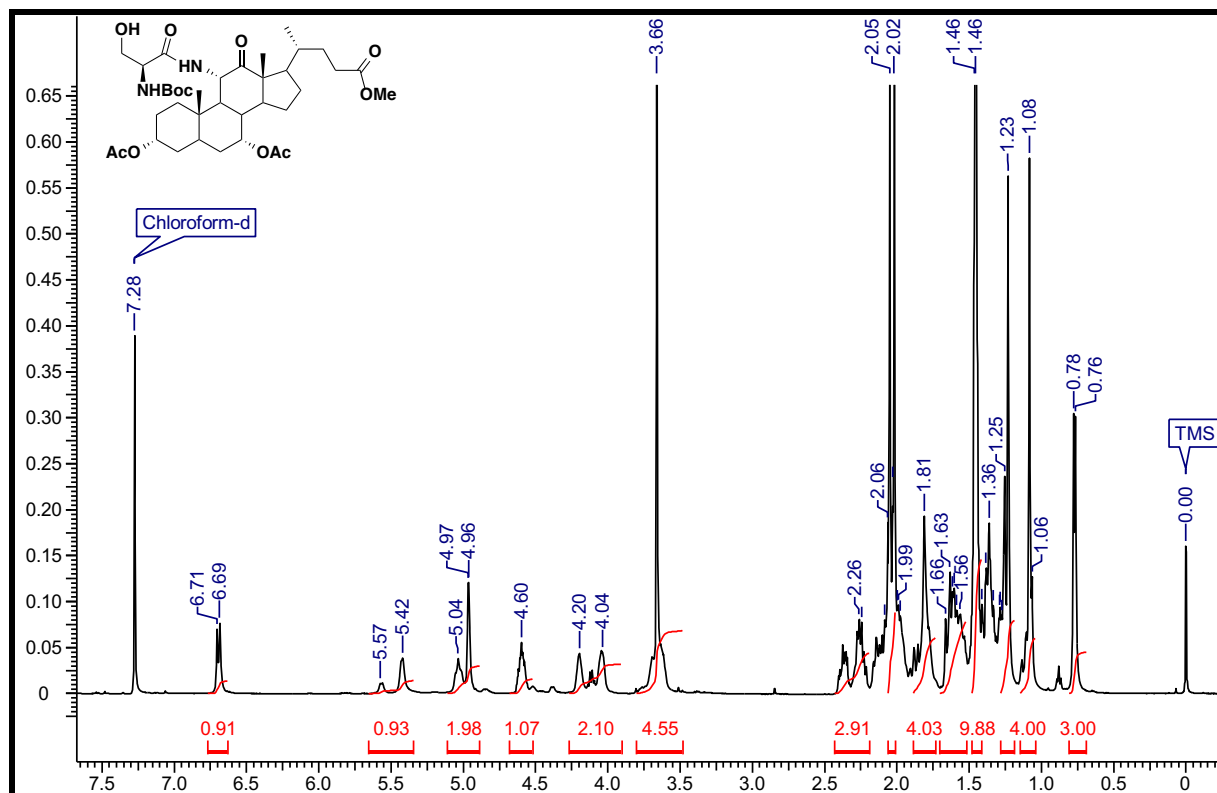
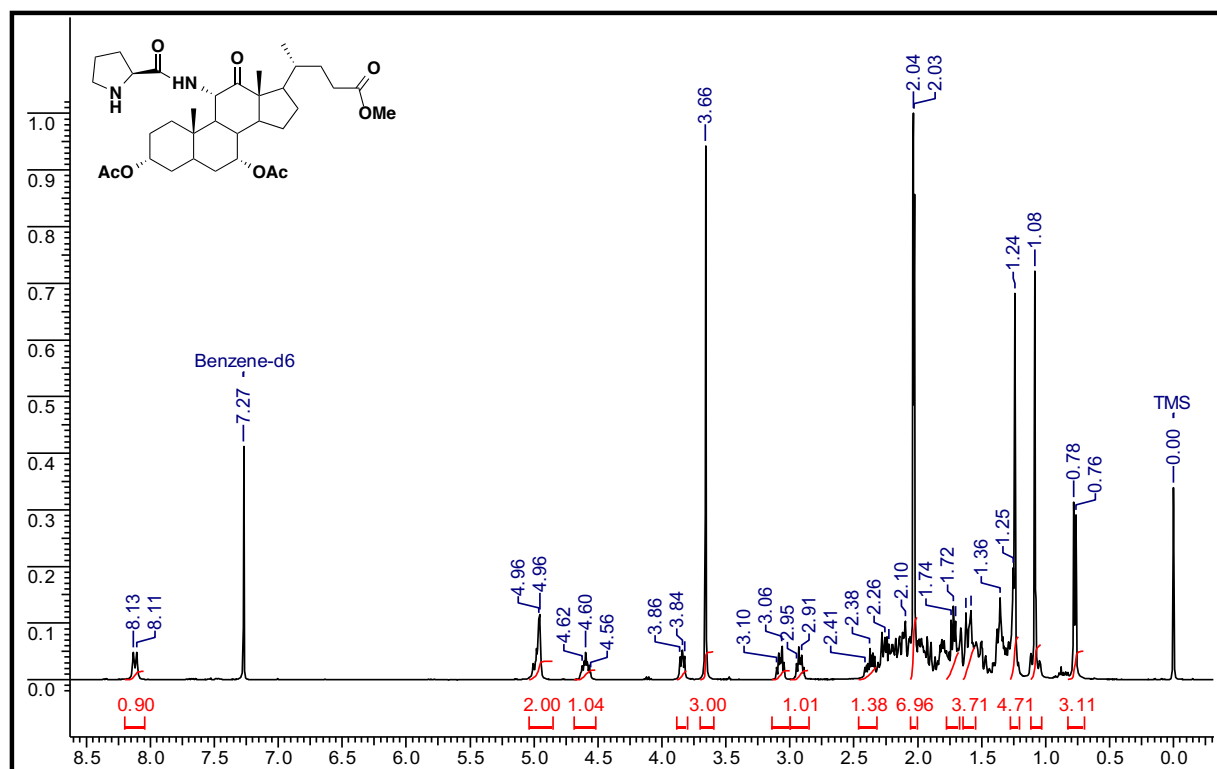
^1H and ^{13}C NMR of 36c (200 MHz, 101 MHz; CDCl_3)

^1H and ^{13}C NMR of 36d (200 MHz, 101 MHz; CDCl_3)

^1H and ^{13}C NMR of 41 (500 MHz, 101 MHz; CDCl_3)

^1H and ^{13}C NMR of 42 (200 MHz, 101 MHz; CDCl_3)

^1H and ^{13}C NMR of 43 (500 MHz, 101 MHz; CDCl_3)

¹H NMR of 44 (400 MHz; CDCl₃)**¹H NMR of 45 (200 MHz; CDCl₃)**

2.8 References

1. V. S. Pore, J. M. Divse, C. R. Charolkar, L. U. Nawale, V. M. Khedkar, D. Sarkar, *Bioorganic & medicinal chemistry letters*, **2015**, 25, 4185-4190.
2. (a) M. J. Genin, D. A. Allwine, D. J. Anderson, M. R. Barbachyn, D. E. Emmert, S. A. Garmon, D. R. Graber, K. C. Grega, J. B. Hester, D. K. Hutchinson, J. Morris, R. J. Reischer, C. W. Ford, G. E. Zurenko, C. J. Hamel, R. D. Schaadt, D. Stapert, B. H. Yagi; *J. Med. Chem.* **2000**, 43, 953; (b) H. Wamhoff, In *Comprehensive Heterocyclic Chemistry*; A. R. Katritzky, C. W. Rees, Eds.; Pergamon: Oxford, 1984; pp 669–732; (c) D. R. Buckle, C. J. M. Rockell, H. Smith, B. A. Spicer, *J. Med. Chem.* **1986**, 29, 2262; (d) R. Alvarez, S. Velazquez, A. San-Felix, S. Aquaro, E. De Clercq, C. F. Perno, A. Karlsson, J. Balzarini, M. J. Camarasa; *J. Med. Chem.* **1994**, 37, 4185.
3. (a) H. C. Kolb, K. B. Sharpless; *Drug Discov. Today*, **2003**, 8, 1128; (b) N. Nicolaus, J. Zapke, P. Riesterer, J. -M. Neud€orfl, A. Prokop, H. Oschkinat, H.-G. Schmalz, *Chem. Med. Chem.*, **2010**, 5, 661; (c) E. N. da Silva Jr., I. M. M. de Melo, E. B. T. Diogo, V. A. Costa, J. D. de Souza Filho, W. O. Valen~ca, C. A. Camara, R. N. de Oliveira, A. S. de Araujo, F. S. Emery, M. R. dos Santos, C. A. de Simone, R. F. S. Menna-Barreto, S. L. de Castro; *Eur. J. Med. Chem.*, **2012**, 52, 304; (d) M. G. Chini, R. De Simone, I. Bruno, R. Riccio, F. Dehm, C. Weinigel, D. Barz, O. Werz, G. Bifulco; *Eur. J. Med. Chem.*, **2012**, 54, 311; (e) V.F. Ferreira, D. R. da Rocha, F. C. da Silva, P. G. Ferreira, N. A. Boechat, J. L. Magalh~aes; *Expert Opin. Ther. Pat. Engl.*, **2013**, 23, 319; (f) S. N. Sunassee, C. G. L. Veale, N. Shunmoogam-Gounden, O. Osoniyi, D. T. Hendricks, M. R. Cairra, J. -A. de la Mare, A. L. Edkins, A. V. Pinto, E. N. da Silva Jr., M. T. Davies-Coleman; *Eur. J. Med. Chem.*, **2013**, 62, 98; (g) S. Terracciano, M. G. Chini, F. Dal Piaz, A. Vassallo, R. Riccio, I. Bruno, G. Bifulco, *Eur. J. Med. Chem.*, **2013**, 65, 464; (h) Z. -H. Huang, S. -T. Zhuo, C. -Y. Li, H. -T. Xie, D. Li, J. -H. Tan, T. -M. Ou, Z. -S. Huang, L. -Q. Gu, S. -L. Huang; *Eur. J. Med. Chem.*, **2013**, 68, 58; (i) B. Garudachari, A. M. Isloor, M. N. Satyanarayana, H. -K. Fun, G. Hegde; *Eur. J. Med. Chem.*, **2014**, 74, 324; (j) K. Pyta, K. Klich, J. Domagalska, P. Przybylski; *Eur. J. Med. Chem.*, **2014**, 84, 651; (k) P. K. Mandal; *RSC Adv.*, **2014**, 4, 5803.
4. (a) N. Applezweig; *Steroid Drugs*, McGraw-Hill Book Company, New York, **1962**; (b) F. J. Zeelen, *Medicinal Chemistry of Steroids*, Elsevier Science B. V: New York, **1990**.

5. U. Kerlo, M. Stahnke, P. E. Schulze, R. Wiechert; *Angew. Chem. Int. Ed. Engl.*, **1981**, 20, 88.
6. K. Pandya, D. Dietrich, J. Seibert, J. C. Vederas, A. Odermatt; *Bioorg. Med. Chem.*, **2013**, 21, 6274.
7. (a) D. K. Dalvie, A. S. Kalgutkar, S. C. Khojasteh-Bakht, R. S. Obach, J. P. O'Donnell; *Chem. Res. Toxicol*, **2002**, 15, 269; (b) W. S. Horne, M. K. Yadav, C. D. Stout, M. R. Ghadiri; *J. Am. Chem. Soc.*, **2004**, 126, 15366.
8. A. García, V. Bocanegra-García, J. P. Palma-Nicolás, G. Rivera; *Eur. J. Med. Chem.*, **2012**, 49, 1.
9. (a) M. Singh, A. Singh, S. Kundu, S. Bansal and A. Bajaj, *Biochim. Biophys. Acta, Biomembr.*, **2013**, 1828, 1926; (b) L. Huang, Y. Sun, H. Zhu, Y. Zhang, J. Xu and Y. Shen, *Steroids*, **2009**, 74, 701; (c) A. Gioiello, F. Venturoni, S. Tamimi, C. Custodi, R. Pellicciari and A. Macchiarulo, *Med.Chem.Comm.*, **2014**, 5, 750.
10. X. Lai, Y. Feng, J. Pollard, J. N. Chin, M. J. Bybak, R. Bucki, R. F. Epanand, R. M. Epanand and P. B. Savage, *Acc. Chem. Res.*, **2008**, 41, 1233.
11. A. P. Davis, R. P. Bonar-Law, J. K. M. Sanders, in *Comprehensive Supramolecular Chemistry* (Eds.: J. L., Atwood, J. E. D. Davies, D. D. Macnicol, F. Vögtle), Elsevier, Oxford, **1996**, vol. 4, pp. 257-286.
12. Nonappa, U.Maitra, *Org. Biomol. Chem.* **2008**, 6, 657-669.
13. J. Ropponen, J. Tamminen, E. Kolehmainen, K. Rissanen, *Synthesis* **2003**, 2226-2230.
14. A. F. Hofmann, *Ital. J. Gastroenterol.* **1995**, 27, 106-113.
15. A. J. Geall, D. Al-Hadithi, I. S. Blagbrough, *Chem. Commun.* **1998**, 2035-2036.
16. I. S. Blagbrough, D. Al-Hadithi, A. J. Geall, *Pharm. Pharmacol. Commun.* **1999**, 5, 139-144.
17. I. S. Blagbrough, D. Al-Hadithi, A. J. Geall, *Tetrahedron* **2000**, 56, 3439-3447.
18. A. J. Geall, D. Al-Hadithi, I. S. Blagbrough, *Bioconjugate Chem.* **2002**, 13, 481-490.
19. (a) H. Danielsson, In *The Bile Acids: Chemistry, Physiology and Metabolism* (eds P. P. Nair, and D. Kritchevsky,), Plenum Press, New York, 1973, vol. 2, pp. 1-32; (b) *The Bile Acids: Chemistry, Physiology and Metabolism* (eds P. P. Nair, and D. Kritchevsky,), Plenum Press, New York, 1971-73, vol. 1-3; (c) A. F. Hofmann; In *Bile Acids and Hepatobiliary Disease* (eds T. Northfield, P. L. Zentler-Munro, and R. P. Jazrawi,), Kluwer, Boston, 1999, pp. 303-332 and references therein; (d) M. C. Carey; In *Phospholipids and Atherosclerosis* (ed. P. Avogaro,), Raven Press, New York, 1983, pp. 33-63.

20. (a) A. F. Hofmann; In *The Liver: Biology and Pathology* (eds I. M. Arias et. al.), Raven Press, New York, 1994, 3rd edn, p. 677; (b) A. F. Hofmann; *News Physiol. Sci.*, 1999, 14, 24-29.
21. M. Stojančević et al.; *Frontiers in Life Science*, **2013**, Vol. 7, 3–4, 112–122.
22. A. Enhsen, W. Kramer, G. Wess, *Drug Discovery Today* **1998**, 3, 409-418.
23. A. F. Hofmann, in *Bile Acids in Hepatobiliary Disease* (Eds.: Northfield, T. C.; Ahmed, H.; Jazwari, R.; Zentler-Munro, P.), Kluwer Academic Publishers, Lancaster, Hardbound, **2000**, vol. 110a, p. 303-332.
24. J. Tamminen, E. Kolehmainen, *Molecules* **2001**, 6, 21-46.
25. X. -X. Zhu, M. Nichifor, *Acc. Chem. Res.* **2002**, 35, 539-546.
26. D. B. Salunke, B. G. Hazra, V. S. Pore, *Arkivoc* **2003**, ix, 115-125.
27. A. P. Davis, J.-B. Joos, *Coordination Chemistry Reviews* **2003**, 240, 143-156.
28. E. Virtanen, E. Kolehmainen, *Eur. J. Org. Chem.* **2004**, 3385-3399.
29. S. Mukhopadhyay, U. Maitra, *Curr. Sci.*, **2004**, 87, 1666-1683.
30. Y. Fujii, T. Kanamaru, H. Kikuchi, H. Nakagami, S. Yamashita, M. Akashi, S. Sakuma ; *Int J Pharm.*, **2011**, 421, 244–251.
31. Y. Chen, Y. Lu, J. Chen, J. Lai, J. Sun, F. Hu, W. Wu ; *Int J Pharm.*, **2009**, 376,153–160.
32. P. Guan, Y. Lu, J. Qi, M. Niu, R. Lian, F. Hu, W. Wu ; *Int J Nanomedicine.* **2011**. 6, 965–674.
33. D. Verzele, S. Figaroli, A. Maddar ; *Molecules*, **2011**, 16, 10168–10186.
34. W. Kramer ; *Biol Chem.* **2011**, 392, 77–94.
35. S. Tolle-Sander, K.A. Lentz, D.Y. Maeda, A. Coop, J.E. Polli ; *Mol. Pharm.* **2004**, 1, 40–48.
36. J.J. Criado, M.C. Herrera, M.F. Palomero, M. Medarde, E. Rodriguez, J.J. Marin ; *J Lipid Res.*, **1997**, 38, 1022–1032.
37. K. S. Moore, S. Wehrli, H. Roder, M. Rogers, J. N. Forrest, D. McCrimmon, M. Zasloff ; *Proceedings of the National Academy of Sciences of the United States of America.* **1993**, 90 1354–8.
38. S. Bansal, M. Singh, S. Kidwai, P. Bhargava, A. Singh, V. Sreekanth, R. Singh and A. Bajaj ; *Med. Chem. Commun.*, **2014**, 5, 1761–1768.
39. Antinarelli et. al., *Organic and Medicinal Chemistry Letters*, **2012**, 2, 16.
40. S. N. Bavikar et. al. / *Bioorg. Med. Chem. Lett.*, **2008**, 18, 5512–5517.

41. D. B. Salunke, B. G. Hazra, V. S. Pore, M. K. Bhat, P. B. Nahar, and M. V. Deshpande ; *J. Med. Chem.* **2004**, 47, 1591-1594.
42. J. J. Harburn, G. C. Loftus, B. A. Marples ; *Tetrahedron*, **1998**, 54, 11907- 11924.
43. D. B. Salunke, D. S. Ravi, V. S. Pore, D. Mitra, and B. G. Hazra ; *J. Med. Chem.* **2006**, 49, 2652-2655.
44. A. Alsayari, L. Kopel, M. Salama Ahmed, A. Pay, T. Carlson, F. T. Halaweish ; *Steroids*, **2017**, 118, 32–40.
45. R. V. Somu, H. Boshoff, C. Qiao, E. M. Bennett, C. E. Barry III, C. C. Aldrich, J. Med. Chem. 2006, 49, 31-34.
46. M. S. Costa, N. b. Boechat, E. A. Rangel, F. de C. da Silva, A. M. T. de Souza, C. R. Rodrigues, H. C. Castro, I. N. Junior, M. C. S. Lourenc, S. M. S. V. Wardell , V. F. Ferreira , *Bioorg. Med. Chem.* **2006**, 14, 8644–8653.
47. R. P. Tripathi, A. K. Yadav, A. Ajay, S. S. Bisht, V. Chaturvedi, S. K. Sinha, *Eur. J. Med. Chem.*, **2010**, 45 , 142-148.
48. K. Dabak, O. Sezer, A. Akar, O. Anac, *Eur. J. Med. Chem.* **2003**, 38, 215-218.
49. H. R. Ferhat Karabulut, S. A. Rashdan, J. R. Dias, *Tetrahedron* **2007**, 63, 5030-5035.
50. M. L. Conte, A. Marra, A. Chambery, S. S. Gurcha, G. S. Besra, A. Dondoni, *J. Org. Chem.* **2010**, 75, 6326–6336.
51. C. Gill, G. Jadhav, M. Shaikh, R. Kale, A. Ghawalkar, D. Nagargoje, M. Shiradkar *Bioorg. Med. Chem. Lett.* **2008**, 18, 6244–6247.
52. M. L. Conte, A. Marra, A. Chambery, S. S. Gurcha, G. S. Besra, A. Dondoni, *J. Org. Chem.* **2010**, 75, 6326–6336.
53. D. Kumar, Beena, G. Khare, S. Kidwai, A. K. Tyagi, R. Singh, D. S. Rawat, *Eur. J. Med. Chem.* **2014**, 81, 301-313.
54. C. Menendez, F. Rodriguez, A. L. Ribeiro, F. Zara, C. Frongia, V. Lobjois, N. Saffon, M. R. Pasca, C. Lherbet, M. Baltas, *Eur. J. Med. Chem.* **2013**, 69, 167-173.
55. (a) N. Applezweig, *Steroid Drugs*, McGraw-Hill Book Company, New York, 1962;
(b) F. J. Zeelen, *Medicinal Chemistry of Steroids*, Elsevier Science B. V: New York, 1990.
56. U. Kerlo, M. Stahnke, P. E. Schulze, R. Wiechert, *Angew. Chem. Int. Ed. Engl.*, **1981**, 20, 88.
57. (a) M. J. Genin, D. A. Allwine, D. J. Anderson, M. R. Barbachyn, D. E. Emmert, S. A. Garmon, D. R. Graber, K. C. Grega, J. B. Hester, D. K. Hutchinson, J. Morris, R. J. Reischer, C. W. Ford, G. E. Zurenko, C. J. Hamel, R. D. Schaadt, D. Stapert, B. H.

- Yagi; *J. Med. Chem.* **2000**, 43, 953; (b) H. Wamhoff, In *Comprehensive Heterocyclic Chemistry*; A. R. Katritzky, C. W. Rees, Eds.; Pergamon: Oxford, 1984; pp 669–732; (c) D. R. Buckle, C. J. M. Rockell, H. Smith, B. A. Spicer, *J. Med. Chem.* **1986**, 29, 2262; (d) R. Alvarez, S. Velazquez, A. San-Felix, S. Aquaro, E. De Clercq, C. F. Perno, A. Karlsson, J. Balzarini, M. J. Camarasa; *J. Med. Chem.* **1994**, 37, 4185.
58. (a) H. C. Kolb, K. B. Sharpless; *Drug Discov. Today*, 2003, 8, 1128; (b) N. Nicolaus, J. Zapke, P. Riesterer, J. -M. Neudörfl, A. Prokop, H. Oschkinat, H.-G. Schmalz, *Chem. Med. Chem.*, **2010**, 5, 661; (c) E. N. da Silva Jr., I. M. M. de Melo, E. B. T. Diogo, V. A. Costa, J. D. de Souza Filho, W. O. Valença, C. A. Camara, R. N. de Oliveira, A. S. de Araujo, F. S. Emery, M. R. dos Santos, C. A. de Simone, R. F. S. Menna-Barreto, S. L. de Castro; *Eur. J. Med. Chem.*, **2012**, 52, 304; (d) M. G. Chini, R. De Simone, I. Bruno, R. Riccio, F. Dehm, C. Weinigel, D. Barz, O. Werz, G. Bifulco; *Eur. J. Med. Chem.*, **2012**, 54, 311; (e) V.F. Ferreira, D. R. da Rocha, F. C. da Silva, P. G. Ferreira, N. A. Boechat, J. L. Magalhães; *Expert Opin. Ther. Pat. Engl.*, **2013**, 23, 319; (f) S. N. Sunassee, C. G. L. Veale, N. Shunmoogam-Gounden, O. Osoniyi, D. T. Hendricks, M. R. Caira, J. -A. de la Mare, A. L. Edkins, A. V. Pinto, E. N. da Silva Jr., M. T. Davies-Coleman; *Eur. J. Med. Chem.*, **2013**, 62, 98; (g) S. Terracciano, M. G. Chini, F. Dal Piaz, A. Vassallo, R. Riccio, I. Bruno, G. Bifulco, *Eur. J. Med. Chem.*, **2013**, 65, 464; (h) Z. -H. Huang, S. -T. Zhuo, C. -Y. Li, H. -T. Xie, D. Li, J. -H. Tan, T. -M. Ou, Z. -S. Huang, L. -Q. Gu, S. -L. Huang; *Eur. J. Med. Chem.*, **2013**, 68, 58; (i) B. Garudachari, A. M. Isloor, M. N. Satyanarayana, H. -K. Fun, G. Hegde; *Eur. J. Med. Chem.*, **2014**, 74, 324; (j) K. Pyta, K. Klich, J. Domagalska, P. Przybylski; *Eur. J. Med. Chem.*, **2014**, 84, 651; (k) P. K. Mandal; *RSC Adv.*, **2014**, 4, 5803.
59. (a) V. S. Pore, N. G. Aher, M. Kumar, P. K. Shukla, *Tetrahedron*, **2006**, 62, 11178; (b) B. G. Hazra, N. S. Vatmurge, V. S. Pore, F. Shirazi, P. S. Chavan, M. V. Deshpande, *Bioorg. Med. Chem. Lett.*, **2008**, 18, 2043; (c) N. S. Vatmurge, B. G. Hazra, V. S. Pore, F. Shirazi, M. V. Deshpande, S. Kadreppa, S. Chattopadhyay, *Org. Biomol. Chem.*, **2008**, 6, 3823; (d) S. N. Bavikar, D. B. Salunke, B. G. Hazra, V. S. Pore, R. H. Dodd, J. Thierry, F. Shirazi, M. V. Deshpande, S. Kadreppa, S. Chattopadhyay, *Bioorg. Med. Chem. Lett.*, **2008**, 18, 5512; (e) N. G. Aher, V. S. Pore, G. B. Shiva Keshava, A. Kumar, N. N. Mishra, P. K. Shukla, A. Sharma, M. K. Bhat, *Bioorg. Med. Chem. Lett.*, **2009**, 19, 759.

60. (a) D. B. Salunke, B. G. Hazra, R. G. Gonnade, M. M. Bhadbhade, V. S. Pore, *Tetrahedron*, **2005**, 61, 3605; (b) D. B. Salunke, D. S. Ravi, V. S. Pore, D. Mitra, B. G. Hazra, *J. Med. Chem.*, **2006**, 49, 2652.
61. J. P. Dzoyem, S. K. Guru, C. A. Pieme, V. Kuete, A. Sharma, I. A. Khan, A. K. Saxena, R. A. Vishwakarma, *BMC Complement. Alternat. Med.*, **2013**, 13, 78.
62. D. Sarkar, U. Singh, *J. Microbiol. Methods*. **2011**, 84, 202.
63. (a) A. Khan, S. Sarkar, D. Sarkar, *Int. J. Antimicrob. Agents.*, **2008**, 32, 40; b) S. Sarkar, D. Sarkar, *J. Biomol. Screen.*, **2012**, 17, 966.
64. S. A. Stanley, S. S. Grant, T. Kawate, N. Iwase, M. Shimizu, C. Wivagg, M. Silvis, E. Kazyanskaya, J. Aquadro, A. Golas, M. Fitzgerald, H. Dai, L. Zhang, D. T. Hung, *ACS Chem. Biol.*, **2012**, 7, 1377.
65. G. Riccardi, M. R. Pasca, L. R. Chiarelli, G. Manina, A. Mattevi, C. Binda, *Appl. Microbiol. Biotechnol.*, **2013**, 97, 8841.
66. A. A. Loosdrecht, van de, R. H. Beelen, G. I. Ossenkoppele, M. G. Broekhoven, M. M. Langenhuijsen, *J. Immunol. Methods*, **1994**, 174, 311.
67. M. C. Alley, D. A. Scudiere, A. Monks, M. L. Hursey, M. J. Czerwinski, D. L. Fine, B. J. Abbott, J. G. Mayo, R. H. Shoemaker, M. R. Boyd, *Cancer Res.*, **1988**, 48, 589.
68. G. Riccardi, M. R. Pasca, L. R. Chiarelli, G. Manina, A. Mattevi, C. Binda, *Appl. Microbiol. Biotechnol.*, **2013**, 97, 8841.
69. B.A. Wolucka, *FEBS Journal* , **2008**, 275, 2691.
70. P. K. Crellin, R. Brammananth, R. L. Coppel, *PLoS ONE*, **2011**, 6, e16869.
71. F. Mir, S. Shafi, M.S. Zaman, N. P. Kalia, V. S. Rajput, C. Mulakayala, N. Mulakayala, I. A. Khan, M. S. Alam, *Eur. J. Med. Chem.* **2014**, 76, 274.

Chapter 3

Cholic acid based *trans*-4-hydroxy-(L)- proline derivative as recyclable organocatalyst for highly *diastereo*- and *enantioselective* asymmetric direct aldol reactions in water

Chapter 3

Cholic acid based *trans*-4-hydroxy-(L)- proline derivative as recyclable organocatalyst for highly *diastereo*- and *enantioselective* asymmetric direct aldol reactions in water

3.1 Abstract

A new cholic acid derived organocatalyst is prepared by linking it with *trans*-4-hydroxy-L-proline through 1, 2, 3-triazole using click reaction. The resulting catalyst was found to be most active against asymmetric direct aldol reaction between *para*-nitro benzaldehyde and cyclohexanone in water without the need for organic solvents and toxic co-catalysts and additives. The results obtained were excellent giving diastereoselectivity *up to* 99:1 and *up to* >99% *ee* in comparatively lesser time using 10 mol % of the catalyst. Low catalyst loading *i.e.*, just 1 mol % of the catalyst was also found efficient regarding enantioselectivity for *para*-nitrobenzaldehyde and cyclohexanone. Furthermore, the catalyst can be recycled at least three times without substantial loss in catalytic activity.

3.2 Introduction

Wurtz first discovered the aldol reaction in 1872,¹ it is one of the most powerful transformations in organic chemistry. The process combines two carbonyl partners to give β -hydroxyketones with up to two new stereocenters (Figure. 1). Aldol condensation plays an important role in nature as a source of carbohydrates and is used for the synthesis of chiral hydroxy carbonyl compounds or α , β -unsaturated ketones, which in turn have great potential as valuable intermediates in organic synthesis.² Proper design of acid-base catalysis has been shown to be effective for achieving high reactivity and selectivity in the asymmetric aldol reaction. There have been numerous reports on small-molecule catalyzed direct aldol reactions.³ The discovery of the versatile catalytic nature of L-proline² occurring via enamine intermediates has undoubtedly been the biggest breakthrough in this field of research. The acidic part of amino acid catalysts seems to be largely responsible for rapidly promoting the steps of enamine and carbon-carbon bond formation. The excellent enantioselectivity of proline as a catalyst can be accounted for due to the formation of a highly organized transition state with a systematic framework of hydrogen bonding.

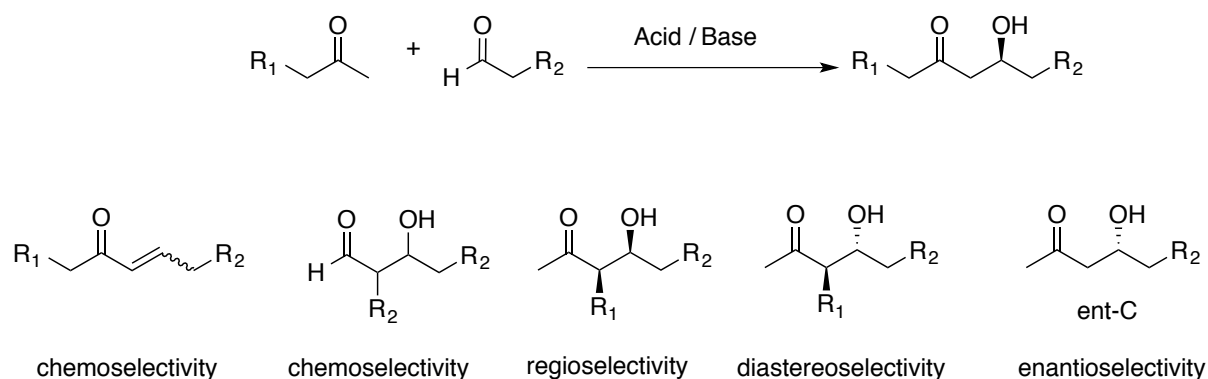


Figure 1. Aldol reaction between aliphatic ketones and aldehydes

A slight modification in the catalyst structure may change the pK_a value of the catalyst affecting the strength of hydrogen bonding to such an extent that a high degree of enhancement of the catalytic activity coupled with stereoselectivity could be observed.⁴ There is a report on chloride salts from group 12 elements (Zn, Cd, Hg) as co-catalyst leading to the highest stereoselectivities.⁵

3.3 Review of Literature

Asymmetric aldol reactions are a robust way for the construction of carbon–carbon bonds in an enantioselective manner. Previously, this reaction has been performed in a stoichiometric manner to control the multiple aspects of *chemo*-, *diastereo*-, *regio*- and enantioselectivity. Nevertheless, a more atom economical approach would strengthen high selectivity with the use of only a catalytic amount of a chiral promoter.⁶ There are so many reports on aldol reactions carried out by different types of acids, bases, enzymes,⁷ catalytic antibodies⁸ and small molecules,^{9–11} but we will only highlight here few proline based catalysts for direct aldol reactions.

3.3.1 Proline-based catalyst for direct aldol reactions.

Hajos–Parrish–Eder–Sauer–Wiechert published the first report of direct asymmetric aldol reaction catalyzed by a small molecule in 1971 (Figure. 2).^{12,13} The reaction was known as Hajos–Parrish–Eder–Sauer–Wiechert cyclization. Only 3mol % of proline was required to proceed this intramolecular aldol cyclization product (Figure. 2) in excellent yield and enantioselectivity. Unfortunately, both the yield and the enantioselectivity was found to be reduced for the 6-membered ring substrate (Figure. 2). Amino acids such as proline are particularly appealing catalysts, due to their natural abundance and low cost. List and co-workers first described the first intermolecular proline-catalyzed direct aldol reaction

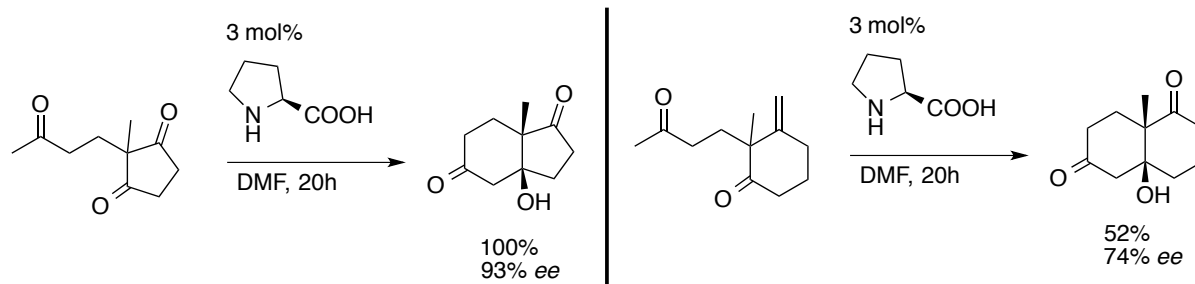


Figure 2. Intramolecular aldol cyclization reaction

in 2000¹⁴, Using 20–30 mol% L-proline in a 4:1 solution of DMSO: acetone, the desired aldol products were obtained. Aromatic aldehydes were proved to be good substrates for this reaction, as were branched aliphatic substrates, which gave the highest yields and enantioselectivities. Whereas, results found to be low to moderate regarding yields and enantioselectivities were observed for α -unbranched aldehydes after harmonizing of the reaction conditions to prevent aldehyde self-condensation.¹⁵ They screened several catalysts for the asymmetric aldol of acetone with *p*-nitrobenzaldehyde demonstrated the effect of many different modifications of the proline structure (Figure 3). Primary amino acids histidine and phenylalanine were inferior to the derivatives of proline. Changing the carboxylic acid to an amide provide little reactivity. The thiazolidine carboxylate worked similar to proline, though slightly inferior results. Interestingly, *trans*-hydroxyproline gave a higher yield and enantioselectivity than proline itself. The *tert*-butyl ether derivative gave lower yield and enantioselectivity, as did the acylated derivative, though to a lesser extent.

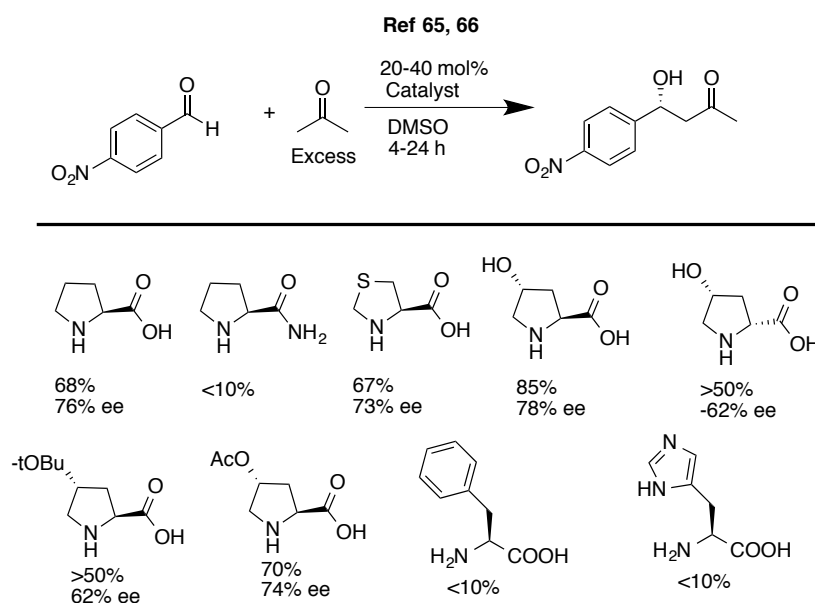


Figure 3. Aldol reaction between *p*-nitrobenzaldehyde and acetone

Whereas, *cis*-hydroxyproline provided the opposite enantiomer, with reduced yield and selectivity.^{14,15}

Lots of research has explained the mechanism of the proline-catalyzed aldol reaction, (Figure 4).^{12,16,17} The accepted mechanism for the intermolecular process starts with the rate-limiting enamine formation (A), followed by the addition of carbonyl compound, activated by the carboxylic acid group of proline (B). The rearrangement of stable six membered intermediate (B) into iminium ion (C) was followed by hydrolysis (C) to give desired aldol product. The addition step has almost similar energy barrier as the enamine formation, showing that under different conditions or with different substrates, the rate-determining step may be the addition step.

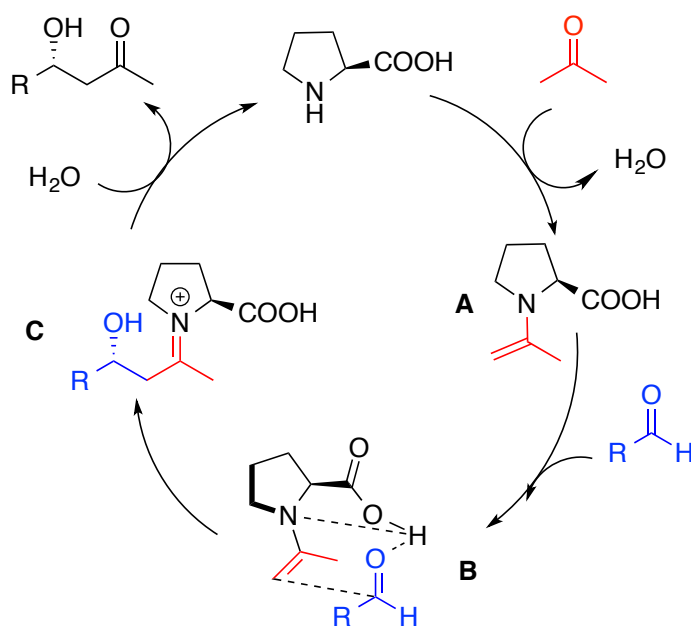


Figure 4. Proposed mechanism of direct aldol reaction

Several other amino acids and peptides have been evaluated as alternate catalysts for the direct catalytic asymmetric aldol reaction.¹⁸⁻²⁷ The reaction between acetone and *p*-nitrobenzaldehyde has been used as a model reaction to evaluate the catalyst and to compare the performance of the multitude of available catalysts. Among the amino acids and peptides screened, L-Pro-L-Pro-L-Asp-NH₂, reported by Wennemers and co-workers, gave the best outcomes.²⁶ The catalyst loading was significantly decreased to 1 mol% to provide the desired *anti*-aldol product in 99% yield and 80% *ee* after 4 hours, using acetone in the excess amount. This catalyst was found to be effective as compared to other reported amino acids

and peptides. Interestingly, it was found that this catalyst furnishes the opposite enantiomer, *i.e.* *syn*-isomer than that obtained *via* proline catalysis.

Several modifications have been developed based on the structure of proline (Figure 5). Some are done by increasing the hydrophobicity to improve solubility in organic solvents and modification of the carboxylic acid with a variation of other hydrogen-bonding groups. Other modifications involve adding stereocenters and steric bulk to improve the enantioselectivity.

Zhao *et al.*²⁹ found *trans*-hydroxy-L-proline derivative to be an efficient catalyst with impressive results. Similarly, G. D. Yadav and S. Singh found excellent results regarding reactivity and found diastereoselectivity up to 100:0, which was really impressive.³⁰ Apart from these, Yu Kong³¹ and Kwang Soo Lee³² developed a proline based catalyst which was supported on magnetic nanoparticle and other worked as self assembled nanotube respectively (Figure 5).

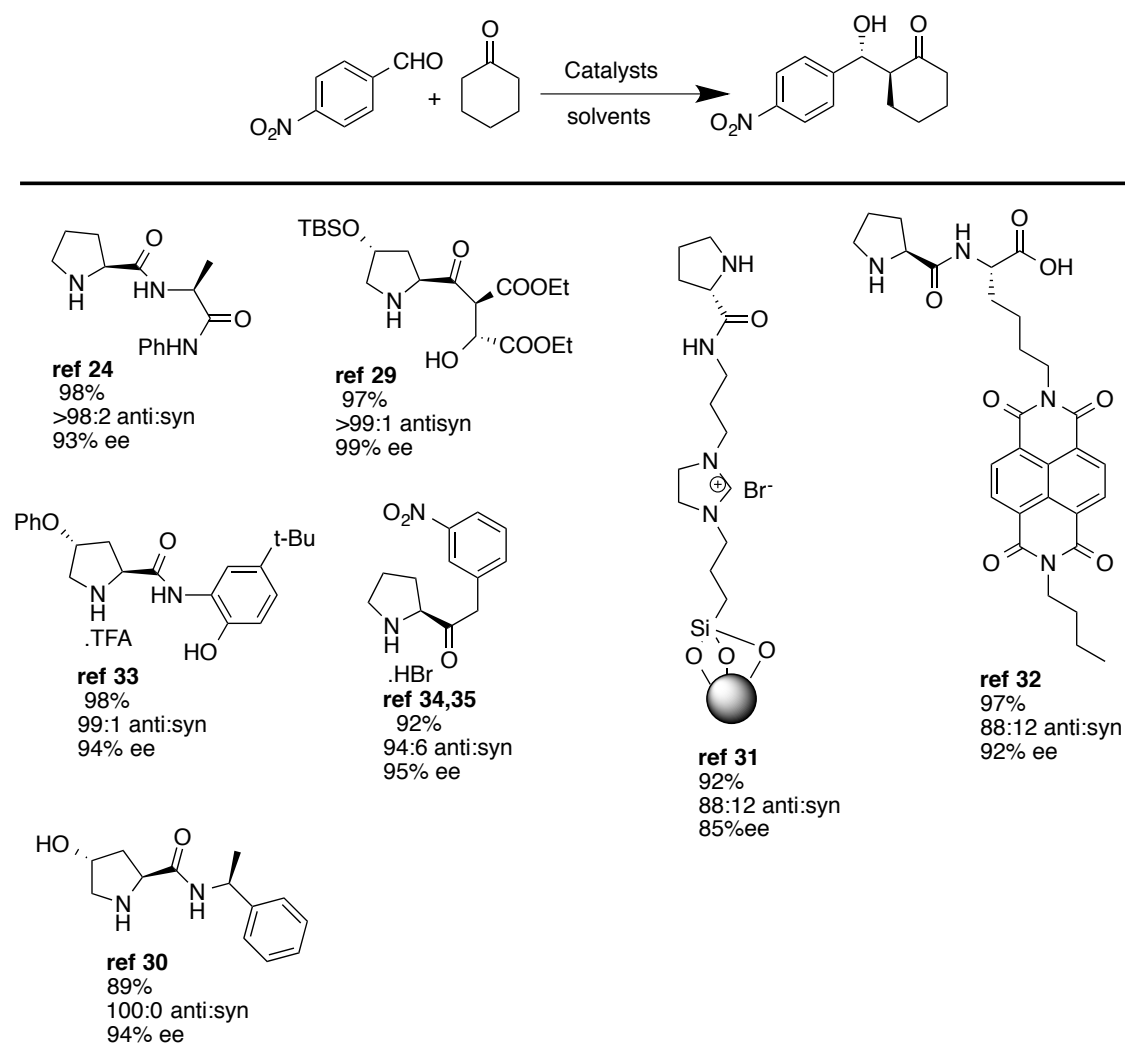


Figure 5. Aldol reaction between *p*-nitrobenzaldehyde and cyclohexanone

Hayashi and co-workers reported a series of proline-surfactant conjugates such as **4** and **5** as organocatalysts for asymmetric aldol reactions.³⁶ There is a report on proline-cholesterol and proline-diosgenin conjugates, as amphiphilic catalysts for highly stereoselective direct aldol reactions between hydrophobic reagents in water.³⁷ Fu *et al.* have replaced carboxylic group in 4-*tert*-butyldimethylsilyloxy proline (**4c**) with sulphonamides and used them for this reactions to get very high enantiomeric excess.³⁸ Attachment of proline at different positions of bile acids (C-3, C-7 or C-12) resulted in the synthesis of organocatalysts **6a-9c** with very low enantioselectivity (Figure 6).³⁹

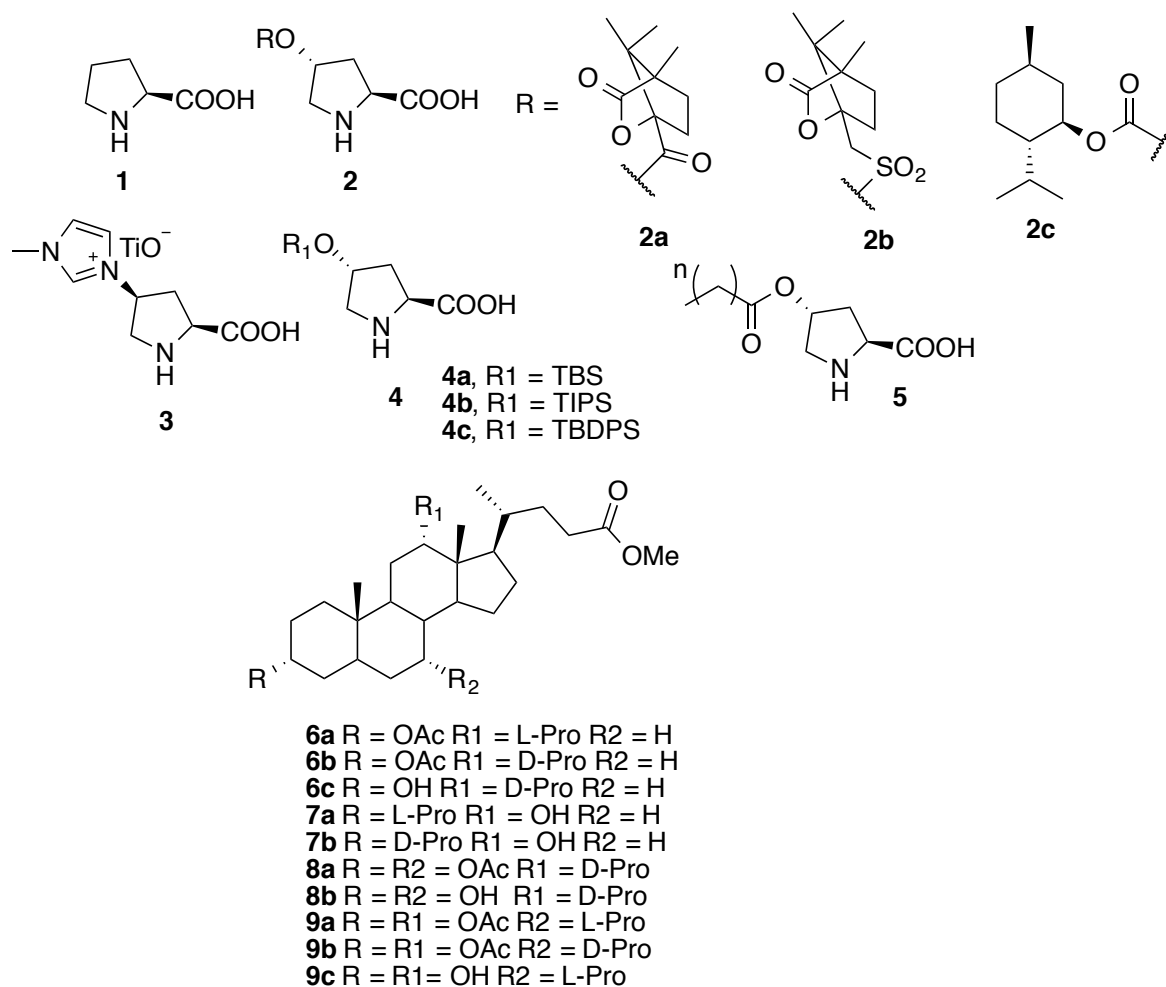


Figure 6. Structure of proline derived organocatalyst.

Unfortunately, proline may not be convenient for many reactions because of its low solubility in number of solvents. 4-Substituted proline such as **2a**, **2b** and **2c** gave much greater enantiomeric excesses and low catalyst loading due to improved solubility of the catalyst in comparison to proline in aldol reactions.⁴⁰ Direct asymmetric α -amination of unmodified aldehydes with azodicarboxylates in ionic liquids in the presence of 4-

imidazolium ion-tagged L-proline recyclable organocatalyst **3** has been reported to furnish excellent enantioselectivities coupled with high chemical yields.⁴¹ There is a report on polystyrene supported 4-hydroxyproline as an insoluble, recyclable organocatalyst for the asymmetric aldol reaction in water.⁴²

Puleo *et al*⁴³ have derived organocatalyst based on bile acids like cholic and deoxycholic acid by linking it to L- or D-proline at various positions i.e 3, 7 and 12 on bile acids (Figure 6). They have observed the best results when D- prolinamide moiety was linked at 12- position of steroid skeleton **8b** with ee upto 80% in 48 hrs using DMF: Water as solvent. Proline catalyzed asymmetric aldol reactions are usually carried out in polar solvents such as DMSO or DMF. However, since the use of water as a solvent is highly beneficial for the reaction and enantioselectivity.

There are several reports in which water is used as a solvent for direct aldol reaction, but there were addition of toxic co-catalysts or harmful additives also were added in almost all the cases. Undesired formation of α , β -unsaturated products arised from dehydration of aldol have also been eliminated by using aqueous solvent, which also directly increases the yield of desired aldol. Bearing this in mind, to reduce the longer duration of the reaction, use of eco-friendly solvent and to increase enantiomeric excess, we designed our organocatalyst in such a way that it will coordinate effortlessly in water only, and gives out the best enantioselectivity and diastereoselectivity in a possible shorter duration.

One of the limitations of these catalysts is that they require various steps for their preparation which makes them expensive. Proline, on the opposite hand, is abundant and cheap, and therefore design and synthesis of the new catalyst which may include proline/hydroxy-proline must be cheaper and easier without compromising selectivity and reactivity.

3.4 Present work

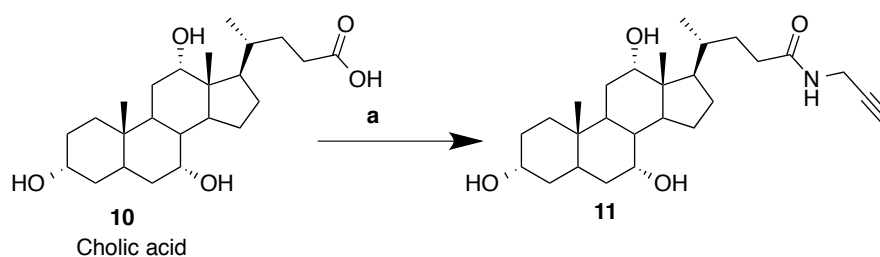
3.4.1 Objective

All the proline organocatalysts discussed above have some drawbacks or limitations regarding yield, enantioselectivity or diastereoselectivity. The synthesis of these catalysts are either highly tedious or require longer reaction time for their preparation. Catalyst loading or quantitative amount of catalysts itself is needed for excellent results. Mostly, the effect of solvents also severely alter the results, similarly use of organic solvents and toxic additives or co-catalysts harms the way of green chemistry. Catalyst reusability is also a big question in

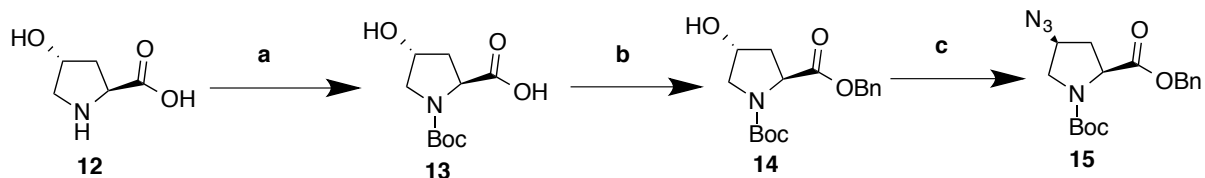
front of chemists, because it needs plenty of solvents and time to extract and reactivation. Hence, many problems need to be solved, and there is still a scope for improvement. Therefore, we endeavoured to develop a new cholic acid based organocatalyst which may overcome the limitations which were described previously. The reasons for which we have selected cholic acid is that it has a rigid backbone which already contains hydrophilic and hydrophobic moiety which can help in increasing the hydrogen bonding in polar solvents and also better interaction with the reactants because of its chiral structure.

3.4.2 Results and Discussion

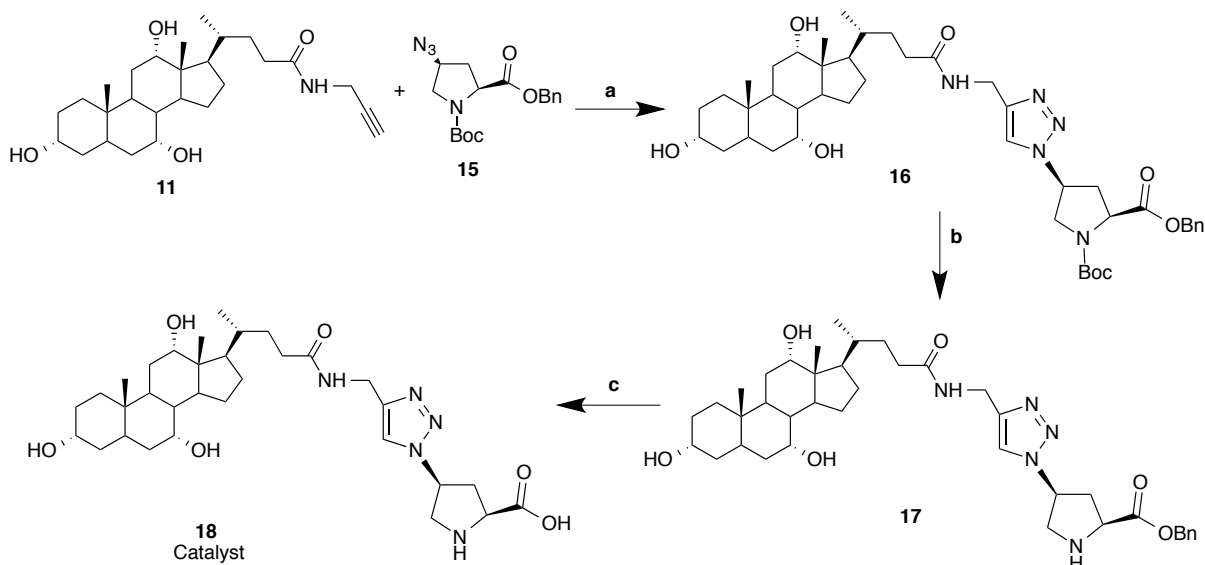
One of the primary objectives of green chemistry is to use environmentally benign solvents and catalysts, and this purpose leads us to perform the reaction in water with benefits concerning cost, safety and environmental impact.² Bearing in mind our ultimate goal of efficient operation in water, we decided to introduce a cholic acid moiety that will hold the hydroxy proline in a chiral cleft, so that more hydrogen bonding can take place efficiently through its three hydroxyl groups present at 3, 7 and 12 positions with the aqueous solvent and the reactants. The synthesis of our organocatalyst starts from cholic acid **10**, which on amidation with propargyl bromide in the presence of 1-Ethyl-3-(3-dimethylaminopropyl) carbodiimide and hydroxybenzotriazole in DMF at 0 °C to RT gives alkyne **11** with 82% yield as previously reported by our group (scheme 1).⁴⁴ From the other side, we converted 4-*trans*-hydroxy-L-proline **12** into azide **15** through previously reported literature (scheme 2).^{45,59,60} The obtained alkyne **11** and azide **15** was then reacted by click reaction to get intermediate **16** which was Boc protected as well as benzyl protected. Intermediate **16** on treatment with trifluoroacetic acid and DCM at 0 °C gives out boc deprotected compound **17**. Finally, the desired catalyst **18** was obtained from **17** by debenzylation with H₂/Pd-C in methanol with 85% yield (scheme 3). The obtained desired catalyst **18** was found to be insoluble in various non-polar organic solvents like chloroform, benzene, toluene, diethyl ether *etc.* But soluble in some polar protic and aprotic solvents like DMF, methanol, DMSO, ethanol *etc.* It was found to be soluble in 1:1 mixture of water and acetone also.



Scheme 1. a) EDC.HCl, HOBT, DMAP, propargyl amide, DMF, 0 °C- rt, overnight, 82%.



Scheme 2. a) i) Boc_2O , Et_3N , MeOH , Reflux, 2 h; ii) NaH_2PO_4 , 0°C Dil. HCl $\text{pH}=2$, 85%; b) BnBr , aq. Cs_2CO_3 0°C , 2 h, DMF , 95%; c) DPPA , PPH_3 , DEAD , 0°C – rt, THF , 24 h, 96%



Scheme 3. a) $\text{CuSO}_4 \cdot 5\text{H}_2\text{O}$, Na-Asc , $\text{DMF}:\text{H}_2\text{O}$ (4:1) Microwave 540W, 10 min, 93%; b) TFA , DCM , 0°C – rt, 4 h, 81%; c) Pd/C , MeOH , H_2 1atm, rt, 5 h, 85%

The asymmetric cross-aldol reaction between *para*-nitrobenzaldehyde and cyclohexanone was chosen as a model to optimize the reaction conditions. As highlighted in **Table 1**, for the screening of the catalyst, we have chosen the condition for performing the reaction at room temperature with 10 mol% of various catalysts **17-21**, in the aqueous solvent system (Figure. 7). Catalysts **19**, **20**, and **17** were intermediates from our scheme, whereas catalyst **21** was prepared from many steps as per our previously reported procedure (Scheme 5).⁴⁶ Using water as the only solvent (**Table 1, Entry 2**) the catalyst **20** gives aldol product with 85% yield and 46% *ee*, similarly, catalyst **17** gives aldol product without any improvement in 89% yields and 44% *ee* (**Table 1, Entry 4**). However, catalyst **21** was screened at different conditions and found to be inactive when concerning enantioselectivity, it gives only upto 31% *ee* (scheme 4) (**Table 1, Entry 3**). To our delight, our desired catalyst **18** was found to be most efficient in terms of yield, enantioselectivity and diastereoselectivity

(Table 1, Entry 5). The time taken for the model reaction was only 10 hours, which is comparatively lesser to the other organocatalysts (24-120 hrs) reported previously⁴⁷ Such efficiency is attributed to the fact that the cholic acid moiety containing amide and a triazole ring facilitated the accessibility of hydrophobic reactants to active sites in water and stabilized the formed enamine intermediate during the reaction. The presence of three hydroxyl groups in cholestanic backbone enhances the hydrogen bonding of catalyst with aqueous solvent and reactants to produce best results.

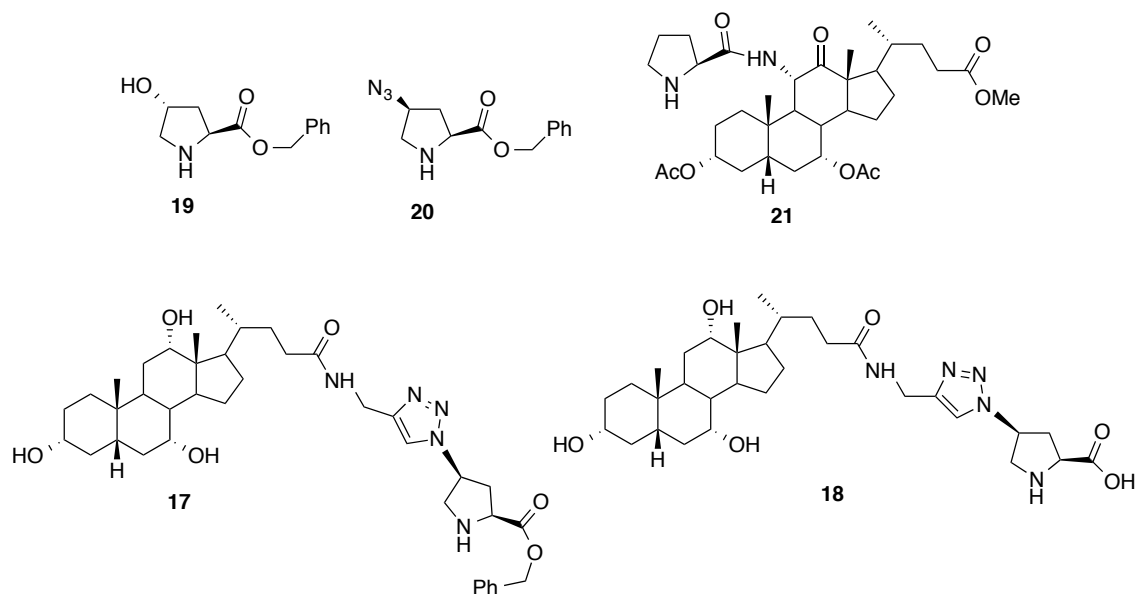
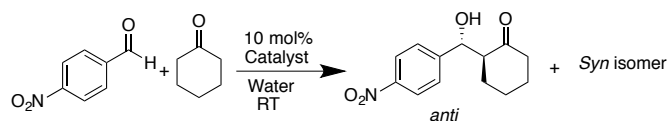


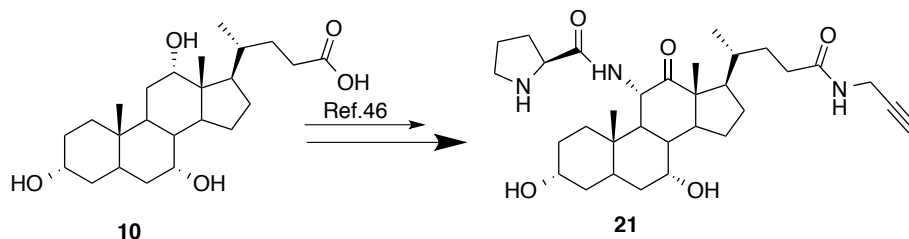
Figure 7. Screening of the catalysts

Table 1: Screening of different catalysts for direct asymmetric aldol reaction between cyclohexanone and *para*-nitro benzaldehyde in water.^a



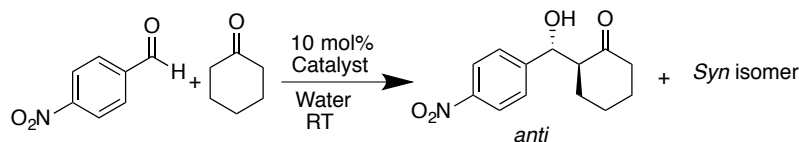
Entry ^a	Catalyst	Yield ^b (%)	<i>anti:syn</i> ^c	<i>ee</i> ^d %
1	19	-	-	nd ^e
2	20	85	76:24	46
3	21	56	-	31
4	17	89	78:22	44
5	18	97	95:5	97

^aCatalyst (10 mol% of aromatic aldehydes), aromatic aldehyde (0.25 mmol), cycloalkanone (1.25 mmol), H₂O (1.2mL), 9-48 h, 28 °C. ^bIsolated yield after column chromatography. ^cDetermined by ¹H nmr of the crude product. ^dDetermined by HPLC (Kromasil 5-cellicoat column) for the *anti*-isomer product. ^eNot determined.

Scheme 5. Synthesis of catalyst **21**

In contrast to the known reactions using a large excess of ketone, only 5 equiv. of ketone to the aldehyde was used in this case. By using brine as a solvent (Table 2, entry 8), the results obtained was pretty good, but not up to the mark as it was in the case of aldol reaction carried out neat (Table 2, entry 9). It must be noted, that our catalyst also gave best results in the absence of any solvent, even water itself (Table 2, Entry 9). The results obtained for aldol reaction with neat condition was outstanding, giving 99% yield and 98% enantioselectivity, with slight loss of diastereoselectivity. To our delight, by using pure water as the solvent, our catalyst **18** was efficient enough to catalyze the aldol reaction in a quantitative yield with an excellent diastereomeric ratio of 95:5 in favor of *anti*-diastereomer as well as a high enantioselectivity of 97% *ee* (Table 2, entry 7).

Table 2: Solvent screening for catalyst **18**^a for the direct asymmetric aldol reaction between cyclohexanone and *para*-nitrobenzaldehyde at room temperature.



Entry	Time(hrs)	Solvent	Yield ^b (%)	<i>anti</i> : <i>syn</i> ^c	<i>ee</i> ^d %
1	32	DMF	5	46:54	94
2	32	THF	25	50:50	83
3	32	PEG-400	Trace	nd ^e	nd ^e
4	27	DCM	27	69:31	54
5	28	MeOH	53	80:20	90
6	27	Toluene	51	67:33	84
7	9	Water	97	95:5	97
8	8	brine	95	93:7	98
9	5	Neat	92	92:8	98

^aCatalyst (10 mol% of aromatic aldehydes), aromatic aldehyde (0.25 mmol), cycloalkanone (1.25 mmol), 9-48 h, 28 °C. ^bIsolated yield after column chromatography. ^cDetermined by ¹H nmr of the crude product. ^dDetermined by HPLC (Kromasil 5-cellicoat column) for the *anti*-isomer product. ^eNot determined

3.4.3 Effect of concentration of water

Natural aldolases are well known for their efficiency for the aldol reaction in water⁴⁸, however with proline as an organocatalyst an excess of ketone,⁴⁹ or organic solvent is generally used.^{50,51} Unfortunately, sometimes use of excess amount of water may lead to low reactivity or even no reaction progress probably because of the limited affinity between the hydrophobic reactants and proline/proline based organocatalyst in water.^{52,53} To overcome this limitation, we have introduced cholic acid **10** moiety which already contains aliphatic hydrophobic hydrocarbon fragments, hydrophilic fragments containing three hydroxyl groups and also a long chain flexible acid as a functional group into the framework of proline to make hydrophobic substrates compatible in an aqueous medium. The model reaction between *para*-nitrobenzaldehyde and cyclohexanone was chosen to check whether the concentration of water has any role in the outcome of the result. It was found that at the concentrations 0 and 100 equivalent of water, both give product with excellent yields and *ee*, but the only difference was the diastereomeric ratio. When the reaction was carried out neat with 0 equivalent of water, the *dr* was found to be 95:5 for *anti*:*syn*. While with 25 and 50 equivalents of water, the product was found with yields 94% and 95% having 96.3% and 95.5% *ee* and *dr* 86:14 and 94:6 respectively (Table 3). To our delight, we found our best ever result while using 100 equivalents of water, which gave us >99% *ee* and *dr* as 99:1 in just 9 hrs. We have also found that, after certain extent water affected the yields,

Table 3: Effect of concentration of water at room temperature using catalyst **18**^a.

Entry	H ₂ O (equi)	Yield ^b (%)	<i>anti</i> : <i>syn</i> ^c	<i>ee</i> ^d %
1	0	95	95:5	98
2	25	94	86:14	96.3
3	50	95	94:6	95.5
4	100	99	98:2	99
5	200	97	95:5	97
6	300	99	95:5	96

^a Catalyst (10 mol% of aromatic aldehydes), aromatic aldehyde (0.25 mmol), cycloalkanone (1.25 mmol), 9-48 h, 28 °C. ^b Isolated yield after column chromatography. ^c Determined by ¹H nmr of the crude product. ^d Determined by HPLC (Kromasil 5-cellicoat column) for the *anti*-isomer product.

enantioselectivity and diastereoselectivity, these decreases with increase in the equivalents of water (Table 3).

Hence, catalyst **18** proved useful in the formation of the β -hydroxy ketone adducts with high stereoselectivity in the aqueous environment. Furthermore, dehydration products were not observed, probably as a consequence of the aqueous reaction conditions in the presence of water, dehydration is much less favorable than using other dry organic solvents.

3.4.4 Effect of catalyst loading on direct aldol reaction

Previous studies on the proline-mediated aldol reaction of *para*-nitrobenzaldehyde and cyclohexanone in water indicated that the reaction hardly proceeds in the presence of 10 mol% of proline,^{54,55} and **18** as a catalyst, we investigated the effects of catalyst loading on the reactions of cyclohexanone with 4-nitrobenzaldehyde (Table 4). When 1 mol % of the catalyst was used (Table 4, entry 3), the reaction proceeded slower, and the *ee* /*dr* values were slightly lower than that using 5 and 10 mol % of the catalyst (Table 4, 3). By using 5 mol% of the catalyst, there was only decrease in the yield (Table 4, entry 2) without affecting enantioselectivity and diastereoselectivity. When using 10 mol % of the catalyst after nine hours, the aldol reaction proceeded smoothly with excellent diastereoselectivity and enantioselectivity (Table 4, Entry 1).

Direct aldol reactions of variously substituted benzaldehydes with cyclohexanone were carried out in the presence of 10 mol % of **18** under the optimal conditions to examine the scope and limitation. The results are summarized in Table 5. The aldol reactions of both electron-deficient and electron-rich benzaldehydes with cyclohexanone proceeded smoothly

Table 4: Screening of the Catalyst loading **18**

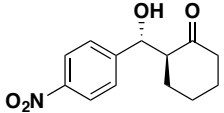
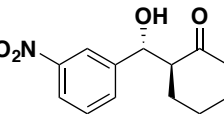
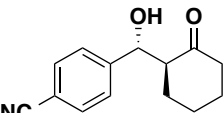
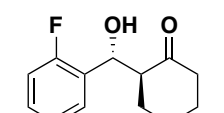
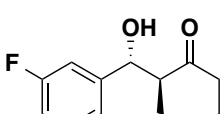
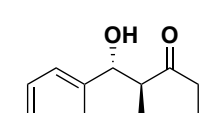
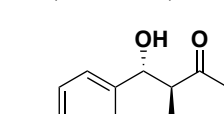
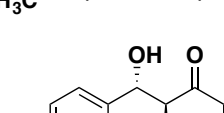
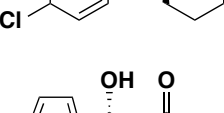
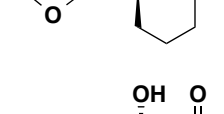
Entry	Catalyst Loading (mol%)	Time (hrs)	Yield ^a %	<i>anti:syn</i> ^b	<i>ee</i> ^c %
1	10	9	99	98:2	>99
2	5	24	86	97:3	>99
3	1	40	59	98:2	98

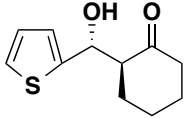
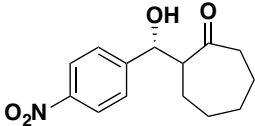
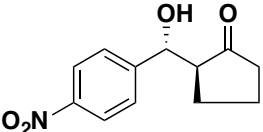
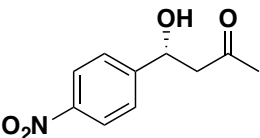
^aIsolated yield after column chromatography. ^bDetermined by ¹H nmr of the crude product.

^cDetermined by HPLC (Kromasil 5-cellicoat column) for the *anti*-isomer product.

to give the aldol adducts with excellent diastereoselectivities (*up to* 99:1) and enantioselectivities (*up to* >99%).

Table 5. Asymmetric aldol reactions with different aldehydes and ketones catalyzed by Catalyst 18.^[a]

Entry	Product	Time	Yield ^[b]	<i>anti:syn</i> ^[c]	<i>ee</i> ^[d]
1		9	99	98:2	>99
2		12	97	74:26	98
3		18	95	96:4	92
4		18	91	>99:1	98
5		20	90	68:32	95
6		15	95	97:3	93
7		36	59	88:12	96
8		18	85	84:16	98.7
9		24	77	94:6	94
10		20	88	98:2	98

11		24	61	85:15	94
12		48	89	65:35	30
13		10	98	68:32	95
14		40	64	-	97.5

^a Catalyst (10 mol% of aromatic aldehydes), aromatic aldehyde (0.25 mmol), cycloalkanone (1.25 mmol), 9-48 h, 28 °C; ^b isolated yield after column chromatography. ^c Determined by ¹H nmr of the crude product. ^d Determined by HPLC, only for the *anti*-isomer product.

From the results obtained from direct intermolecular aldol reaction between the cyclic ketones and different aldehydes, we investigated that when cyclohexanone was used as a donor, the electron-deficient aldehydes (*p*-nitro/*m*-nitro/*p*-cyano/*o*-fluoro/*m*-fluoro benzaldehyde) were converted to the corresponding aldol products with up to >99:1 *de* values in 99% yield and with high enantioselectivities up to 99% (Table 5, entries 1-5); for the electron-rich aldehydes (benzaldehyde, *p*-methyl/*p*-chloro benzaldehyde) the corresponding aldol products with moderate to high diastereoselectivities up to 97:3 in moderate to excellent yields and with up to 98% *ee* values (Table 5, entries 6–8). When cyclohexanone is used with heterocyclic aldehydes the aldol product is obtained with moderate to high reactivity in terms of both enantioselectivity and diastereoselectivity with lowering in product yields (Table 5, entries 9 and 11). When cyclopentanone was used as a donor with *p*-nitrobenzaldehyde, the corresponding aldol products were isolated in 98% yield with 68% *de* and 95% *ee* values (Table 5, entry 13). Enantioselectivity and diastereoselectivity was found to be lowest in the case where cycloheptanone was used as a donor with *p*-nitrobenzaldehyde, might be because of the unstable seven-membered ring which did not interacted well with the catalyst in water.

3.4.5 Recyclability and Stability of the catalyst 18.

For industrial applications of such important reactions, the lifetime of the catalyst and its level of reusability are very significant factors. Efficient recovery of the catalyst and high purity of products are also difficult to achieve.⁵² Plenty of organic solvents is often required

to precipitate the catalyst out of the reaction mixture selectively.⁵⁶ Most of the catalysts are grafted/supported on metallic nanoparticles or polymers which can be precipitated sometimes or extracted by filtration and then washed to remove impurities followed by heating in a vacuum oven to reactivate them.⁵⁷ At present, the preparation of an efficient and recoverable proline based catalyst for direct asymmetric aldol reaction in water remains challenging.

An obvious advantage of our catalytic system is the facile recyclability of the catalyst. After completion of the reaction and subsequent extraction of the product with ethyl acetate the catalyst remaining in the aqueous phase and can be reused for the next cycle of reaction. Several recycling experiments for the reaction between *p*-nitrobenzaldehyde and cyclohexanone were conducted, and the results are summarized in Table 6. Catalyst **18** has been recycled and reused for three times without substantial change in reactivity and enantioselectivity (entries 1–3, Table 6).

Table 6 Reuse of catalyst **18** after 1st use in the direct asymmetric aldol reaction of cyclohexanone with *p*-nitrobenzaldehyde in water

Entry ^a	Cycle ^b	Yield ^c	<i>anti:syn</i> ^d	<i>ee</i> ^e %
1	1	90	97:3	98
2	2	77	98:2	98
3	3	54	98:2	>99

^a Catalyst (10 mol% of aromatic aldehydes), aromatic aldehyde (0.25 mmol), cycloalkanone (1.25 mmol), 9-48 h, 28 °C; ^bAfter first use, the products has been extracted in ethyl acetate 4-5 times followed by the addition of both the reactants only; ^cisolated yield after column chromatography. ^dDetermined by ¹H nmr of the crude product. ^eDetermined by HPLC (Kromasil 5-cellucoat column) for the *anti*-isomer product.

Although several unique chiral catalysts have been developed for aldol reactions, and the other transformations, but they are often unstable in the air or in the presence of water. This occurs especially the case in chiral Lewis acid based catalysts because most of the Lewis acids are air- and moisture sensitive.⁵⁸ Therefore, many catalysts have to be prepared in *in-situ* in an appropriate solvent just before use, and they cannot be stored for extended periods.

However, our desired catalyst **18** is highly stable in the air at room temperature for almost a year. We have performed our model reaction of aldol between *para*-nitrobenzaldehyde and cyclohexanone using our catalyst **18** which was kept in a round bottom flask for nearly a year at room temperature. To our delight, catalyst **18** (Figure 8) performed well giving excellent results without significant loss of reactivity, enantioselectivity and diastereoselectivity. After prolonged period, little amount of moisture may affect the reactivity, but that can be simply overcome by allowing our catalyst **18** to be dried up in an oven at 120 °C, for 4-5 hours followed by applying it for a high vacuum for 1-2 hrs.

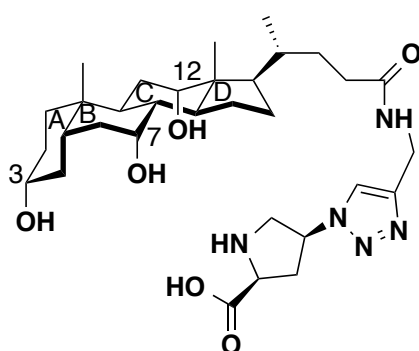


Figure 8. Structure of Catalyst 18

3.4.6 Plausible mechanism for the mode of action of the Catalyst 18.

The idea of using cholestanic backbone of cholic acid is because of its concave like structure, caused by the *cis* junction of the A and B cyclohexane rings, which provide a chiral cleft to hold hydroxy proline that can help enantioselection. Furthermore, the presence of three free hydroxyl groups and a flexible long acid chain will enhance the hydrogen bonding with water and could control the position of the substrate in the cavity of organocatalyst (Figure 8, 9). Furthermore, the presence of amide linkage, triazole ring also supports strong hydrogen bonding between water and substrates to give excellent results in water only (Figure 9, 10).

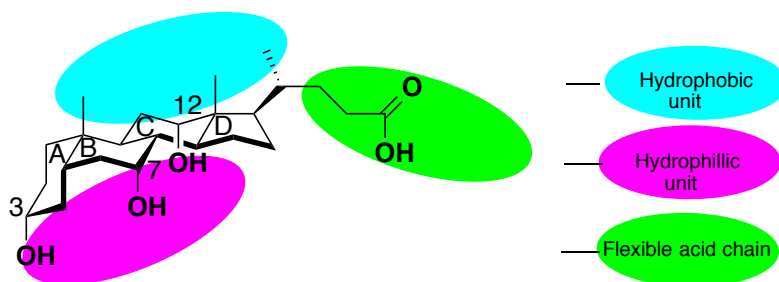


Figure 9. Structure of cholic acid

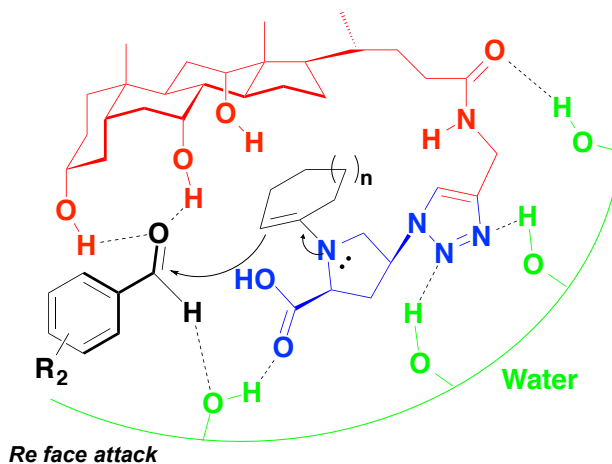


Figure 10. Proposed mechanism for aldol reaction by using catalyst **18** in the presence of water

3.5 Conclusions

An efficient and reusable cholic acid derived *trans*-4-hydroxy-(L)-proline catalyst was successfully prepared through triazole linkage using click chemistry. The presence of the cholic acid moiety with an amide and a triazole functionalization supported proline-based catalyst resulted in an excellent catalytic activity for a wide range aromatic aldehydes and ketones in direct asymmetric aldol reaction in water without the need for any organic solvent or additional toxic additives. The catalyst can also be well dispersed in the reaction medium, easily reused several times without significant loss of activity from the reaction mixture by simple extraction of the product by diethyl ether or ethyl acetate, and later addition of both the reactants only. All these benefits made the cholic acid derived *trans*-4-hydroxy-(L)-proline catalyst becomes a green, promising and convenient organocatalyst for aldol and other relevant aqueous reactions. Significantly, quantitative yield, excellent diastereoselectivity (up to 99:1), and enantioselectivity (up to >99%) were obtained by performing the reaction at room temperature. Such efficiency is attributed to the fact that the cholic acid moiety containing amide and a triazole ring facilitated the accessibility of hydrophobic reactants to active sites in water and stabilized the formed enamine intermediate during the reaction.

3.6 Experimental

Synthesis of 2-benzyl 1-(tert-butyl) (2*S*,4*S*)-4-(4-(((4*R*)-4-(((3*R*,7*R*,10*S*,12*S*,13*R*,17*R*)-3,7,12-trihydroxy-10,13-dimethylhexadecahydro-1*H*-cyclopenta[*a*]phenanthren-17-yl)pentanamido)methyl)-1*H*-1,2,3-triazol-1-yl)pyrrolidine-1,2-dicarboxylate (16): The

alkyne of cholic acid **11** (1.5 equiv) and the azide of *trans*- hydroxyl L-proline **15** (1equiv) were dissolved in DMF:H₂O (4:1). To this solution CuSO₄·5H₂O (0.05 equiv.) and sodium ascorbate (0.5 equiv.) were added. The reaction mixture was placed in a microwave reactor and irradiated for 10 mins at 540W. It was then cooled to room temperature, quenched with crushed ice and filtered it on celite followed by extraction with dichloromethane. The extract was then washed with water and brine, dried over anhydrous sodium sulphate. Solvent was evaporated under reduced pressure and crude product was purified by column chromatography using methanol/dichloromethane (10:90), to obtain compound **16** with 93% yields.

Synthesis of benzyl (2S,4S)-4-(4-(((4R)-4-((3R,7R,10S,12S,13R,17R)-3,7,12-trihydroxy-10,13-dimethylhexadecahydro-1H-cyclopenta[a]phenanthren-17-yl) pentanamido)methyl)-1H-1,2,3-triazol-1-yl)pyrrolidine-2-carboxylate(17): The compound **16** (1 equiv.) was dissolved in dry dichloromethane (10 mL), after which trifluoroacetic (3 mL) was added, then stirred at room temperature for 4 h. The reaction mixture was quenched by crushed ice and organic layer was washed with NaHCO₃ solution and brine several times. Finally, the organic layer was dried over MgSO₄ and concentrated in vacuo to yield an sticky solid, which was purified by column chromatography using methanol/dichloromethane (10:90), to afford product **17** with yield of 81%.

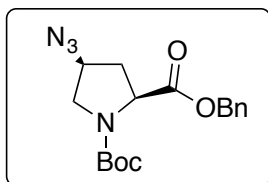
Synthesis of (2S,4S)-4-(4-(((4R)-4-((3R,7R,10S,12S,13R,17R)-3,7,12-trihydroxy-10,13-dimethylhexadecahydro-1H-cyclopenta[a]phenanthren-17-yl)pentanamido)methyl)-1H-1,2,3-triazol-1-yl)pyrrolidine-2-carboxylic acid (18): Boc-protected compound **17** was dissolved in MeOH (10 mL) and palladium on carbon (10 mol%) was added. The reaction vessel was fitted with hydrogen balloon, and the resulting heterogeneous mixture was stirred for 5 h at room temperature. The mixture was filtered through a pad of Celite and the pad was washed with MeOH. The filtrate was concentrated in vacuo and the round bottom flask containing the crude solid mixture was added Pet-ether: ethyl acetate (05:95) solution and decanted several times to remove unwanted impurities. The obtained white powder was then concentrated again in vacuo to remove excess solvent traces. Finally, the round bottom flask was kept in the preheated oven at 100 °C for 4-5 hrs to give our desired catalyst **18** as a cream coloured powder with 85% yield without further purification.

General Procedure for the Asymmetric Aldol Reactions

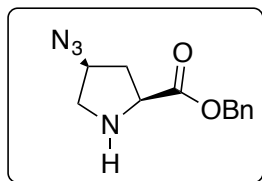
The cholic acid based hydroxyl L-proline catalyst (10 mol%) was suspended in H₂O (100equiv.), ketone (5.0 equiv.) was added, and the suspension was shaken at room temperature for 10-15 mins. After the indicated time, aldehyde (1equiv.) was added and the reaction mixture was allowed to stir at room temperature for the time indicated. The reaction was monitored by TLC, and after finish, the aqueous phosphate buffer (pH=7) 1-2 ml was added to quench the reaction. Ethyl acetate was added for aldol extraction, and the organic liquid phases were dried over anhydrous magnesium sulfate and concentrated under reduced pressure. The aldol products were purified by column chromatography. The enantiomeric excess and diastereomeric ratio were determined by HPLC on a chiral stationary phase after purification. For the recycling experiments, after reaction completion there is no need to quench reaction mixture with phosphate buffer, aldol was simply extracted using ethyl acetate and only need to add the reactants at the required amount.

Synthesis and characterization of the proline derivative

(2*S*,4*S*)-1-(*tert*-Butoxycarbonyl)-4-azidoproline Benzyl Ester **15**^{59,60}

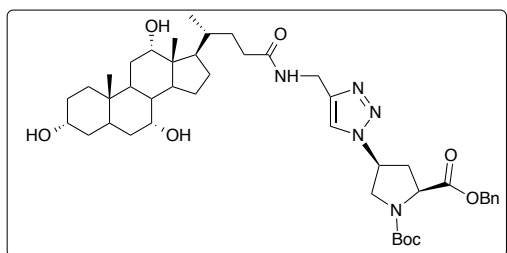


A solution of DEAD (7.9 mL of a 40% solution in toluene, 3 equiv.) and DPPA (3.9 mL, 3 equiv.) in THF (15 mL) was added to a solution of proline **14** (1.95 g, 1equiv.) and PPh₃ (4.77 g, 3equiv.) in THF (50 mL) dropwise over 30 min at 0 °C under argon. The mixture was then allowed to stir for 24 h at room temperature. Finally, EtOH (20 mL) was added to the reaction mixture and the solvent was concentrated to dryness in vacuo. The residue was purified by silica gel flash chromatography (hexanes/EtOAc 80:20) to afford azidoproline **15** (2.0g 98%) as a yellowish oil: $[\alpha]_D^{25} -39.9$ (*c* 1.1, CHCl₃); [lit.² $[\alpha]_D^{24} = -32.2$ (*c* =1.5, CHCl₃)]; ¹H NMR (200 MHz, CDCl₃, mixture of rotamers) 7.36 (m, 5H), 5.19 (m, 2H), 4.38 (m, 1H), 4.14 (m, 1H), 3.64 (m, 1H), 3.53 (m, 1H), 2.55-2.39 (m, 1H), 2.20-2.14 (m, 1H), 1.47 and 1.34 (2s, 9H, Bu^t); ¹³C NMR (75.4 MHz, CDCl₃, mixture of rotamers, major isomer) 171.4, 153.4, 135.3, 128.1, 80.4, 66.9, 59.2, 57.4, 50.84, 42.7, 36.0, 35.0, 27.8. HRMS: [M+Na] calcd for [C₁₇H₂₂O₄Na] 369.1533, found 369.1534.

Benzyl (2S,4S)-4-azidopyrrolidine-2-carboxylate 20

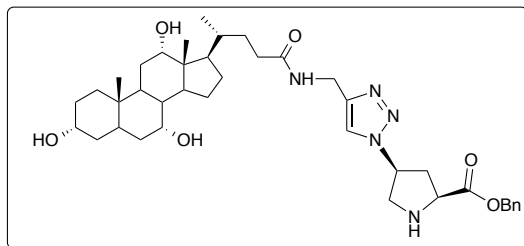
The compound **15** (1 equiv.) was dissolved in dry dichloromethane (10 mL), after which trifluoroacetic acid (3 mL) was added, then stirred at room temperature for 4 h. The reaction mixture was quenched by crushed ice and organic layer was washed with NaHCO₃ solution and brine several times. Finally, the organic layer was dried over MgSO₄ and concentrated in vacuo to yield a sticky liquid, which was purified by column chromatography using pet-ether/ethyl acetate (90:10), to afford product **20** with yield of 78%. colorless oil: $[\alpha]_D^{24} = -40.5$ ($c = 1.0$, CHCl₃); ¹H NMR (200 MHz, CDCl₃) 7.34 (m, 5H, Ph), 5.21 (m, 2H), 4.10 (m, 1H), 3.83 (m, 1H), 3.12-2.96 (m, 2H), 2.45-2.30 (m, 1H), 2.38-2.10 (m, 3H), 1.26-1.22 (m, 2H), 0.85 (m, 1H); LC-MS calcd. for [C₁₂H₁₄N₄O₂] 246.11, found 247.11.

2-benzyl 1-(tert-butyl) (2S,4S)-4-(4-(((4R)-4-((3R,7R,10S,12S,13R,17R)-3,7,12-trihydroxy-10,13-dimethylhexadecahydro-1H-cyclopenta[a]phenanthren-17-yl)pentanamido)methyl)-1H-1,2,3-triazol-1-yl)pyrrolidine-1,2-dicarboxylate (16): Brown coloured sticky solid 93%,



$[\alpha]_D^{24} = -7.4$ ($c = 1.7$, CHCl₃); IR (KBr, CHCl₃, cm⁻¹) 3391, 2934, 1743, 1693, 1540, 1402, 1216, 1080, 768, 668; ¹H NMR (200 MHz, CDCl₃, mixture of rotamer, major product) δ 7.62 (d, $J = 2.15$ Hz, 1H), 7.36 (s, 5H), 5.30 (s, 1H), 5.19 (s, 2H), 5.01-5.15 (m, 2H), 4.44 (d, $J = 5.31$ Hz, 2H), 3.91-4.08 (m, 2H), 3.41 (d, $J = 5.05$ Hz, 3H), 2.70-2.90 (m, 1H), 2.29-2.51 (m, 5H), 2.23 (br. s., 2H), 1.90-2.16 (m, 5H), 1.58-1.85 (m, 9H), 1.38-1.49 (m, 4H), 1.21-1.30 (m, 9H), 0.86-0.96 (m, 5H), 0.76-0.83 (m, 2H), 0.67 (s, 2H); ¹³C NMR (101 MHz, CHLOROFORM-D, mixture of rotamer) δ 174.71, 171.65, 153.45, 145.56, 135.30, 128.78, 128.69, 128.27, 121.89, 81.25, 77.16, 73.17, 71.89, 68.51, 67.39, 57.90, 57.27, 51.25, 46.45, 46.03, 41.74, 41.63, 39.85, 39.59, 36.03, 35.51, 35.40, 34.88, 32.41, 31.47, 30.45, 29.81, 28.43, 28.21, 27.67, 26.45, 23.40, 22.58, 17.55, 14.31, 12.52; HRMS: [M+H] calcd for [C₄₄H₆₆O₈N₅] 792.4906, found 792.4903, [M+Na] calcd for [C₄₄H₆₅O₈N₅Na] 814.4725, found 814.4719.

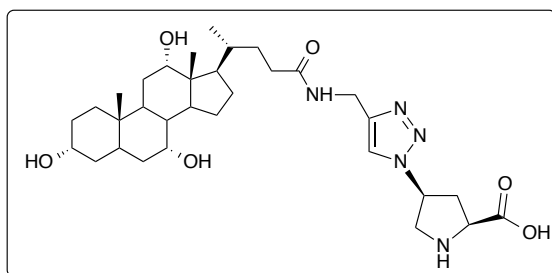
benzyl (2S,4S)-4-(4-(((4R)-4-((3R,7R,10S,12S,13R,17R)-3,7,12-trihydroxy-10,13-dimethylhexadecahydro-1H-cyclopenta[a]phenanthren-17-yl)pentanamido)methyl)-1H-1,2,3-triazol-1-yl)pyrrolidine-2-carboxylate(17): Brown coloured sticky solid 81%, $[\alpha]_D^{24} =$



+8.9 ($c=1.5$, CHCl_3); IR (KBr, CHCl_3 , cm^{-1}) 3683, 3443, 3021, 2946, 2403, 1773, 1665, 1519, 1435, 1217, 1170, 769, 672; ^1H NMR (500 MHz, CDCl_3 , mixture of rotamer, major product) δ 7.60 (s, 1H), 7.30 - 7.42 (m, 5H), 6.34 (d, $J=6.71$ Hz,

1H), 5.31 (br. s., 1H), 5.20 (s, 2H), 5.04 - 5.13 (m, 2H), 4.70 - 4.84 (m, 1H), 4.38 - 4.48 (m, 2H), 3.95 - 4.04 (m, 2H), 3.89 (br. s., 1H), 3.36 - 3.48 (m, 2H), 2.75 - 2.86 (m, 1H), 2.40 - 2.52 (m, 2H), 2.19 - 2.29 (m, 2H), 2.15 - 2.19 (m, 1H), 2.04 - 2.13 (m, 4H), 1.95 - 2.02 (m, 2H), 1.91 (d, $J=11.60$ Hz, 2H), 1.74 - 1.84 (m, 5H), 1.70 (d, $J=14.65$ Hz, 3H), 1.63 (br. s., 2H), 1.49 - 1.60 (m, 4H), 1.42 (br. s., 2H), 1.34 (dd, $J=14.65, 18.62$ Hz, 3H), 1.26 (s, 1H), 1.17 - 1.22 (m, 1H), 1.03 - 1.16 (m, 2H), 0.86 - 1.01 (m, 6H), 0.73 - 0.85 (m, 4H), 0.69 (s, 2H); ^{13}C NMR (126 MHz, CDCl_3 , mixture of rotamer, major product) δ 173.4, 173.2, 173.1, 144.7, 135.2, 128.7, 128.6, 128.4, 121.0, 80.6, 78.8, 78.3, 72.1, 67.5, 67.3, 60.1, 59.1, 53.4, 53.4, 47.3, 46.7, 46.6, 45.1, 43.3, 41.7, 41.0, 40.4, 39.1, 38.1, 36.2, 36.2, 35.0, 34.8, 34.5, 34.4, 34.3, 34.3, 34.2, 34.0, 33.5, 33.0, 32.7, 31.3, 31.1, 31.0, 29.7, 28.5, 28.1, 27.5, 27.2, 27.1, 26.0, 25.9, 25.3, 22.8, 22.7, 22.3, 17.6, 17.4, 12.4, 12.2; HRMS: $[\text{M}+\text{H}]$ calcd for $[\text{C}_{39}\text{H}_{58}\text{O}_6\text{N}_5]$ 692.4382, found 692.4380.

(2*S*,4*S*)-4-(4-(((4*R*)-4-((3*R*,7*R*,10*S*,12*S*,13*R*,17*R*)-3,7,12-trihydroxy-10,13-dimethylhexadecahydro-1*H*-cyclopenta[*a*]phenanthren-17-yl)pentanamido)methyl)-1*H*-1,2,3-triazol-1-yl)pyrrolidine-2-carboxylic acid (18): Cream coloured solid, M.P = 228.3 $^{\circ}\text{C}$,

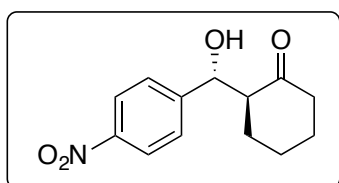


85%, $[\alpha]_{\text{D}}^{24} = +38.7$ ($c=1.0$, MeOH); IR (KBr, Nujol, cm^{-1}) 3362, 2850, 2726, 1776, 1670, 1543, 1456, 1374, 1211, 1164, 1030, 836, 770, 725; IR Solid state cm^{-1} 3756, 3678, 3077, 2890, 2376, 2341, 1845, 1697, 1674, 1522,

1299, 1206, 1142, 1142, 968, 835, 672, 669; (^1H NMR (500MHz, MeOD- d_4) δ 7.88 (s, 1H), 5.36 (m, 1H), 5.27(s, 0.6H), 5.06 (s, 0.4H), 4.37-4.32 (m, 3H), 3.88 (m, 1H), 3.82-3.77 (m, 2H), 3.23 (s, 2H), 2.95 (m, 1H), 2.68-2.64 (m, 1H), 2.21-2.18 (m, 2H), 2.05 (m, 2H), 1.88 (m, 2H), 1.78-1.64 (m, 5H), 1.60-1.45 (m, 5H), 1.38-1.30 (m, 3H), 1.22 (m, 1H), 1.12 (m, 2H), 0.93 (d, $J=6.1$ Hz, 2H), 0.88 (d, $J=10.99$ Hz, 3H), 0.76 (m, 4H), 0.64 (m, 1H); ^{13}C NMR (101MHz, MeOD- d_4) δ 176.9, 176.6, 157.8, 147.0, 124.4, 114.8, 82.9, 82.01, 78.9, 73.3, 72.7, 72.4, 68.4, 61.1, 59.8, 51.4, 47.9, 47.7, 44.7, 44.3, 43.3, 43.1, 42.4, 42.1, 40.6, 40.4, 39.8,

39.5, 37.0, 36.9, 36.3, 36.2, 36.1, 36.0, 35.8, 35.7, 35.5, 33.8, 33.1, 33.0, 32.9, 32.4, 32.3, 31.3, 31.1, 29.9, 29.5, 29.0, 28.6, 28.3, 28.1, 26.5, 26.2, 18.2, 17.7, 13.0, 12.6, 12.3 ; HRMS: [M+H] calcd for [C₃₂H₅₂O₆N₅] 602.3912, found 602.3918; [M+Na] calcd for [C₃₂H₅₁O₆N₅Na] 624.3732, found 624.3735.

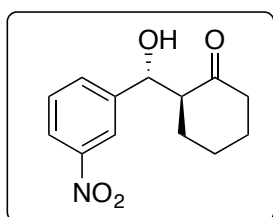
(S)-2-((R)-Hydroxy(4-nitrophenyl)methyl)cyclohexanone (Table 5, Entry 1)



$[\alpha]_D^{25} = +13.2$ ($c = 1.1$, CHCl₃), >99% *ee*; ¹H NMR (200 MHz, CDCl₃): δ 8.20 (d, $J = 8.7$ Hz, 2H), 7.53 (d, $J = 8.7$ Hz, 2H), 5.27 (t, $J = 7.3$ Hz, 1H), 3.58 (s, 1H), 2.85 (d, $J = 7.2$ Hz, 2H), 2.22 (s, 3H). Enantiomeric excess was determined by HPLC

with a Kromasil -5-cellicoat column, hexane/2-propanol 95:05, 1 mL·min⁻¹, $\lambda = 254$ nm, *tr* (minor): 29.5 min, *tr* (major): 14.16 min.

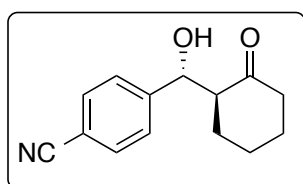
(S)-2-((R)-hydroxy(3-nitrophenyl)methyl)cyclohexan-1-one (Table 5, Entry 2)



$[\alpha]_D^{24} = +32.8$ ($c=1.30$, CHCl₃), 98% *ee*; ¹H NMR (200MHz, CDCl₃): δ 8.22-8.14 (2H, m), 7.66-7.49 (2H, m), 4.88 (1H, d, $J = 8.4$ Hz), 4.12 (1H, bs), 2.67-2.56 (1H, m), 2.48-2.36 (2H, m), 2.17-2.1 (1H, m), 1.85-1.8 (1H, m), 1.74-1.47 (1H, m). Enantiomeric excess

was determined by HPLC with a Kromasil -5-cellicoat column, hexane/2-propanol (90:10), 1 mL·min⁻¹, $\lambda = 220$ nm, *tr* (minor): 15.9 min, *tr* (major): 12.1 min

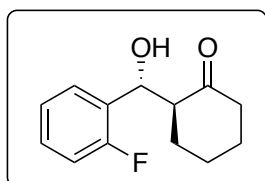
(2S, 1'R)-2-(Hydroxy-(p-cyanophenyl)methyl)cyclohexan-1-one (Table 5, Entry 3)



$[\alpha]_D^{22} = +23.3$ ($c = 1.55$, CHCl₃), 92% *ee*; ¹H NMR (200MHz, CDCl₃): δ 7.63 (2H, d, $J = 8.3$ Hz), 7.43 (2H, d, $J = 8.2$ Hz), 4.85 (1H, dd, $J = 8.4, 2.4$ Hz), 4.05 (1H, d, $J = 2.91$ Hz), 2.61-2.35 (3H, m), 2.17-2.05 (1H, m), 1.86-1.81 (1H, m), 1.64-1.53 (3H, m),

1.39-1.33 (1H, m). Enantiomeric excess was determined by HPLC with a Chiralcel-IA column, Pet Ether/2-propanol (90:10), 1 mL·min⁻¹, $\lambda = 220$ nm, *tr* (minor): 12.2 min, *tr* (major): 16.7 min.

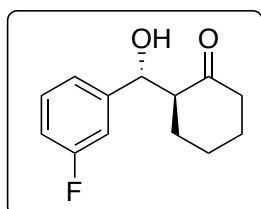
(S)-2-((R)-Hydroxy(2-fluoro-phenyl)methyl)cyclohexanone (Table 5, Entry 4)



$[\alpha]_D^{25} = +19.2$ ($c = 0.5$, CHCl₃), 98% *ee*; ¹H NMR (200 MHz, CDCl₃): δ =7.47–7.38 (m, 1H), 7.24–7.08 (m, 2H), 7.01-6.91 (m, 1H), 5.11 (d, $J = 8.72$ Hz, 1H), 3.22 (br s, 1H), 2.69–2.56 (m, 1H), 2.42–

2.26 (m, 2H), 2.04–2.01 (m, 1H), 1.77–1.72 (m, 1H), 1.65–1.53 (m, 2H), 1.48–1.37 (m, 1H), 1.20 (m, 1H) ppm. Enantiomeric excess was determined by HPLC with a Kromasil -5-cellucoat column, hexane/2-propanol (95:05), 1 mL·min⁻¹, λ = 254 nm, tr (minor): 10.1 min, tr (major): 8.1 min

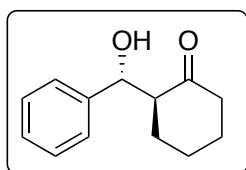
(S)-2-((R)-(3-fluorophenyl)(hydroxy)methyl)cyclohexan-1-one (Table 5, Entry 5)



95% *ee*; ¹H NMR (500 MHz, CDCl₃): δ 7.25–7.20 (1H, m), 7.02–6.98 (2H, m), 6.93–6.87 (1H, m), 4.70 (1H, d, *J* = 8.39 Hz), 2.54–2.48 (1H, m), 2.43–2.38 (1H, m), 2.33–2.26 (1H, m), 2.05–2.01 (1H, m), 1.77–1.73 (1H, m), 1.66–1.58 (1H, m), 1.45–1.56 (2H, d), 1.30–1.19 (1H, m).

Enantiomeric excess was determined by HPLC with a Kromasil -5-cellucoat column, hexane/2-propanol (95:05), 1 mL·min⁻¹, λ = 254 nm, tr (minor): 13.0 min, tr (major): 10.3 min

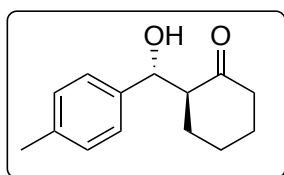
(2S, 1'R)-2-(Hydroxy(phenyl)methyl)cyclohexan-1-one (Table 5, Entry 6)



$[\alpha]_D^{25}$ = +24.3 (*c* = 1.35, CHCl₃), 98% *ee*; ¹H NMR (200MHz, CDCl₃): δ 7.25–7.19 (m, 5H), 4.70 (d, *J* = 8.71 Hz, 1H), 3.91 (m, 1H), 2.65–2.48 (m, 1H), 2.40–2.30 (m, 1H), 2.01 (m, 1H), 1.67 (m, 1H), 1.56–1.43 (m, 2H), 1.31–1.15 (m, 2H), 1.0–0.84 (m, 1H). Enantiomeric excess was

determined by HPLC with a Chiralcell OD-H column, Pet Ether/2-propanol 95:05, 1 mL·min⁻¹, λ = 220 nm, tr (minor): 17.08 min, tr (major): 11.26 min

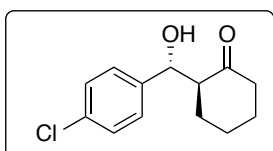
(S)-2-((R)-hydroxy(p-tolyl)methyl)cyclohexan-1-one (Table 5, Entry 7)



$[\alpha]_D^{24}$ = +12.6 (*c* = 0.15, CHCl₃), 96% *ee*; ¹H NMR (200MHz, CDCl₃): δ 7.24–7.13 (4H, dd, *J* = 12.6, 8.2 Hz), 4.74 (1H, d, *J* = 8.9 Hz), 2.62–2.55 (1H, m), 2.35(3H, m), 2.08 (1H, m), 1.79–1.76 (1H, s), 1.63–1.57 (2H, m), 1.38–1.31 (1H, m). Enantiomeric excess was

determined by HPLC with a Kromasil -5-cellucoat column, hexane/2-propanol (95:05), 1 mL·min⁻¹, λ = 220 nm, tr (minor): 10.1 min, tr (major): 8.1 min

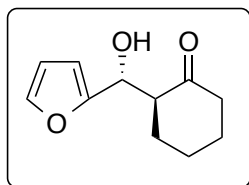
(2S, 1'R)-2-(Hydroxy-(p-chlorophenyl)methyl)cyclohexan-1-one (Table 5, Entry 8)



$[\alpha]_D^{25}$ = +22.5 (*c* = 1.2, CHCl₃), 98.7% *ee*; ¹H NMR (200MHz, CDCl₃): δ 7.21 (4H, dd, *J* = 14.7, 7.45 Hz), 4.67 (1H, d, *J* = 8.7 Hz),

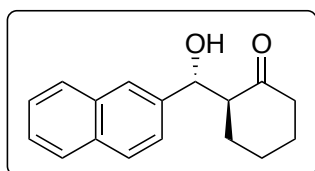
3.93 (1H, s), 2.49-2.36 (2H, m), 1.99 (1H, m), 1.63-1.41 (3H, m), 1.13-1.25 (2H, m), 0.80 (1H, m). Enantiomeric excess was determined by HPLC with a Chiralcell OJ-H column, Pet Ether/2-propanol 98.5:1.5, 1 mL·min⁻¹, λ = 220 nm, tr (minor): 31.2 min, tr (major): 24.8 min

(2*S*, 1'*R*)-2-(Hydroxy-(furan-2-yl)propyl)cyclohexan-1-one (Table 5, Entry 9)



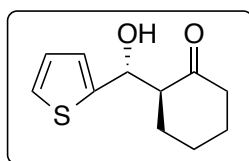
94% *ee*; ¹H NMR (500 MHz, CDCl₃): δ 7.40 (1H, s), 6.30 (1H, d, *J* = 22.5 Hz), 4.83 (1H, d, *J* = 7.63 Hz), 3.88 (1H, s), 2.93 (1H, m), 2.47 (1H, m), 2.38 (1H, m), 2.12 (1H, m), 1.85 (1H, m), 1.71-1.58 (4H, m), 1.37-1.35 (1H, m). Enantiomeric excess was determined by HPLC with a Chiralcel-IA column, n-hexane/2-propanol (95:05), 1 mL·min⁻¹, λ = 220 nm, tr (minor): 14.8 min, tr (major): 13.6 min.

(*S*)-2-((*R*)-hydroxy(naphthalen-2-yl)methyl)cyclohexan-1-one (Table 5, Entry 10)



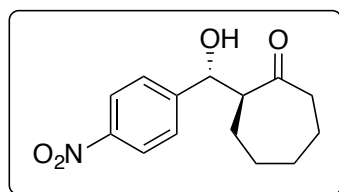
[α]_D²⁴ = +6.7 (c = 1.6, CHCl₃), 98% *ee*; ¹H NMR (200 MHz, CDCl₃): δ 7.88-7.82 (3H, m), 7.76 (1H, m), 7.53-7.47 (3H, m), 4.96 (1H, d, *J* = 8.8 Hz), 4.10 (1H, s), 2.74-2.69 (1H, m), 2.51-2.37 (2H, m), 2.10-2.05 (1H, m), 1.80-1.72 (2H, m), 1.67-1.48 (2H, m), 1.36-1.31 (1H, m). Enantiomeric excess was determined by HPLC with a Chiralcel OD-H column, hexane/2-propanol (90:10), 1 mL·min⁻¹, λ = 220 nm, tr (minor): 14.8 min, tr (major): 11.8 min

(*S*)-2-((*R*)-hydroxy(thiophen-2-yl)methyl)cyclohexan-1-one (Table 5, Entry 11)



94% *ee*; ¹H NMR (200 MHz, CDCl₃): δ = 7.3 (1H, m), 6.93-6.97 (2H, m), 5.06 (1H, d, *J* = 8.4 Hz), 2.67 (3H, m), 2.47-2.36 (2H, m), 2.0 (1H, m), 1.88-1.62 (4H, m), 1.38 (1H, m); Enantiomeric excess was determined by HPLC with a Kromasil -5-cellicoat column, hexane/2-propanol (95:05), 1 mL·min⁻¹, λ = 220 nm, tr (minor): 14.1 min, tr (major): 11.1 min

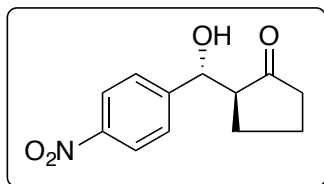
(*S*)-2-((*R*)-hydroxy(4-nitrophenyl)methyl)cycloheptan-1-one (Table 5, Entry 12)



[α]_D²⁸ = -7.9 (c = 0.35, CHCl₃), 30% *ee*; ¹H NMR (400 MHz, CDCl₃): δ 8.21 (2H, d, *J* = 8.54 Hz), 7.52 (2H, d, *J* = 7.93 Hz), 4.91 (1H, d, *J* = 7.93 Hz), 2.98 (1H, m), 2.86 (1H, m), 2.53-2.47 (2H, m), 1.89-1.81 (2H, m), 1.69-1.60 (2H, m), 1.42-1.69 (1H,

m) 1.30-1.26 (2H, m). Enantiomeric excess was determined by HPLC with a Kromasil -5-cellucoat column, hexane/2-propanol (98:2), $1 \text{ mL} \cdot \text{min}^{-1}$, $\lambda = 254 \text{ nm}$, tr (minor): 14.1 min, tr (major): 11.1 min

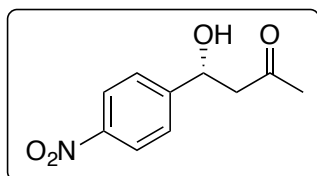
(S)-2-((R)-hydroxy(4-nitrophenyl)methyl)cyclopentan-1-one (Table 5, Entry 13)



$[\alpha]_{\text{D}}^{25} = -29.9$ ($c = 0.7$, CHCl_3), $^1\text{H NMR}$ (400 MHz, CDCl_3): $ee = 95\%$; $\delta = 8.20$ (d, $J = 8.72 \text{ Hz}$, 2H), 7.56-7.50 (m, 2H), 4.83 (d, $J = 9.22 \text{ Hz}$), 2.60-2.32 (m, 2H), 2.16-1.96 (m, 1H), 1.79-1.69 (m, 2H). Enantiomeric excess was determined by HPLC with a

Chiralcel-IA column, Pet Ether/2-propanol (95:05), $1 \text{ mL} \cdot \text{min}^{-1}$, $\lambda = 265 \text{ nm}$, tr (minor): 23.7 min, tr (major): 25.5 min.

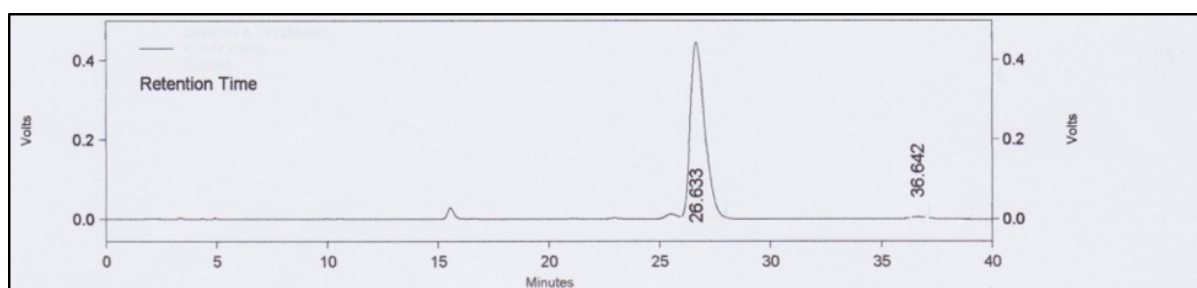
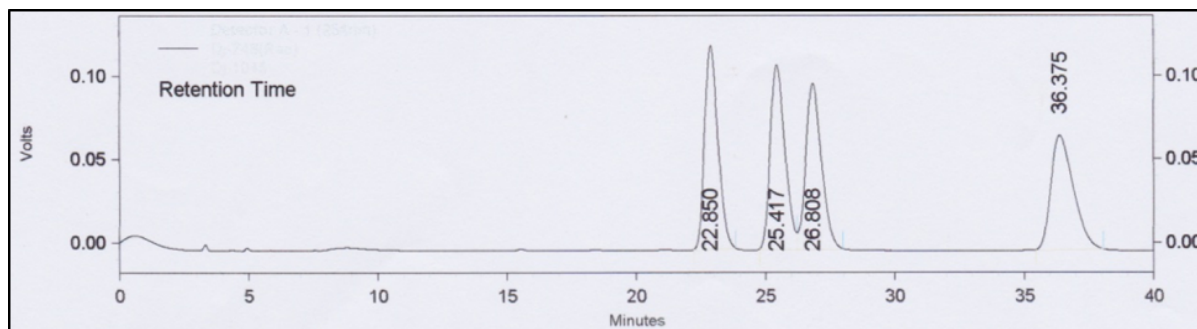
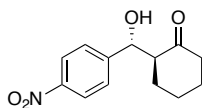
(R)-4-Hydroxy-4-(4-nitrophenyl)butan-2-one (Table 5, Entry 14)



$[\alpha]_{\text{D}}^{25} = +40.2$ ($c = 1.1$, CHCl_3), 97.5% ee ; $^1\text{H NMR}$ (200 MHz, CDCl_3): $\delta = 8.20$ (d, $J = 8.7 \text{ Hz}$, 2H), 7.53 (d, $J = 8.7 \text{ Hz}$, 2H), 5.27 (t, $J = 7.3 \text{ Hz}$, 1H), 3.58 (s, 1H), 2.85 (d, $J = 7.2 \text{ Hz}$, 2H), 2.22 (s, 3H). Enantiomeric excess was determined by HPLC with a

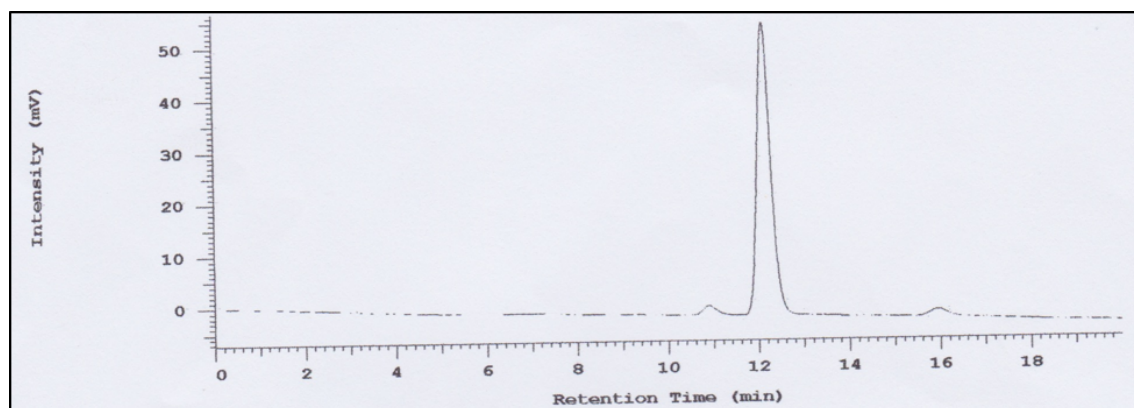
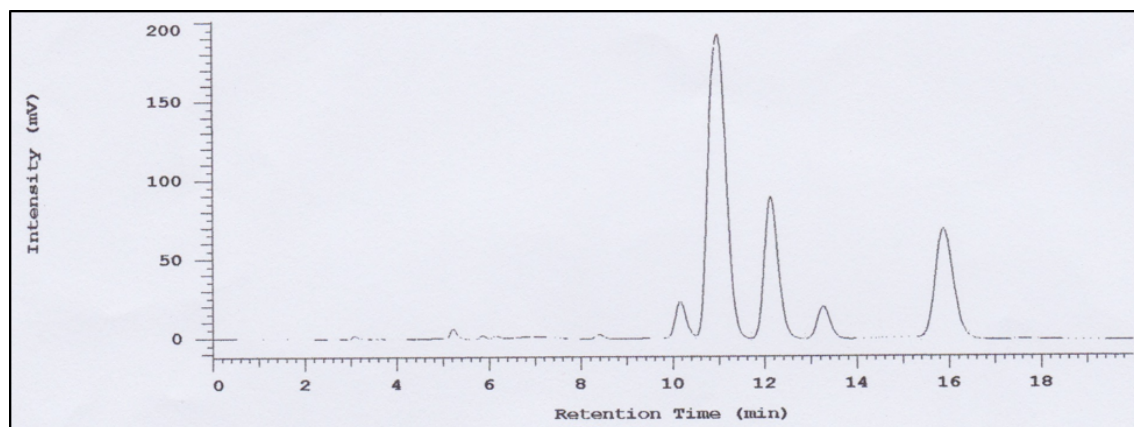
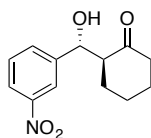
Kromasil -5-cellucoat column, hexane/2-propanol 95:05, $1 \text{ mL} \cdot \text{min}^{-1}$, $\lambda = 254 \text{ nm}$, tr (minor): 29.5 min, tr (major): 14.16 min

3.7 HPLC Spectra for compounds in Table 5 (Entries 1-14)

(S)-2-((R)-Hydroxy(4-nitrophenyl)methyl)cyclohexanone (Table 5, Entry 1)

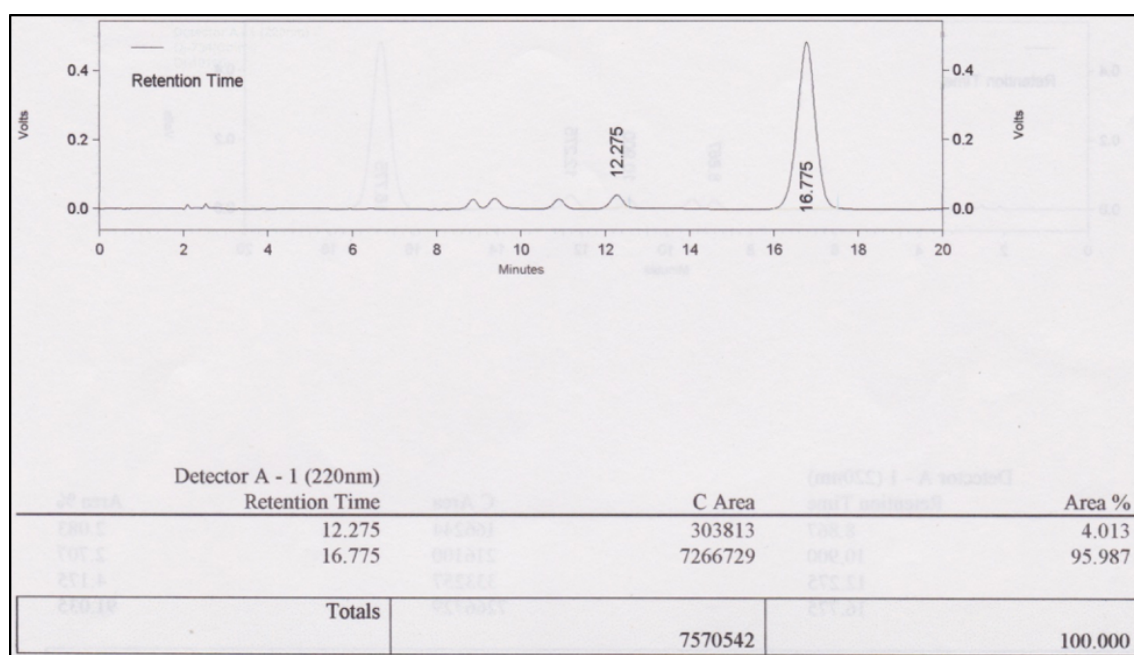
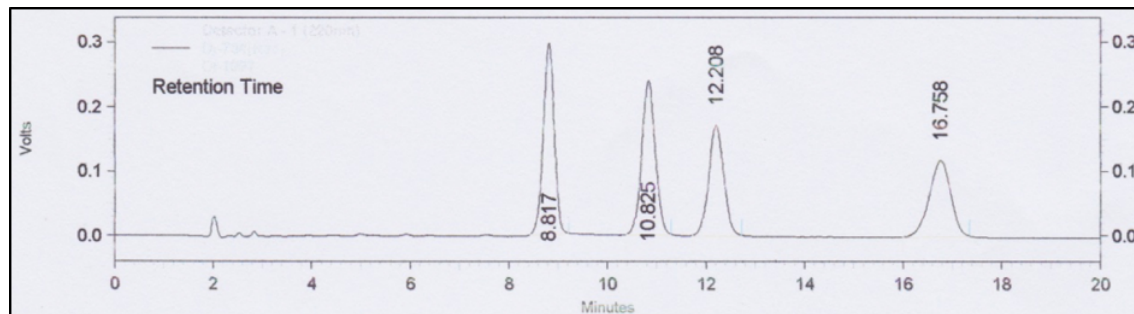
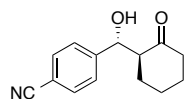
Detector A - 1 (254nm)		
Retention Time	C Area	Area %
26.633	9793584	99.577
36.642	41584	0.423
Totals	9835168	100.000

Kromasil -5-cellicoat column, hexane/2-propanol 95:05, $1 \text{ mL} \cdot \text{min}^{-1}$, $\lambda = 254 \text{ nm}$, tr (minor): 36.6 min, tr (major): 26.6 min

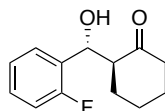
(S)-2-((R)-hydroxy(3-nitrophenyl)methyl)cyclohexan-1-one (Table 5, Entry 2)

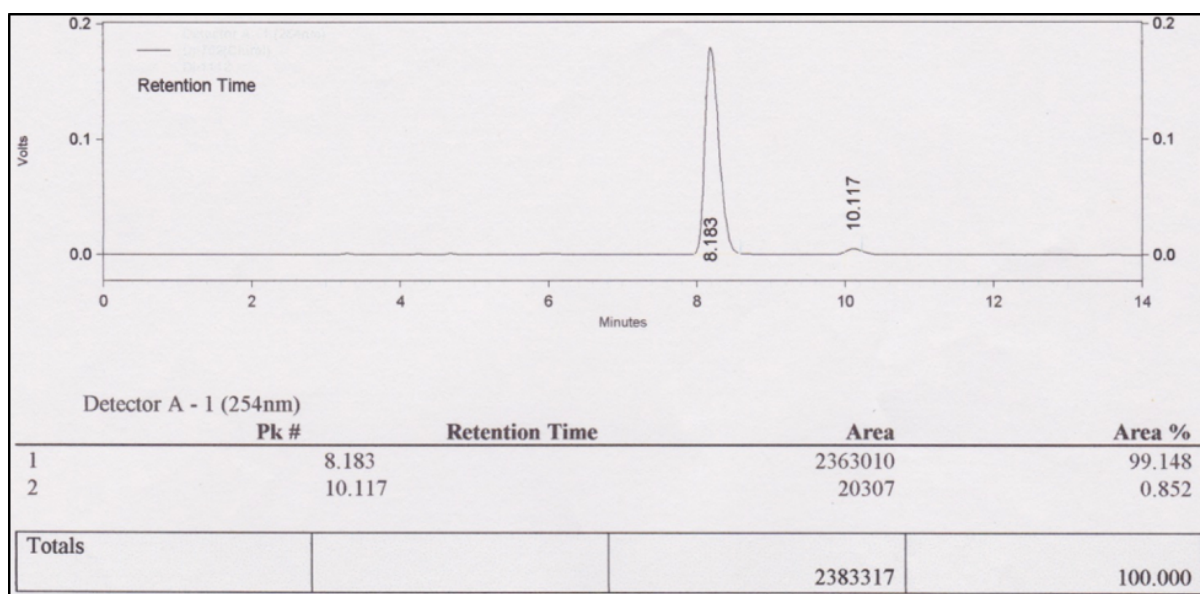
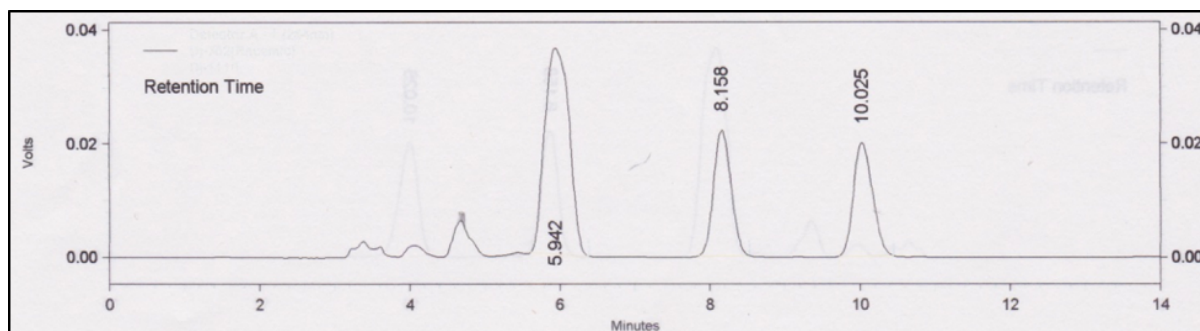
No.	RT	Area	Conc 1
1	12.14	1186764	98.871
2	15.95	13545	1.129
		1200309	100.000

Kromasil -5-cellucoat column, hexane/2-propanol (90:10), $1 \text{ mL} \cdot \text{min}^{-1}$, $\lambda = 220 \text{ nm}$, tr (minor): 15.9 min, tr (major): 12.1 min

(2*S*, 1'*R*)-2-(Hydroxy-(4-cyanophenyl)methyl)cyclohexan-1-one (Table 5, Entry 3)

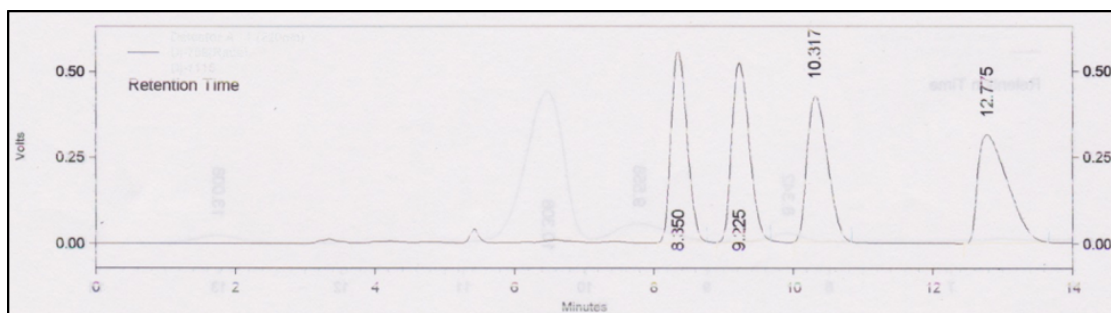
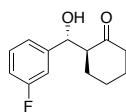
Chiralcel-IA column, Pet Ether/2-propanol (90:10), 1 mL·min⁻¹, λ = 220 nm, tr (minor): 12.2 min, tr (major): 16.7 min.

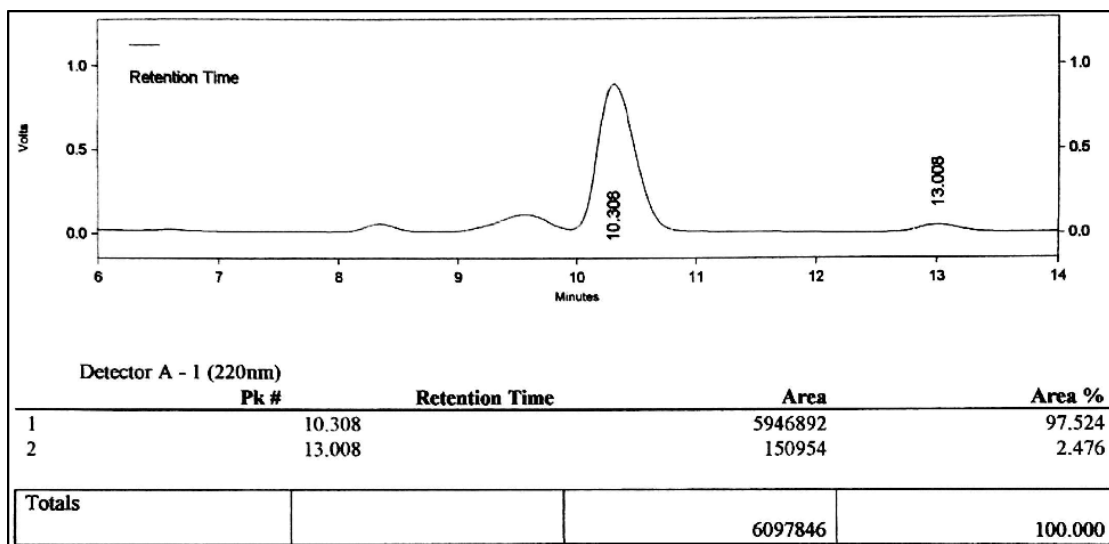
(*S*)-2-((*R*)-Hydroxy(2-fluoro-phenyl)methyl)cyclohexanone (Table 5, Entry 4)



Kromasil -5-cellicoat column, hexane/2-propanol (95:05), $1 \text{ mL} \cdot \text{min}^{-1}$, $\lambda = 254 \text{ nm}$, tr (minor): 10.1 min, tr (major): 8.1 min

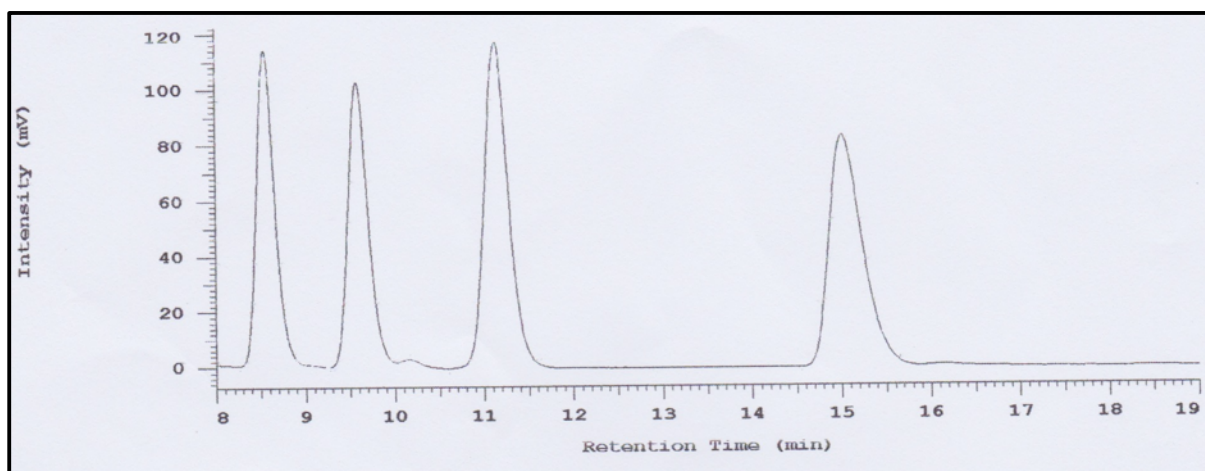
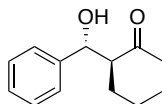
(S)-2-((R)-(3-fluorophenyl)(hydroxy)methyl)cyclohexan-1-one (Table 5, Entry 5)

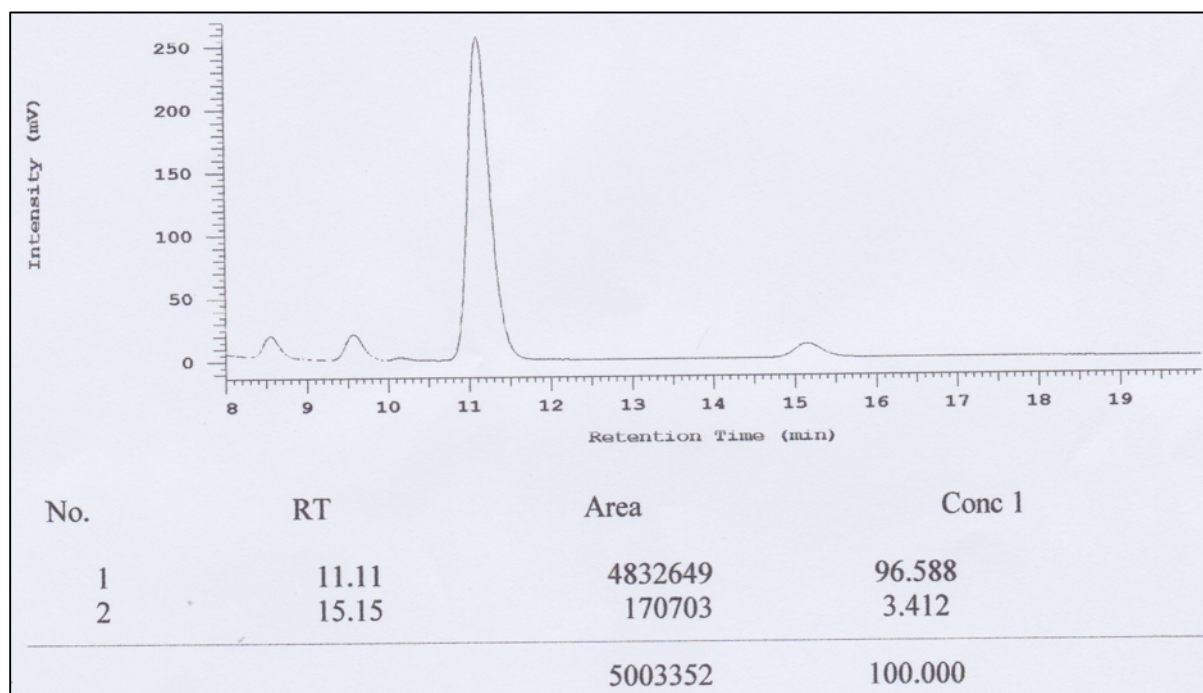




Kromasil -5-cellucoat column, hexane/2-propanol (95:05), $1 \text{ mL} \cdot \text{min}^{-1}$, $\lambda = 254 \text{ nm}$, tr (minor): 13.0 min, tr (major): 10.3 min

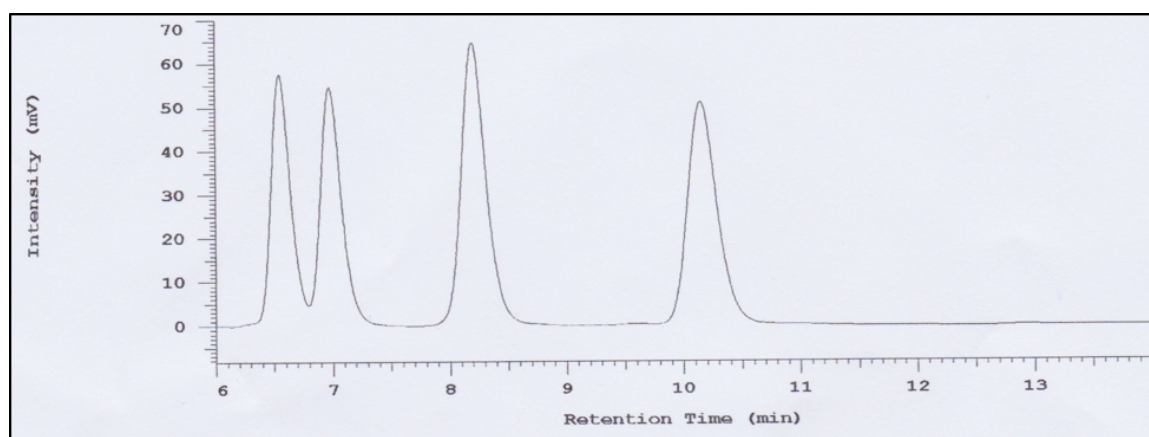
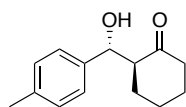
(2*S*, 1'*R*)-2-(Hydroxy(phenyl)methyl)cyclohexan-1-one (Table 5, Entry 6)

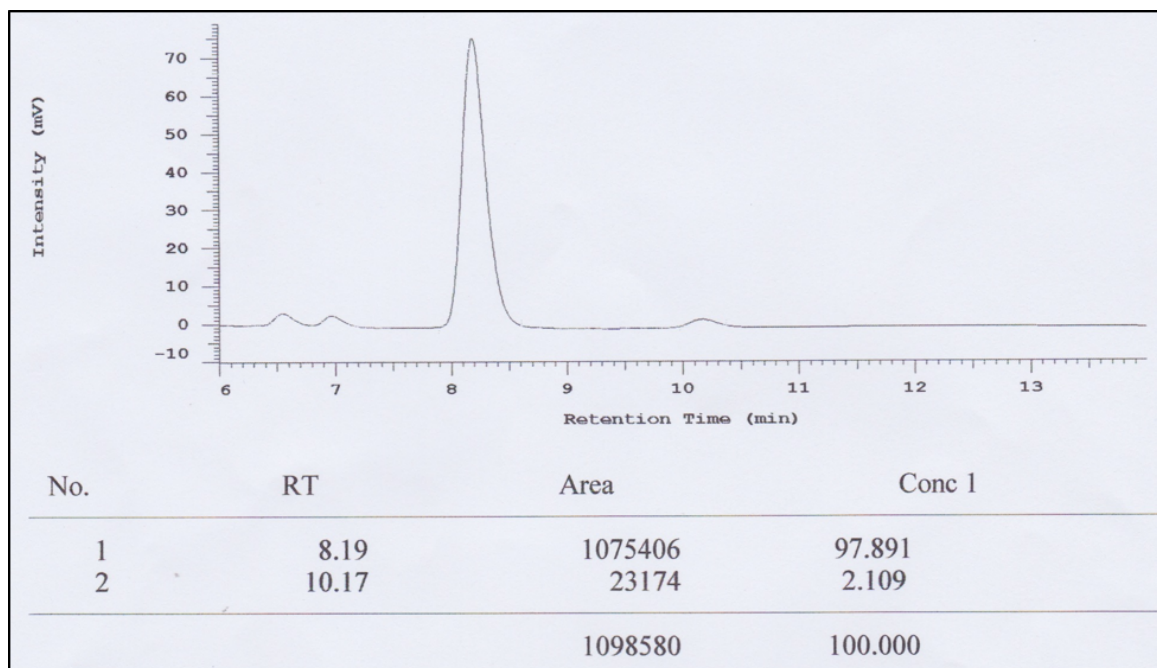




Kromasil Cellucoat column, IPA/n-hexane 04:96, $1 \text{ mL} \cdot \text{min}^{-1}$, $\lambda = 213 \text{ nm}$, tr (minor): 15.15 min, tr (major): 11.11 min

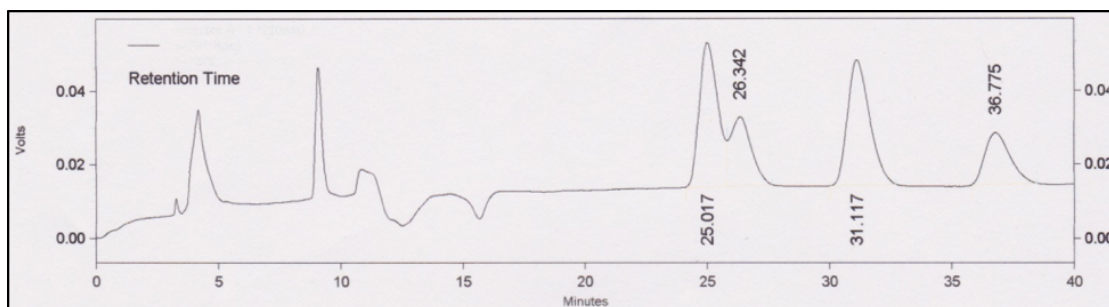
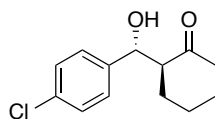
(S)-2-((R)-hydroxy(*p*-tolyl)methyl)cyclohexan-1-one (Table 5, Entry 7)

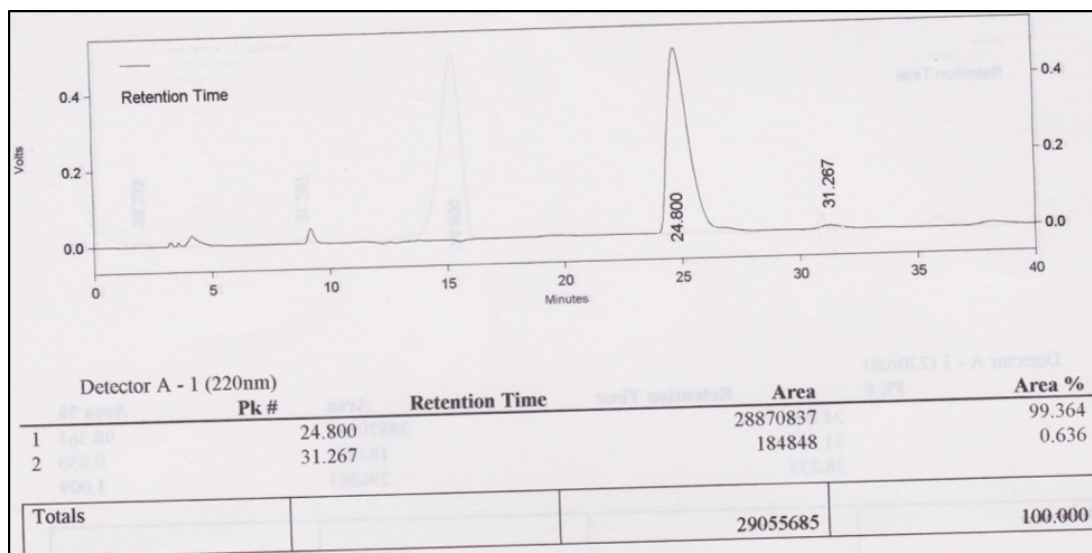




Kromasil -5-cellucoat column, hexane/2-propanol (95:05), $1 \text{ mL} \cdot \text{min}^{-1}$, $\lambda = 220 \text{ nm}$, tr (minor): 10.1 min, tr (major): 8.1 min

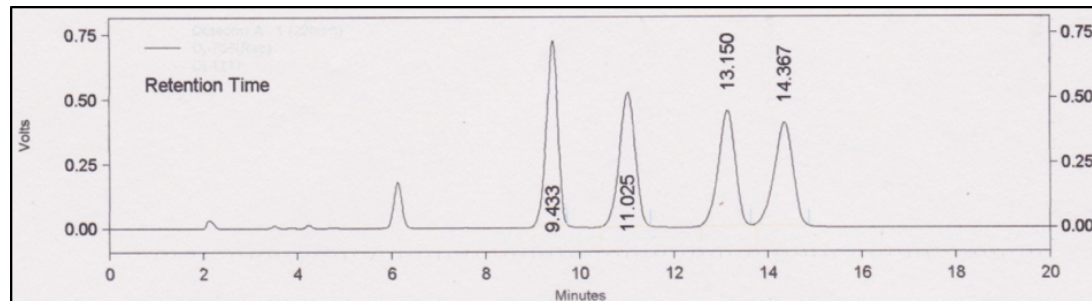
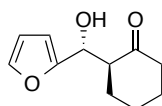
(2*S*, 1'*R*)-2-(Hydroxy-(4-chlorophenyl)methyl)cyclohexan-1-one (Table 5, Entry 8)

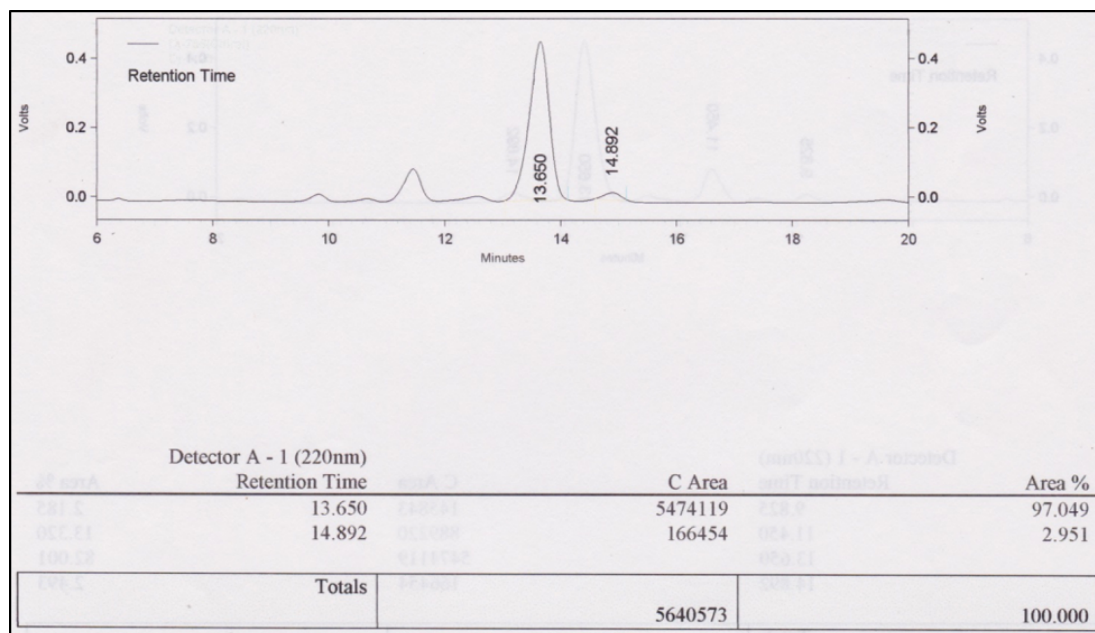




Chiralcell OJ-H column, Pet Ether/2-propanol 98.5:1.5, $1 \text{ mL} \cdot \text{min}^{-1}$, $\lambda = 220 \text{ nm}$, tr (minor): 31.2 min, tr (major): 24.8 min

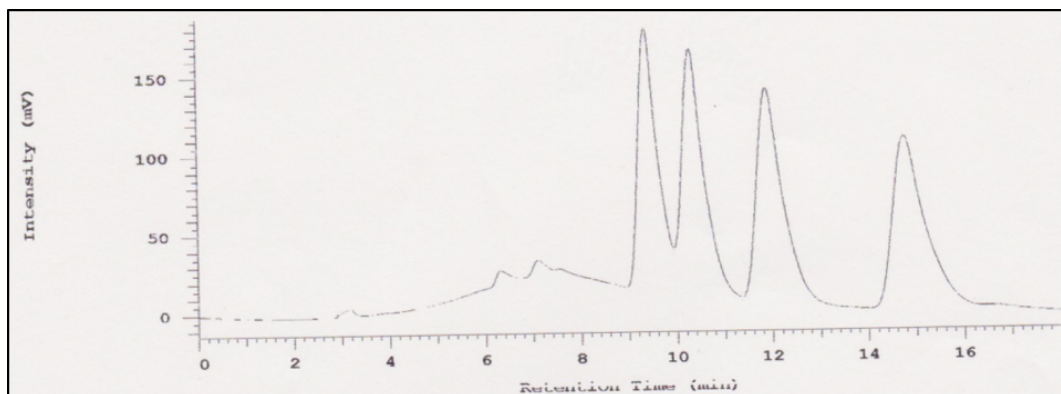
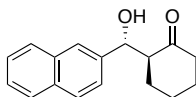
(2*S*, 1'*R*)-2-(Hydroxy-(furan-2-yl)propyl)cyclohexan-1-one (Table 5, Entry 9)

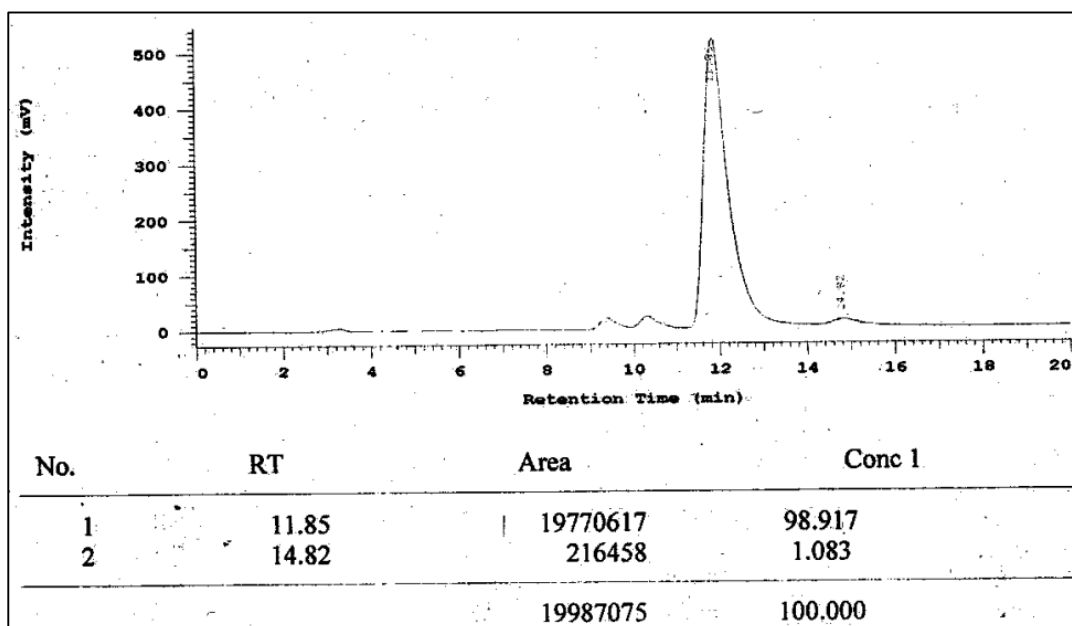




Chiralcel-IA column, n-hexane/2-propanol (95:05), $1 \text{ mL} \cdot \text{min}^{-1}$, $\lambda = 220 \text{ nm}$, tr (minor): 14.8 min, tr (major): 13.6 min.

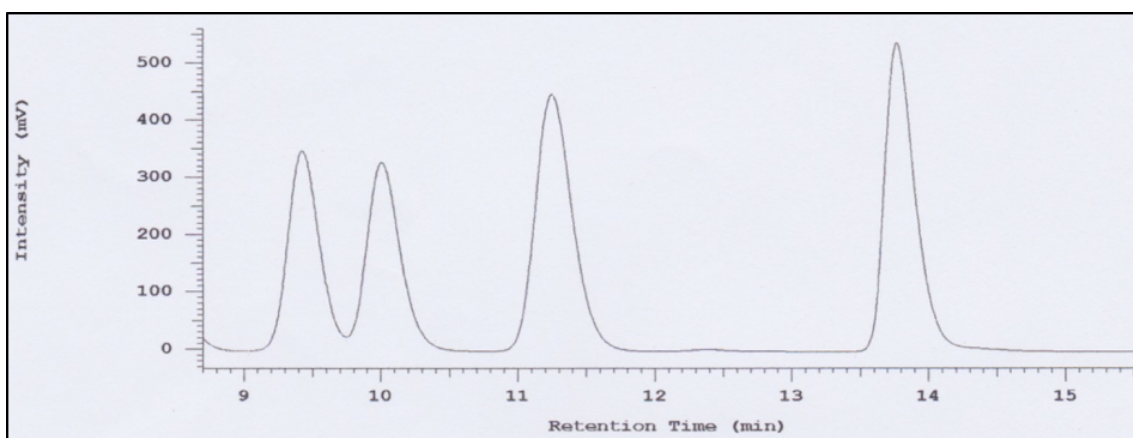
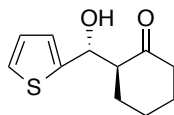
(S)-2-((R)-hydroxy(naphthalen-2-yl)methyl)cyclohexan-1-one (Table 5, Entry 10)

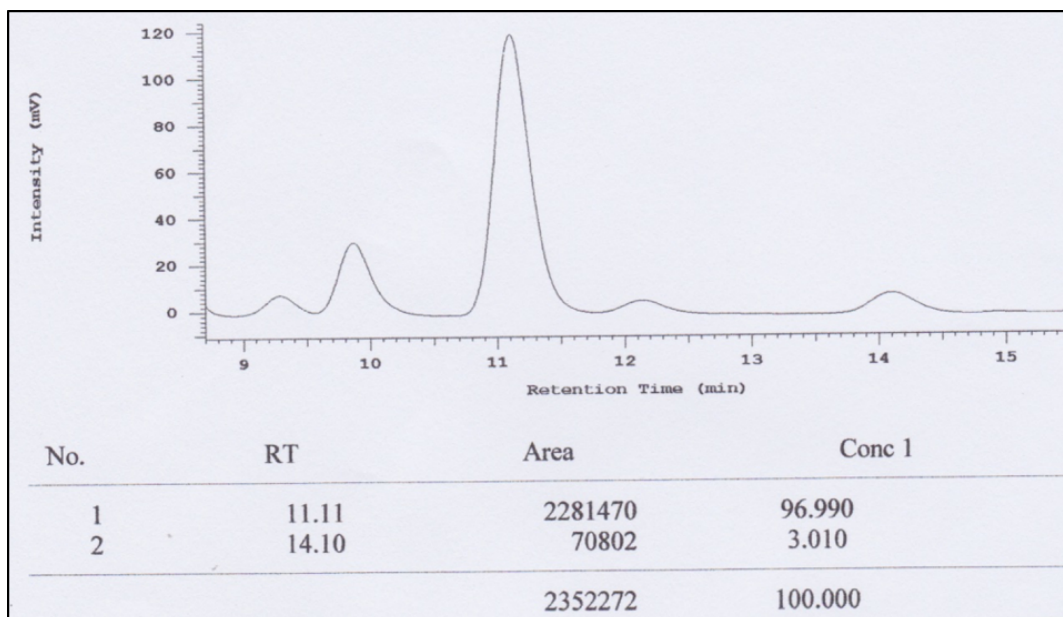




Chiralcel OD-H column, hexane/2-propanol (90:10), $1 \text{ mL} \cdot \text{min}^{-1}$, $\lambda = 220 \text{ nm}$, tr (minor): 14.8 min, tr (major): 11.8 min

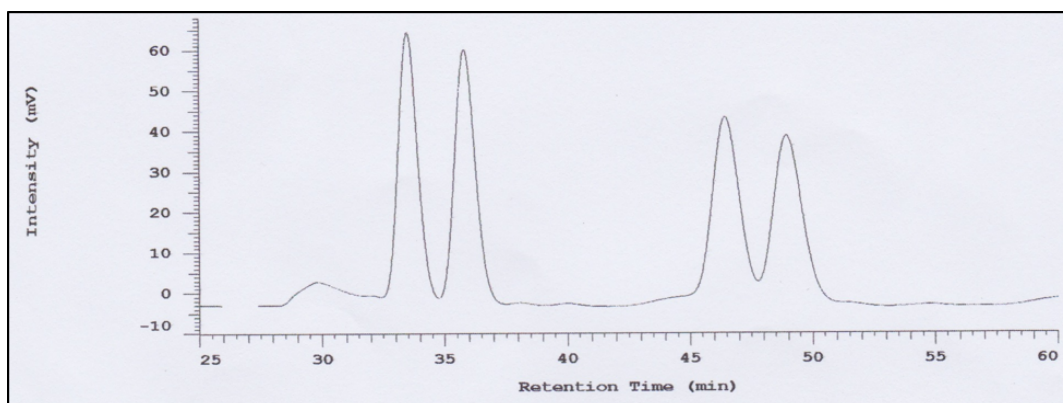
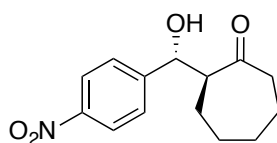
(S)-2-((R)-hydroxy(thiophen-2-yl)methyl)cyclohexan-1-one (Table 5, Entry 11)

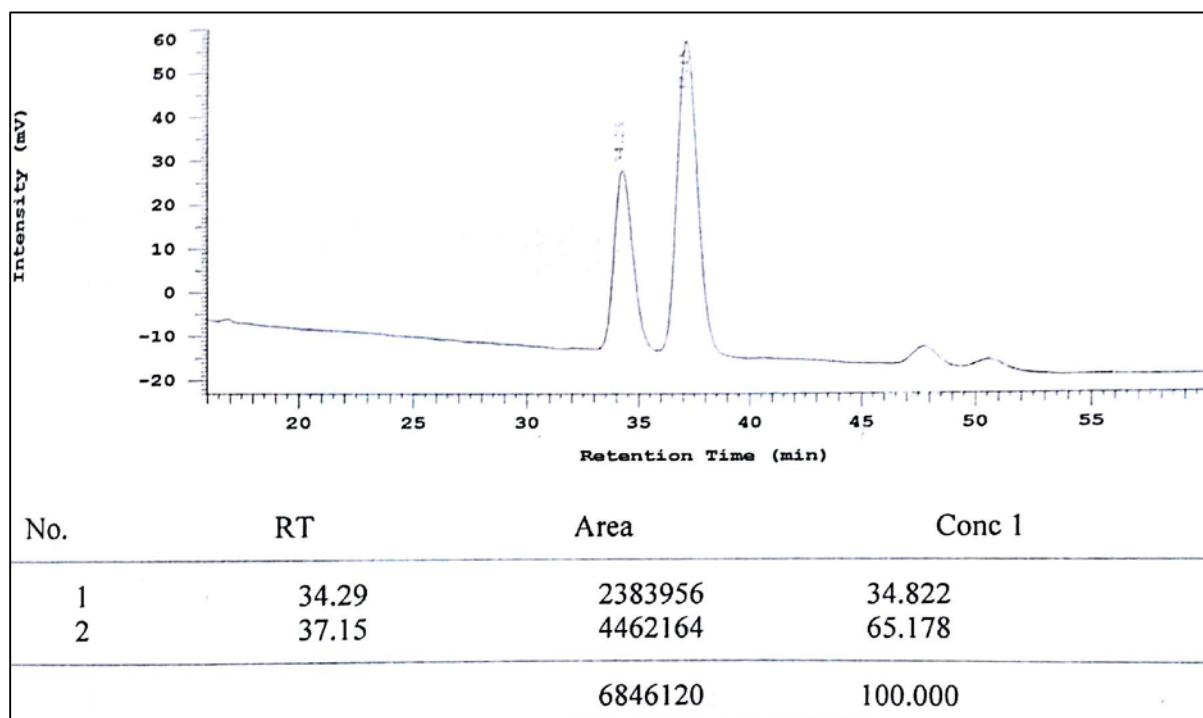




Kromasil -5-cellucoat column, hexane/2-propanol (95:05), $1 \text{ mL} \cdot \text{min}^{-1}$, $\lambda = 220 \text{ nm}$, tr (minor): 14.1 min, tr (major): 11.1 min

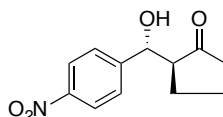
(S)-2-((R)-hydroxy(4-nitrophenyl)methyl)cycloheptan-1-one (Table 5, Entry 12)

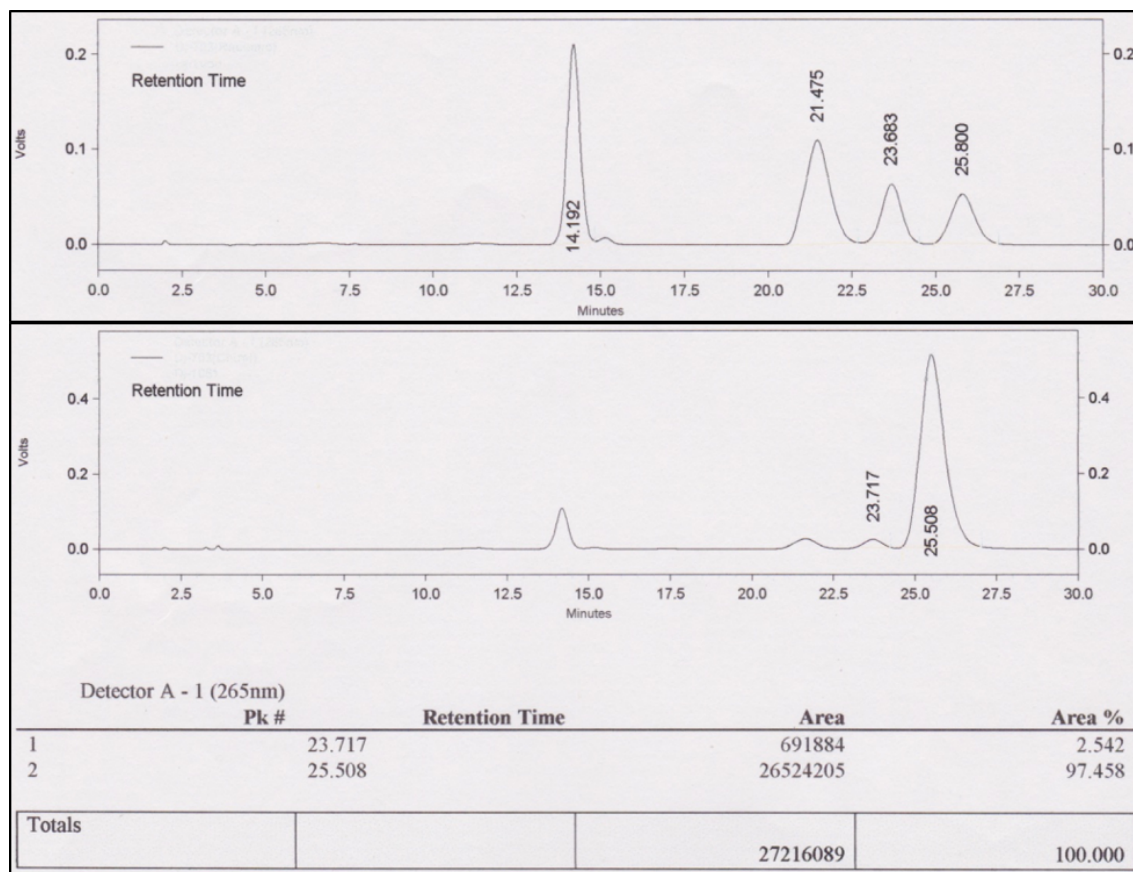




Kromasil -5-cellicoat column, hexane/2-propanol (98:2), $1 \text{ mL} \cdot \text{min}^{-1}$, $\lambda = 254 \text{ nm}$, tr (minor): 34.2 min, tr (major): 37.1 min

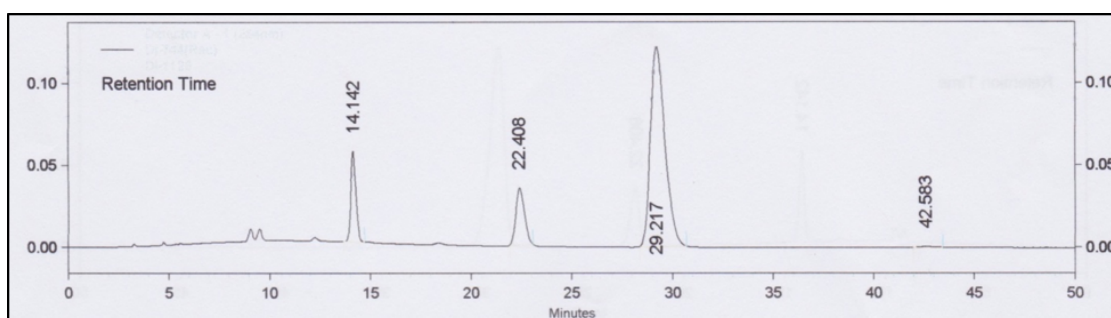
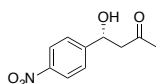
(S)-2-((R)-hydroxy(4-nitrophenyl)methyl)cyclopentan-1-one (Table 5, Entry 13)

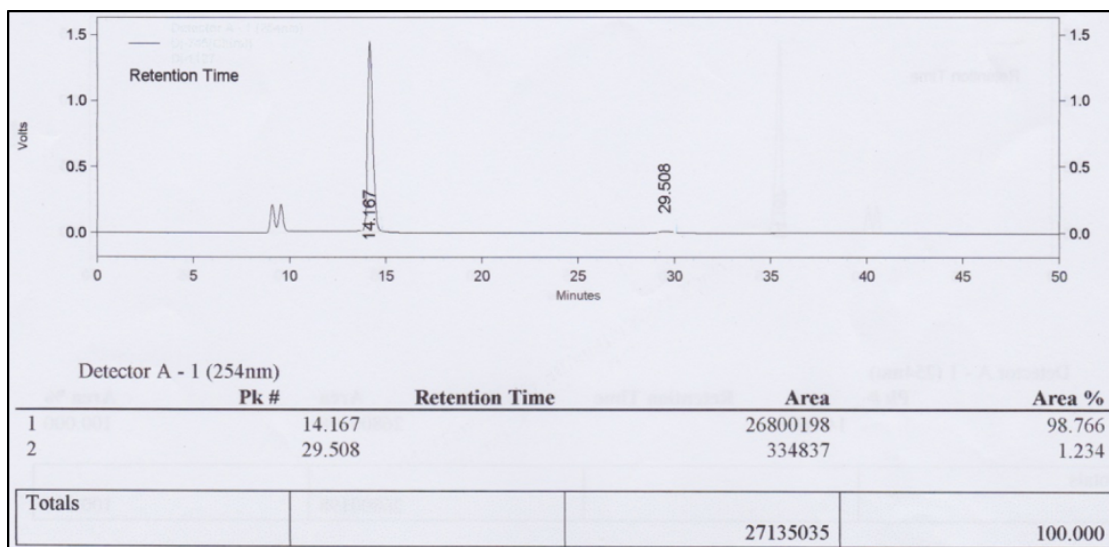




Chiralcel-IA column, Pet Ether/2-propanol (95:05), $1 \text{ mL} \cdot \text{min}^{-1}$, $\lambda = 265 \text{ nm}$, tr (minor): 23.7 min, tr (major): 25.5 min.

(R)-4-Hydroxy-4-(4-nitrophenyl)butan-2-one (Table 5, Entry 14)

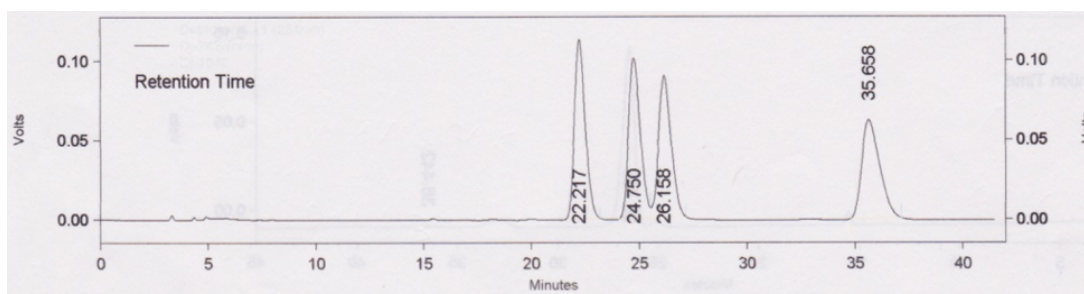




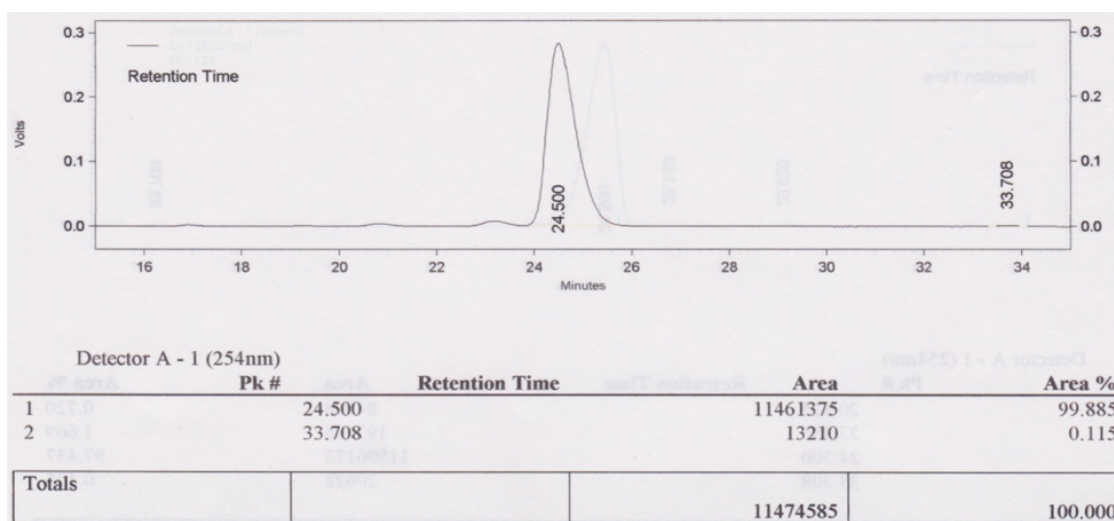
Kromasil -5-cellucoat column, hexane/2-propanol 95:05, $1 \text{ mL} \cdot \text{min}^{-1}$, $\lambda = 254 \text{ nm}$, tr (minor): 29.5 min, tr (major): 14.16 min

Table 4. Entry 2.

Racemic

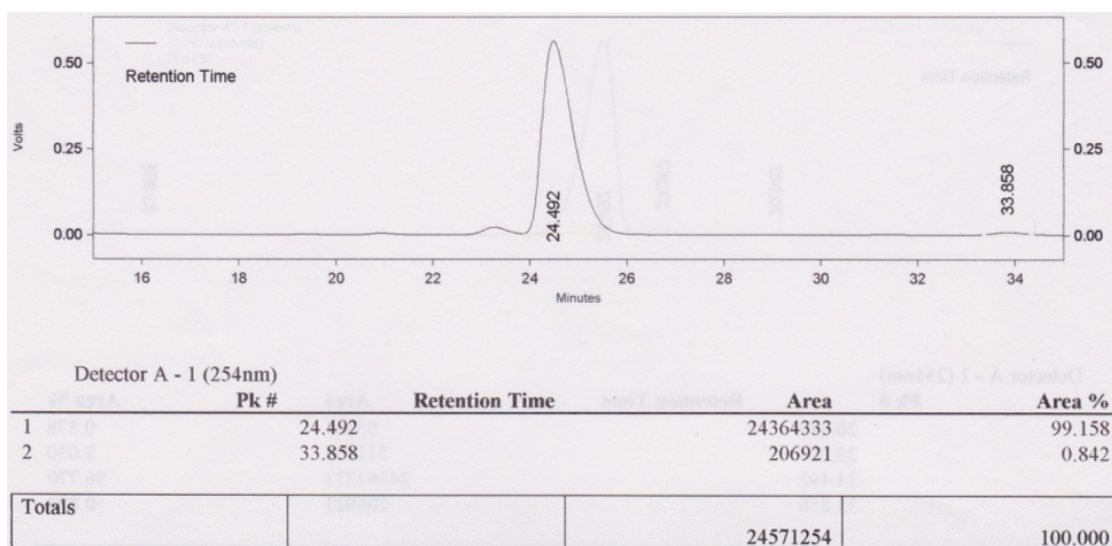


Chiral



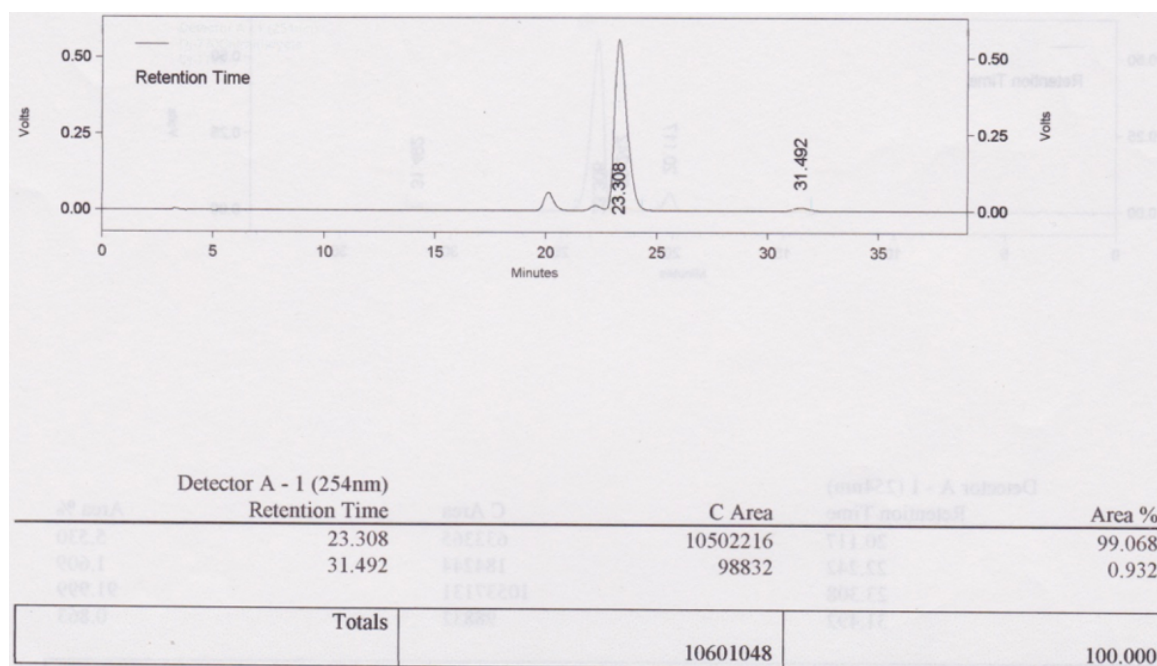
Kromasil -5-cellucoat column, hexane/2-propanol (95:05), $1 \text{ mL} \cdot \text{min}^{-1}$, $\lambda = 254 \text{ nm}$, tr (minor): 33.7 min, tr (major): 24.5 min.

Table 4. Entry 3.



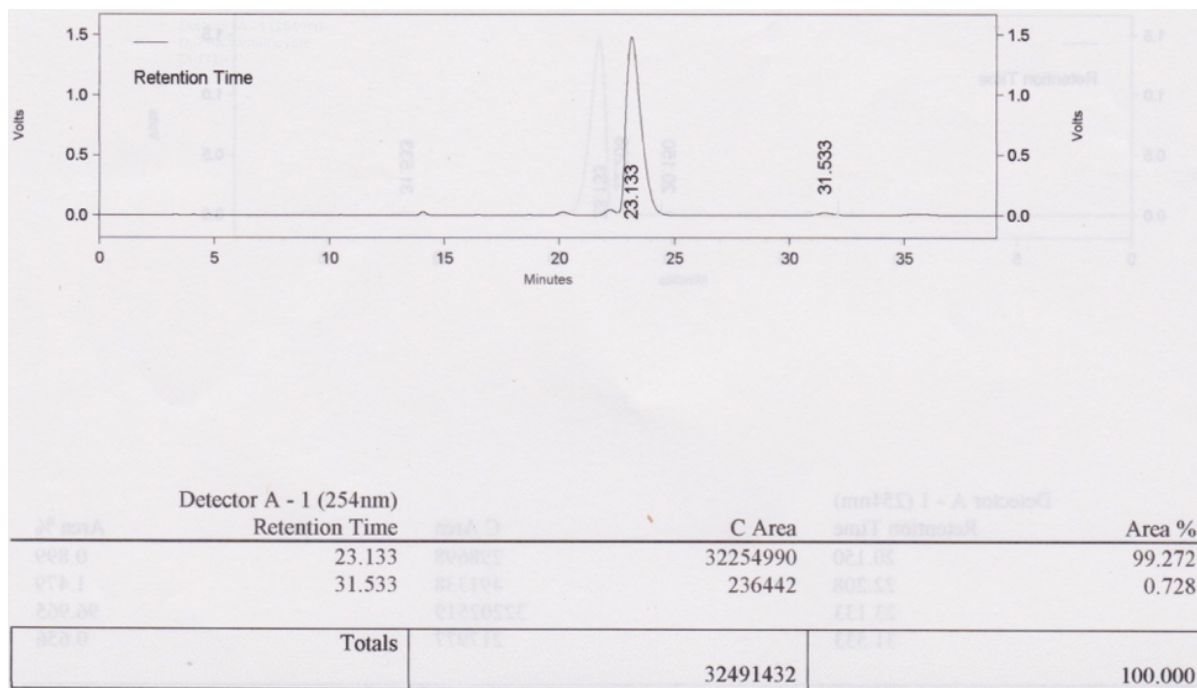
Kromasil -5-cellucoat column, hexane/2-propanol (95:05), $1 \text{ mL} \cdot \text{min}^{-1}$, $\lambda = 254 \text{ nm}$, tr (minor): 33.8 min, tr (major): 24.4 min.

Table 6, Entry 1.



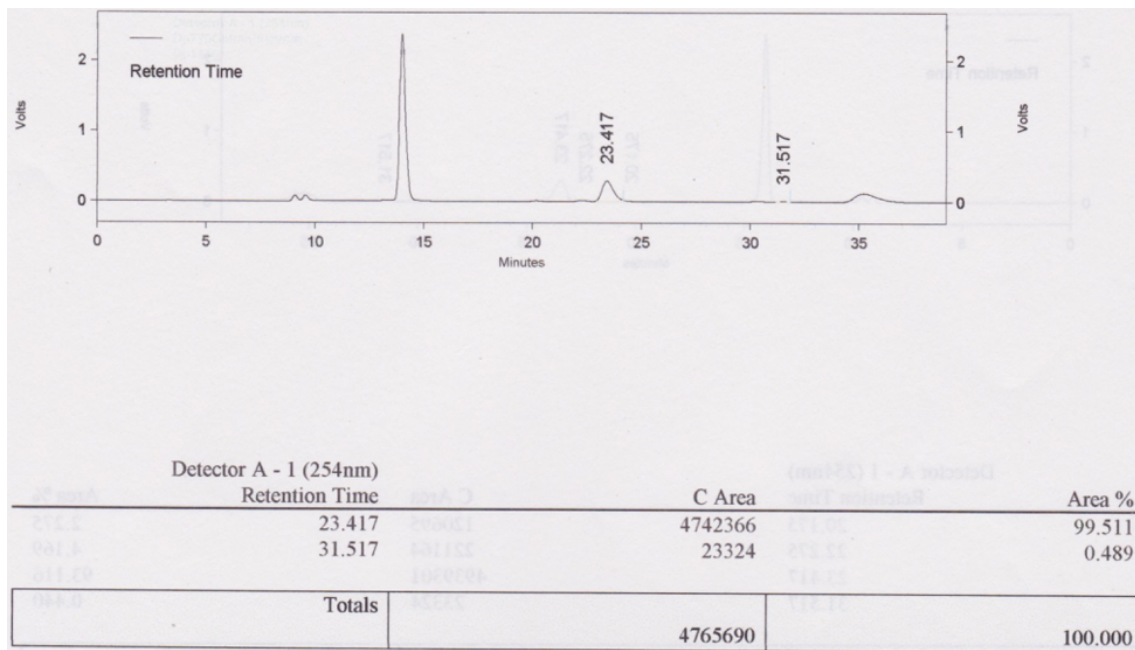
Kromasil -5-cellucoat column, hexane/2-propanol (95:05), $1 \text{ mL} \cdot \text{min}^{-1}$, $\lambda = 254 \text{ nm}$, tr (minor): 31.4 min, tr (major): 23.3 min.

Table 6, Entry 2



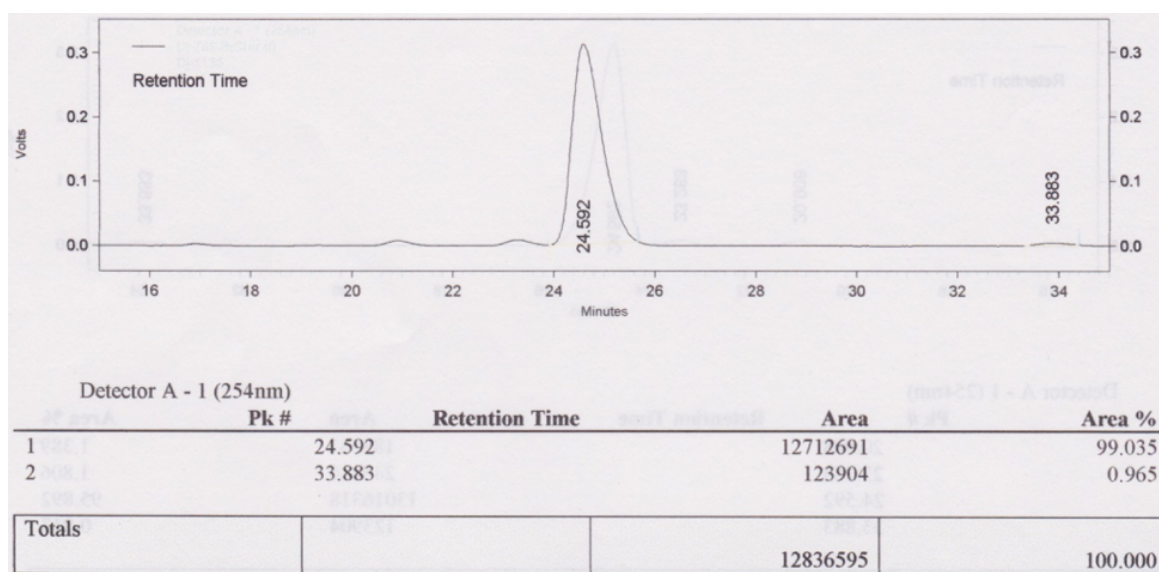
Kromasil -5-cellucoat column, hexane/2-propanol (95:05), $1 \text{ mL} \cdot \text{min}^{-1}$, $\lambda = 254 \text{ nm}$, tr (minor): 31.5 min, tr (major): 23.3 min.

Table 6, Entry 3



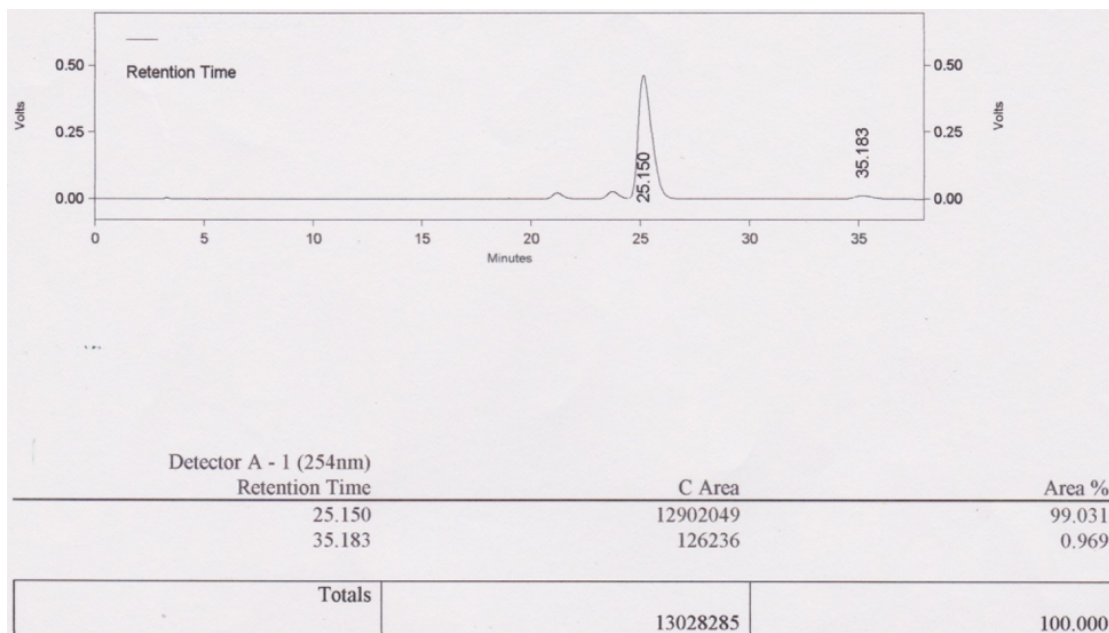
Kromasil -5-cellicoat column, hexane/2-propanol (95:05), $1 \text{ mL} \cdot \text{min}^{-1}$, $\lambda = 254 \text{ nm}$, t_r (minor): 31.5 min, t_r (major): 23.4 min. (HPLC of crude rxn mixture without purification, peaks at 14 & 35 are for impurities).

Table 2, Entry 8.



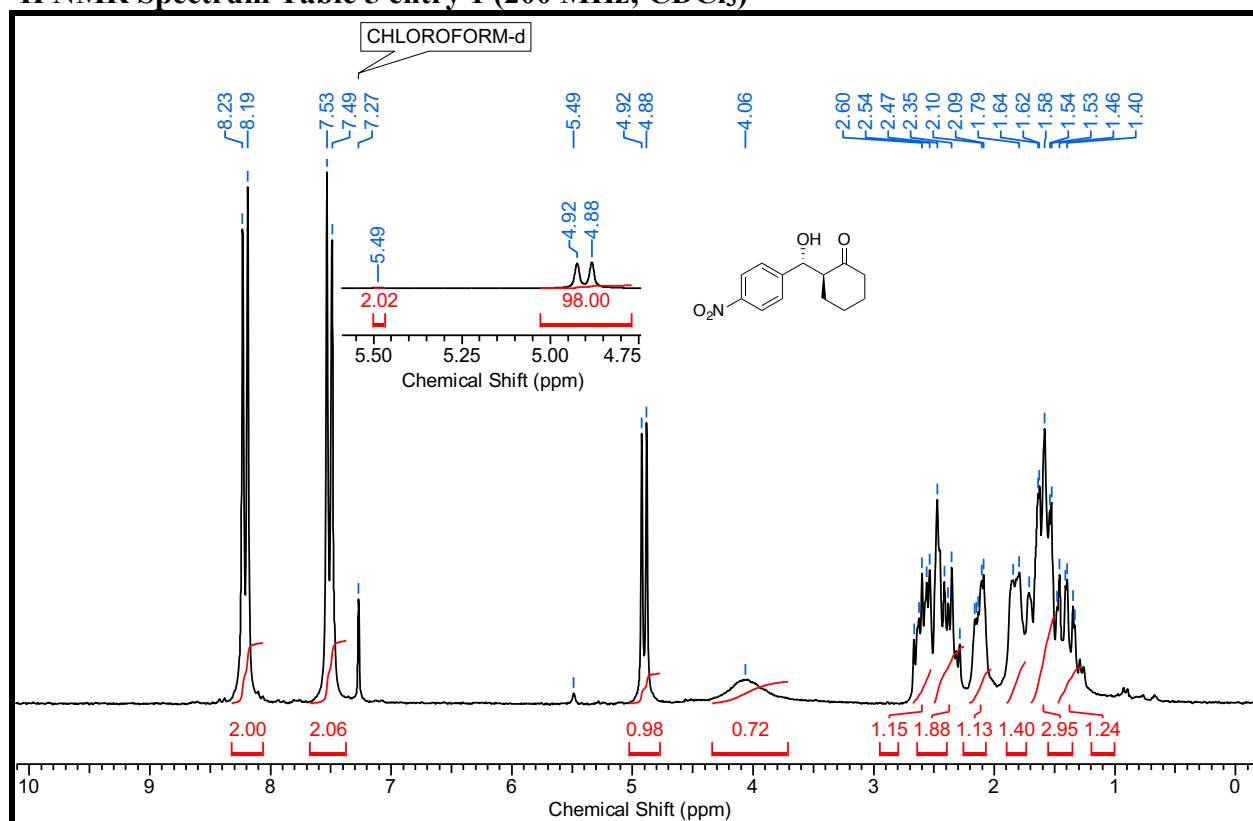
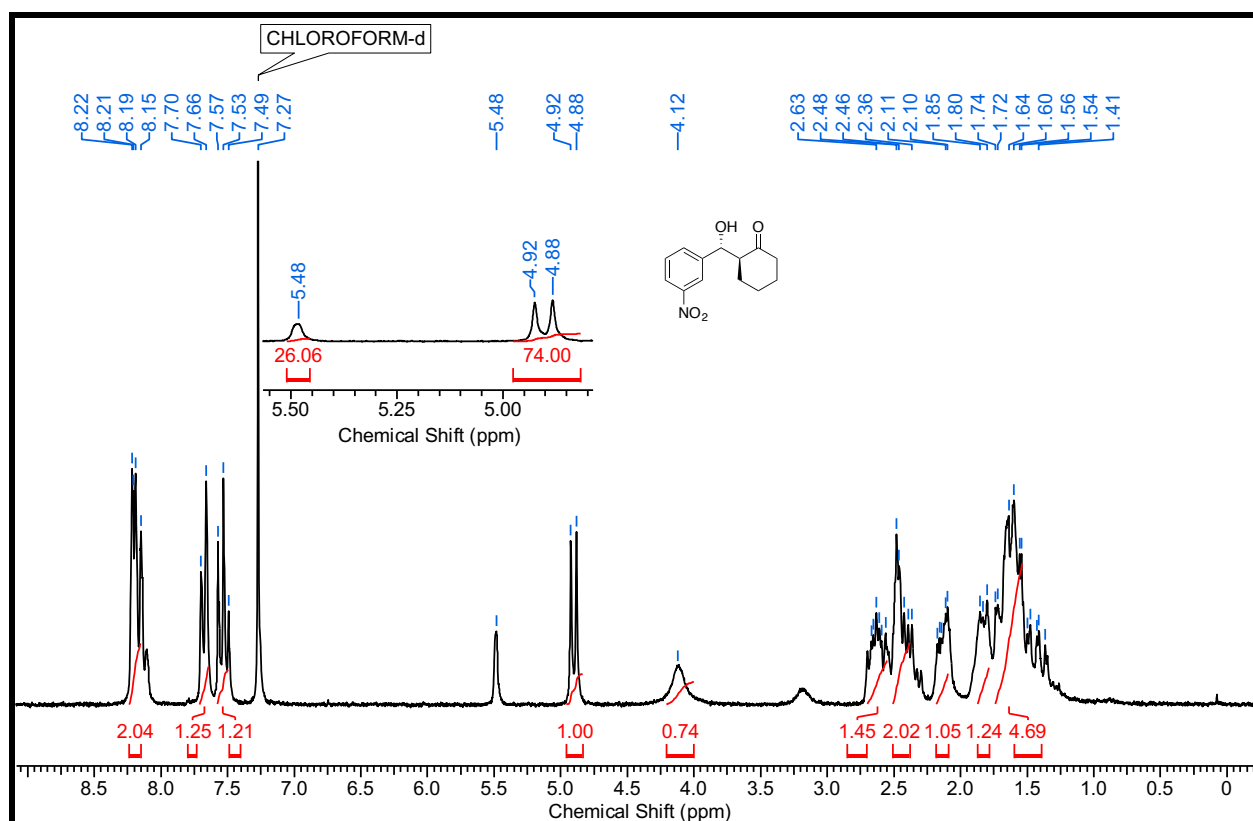
Kromasil -5-cellucoat column, hexane/2-propanol (95:05), $1 \text{ mL} \cdot \text{min}^{-1}$, $\lambda = 254 \text{ nm}$, tr (minor): 33.8 min, tr (major): 24.5 min.

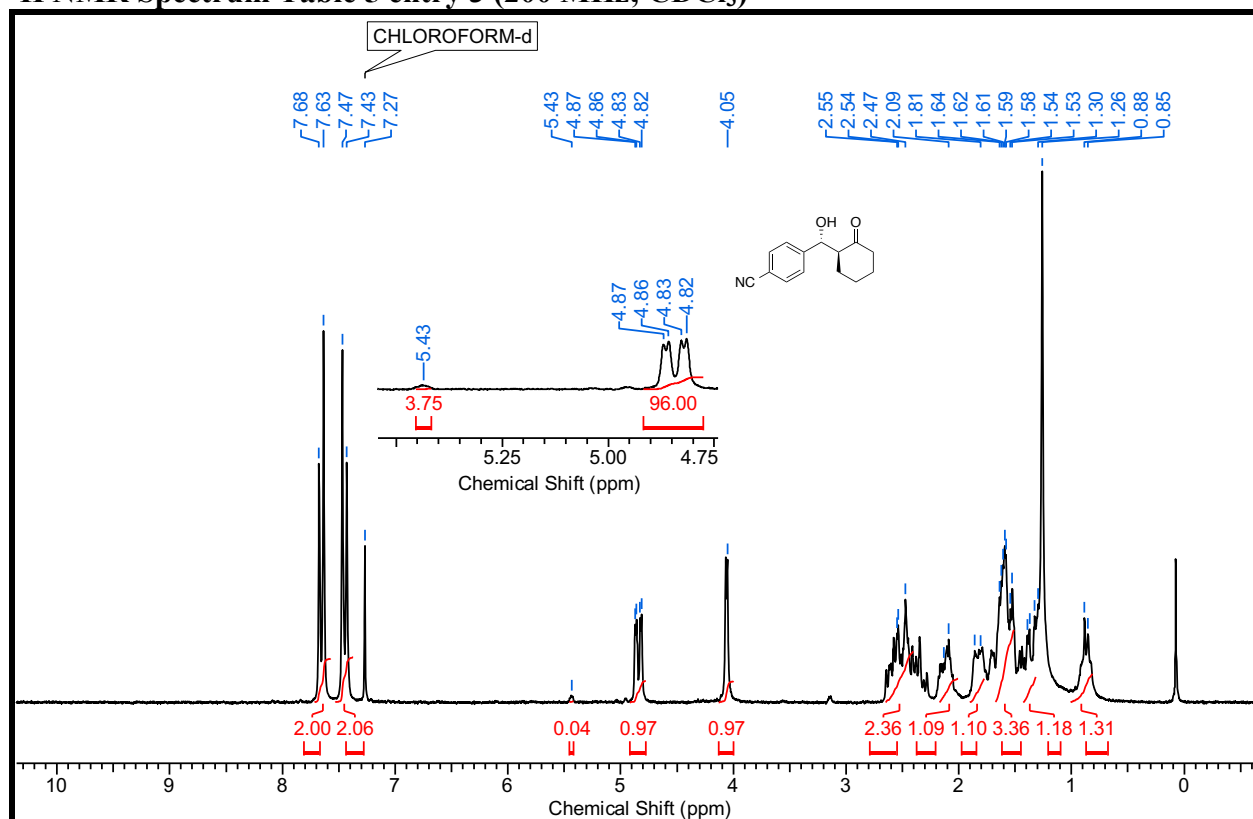
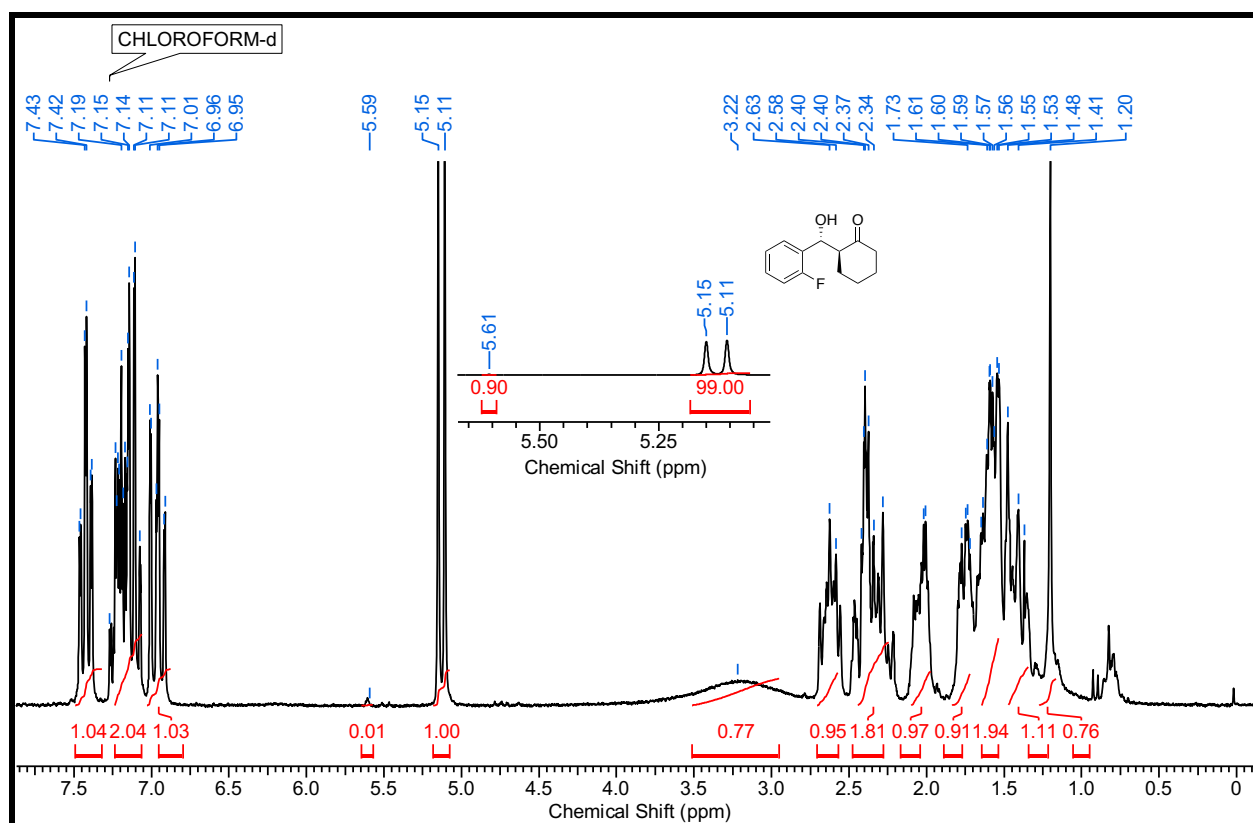
Table 2, Entry 9.

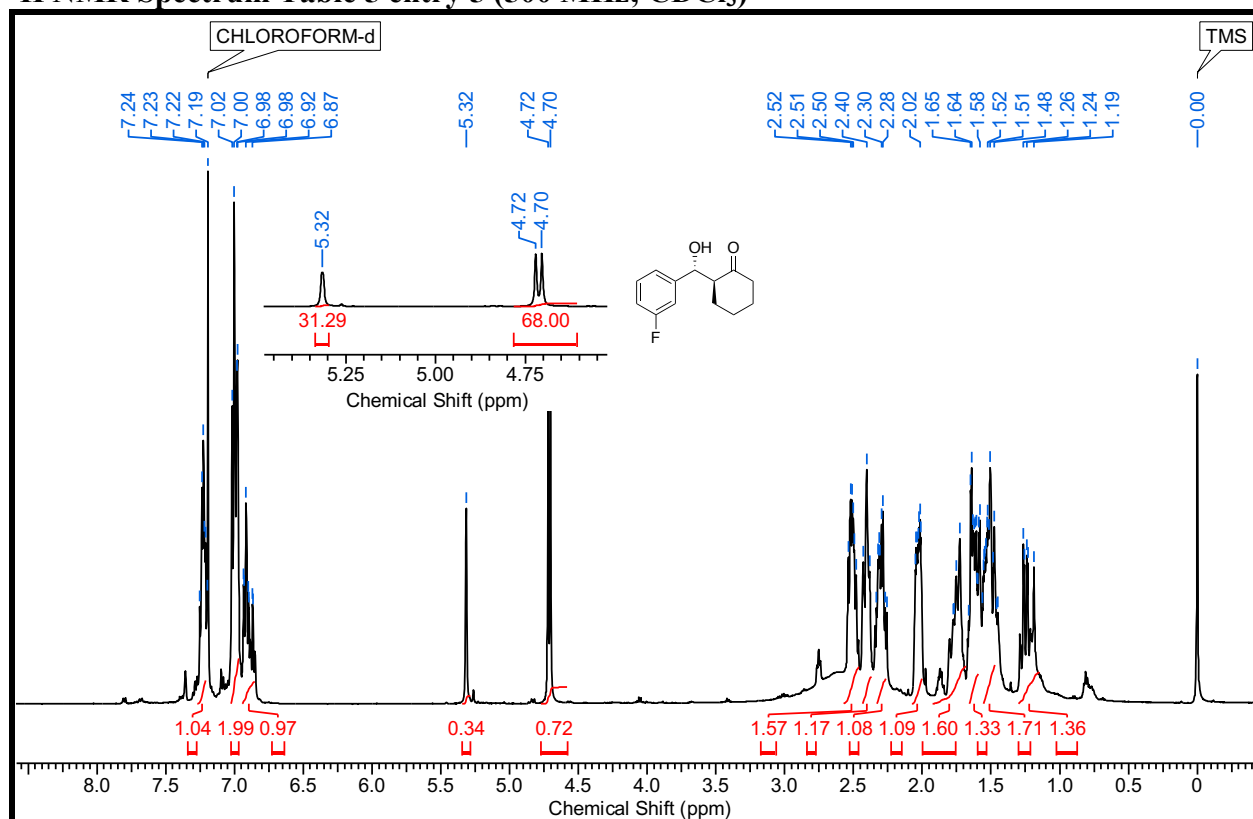
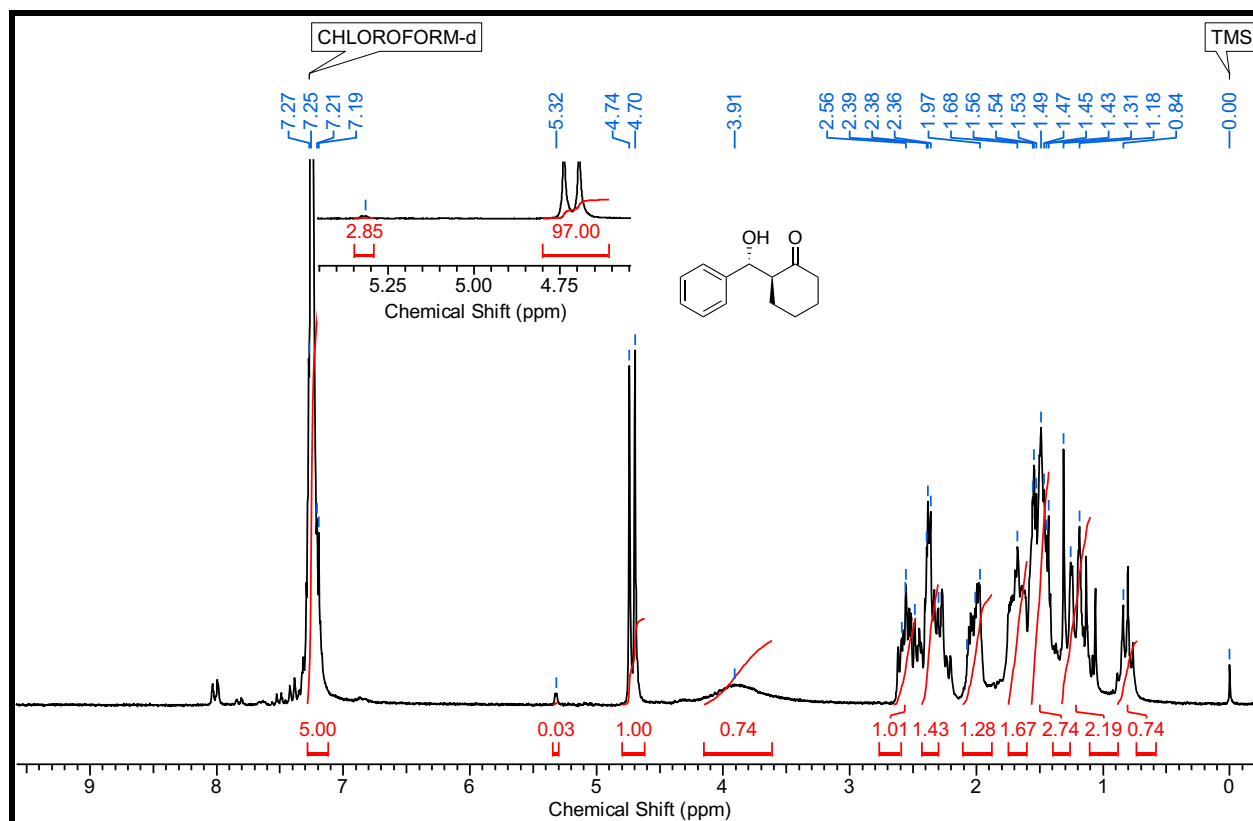


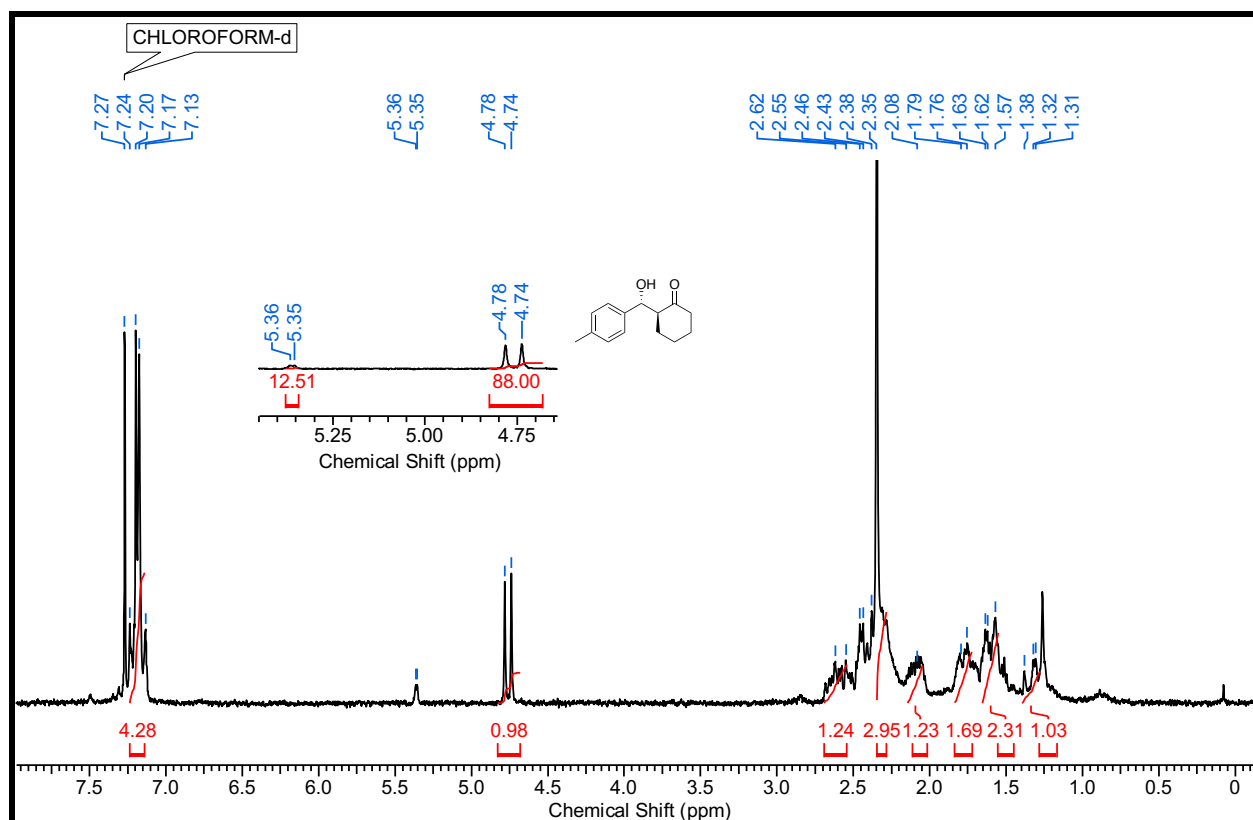
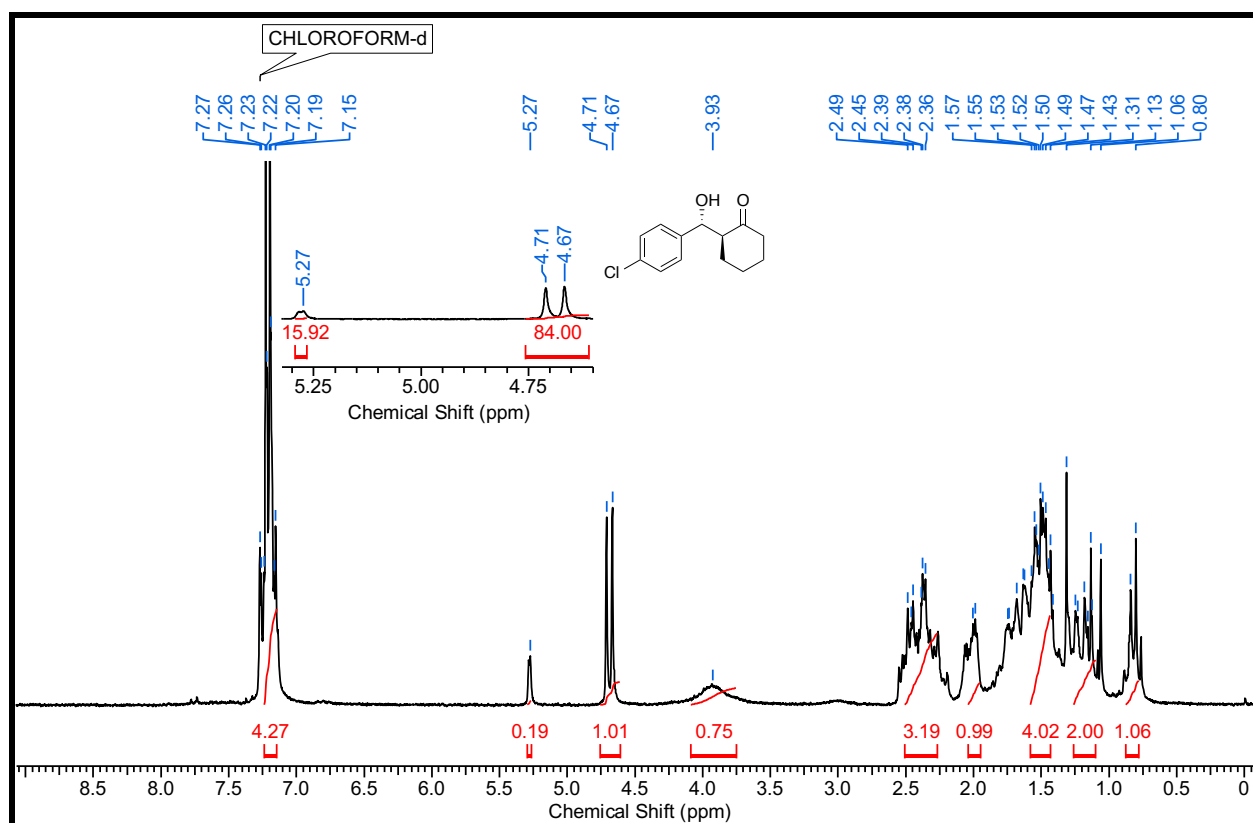
Kromasil -5-cellucoat column, hexane/2-propanol (95:05), $1 \text{ mL} \cdot \text{min}^{-1}$, $\lambda = 254 \text{ nm}$, tr (minor): 35.1 min, tr (major): 25.1 min.

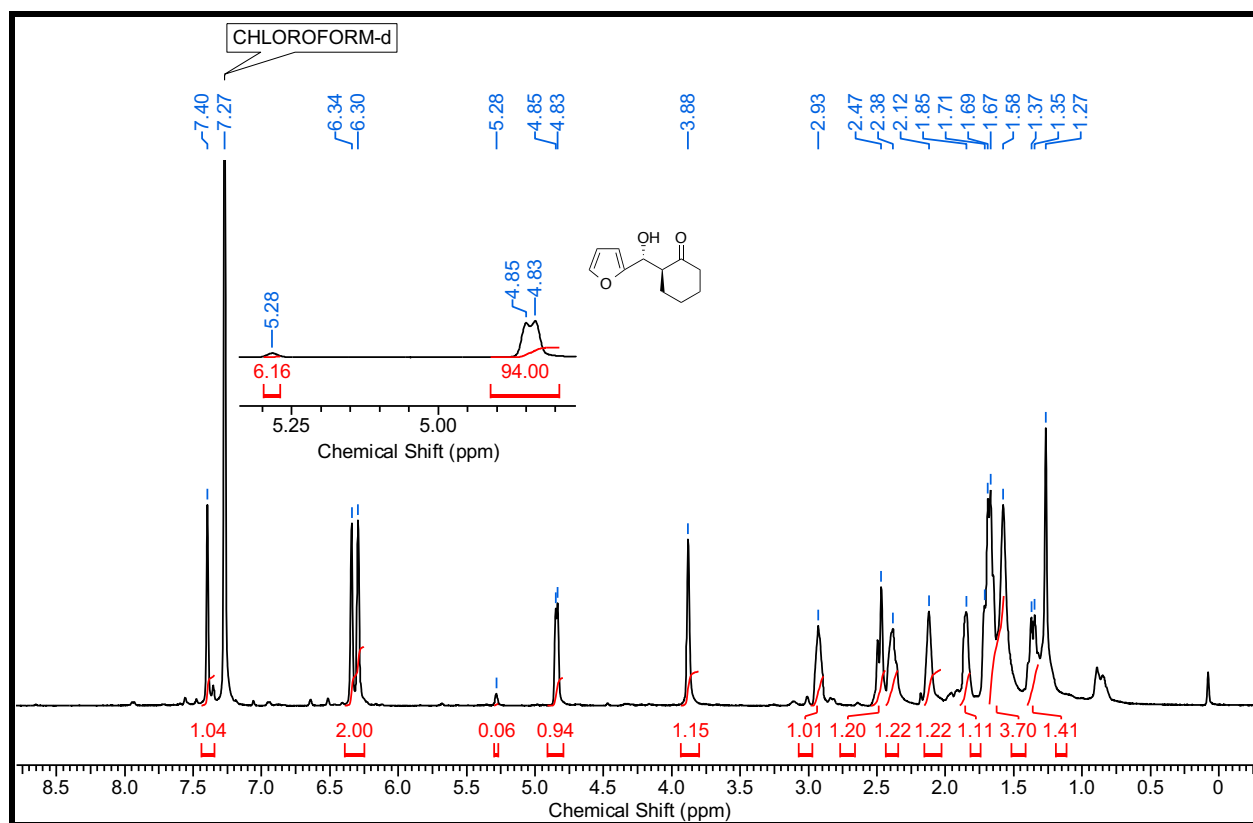
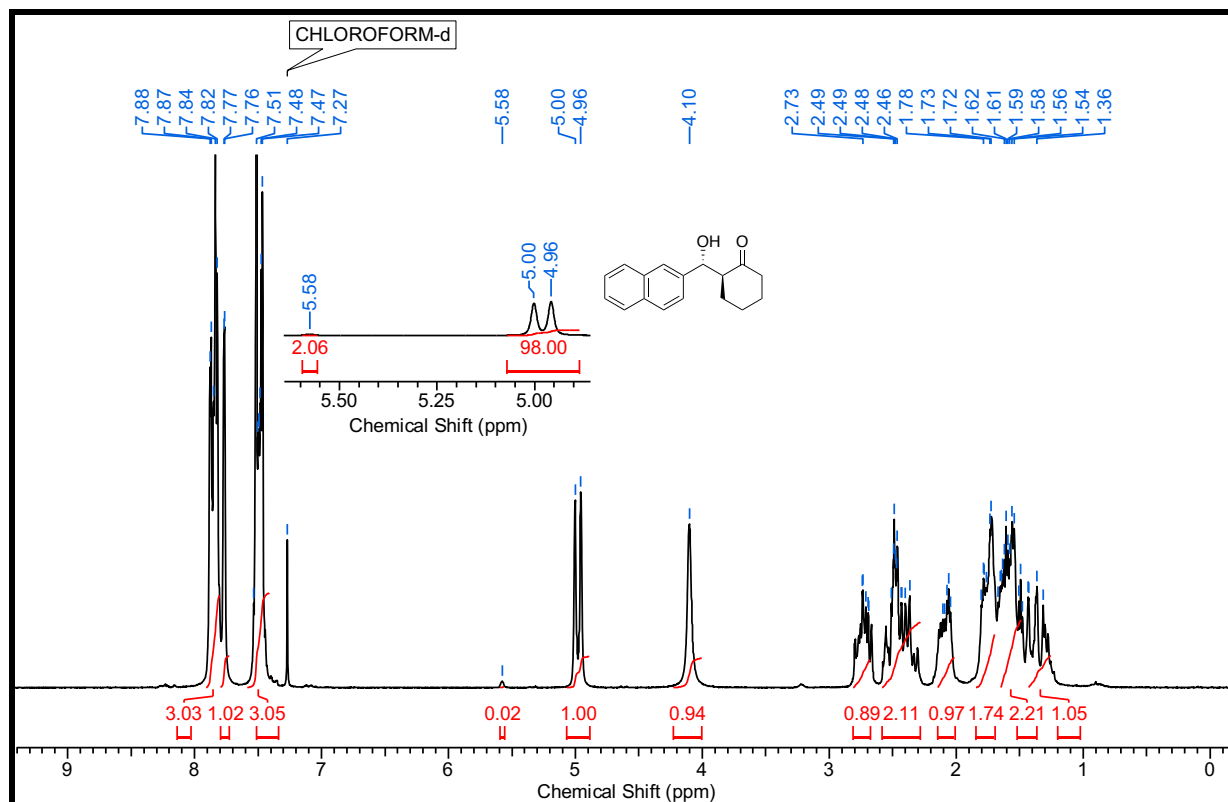
3.8 NMR Spectra's

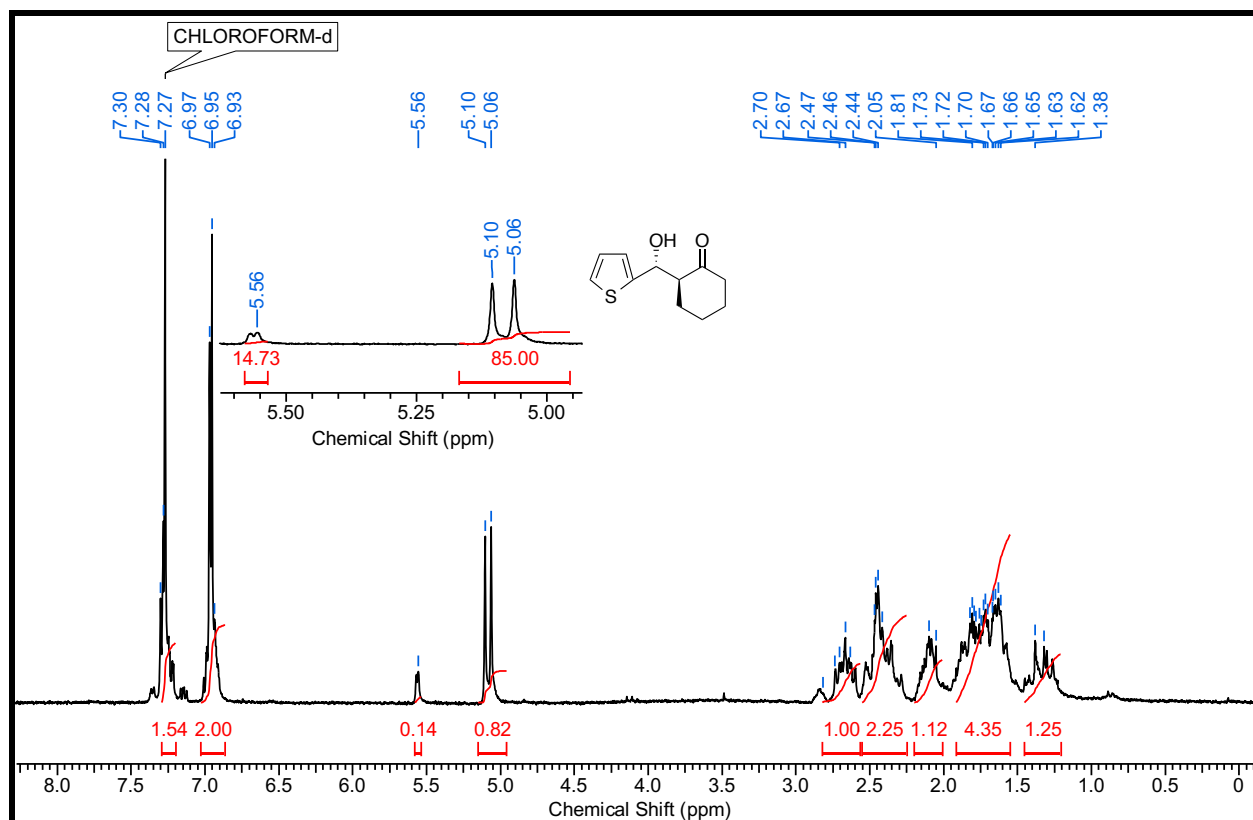
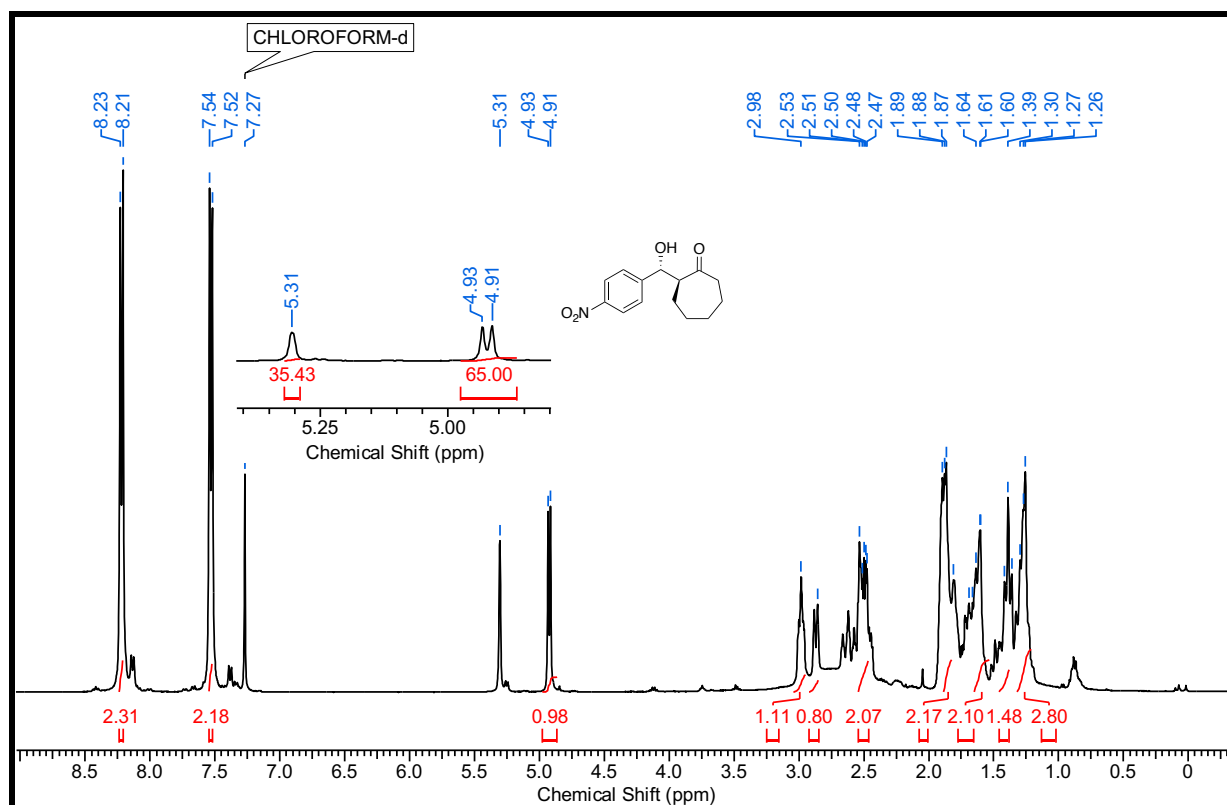
¹H NMR Spectrum Table 5 entry 1 (200 MHz; CDCl₃)¹H NMR Spectrum Table 5 entry 2 (200 MHz; CDCl₃)

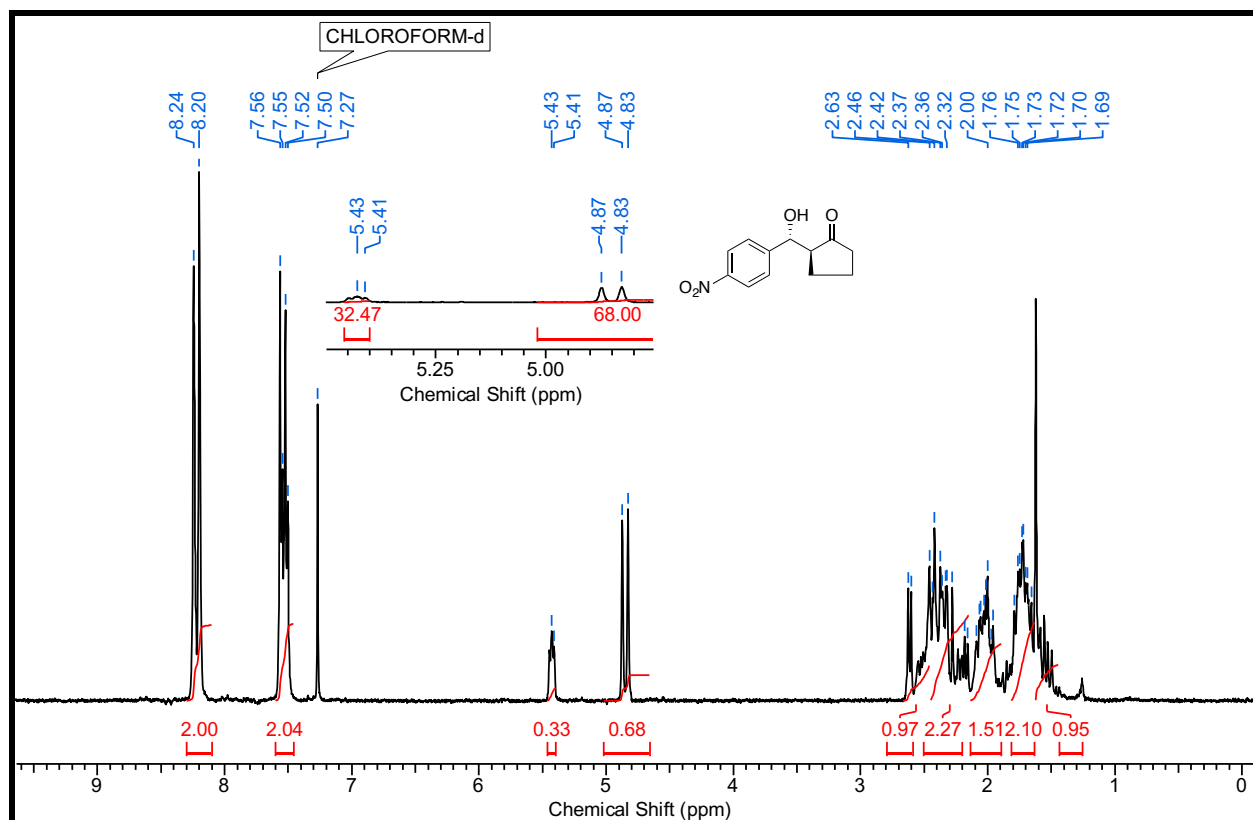
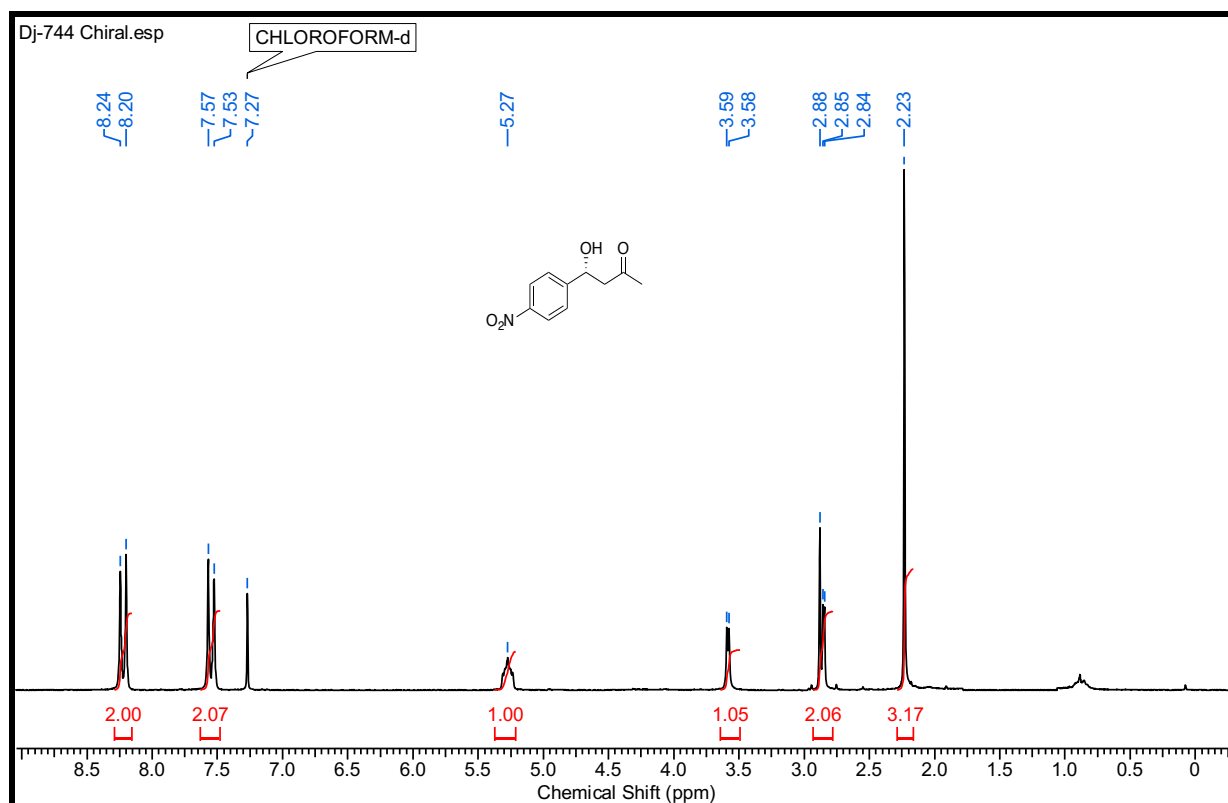
¹H NMR Spectrum Table 5 entry 3 (200 MHz; CDCl₃)¹H NMR Spectrum Table 5 entry 4 (200 MHz; CDCl₃)

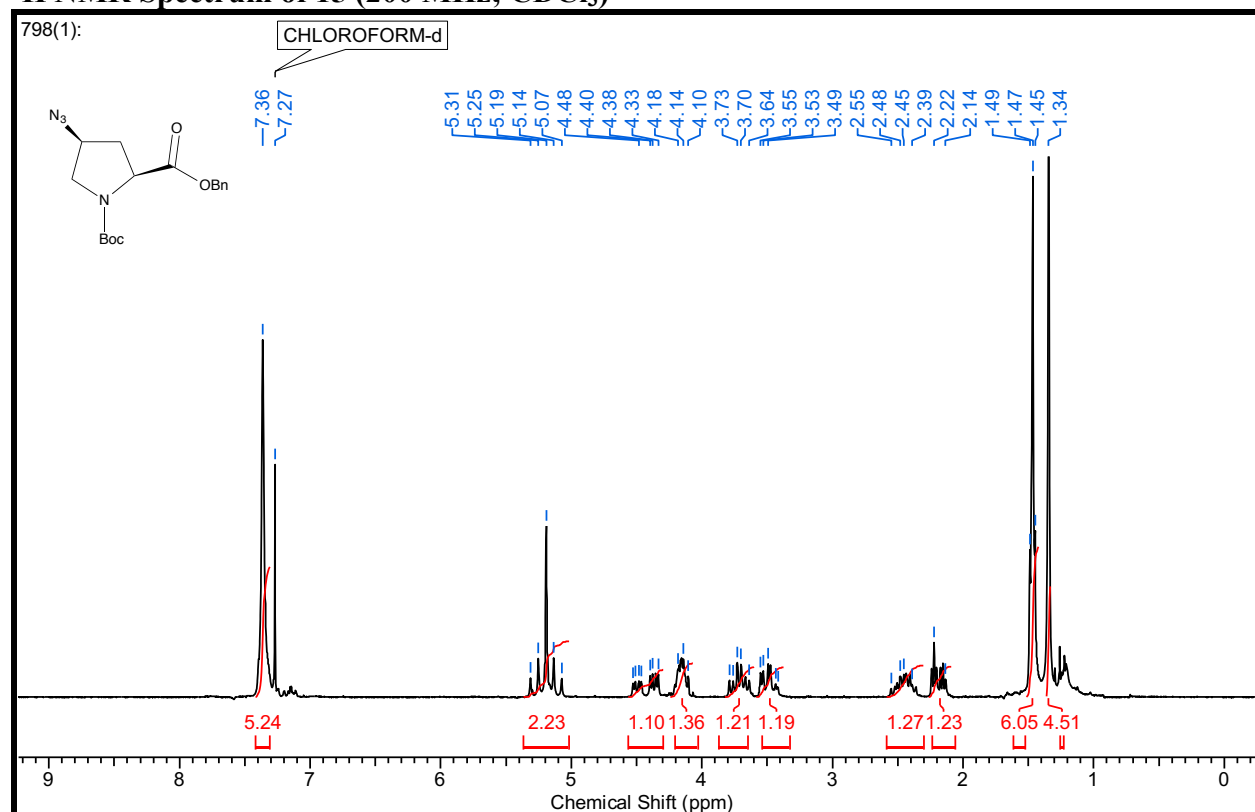
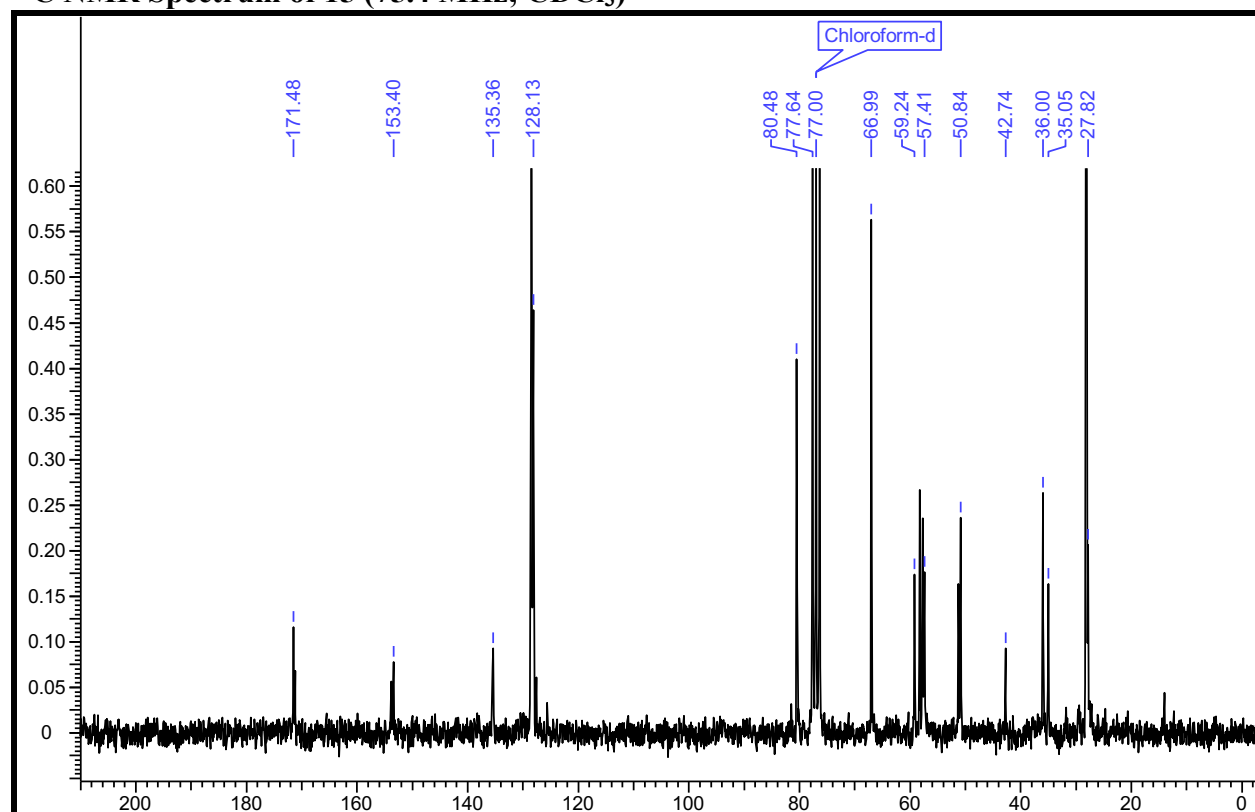
^1H NMR Spectrum Table 5 entry 5 (500 MHz; CDCl_3) ^1H NMR Spectrum Table 5 entry 6 (200 MHz; CDCl_3)

¹H NMR Spectrum Table 5 entry 7 (200 MHz; CDCl₃)¹H NMR Spectrum Table 5 entry 8 (200 MHz; CDCl₃)

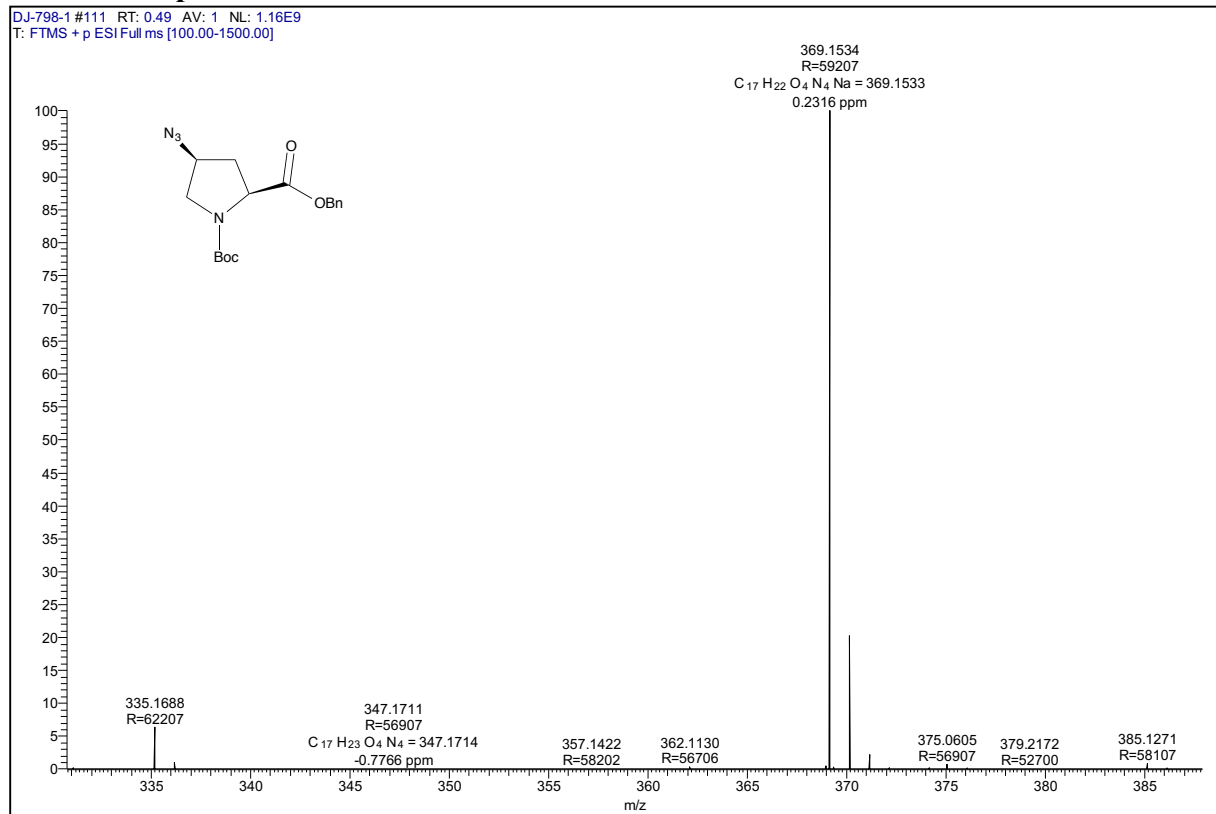
^1H NMR Spectrum Table 5 entry 9 (500 MHz; CDCl_3) ^1H NMR Spectrum Table 5 entry 10 (200 MHz; CDCl_3)

¹H NMR Spectrum Table 5 entry 11 (200 MHz; CDCl₃)¹H NMR Spectrum Table 5 entry 12 (400 MHz; CDCl₃)

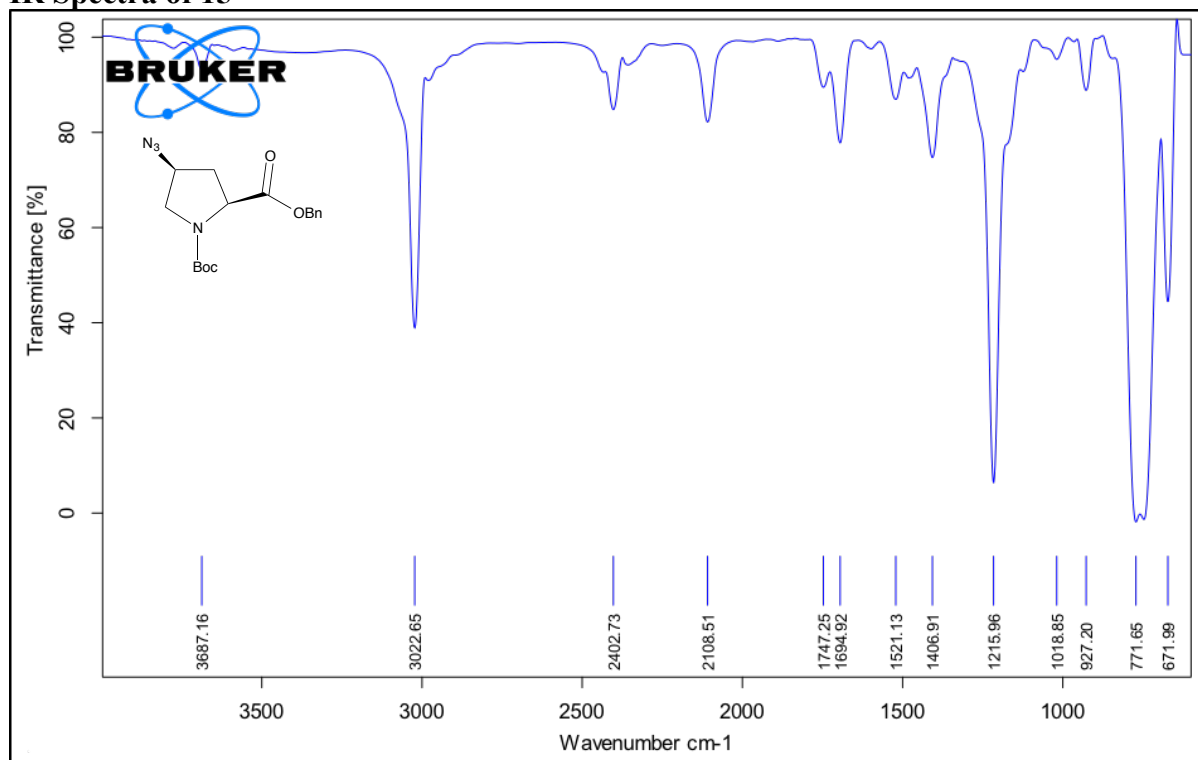
^1H NMR Spectrum Table 5 entry 13 (400 MHz; CDCl_3) ^1H NMR Spectrum Table 5 entry 14 (200 MHz; CDCl_3)

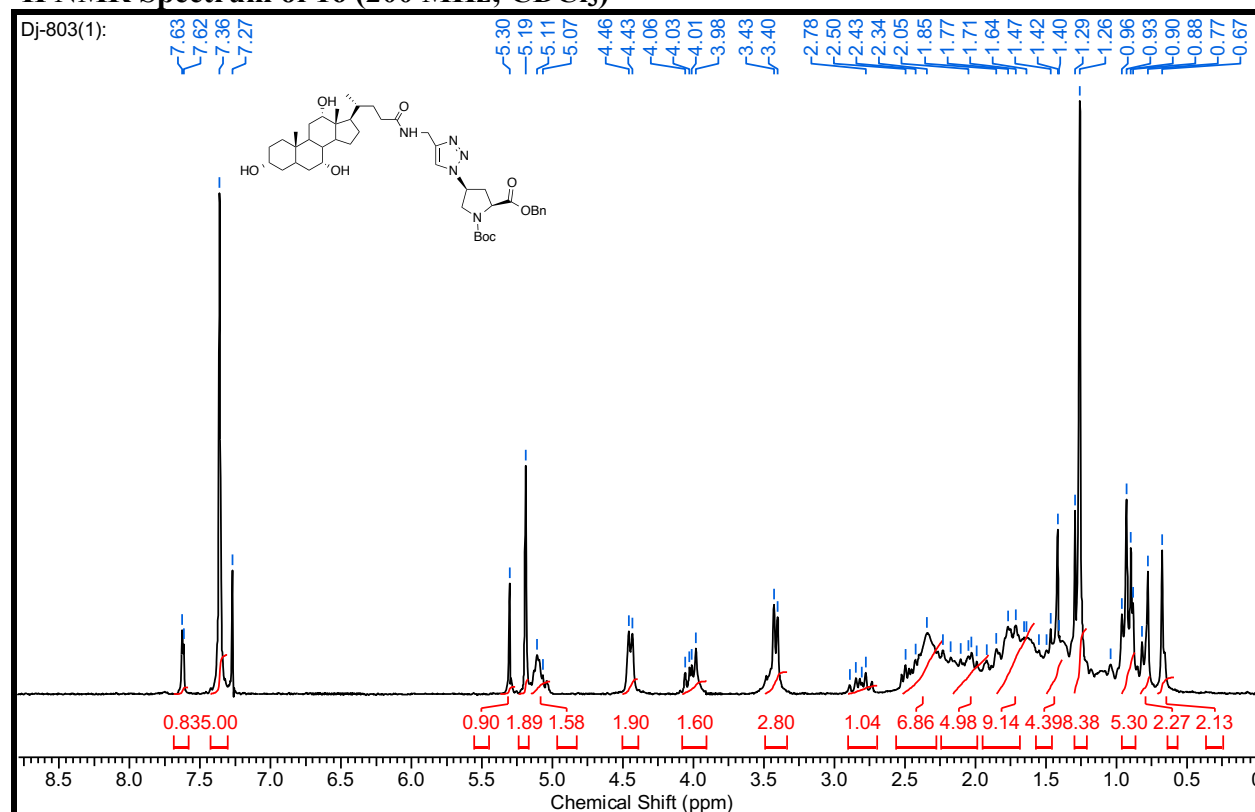
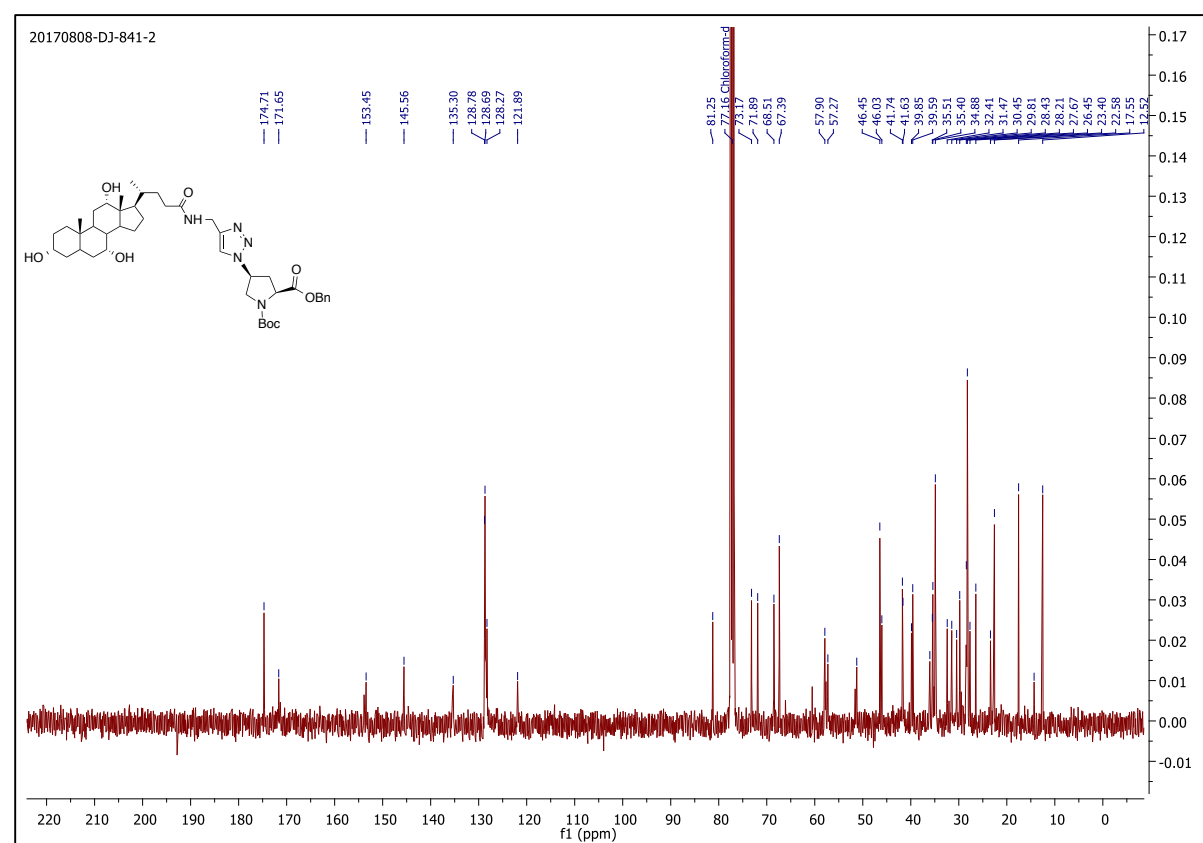
¹H NMR Spectrum of 15 (200 MHz; CDCl₃)**¹³C NMR Spectrum of 15 (75.4 MHz; CDCl₃)**

3.9 HRMS Spectra of 15

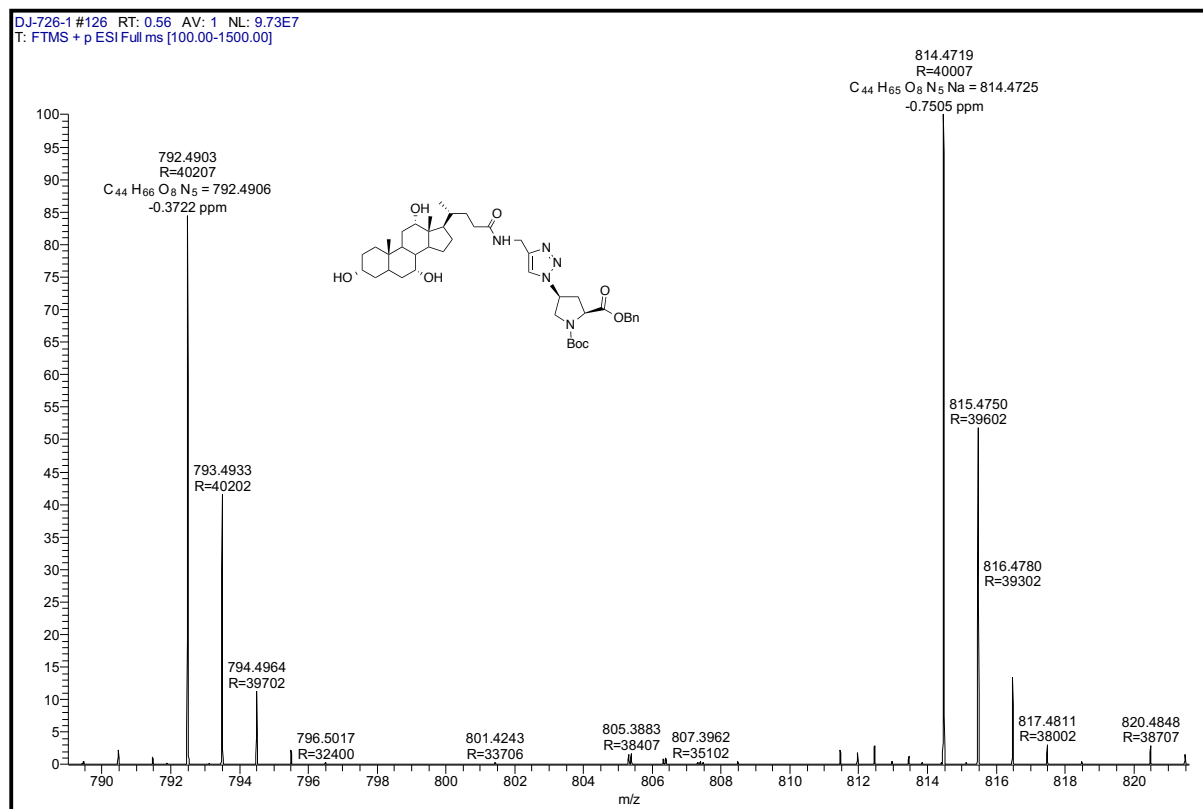


IR Spectra of 15

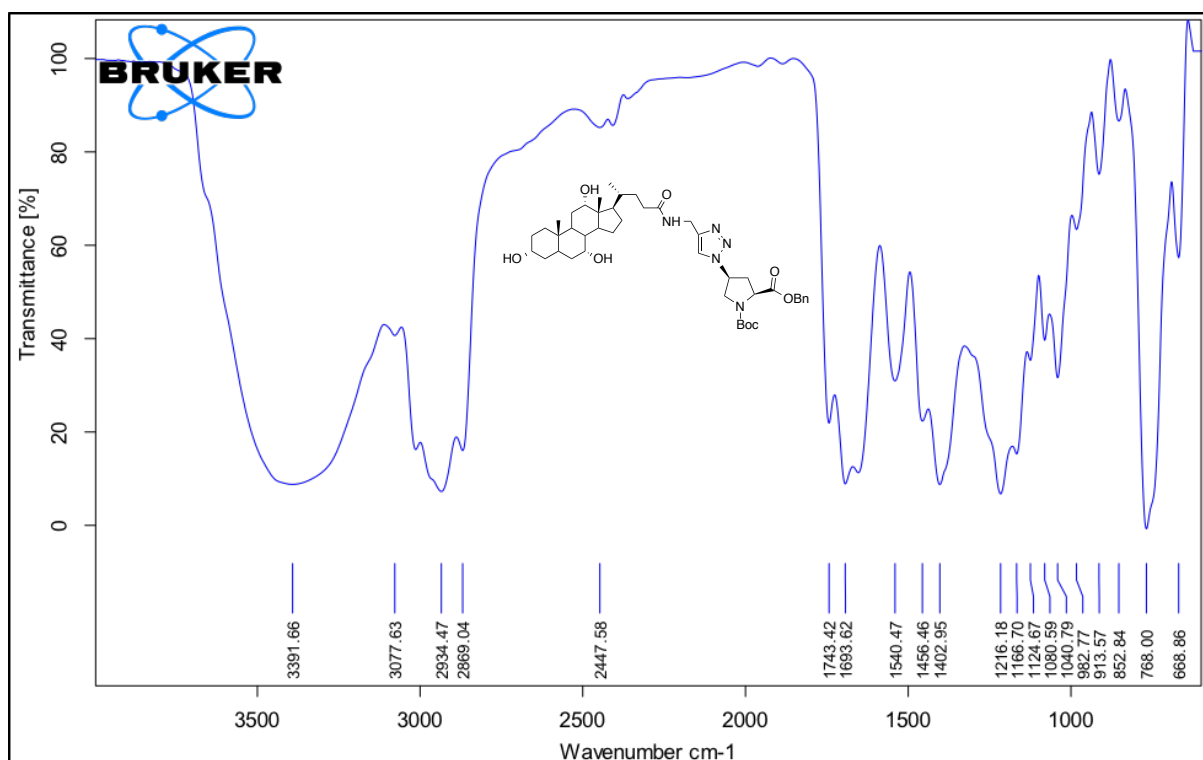


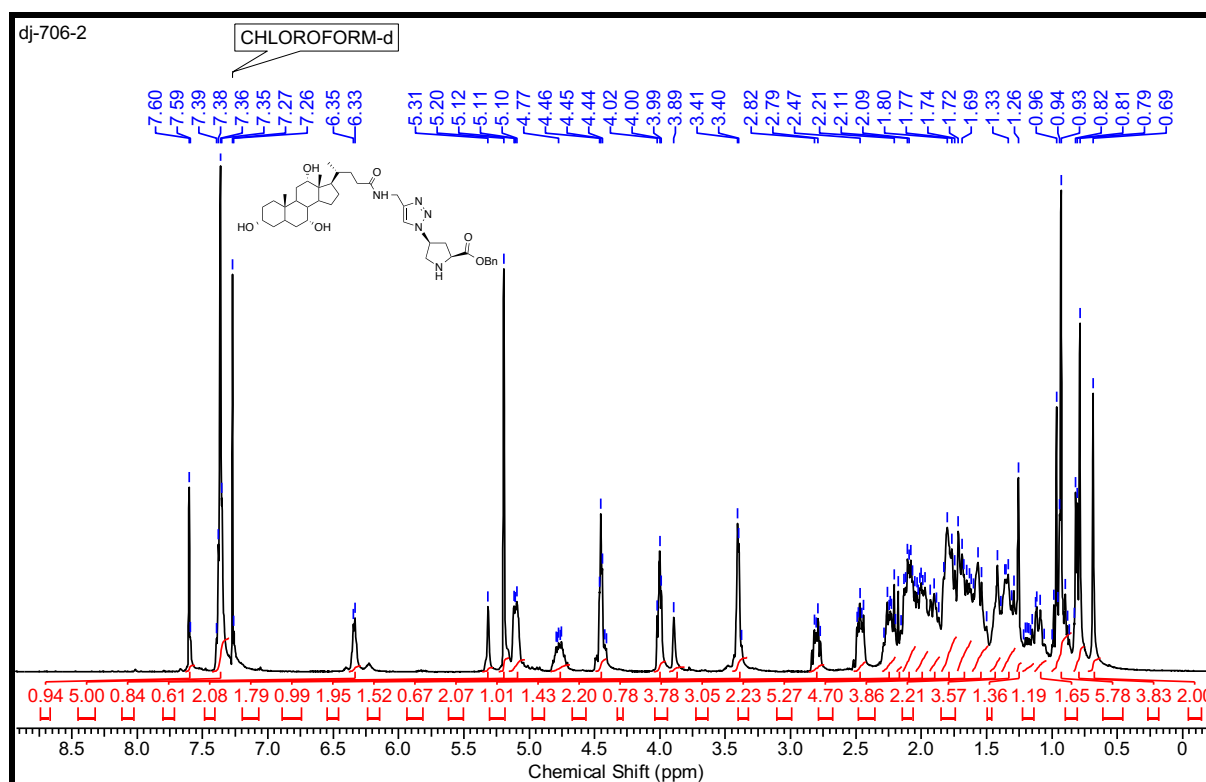
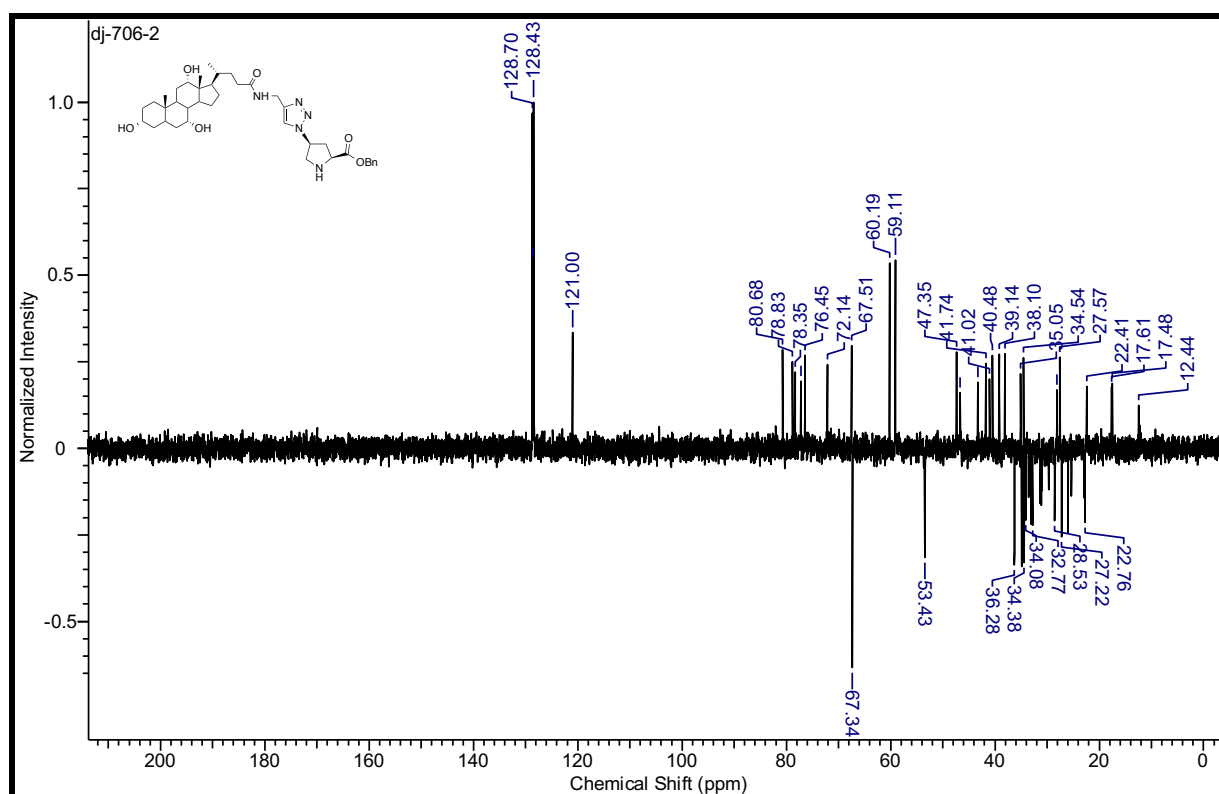
¹H NMR Spectrum of 16 (200 MHz; CDCl₃)**¹³C NMR Spectrum of 16 (101 MHz; CDCl₃)**

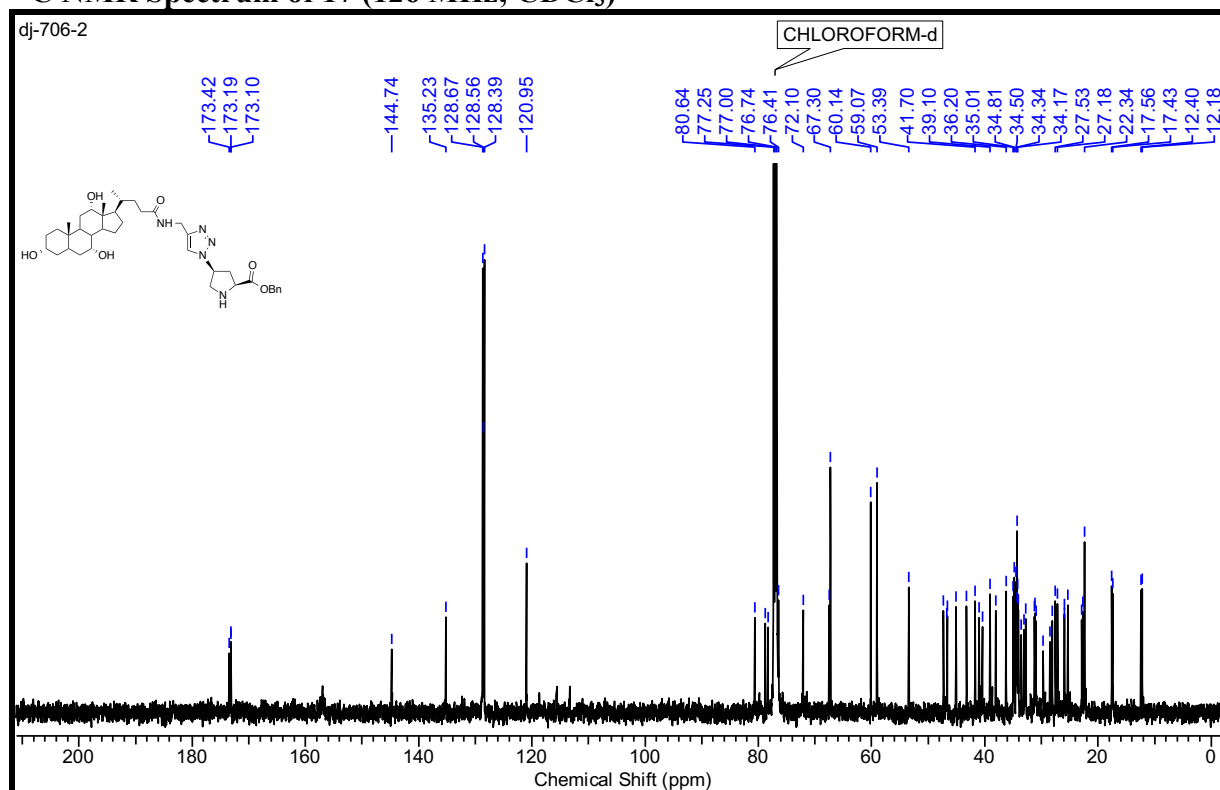
HRMS Spectra of 16



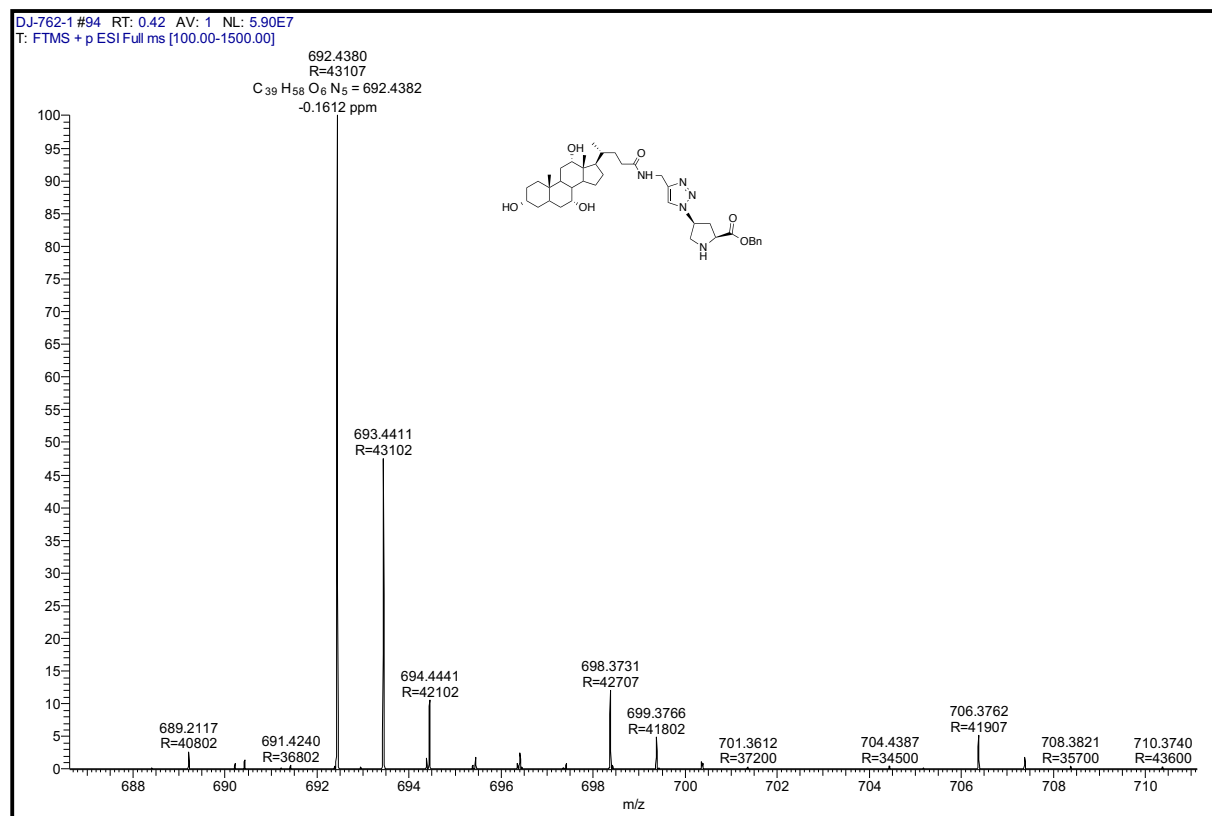
IR Spectrum of 16



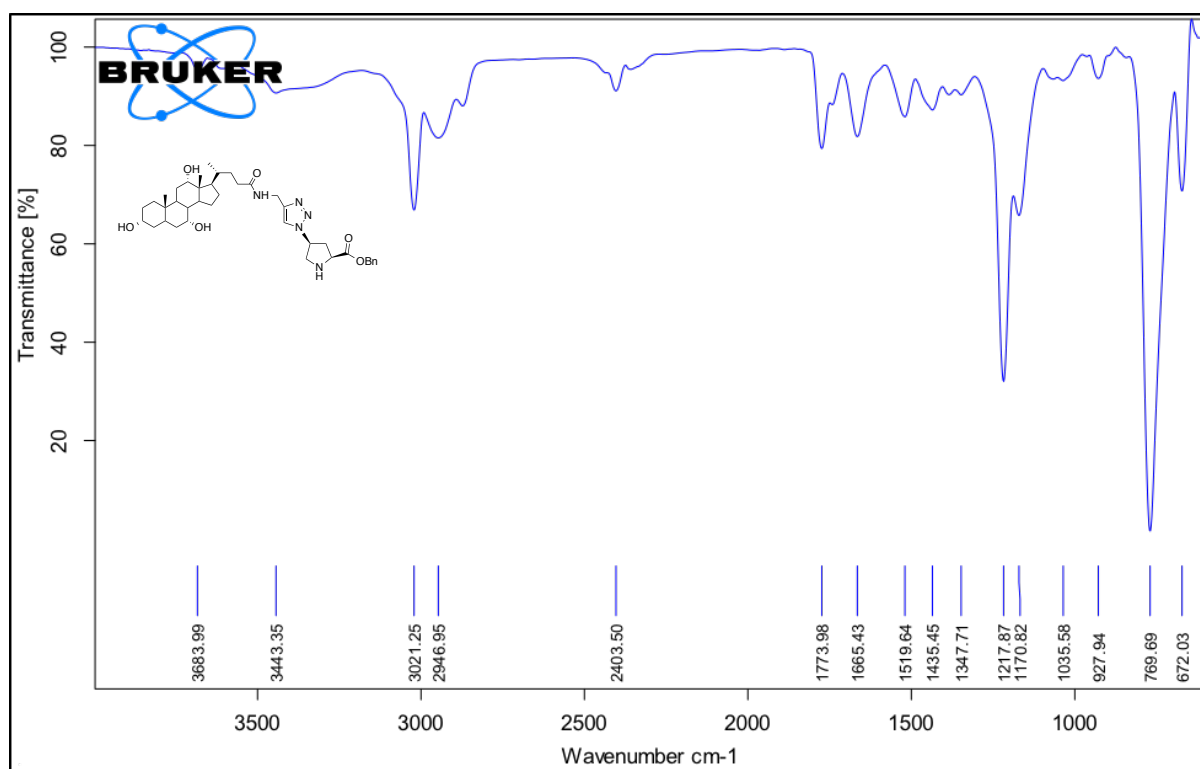
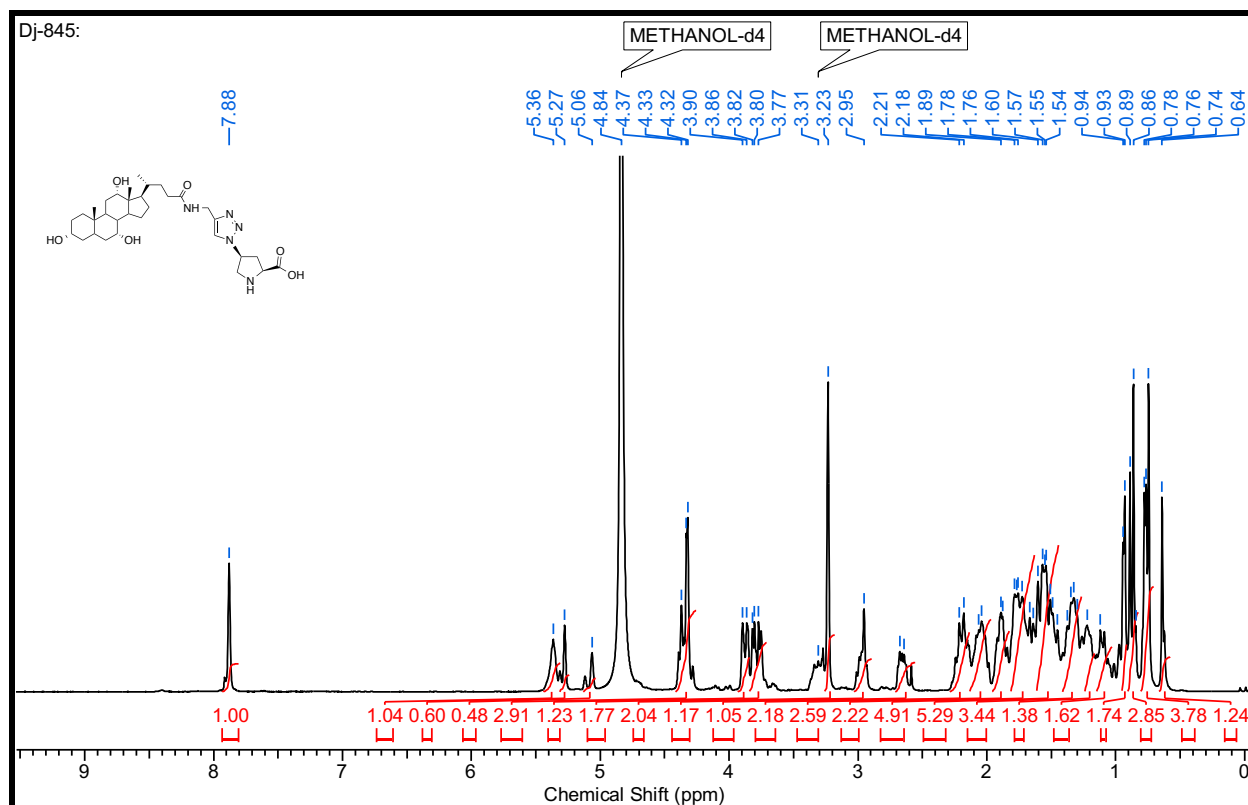
^1H NMR Spectrum of 17 (500 MHz; CDCl_3) ^{13}C -Dept NMR Spectrum of 17 (126 MHz; CDCl_3)

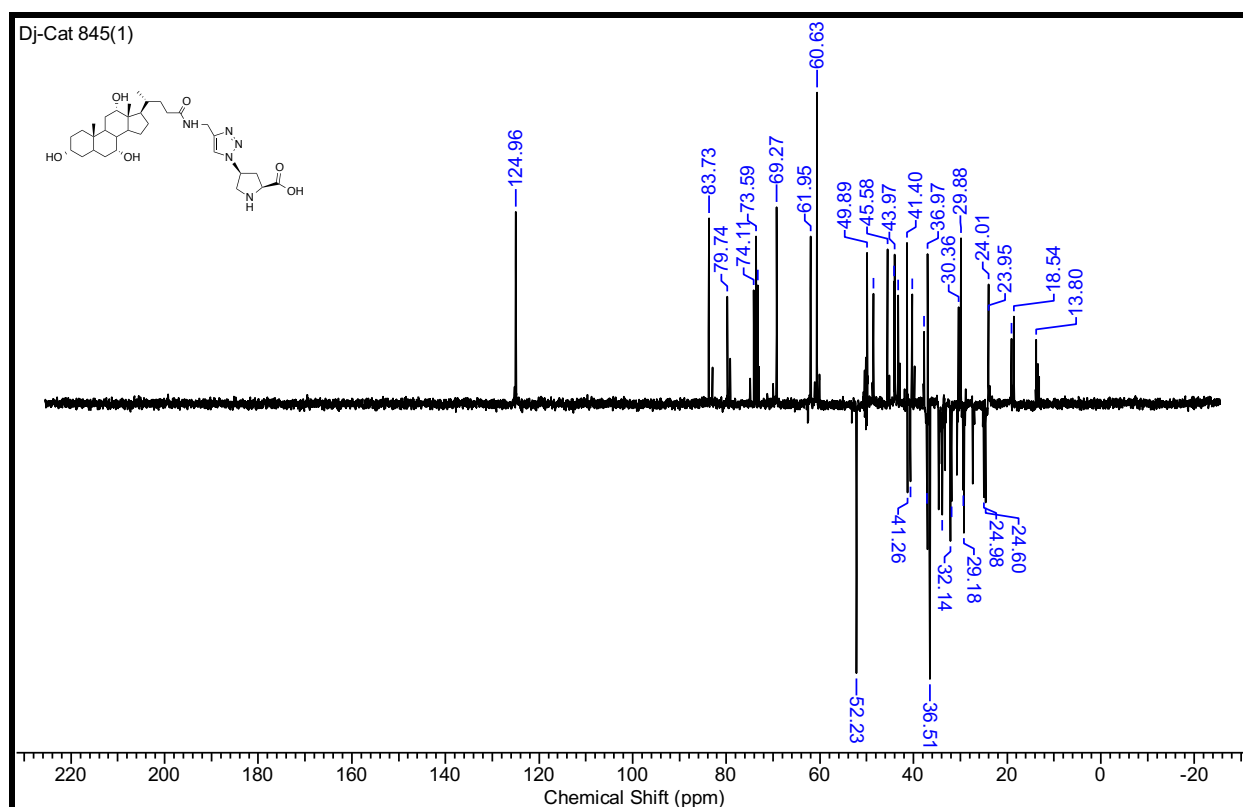
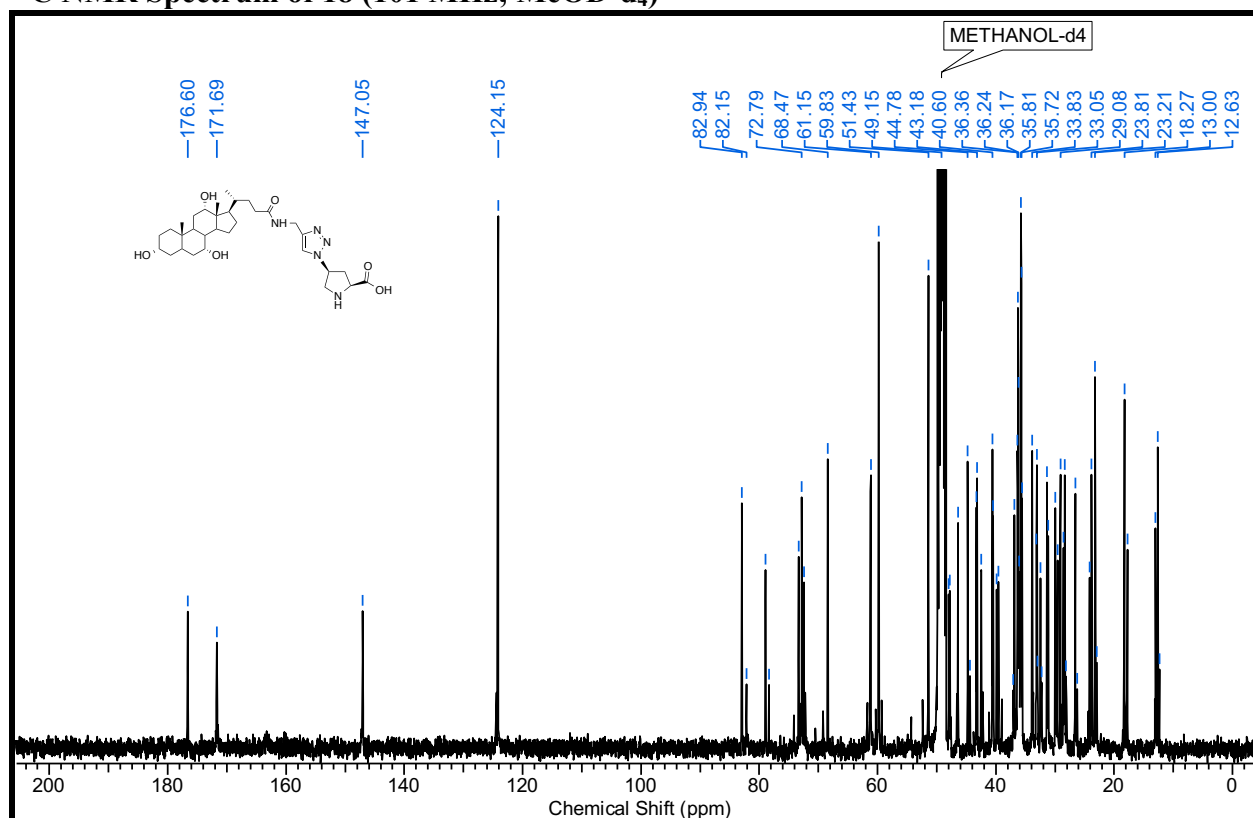
^{13}C NMR Spectrum of 17 (126 MHz; CDCl_3)

HRMS of 17

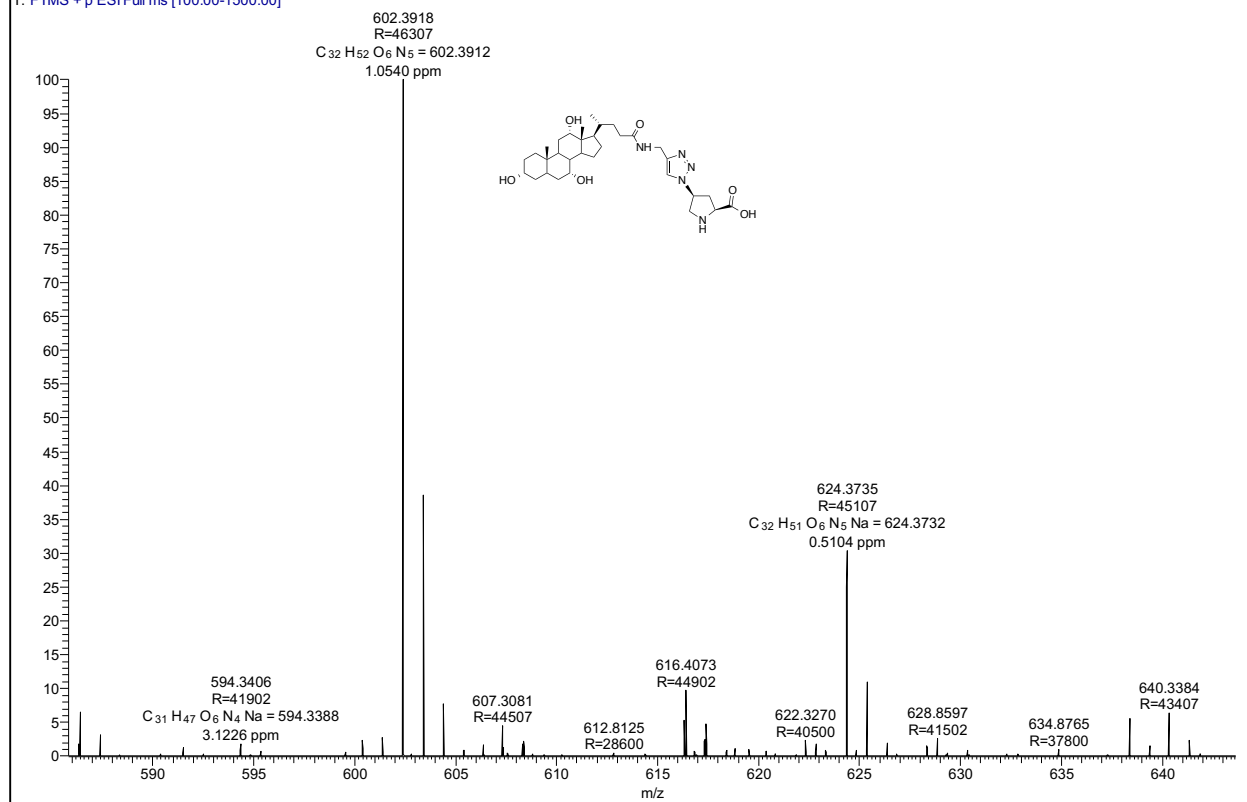


IR Spectra of compound 17

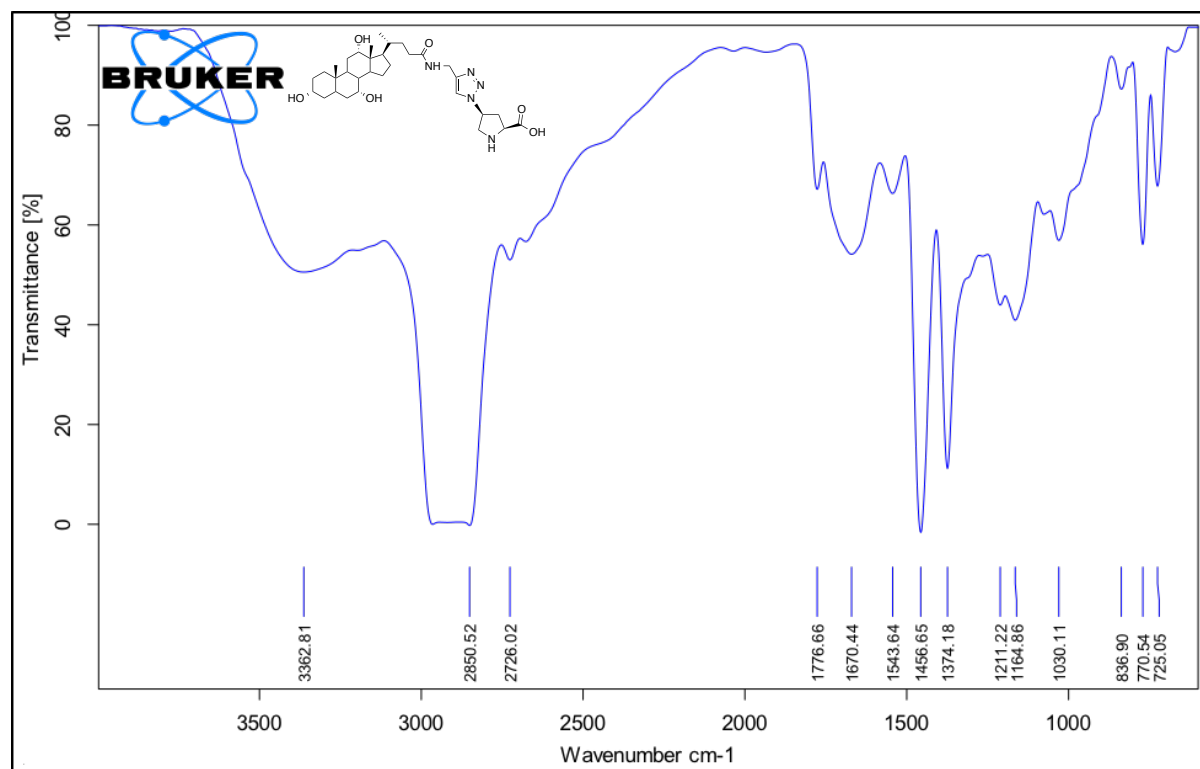
¹H NMR Spectrum of 18 (500 MHz; MeOD-d₄)

^{13}C -Dept NMR Spectrum of 18 (101 MHz; MeOD- d_4) **^{13}C NMR Spectrum of 18 (101 MHz; MeOD- d_4)**

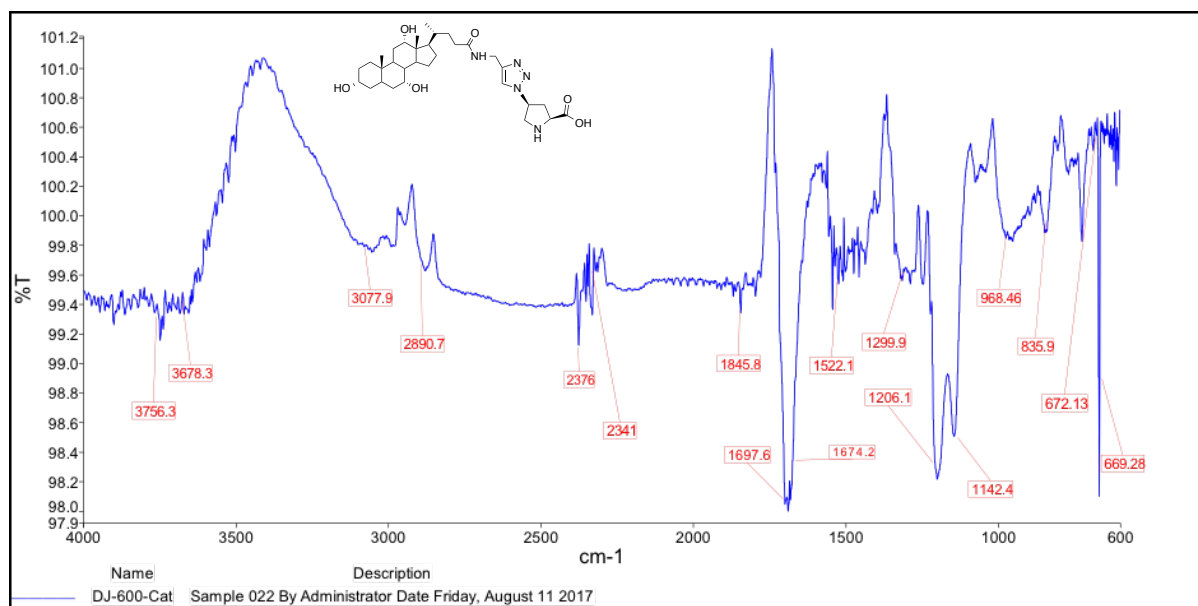
HRMS of catalyst 18

DJ-CAT #129 RT: 0.57 AV: 1 NL: 5.16E6
T: FTMS + p ESI Full ms [100.00-1500.00]

IR spectra of Catalyst 18



Solid IR of Catalyst



3.10 References

1. A. Wurtz; *Bull. Soc. Chim. Fr.*, **1872**, 17, 436.
2. (a) S. Narayan, J. Muldoon, M. G. Finn, V. V. Fokin, H. C. Kolb, K. B. Sharpless; *Angew. Chem. Int. Ed. Engl.*, **2005**, 44, 3275-3279. (b) X. Chen, J. She, Z. -C. Shang, J. Wu, P. Z. Zhang; *Synthesis*, **2008**, 21, 3478-3486. (c) C.-J. Li; *Chem. Rev.*, **2005**, 105, 3095-3165. (d) Y. Shiraishi, D. Tsukamoto, T. Hirai; *Org. Lett.*, **2008**, 10, 3117-3120. (e) N. Azizi, L. Torkian, M. R. Saidi; *J. Mol. Catal. A Chem.*, **2007**, 275, 109-112
3. (a) Z. G. Hajos, D. R. Parrish; *J. Org. Chem.* **1974**, 39, 1615–1621 (b) U. Eder, R. Sauer, R. Wiechert; *Angew. Chem., Int. Ed.* **1971**, 10, 496–497; (c) B. List, R. A. Lerner, C. F. Barbas III; *J. Am. Chem. Soc.* **2000**, 122, 2395–2396; (d) K. Sakthivel, W. Notz, T. Bui, C. F. Barbas III, *J. Am. Chem. Soc.* **2001**, 123, 5260–5267. (e) S. Saito and H. Yamamoto, *Acc. Chem. Res.* **2004**, 37, 570-579
4. (a) P. K. Jaiswal, D. K. Dikshit, International Symposium on ‘Current Trends in Drug Discovery and Research (CTDDR- 2010)’ held at Central Drug Research Institute, Lucknow, India; February 17–21, **2010**; Abstract published in special issue of *Med. Chem. Res.* **2010**, 19, S 99; (b) V. I. Maleev, Z. T. Gugkaeva, M. A. Moskalenko, A. T. Tsalojev, K. A. Lyssenko, *Russ. Chem. Bull.* **2009**, 58, 1903. and references cited there in; (c) Z. Tang, F. Jiang, L. -T. Yu, X. Cui, L.-Z. Gong, A. -Q. Mi, Y. -Z. Jiang, Y. -D. Wu, *J. Am. Chem. Soc.* **2003**, 125, 5262; (d) Z. Tang, F. Jiang, X. Cui, L.-Z. Gong, A.- Q. Mi, Y.-Z. Jiang, Y.-D. Wu, *Proc. Natl. Acad. Sci. U. S. A.* **2004**, 101, 5755; (e) X. Chen, J. Yu, L. -Z. Gong, *Chem. Commun.* **2010**, 46, 6437; (f) M. Penhoat, D. Barbry, C. Rolando, *Tetrahedron Lett.* **2011**, 52, 159 (g) J. Franzen, A. Fisher, *Angew. Chem., Int. Ed.* **2009**, 48, 787 and references cited therein (h) A. J. A. Cobb, D. M. Shaw, D. A. Longbottom, J. B. Gold, S. V. Ley, *Org. Biomol. Chem.* **2005**, 3, 84.
5. M. Penhoat, D. Barbry, C. Rolando, *Tetrahedron Lett.* **2011**, 52, 159.
6. Trost, B. M.; Brindle, C. S., The direct catalytic asymmetric aldol reaction. *Chem Soc Rev* **2010**, 39 (5), 1600-32.
7. W.-D. Fessner, in *Modern Aldol Reactions*, ed. R. Mahrwald, *Wiley-VCH, Berlin*, **2004**, vol. 1, ch. 5, pp. 201–272.
8. A. Tanaka and C. F. Barbas, III, in *Modern Aldol Reactions*, ed. R. Mahrwald, *Wiley-VCH, Berlin*, **2004**, vol. 1, ch. 6, pp. 273–310.
9. B. List, in *Modern Aldol Reactions*, ed. R. Mahrwald, *Wiley-VCH, Berlin*, **2004**, vol. 1, ch. 4, pp. 161–200.
10. M. Shibasaki, S. Matsunaga and N. Kumagai, in *Modern Aldol Reactions*, ed. R. Mahrwald, *Wiley-VCH, Berlin*, **2004**, vol. 2, ch. 6, pp. 197–227.
11. 8 A. Yanagisawa, in *Modern Aldol Reactions*, ed. R. Mahrwald, *Wiley-VCH, Berlin*, **2004**, vol. 2, ch. 1, pp. 1–23.
12. Z. G. Hajos and D. R. Parrish, German Pat., DE 2 102 623, **1971**. 62
13. U. Eder, G. R. Sauer and R. Wiechert, German Pat., DE 2 014 757, **1971**.

14. B. List, R. A. Lerner and C. F. Barbas, III, *J. Am. Chem. Soc.*, **2000**, 122, 2395.
15. B. List, P. Pojarliev and C. Castello, *Org. Lett.*, **2001**, 3, 573.
16. B. List, *Acc. Chem. Res.*, **2004**, 37, 548.
17. C. Agami, *Bull. Soc. Chim. Fr.*, **1988**, 3, 499.
18. C. Agami, J. Levisalles and C. Puchot, *J. Chem. Soc., Chem. Commun.*, **1985**, 441.
19. H. Wennemers, *Chimia*, **2007**, 61, 276.
20. M. Amedjkouh, *Tetrahedron: Asymmetry*, **2005**, 16, 1411.
21. H. J. Martin and B. List, *Synlett*, **2003**, 1901.
22. S. B. Tsogoeva, S. B. Jagtap and Z. A. Ardemasova, *Tetrahedron: Asymmetry*, **2006**, 17, 989.
23. S. B. Tsogoeva and S. Wei, *Tetrahedron: Asymmetry*, **2005**, 16, 1947.
24. F. Chen, S. Huang, H. Zhang, F. Liu and Y. Peng, *Tetrahedron*, **2008**, 64, 9585.
25. S. Chandrasekhar, K. Johny and C. R. Reddy, *Tetrahedron: Asymmetry*, **2009**, 20, 1742.
26. P. Krattiger, R. Kovasy, J. D. Revell, S. Ivan and H. Wennemers, *Org. Lett.*, **2005**, 7, 1101.
27. J. D. Revell, D. Gantenbein, P. Krattiger and H. Wennemers, *Biopolymers*, **2006**, 84, 105.
28. J. D. Revell and H. Wennemers, *Adv. Synth. Catal.*, **2008**, 350, 1046.
29. J. F. Zhao, L. He, J. Jiang, Z. Tang, L. F. Cun and L. Z. Gong, *Tetrahedron Lett.*, **2008**, 49, 3372.
30. G. D. Yadav, S. Singh / *Tetrahedron: Asymmetry*, **2015**, 26, 1156–1166
31. Y. Kong, R. Tan, L. Zhao and D. Yin, *Green Chem.*, **2013**, 15, 2422
32. K. S. Lee and J. R. Parquette, *Chem. Commun.*, **2015**, 51, 15653
33. S. -P. Zhang, X. -K. Fu and S. -D. Fu, *Tetrahedron Lett.*, **2009**, 50, 1173.
34. S. S. Chimni, S. Singh and D. Mahajan, *Tetrahedron: Asymmetry*, **2008**, 19, 2276.
35. S. S. Chimni, S. Singh and A. Kumar, *Tetrahedron: Asymmetry*, **2009**, 20, 1722.
36. (a) Hayashi, Y.; Sumiya, T.; Takahashi, J.; Gotoh, H.; Urushima, T.; Shoji, M. *Angew. Chem., Int. Ed.*, **2006**, 45, 958; (b) Y. Hayashi, S. Aratake, T. Okano, J. Takahashi, T. Sumiya, M. Shoji, *Angew. Chem., Int. Ed.*, **2006**, 45, 5527.
37. T. He, K. Li, M. Y. Wu, M. B. Wu, N. Wang, L. Pu, X. Q. Yu, *Tetrahedron* **2013**, 69, 5136-5143.
38. S. Fu, X. Fu, S. Zhang, X. Zou, X. Wu, *Tetrahedron Asymmetry*, **2009**, 20, 2390–2396
39. G. L. Puleo, M. Masi and A. Iuliano, *Tetrahedron Asymmetry*, **2007**, 18, 1364–1375

40. E. Bellis, G. Kakotos, *Tetrahedron*, **2005**, 61, 8669.
41. X. Ding, H. -L. Jiang, C. -J. Zhu, Y. -X. Cheng, *Tetrahedron Lett.* **2010**, 51, 6105.
42. D. Font, C. Jimeno, M. A. Pericàs, *Org. Lett.*, **2006**, 8, 4653- 4655.
43. G. L. Puleo, M. Masi and A. Iuliano, *Tetrahedron Asymmetry*, **2007**, 18, 1364–1375
44. N. S. Vatmurge, B. G. Hazra, V. S. Pore, F. Shirazi, M. V. Deshpande, S. Kadreppa, S. Chattopadhyay and R. G. Gonnade, *Org. Biomol. Chem.*, **2008**, 6, 3823–3830
45. (a) F. Zanardi, P. Burreddu, G. Rassu, L. Auzzas, L. Battistini, C. Curti, A. Sartori, G. Nicastro, G. Menchi, N. Cini, A. Bottonocetti, S. Raspanti, and G. Casiraghi, *J. Med. Chem.*, **2008**, 51, 1771–1782; b) L. Battistini, P. Burreddu, P. Carta, G. Rassu, L. Auzzas, C. Curti, F. Zanardi, L. Manzoni, E. M. V. Araldi, C. Scolastico and G. Casiraghi, *Org. Biomol. Chem.*, **2009**, 7, 4924–4935
46. V. S. Pore, J. M. Divse, C. R. Charolkar, L. U. Nawale, V. M. Khedkar, D. Sarkar, *Bioorg. & medicinal chemistry lett.*, **2015**, 19, 4185-4190
47. (a) C. Ayats, A. H. Henseler, and M. A. Pericàs, *Chem. Sus. Chem.*, **2012**, 5, 320–325, b) K. S. Lee and J. R. Parquette, *Chem. Commun.*, **2015**, 51, 15653-15656, c) A. H. Henseler, C. Ayats, and M. A. Pericàs, *Adv. Synth. Catal.* **2014**, 356, 1795 – 1802
48. R. Schoevaart, F. V. Rantwijk, and R. A. Sheldon, *J. Org. Chem.* **2001**, 66, 4559-4562.
49. A. Berkessel, B. Koch and J. Lex, *Adv. Synth. Catal.*, **2004**, 346, 1141; (b) Z. Tang, F. Jiang, X. Cui, L. Gong, A. Mi, Y. Jiang and Y. Wu, *Proc. Natl. Acad. Sci. U. S. A.*, **2004**, 101, 5755; (c) D. Gryko and R. Lipinski, *Eur. J. Org. Chem.*, **2006**, 3864.
50. (a) B. List, R. A. Lerner and C. F. Barbas III, *J. Am. Chem. Soc.*, **2000**, 122, 2395; (b) S. Calogero, D. Lanari, M. Orrù, O. Piermatti, F. Pizzo and L. Vaccaro, *J. Catal.*, **2011**, 282, 112
51. (a) G. Yang, Z. Yang, L. Zhou, R. Zhuand, C. Liu, *J. Mol. Catal. A: Chem.*, **2010**, 316, 112; (b) H. Yang, S. Li, X. Wang, F. Zhang, X. Zhong, Z. Dong and J. Ma, *J. Mol. Catal. A: Chem.*, **2012**, 363, 404.
52. N. Mase, Y. Nakai, N. Ohara, H. Yoda, K. Takabe, F. Tanaka and C. F. Barbas III, *J. Am. Chem. Soc.*, **2006**, 128, 734;
53. (a) S. Aratake, T. Itoh, T. Okano, N. Nagae, T. Sumiya, M. Shoji and Y. Hayashi, *Chem.–Eur. Jour.*, **2007**, 13, 10246; (b) M. Amedjkouh, *Tetrahedron Asymmetry*, **2007**, 18, 390; (c) D. E. Siyutkin, A. S. Kucherenko and S. G. Zlotin, *Tetrahedron*, **2009**, 65, 1366.
54. Y. Hayashi, S. Aratake, T. Itoh, T. Okano, T. Sumiya and M. Shoji, *Chem. Commun.*, **2007**, 0, 957–959
55. K. Sakthivel, W. Notz, T. Bui, and C. F. Barbas III, *J. Am. Chem. Soc.*, **2001**, 123, 5260-5267

56. Z. Zheng, B. L. Perkins and B. Ni, *J. Am. Chem. Soc.*, **2010**, 132, 50–51.
57. a) Y. Kong, R. Tan, L. Zhao and D. Yin, *Green Chem.*, **2013**, 15, 2422–2433; b) C. Yeh, Y.-R. Sun, S.-J. Huang, Y.-M. Tsai and S. Cheng, *Chem. Commun.*, **2015**, 51, 17116–17119 ; c) P. Llanes, S. Sayalero, C. Rodríguez-Escricha and M. A. Pericàs, *Green Chem.*, **2016**, 18, 3507–3512; d) Y. Wu, Y. Zhang, M. Yu, G. Zhao, and S. Wang, *Org. Lett.*, **2006**, 8, 4419 ; d) A. H. Henseler, C. Ayats, and M. A. Pericàs, *Adv. Synth. Catal.*, **2014**, 356, 1795 – 1802.
58. Yamamoto H., ed. (2000) Lewis Acid in Organic Synthesis (*Wiley-VCH*, **2000**), Vols. 1 and 2.
59. L. Battistini, P. Burreddu, P. Carta, G. Rassu, L. Auzzas, C. Curti, F. Zanardi, L. Manzoni, Elena M. V. Araldi, C. Scolastico and G. Casiraghi; *Org. Biomol. Chem.*, **2009**, 7, 4924–4935
60. F. Zanardi, P. Burreddu, G. Rassu, L. Auzzas, L. Battistini, C. Curti, A. Sartori, G. Nicastro, G. Menchi, N. Cini, A. Bottonocetti, S. Raspanti and G. Casiraghi, *J. Med. Chem.*, **2008**, 51, 1771–1782

Chapter 4

Design and synthesis of one-pot click derivatives of pregnenolone by epoxide opening of 20'(*R*)-Spiro[oxirane-2,20'-pregn-5'-en]-3' -ol and their bioevaluation as anticancer agents

Chapter 4

Design and Synthesis of one-pot click derivatives of Pregnenolone by epoxide opening of 20'(R)-Spiro[oxirane-2,20'-pregn-5'-en]-3' -ol and their bioevaluation as anticancer agents

4.1 Abstract

Synthesis of 1, 2, 3-triazole containing click derivatives of pregnenolone by three component “one-pot” click reaction from epoxide opening of 20'(R)-spiro[oxirane-2,20'-pregn-5'-en]-3' -ol is presented in this chapter. This chapter includes cheaper and convenient method for synthesizing click derivatives directly from epoxide in one-pot conditions in good to excellent yields. Besides, this method is rapid and efficient because of the use of microwave. The use of eco-friendly solvent PEG-400 and water as a reaction medium also adds charm to this method. All the synthesized compounds are expected to show anticancer and antifungal activities because of the presence of 1, 2, 3-triazole as a pharmacophore which is responsible for anti-fungal and anti-cancer activities in most of the existing drugs.

4.2 Introduction

Steroids are broadly used drugs in the modern pharmaceutical industry. In spite of debate about their side effects, the global markets of steroidal drugs and intermediates are worth more than a billion dollars.¹ Among numerous reported steroidal compounds, 16-dehydropregnenolone (16-DHP) and 16-dehydropregnenolone acetate (16-DPA) and their analogs, as valuable drugs and intermediates for providing various steroid drugs, have gained much attention (Figure 1). More than 65 % of steroid drugs are derived from 16-DPA and its analogs.¹ 16-DPA is widely used as prime intermediate or building block for the synthesis of a vast number of steroidal drugs including anabolic steroids, corticosteroids, sex hormones, and contraceptives.^{2,3} Steroids are a broad group of naturally occurring and synthetic lipids with a magnificent diversity of physiological activity. Included among the steroids are many important hormones. Steroid hormones include cortisone, progesterone, and the female and male sex hormones (estradiol; testosterone) (Figure 1). Perhaps the most widely used steroids in medicine are cortisone and progesterone and their various synthetic derivatives. These steroids are prescription drugs used for a variety of skin ailments, rheumatoid arthritis, asthma and allergies, and various eye diseases, and in cases of adrenal insufficiency, or the

malfunctioning of the adrenal cortex. It is an ideal platform for preparation of dexamethasone, β -methasone, 5α -reductase inhibitor, γ -aminobutyric acid type A (GABAA) receptor, inhibitor of steroid C17(20) lyase, dipeptidyl peptidase (DPP)-IV, and other related steroidal pharmacophores⁴⁻⁸ 16-DHP is an efficient inhibitor of 17α -hydroxylase and 15α -reductase.⁹ The 16-DPA and 16-DHP are key intermediates used for making residual hormone medicines such as cortisone, progesterone, testosterone (Figure 1), floucinolone acetonide *etc.* This chapter includes the synthesis of several molecules deived from 16-DPA through a convinient one-pot click reaction, which are expected to have several biological activities including anticancer and antifungal.

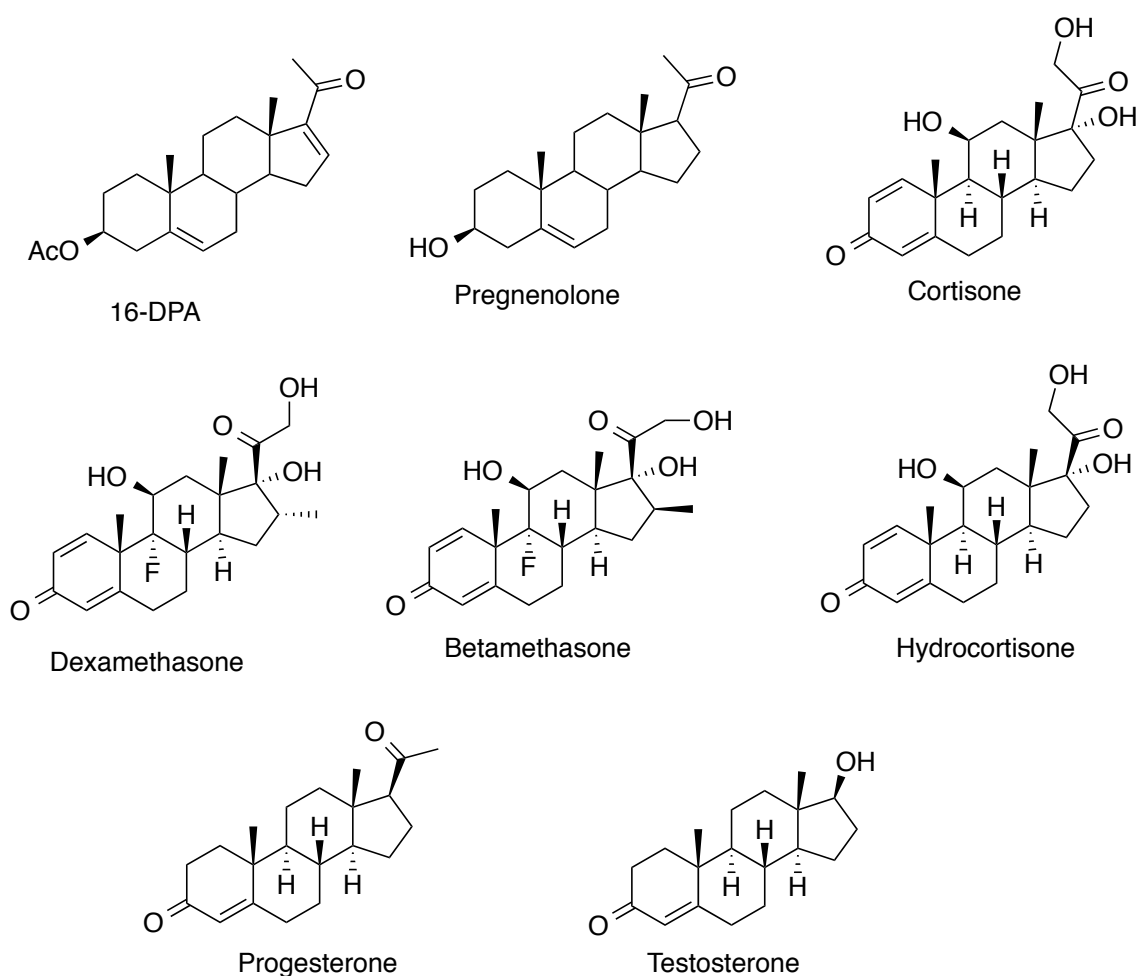


Figure 1. Structures of various steroids.

4.3 Review of Literature

4.3.1 Steroids with various biological activities.

Steroids, a broad class of natural organic compounds occurring in animals, plants and fungi, have exhibited high therapeutic value for a wide array of pathologies, which is very characteristic of a rich structural molecular diversity and capability to interact with various biological targets and with pathways. Steroids comprise a vast repertoire of structurally related natural compounds with significant functions *in vivo*, such as physiological regulators, hormones, and provitamins. The reason for such activity is probably because of the various advantages associated with the steroid-based chemotherapeutics. These compounds transpose to be non-toxic, less exposed to multi-drug resistance (MDR) and highly bioavailable because of being proficient of cell wall penetration. This can be true for modified steroids having heterocyclic systems as a part of their skeleton. This has been confirmed by modification of different rings. Studies of steroidal molecules in which A- and D-ring are modified by inclusion of heteroatom (N or O), have been reported to improve the biological activities of these molecules. Such modifications have revealed a lot of different biological activities such as anti-microbial, anti-inflammatory, hypotensive, hypocholesterolemic and diuretic activities.¹⁰⁻¹⁴ Based on these reports, many different heterocyclic systems have been incorporated into the core structure of steroids such as pyrazoles, pyrazolines, isoxazoles, isoxazolines, thiazoles, thiadiazoles, pyridines, pyrimidines, imidazoles, *etc.* to improve or modify their activity.¹⁵

Abid H. Banday *et al.*¹⁵ synthesized 17-pyrazolinyl derivatives of pregnenolone and evaluated their potential as anticancer agents against various human cancer cell lines (**1**, **2** Figure 2). Compound **2** was found to be the most active especially against *HT-29* and *HCT-15* cancer cell lines. Hongqi Li *et al.*¹⁶ synthesized a series of new phenyl esters based on a 5,16-pregnadiene-20-one skeleton starting from diosgenin, namely 3 β -benzoyloxy-5,16-pregnadiene-20-ones (**3**, Figure 2), which might be good inhibitors of 17 α -hydroxylase and 5 α -reductase enzyme or useful intermediates for producing steroidal drugs. Several 16-DPA derivatives containing a triazole ring at C-21 and a linear or alicyclic ester moiety at C-3 of the steroidal skeleton have been synthesized by A. V. Silva-Ortiz *et al.*¹⁷ (**4a-i**, Figure 2). These steroids were designed as potential inhibitors of the activity of both types (**1** and **2**) of 5 α -reductase. The compounds are found to be cytotoxic for a panel of PC-3, MCF7, and SK-LU-1 human cancer cell lines. The results showed that the compounds exhibit a lower inhibitory activity for both isoenzymes of 5 α -reductase than finasteride with the exception of steroids 20-oxo-21-(1H-1,2,4-triazole-1-yl)pregna-5,16-dien-3 β -yl-propionate and 20-oxo-21-(1H-1,2,4-triazole-1-yl)pregna-5,16-dien-3 β -yl-pentanoate. The results also indicated that

the triazole derivatives, which have a hydroxyl or acetoxy group at C- 3 (**4i**, Figure 2), could have an anticancer effect, whereas the derivatives with an alicyclic ester group at C-3 do not possess biological activity (Figure 2).

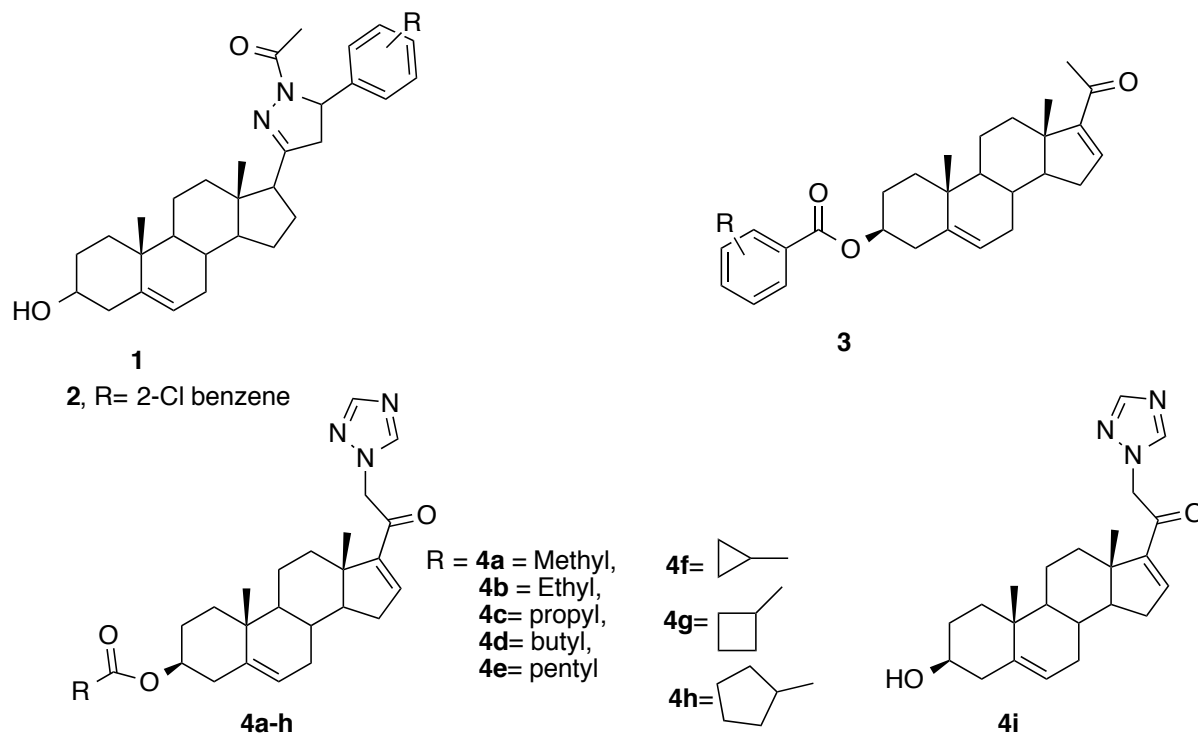


Figure 2. Structures 1-4i

A. Cammarata *et al.*¹⁸ observed that antifungal activity of $2\alpha, 3\beta$ -functionalized steroids stereoselectively increases by the addition of oligosaccharides. (Figure 3). They outline a novel approach for the synthesis of glycoside-linked functionalized $2\alpha, 3\beta$ -cholestane and spirostane molecules and reported data from *in vitro* screenings of the antifungal activities against human fungal pathogens as well as mammalian cell toxicity of those derivatives (**5**, **6**, **7** and **8** Figure 3).

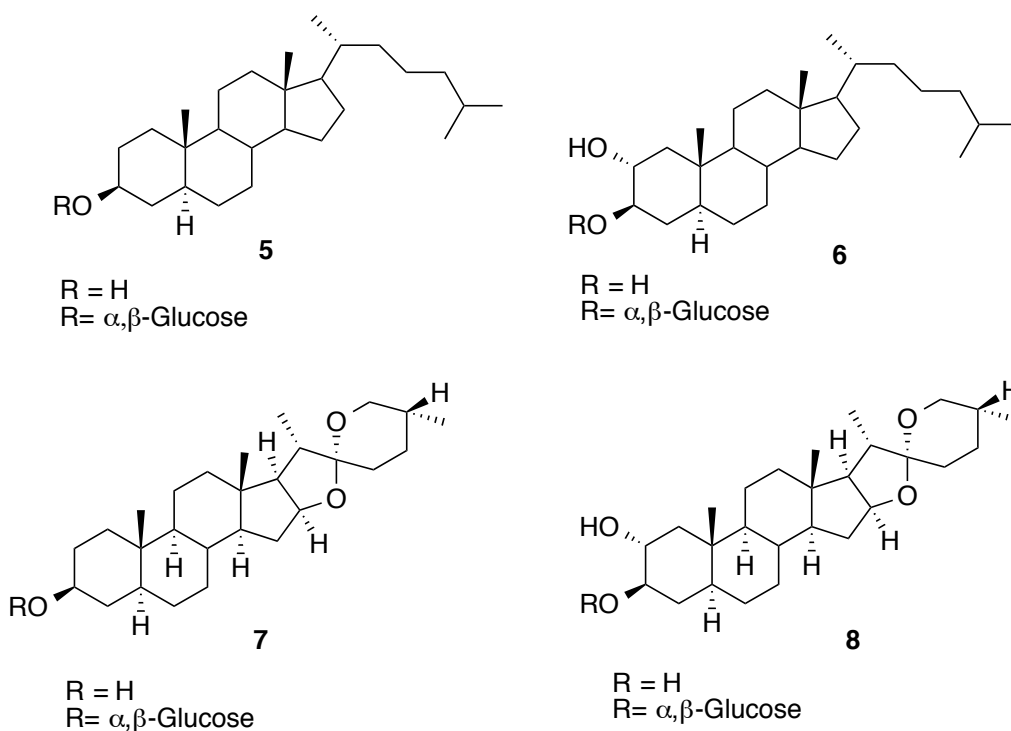


Figure 3. Structures 5-8

Recently there is a report¹⁹ from our group on synthesis of a series of pregnane derivatives incorporating 1,3-dithiane. The products were evaluated *in vitro* for their antifungal and antibacterial activities (**9-14**, Figure 4). The compounds were found to show good to moderate antifungal and antibacterial activity against all the tested fungal and bacterial strains. This was the first report of screening the biological activity of 1,3-dithiane-pregnane conjugates. Lei Ma *et al.*²⁰ synthesized a series of Sarsasapogenin derivatives and evaluated them for their neuroprotective activity in PC12 cells and NO production inhibitory activity in RAW264.7 cell lines. They found that introduction of carbamate groups (various substituted benzyl amine, cyclic amines and aliphatic amines) at the 3-hydroxyl position of Sarsasapogenin have improved the neuroprotective activity (**15** Figure 4). A series of steroidal hybrids with different terminal bioactive scaffolds linked *via* substituted 1,2,3-triazole at C-3 position of the steroidal skeleton were synthesized by Hong-Min Liu *et al.*²¹ and further evaluated for their antiproliferative activity against several cancer cell lines of different origins using the MTT assay (**16**, Figure 4). Their results indicated that most of the compounds with the terminal isatin motif **16a** were remarkably sensitive to SH-SY5Y cells, through exerting potent growth inhibition *in vitro*.

Edward T. Petri *et al.*²² reported a convenient “click” synthesis for D-homo fused steroidal

tetrazoles (**17a**, **17b** Figure 4) derived from androstane and estratriene via intramolecular 1,3-dipolar cycloaddition, and most of the synthesized compounds were evaluated as potential antiproliferative agents against a panel of human cancer cell lines. Adrian Salic *et al.*²³ found that oxysterols activate vertebrate Hedgehog (Hh) signaling, a pathway essential in embryonic development, adult stem cell maintenance and cancer. They developed azasterols that block Hh signaling triggered by the Hh ligand and by 20-Hydroxy steroids (**18a**, **18b**, Figure 4).

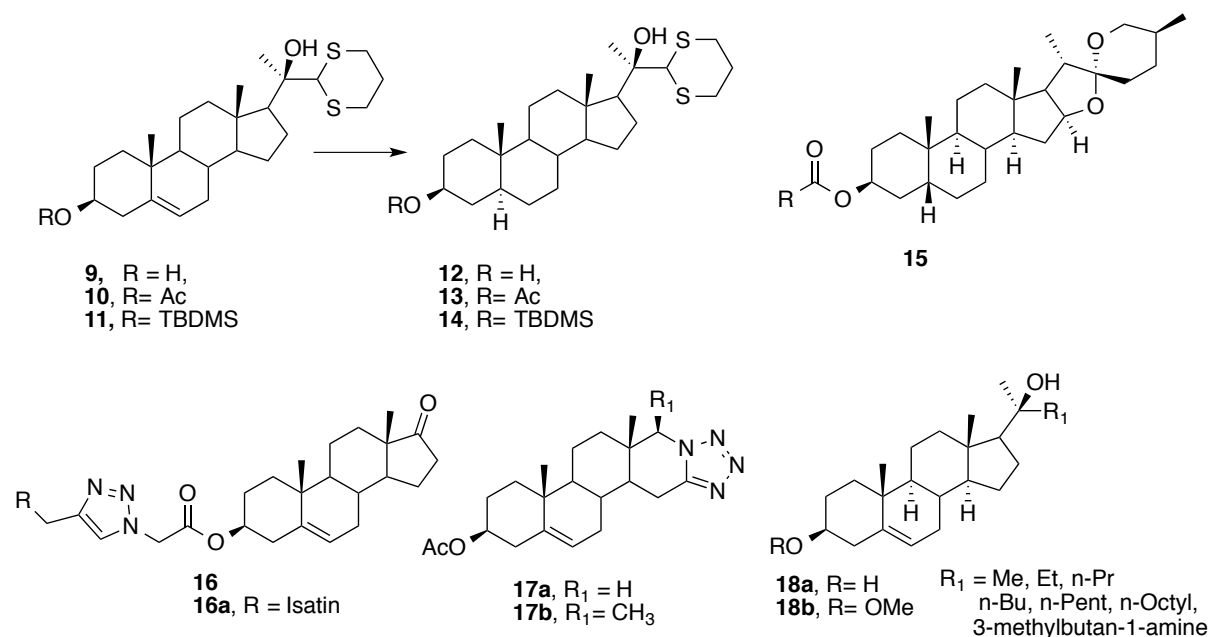
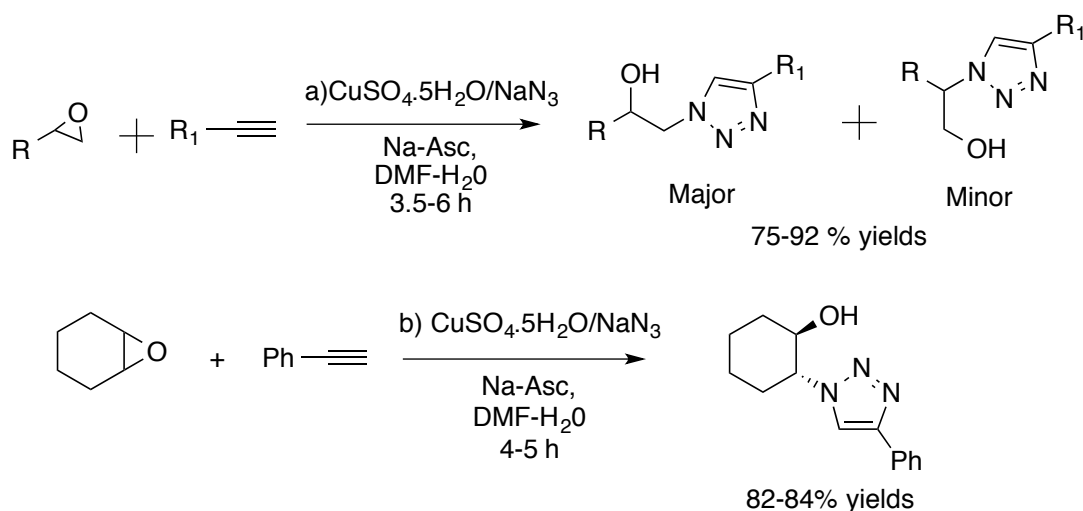


Figure 4. Structures 9-18b

4.3.2 Literature on One-pot click reaction

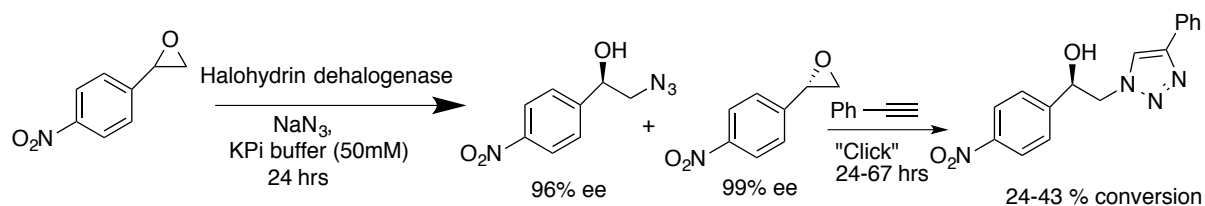
There are plenty of reports on one-pot click reactions between halides/azides and alkynes, but there are only a few reports on direct one-pot between epoxides and alkynes for the 1,2,3-triazole synthesis through the *in-situ* formation of azides from epoxides. A few recent reports are discussed below.

J.S Yadav *et al.*²⁴ have derived 2-azidoalcohols *in situ* from epoxides and sodium azide, undergo smooth coupling with alkynes under neutral conditions employing 'click reaction' conditions to provide β -hydroxytriazoles in excellent yields and with high regioselectivity (Scheme 1). This reaction proceeds readily in water at room temperature without the need for acid catalysis. This reaction undergoes well in about 3-4 hours.



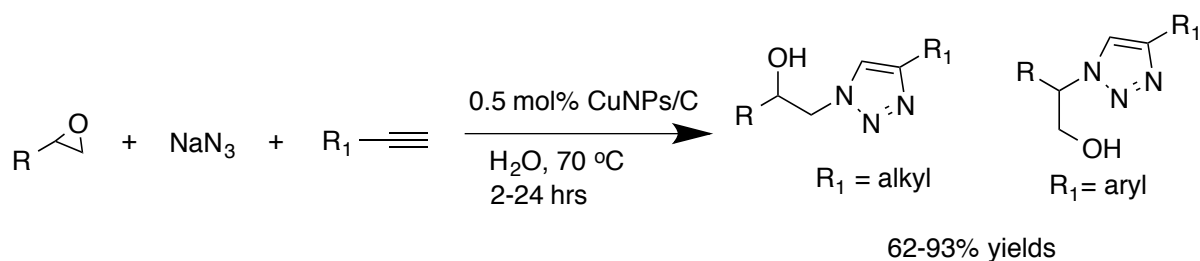
Scheme 1.

Ben L. Feringa *et al.*²⁵ found Halohydrin dehalogenase (HheC) to be efficient to complete enantioselective azidolysis of aromatic epoxides to 1,2-azido alcohols which are consequently ligated to alkynes providing chiral hydroxy triazoles in a one-pot procedure with excellent enantiomeric excess (Scheme 2).



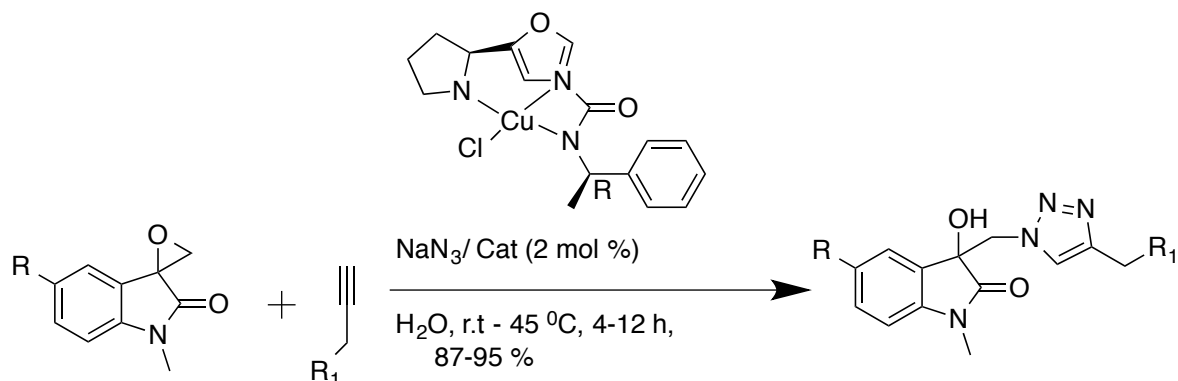
Scheme 2.

Miguel Yus *et al.*²⁶ found that by adsorbing copper nanoparticles on activated carbon efficiently catalyze the multicomponent synthesis of β -hydroxy-1,2,3-triazoles from a diversity of epoxides and alkynes in water. The regio- and stereochemistry of the reaction has also been reviewed and unequivocally established from X-ray crystallographic analyses (Scheme 3).



Scheme 3.

Nagula Shankaraiah *et al.*²⁷ found an efficient Cu(I)-pyrrolidinyl-oxazolo-carboxamide catalyst for the ‘one-pot’ synthesis of novel 3-substituted-1,2,3-triazolo-3-hydroxy-indolin-2-ones. The reaction comprises an *in-situ* azide formation from spiro-epoxide by a simultaneous ‘click’ reaction in aqueous medium (Scheme 4). The reaction performed well within 4-12 hrs at 45 °C.



Scheme 4.

4.4 Present Work

4.4.1 Objective

As we have discussed earlier in the literature review, there are plenty of reports on various biologically active steroids out of which a few derived from 16-dehydropregnenolone acetate exhibited variety of biological activities including anticancer and antifungal. In addition, we have also seen various methods for one-pot click reactions for producing 1,2,3-triazole based products *via in-situ* generation of azides from epoxides. But, one of the limitations was observed in previous methods was the time required for almost all the products are ranging from 3-67 hrs. We wanted to increase the rate of reaction in an effective way. By keeping this in mind, we planned to synthesize a few steroid based 1,2,3-triazole containing molecules derived from 16-dehydropregnenolone acetate (16-DPA) through an efficient one-pot click reaction in microwave using PEG-400 as another greener alternative for solvent in a very short time with excellent yields. The followings are the objectives for this work,

1. Synthesize new molecules derived from 16-DPA containing 1,2,3-triazole in their structure to enhance their biological activity.
2. Develop efficient and quick one-pot click reaction.
3. Regioselectively *in-situ* generation of β -hydroxy azides for the synthesis of regioselective β -hydroxy 1,2,3-triazole functionality based steroids.

4. β -hydroxy 1,2,3-triazole functionality is very important, which may act as pharmacophores. Hence, may enhances biological activities.
5. Synthesized molecules are expected to exhibit anticancer and antifungal activity.

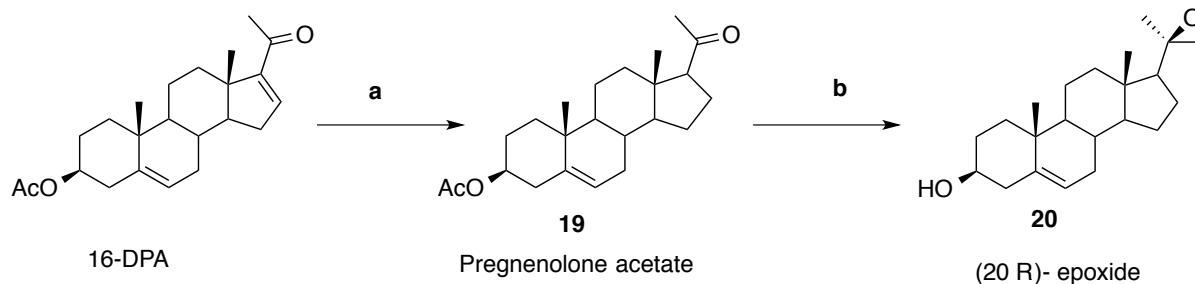
4.4.2 Result and discussion

In addition to our work on microwave assisted 1,2,3- triazole containing biologically active bile acid derivatives,^{28,29} now we report here a novel and practical approach for the synthesis of small steroidal molecules possessing β -hydroxy 1,2,3- triazole functionality by *in-situ* azidation of epoxides with sodium azide followed by “click reaction” utilizing eco-friendly PEG-400:Water as a reaction medium in the presence of 5 mol % of CuI under microwave conditions.

4.4.3 Chemistry

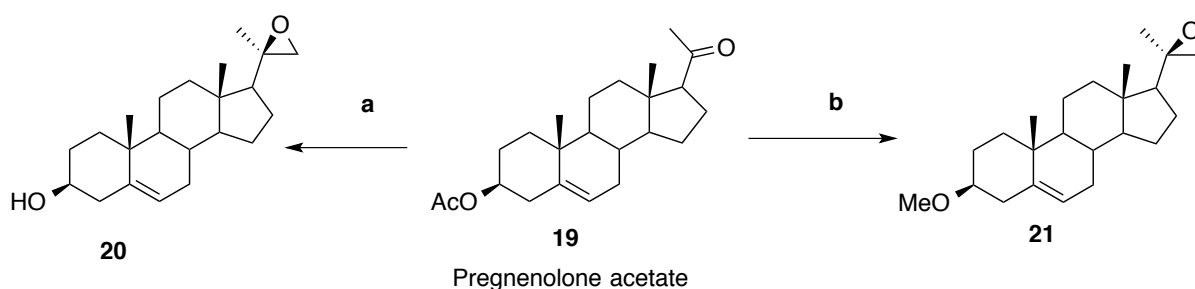
A) Synthesis of (20-*R*) chiral epoxide from 16-DPA

The synthesis of (20-*R*) chiral epoxide **20** was done by previously reported procedure from 16-dehydropregnenolone acetate in two steps with 45% yield.³⁰ Preparation of 20-*R* epoxide **20** from 16-DPA is described in Scheme 5. 16-Dehydropregnenolone acetate on hydrogenation using H₂-Pd/C in ethyl acetate at 55-60 psi for 4-6 hrs afforded pregnenolone acetate **19** in good yield (Scheme 5). It must be noted that, under these conditions double at C-16 was selectively reduced. If methanol is used as a as solvent, both the double bonds at C-3 and C-16 were found to get reduced. The sulfur ylide (dimethylsulfonium methylide)³¹ was used to transform the 20-ketone of pregnenolone 3-acetate **19** to the (20*R*)-epoxide **20** (Scheme 5). The dimethylsulfonium methylide solution was prepared from trimethylsulfonium iodide and sodium hydride in DMSO at 0 °C. The reaction was conducted at room temperature for 12h. Under these conditions, the stereoisomer (20*R*)- **20** was obtained as the major product. The selectivity found for this stereospecifically product is believed to be due to the high reactivity of the dimethylsulfonium methylide.^{31,32} This sulfur ylide is very unstable and may immediately attack the less hindered *R*-side of 20-ketone to form the (20*R*)-epoxide. The configuration of the 20-*R* epoxide was confirmed by the two oxirane proton signals in its ¹H-NMR spectrum (ppm: 2.33 doublet and 2.50 doublet), which coincides with the reported data for the 3-acetate of **20**.³³



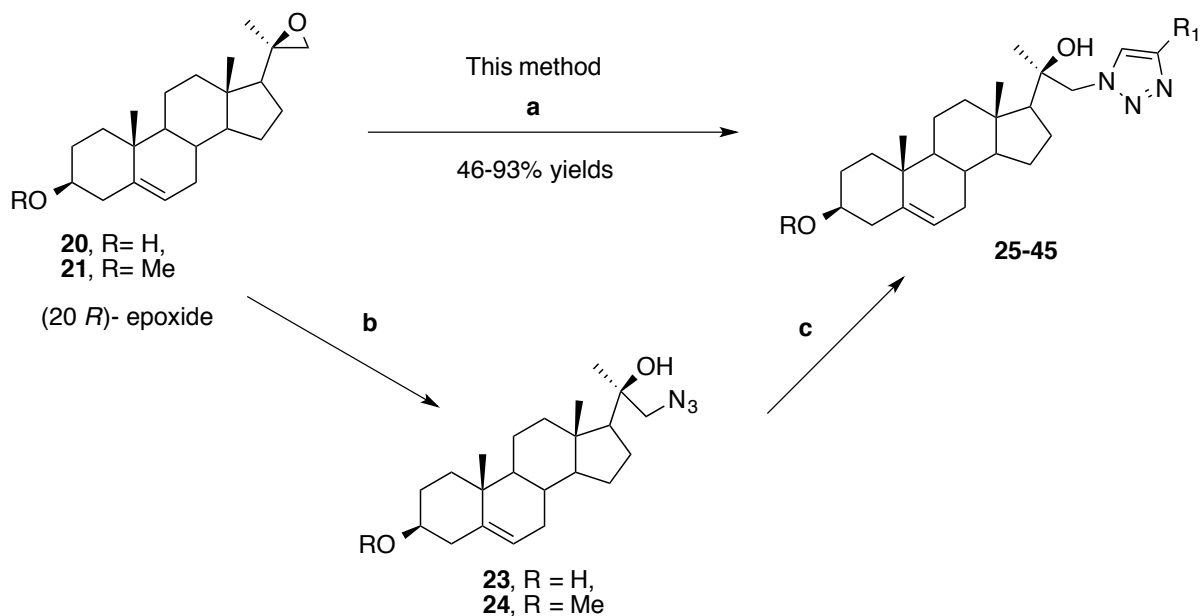
Scheme 5. a) H_2 -Pd/C, EtOAc, 55 psi, 6 h, 90%; b) TMSOI, NaH, DMSO: THF, -5 to 28 °C, 12 h, 45%

Interestingly, methyl protected 20-*R* epoxide **21** at C-3 hydroxy position was also obtained as major product from pregnenolone acetate **19** when sodium hydride was used in excess quantity along with trimethylsulfonium iodide under extended time period (Scheme 6).



Scheme 6. a) TMSOI, NaH (1:2) DMSO: THF, -5 to 28 °C, 12 h, 46%; b) TMSOI, NaH (1:2.5) DMSO: THF, -5 to 28 °C, 18-20 h, 49%

Once we obtained our desired 20*R*-epoxides **20** and **21**, we had option for traditional route for click reaction, *i.e.* by converting epoxide to azide **23**, **24** using sodium azide in dry DMF, which includes purification of toxic azides, followed by click reaction using copper sulphate, sodium ascorbate in DMF and water. This traditional route was going to be lengthy which includes isolation of hazardous azides by column chromatography and use of DMF as a solvent in click reaction. To overcome these issues, we developed new strategy for direct click reaction from epoxide to 1,2,3-triazole containing compounds in good to excellent yields *via in-situ* generation of regioselective β -hydroxy azides **23** and **24** (Scheme 7). To confirm the regioselective formation of azide **23**, we have isolated the intermediate and confirmed it by ^1H , ^{13}C NMR and X-ray crystallographic study shown in figure 5.



Scheme 7. a) NaN₃, alkyne, CuI, PEG-400: H₂O (2:1), Microwave (P 80), 10-40 min 46-93%; b) NaN₃, Dry DMF, 80 °C, 8-10 h, 55-60%; c) CuSO₄·5H₂O, sodium ascorbate, alkynes, DMF: H₂O (4:1), Microwave (P 80) 10-30 min.

Initially, we performed the one-pot epoxide-azide-click reaction employing epoxide **20**, sodium azide, and terminal alkyne 1-octyne using few solvents and their combination, but we got excellent results by employing polyethylene glycol (PEG-400: Water) in 2:1 ratio as the reaction medium in the presence of 5 mol % of CuI. After completion of the reaction in 20 minutes confirmed by TLC in the microwave, the desired product **27** was obtained in 90% isolated yield (Entry 6, Table 1).

Table 1. Investigation of various solvents effect on the “one-pot” reaction^a

Entry	Solvent	Time (Min)	Yield ^b (%)
1	THF	30	-
2	DMF	30	5
3	PEG-400	30	30
4	H ₂ O	30	14
5	DMF:H ₂ O (2:1)	30	55
6	PEG-400:H ₂ O (2:1)	5	90

^aThe reaction was performed with epoxide (**20**, 0.2 mmol), sodium azide (0.6 mmol), alkyne (1-octyne, 0.6 mmol), in the presence of CuI (5mol%) in a microwave (P 80). Reaction progress of the reaction was monitored by TLC. ^bIsolated yields.

Next, we measured the catalyst loading and found that 5 mol % of CuI was enough to drive the reaction to completion with the same efficacy. Among the solvents surveyed, PEG-400 turned out to be the solvent of choice (Table 1). We have also evaluated other reaction media such as THF, DMF and water alone for this transformation. To our surprise, the reaction in water, DMF and THF did not progress even after long time. These results demonstrate that PEG-400 and water not only acts as a reaction medium but also presumably activates epoxide (Table 1).

B) Regiochemistry

It could be delighted that the multicomponent synthesis of novel steroidal molecules containing 1,2,3-triazoles catalyzed by a Cu(I) complex in PEG: Water medium was regiospecific concerning both azidolysis of the epoxide and 1,3-dipolar cycloaddition with terminal alkynes. However, we have used chiral epoxides **20/21** obtained by a reported procedure³⁴ which on azidolysis resulted in chiral products and moreover no enantiomeric excess experiments were done. The NMR data were matched for the chiral epoxides in the reported procedure.³⁴ It was speculated that PEG enhances the electrophilicity of the epoxide-ring through hydrogen-bonding and facilitates the nucleophilic attack of the azide (Figure 5). Besides, hydrogen bonding between azide and water may provide additional stabilization and allows the epoxide to be explicitly opened from the less-hindered side. Another hypothesis is that the role of PEG is to form complexes with the cation (Sodium), much like crown ethers possibly, and these complexes cause the anion to be activated. However, the Cu(I) catalyst might also play an important role in the fate of regioselectivity due to the additional coordination of the epoxide ring oxygen with the metal center,³⁵ since it was observed to accelerate the azidolysis of the epoxide ring. The isolation of intermediate azides **23** and **24** formed in *in-situ* conditions were confirmed by proton and carbon NMR,

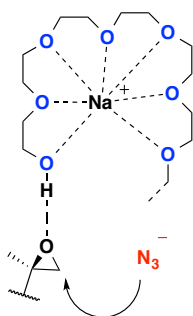


Figure 5. Plausible mechanism of regioselectivity using PEG-400

whereas the regioselective synthesis of intermediate **23** was also confirmed by single X-ray crystallographic study (Figure 6). Moreover, the regiochemistry of the final product **41** in which methylation of hydroxyl group of epoxide **20** was confirmed by single X-ray crystallographic study which shows the exclusive formation of one regioisomer as shown in the Figure 7.

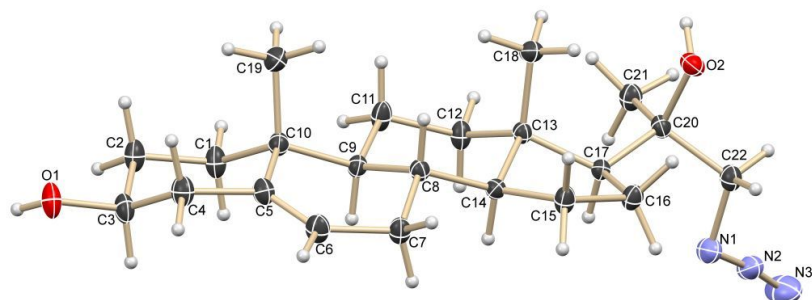


Figure 6. ORTEP diagram of intermediate **23**

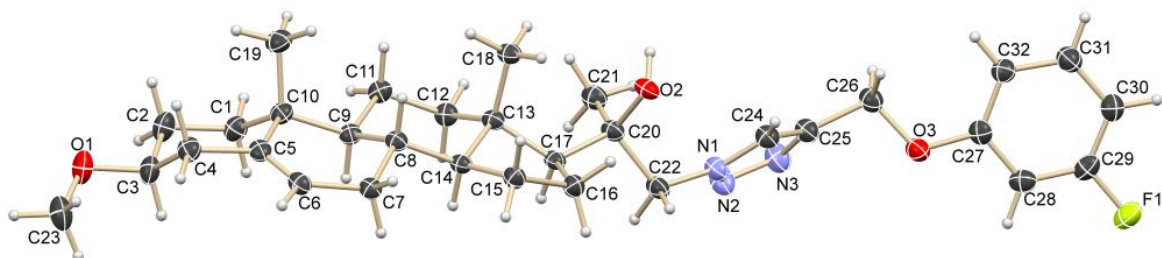
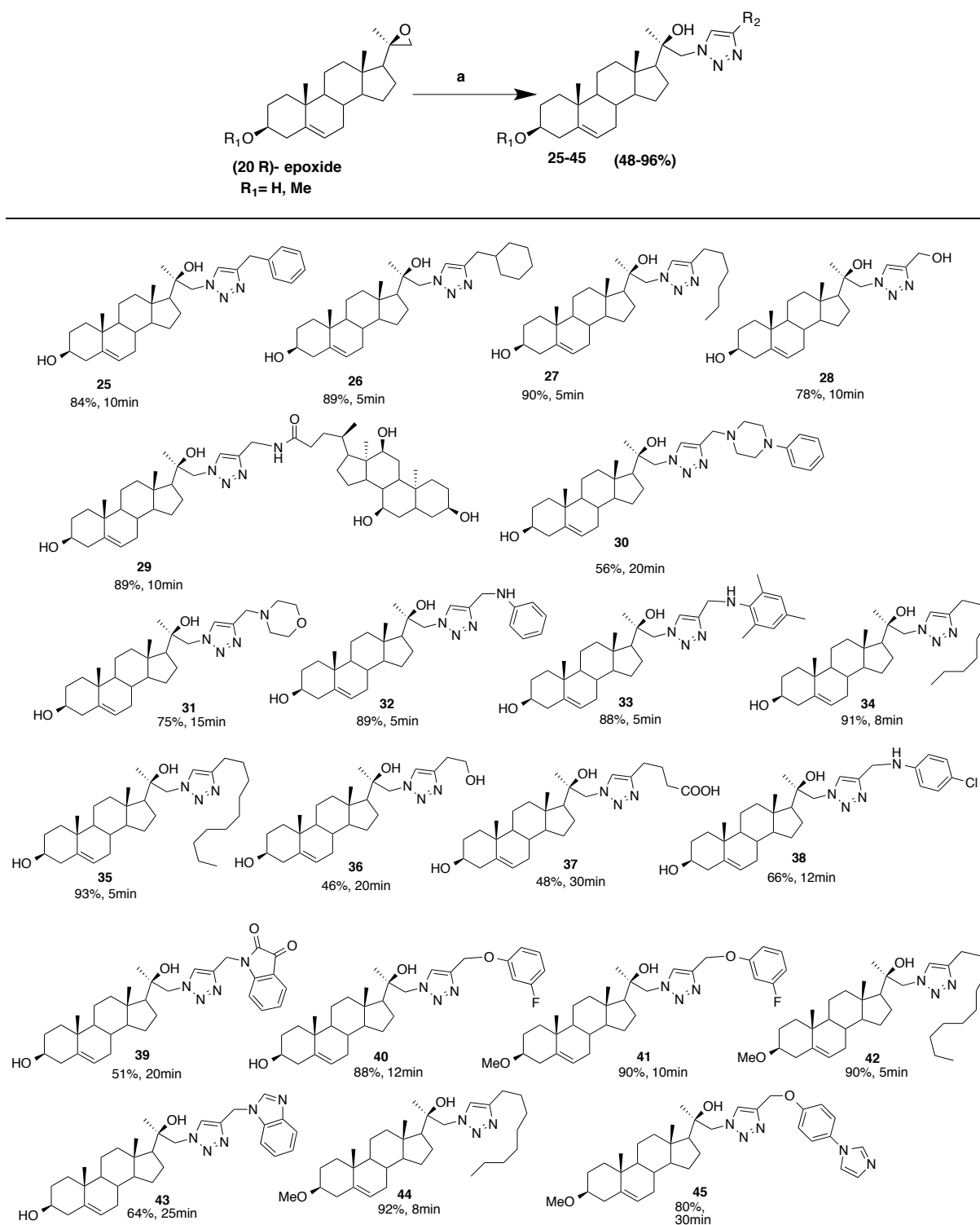


Figure 7. ORTEP diagram of **41**

Table 2. Epoxy-Azide-Cu(I)-Catalyzed [3+2] Huisgen Reaction with Various Acetylenes

^a All reactions were carried out in microwave at (P80) with 5 mol % of CuI, 3 equiv of NaN₃ and 3 equiv of alkynes in PEG-400:H₂O (2:1) for the given time. Yield and time are indicated below each structure. All compounds are purified using column chromatography.

4.4.4 Biological activity [Anticancer]

All the synthesized compounds **25-45** were further tested against human breast adenocarcinoma cell line and almost all the compounds were found to be potent except **37**, **41** and **43**. All the compounds were compared with two drugs *i.e* Cisplatin and Doxorubicin HCl as a standard. IC₅₀ determination at concentrations were 0.01, 0.1, 1, 10, 50 and 100 μ M (Table 3).

Table 3. Anticancer activity of compounds **25-45** against MDA-MB-231

Sample Code	Molecular weight	IC ₅₀ (μ M)
		MDA-MB--231
Cisplatin	300.05	50.40
Doxorubicin HCl	579.98	0.54
25	489.70	1.64
26	495.75	5.58
27	483.74	5.87
28	429.60	3.52
29	819.19	0.71
30	573.83	1.42
31	498.71	7.31
32	504.72	44.71
33	546.80	6.55
34	511.80	2.84
35	539.85	43.72
36	443.63	23.10
37	485.67	>100
38	539.16	50.4
39	558.72	40.44
40	523.69	21.22
41	537.72	>100
42	553.87	42.69
43	529.72	>100
44	525.82	63.43
45	585.79	2.48

4.4.5 MTT Assay protocol

Cells were seeded into 96-well tissue culture plates at a density of 1×10^4 cells/well and were incubated at 5% CO₂ at 37 °C for 24 h. After, incubation 6 concentrations (triplicate) of test compounds (prepared in DMSO) was added to the cells and incubated at 37 °C and 5% CO₂ for 48 h. Then, 20 µL of MTT solution (5 mg/mL) was added to each well. Plate was further incubated for a period of about 4 h, the supernatant was removed and 200 µL per well DMSO was added to solubilize formazan crystals. Plate was incubated for 10 mins and absorbance was measured at 540 nm. IC₅₀ determination at concentrations 0.01, 0.1, 1, 10, 50 and 100 µM.

4.4.6 Molecular Docking

Molecular docking is now a well established computational technique and has become an integral part of drug discovery research to predict the predominant binding mode(s) of a ligand within a protein (biological target) of a known three-dimensional structure. It imparts knowledge on binding affinities, binding modes, type of interactions guiding the protein–ligand complexation which provides immense opportunity to researchers for generating and analyzing the potential of existing lead molecules and their analogues. In the absence of available resources to carry out the enzymatic assays, *in silico* computational chemistry techniques like molecular docking have become very essential to identify the targets for different molecules and their associated thermodynamic interactions with the target enzyme that govern the inhibition of the pathogen. Therefore, with the aim of rationalizing the promising anticancer results and to investigate the possible interactions of the studied compounds, 3D structure of human placental aromatase cytochrome P450 complexed with its inhibitor was selected as target protein to carry out the molecular docking study for the series. Aromatase cytochrome P450 is the only enzyme in vertebrates known to catalyse the biosynthesis of all oestrogens from androgens. Estrogen is important and promotes the growth and survival of normal and cancer epithelial cells. The chemical compound estrogen binds to the estrogen receptor (ER) and the activation of the cell progression takes place. The active estrogen receptor tends to bind with promoter gene present in the nucleus, which regulates the gene activity and translates the protein. The activated receptor in turn binds to gene promoters in the nucleus and activates many other genes. The activated gene products are thereby responsible for cell division, inhibition of cell death, new blood vessels formation and protease activity. Rapid expression of estrogen receptor is found at earlier stages of

breast cancer. Nearly 70% cancer mainly depends on the over-expression of estrogen receptor. Aromatase inhibitor inactivates the production of estrogen from androgens, by suppressing aromatase enzyme activity. The breast cancer patients treated with aromatase inhibitors show, low level of estrogen secretion in the tumor cells. The aromatase enzyme is responsible for the conversion of androstenedione to estrone and testosterone to estradiol, any mutation or overexpression of estrogen can be controlled only by inhibiting the conversion process. Hence, aromatase is chosen as important drug target protein in breast cancer treatment. The molecular docking of the most active compound **30** is shown in Figure 8.

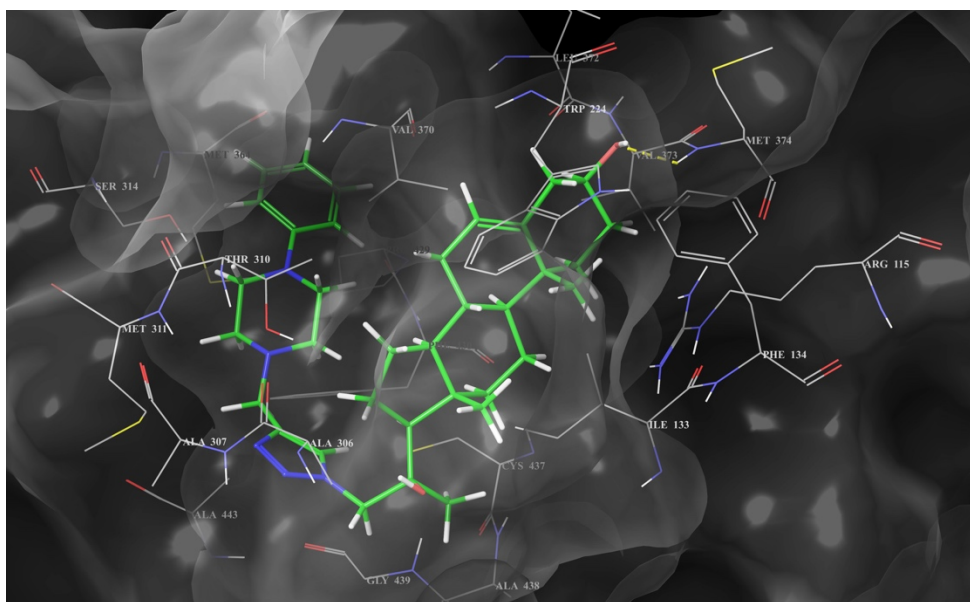


Figure 8. Binding mode of **30** into the active site of Aromatase cytochrome P450.

The outcome of molecular docking study revealed that all the studied compounds were successfully docked making a snug fit into the active site of Aromatase cytochrome P450 at co-ordinates very close to that of the native ligand in the crystal structure with varying degree of affinities (Figure 8). Their complexes with protein structure were stabilized by several bonded and non-bonded interactions with the amino acids surrounding the active site. The results of molecular docking study are summarized in Table 4 where a significant correlation was found in between the docking scores and the obtained biological activity (expressed as MIC($\mu\text{g}/\text{mL}$)) with the active compounds producing lower scores and lower glide energy in Kcal/mol (most active compound **30** produced lowest score -10.204 with lowest glide energy -79.392 kcal/mol) while those with relatively low activity are also predicted to produce a high docking score. Their binding energies were also found to be negative

(-79.392 to -34.528Kcal/mol) qualifying them to be pertinent starting point for the rational design of drugs targeting Aromatase cytochrome P450.

Table 4. Summary of molecular docking study of compounds **25-45**

Sample Code	Molecular weight	IC ₅₀ (μM)	Docking Score (Glide Score)	Glide energy (kcal/mol)	H-bond	π-π stacking
		MDA-MB--231				
Cisplatin	300.05	50.40				
Doxorubicin HCl	579.98	0.54				
25	489.70	1.64	-10.007	-75.280	<i>Met374</i>	
26	495.75	5.58	-8.569	-65.045	<i>Met374</i>	
27	483.74	5.87	-8.177	-64.853	<i>Met374</i>	
28	429.60	3.52	-8.966	-67.854	<i>Ala307</i>	
29	819.19	0.71	-	-	-	
30	573.83	1.42	-10.204	-79.392	<i>Met374</i>	
31	498.71	7.31	-7.917	-61.723	<i>Met374</i>	
32	504.72	44.71	-7.241	-54.913	<i>Met374</i>	<i>Phe430</i>
33	546.80	6.55	-8.071	-62.572	<i>Met374, Leu477</i>	<i>Arg115, Trp224</i>
34	511.80	2.84	-9.196	-69.180	<i>Met374</i>	
35	539.85	43.72	-	-	-	
36	443.63	23.10	-7.878	-59.367	<i>Leu372, Thr310</i>	
37	485.67	>100	-4.467	-37.891	-	-
38	539.16	50.4	-7.220	-53.868	<i>Met374</i>	<i>Phe430</i>
39	558.72	40.44	-7.747	-57.777	<i>Ser314</i>	-
40	523.69	21.22	-7.988	-60.467	<i>Met374</i>	<i>Phe430</i>
41	537.72	>100	-3.706	-37.609	<i>Met374</i>	<i>Phe430</i>
42	553.87	42.69	-7.395	-55.880	-	<i>Phe134</i>

43	529.72	>100	-3.139	-34.528	<i>Met374</i>	<i>Phe430</i>
44	525.82	63.43	-6.871	-50.081	<i>Met374</i>	-
45	585.79	2.48	-9.217	-70.228	<i>Met374</i>	<i>Phe430</i>

4.4.7 Molecular docking Assay

The molecular docking study was performed with Glide (Grid-Based Ligand Docking with Energetics) [Friesner RA, Banks JL, Murphy RB, Halgren TA, Klicic JJ, Mainz DT, et al. Glide: a new approach for rapid, accurate docking and scoring. 1. Method and assessment of docking accuracy. *Journal of medicinal chemistry*. 2004; 47: 1739-49. Halgren TA, Murphy RB, Friesner RA, Beard HS, Frye LL, Pollard WT, et al. Glide: a new approach for rapid, accurate docking and scoring. 2. Enrichment factors in database screening. *Journal of medicinal chemistry*. 2004;47:1750-9.] module incorporated in the Schrödinger molecular modeling software (Schrödinger, Inc., USA, 2016) to gain an insight into the binding modes of the oxadiazole derivatives (KB01-KB20) into the active site of human placental aromatase cytochrome P450 enzyme. With this purpose the crystal structure of human placental aromatase cytochrome P450 in complex with androstenedione (code ID: 3EQM, resolution [Å]: 2.90) was retrieved from protein data bank. (<http://www.rcsb.org/pdb/>).

4.5 Conclusions

In the present work, we have developed the synthesis of novel steroidal molecules containing 1,2,3-triazole through a sustainable ‘one-pot’ click protocol directly from epoxides in good to excellent yields. It involves a regioselective multi-component reaction between steroidal 20-*R* epoxides, terminal alkynes, sodium azide and CuI towards the synthesis of a library of novel 1,2,3-triazole containing pregnene derivatives **25-45**. This method affords a significant advantage by avoiding the isolation and handling of hazardous organic azide intermediates. The reaction offers regiospecificity, high yields, cost-effective, and easy isolation of final products including a broad substrate scope. The overall modularity of this “one-pot” sequence is greener and noteworthy. Almost all the synthesized compounds were found to be active against human breast adenocarcinoma cell line **MDA-MB-231** except **37**, **41** and **43**. Molecular docking study also supports the biological findings.

4.6 Experimental section

4.6.1 General methods

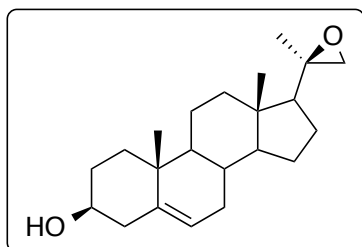
All chemicals were obtained from commercial sources and used as received without further purification. All the reactions were carried out under nitrogen atmosphere. Column chromatography was carried out by using silica gel (60-120/240-400 mm, Merck). All reactions were monitored by TLC with silica gel coated plates; spots were visualized by UV light and/or with dipping in a phosphomolybdic acid and ninhydrin solution and charring on a hot plate. All the liquid state 1D-NMR spectra (^1H , ^{13}C NMR) were recorded in CDCl_3 (for compound **22**), and CD_3OD (for compounds **23**, **24** and **25**) on AC 200 MHz and AV-500 MHz Bruker NMR spectrometers. Chemical shifts are reported in ppm. Coupling constants J are reported in Hz. The ^1H chemical shifts were referenced to TMS as internal standard. Infrared (IR) spectra were recorded on liquid cell with KBr plates. Only diagnostic bands are reported on cm^{-1} scale. High-resolution mass spectra (HR-MS) were recorded on an Agilent 6520 (QTOF) ESI-HRMS instrument and LC-MS spectrometer.

4.6.2 Synthesis of 20-(*R*) epoxide 20.

(3S,10R,13S)-10,13-dimethyl-17-((R)-2-methyloxiran-2-yl)-

2,3,4,7,8,9,10,11,12,13,14,15,16,17-tetradecahydro-1H-cyclopenta[a]phenanthren-3-ol

(20):

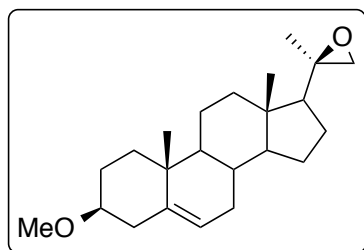


A suspension of sodium hydride (80%, 5.6 mmol), anhydrous DMSO (3 mL), and THF (3 mL) was stirred for 5 min and then cooled to -5 to 0°C in an ice bath. Trimethylsulfoniumiodide (2.8 mmol) was added, and the mixture was stirred for 2 h. Pregnenolone acetate (**19**; Scheme 1) (0.5 g, 1.4 mmol, in DMSO (4 mL) and THF (2 mL)) was added dropwise into the reaction mixture, and the ice bath was removed. The reaction was continued for 12 h at room temperature. Water (5 mL) was then added, and the mixture was stirred for another 2 h. The reaction mixture was poured onto ice (10 g), and the product was extracted with dichloromethane. After the removal of solvent, the residue was recrystallized from acetone and then methanol to give white crystals of **20** (Yield 46%), IR (CHCl_3 , cm^{-1}) 3417, 3020, 2929, 2400, 1737, 1641, 1439, 1378, 1215, 770; M.P $162-63^\circ\text{C}$. ^1H NMR (200 MHz, CHLOROFORM-d) δ 5.35 (d, $J = 5.31$ Hz, 1H), 3.40 - 3.64 (m, 1H), 2.51 (d, $J = 5.05$ Hz, 1H), 2.33 (d, $J = 4.93$ Hz, 1H), 2.19 - 2.30 (m, 2H), 1.98 - 2.13 (m, 2H), 1.75 - 1.92 (m, 3H), 1.70 (d, $J = 8.59$ Hz, 1H), 1.57 - 1.64 (m, 3H), 1.44 - 1.56 (m, 5H), 1.37 - 1.41 (m, 3H), 1.05 - 1.32 (m, 4H), 1.02 (s, 4H), 0.91 (d, $J = 6.95$ Hz, 1H), 0.82 (s, 3H) ^{13}C NMR (50 MHz,

CHLOROFORM-d) δ 140.8, 121.5, 71.7, 56.6, 56.2, 54.1, 51.5, 50.0, 43.1, 42.2, 39.4, 37.2, 36.5, 31.7, 31.6, 23.8, 22.5, 21.8, 20.9, 19.4, 12.9

4.6.3 Synthesis of 20-(*R*) epoxide 21.

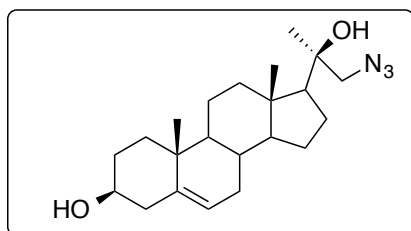
(2*R*)-2-((3*S*,10*R*,13*S*)-3-methoxy-10,13-dimethyl-2,3,4,7,8,9,10,11,12,13,14,15,16,17-tetradecahydro-1*H*-cyclopenta[*a*]phenanthren-17-yl)-2-methyloxirane (**21**):



A suspension of sodium hydride (80%, 7 mmol), anhydrous DMSO (3 mL), and THF (3 mL) was stirred for 5 min and then cooled to -5 to 0 °C in an ice bath. Trimethylsulfonium iodide (2.8 mmol) was added, and the mixture was stirred for 2 h. Pregnenolone acetate (**19**; Scheme 1) (0.5 g, 1.4 mmol, in DMSO (4 mL) and THF (2 mL)) was added dropwise into the reaction mixture, and the ice bath was removed. The reaction was continued for 12 h at room temperature. Water (5 mL) was then added, and the mixture was stirred for another 2 h. The reaction mixture was poured onto ice (50 g), and the product was extracted with dichloromethane. After the removal of solvent, the residue was recrystallized from acetone and then methanol to give white crystals of **21** (Yield 49%), ¹H NMR (200 MHz, CHLOROFORM-d) δ 5.35 (d, *J* = 5.31 Hz, 1H), 3.40 - 3.64 (m, 1H), 3.36 (s, 3H), 2.51 (d, *J* = 5.05 Hz, 1H), 2.33 (d, *J* = 4.93 Hz, 1H), 2.19 - 2.30 (m, 2H), 1.98 - 2.13 (m, 2H), 1.75 - 1.92 (m, 3H), 1.70 (d, *J* = 8.59 Hz, 1H), 1.57 - 1.64 (m, 3H), 1.44 - 1.56 (m, 5H), 1.37 - 1.41 (m, 3H), 1.05 - 1.32 (m, 4H), 1.02 (s, 4H), 0.91 (d, *J* = 6.95 Hz, 1H), 0.82 (s, 3H); ¹³C NMR (50 MHz, CHLOROFORM-d) δ 140.9, 121.4, 80.3, 75.1, 61.5, 56.7, 56.2, 55.6, 50.0, 42.8, 39.9, 38.6, 37.1, 36.8, 31.7, 31.3, 28.0, 24.9, 23.8, 22.3, 20.9, 19.3, 13.5

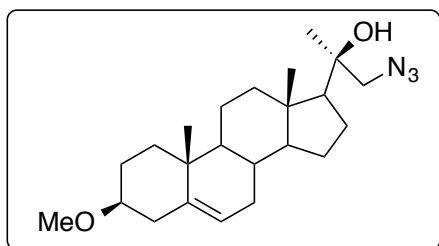
(3*S*,10*R*,13*S*)-17-((*R*)-1-azido-2-hydroxypropan-2-yl)-10,13-dimethyl-2,3,4,7,8,9,10,11,12,13,14,15,16,17-tetradecahydro-1*H*-cyclopenta[*a*]phenanthren-3-ol

(**23**): ¹H NMR (200 MHz, CHLOROFORM-d) δ 5.36 (d, *J* = 4.80 Hz, 1H), 3.42 - 3.64 (m, 1H), 3.31 (d, *J* = 11.87 Hz, 1H), 3.12 (d, *J* = 11.87 Hz, 1H), 2.21 - 2.36 (m, 2H), 2.04 (br. s., 1H), 1.85 (d, *J* = 11.87 Hz, 3H), 1.69 (d, *J* = 6.44 Hz, 2H), 1.42 - 1.62 (m, 8H), 1.35 (s, 3H), 1.25 (d, *J* = 4.80 Hz, 2H), 1.06 - 1.16 (m, 2H), 1.02 (s, 3H), 0.86 (s, 3H); ¹³C NMR (50 MHz, CHLOROFORM-d)



δ140.8, 121.5, 75.2, 71.7, 61.5, 56.7, 56.2, 49.9, 42.8, 42.2, 39.9, 37.2, 36.5, 31.7, 31.6, 31.3, 24.9, 23.8, 22.3, 20.9, 19.4, 13.6

(2R)-1-azido-2-((3S,10R,13S)-3-methoxy-10,13-dimethyl-2,3,4,7,8,9,10,11,12,13,14,15,16,17-tetradecahydro-1H-cyclopenta[a]phenanthren-17-yl)propan-2-ol (24):



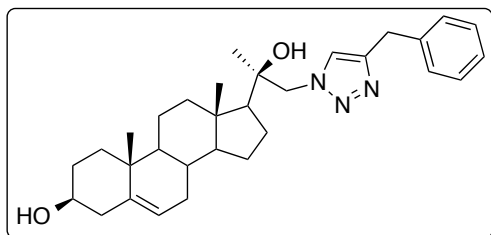
IR (CHCl₃, cm⁻¹) 3437, 3173, 2842, 2724, 2189, 2107, 1712, 1464, 1377, 1306, 1155, 1070, 723; ¹H NMR (400 MHz, CHLOROFORM-d) δ 5.36 (d, *J* = 5.50 Hz, 1H), 3.36 (s, 3H), 3.30 (d, *J* = 11.91 Hz, 1H), 3.12 (d, *J* = 11.91 Hz, 1H), 3.01 - 3.09 (m, 1H), 2.35 - 2.45 (m, 1H), 2.11 - 2.21 (m, 1H), 2.03 - 2.10 (m, 1H), 2.01 (d, *J* = 2.75 Hz, 1H), 1.95 (d, *J* = 10.53 Hz, 1H), 1.76 - 1.90 (m, 2H), 1.61 - 1.71 (m, 3H), 1.39 - 1.60 (m, 7H), 1.32 - 1.36 (m, 3H), 1.10 - 1.29 (m, 3H), 1.03 - 1.09 (m, 1H), 1.01 (s, 4H), 0.89 - 0.97 (m, 1H), 0.84 - 0.88 (m, 3H); ¹³C NMR (50 MHz, CHLOROFORM-d) δ 140.9, 121.4, 80.3, 75.1, 61.5, 56.7, 56.2, 55.6, 50.0, 42.8, 39.9, 38.6, 37.1, 36.8, 31.7, 31.3, 28.0, 24.9, 23.8, 22.3, 20.9, 19.3, 13.5.

4.6.4 General procedure for the “one-pot” synthesis of click derivatives 25-45.

The epoxide (1 mmol) and NaN₃ (3 mmol) were first dissolved in PEG-400 (2 mL) and water (1 mL) and allowed to keep in a traditional microwave at P100 for 2 minutes. To this mixture, Alkyne (3 mmol) and CuI (5 mol %) were added and kept again in a microwave at P80 for a specified period of time. The reaction mixture was filtered through celite and the filtrate was quenched with ice (5 mL) and extracted with ethyl acetate (3 × 10 mL). The organic layer was dried over anhydrous Na₂SO₄, followed by concentration under reduced pressure resulting in the crude product. The crude residue was purified by column chromatography (silica gel 240-400 mesh) with hexane: EtOAc (6:4) elutant to give the triazole product. These were recrystallized with hexane: EtOAc (6:4).

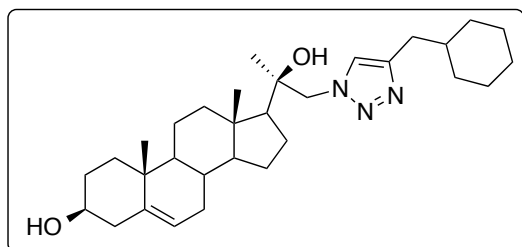
(3S,10R,13S)-17-((R)-1-(4-benzyl-1H-1,2,3-triazol-1-yl)-2-hydroxypropan-2-yl)-10,13-dimethyl-2,3,4,7,8,9,10,11,12,13,14,15,16,17-tetradecahydro-1H-cyclopenta[a]phenanthren-3-ol (25):

White coloured solid, M.P= 177.5 °C, S.R= -9.98 (c=0.2, CHCl₃): ¹H NMR (200 MHz, CHLOROFORM-d) δ 7.88 (s, 1H), 7.82-7.77(m, 1H), 7.48- 7.36(m, 4H), 5.35(d, *J* = 4.93



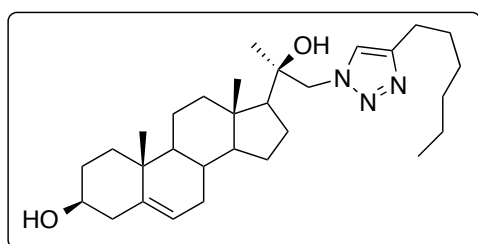
Hz, 1H), 4.52 - 4.36 (m, 2H), 3.56 - 3.51 (m, 1H), 2.74-2.65 (m, 2H), 2.30 (m, 2H), 2.13 (m, 2H), 2.05 (m, 2H), 1.87-1.82 (m, 2H), 1.70 (m, 2H), 1.56-1.49 (m, 6H), 1.26-1.20 (m, 2H), 1.14 (s, 3H), 1.02 (s, 3H), 0.90 (s, 3H); ^{13}C NMR (101 MHz, CHLOROFORM-D) δ 147.8, 140.7, 130.8, 129.9, 128.8, 128.5, 125.8, 121.5, 74.9, 71.7, 64.3, 57.3, 56.7, 49.9, 43.1, 42.2, 40.0, 37.1, 36.4, 31.7, 31.3, 24.7, 23.9, 22.3, 20.8, 19.3, 13.3; HRMS (ESI-qTOF): calcd for $\text{C}_{31}\text{H}_{44}\text{N}_3\text{O}_2$ $[\text{M}+\text{H}]^+$, 490.3430; found: 490.3428.

(3S,10R,13S)-17-((R)-1-(4-(cyclohexylmethyl)-1H-1,2,3-triazol-1-yl)-2-hydroxypropan-2-yl)-10,13-dimethyl-2,3,4,7,8,9,10,11,12,13,14,15,16,17-tetradecahydro-1H-cyclopenta[a]phenanthren-3-ol (26):



White coloured solid, M.P= 118.2 $^{\circ}\text{C}$, S.R = -20.37 ($c=1$, CHCl_3), ^1H NMR (400 MHz, Chloroform-d) δ 7.36 (s, 1H), 5.34 (d, $J = 5.2$ Hz, 1H), 4.24 (s, 2H), 3.56 - 3.46 (m, 1H), 2.57 (d, $J = 6.8$ Hz, 2H), 2.32 - 2.19 (m, 2H), 2.18 - 2.01 (m, 3H), 1.95 (s, 2H), 1.82 (d, $J = 10.0$ Hz, 3H), 1.68 (d, $J = 12.7$ Hz, 10H), 1.50 (s, 4H), 1.17 (d, $J = 10.7$ Hz, 5H), 1.11 (s, 3H), 1.05 (s, 1H), 1.00 (s, 3H), 0.93 (d, $J = 11.0$ Hz, 3H), 0.88 (s, 3H); ^{13}C NMR (101 MHz, CHLOROFORM-D) δ 146.61, 140.94, 123.32, 121.54, 74.86, 71.79, 59.88, 57.49, 56.80, 50.03, 43.28, 42.35, 40.15, 38.18, 37.34, 36.59, 33.47, 33.15, 31.82, 31.70, 31.41, 26.55, 26.29, 24.65, 24.03, 22.45, 20.99, 19.51, 13.66; HRMS (ESI-qTOF): calcd for $\text{C}_{31}\text{H}_{50}\text{N}_3\text{O}_2$ $[\text{M}+\text{H}]^+$, 496.3904; found: 496.3898.

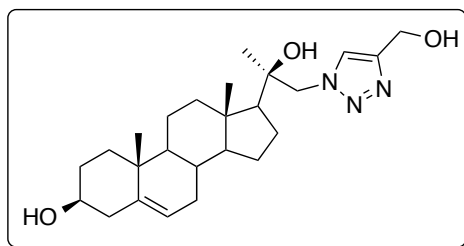
(3S,10R,13S)-17-((R)-1-(4-hexyl-1H-1,2,3-triazol-1-yl)-2-hydroxypropan-2-yl)-10,13-dimethyl-2,3,4,7,8,9,10,11,12,13,14,15,16,17-tetradecahydro-1H-cyclopenta[a]phenanthren-3-ol (27):



Cream coloured solid, mp= 112.2 $^{\circ}\text{C}$; ^1H NMR (400 MHz, Chloroform-d) δ 7.36 (s, 1H), 5.35 (d, $J = 5.1$ Hz, 1H), 4.43 - 4.16 (m, 2H), 3.52 (m, 1H), 3.15 - 3.06 (m, 1H), 2.70 (t, $J = 7.7$ Hz, 1H), 2.34 - 2.19 (m, 2H), 2.10 (m, 1H), 1.98 (m, 3H), 1.83 (m, 3H), 1.68 (m, 7H), 1.57 - 1.44 (m, 6H), 1.37 (s, 3H), 1.28 (d, $J = 21.8$ Hz, 7H), 1.13 (d, $J = 6.0$ Hz, 3H), 1.00 (s, 3H), 0.88 (m, 6H); ^{13}C NMR (101 MHz, CHLOROFORM-D) δ 148.26, 147.82,

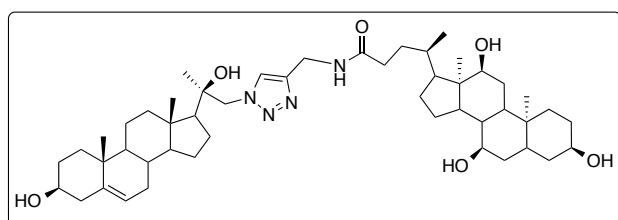
140.92, 127.35, 122.66, 121.59, 121.54, 74.89, 74.73, 71.85, 60.0, 59.89, 57.46, 56.80, 50.03, 49.9, 43.35, 42.36, 40.15, 39.68, 37.34, 31.72, 25.77, 24.62, 23.77, 22.47, 19.52, 14.0, 14.21, 13.74, 13.68; HRMS (ESI-qTOF): calcd for $C_{30}H_{49}N_3O_2$ $[M+H]^+$, 484.3902; found: 484.3898.

(3*S*,10*R*,13*S*)-17-((*R*)-2-hydroxy-1-(4-(hydroxymethyl)-1*H*-1,2,3-triazol-1-yl)propan-2-yl)-10,13-dimethyl-2,3,4,7,8,9,10,11,12,13,14,15,16,17-tetradecahydro-1*H*-cyclopenta[*a*]phenanthren-3-ol (28):



White coloured solid, M. P = 212 °C, S.R = -31.96 (c=0.2, MeOH); 1H NMR (400 MHz, DMSO- d_6) δ 7.83 (s, 1H), 5.26 (d, J = 4.8 Hz, 1H), 5.15 (s, 1H), 4.59 (d, J = 4.5 Hz, 1H), 4.52 – 4.45 (m, 3H), 4.15 (dd, J = 68.5, 13.7 Hz, 2H), 3.24 (d, J = 10.4 Hz, 1H), 2.13 (s, 1H), 2.00 (s, 1H), 1.88 (s, 1H), 1.77 – 1.63 (m, 3H), 1.38 (d, J = 20.6 Hz, 4H), 1.07 (s, 2H), 1.02 (s, 3H), 0.93 (s, 4H), 0.81 (s, 3H); ^{13}C NMR (101 MHz, DMSO) δ 147.37, 141.27, 123.89, 120.41, 72.92, 70.00, 56.36, 56.30, 55.07, 49.56, 42.34, 42.22, 36.92, 36.08, 31.42, 31.28, 30.91, 30.71, 24.23, 23.60, 21.69, 20.48, 19.15, 13.21; HRMS (ESI-qTOF): calcd for $C_{25}H_{40}N_3O_3$ $[M+H]^+$, 430.3066; found: 430.3064.

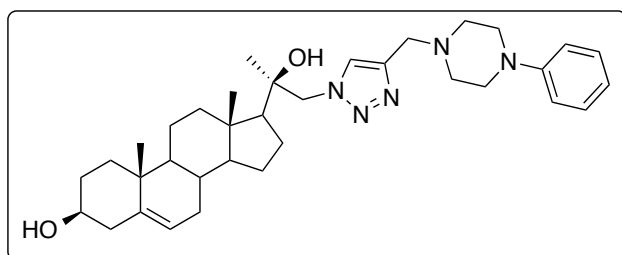
(4*R*)-*N*-((1-((2*R*)-2-hydroxy-2-((3*S*,10*R*,13*S*)-3-hydroxy-10,13-dimethyl-2,3,4,7,8,9,10,11,12,13,14,15,16,17-tetradecahydro-1*H*-cyclopenta[*a*]phenanthren-17-yl)propyl)-1*H*-1,2,3-triazol-4-yl)methyl)-4-((3*R*,7*R*,10*S*,12*S*,13*R*)-3,7,12-trihydroxy-10,13-dimethylhexadecahydro-1*H*-cyclopenta[*a*]phenanthren-17-yl)pentanamide (29):



Cream coloured solid, M.P = 220 °C, S.R = 0.99 (c= 0.4, MeOH), 1H NMR (400 MHz, DMSO- d_6) δ 8.28 (s, 1H), 7.75 (s, 1H), 5.28 – 5.22 (m, 1H), 4.60 (d, J = 4.6 Hz, 1H), 4.48 – 4.31 (m, 2H), 4.24 (m, 3H), 4.09 – 4.00 (m, 5H), 3.79 – 3.58 (m, 2H), 3.18 (m, 1H), 2.08 (s, 4H), 1.98 (s, 4H), 1.79 – 1.72 (m, 5H), 1.64 (m, 7H), 1.35 (s, 11H), 1.26 – 1.20 (m, 5H), 1.17 (s, 3H), 1.00 (s, 6H), 0.92 (m, 7H), 0.81 (m, 7H), 0.56 (s, 3H); ^{13}C NMR (101 MHz, DMSO- D_6) δ 172.60, 144.65, 141.26, 123.95, 120.40, 72.89, 71.02, 70.44, 70.01, 66.26, 59.46, 56.37, 49.57, 46.10, 45.74, 42.34, 42.22, 41.53, 41.37, 36.94, 36.07, 35.32, 35.05, 34.91, 34.40, 34.16, 32.29, 31.66, 31.41, 30.91, 30.71, 30.41, 28.57, 27.32, 26.22, 24.20, 23.60, 22.82, 22.62, 21.72, 20.78, 20.48,

19.14, 17.14, 14.10, 13.20, 12.38; HRMS (ESI-qTOF): calcd for $C_{49}H_{79}N_4O_6$ $[M+H]^+$, 819.5999; found: 819.5994.

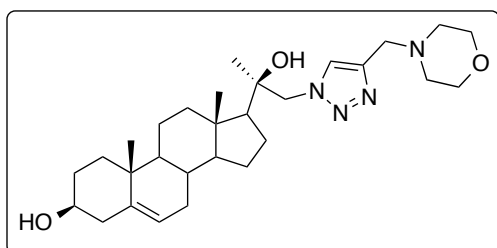
(3*S*,10*R*,13*S*)-17-((*R*)-2-hydroxy-1-(4-((4-phenylpiperazin-1-yl)methyl)-1*H*-1,2,3-triazol-1-yl)propan-2-yl)-10,13-dimethyl-2,3,4,7,8,9,10,11,12,13,14,15,16,17-tetradecahydro-1*H*-cyclopenta[*a*]phenanthren-3-ol (30):



Brown solid, mp = 207 °C, S.R = -13.48 (c= 1.2, $CHCl_3$), 1H NMR (400 MHz, Chloroform-*d*) δ 7.64 (s, 1H), 7.26 – 7.20 (m, 2H), 6.95 – 6.89 (m, 2H), 6.88 – 6.81 (m, 1H), 5.35 (d, J = 4.9 Hz, 1H), 4.28 (d, J

= 3.8 Hz, 2H), 3.77 (s, 2H), 3.52 (m, 1H), 3.20 (t, J = 5.0 Hz, 4H), 2.69 (m, 2H), 2.63 (m, 2H), 2.34 – 2.21 (m, 2H), 2.10 (d, J = 12.3 Hz, 1H), 2.05 – 1.90 (m, 4H), 1.83 (d, J = 10.2 Hz, 4H), 1.71 (m, 3H), 1.56 – 1.45 (m, 6H), 1.13 (s, 3H), 1.00 (s, 3H), 0.89 (s, 3H); ^{13}C NMR (101 MHz, $CDCl_3$) δ 151.19, 140.80, 129.10, 124.70, 121.42, 119.77, 116.09, 74.72, 71.69, 69.53, 59.88, 57.38, 56.71, 53.80, 52.83, 49.93, 49.00, 43.20, 42.25, 40.05, 37.22, 36.48, 31.74, 31.71, 31.61, 31.30, 29.28, 24.56, 23.91, 22.34, 20.88, 19.39, 13.56; HRMS (ESI-qTOF): calcd for $C_{35}H_{52}N_5O_2$ $[M+H]^+$, 574.4122; found: 574.4116.

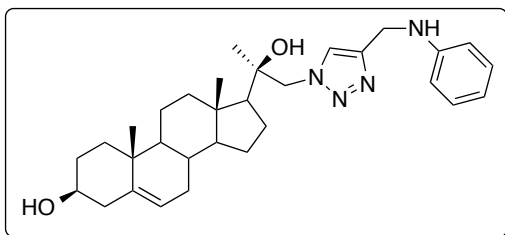
(3*S*,10*R*,13*S*)-17-((*R*)-2-hydroxy-1-(4-(morpholinomethyl)-1*H*-1,2,3-triazol-1-yl)propan-2-yl)-10,13-dimethyl-2,3,4,7,8,9,10,11,12,13,14,15,16,17-tetradecahydro-1*H*-cyclopenta[*a*]phenanthren-3-ol (31):



Cream coloured solid, M.P= 222.8 °C, S.R = -21.64 (c=0.5, $CHCl_3$); 1H NMR (400 MHz, Chloroform-*d*) δ 7.62 (s, 1H), 5.36 (m, 1H), 4.28 (m, 2H), 3.71 (m, 6H), 3.55 – 3.46 (m, 1H), 2.53 (m, 4H), 2.29-2.24 (m, 2H), 2.12– 2.09 (m, 1H), 1.96 (m, 3H), 1.85 – 1.83

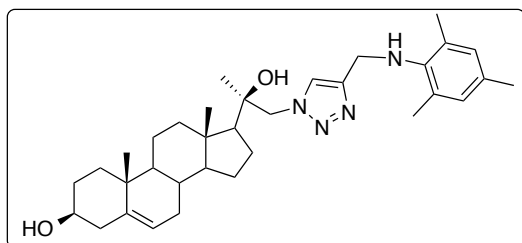
(m, 3H), 1.76-1.68 (m, 3H), 1.52 – 1.46 (m, 5H), 1.25-1.20 (m, 3H), 1.12 (s, 3H), 1.02 (s, 3H), 0.90 (s, 3H); ^{13}C NMR (101 MHz, $CDCl_3$) δ 140.7, 121.3, 74.6, 71.6, 57.3, 56.6, 49.8, 43.1, 42.2, 40.0, 37.1, 36.4, 31.6, 31.5, 31.2, 24.4, 23.8, 22.2, 20.8, 19.3, 13.5; HRMS (ESI-qTOF): calcd for $C_{29}H_{47}N_4O_3$ $[M+H]^+$, 499.3647; found: 499.3643.

(3*S*,10*R*,13*S*)-17-((*R*)-2-hydroxy-1-(4-((phenylamino)methyl)-1*H*-1,2,3-triazol-1-yl)propan-2-yl)-10,13-dimethyl-2,3,4,7,8,9,10,11,12,13,14,15,16,17-tetradecahydro-1*H*-cyclopenta[*a*]phenanthren-3-ol (32):



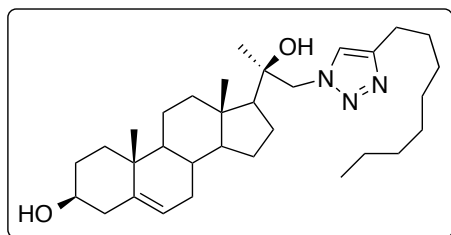
Cream coloured solid, M.P= 214.3 °C, S.R = -19.69 (c=0.7, CHCl₃); ¹H NMR (500 MHz, Chloroform-d) δ 7.56 (s, 1H), 7.18 (t, *J*= 7.63 Hz, 2H), 6.74 (t, *J*= 7.63 Hz, 1H), 6.66 (d, *J*= 8.01 Hz, 2H), 5.35 (d, *J*= 4.58 Hz, 1H), 4.46 (m, 2H), 4.28-4.21 (m, 2H), 3.53 – 3.52 (m, 1H), 2.32-2.24 (m, 2H), 2.10-2.05 (m, 2H), 2.01– 1.97 (m, 1H), 1.92-1.90 (m, 1H), 1.85 – 1.83 (m, 2H), 1.74-1.66 (m, 2H), 1.58 – 1.45 (m, 6H), 1.29-1.19 (m, 4H), 1.11 (s, 3H), 1.01 (s, 3H), 0.89 (s, 3H); ¹³C NMR (101 MHz, CDCl₃) δ 147.5, 145.7, 140.7, 129.2, 123.4, 121.3, 118.0, 113.2, 74.6, 71.6, 59.8, 57.2, 56.6, 49.8, 43.1, 42.1, 39.9, 37.1, 36.4, 31.6, 31.5, 31.2, 24.4, 23.8, 22.2, 20.8, 19.3, 13.5; HRMS (ESI-qTOF): calcd for C₃₁H₄₅N₄O₂ [M+H]⁺, 505.3546; found: 505.3537.

(3*S*,10*R*,13*S*)-17-((*R*)-2-hydroxy-1-(4-((mesitylamino)methyl)-1*H*-1,2,3-triazol-1-yl)propan-2-yl)-10,13-dimethyl-2,3,4,7,8,9,10,11,12,13,14,15,16,17-tetradecahydro-1*H*-cyclopenta[*a*]phenanthren-3-ol (33):



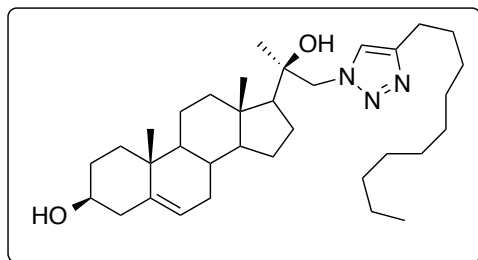
Sticky thick liquid, S.R = -19.69 (c= 0.7, CHCl₃); ¹H NMR (400 MHz, Chloroform-d) δ 7.31 (s, 1H), 6.79 (s, 2H), 5.34 (d, *J*= 4.27 Hz, 1H), 4.24-4.21 (m, 2H), 4.20-4.17 (m, 2H), 3.54 – 3.49 (m, 1H), 2.95 (s, 1H), 2.88 (s, 2H), 2.29-2.26 (m, 2H), 2.21 (s, 9H), 2.18-2.15 (m, 1H), 2.10-2.05 (m, 1H), 2.0-1.96 (m, 1H), 1.92-1.89 (m, 1H), 1.85-1.82 (m, 2H), 1.70-1.68 (m, 2H), 1.55-1.52 (m, 2H), 1.49-1.46 (m, 3H), 1.21-1.18 (m, 1H), 1.13 (m, 1H), 1.01(d, *J*= 4.27 Hz, 6H), 1.01 (s, 3H), 0.87 (s, 3H); ¹³C NMR (101 MHz, CDCl₃) δ 162.5, 145.7, 142.1, 140.7, 131.7, 130.1, 129.3, 123.3, 121.3, 74.4, 71.5, 59.7, 57.0, 56.6, 49.8, 43.2, 43.0, 42.1, 39.9, 37.1, 36.4, 31.6, 31.5, 31.5, 31.5, 31.2, 24.2, 23.8, 22.2, 20.8, 20.5, 19.3, 18.3, 13.4; HRMS (ESI-qTOF): calcd for C₃₄H₅₁N₄O₂ [M+H]⁺, 547.4014; found: 547.4007.

(3*S*,10*R*,13*S*)-17-((*R*)-2-hydroxy-1-(4-octyl-1*H*-1,2,3-triazol-1-yl)propan-2-yl)-10,13-dimethyl-2,3,4,7,8,9,10,11,12,13,14,15,16,17-tetradecahydro-1*H*-cyclopenta[*a*]phenanthren-3-ol (34):



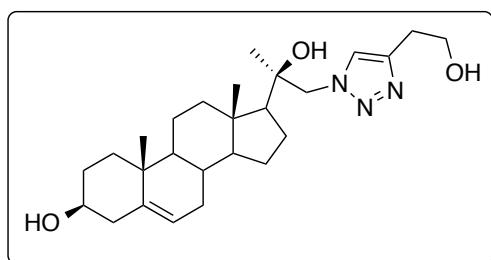
White crystalline solid, M.P = 147.8 °C, S.R = -32.36 (c= 0.5, CHCl₃); ¹H NMR (400 MHz, Chloroform-d) δ 7.38 (s, 1H), 5.36 (bs, 1H), 4.25 (m, 2H), 3.56 – 3.51 (m, 1H), 2.74-2.70 (m, 2H), 2.30-2.24 (m, 2H), 2.13-2.10(m, 1H), 2.01-1.93(m, 2H), 1.86-1.83 (m, 2H), 1.77-1.67(m, 5H), 1.53-1.47(m, 5H), 1.32-1.21(m, 14H), 1.13 (s, 3H), 1.02(s, 3H), 0.89 (m, 6H); ¹³C NMR (101 MHz, CDCl₃) δ 148.1, 140.7, 122.5, 121.4, 74.7, 71.6, 59.7, 57.3, 56.6, 49.8, 43.1, 42.2, 40.0, 37.1, 36.4, 31.8, 31.6, 31.5, 31.2, 29.4, 29.3, 29.2, 25.6, 23.8, 22.6, 22.3, 19.3, 14.0, 13.5; HRMS (ESI-qTOF): calcd for C₃₂H₅₄N₃O₂ [M+H]⁺, 512.4219; found: 512.4211.

(3S,10R,13S)-17-((R)-1-(4-decyl-1H-1,2,3-triazol-1-yl)-2-hydroxypropan-2-yl)-10,13-dimethyl-2,3,4,7,8,9,10,11,12,13,14,15,16,17-tetradecahydro-1H-cyclopenta[a]phenanthren-3-ol (35):



Cream coloured solid, M.P = 143.6 °C, S.R = -28.21 (c= 0.8, CHCl₃); ¹H NMR (500 MHz, Chloroform-d) δ 7.38 (s, 1H), 5.33 (d, J= 4.20 Hz, 1H), 4.24 (m, 2H), 3.52–3.49 (t, J= 7.63 Hz, 1H), 2.28-2.23 (m, 3H), 2.11-2.08 (m, 2H), 1.99-1.92 (m, 2H), 1.84-1.81 (m, 2H), 1.71-1.63 (m, 4H), 1.55-1.45 (m, 6H), 1.3-1.19(m, 17H), 1.11 (s, 3H), 1.0 (s, 3H), 0.87 (m, 6H); ¹³C NMR (101 MHz, CDCl₃) δ 148.0, 140.8, 122.5, 121.3, 74.6, 71.5, 59.7, 57.3, 56.6, 56.4, 49.8, 44.7, 43.1, 42.1, 39.9, 37.1, 36.4, 31.8, 31.5, 31.2, 29.5, 29.3, 29.2, 29.1, 25.5, 22.6, 22.2, 19.3, 14.0, 13.4; HRMS (ESI-qTOF): calcd for C₃₄H₅₈N₃O₂ [M+H]⁺, 540.4519; found: 512.4524.

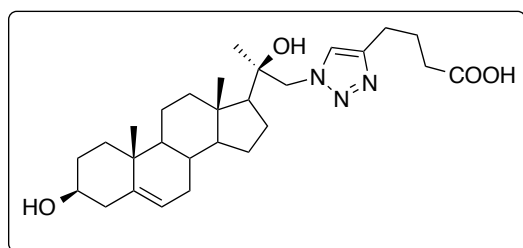
(3S,10R,13S)-17-((R)-2-hydroxy-1-(4-(2-hydroxyethyl)-1H-1,2,3-triazol-1-yl)propan-2-yl)-10,13-dimethyl-2,3,4,7,8,9,10,11,12,13,14,15,16,17-tetradecahydro-1H-cyclopenta[a]phenanthren-3-ol (36):



White solid, M. P = 212.2 °C, S.R = -31.96 (c= 0.3, MeOH), ¹H NMR (400 MHz, DMSO-d₆) δ 7.74 (s, 1H), 5.26 (d, J = 4.9 Hz, 1H), 4.66 (t, J = 5.3 Hz, 1H), 4.61 – 4.40 (m, 2H), 4.12 (m, 2H), 3.61 (td, J = 6.9, 5.1 Hz, 2H), 3.24 (m, 1H), 2.75 (t, J = 7.0 Hz, 2H), 2.17 – 2.02 (m, 2H), 2.02 – 1.83 (m, 3H), 1.76 – 1.63 (m, 3H), 1.56 (m, 2H), 1.34 (m,

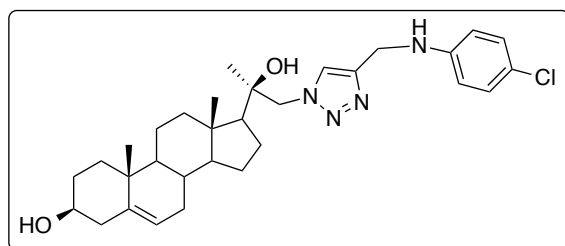
4H), 1.23 (s, 2H), 1.09 (s, 2H), 1.01 (s, 3H), 0.92 (s, 3H), 0.81 (s, 3H); ^{13}C NMR (101 MHz, DMSO) δ 144.17, 141.72, 124.12, 120.86, 73.36, 70.46, 60.92, 59.91, 56.80, 56.76, 50.01, 42.80, 42.68, 37.37, 36.53, 31.87, 31.74, 31.36, 29.64, 24.70, 24.06, 22.13, 20.93, 19.61, 13.65; HRMS (ESI-qTOF): calcd for $\text{C}_{26}\text{H}_{42}\text{N}_3\text{O}_3$ $[\text{M}+\text{H}]^+$, 444.3215; found: 444.3221.

4-(1-((2R)-2-hydroxy-2-((3S,10R,13S)-3-hydroxy-10,13-dimethyl-2,3,4,7,8,9,10,11,12,13,14,15,16,17-tetradecahydro-1H-cyclopenta[a]phenanthren-17-yl)propyl)-1H-1,2,3-triazol-4-yl)butanoic acid (37):



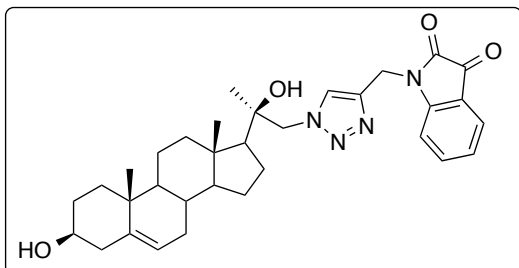
Cream coloured solid, M.P = 201.8 $^{\circ}\text{C}$, S.R = -26.96 ($c=0.4$, MeOH); ^1H NMR (400 MHz, DMSO- d_6) δ 7.75 (s, 1H), 5.27 (d, $J=4.9$ Hz, 1H), 4.13 (m, 2H), 3.23 (m, 1H), 2.63 (t, $J=7.5$ Hz, 2H), 2.25 (t, $J=7.4$ Hz, 2H), 2.09 (s, 2H), 1.99 (m, 1H), 1.91 (s, 2H), 1.81 (s, 2H), 1.68 (m, 3H), 1.55 (m, 2H), 1.48 – 1.28 (m, 6H), 1.23 (s, 1H), 1.09 (s, 2H), 1.02 (s, 3H), 0.94 (s, 3H), 0.82 (s, 3H); ^{13}C NMR (101 MHz, DMSO- d_6) δ 174.77, 146.06, 141.71, 123.66, 120.87, 73.35, 70.46, 59.97, 56.80, 56.72, 50.00, 42.79, 42.68, 37.36, 36.53, 33.45, 31.87, 31.74, 31.36, 31.16, 24.89, 24.80, 24.74, 24.06, 22.11, 20.93, 19.60, 13.63; HRMS (ESI-qTOF): calcd for $\text{C}_{28}\text{H}_{44}\text{N}_3\text{O}_4$ $[\text{M}+\text{H}]^+$, 486.3323; found: 486.3326.

(3S,10R,13S)-17-((R)-1-(4-(((4-chlorophenyl)amino)methyl)-1H-1,2,3-triazol-1-yl)-2-hydroxypropan-2-yl)-10,13-dimethyl-2,3,4,7,8,9,10,11,12,13,14,15,16,17-tetradecahydro-1H-cyclopenta[a]phenanthren-3-ol (38):



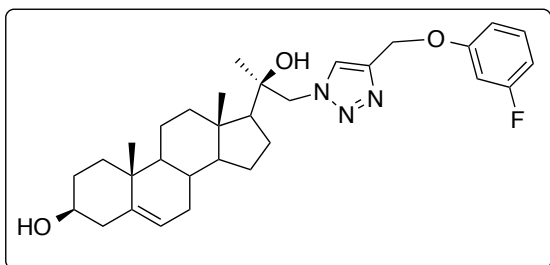
Brown solid, M.P = 217.2 $^{\circ}\text{C}$, S.R = -24.63 ($c=0.3$, CHCl_3), ^1H NMR (400 MHz, Chloroform- d) δ 7.56 (s, 1H), 7.11 (d, $J=8.6$ Hz, 2H), 6.57 (d, $J=8.4$ Hz, 2H), 5.34 (dd, $J=4.9, 2.6$ Hz, 1H), 4.47 – 4.36 (m, 2H), 4.30 – 4.19 (m, 2H), 3.58 – 3.45 (m, 1H), 2.63 (s, 1H), 2.26 (m, 2H), 2.17 (s, 1H), 2.07 (m, 2H), 2.01 – 1.93 (m, 2H), 1.92 – 1.77 (m, 4H), 1.69 (m, 3H), 1.54 – 1.42 (m, 6H), 1.18 (s, 2H), 1.10 (s, 3H), 1.00 (s, 3H), 0.88 (s, 3H); ^{13}C NMR (101 MHz, CHLOROFORM-D) δ 140.86, 129.15, 121.50, 114.46, 74.78, 71.78, 59.98, 57.37, 56.73, 53.85, 49.94, 43.25, 42.30, 40.07, 37.28, 36.55, 31.83, 31.76, 31.67, 31.35, 29.34, 24.58, 23.97, 22.39, 20.93, 19.46, 13.64; HRMS (ESI-qTOF): calcd for $\text{C}_{31}\text{H}_{44}\text{ClN}_4\text{O}_2$ $[\text{M}+\text{H}]^+$, 439.3149; found: 439.3147.

1-((1-((2R)-2-hydroxy-2-((3S,10R,13S)-3-hydroxy-10,13-dimethyl-2,3,4,7,8,9,10,11,12,13,14,15,16,17-tetradecahydro-1H-cyclopenta[a]phenanthren-17-yl)propyl)-1H-1,2,3-triazol-4-yl)methyl)indoline-2,3-dione (39):



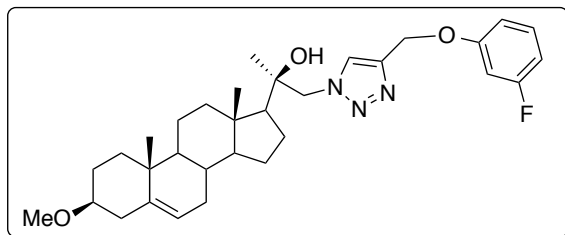
Orange solid, mp = 234.4 °C, S.R = -16.64 (c= 0.3, CHCl₃), ¹H NMR (400 MHz, Chloroform-d) δ 7.74 (s, 1H), 7.57 (t, *J* = 7.7 Hz, 2H), 7.28 (d, *J* = 1.0 Hz, 1H), 7.10 (td, *J* = 7.6, 0.8 Hz, 1H), 5.34 (dd, *J* = 4.7, 2.6 Hz, 1H), 5.09 – 4.95 (m, 2H), 4.31 – 4.16 (m, 2H), 3.58 – 3.45 (m, 1H), 2.63 (s, 1H), 2.33 – 2.20 (m, 2H), 2.17 (s, 1H), 2.10 – 1.97 (m, 2H), 1.97 – 1.89 (m, 1H), 1.88 – 1.78 (m, 3H), 1.66 (m, 5H), 1.49 (m, 6H), 1.23 – 1.12 (m, 2H), 1.09 (s, 3H), 1.00 (s, 3H), 0.87 (s, 3H); ¹³C NMR (101 MHz, CDCl₃) δ 210.84, 183.10, 157.94, 150.29, 141.35, 140.79, 138.58, 125.32, 124.77, 124.00, 121.40, 117.56, 111.50, 74.60, 71.71, 59.98, 57.31, 56.66, 53.80, 49.89, 43.19, 42.24, 40.00, 37.21, 36.47, 35.53, 31.74, 31.68, 31.60, 31.27, 29.27, 24.52, 23.87, 22.29, 20.86, 19.38, 13.55; HRMS (ESI-qTOF): calcd for C₃₃H₄₃N₄O₄ [M+H]⁺, 559.3273; found: 559.3279.

(3S,10R,13S)-17-((R)-1-(4-((3-fluorophenoxy)methyl)-1H-1,2,3-triazol-1-yl)-2-hydroxypropan-2-yl)-10,13-dimethyl-2,3,4,7,8,9,10,11,12,13,14,15,16,17-tetradecahydro-1H-cyclopenta[a]phenanthren-3-ol (40):



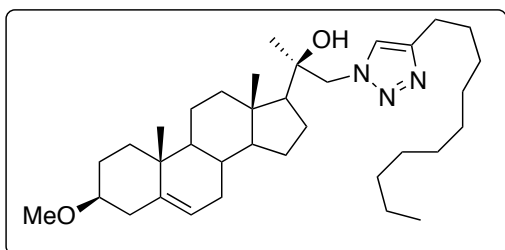
Cream coloured solid, M.P = 174.4 °C, S.R = -25.96 (c= 0.6, CHCl₃), ¹H NMR (400 MHz, Chloroform-d) δ 7.74 (s, 1H), 7.21 (td, *J* = 8.3, 6.8 Hz, 1H), 6.75 (dd, *J* = 8.3, 2.4 Hz, 1H), 6.72 – 6.62 (m, 2H), 5.33 (dd, *J* = 4.7, 2.6 Hz, 1H), 5.17 (s, 2H), 4.28 (q, *J* = 13.8 Hz, 2H), 3.51 (m, 1H), 2.28 (m, 2H), 2.16 (m, 1H), 2.06 (m, 3H), 1.96 – 1.88 (m, 2H), 1.82 (m, 4H), 1.71 (m, 3H), 1.51 (s, 5H), 1.19 (m, 2H), 1.12 (s, 3H), 1.03 (s, 1H), 0.99 (s, 3H), 0.88 (s, 3H); ¹³C NMR (101 MHz, CDCl₃) δ 164.76, 162.32, 159.58, 159.47, 143.28, 140.81, 130.34, 130.24, 124.68, 121.39, 110.49, 110.46, 108.20, 107.98, 102.88, 102.63, 74.67, 71.66, 69.57, 62.29, 59.95, 57.33, 56.66, 53.80, 53.80, 49.88, 43.18, 42.22, 40.00, 37.22, 36.47, 31.74, 31.69, 31.58, 31.28, 29.27, 24.47, 23.90, 22.33, 20.86, 19.38, 13.56; MS (LCMS) *m/z*: 524 (M⁺).

(2R)-1-(4-((3-fluorophenoxy)methyl)-1H-1,2,3-triazol-1-yl)-2-((3S,10R,13S)-3-methoxy-10,13-dimethyl-2,3,4,7,8,9,10,11,12,13,14,15,16,17-tetradecahydro-1H-cyclopenta[a]phenanthren-17-yl)propan-2-ol (41):



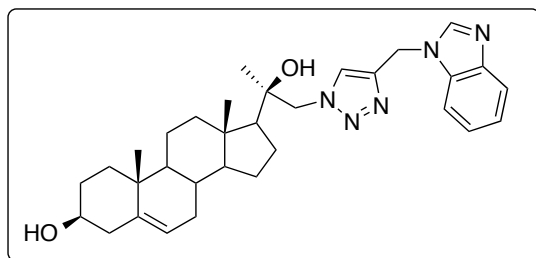
White solid, M.P = 154.6 °C, sr = -40.61 (c= 0.3, CHCl₃), ¹H NMR (400 MHz, Chloroform-d) δ 7.73 (s, 1H), 7.22 (td, *J* = 8.3, 6.8 Hz, 1H), 6.77 (dd, *J* = 8.2, 2.4 Hz, 1H), 6.73 – 6.62 (m, 2H), 5.36 (dt, *J* = 4.2, 1.8 Hz, 1H), 5.20 (s, 2H), 4.37 – 4.21 (m, 2H), 3.35 (s, 3H), 3.11 – 3.00 (m, 1H), 2.39 (m, 1H), 2.17 (s, 2H), 1.83 (m, 5H), 1.64 (m, 4H), 1.52 (m, 6H), 1.23 (m, 1H), 1.14 (s, 3H), 1.00 (s, 3H), 0.89 (s, 3H); ¹³C NMR (101 MHz, CDCl₃) δ 164.91, 162.47, 159.73, 159.62, 143.50, 141.05, 130.47, 130.37, 124.74, 121.44, 110.63, 110.60, 108.33, 108.12, 103.03, 102.79, 80.41, 74.86, 62.47, 60.04, 57.45, 56.82, 55.76, 50.09, 43.34, 40.15, 38.80, 37.28, 37.00, 31.87, 31.42, 29.41, 28.10, 24.69, 24.04, 22.47, 20.99, 19.50, 13.72; MS (LCMS) *m/z*: 538 M⁺).

(2R)-1-(4-decyl-1H-1,2,3-triazol-1-yl)-2-((3S,10R,13S)-3-methoxy-10,13-dimethyl-2,3,4,7,8,9,10,11,12,13,14,15,16,17-tetradecahydro-1H-cyclopenta[a]phenanthren-17-yl)propan-2-ol (42):



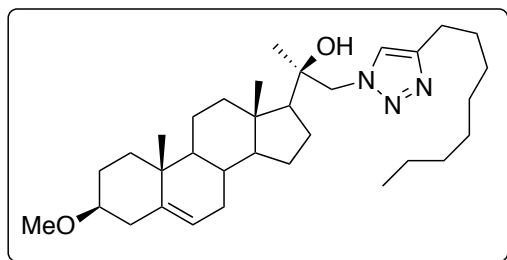
White coloured solid, M.P = 143 °C, S.R = -33.96 (c = 0.4, CHCl₃), ¹H NMR (400 MHz, Chloroform-d) δ 7.36 (s, 1H), 5.36 (d, *J* = 5.2 Hz, 1H), 4.24 (s, 2H), 3.35 (s, 3H), 3.06 (dd, *J* = 15.7, 6.8 Hz, 1H), 2.75 – 2.64 (m, 2H), 2.39 (ddd, *J* = 13.2, 4.7, 2.3 Hz, 1H), 2.20 – 2.06 (m, 2H), 2.03 – 1.81 (m, 5H), 1.78 – 1.59 (m, 6H), 1.49 (m, 6H), 1.31 (m, 6H), 1.25 – 1.17 (m, 7H), 1.12 (s, 3H), 1.08 – 1.01 (m, 2H), 1.00 (m, 4H), 0.88 (m, 6H); ¹³C NMR (101 MHz, CDCl₃) δ 148.28, 141.05, 122.63, 121.48, 80.42, 74.91, 59.91, 57.49, 56.85, 55.76, 50.13, 43.33, 40.19, 38.81, 37.29, 37.01, 32.06, 31.89, 31.44, 29.75, 29.72, 29.58, 29.53, 29.48, 29.38, 28.12, 25.80, 24.73, 24.06, 22.83, 22.48, 21.02, 19.50, 14.26, 13.69; MS (LCMS) *m/z*: 554 (M⁺).

(3S,10R,13S)-17-((R)-1-(4-((1H-benzo[d]imidazol-1-yl)methyl)-1H-1,2,3-triazol-1-yl)-2-hydroxypropan-2-yl)-10,13-dimethyl-2,3,4,7,8,9,10,11,12,13,14,15,16,17-tetradecahydro-1H-cyclopenta[a]phenanthren-3-ol (43):



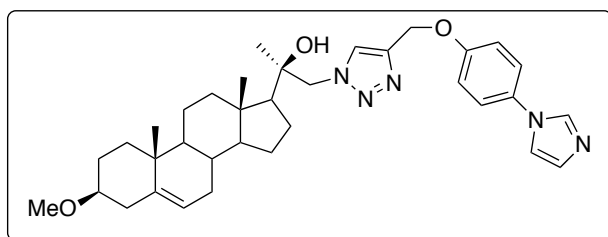
White coloured solid, M.P = >250 °C; ^1H NMR (400 MHz, DMSO- d_6) δ 8.30 (s, 1H), 8.03 (s, 1H), 7.62 (ddd, J = 8.7, 7.1, 1.7 Hz, 2H), 7.19 (m, 2H), 5.55 (s, 2H), 5.25 (d, J = 4.9 Hz, 1H), 4.60 (s, 1H), 4.47 (s, 1H), 4.28 – 4.00 (m, 2H), 2.18 – 1.99 (m, 2H), 1.98 – 1.78 (m, 3H), 1.77 – 1.55 (m, 3H), 1.54 – 1.43 (m, 2H), 1.41 – 1.22 (m, 5H), 1.18 – 1.00 (m, 3H), 0.97 (s, 3H), 0.92 (s, 3H), 0.78 (s, 3H); ^{13}C NMR (101 MHz, DMSO) δ 143.92, 143.49, 141.89, 141.26, 124.90, 122.31, 121.56, 120.39, 119.41, 110.73, 72.79, 70.00, 59.61, 56.30, 56.26, 49.54, 42.31, 42.22, 36.06, 31.42, 31.27, 30.88, 24.18, 21.62, 20.46, 19.14, 13.14; MS (LCMS) m/z : 530 (M^+).

(2R)-2-((3S,10R,13S)-3-methoxy-10,13-dimethyl-2,3,4,7,8,9,10,11,12,13,14,15,16,17-tetradecahydro-1H-cyclopenta[a]phenanthren-17-yl)-1-(4-octyl-1H-1,2,3-triazol-1-yl)propan-2-ol (44):



White coloured solid, M.P = 156.1 °C, S.R = -40.45 (c = 0.4, CHCl_3), ^1H NMR (400 MHz, Chloroform- d) δ 7.37 (s, 1H), 5.35 (d, J = 5.1 Hz, 1H), 4.24 (s, 2H), 3.35 (s, 3H), 3.06 (m, 1H), 2.70 (t, J = 7.7 Hz, 2H), 2.39 (ddd, J = 12.9, 4.8, 2.2 Hz, 1H), 2.14 (m, 2H), 2.03 – 1.82 (m, 5H), 1.75 – 1.63 (m, 6H), 1.58 – 1.40 (m, 6H), 1.31 (m, 10H), 1.12 (m, 3H), 1.05 (m, 1H), 1.00 (s, 3H), 0.88 (m, 6H); ^{13}C NMR (101 MHz, Chloroform- d) δ 148.27, 141.03, 122.64, 121.48, 80.41, 74.89, 59.89, 57.46, 56.83, 55.76, 50.11, 43.32, 40.16, 38.79, 37.27, 37.00, 31.99, 31.88, 31.42, 29.57, 29.48, 29.38, 28.10, 25.79, 24.71, 24.05, 22.81, 22.46, 21.00, 19.50, 14.26, 13.69; MS (LCMS) m/z : 526 (M^+).

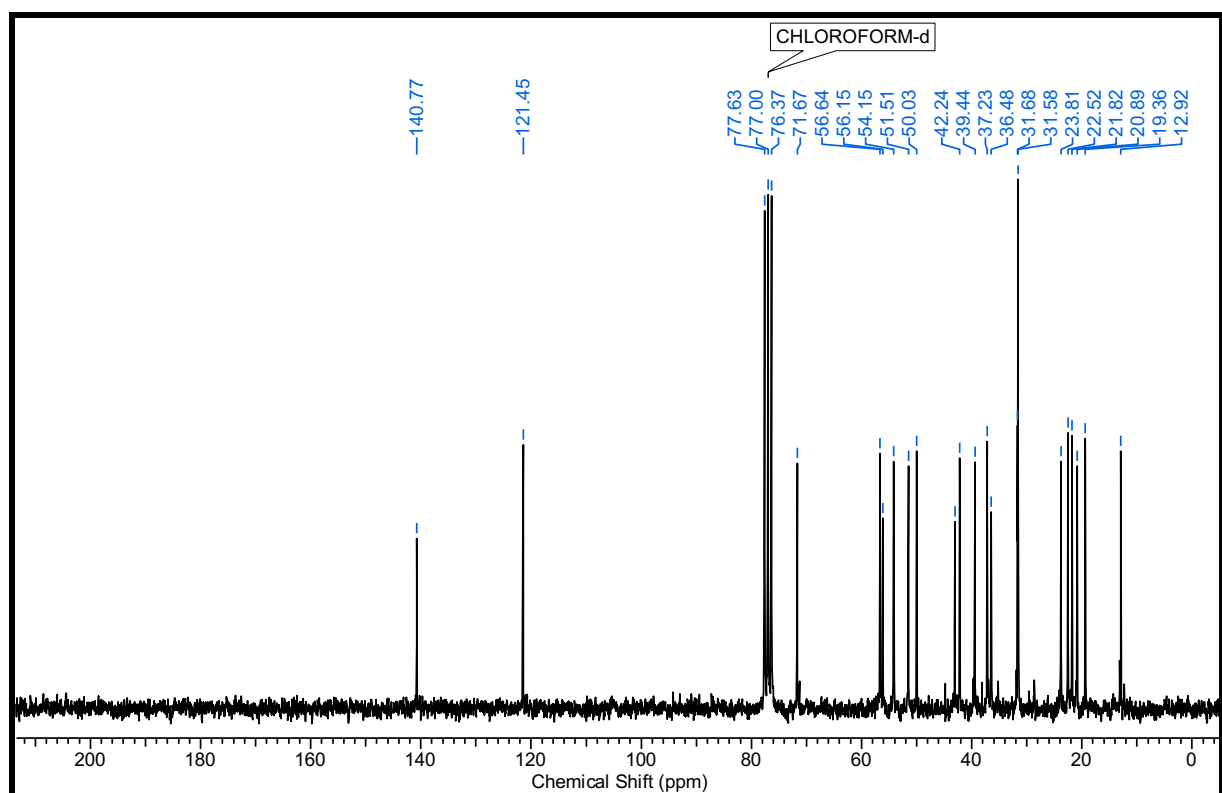
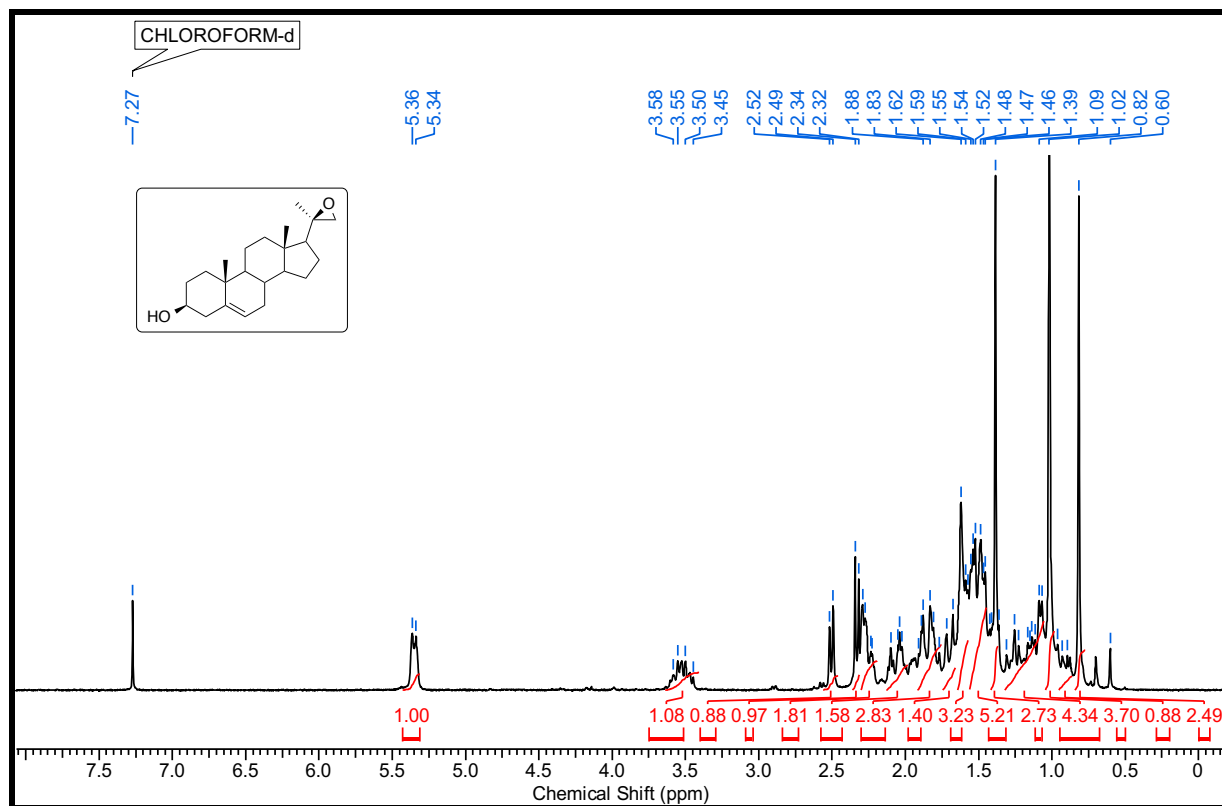
(2R)-1-(4-((4-(1H-imidazol-1-yl)phenoxy)methyl)-1H-1,2,3-triazol-1-yl)-2-((3S,10R,13S)-3-methoxy-10,13-dimethyl-2,3,4,7,8,9,10,11,12,13,14,15,16,17-tetradecahydro-1H-cyclopenta[a]phenanthren-17-yl)propan-2-ol (45):

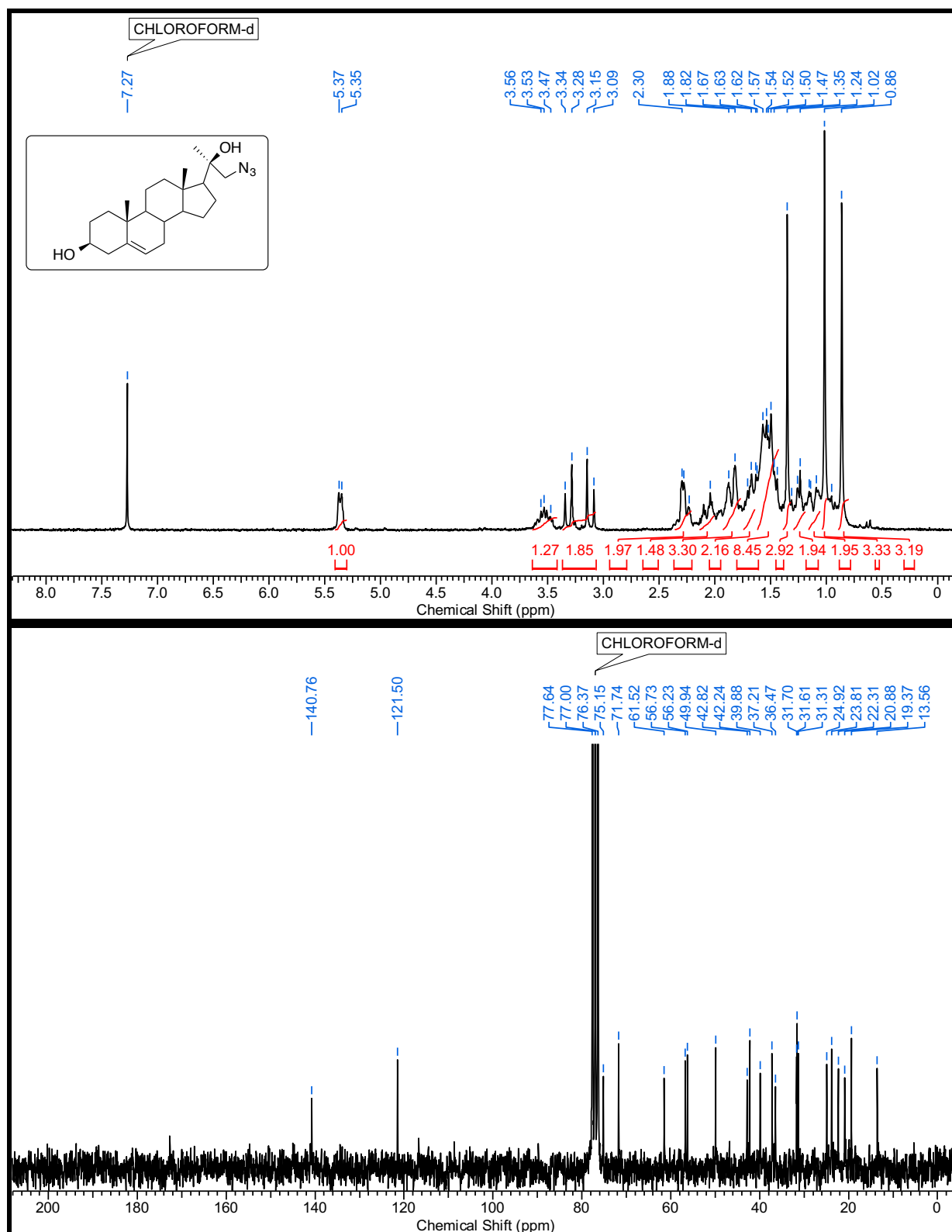


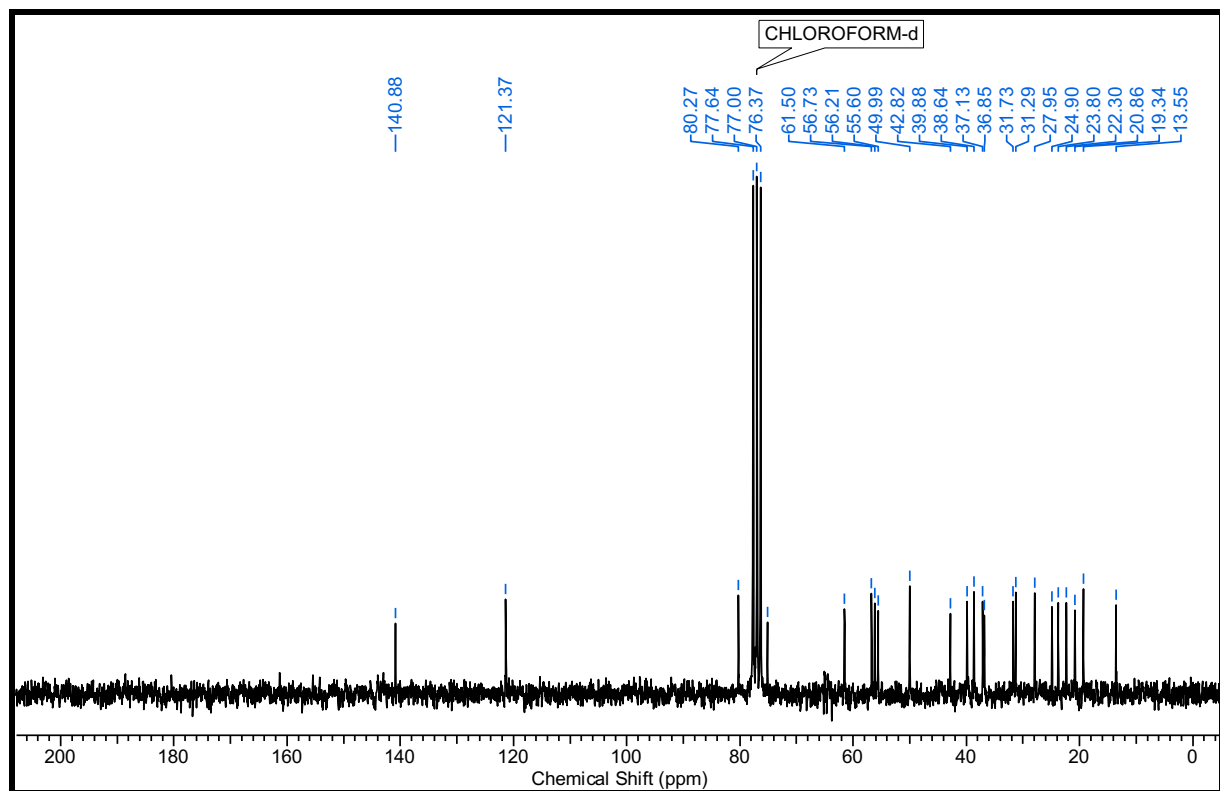
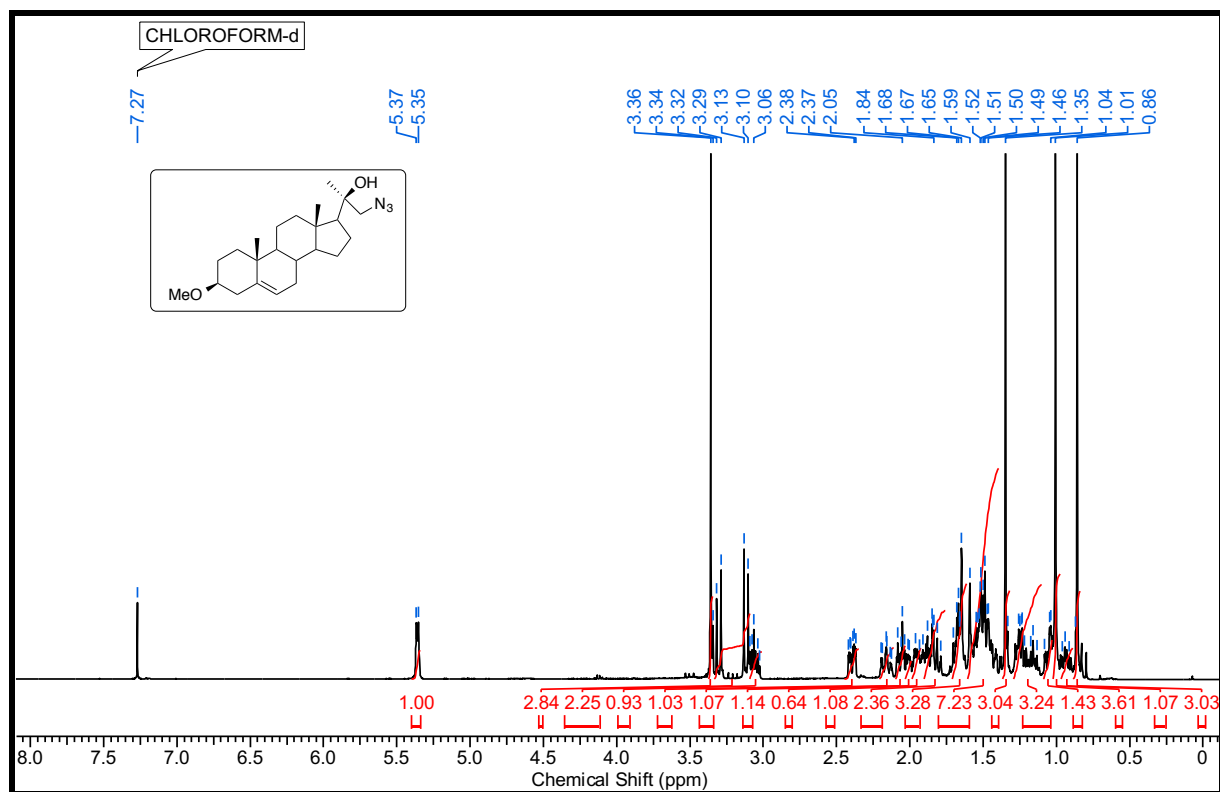
Cream coloured solid, M.P = 216.3 °C, S.R = -31.62 (c = 0.6, CHCl_3), ^1H NMR (400 MHz, Chloroform- d) δ 7.77 (s, 2H), 7.29 (d, J = 8.8 Hz, 2H), 7.07 (d, J = 8.8 Hz, 2H), 5.35 (d, J = 5.0 Hz, 1H), 5.24 (s, 2H), 4.30 (q, J = 13.8 Hz, 2H), 3.35 (s, 3H), 3.12 – 3.00 (m, 1H), 2.63 (s, 1H), 2.39 (ddd, J = 13.0, 4.7,

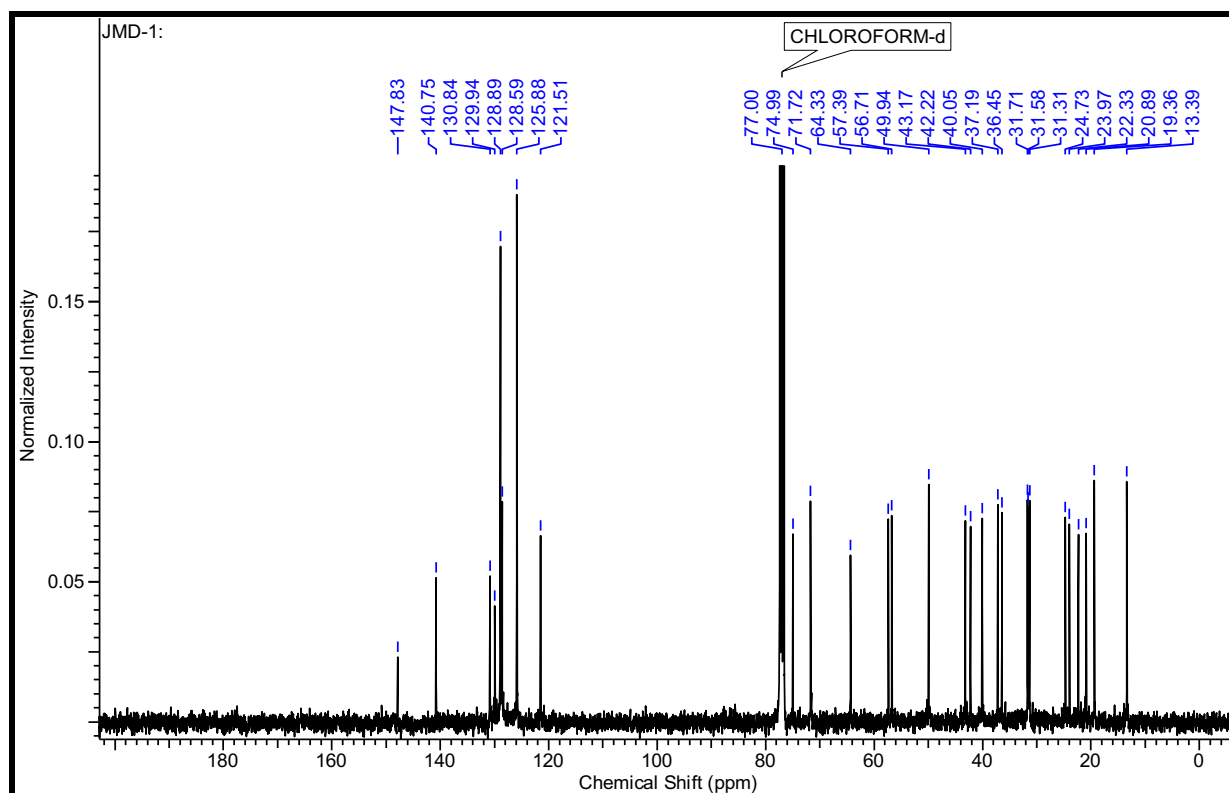
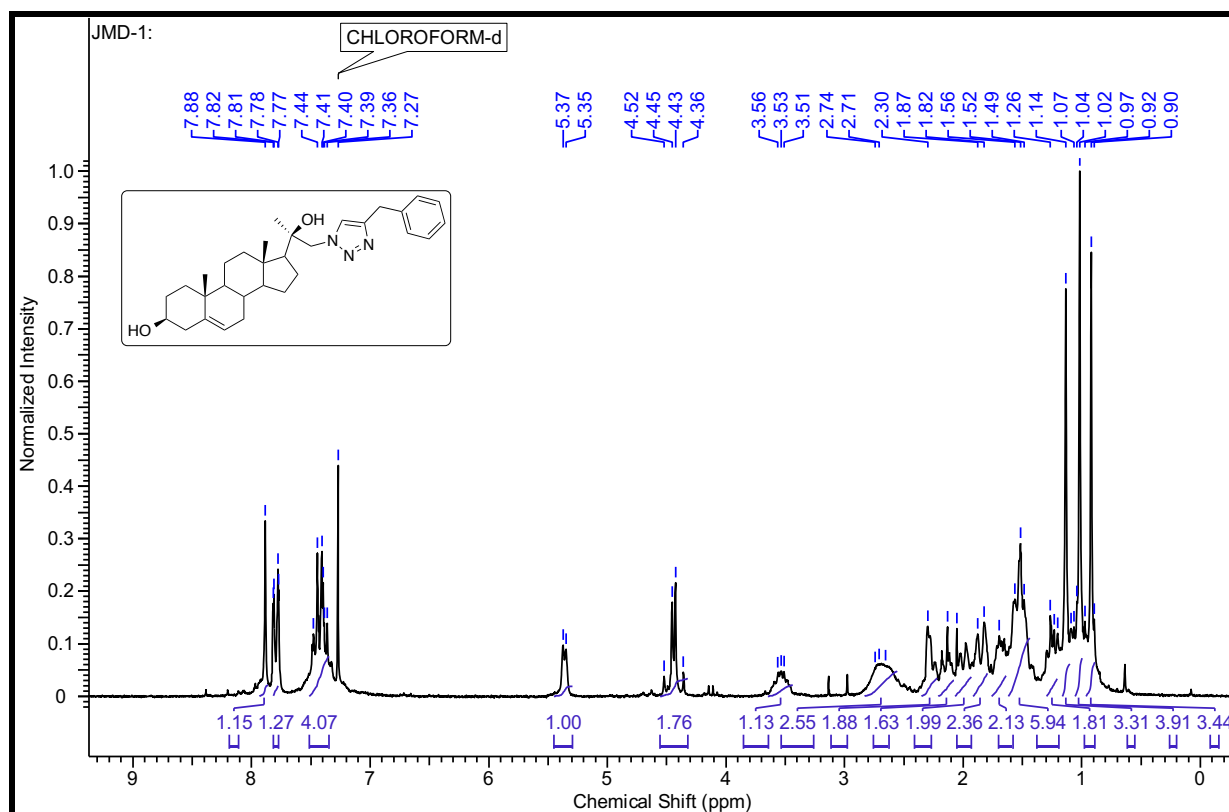
2.1 Hz, 1H), 2.17 (s, 4H), 2.00 – 1.83 (m, 5H), 1.77 – 1.64 (m, 3H), 1.56 – 1.37 (m, 6H), 1.20 (m, 1H), 1.14 (s, 3H), 1.00 (s, 3H), 0.90 (s, 3H); ¹³C NMR (101 MHz, CDCl₃) δ 157.70, 143.41, 141.06, 124.83, 123.34, 121.42, 116.09, 80.40, 74.84, 69.65, 62.56, 60.10, 57.53, 56.84, 55.76, 53.95, 50.11, 43.37, 40.18, 38.80, 37.28, 37.00, 31.88, 31.43, 29.42, 28.10, 24.64, 24.05, 22.49, 21.00, 19.50, 13.73; MS (LCMS) *m/z*: 586 (M⁺¹).

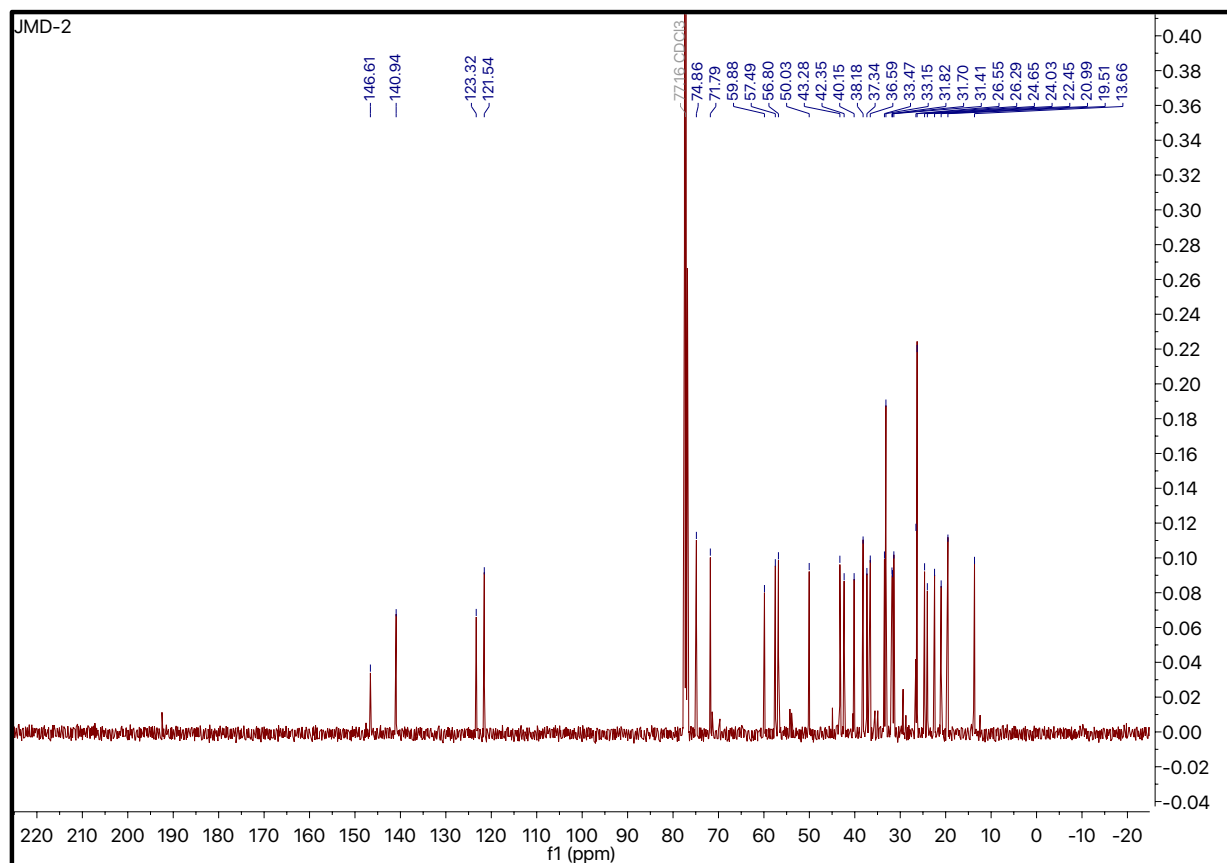
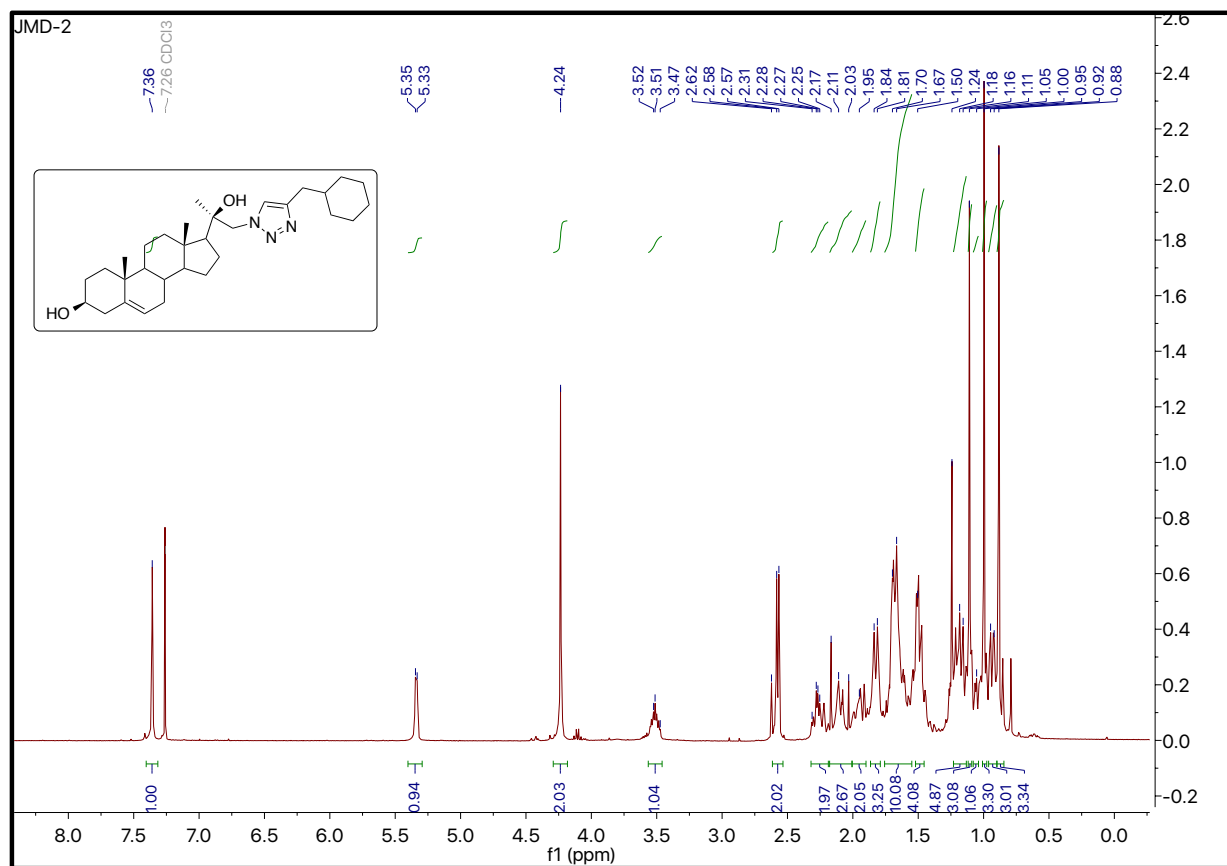
4.7 NMR Spectras

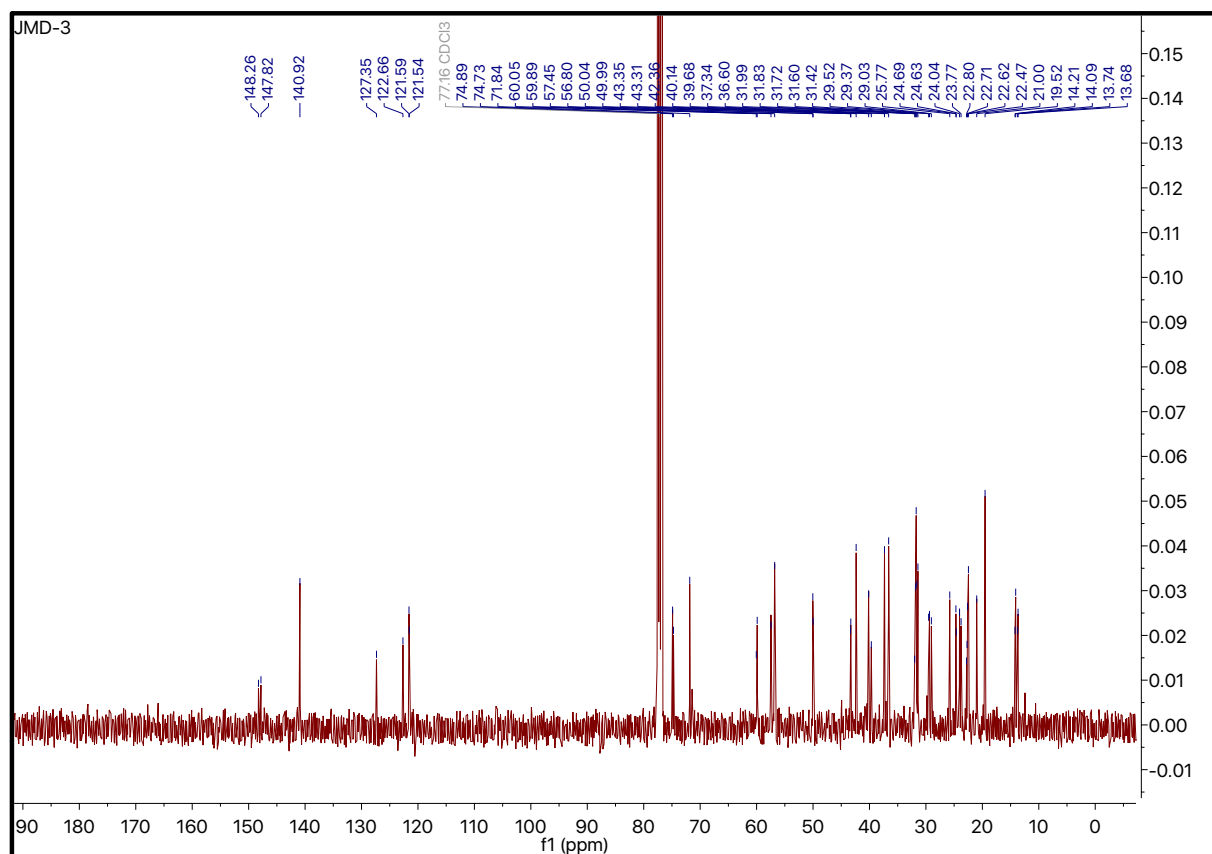
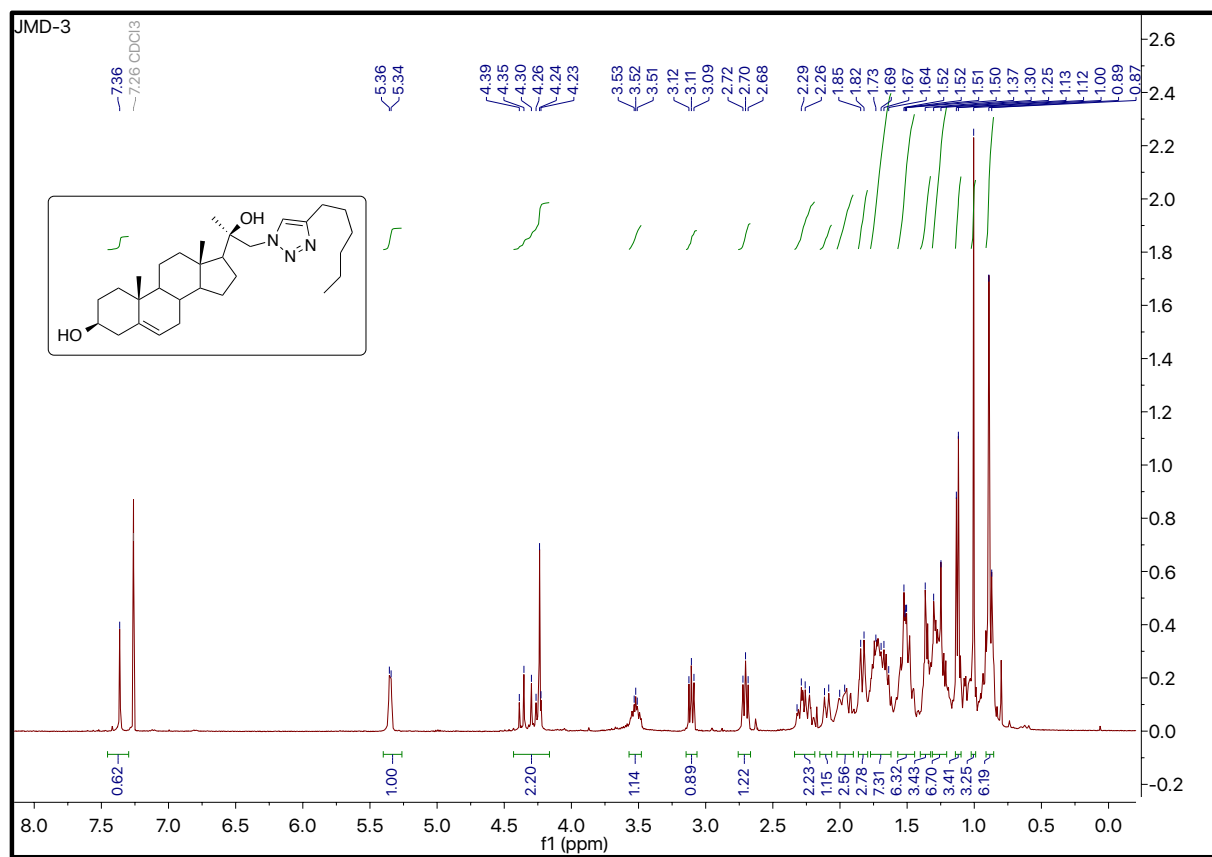
 ^1H and ^{13}C NMR Spectra of 20 (200MHz, 50MHz; CDCl_3)

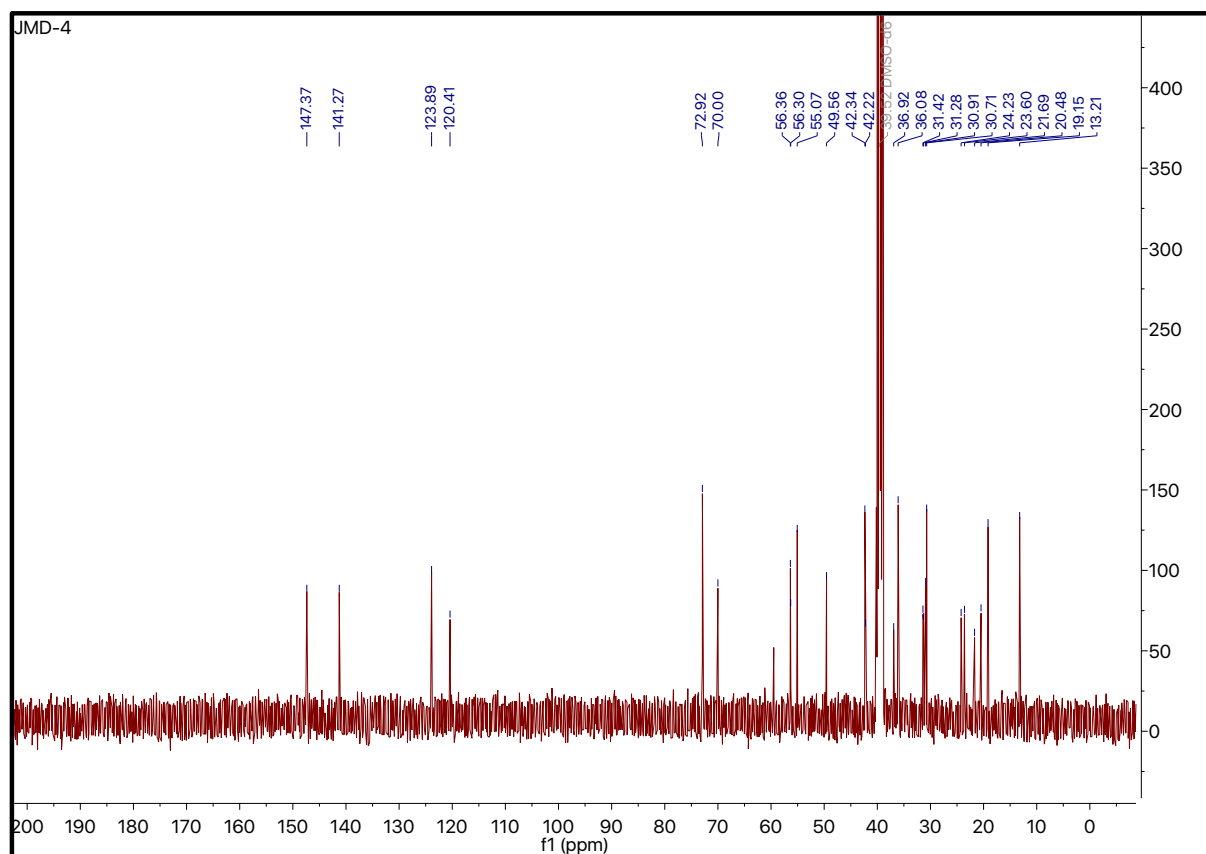
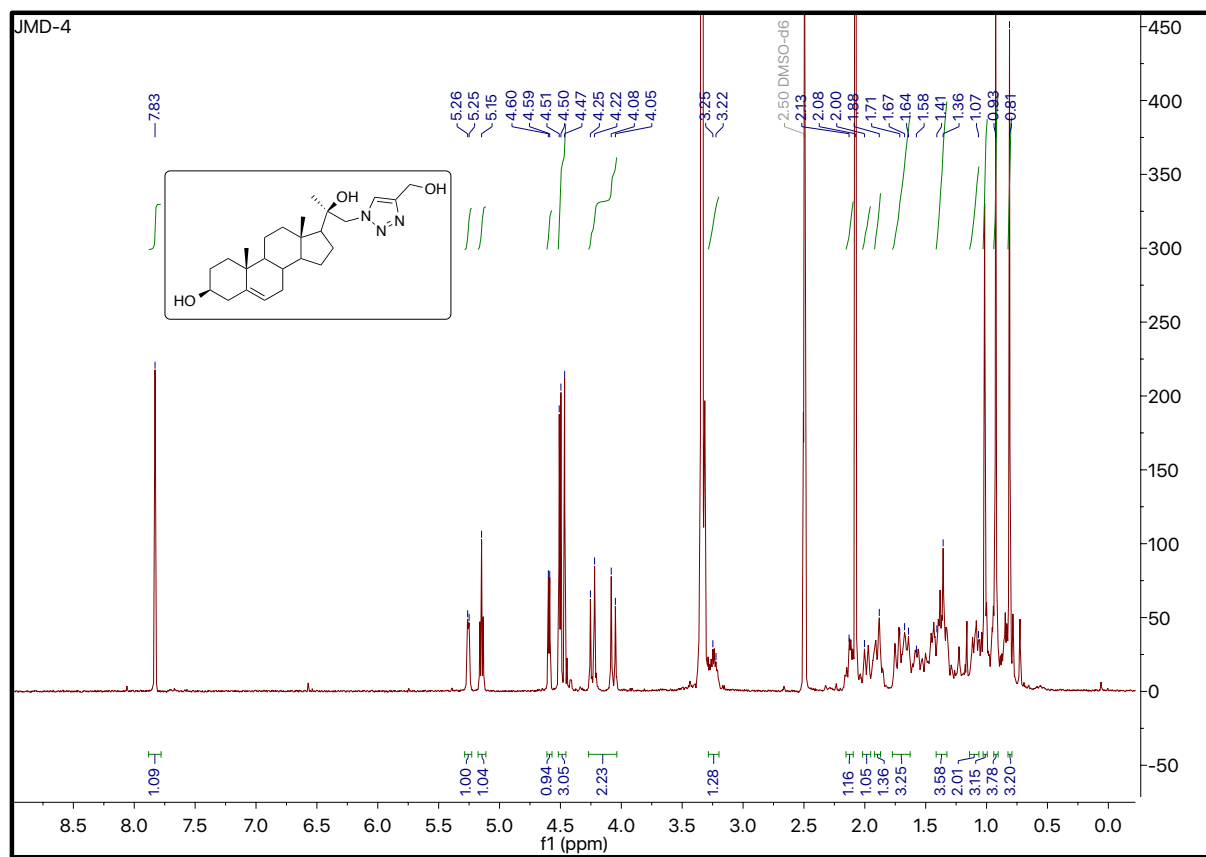
^1H and ^{13}C NMR Spectra of 23 (200 MHz, 50 MHz; CDCl_3)

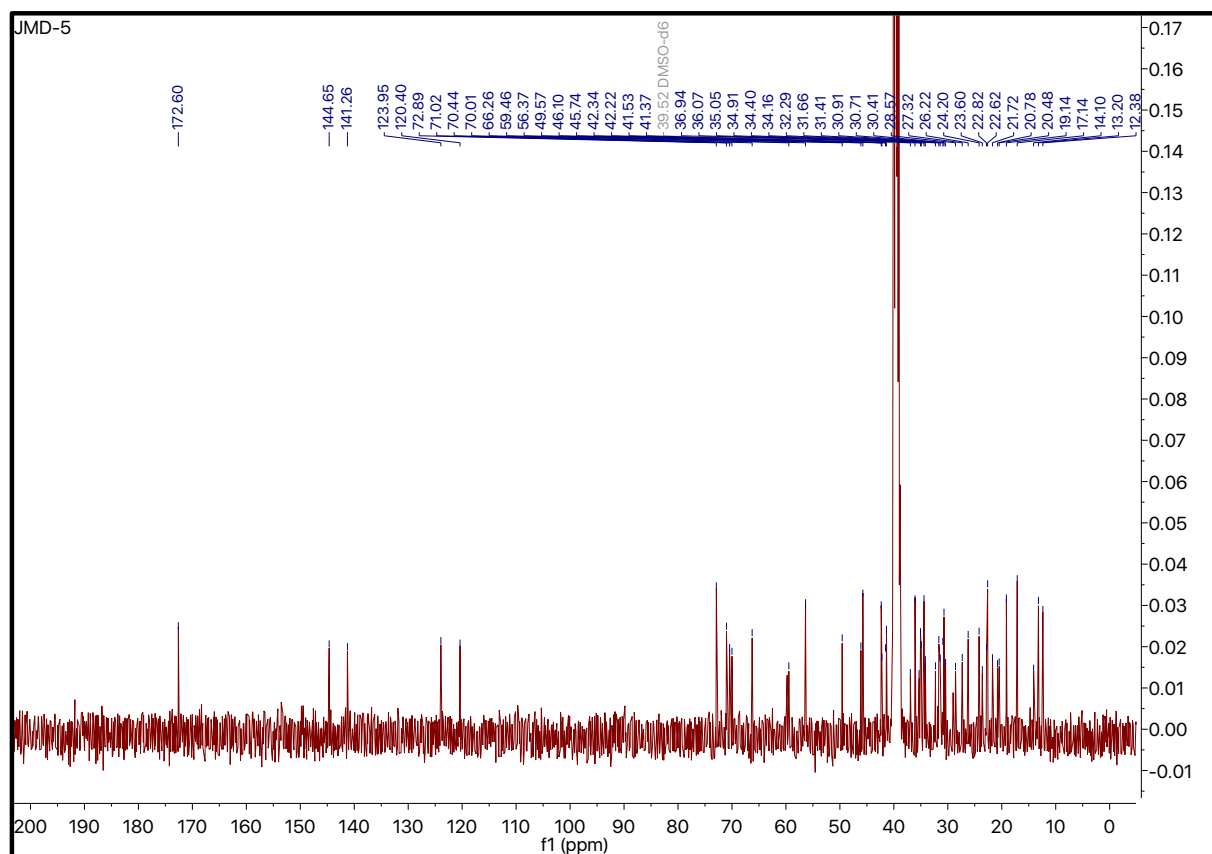
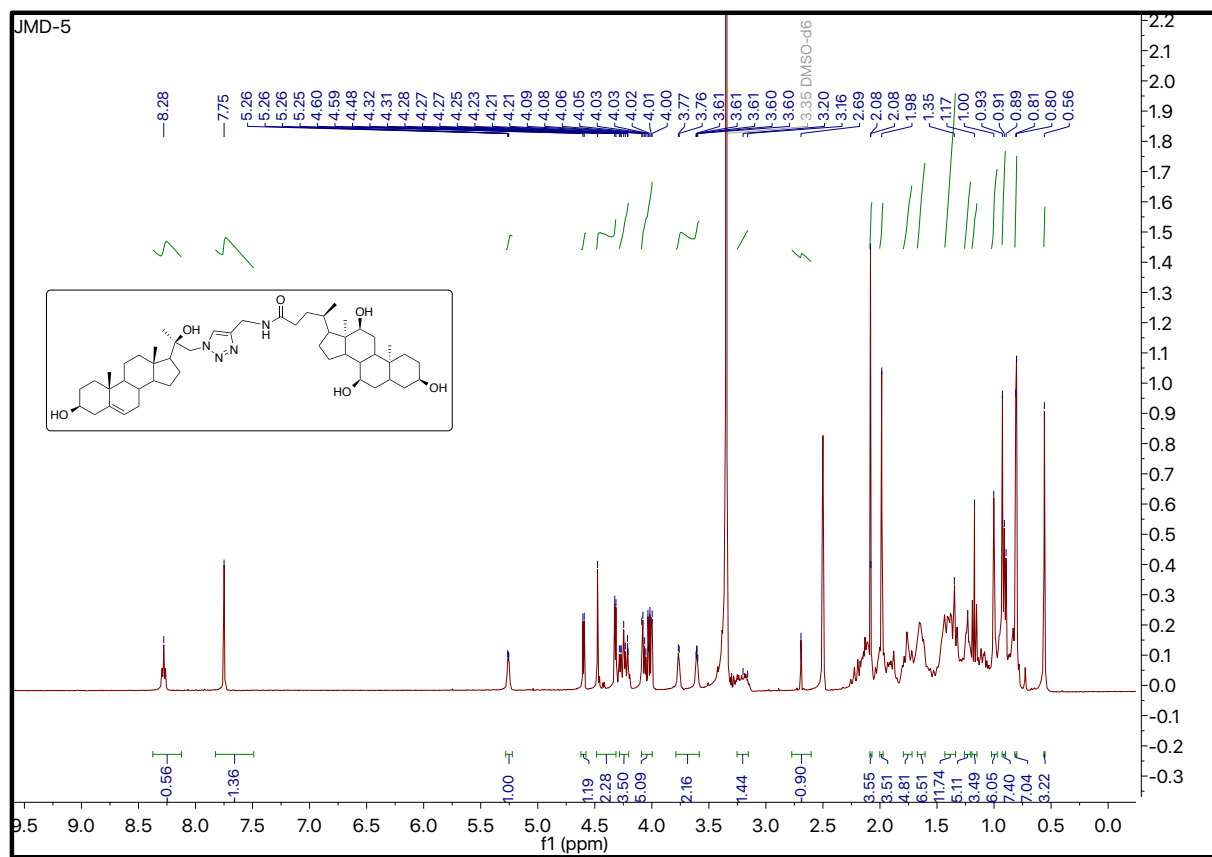
^1H and ^{13}C NMR Spectra of 24 (400MHz, 50MHz; CDCl_3)

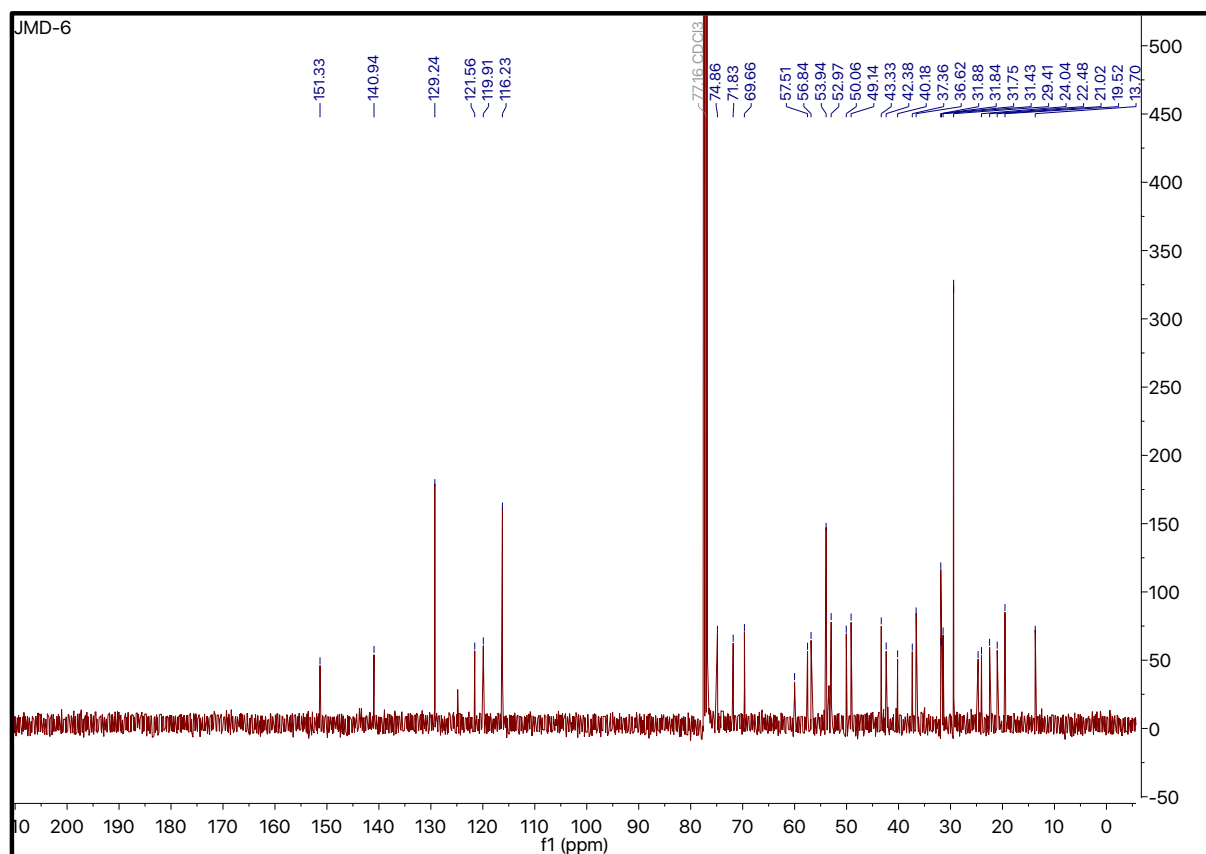
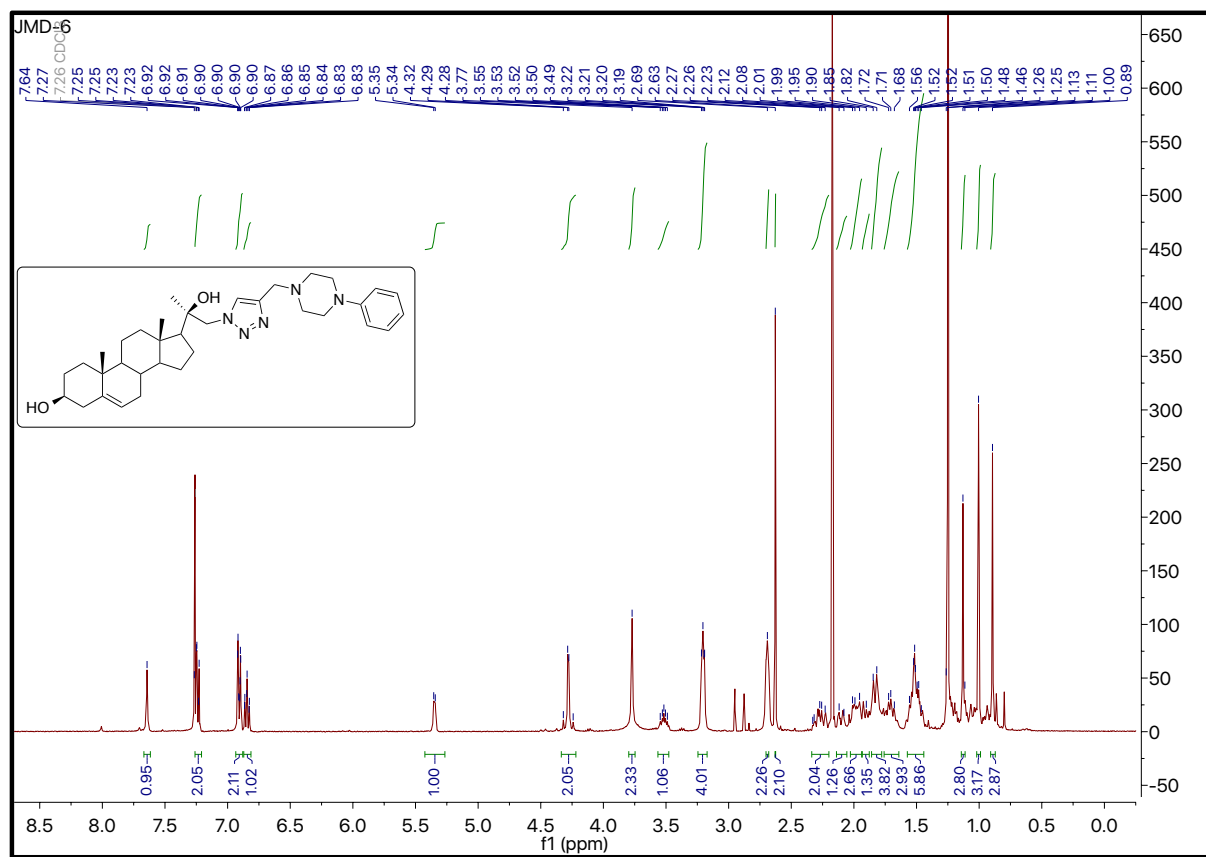
^1H and ^{13}C NMR Spectra of 25 (200MHz, 101MHz; CDCl_3)

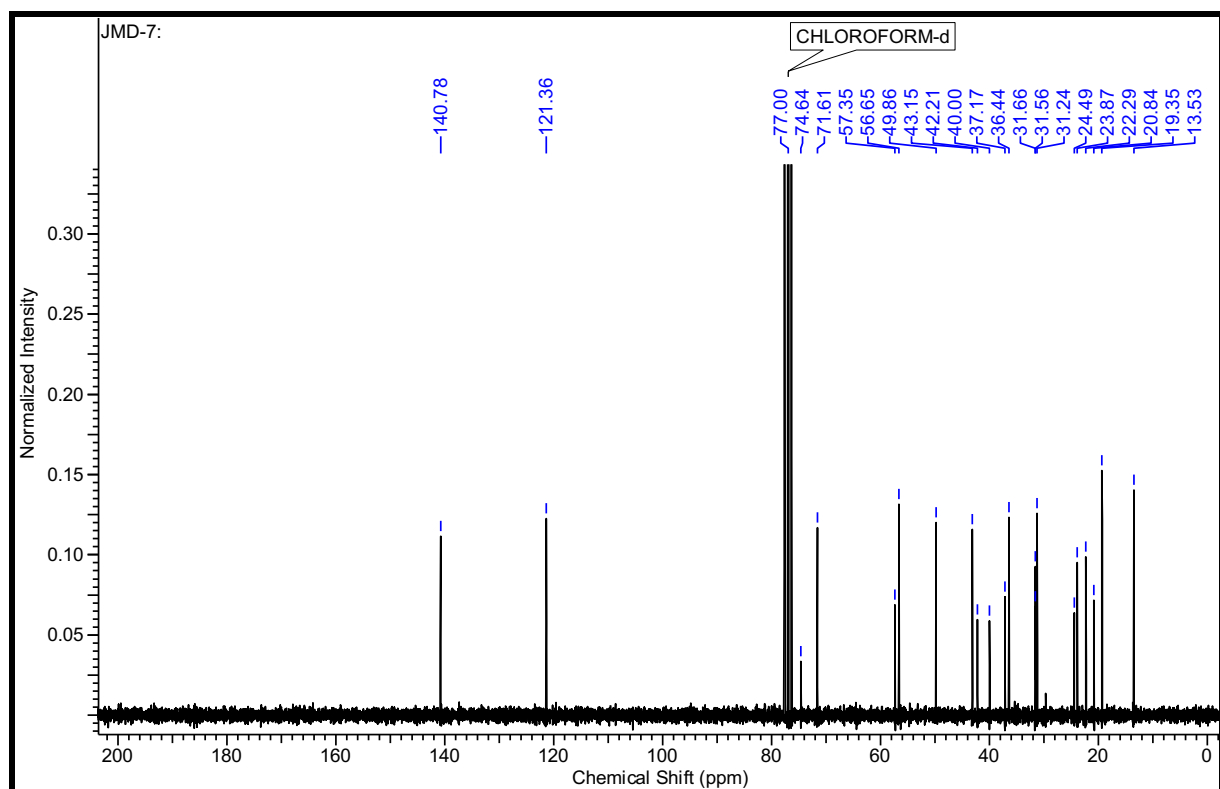
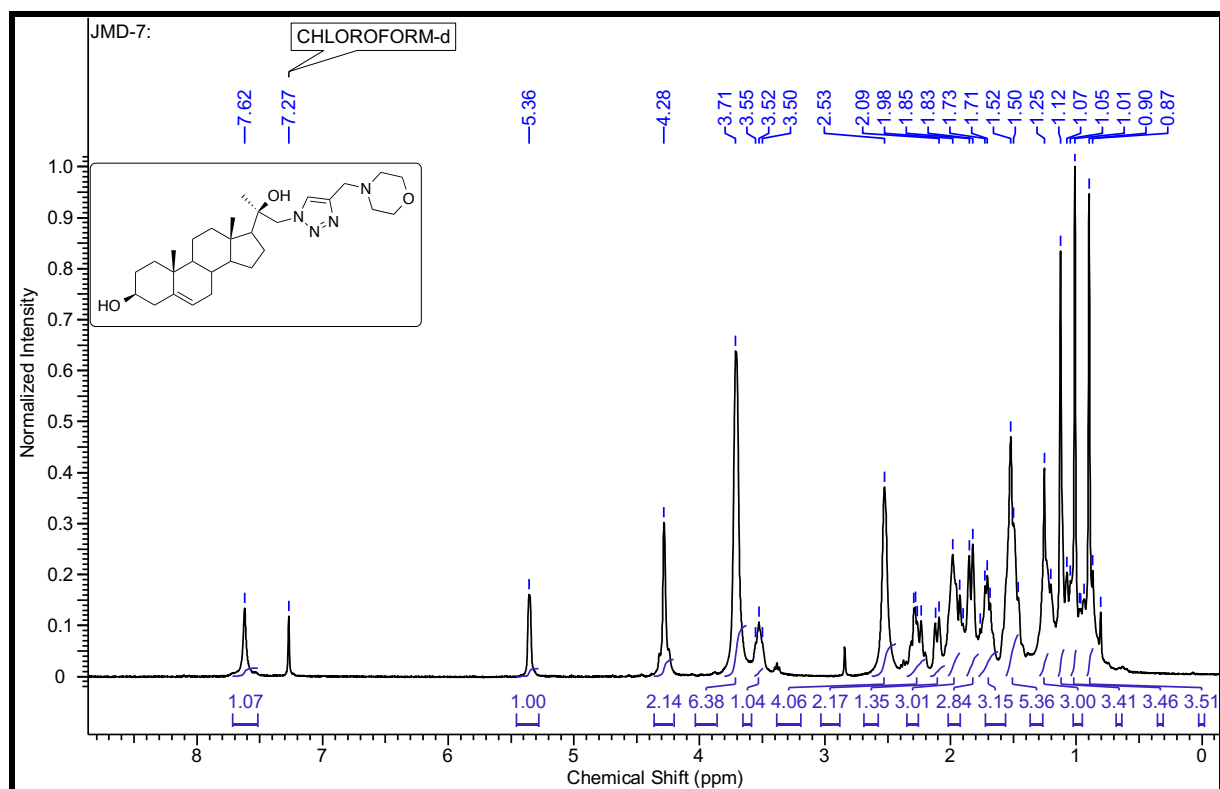
^1H and ^{13}C NMR Spectra of 26 (400MHz, 101MHz; CDCl_3)

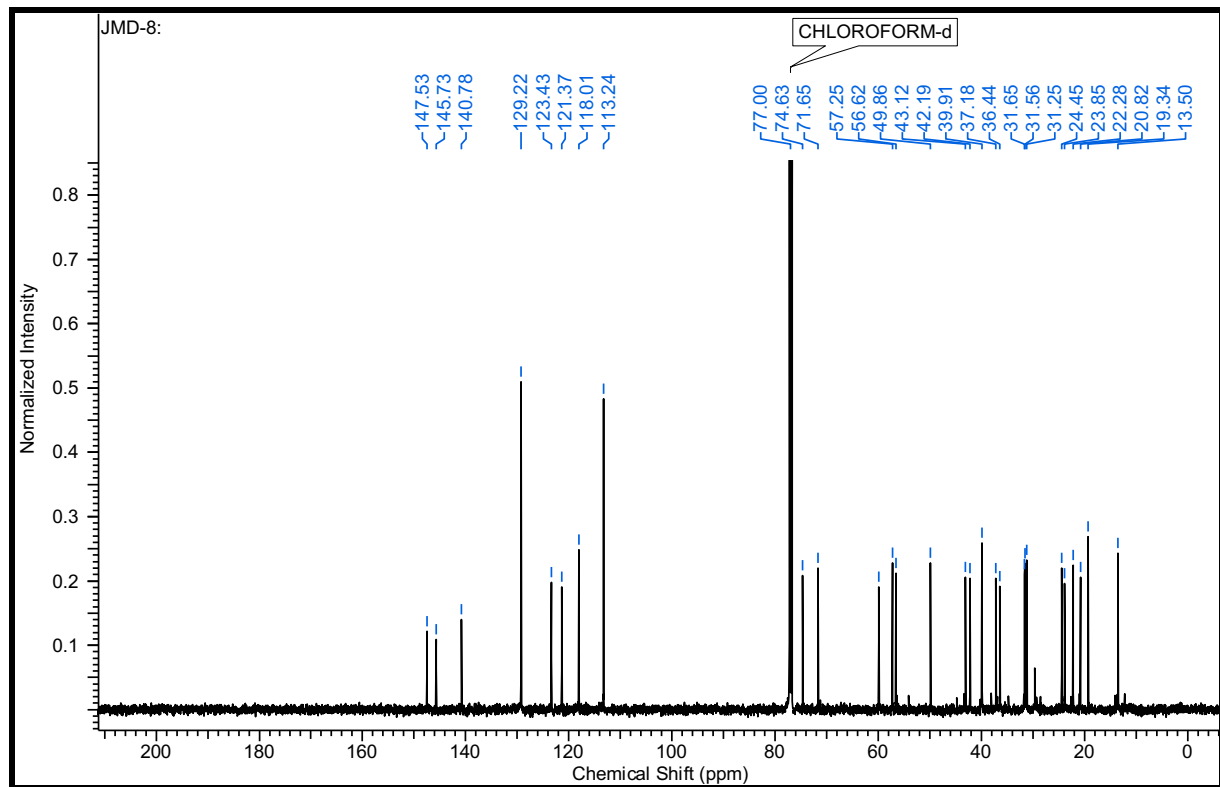
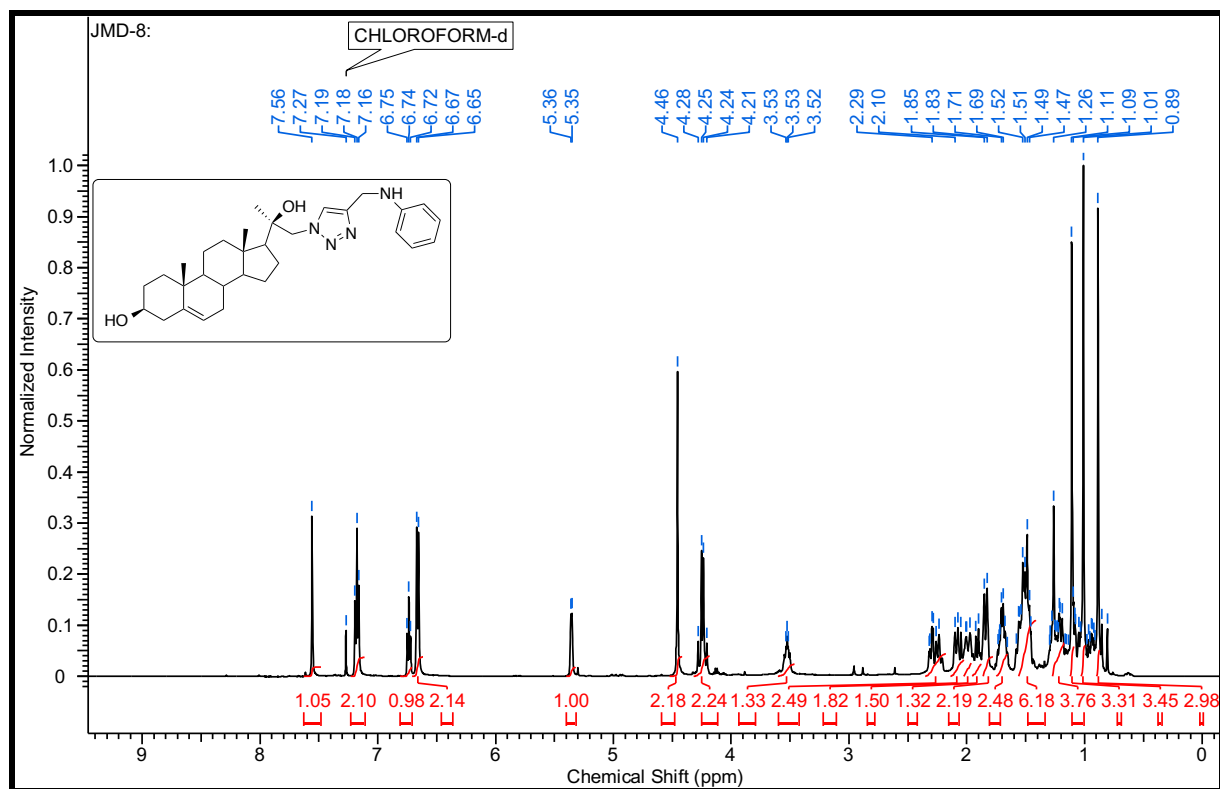
^1H and ^{13}C NMR Spectra of 27 (400MHz, 101MHz; CDCl_3)

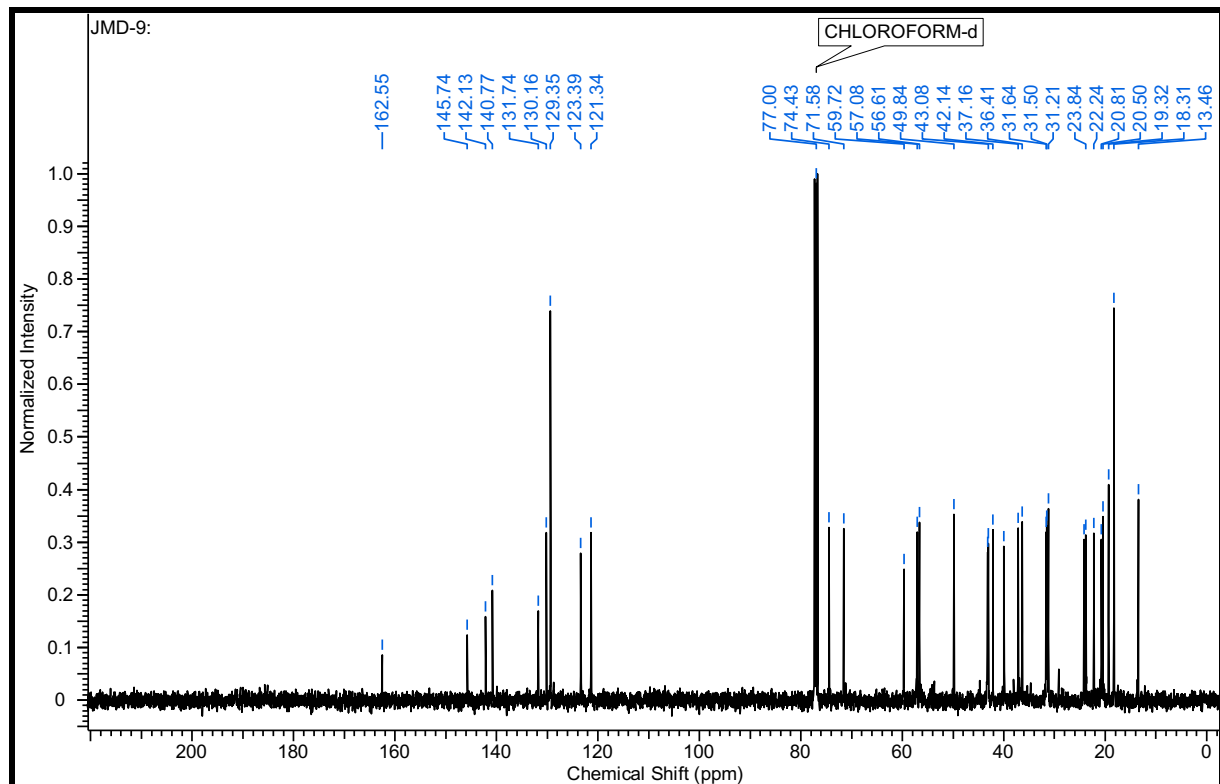
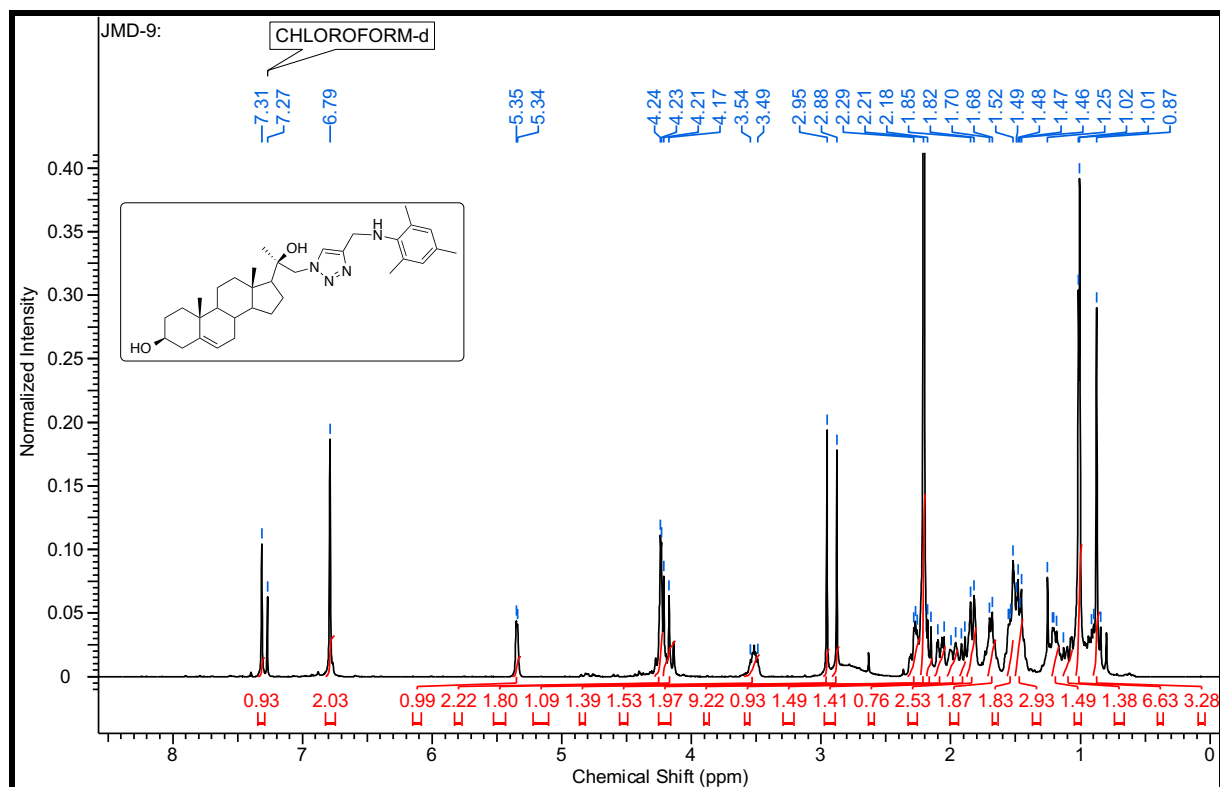
^1H and ^{13}C NMR Spectra of 28 (400MHz, 101MHz; DMSO- d_6)

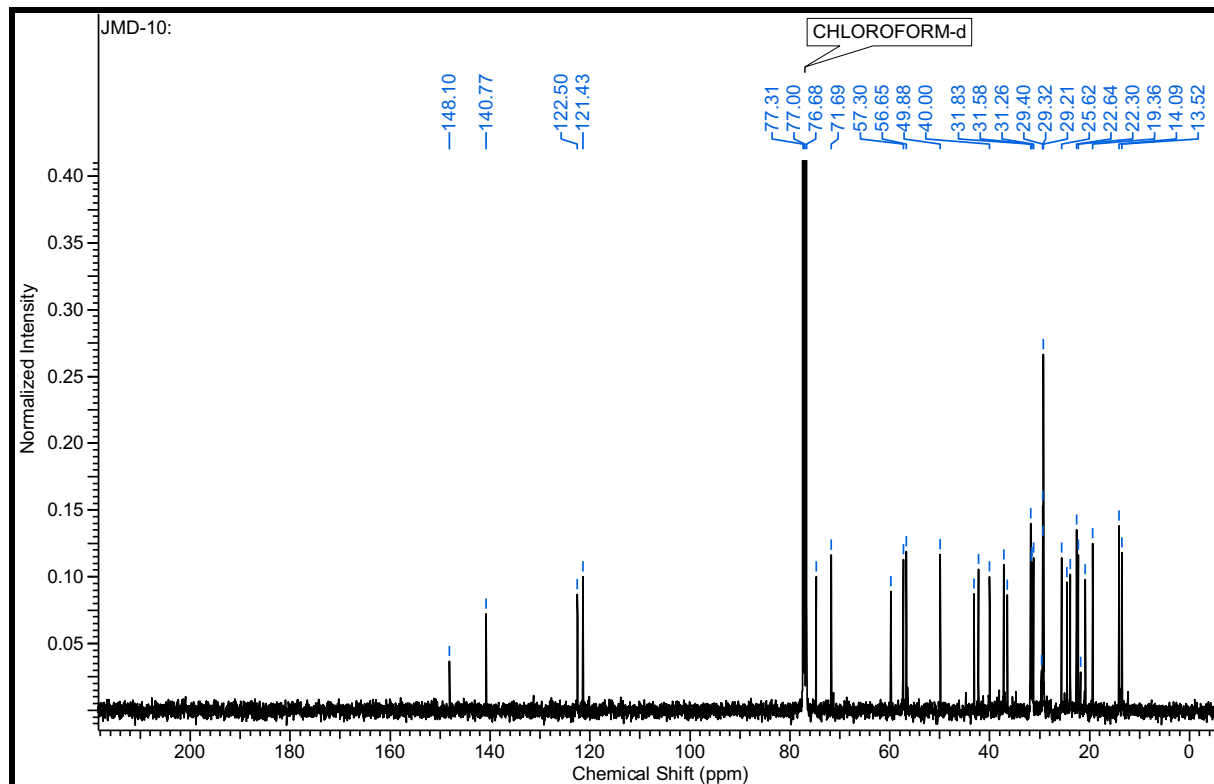
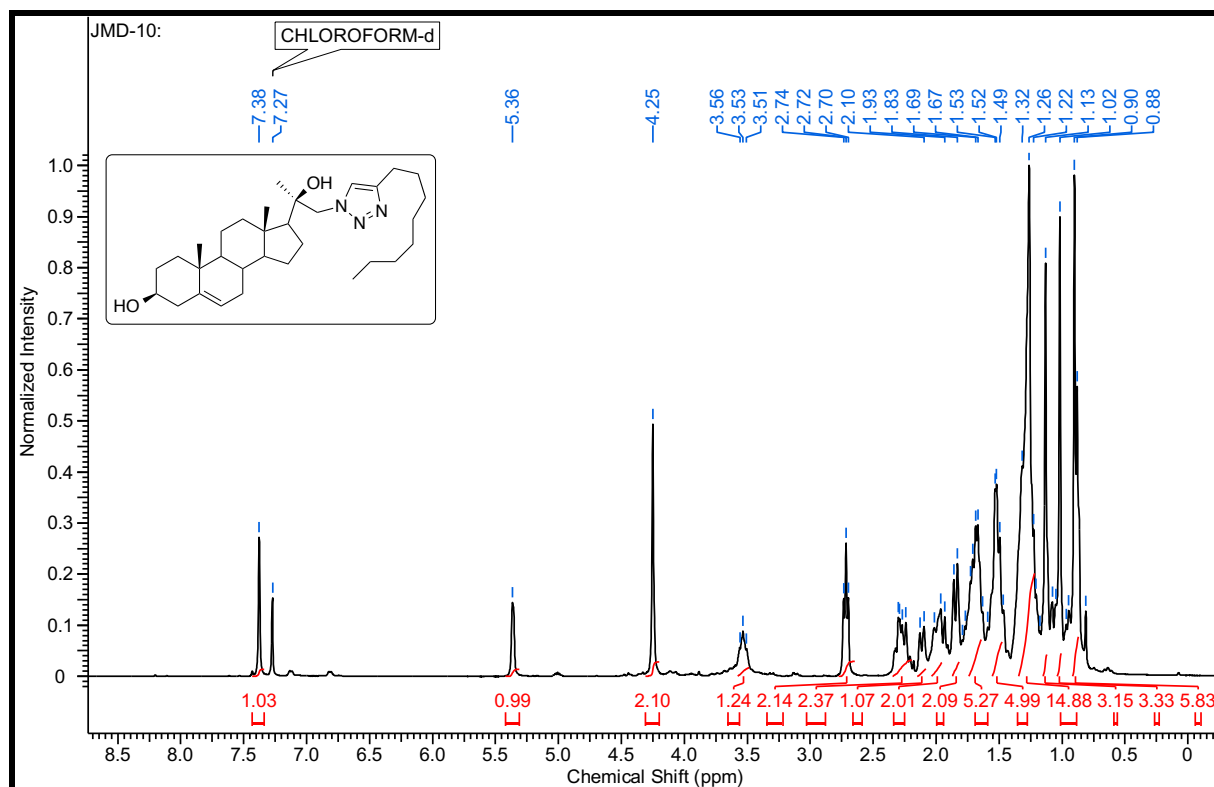
^1H and ^{13}C NMR Spectra of 29 (400MHz, 101MHz; DMSO- d_6)

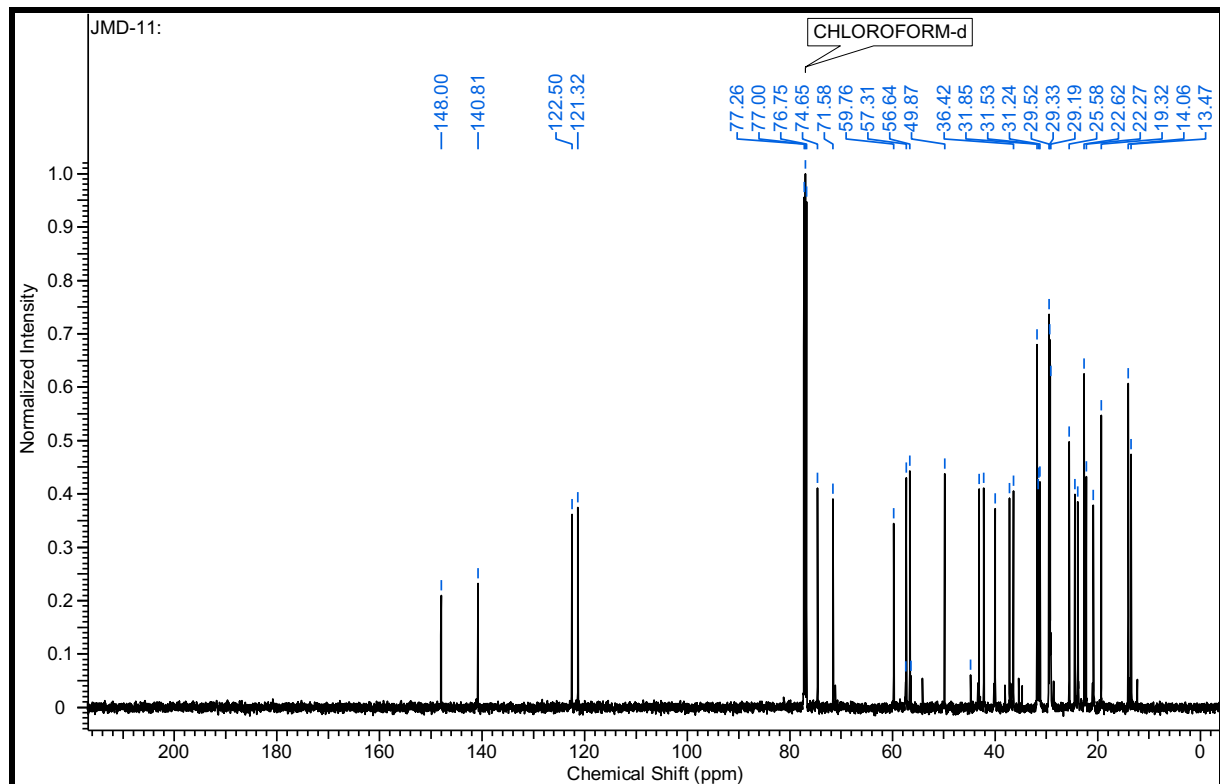
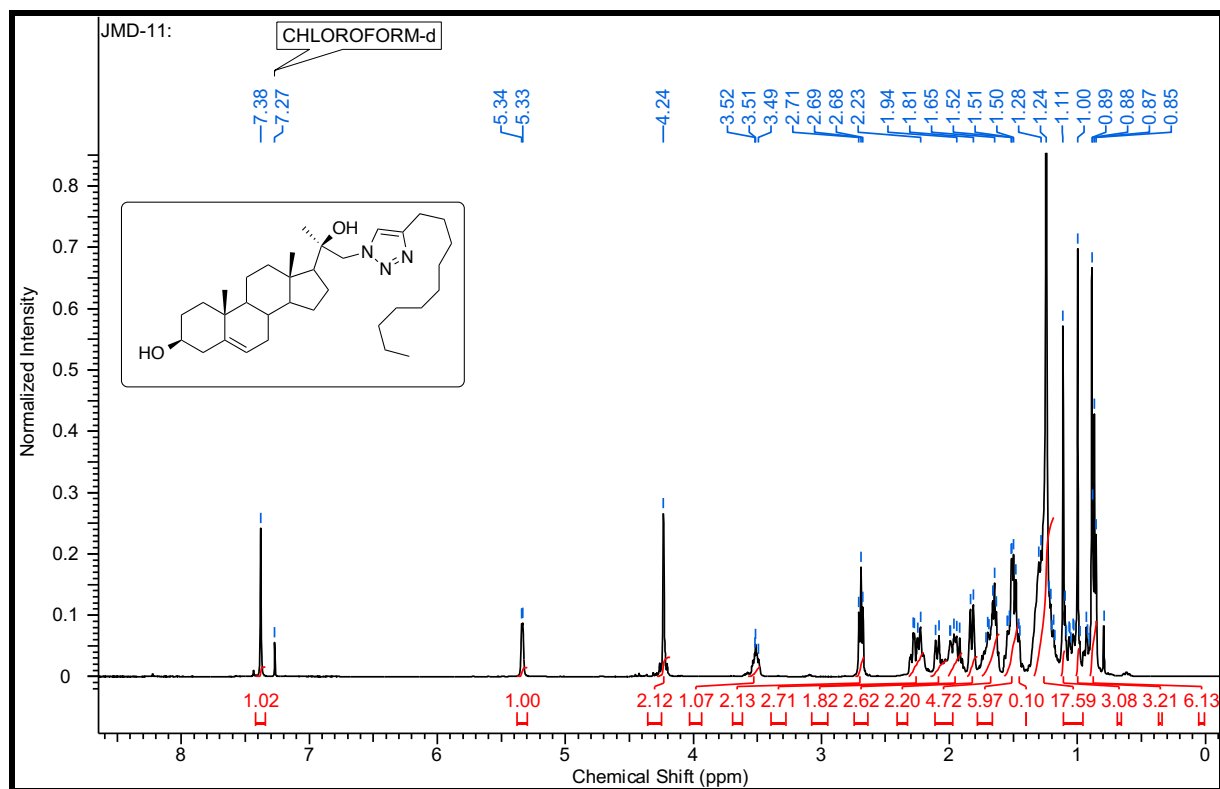
^1H and ^{13}C NMR Spectra of 30 (400MHz, 101MHz; CDCl_3)

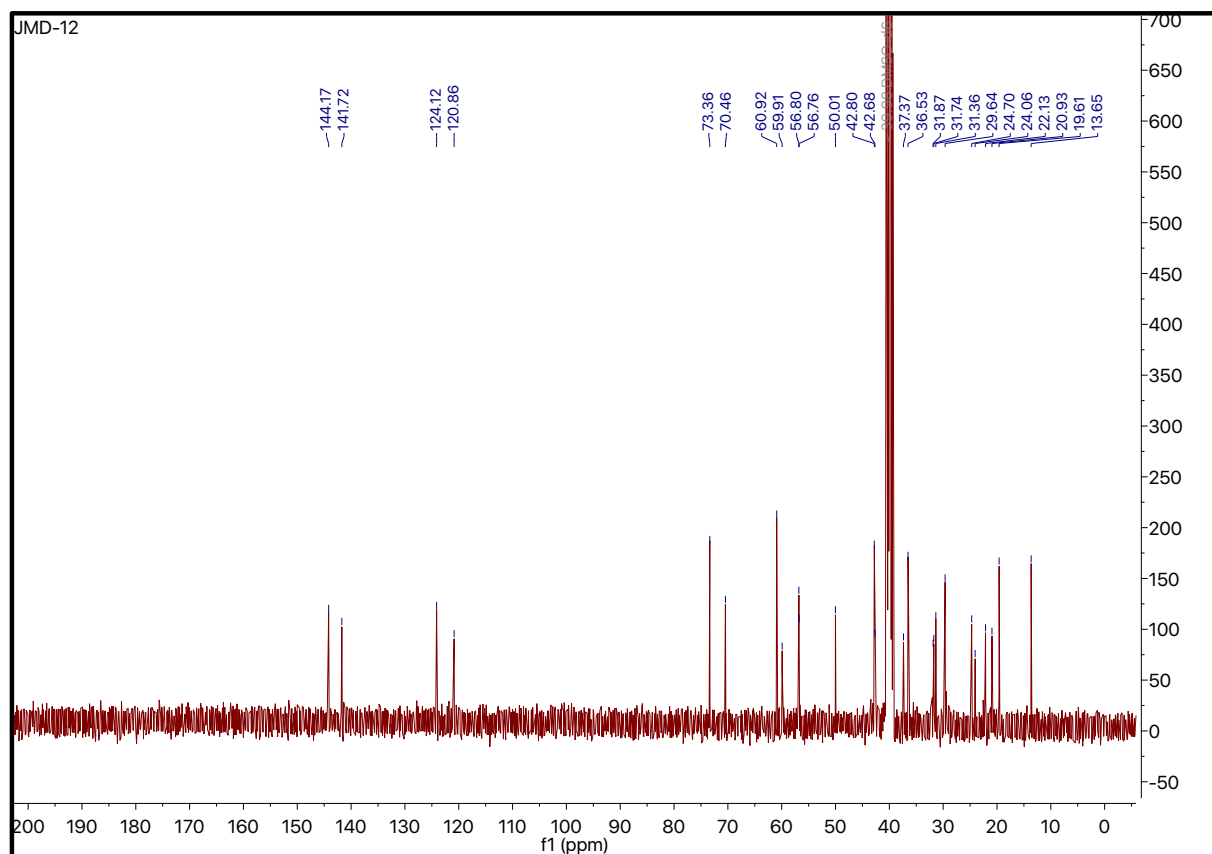
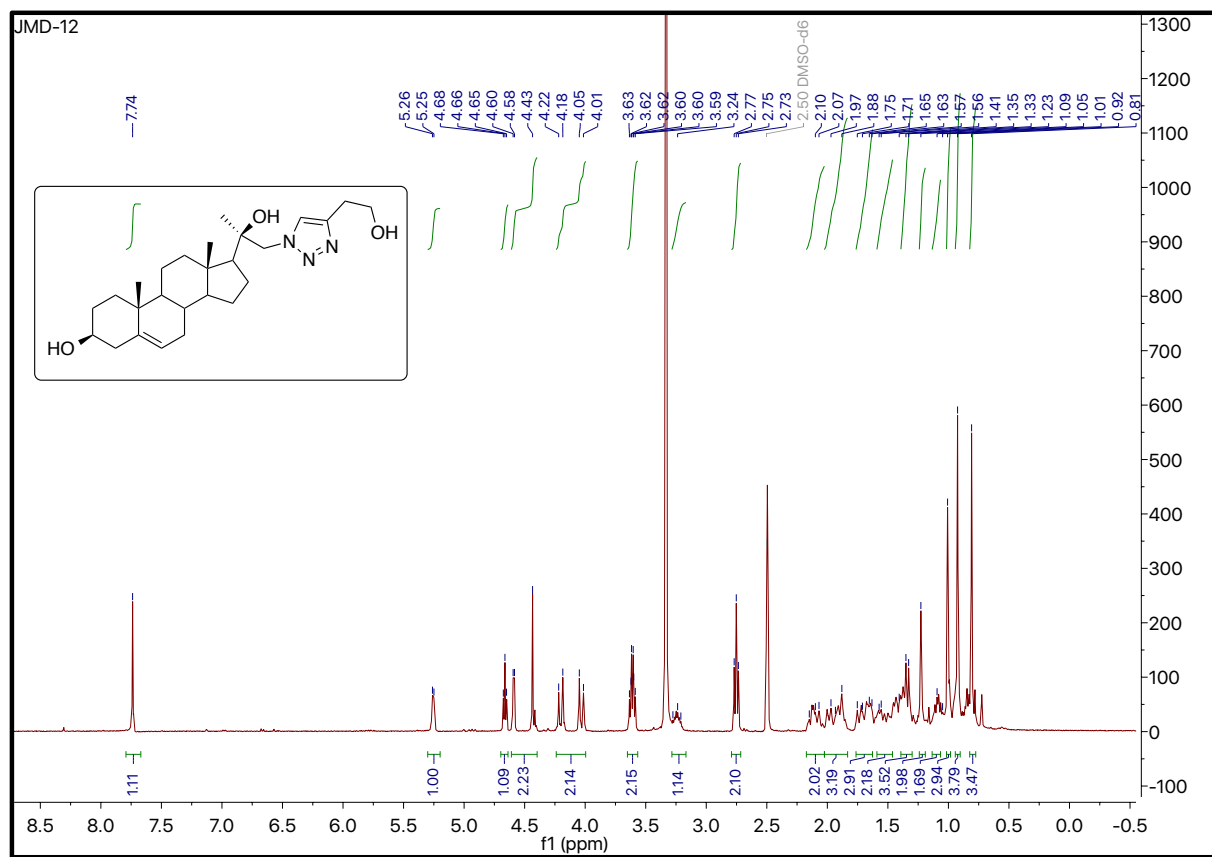
^1H and ^{13}C NMR Spectra of 31 (400MHz, 101MHz; CDCl_3)

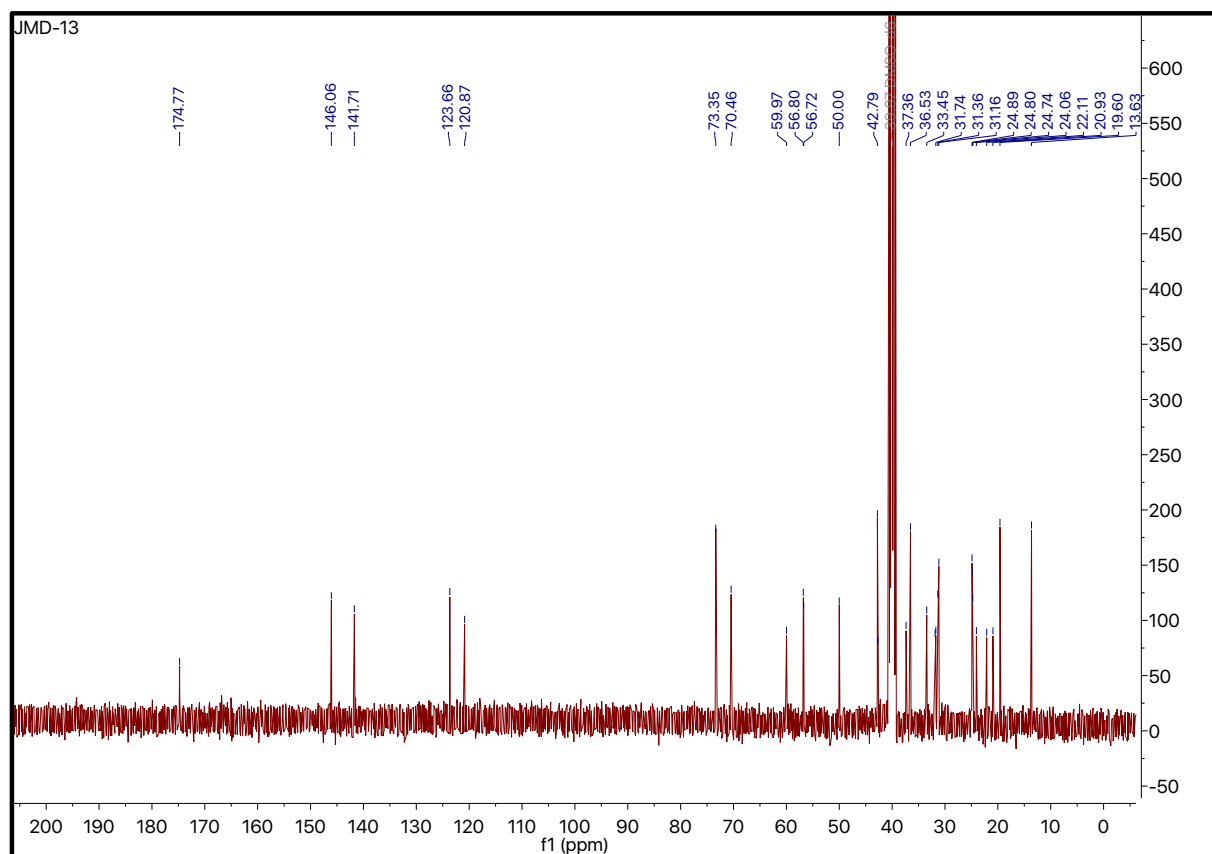
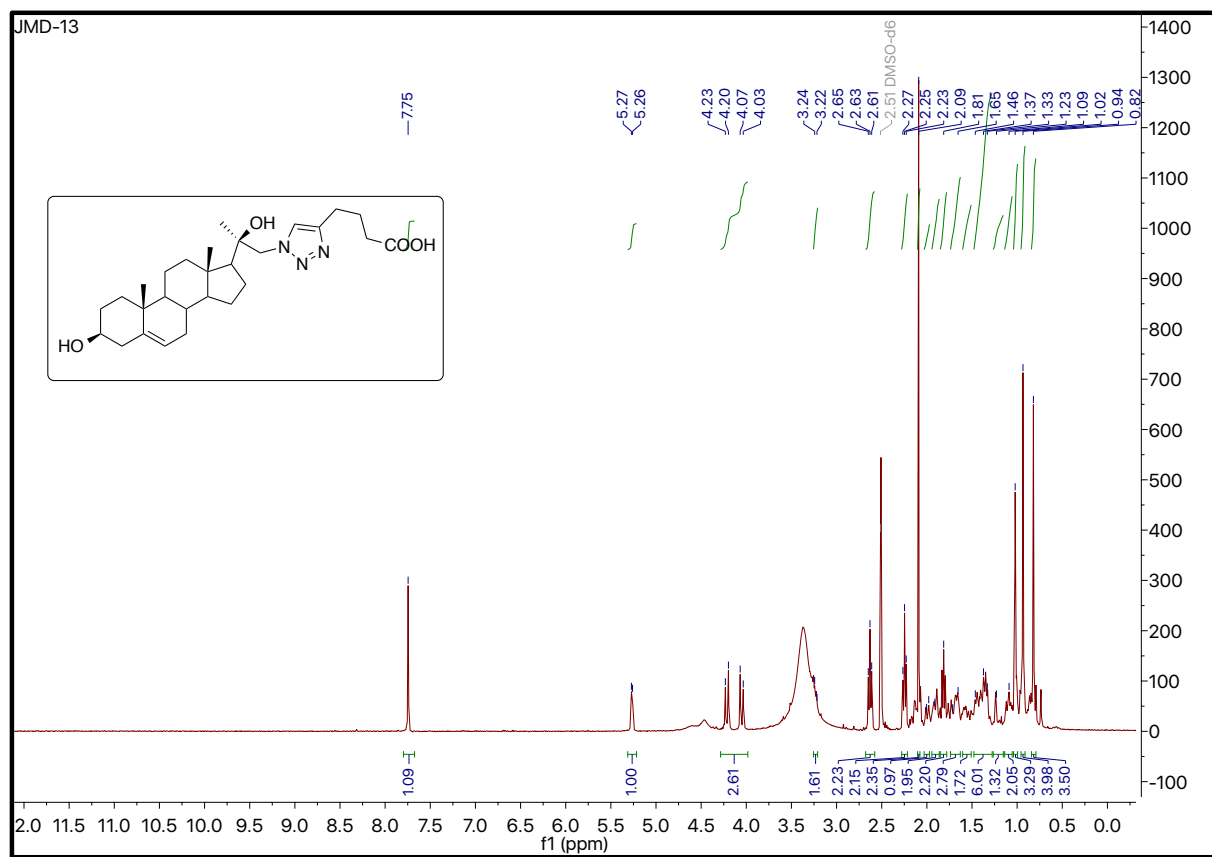
^1H and ^{13}C NMR Spectra of 32 (500MHz, 101MHz; CDCl_3)

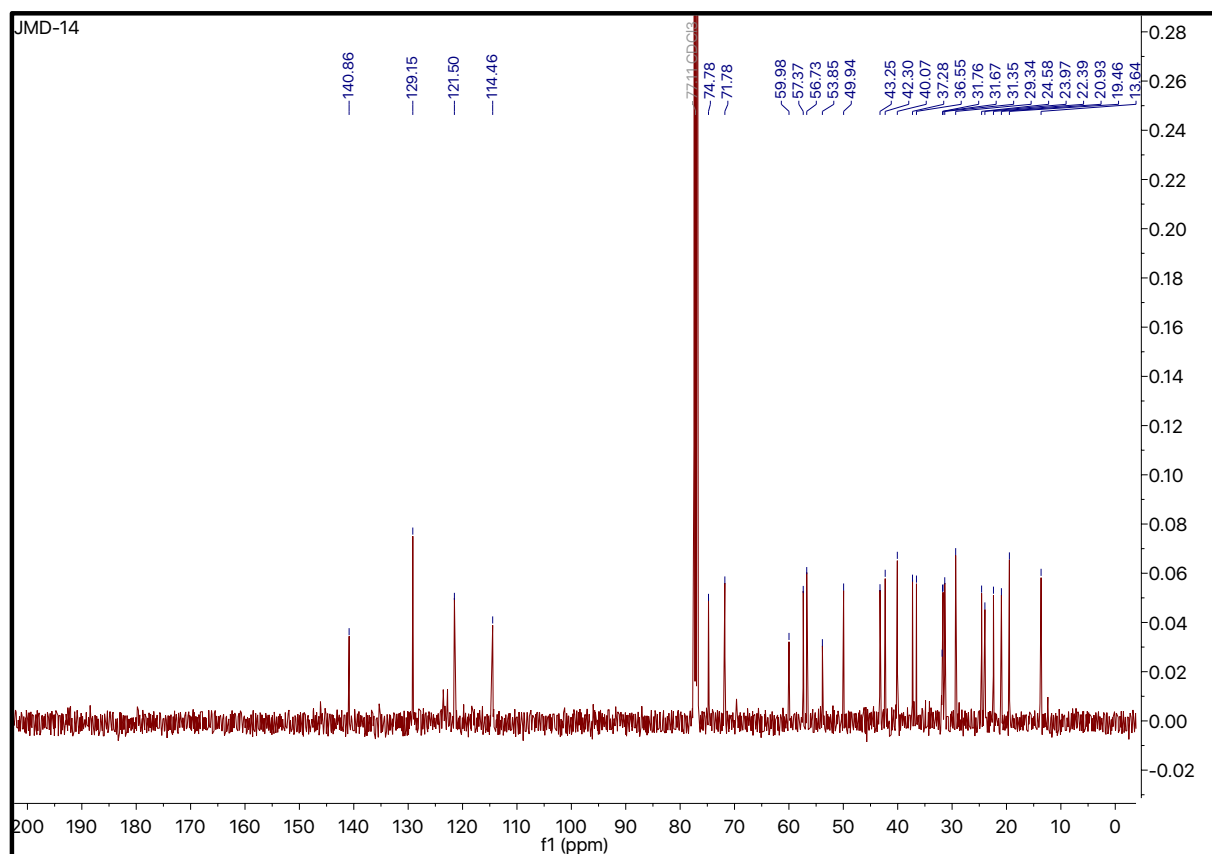
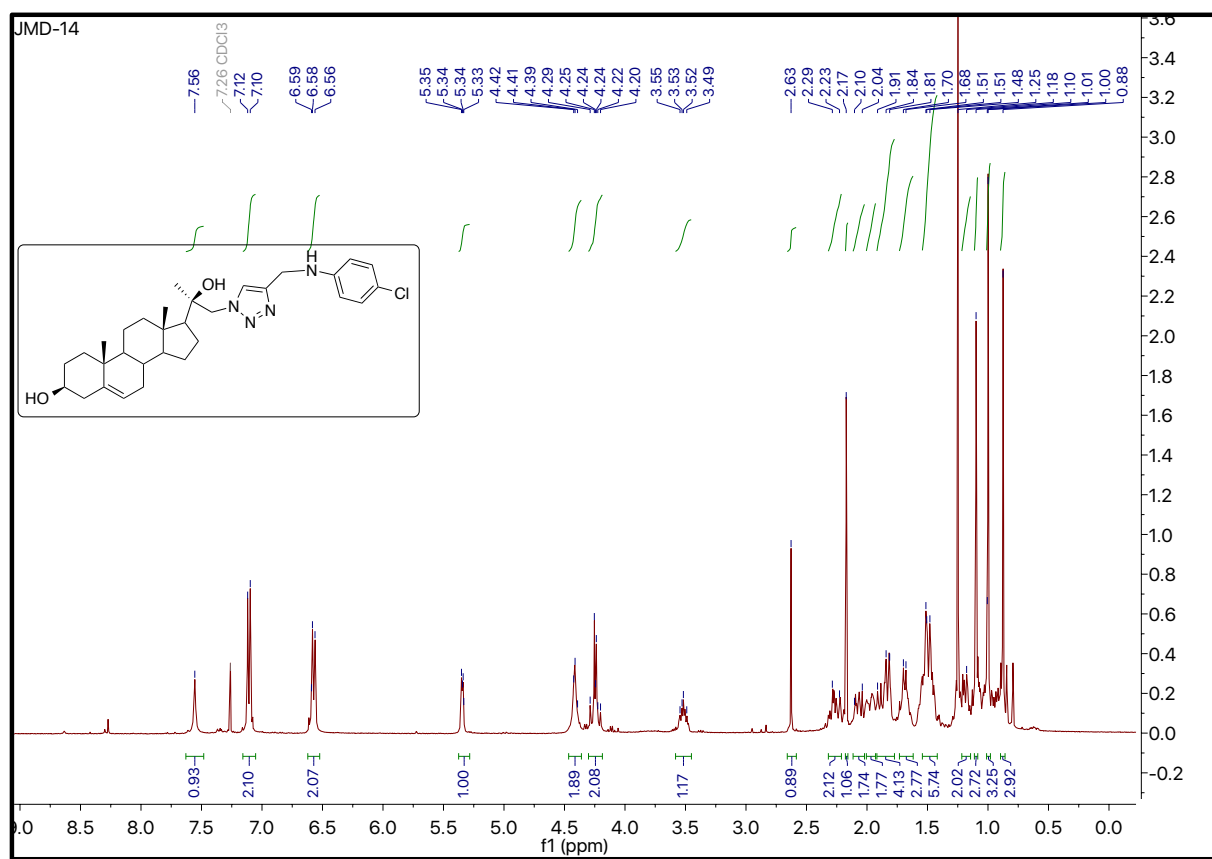
^1H and ^{13}C NMR Spectra of 33 (400MHz, 101MHz; CDCl_3)

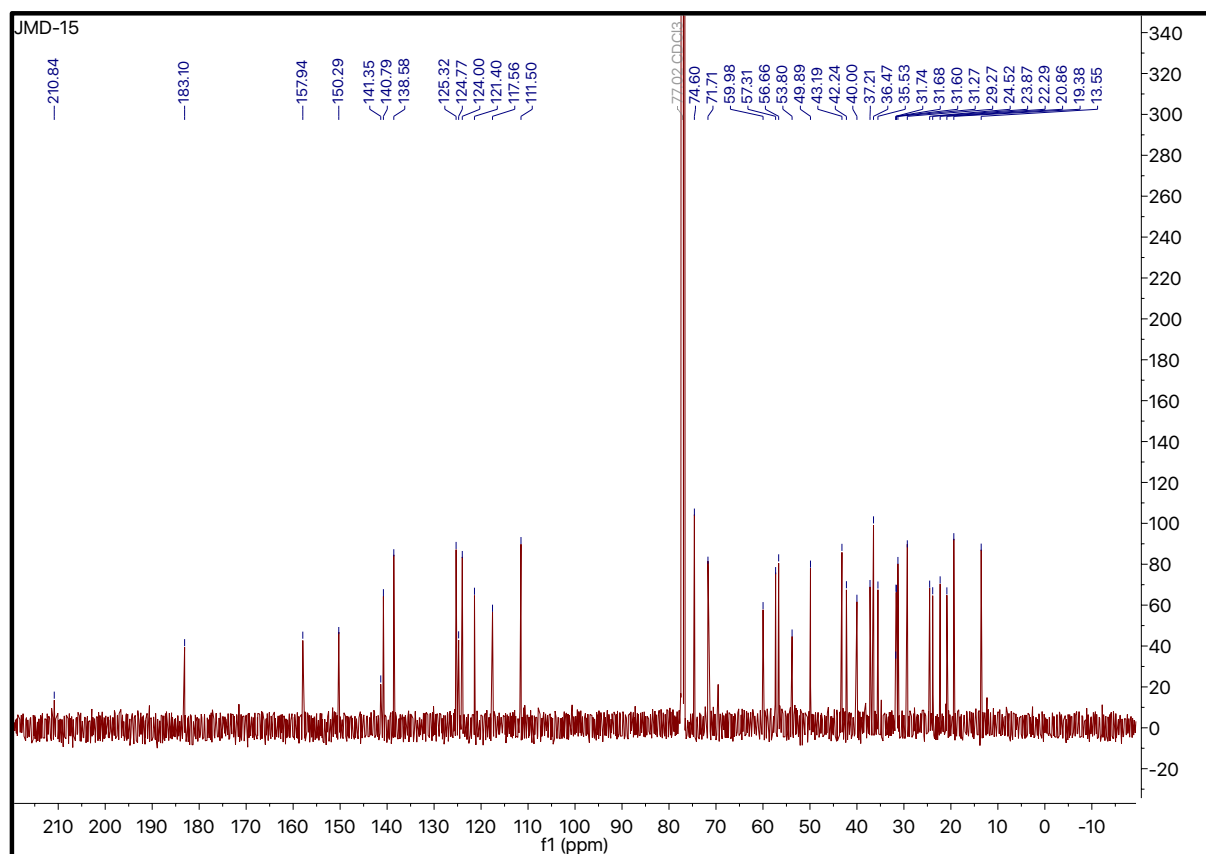
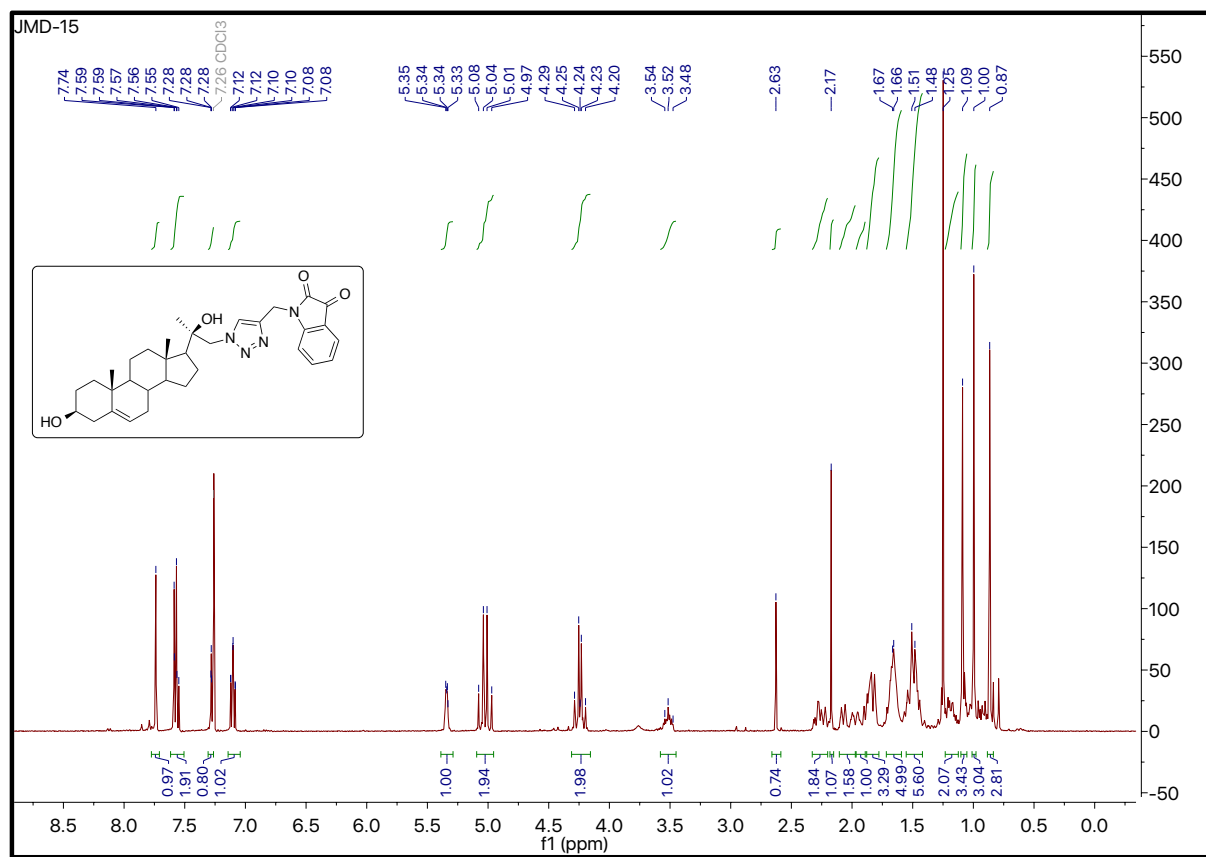
^1H and ^{13}C NMR Spectra of 34 (400MHz, 101MHz; CDCl_3)

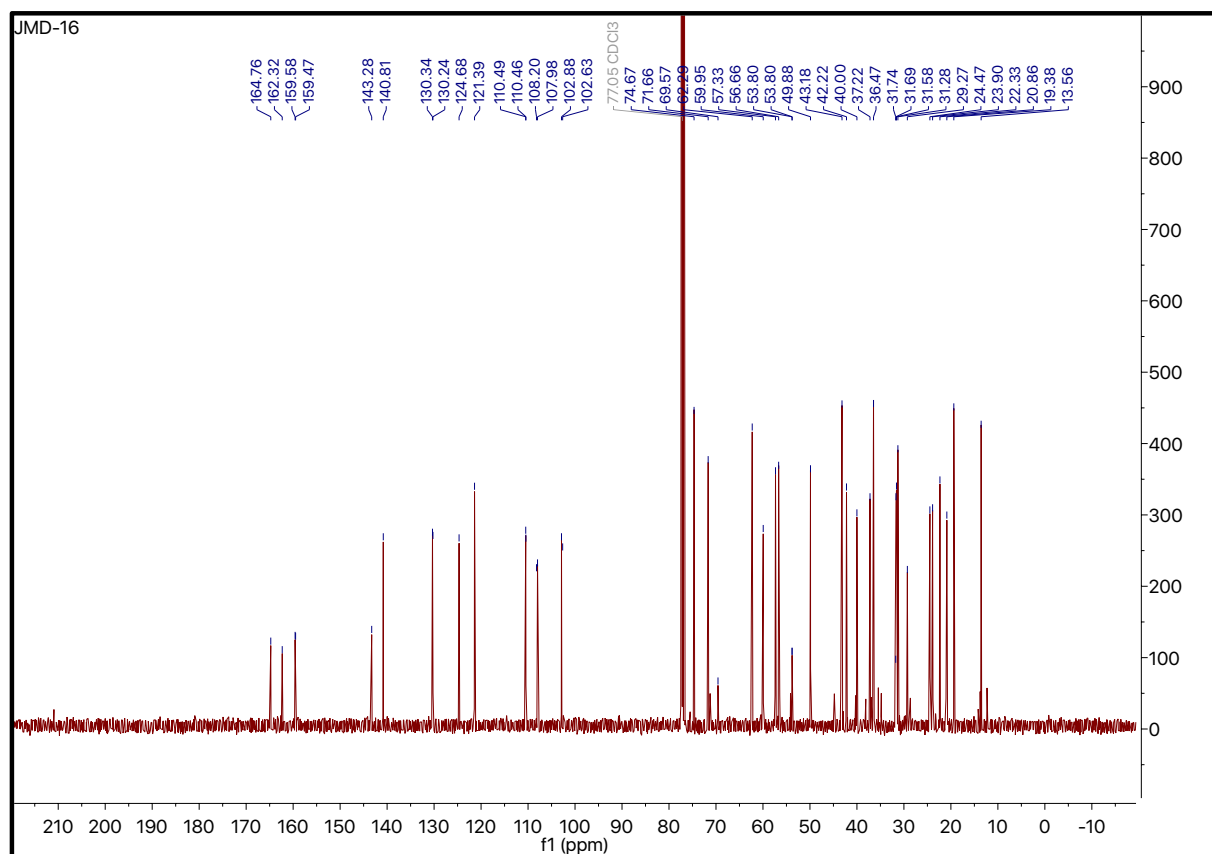
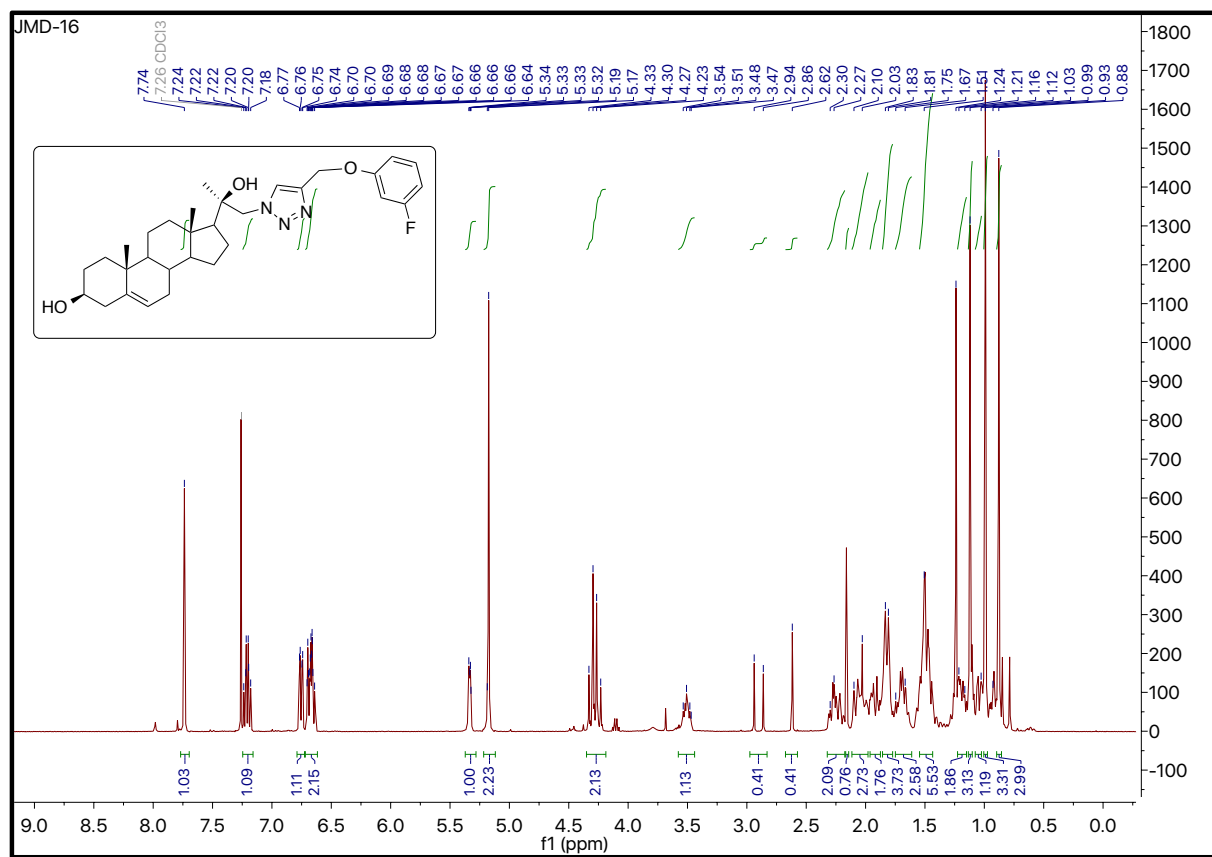
^1H and ^{13}C NMR Spectra of 35 (500MHz, 101MHz; CDCl_3)

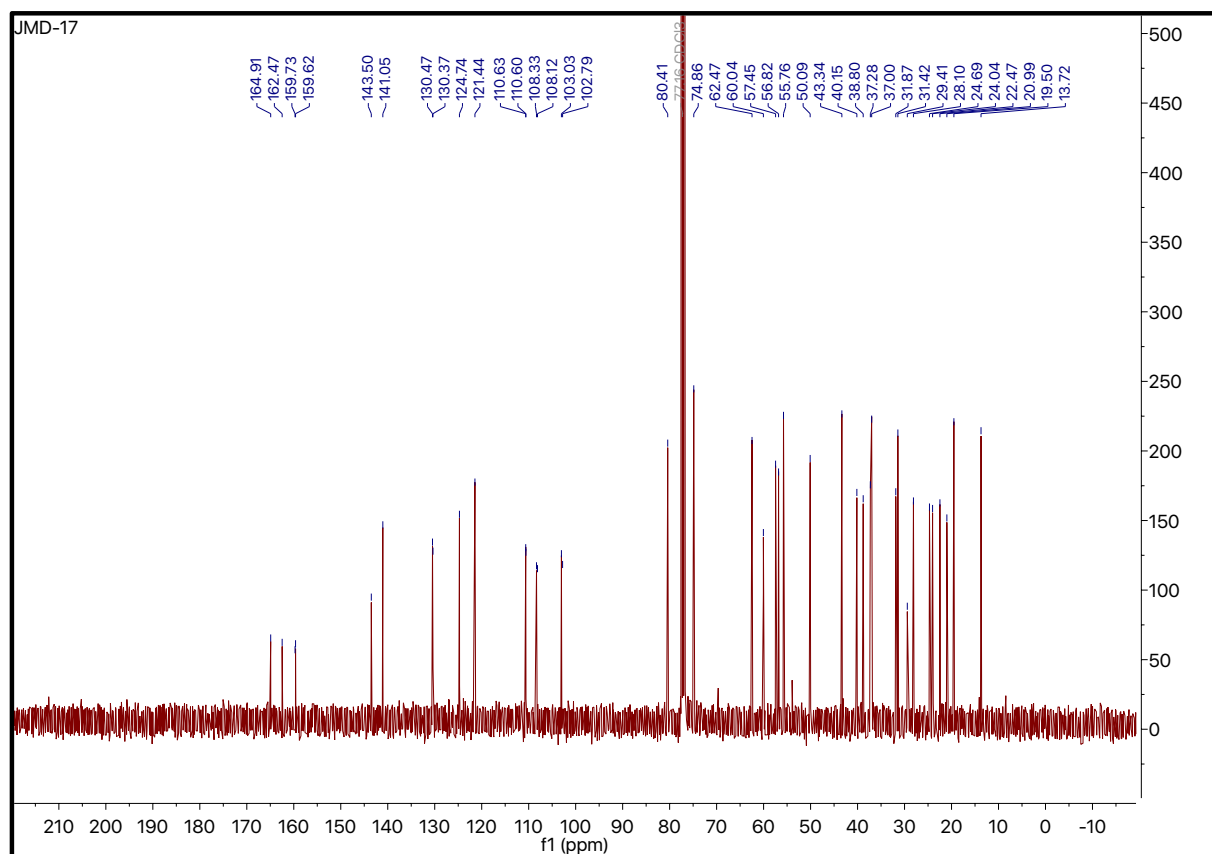
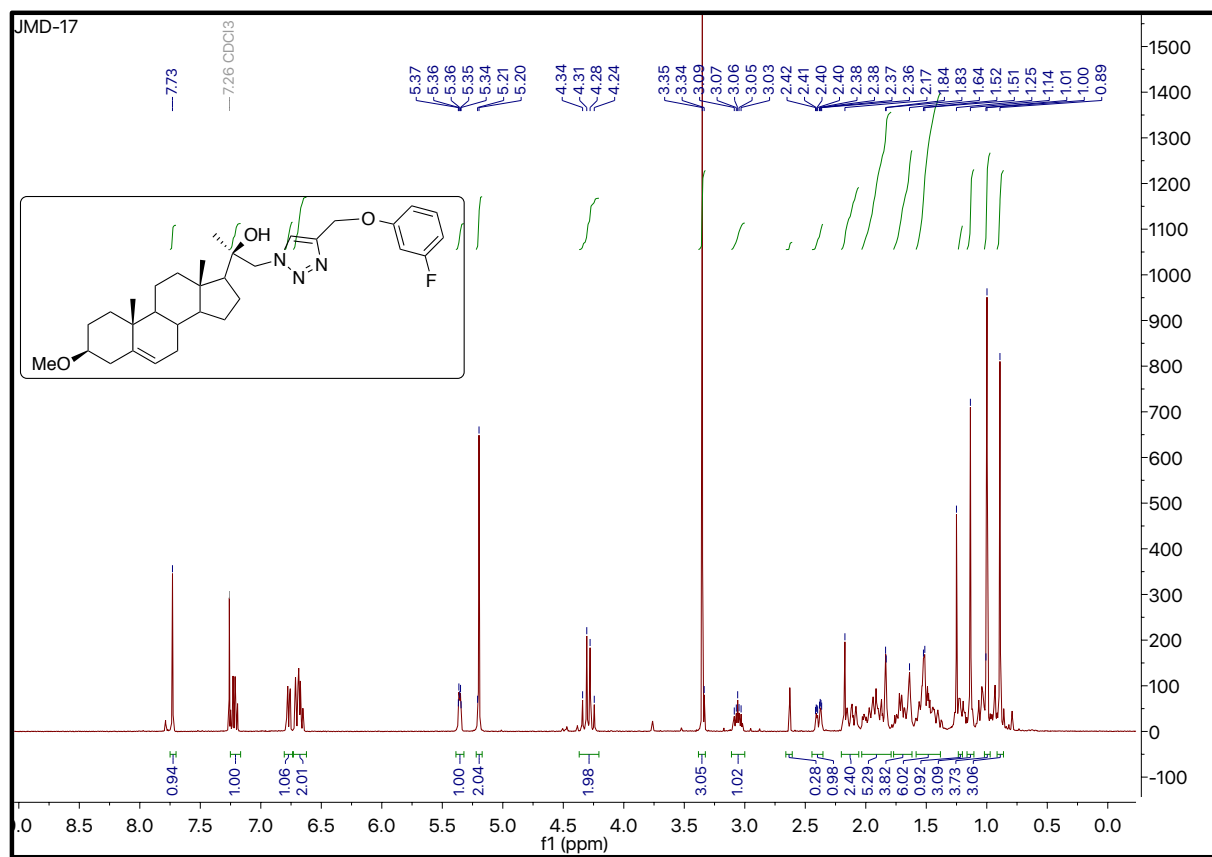
^1H and ^{13}C NMR Spectra of 36 (400MHz, 101MHz; DMSO- d_6)

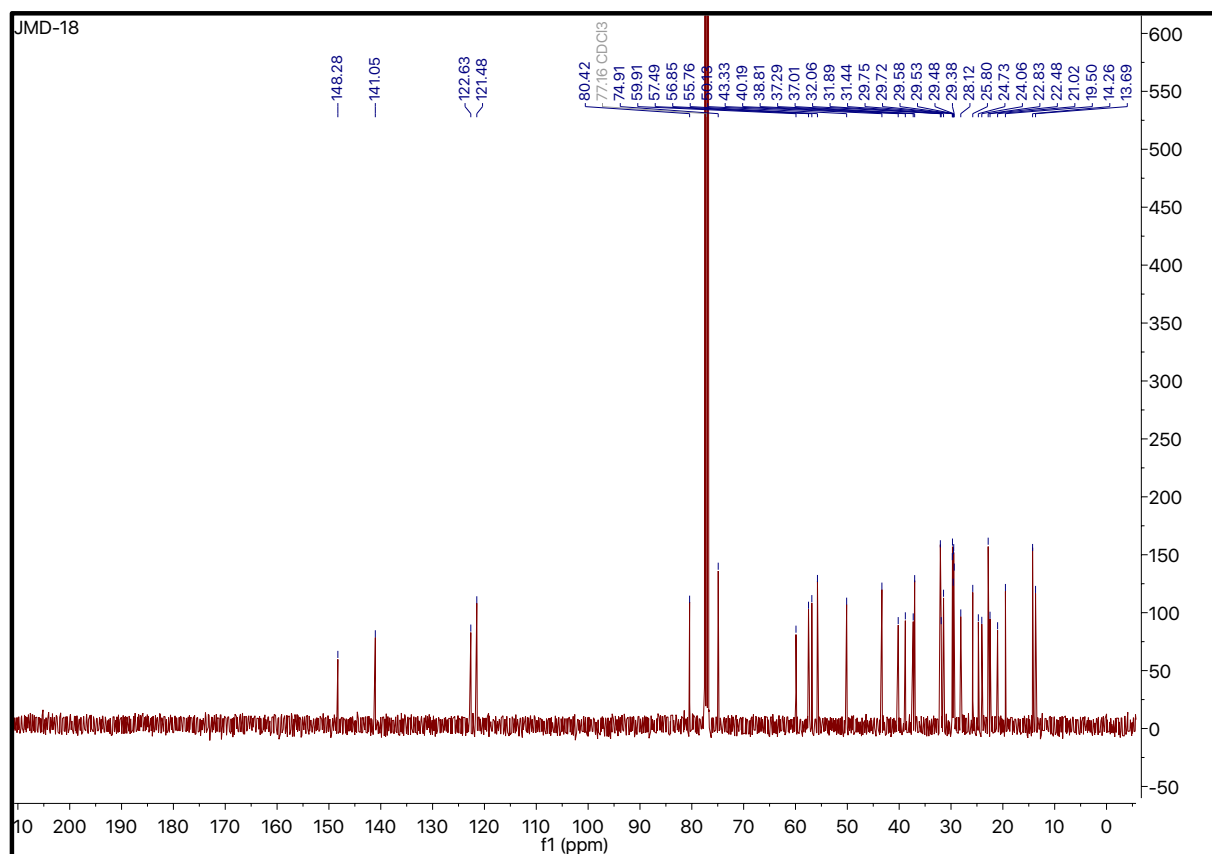
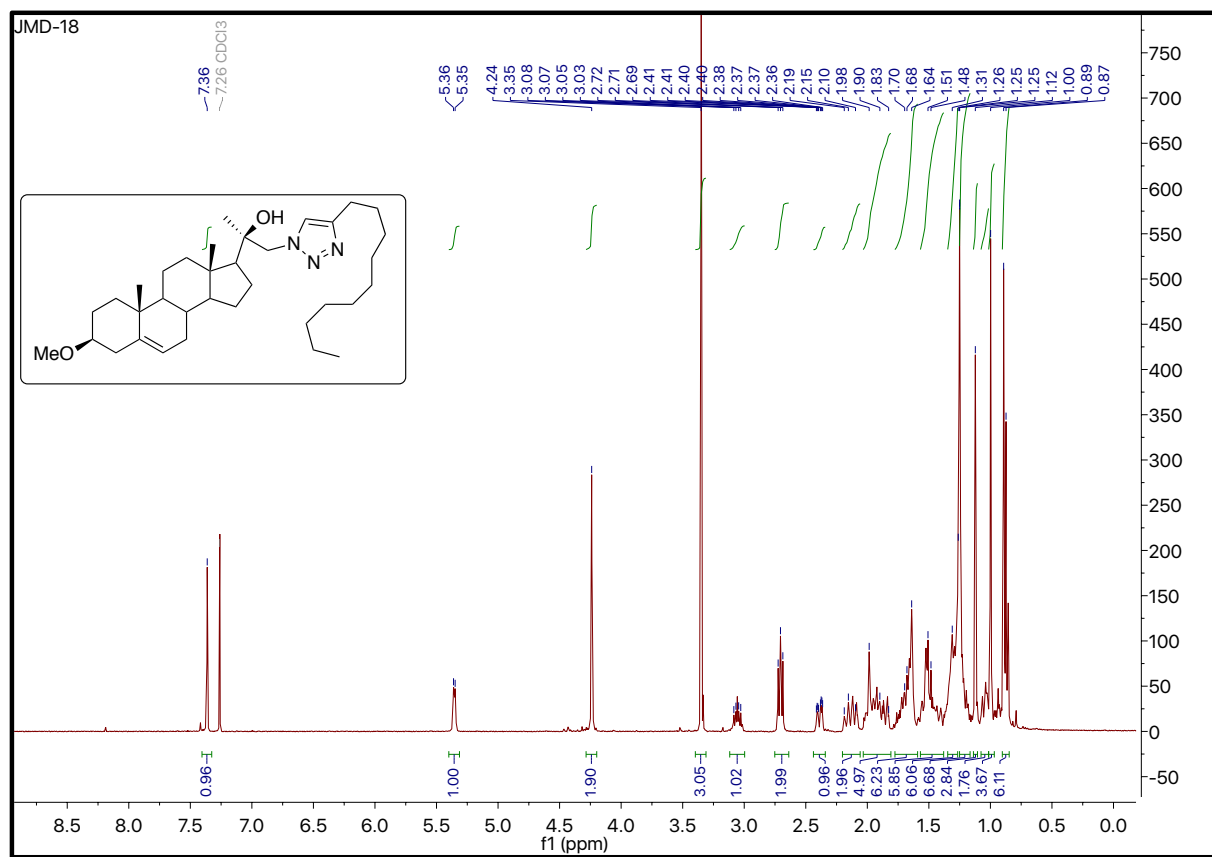
^1H and ^{13}C NMR Spectra of 37 (400MHz, 101MHz; DMSO- d_6)

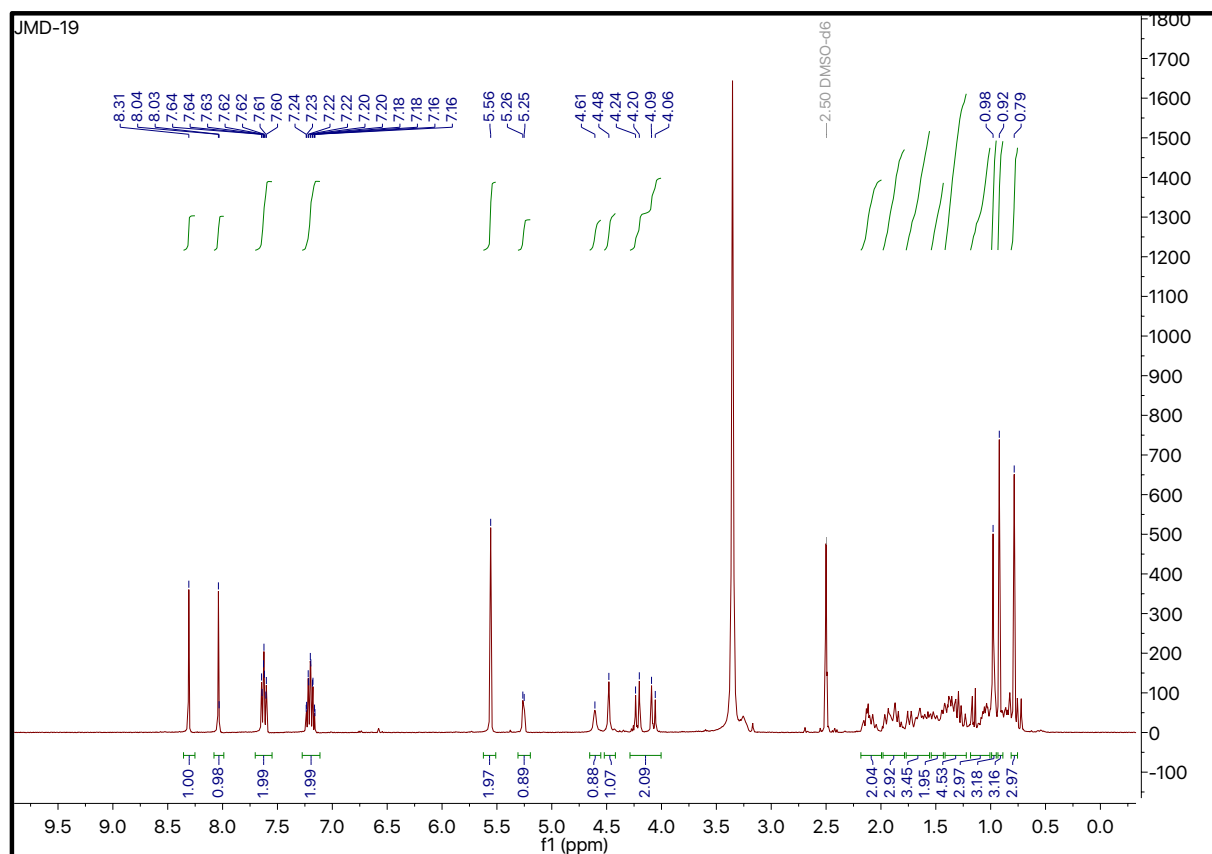
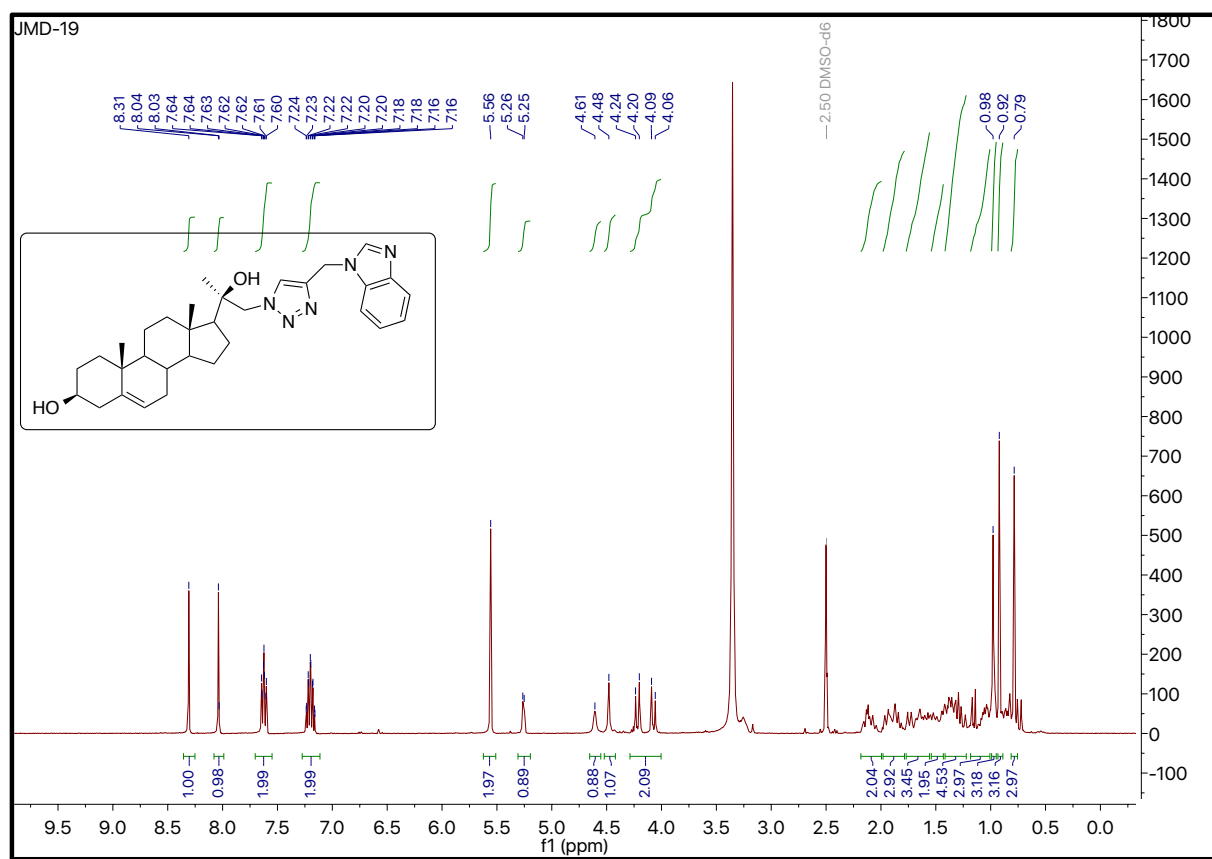
^1H and ^{13}C NMR Spectra of 38 (400MHz, 101MHz; CDCl_3)

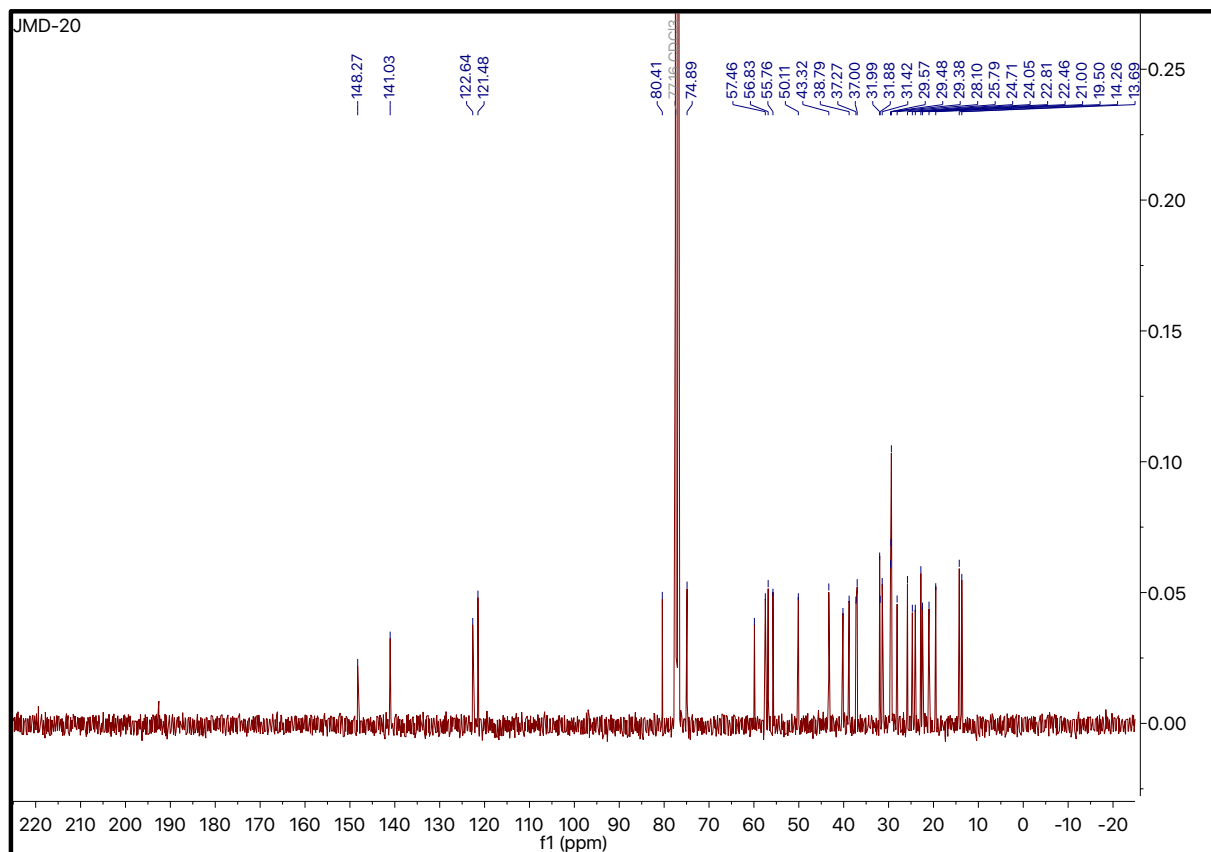
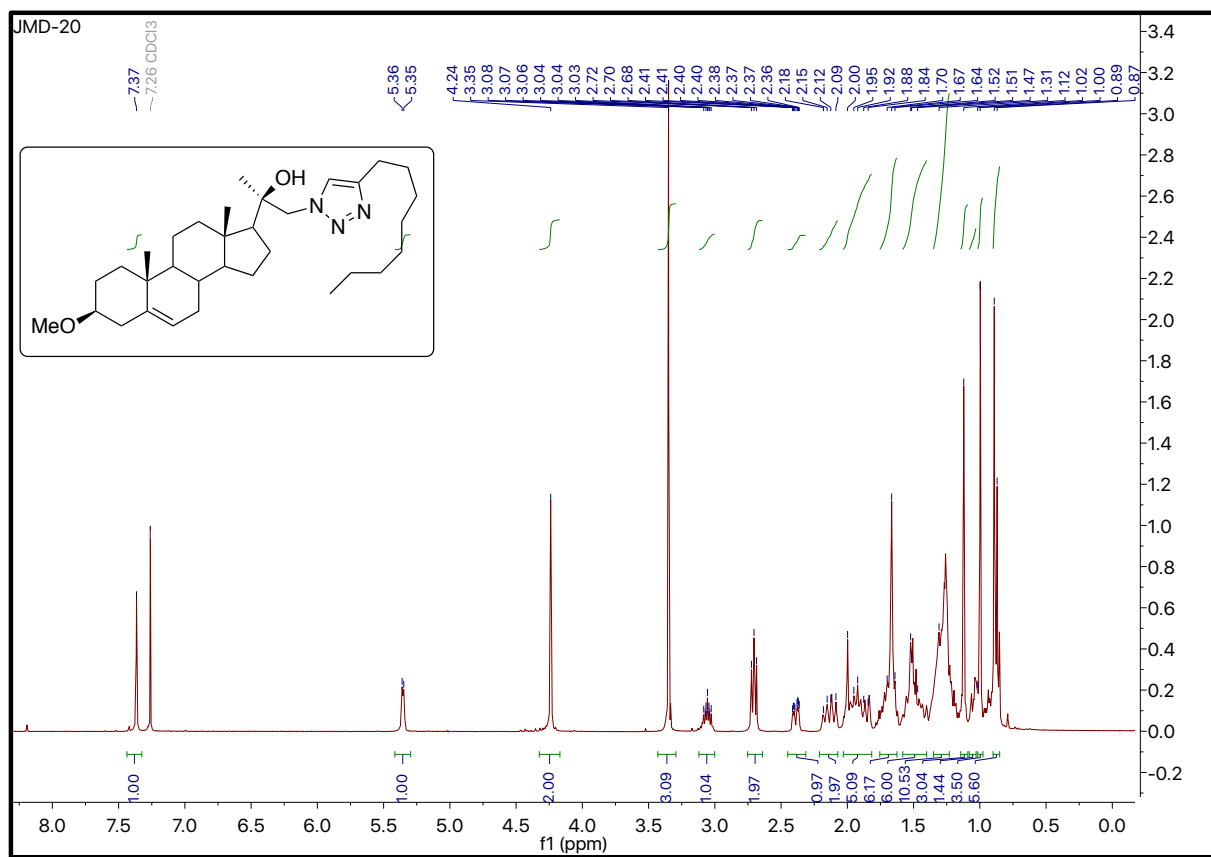
^1H and ^{13}C NMR Spectra of 39 (400MHz, 101MHz; CDCl_3)

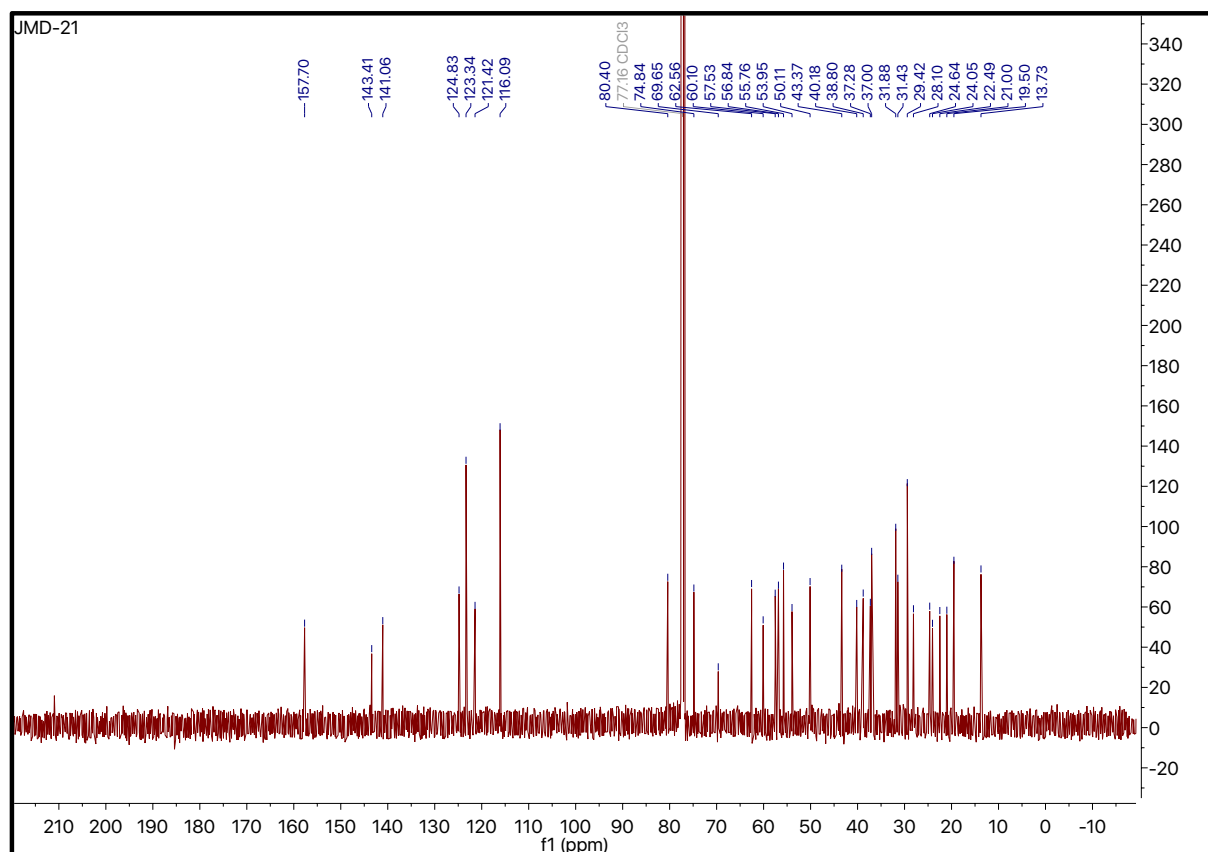
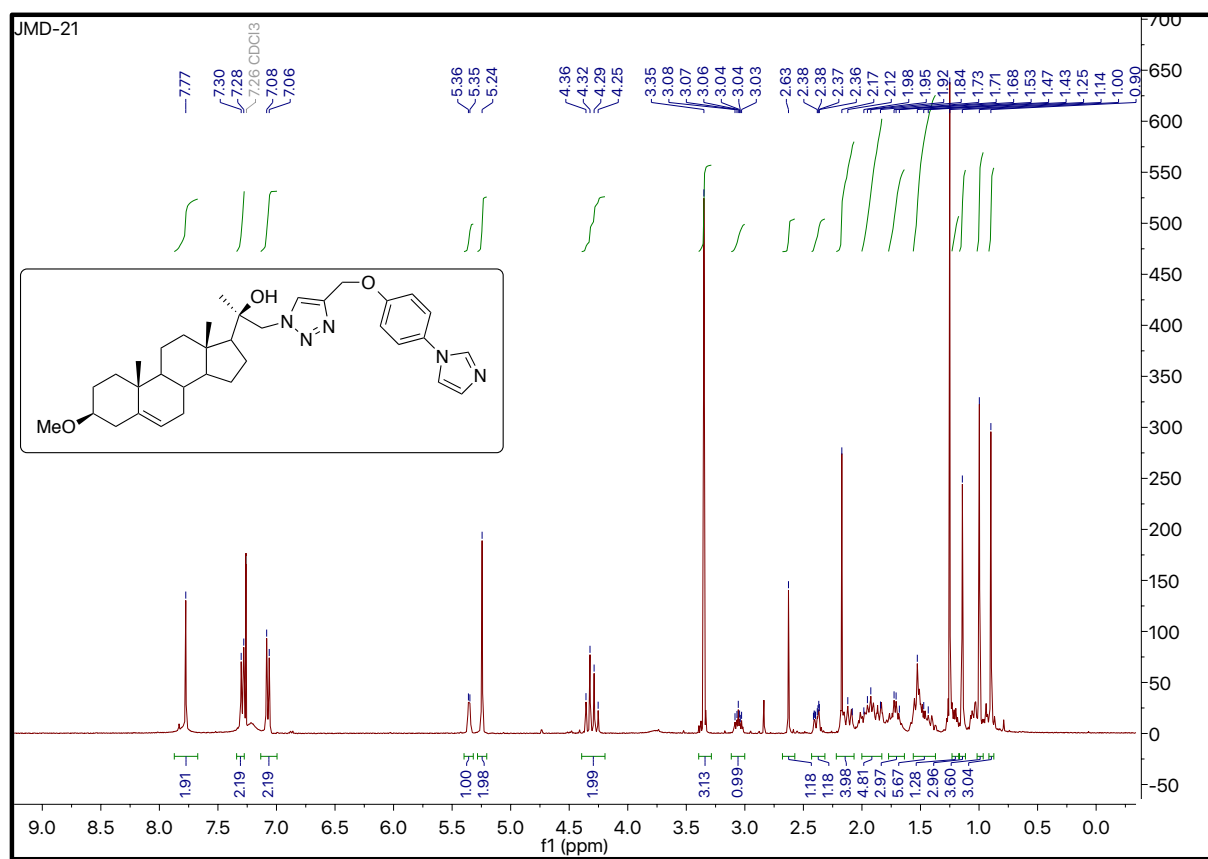
^1H and ^{13}C NMR Spectra of 40 (400MHz, 101MHz; CDCl_3)

^1H and ^{13}C NMR Spectra of 41 (400MHz, 101MHz; CDCl_3)

^1H and ^{13}C NMR Spectra of 42 (400MHz, 101MHz; CDCl_3)

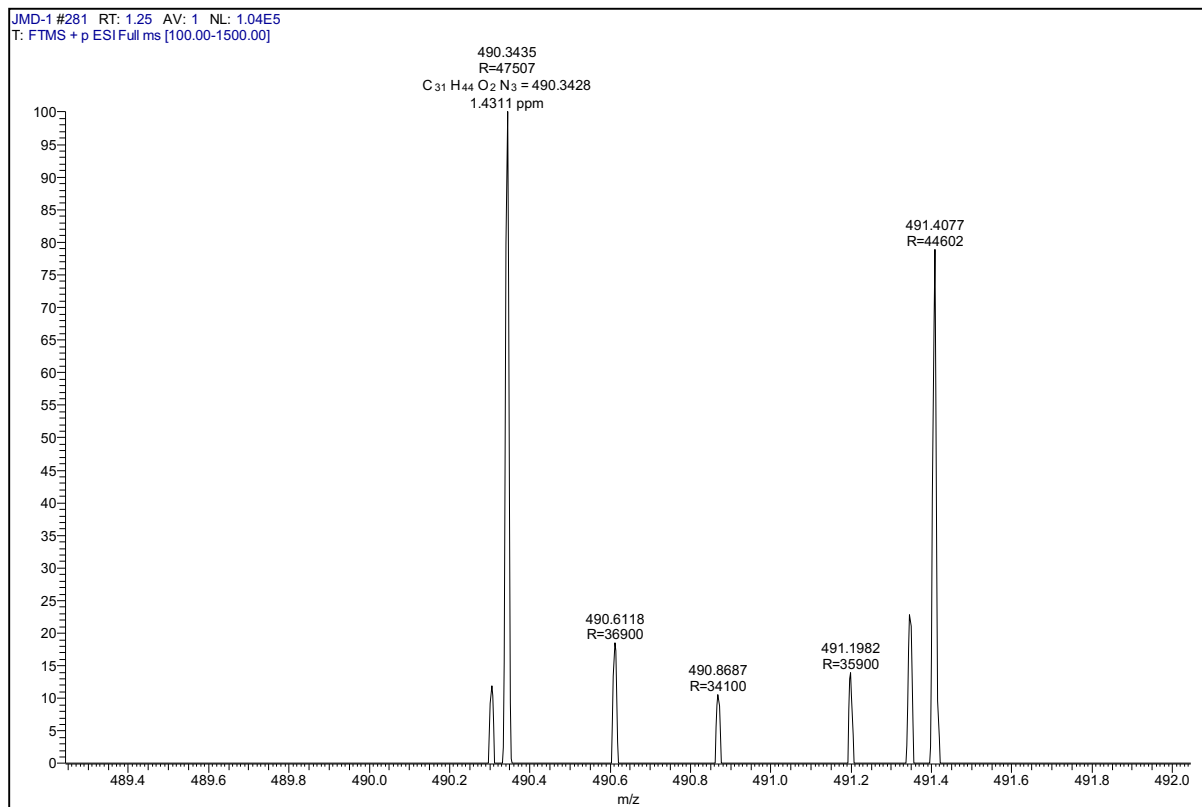
^1H and ^{13}C NMR Spectra of 43 (400MHz, 101MHz; DMSO- d_6)

^1H and ^{13}C NMR Spectra of 44 (400MHz, 101MHz; CDCl_3)

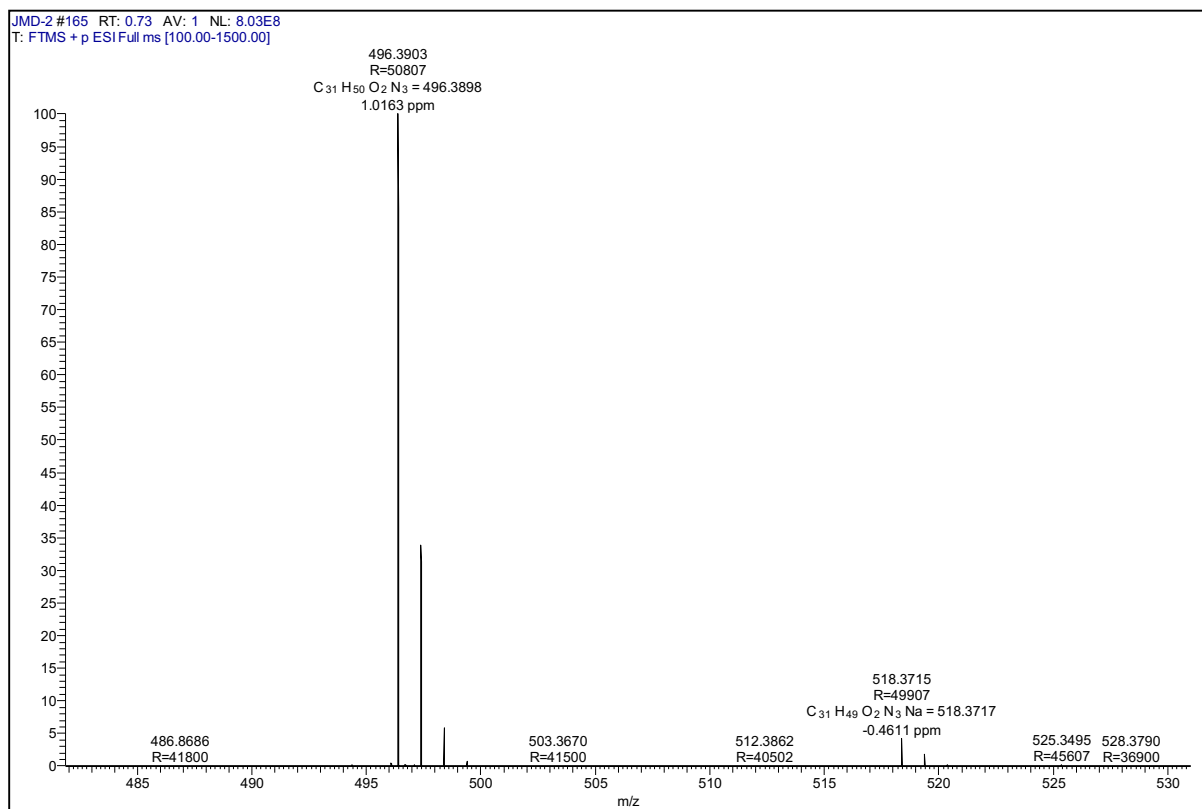
^1H and ^{13}C NMR Spectra of 45 (400MHz, 101MHz; CDCl_3)

4.8 Selected HRMS

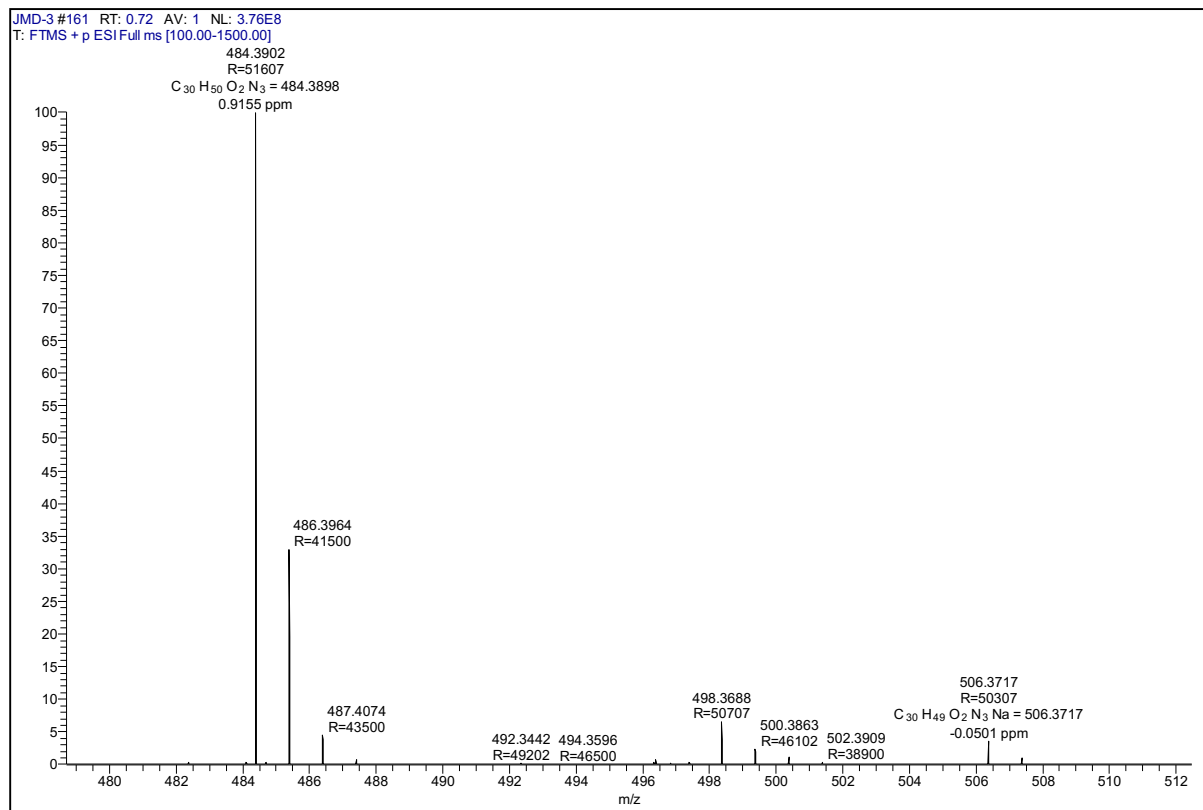
HRMS of 25



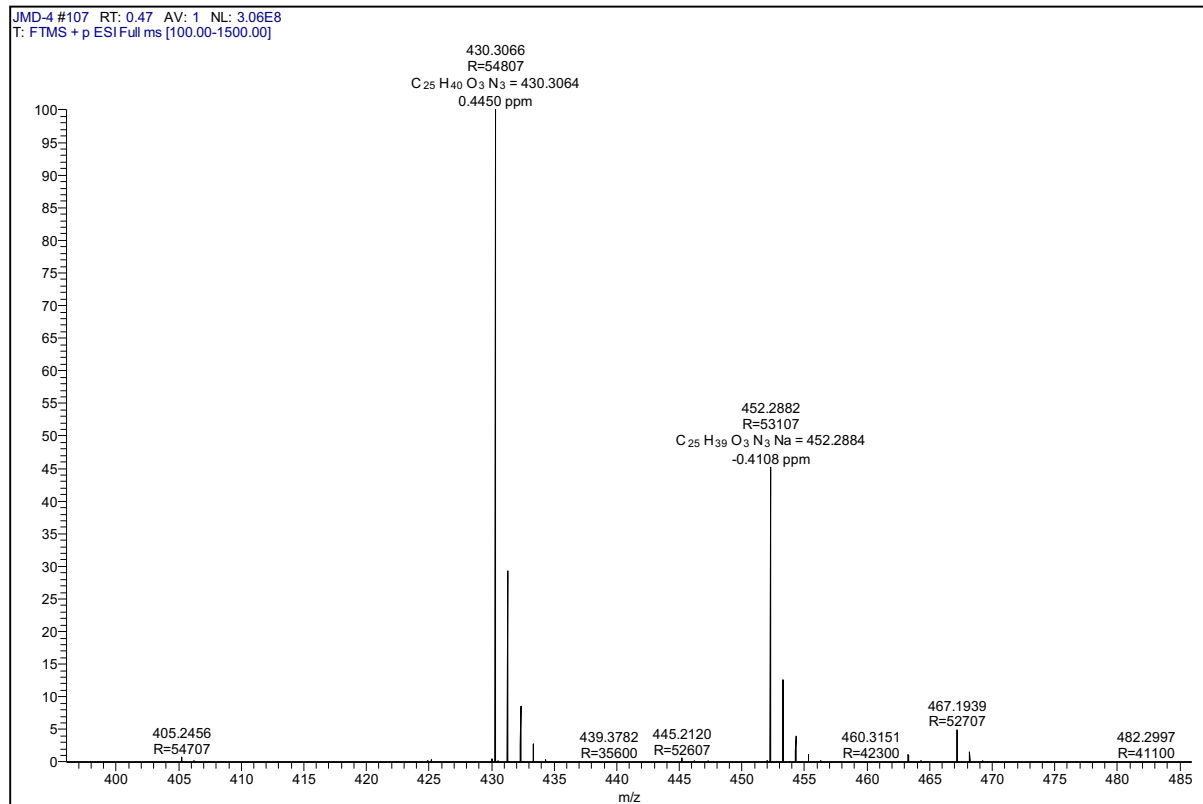
HRMS of 26



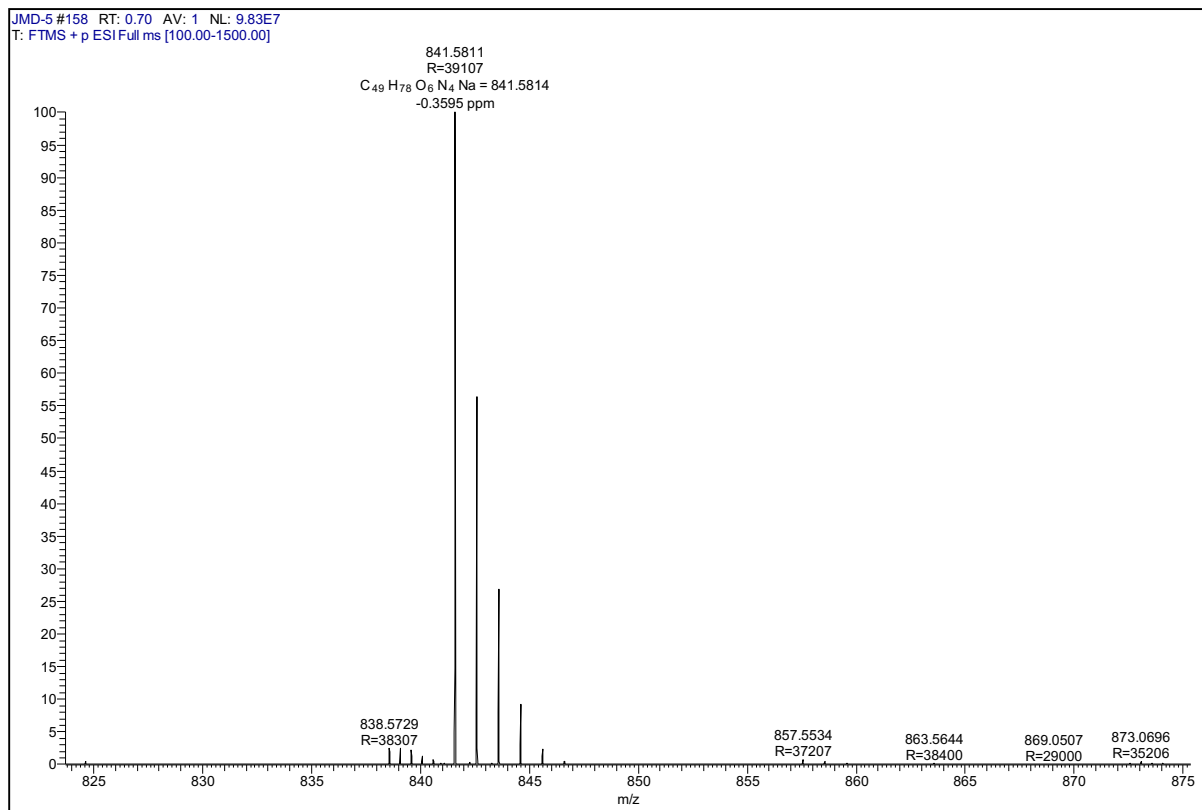
HRMS of 27



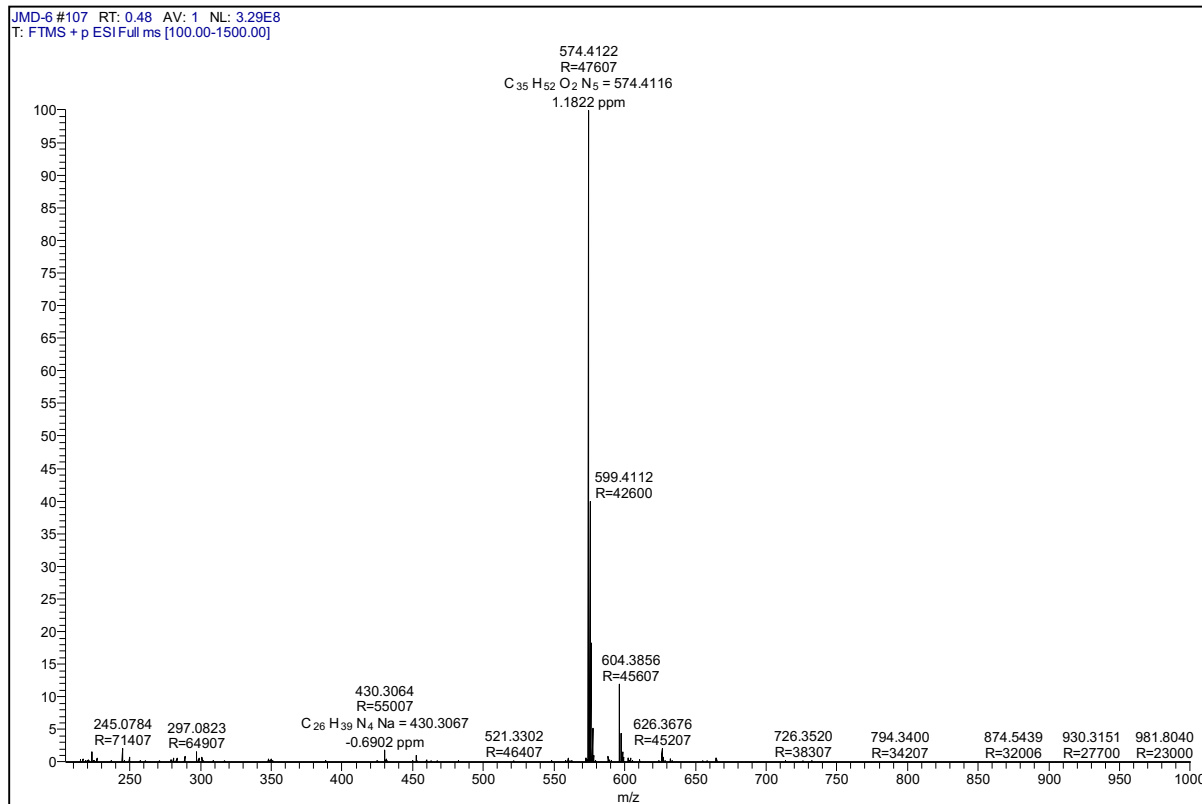
HRMS of 28



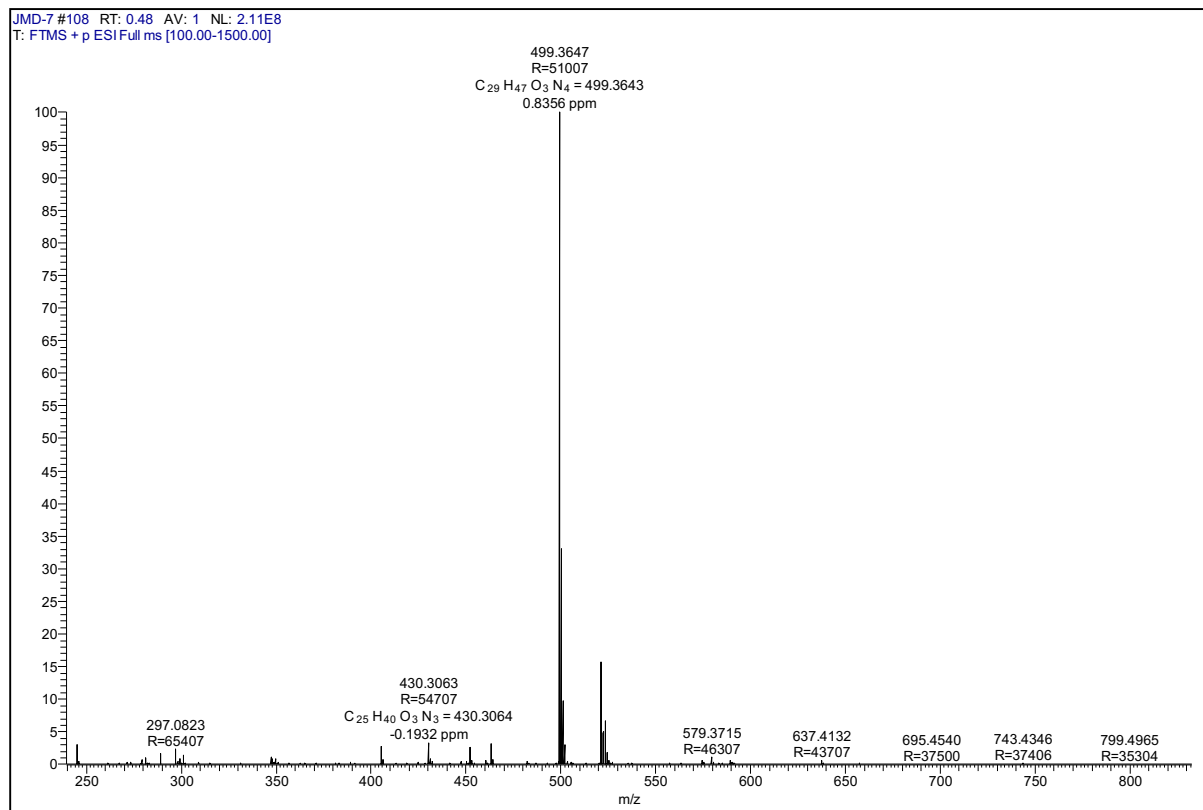
HRMS of 29



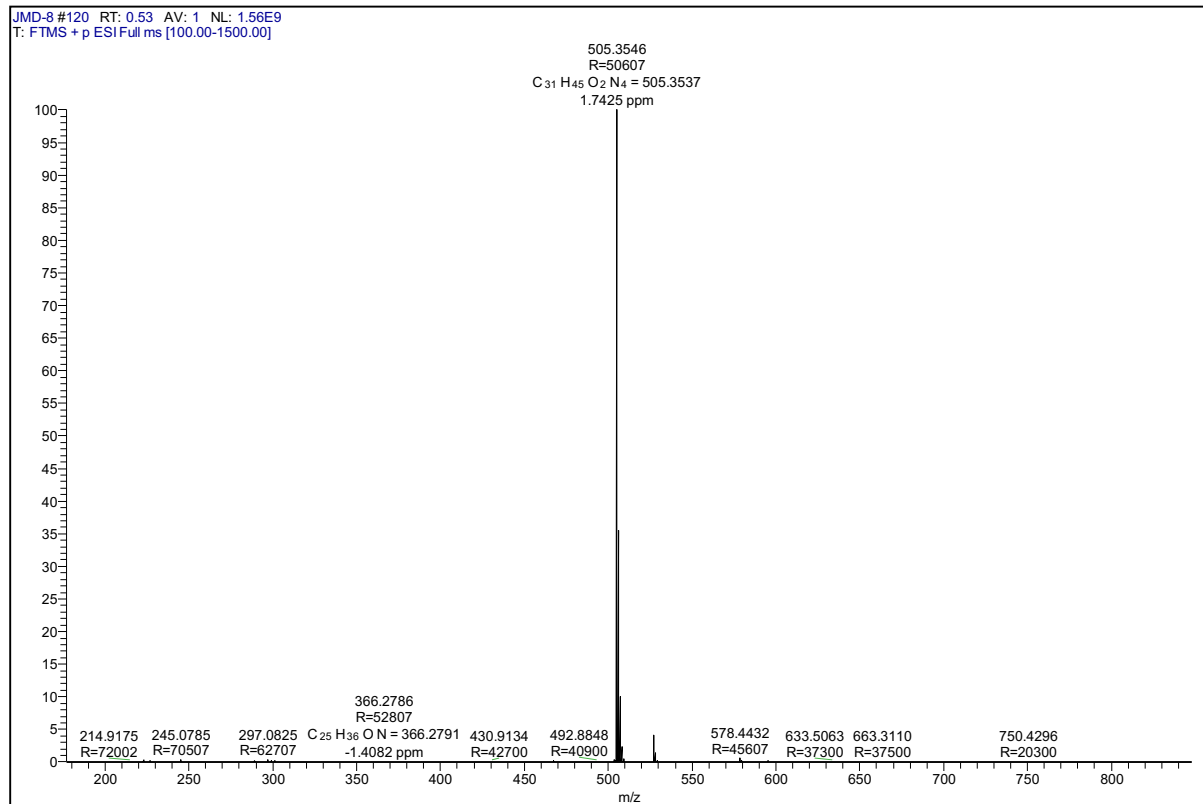
HRMS of 30



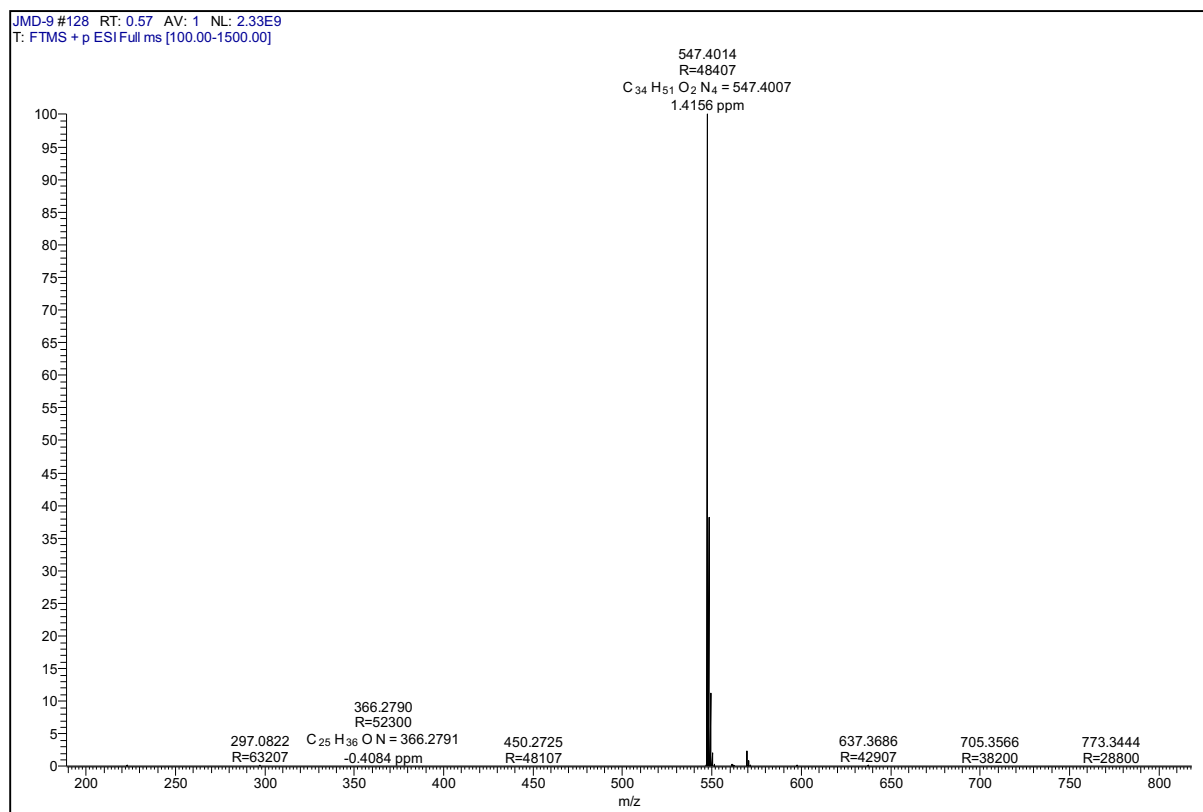
HRMS of 31



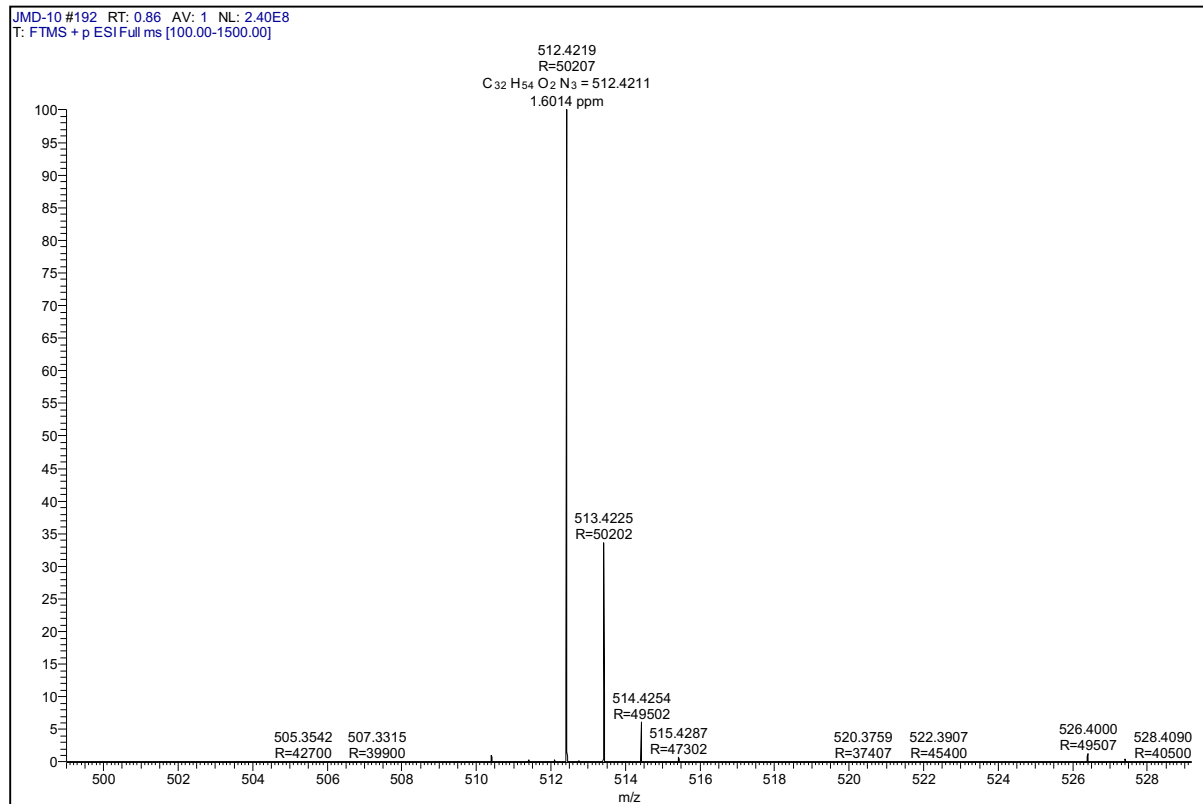
HRMS of 32



HRMS of 33



HRMS of 34



4.9 References

1. D. Baruah, R. N. Das, and D. Konwar, *Synthetic Communications*, **2016**, *46*, 79–84
2. D. Lednicer, In *Steroid Chemistry at a Glance*, Hoboken, NJ: Wiley, **2011**.
3. M. Cabeza, I. Heuze, E. Bratoeff, E. Ramirez, R. Martinez, *Chem. Pharm. Bull.*, **2001**, *49*, 525.
4. M.V. Dansey, P.H. Di Chenna, A.S. Veleiro, Z. Krisťofíková, H. Chodounska, A. Kasal, G. Burton; *Eur. J. Med. Chem.* **2010**, *45*, 3063.
5. M.R. Angelastro, A.L. Marquart, P.M. Weintraub, C.A. Gates, M.E. Laughlin, T.R. Blohm, N.P. Peet, *Bioorg. Med. Chem. Lett.* **1996**, *6*, 97.
6. M. Kumar, P. Rawat, M.F. Khan, A.K. Rawat, A.K. Srivastava, R. Maurya, *Bioorg. Med. Chem. Lett.*, **2011**, *21*, 2232.
7. P. Chowdhury, J.M. Borah, P. Goswami, A.M. Das, *Steroids*, **2011**, *76*, 497.
8. B.B. Shingate, B.G. Hazra, D.B. Salunke, V.S. Pore, F. Shirazi, M.V. Deshpande, *Eur. J. Med. Chem.* **2011**, *46*, 3681.
9. Y.Z. Ling, J.Z. Li, Z. Kato, *Bioorg. Med. Chem.* **1998**, *6*, 1683.
10. R. Hirschmann, P. Buchschacher, N.G. Steinberg, J.H. Fried, R. Ellis, G.J. Kent *et al. J. Am. Chem. Soc.* **1964**, *86*, 1520–7.
11. R. Gupta, D. Pathak, D.P. Jindal, *Eur. J. Med. Chem.* **1996**, *31*, 241–7.
12. A.J. Manson, F.W. Stonner, H.C. Neumann, R.G. Christiansen, R.L. Clarke, J.H. Ackerman *et al. J. Med. Chem.* **1963**, *6*, 1.
13. S. Wang, F. Xie, K. Song, *Chem. Abstr.* **1993**, *119*, 203669y.
14. R. Hirschmann, N.G. Steinberg, P. Buschacher, J.H. Fried, G.J. Kent, M. Tishler, *J. Am. Chem. Soc.* **1963**, *85*, 120–2.
15. A. H. Bandaya, B. P. Mira, J. Khazirb, K.A. Surib, H.M. S. Kumar, *Steroids*, **2010**, *75*, 805-809.
16. Li. Hongqi, F. Jueshu, Li. Juan, W. Yulong, T. Xiujuan, X. Yuanhui, *Res.Chem. Intermed.* **2013**, *39*, 3887–3893.
17. A. V. Silva-Ortiz, E. Bratoeff, T. Ramírez-Apan, Y. Heuze, A. Sánchez, J. Soriano, M. Cabeza, *Bioorganic & Medicinal Chemistry*, **2015**, *23*, 7535–7542.
18. A. Cammarata, S. K. Upadhyay, B. S. Jursic, D. M. Neumann, *Bioorg. Med. Chem. Lett.* **2011**, *21*, 7379–7386.
19. B. Shingate, B.G. Hazra, D.B. Salunke, V.S. Pore, F. Shirazi, M.V. Deshpande, *Chemistry & Biology Interface*, **2015**, *5*, 306-310.
20. H. Pan, P. V. Khang, D. Dong, R. Wang, L. Ma, *Bioorganic & Medicinal Chemistry*

Letters, **2016**.

21. Y. Bin, Q. Ping-Ping, S. Xiao-Jing, H. Ruilei, G. Hao, Z. Yi-Chao, Y. De-Quan, L. Hong-Min, *Eur. J. M. Chem.* **2016**, *117*, 241-255.
22. M.K. Penov-Gašić, A.M. Oklječ, E.T. Petri, A.S. Čelić, E.A. Djurendić, O.R. Klisurić, J.J. Csanadi, G. Batta, A.R. Nikolić, D.S. Jakimovb and M.N. Sakač, *Med. Chem. Commun.*, **2013**, *4*, 317–323.
23. D. Nedelcu, J. Liu, Y. Xu, C. Jao & A. Salic, *NATURE CHEMICAL BIOLOGY*, **2013**, *9*, 557-566.
24. J. S. Yadav, B. V. Subba Reddy, G. Madhusudhan Reddy and D. Narasimha Chary, *Tetrahedron Letters*, **2007**, *48*, 8773–8776.
25. L.S. Campbell-Verduyn, W.S' ski, C.P. Postema, R.A. Dierckx, P.H. Elsinga, D.B. Janssen and B.L. Feringa, *Chem. Commun.*, **2010**, *46*, 898–900.
26. F. Alonso, Y. Moglie, G. Radivoy, and M. Yus, *J. Org. Chem.* **2011**, *76*, 8394–8405.
27. K.R Senwar, P. Sharma, S. Nekkanti, M. Sathish, A. Kamal, B. Sridhard and N. Shankaraiah, *New J. Chem.*, **2015**, *39*, 3973—3981.
28. V. S. Pore, J. M. Divse, C. Charolkar, L. Nawale, V. Khedkar, D. Sarkar; *Bioorganic & Medicinal Chemistry Letters*, **2015**, *25*, 4185–4190.
29. (a) V. S. Pore, N. G. Aher, M. Kumar, P. K. Shukla, *Tetrahedron*, 2006, *62*, 11178; (b) B. G. Hazra, N. S. Vatmurge, V. S. Pore, F. Shirazi, P. S. Chavan, M. V. Deshpande, *Bioorg. Med. Chem. Lett.*, 2008, *18*, 2043; (c) N. S. Vatmurge, B. G. Hazra, V. S. Pore, F. Shirazi, M. V. Deshpande, S. Kadreppa, S. Chattopadhyay, *Org. Biomol. Chem.*, 2008, *6*, 3823; (d) S. N. Bavikar, D. B. Salunke, B. G. Hazra, V. S. Pore, R. H. Dodd, J. Thierry, F. Shirazi, M. V. Deshpande, S. Kadreppa, S. Chattopadhyay, *Bioorg. Med. Chem. Lett.*, 2008, *18*, 5512; (e) N. G. Aher, V. S. Pore, G. B. Shiva Keshava, A. Kumar, N. N. Mishra, P. K. Shukla, A. Sharma, M. K. Bhat, *Bioorg. Med. Chem. Lett.*, 2009, *19*, 759.
30. Ji-song Li, Y. Li, C. Son, and A. M. H. Brodie; *J. Med. Chem.*, **1996**, *39*, 4335-4339.
31. E. J. Corey, M. Chaykovsky; *J. Am. Chem. Soc.* **1965**, *87*, 1353-1364.
32. C. E. Cook, R. C. Corley, M. E. Wall, *Tetrahedron Lett.* **1965**, 891-895.
33. Z. S. Sydykov, G. M. Segal, *Izv. Akad. Nauk. SSSR, Ser. Khim.* **1975**, *11*, 2581-2584.
34. Ji-song Li, Y. Li, C. Son, and A. M. H. Brodie, *J. Med. Chem.* **1996**, *39*, 4335-4339.
35. J. Lewin'ski, J. Zachara, P. Horeglad, D. Glinka, J. Lipkowski and I. Justyniak, *Inorg. Chem.*, **2001**, *40*, 6086.

